CRANFIELD UNIVERSITY

ABDELMANAM ABAAD ABDELSALAM ABAAD

DESIGN, TECHNO-ECONOMIC AND ENVIRONMENTAL RISK ASSESSMENT OF AERO-DERIVATIVE INDUSTRIAL GAS TURBINE

SCHOOL OF ENGINEERING
PhD SCHOOL OF ENGINEERING

PhD
Academic Year: 2011-2012

Supervisor: Prof. Pericles Pilidis

August 2012

CRANFIELD UNIVERSITY

SCHOOL OF ENGINEERING
PhD SCHOOL OF ENGINEERING

PhD

Academic Year 2011-2012

ABDELMANAM ABAAD ABDELSALAM ABAAD

DESIGN, TECHNO-ECONOMIC AND ENVIRONMENTAL RISK ASSESSMENT OF AERO-DERIVATIVE INDUSTRIAL GAS TURBINE

Supervisor: Prof. Pericles Pilidis

August 2012

ABSTRACT

Increased availability of natural gas has boosted research and development efforts to further increase gas turbine performance. Performance has been increased remarkably and unit cost reduced due to achievements gained in improving thermodynamic cycles and cooling technologies. However, increased complexity in power industry regulations and fluctuations in fuel price have indicated that all the aforementioned improvements in gas turbine performance could not cope with the increased competition in the gas turbine industrial market. Innovation within the aero-derivative concept has enabled further significant improvement in the performance of industrial gas turbines. It allows a more beneficial approach than developing new designs of industrial gas turbines owing to reduced designing time and cost. Objectives in this project focus on developing a methodology of design and assessing aero-derivative gas turbine engines derived from a 130-seat aircraft engine. Developed methodology includes techno-economic and environmental assessment, conducted through further developments of models based on Techno-economic and Environmental Risk Assessment (TERA) philosophy, to be applied in further industrial applications.

Tools used in this investigation include a significant literature research on the development of aero-derivative gas turbine technologies, including thermodynamic cycles and its land-based applications. Turbomatch is a home-based code developed in Cranfield University, used in calculating design point and predicting off-design performance of parent aero-engine and the aero-derivative engines developed. Excel and FORTRAN code are also used in calculating engine's design parameters, and creating a model of life estimation Creep. Moreover, FORTRAN code is used for building emission and economic models for power generation and combined heat and power applications. Finally, MATLAP code is used in creating a small model for generating performance TXT files, and running marine integrated models platform.

All models needed to develop the methodology have been created, and calculations of an engine's performance and assessment were conducted based on this developed methodology. Sensible results are generated from the investigated methodology and they show acceptable designs of aero-derivative engines on different thermodynamic cycles. Based on the acceptable level of technology and material thermal barriers, all design and off-design performance limitations of new developed aero-derivative engines have been determined for a wide range of ambient conditions. Techno-economic and environmental assessment performed through implementing the developed aero-derivative engines on power generation and marine applications under different operating scenarios. Results of operating the engines on power generation and marine applications have been investigated and compared. It is observed that engines respond differently when operating under different environmental profiles, depending on the number of units engaged and their thermodynamic cycle as well as mechanical configurations. Also, the selected specific gas turbine engine can be the best economical choice for operating on determined scenario, while it cannot be when operating in different scenarios. Assessment of developed engines on the investigated application shows how the lowest specific cost (small engine size) can constitute important criteria in engine selection.

Keywords:

Cycles, Design, Performance, Derivation, Development, Conditions, Limitations, Emission, Creep, Economics, PG, Marin, Assessment

ACKNOWLEDGEMENTS

I would like to take this opportunity to extend my sincere thanks and gratitude to some of the people who have helped me to complete this project, either by providing academic supervision or by encouraging and supporting me during the whole period of my study.

I would like to express my regards and thanks to Professor Pericles Pilidis and Dr. Georgios Doulgeris for their support, encouragement and guidance since the beginning of my research studies in Cranfield University. I would also like thank all of the administrative staff and secretaries in the Department of Power and Propulsion for their help and support.

To my PhD colleagues in Gas Turbine Group and in my office, thank you for all your support and friendship. I would like to express my special appreciation and thanks to my colleague, Raja Khan.

I wish to convey my gratitude to the University of Sabha in Libya for the lavish funding of my research and providing me with the chance to complete my PhD study and be among its PhD scholars.

I owe huge thanks to my parents and would like to convey my valuable regards for their never-ending support and encouragement throughout my entire life, including my education until I achieved my PhD degree. To my wife and children, I extend my gratitude for your patience and all your support throughout the period of my study.

TABLE OF CONTENTS

LIST OF FIGURES

LIST OF TABLES

LIST OF EQUATIONS

NOMENCLATURE

AVIC	*Aviation Industries Corporation of China*
C	*Constant*
CHAT	*Cascaded Humidified Advanced Turbine*
CPR	*Compressor Pressure Ratio*
C_p	*Constant Pressure specific Heat Energy*
CW	*Compressor Work*
CPL	*Combustor Pressure Losses*
COT	*Combustor outlet Temperature*
CU	*Cranfield University*
CUAVA	*Cranfield University AVIC Aircraft*
D_m	*HPT Blade Mean Diameter*
DD	*Direct Load Driving*
DDV	*Direct Derivation*
Dens	*High Pressure Turbine Blade Material or Metal Density*
DP	*Design Point*
DDE	*Direct Derivation*
EGF	*Exhaust Gas Flow Rate*
EGT	*Exhaust Gas Temperature*
EPNL	*Effective Perceived Noise Level*
FPT	*Free power Turbine*
GT	*Gas Turbine*
GWP	*Global Warming Potential*
H_b	*High Pressure Turbine Blade Height*
HAT	*Humidified Air Turbine*
HEC	*Heat Exchanger Cycle*
HP	*High Pressure*
HPW	*Heat Power*
HPT	*High Pressure Turbine*
HPC	*Low Pressure Turbine*
IC	*Intercooler*
ICRH	*Intercooled Reheat Cycle*
I/C	*Intercooled Cycle*
IPT	*Integrated Power turbine*
$IC\ T_{in}$	*Intercooler Outlet Temperature*
$IC\ T_{out}$	*Intercooler Outlet Temperature*
ICR	*Intercooled Recuperated Cycle*
ISTIG	*Intercooled steam-injected cycle*
LMP	*Larson Millar Parameter*
LP	*Low Pressure*
LPC	*Low Pressure Compressor*
IPC	*Intermediate Pressure Compressor*
IPT	*Intermediate Pressure Turbine*
LPT	*Low Pressure Turbine*
MAST	*Mixed Air Steam*
MTG	*Microturbine Generators*
N_{HT}	*High Pressure Shaft Rotational Speed*
NONDW	*Non-dimensional Mass Flow*
NGV	*Nozzle Guide Van*

OD	*Off Design*
OPR	*Overall Pressure ratio*
P	*Pressure*
PEL	*Project Economic Life of Investment*
PR	*Pressure Ratio*
RH	*Reheat Cycle*
RWI	*Water Injection cycle*
PR_{lc}	*Low Pressure Compressor Pressure Ratio*
PT	*Power Turbine*
Q_{cc}	*Input Heat Energy*
SC	*Simple Cycle*
ShP	*Shaft Power*
SFC	*Specific Fuel consumption*
SFF	*Supplementary Firing Factor*
STIG	*Steam-injected Cycle*
S_P	*Specific*
T	*Temperature*
T_{am}	*Ambient Temperature*
T_b	*Turbine Blade Temperature*
TET	*Turbine Rotor inlet Temperature*
t_f	*Time to Failure*
TIT	*Turbine Rotor inlet Temperature*
T_{ex}	*Gas Turbine Exhaust Temperature*
TW	*Turbine Work*
$VIGVs$	*Variable inlet Guide Vans*
VANs	*Variable area nozzles*
W	*Core Mass Flow*
W_f	*Fuel Flow*
W_{ex}	*Exhaust Gas Flow Rate*
ζ_{ic}	*Compressors Isentropic efficiency*
ζ_{iT}	*Turbine Isentropic Efficiency*
ζ_{th}	*Thermal Efficiency*
α	*Power-to-heat-Ratio*
γ	*Air constant*
ζ_{cc}	*Combined Cycle Efficiency*
ζ_{GT}	*Gas Turbine Efficiency*
ϵ_{HRSG}	*Heat Recovery Steam Generator Effectiveness*
$\zeta_{Rankine}$	*Steam Cycle Efficiency*
$PrCst_t$	*Production Cost*
$RunCst_t$	*Running Cost*
$EmsTax_t$	*Emission Cost*
$DefCst_t$	*Deficit Cost*
$CO2Tax_t$	*Carbon Dioxide Taxation Cost*
δt	*Time Interval*
$CO2TaxR$	*Carbon Dioxide Tax Rate*
$CO2Al$	*Carbon Dioxide Allowance [Percentage of Annual emission Allowed]*
$CO2EmsM_t$	*Mass of Carbon Dioxide Emission*
MFC_t	*Mass of Fuel Consumed*
$CO2SM_t$	*Carbon Dioxide Emission per Unit Mass of Fuel*
$CMCF_t$	*Carbon Content Mass in Fuel*

1 INTRODUCTION

Much concern has recently been made regarding cost and efficiency which has led to seemingly never-ending development and improvement in gas turbine engines. Much effort has been expended by engineers and manufacturing firms in investing more in research and development in order to increase performance of gas turbines. Increased availability of natural gas and the introduction of more sophisticated cooling technologies resulted in further improvements to gas turbines, and success was achieved in reducing unit capital costs. Further improvements in gas turbine thermodynamic performance were achieved due to a range of approaches proposed after the results of extensive research and development. Improving the ability of increasing thermodynamic firing temperature and pressure ratio, achieved through advancement in cooling technologies and emission (NO_X) reduction, is considered as one proposed approach. A further approach used is by modifying Brayton's thermodynamic cycle through the involvement of heat exchanging technology in order to design advanced thermodynamic cycles such as Intercooled, Recuperated, Intercooled Recuperated, and Intercooled Recuperated Reheat Cycles, etc. [16]. Combined gas and steam cycles with high thermal efficiency and output power have dominated the market of base-load power generation.

However, the aforementioned approaches were found insufficient to keep up with the increased competition in the gas turbine market, with the complexity recently experienced in power industry deregulation as well as fluctuations in fuel price. So, the need to develop new gas turbines has increased, but manufacturers are aware that it needs a longer time (probably more than 10 years) to be accomplished.

Therefore, an innovation of aero-derivative ideas indicated in a third approach of developing gas turbine performance, was introduced by gas turbine manufacturer's engineers, i.e. the further development of the performance of industrial gas turbines derived from aero gas turbine engines [10]. This concept

or method results in reducing time and cost needed for designing newly developed gas turbine engines. It is commonly recognised in the gas turbine market that in considering profitability and other benefits, producing sufficient aero gas turbine engines requires much more spending than developing stationary gas turbine engines based on existing design technology of aero engines [63]. In addition, the highly sophisticated design technology of aero gas turbine engines is the most important factor to be considered concerning developing industrial gas turbine engines. The GE LM-6000 is an example of an aero-derivative gas turbine engine developed in the early 1990s by the GE Company. It was derived from the CF6-50 and CF6-80C2 aero engines, where low pressure compressors were imported from the former and high pressure compressors from the latter. Thermal efficiency was improved in the newly developed engine and reached about 40%, its development and design process time being cut down to under five years. Applying advanced material and cooling technology along with aerodynamics on aero-derivative approaches allows the improvement of simple cycle gas turbine operating temperatures to approximately $1500\mathcal{C}^{\circ}$ and a thermal efficiency of 40% or more [9][12]. In addition, aero-derivative technology advantages are observed as achieving remarkably good part-load efficiencies with a higher rate of return and low maintenance downtime [122]. These achievements are gained due to better flexibility provided by aero-derivative removable gas generator technology.

The early years of jet engines was the first time manufacturers and engineers realised the importance of using aero-derivative engines in power generation, mechanical drive and marine applications. Availability of gas turbines in some applications such as land-based applications is increased owing to the aforementioned significant fall in engine operation and maintenance cost [83]**.** Natural gas prices however, were very high in the early years of jet engines and resulted in delays in achieving success in developing gas turbine technology. The first successes in developing gas turbine technology were made and observed slightly later when prices dropped in the 1980s [100].

The assessment methodology used in this project is based on TERA, the philosophy of Technical, Economic, Environmental and Risk Assessment analysis, which was invented in Cranfield University and started as a concept based on the investigation of multi-disciplinary optimisation of power plants, including the effect of designing and operating power plants on atmospheric pollution. In the aero-engine area, TERA is a method introduced in software created at Cranfield University for modelling gas turbine engines along with aircraft performance. It includes different modules integrated with a commercial optimiser [84]. This optimiser is capable of optimising more than one objective function, including global warming potential, gaseous emission, engine noise and engine direct operating cost. Regarding the field of industrial land-based applications however, work is currently on-going to investigate the potential application of TERA philosophy. Objectives are concentrated on the possibilities of modifying and adapting TERA software to suit all land-based applications.

In this project it must be noted that the focus is on thermodynamic design analysis of aero-derivative gas turbine engines. It is worth mentioning that all proposed mechanical design changes and modifications to the existing aircraft gas turbine engines are not considered or addressed in this project.

1.1 Objectives

The main aim of this project is to develop a methodology of evaluating the potential to produce aeroderivative industrial gas turbines from a parent 130-saet aircraft engine using techno-economic and environmental risk assessment TERA. Investigation will include the ability of applying TERA in assessing the designed aero-derivative gas turbine engines on different thermodynamic cycles and applications.

Although the TERA is a complete tool invented and successfully developed for aero-engine applications, it is still not fully adapted for the use in evaluating aero-derivative industrial gas turbine applications. Objectives which lead to achieving the main aim are established in detailed milestones as following:

1. Investigate different aero-derivative cycles in different applications

2. Design different aero-derivative engines for application in different thermodynamic cycles derived from a 130-seat aircraft engine.
3. Simulation analysis for newly developed derivative engines to predict their off-design performance in different environmental conditions and apply them in different land-based applications.
4. Investigate and examine current and future feasibility of the thermodynamic cycle by exceeding turbine entry temperature of 1500°C, which is assumed as the current technology limit.
5. Building economic models for power generation applications used in techno-economic and environmental assessment of the designed derivative engines.
6. Evaluate engine economics and performance outputs using adapted methodology based on TERA philosophy, including environmental emission and engine life consumption considering different scenarios of operation on the plant.

1.2 Thesis Structure

This thesis introduces efforts taken by the author to introduce a methodology of evaluating new development and design of aero-derivative gas turbine engines derived from short-range 130-seat aircraft engines. The methodology considers methods of evaluating the viability of implementing the newly developed derivatives in land-based applications. The thesis consists of eight chapters, briefly described as follows:

Chapter One includes an introduction, defines problems faced in the gas turbine market which justify the need of introducing the innovation of aero-derivative gas turbine technology. Brief clarification of the introduced methodology of evaluation based on TERA philosophy is also included. In addition, the project's aim and objectives are presented along with a clarification of the thesis structure.

Chapter Two consists of a literature research, involving a significant amount of research survey work in the gas turbine field to support the

investigation. It includes an investigation into a variety of gas turbines applicable to thermodynamic cycles and most applications where aero-derivative gas turbine technology is applied. All economic and technical considerations taken in developing and selecting aero-derivative gas turbines are incorporated. The chapter shows how these considerations vary based on engine thermodynamic cycles and plant application. Furthermore, factors affecting the selection of aero-derivative industrial gas turbines are illustrated for marine, power generation and combined heat and power applications. A brief history of already designed aero-derivative gas turbines, including some currently on the market, is presented, including some examples of these engines and their applications.

Chapter Three defines two simulation case studies focusing on conducting design point calculations and predicting off-design performance of two-spool aero gas turbine engines and three-shaft intercooled aero-derivative industrial gas turbine engines. It introduces the process of conducting performance matching for 100kN thrust aircraft engines matching performance outputs of 130-seat aircraft engine CFM56-5B5, and also matching the performance of 100kN output power of three-shaft inter-cooled aero-derivative gas turbine engines LMS100.

Chapter Four is dedicated to clarifying the methodology used to fulfil the introduced objectives and conducting the investigation towards achieving the aim of this study. It shows the different sequential stages and milestones which need to be followed to conduct the whole analysis and generate the expected results. All selected thermodynamic cycles associated with each aero-derivative application are included. The proposed 130-seat aircraft engine is determined with its thermodynamic performance, and all possible mechanical configurations of aero-derivative gas turbine engines based on derivation methodology are sighted. In addition, all necessary tools and software are explained in stages which can be followed in order to investigate the thermodynamic performance, estimating the engine life consumed, environmental effect and economics. The platform of the TERA philosophy for aero-application is explained, including the model's relationships between the inputs and outputs.

Chapter Five determines procedures of performing design point calculation of all selected or proposed aero-derivative gas turbine engines. In this stage of design point calculation, all engine thermodynamic performance outputs of power output, thermal efficiency and heat outputs are calculated. The investigation also includes both proposed derivation concepts of keeping design specification of HP and LP rotor components, or only maintaining HP rotor components. All heat recovered at the assumption of the constant stack temperature of $400K^{\circ}$ or $126.85\mathrm{C}^{\circ}$ for all heat processes. It is based on fuel dew-point curves introduced in [85][6] and takes into consideration avoiding condensation problems at the engine's exhaust. Subject to derivation conditions and material barriers, all design limitations are determined at the design point for all applied thermodynamic cycle technologies of inter-cooling, recuperation and both combined.

Chapter Six attempts to present investigation procedures and results of all off-design performance calculations for selected aero-derivative industrial gas turbines developed in this project. In fact, it is well known that design point performance alone cannot be helpful in selecting gas turbine engines for any application. Thermodynamic outputs at the design point of developed aero-derivative gas turbine engines are not enough to determine whether or not they will be able to satisfy variation in load demand during their daily operation. Therefore, they are simulated at different conditions of expected off-design operating (different ambient pressures and temperatures). So, the effect of ambient conditions' variation on engine performance is investigated in the range of ambient temperature $(45C^{o}\ to - 15\ C^{o})$; hence, an engine's behaviour during its life cycle operation has been preliminarily predicted. The majority of possible control methods for engine surge protection and recuperation conditions are illustrated for all aero-derivative designs where recuperation technology has been applied.

Chapter Seven presents procedures and processes of assessing the developed aero-derivative industrial gas turbine engines. Technical, economic, and environmental evaluation is the major technique used for assessing newly

designed or developed gas turbines. Many aspects are considered for the technical assessment of derivative engines and clarified in this chapter. Hot section life is estimated through the crucial factor of calculating creep and thermal fatigue. Based on the Larson Miler Parameter method which presented in [36], a mathematical model for calculating creep for high pressure turbine blades has been developed using both FORTRAN and Excel software.

Emission components of $CO, CO_2, NO_X \; and \; UHC$ are also estimated at all off-design operation settings for all developed gas turbine engines. The emission model, originally created in FORTRAN code [29], has been modified and adapted in joint work conducted with EngD project [91] to suit the requirements of this project. It matches output format for performance outputs generated by different engines' performance models. All mathematical equations used in the model are based on work introduced by [71], [86]. This adapted model has been used in estimating all emission indices in this project, and it calculates specific values of $CO2, CO, UHC, and \; NOx$ per unit kilogram of fuel burned.

Manufacturing technology of gas turbines has been significantly improved and material cost has also been increased in addition to fuel cost, all resulting in rising manufacturing cost. In fact, the economic assessment is the complement to technical assessment and considering them separately is not possible in order to arrive at sensible assessment. Economic assessment has some factors which vary depending on the gas turbine application itself. Net Present Value NPV is a well-known technique used to compare the financial benefits, especially for long term projects [124]. An overview of NPV technique is given in this chapter. It has been used in the investigation of economic assessment of developed aero-derivative gas turbine engines in selected applications. Selected aero-derivative gas turbine engines have been implemented in this chapter on two applications of marine and power generation for further economic assessment.

In power generation application, an economic model is created in FORTRAN code and all its mathematical equations and considered economic aspects are also explained in Chapter Seven. Economic estimation is made regarding long-term investment projection and is conducted on yearly based calculations. It evaluates economic factors used to determine economic viability of the project through calculating Internal Rate of Return and time of starting generating money by knowing the Discounted Payback period, and calculates NPV as well as Generation Cost. Annual load demand of electricity and heat is taken from realistic records for three sites in Greece, representing three magnitudes of power demands [88]. Hourly demand profile changes with ambient temperature are analysed and manipulated in order to be applied to the designed power generation model. Ambient temperature change profile is figured out based on climate change history records published in Weather Underground [87]. Three typical seasonal days have been chosen to cover the whole year for economic analysis. The hourly variation profile of power demand is estimated hourly according to correlations created based on the monthly average value. The correlations are estimated based on methods for estimating load variation adapted in ERCOT [39]. An Excel worksheet is used to create these correlations for three different seasons of the year. Emission is also included in the economic model and it quantifies relative values of $CO, CO_2, NO_X \; and \; UHC$ per kilogram of consumed fuel.

Regarding marine application, developed derivative engines are involved and applied to an ongoing project of developing a model of investigating the performance of several aero-derivative marine gas turbines [72]. The engines are applied as the prime movers of propulsion system of merchant vessels. The project constitutes an integrated simulation platform for marine propulsion called Poseidon, and consists of numerical models used to evaluate the performance of ship propulsion systems using gas turbines as the prime mover. It is also capable of assessing the techno-economic potentials and environmental impacts of the gas turbine propulsion system. The aim is to contribute to the investigation of further developing the platform to be applied to longer haul ocean-going voyages, where the ship is expected to face diversity of rough and

smooth sea and weather conditions through the manoeuvring from one ocean to another. The contribution is conducted through investigating the performance of a variety of ship prime movers gas turbine propulsion systems implemented in different ship types and configurations. The investigation expresses a comparative analysis of evaluating the effects of varying the voyage's environmental conditions on developed engine performance.

Chapter Eight summarises the conclusions derived from this project research considering the impact of design and development limitations on the ability to produce aero-derivative industrial gas turbine engines. Also, it defines constraints of this research and recommendations for future work which may require further investigation.

Notice: Using isentropic efficiency in the design calculations makes no difference in thermal efficiency at the design point for engines with free power turbine FPT or direct coupling single-shaft.

2 LITERATURE RESEARCH

2.1 Gas Turbine Cycles and Configurations

The Brayton cycle is the base of designing most of the commercially available gas turbine engines. It was first introduced in simple thermodynamic cycles in one-spool direct load drive configuration. An enormous number of gas turbine cycles exist, which are basically considered as variants of the simple Brayton cycle. Some of these variants are implemented in commercial engines and others are still undergoing research for improvement and development. Accordingly, these cycles can be categorised as:

- Dry Cycles (Complex Cycles): modified Brayton cycles of IC, HEx, ICR, Reheat (RH), ICRH, Recuperated ICRH, and Combined cycle [13].

- Wet Cycles: which vary based on the way water is implemented in the dry cycles to increase output power and improve thermodynamic performance. STIG, ISTIG, RWI, HAT and CHAT are examples of wet cycles, and extra detailed review work and parametric thermodynamic analysis are presented in [14; 15].

- Advanced fuel cells based hybrid gas turbine cycles.

Industrial gas turbines are categorised in two groups, relating to their size. The small engines are determined by their use and are always pointed to the small industrial market. The large group machines however, are competitors and dominate most of the base-load power generation market. Gas turbine technologies are being developed and their development leads to enlarging the market for small units, where combinations of power and heat or cooling are needed. The size of industrial gas turbines has grown due to developments in technology and it has become viable to provide over 300MW of output power, as demonstrated in Figure 2-1. It is clearly noticed that increasing gas turbine engine size raises the pressure ratio, which improves engine outputs. However, another option available to improve an engine's output power and performance

is by increasing turbine inlet temperature which can be available through combined development in technologies of materials, cooling and thermal barrier coatings. Much effort has been made in order to improve gas turbine efficiency and plant economics through looking into the different possible technologies and engine configurations. The simple cycle was applied in single-shaft, two-shaft and three-shaft configurations respectively, with and without exhaust heat recuperation and inter-cooled divided compression. Also, combined cycle steam and gas turbines were applied [98].

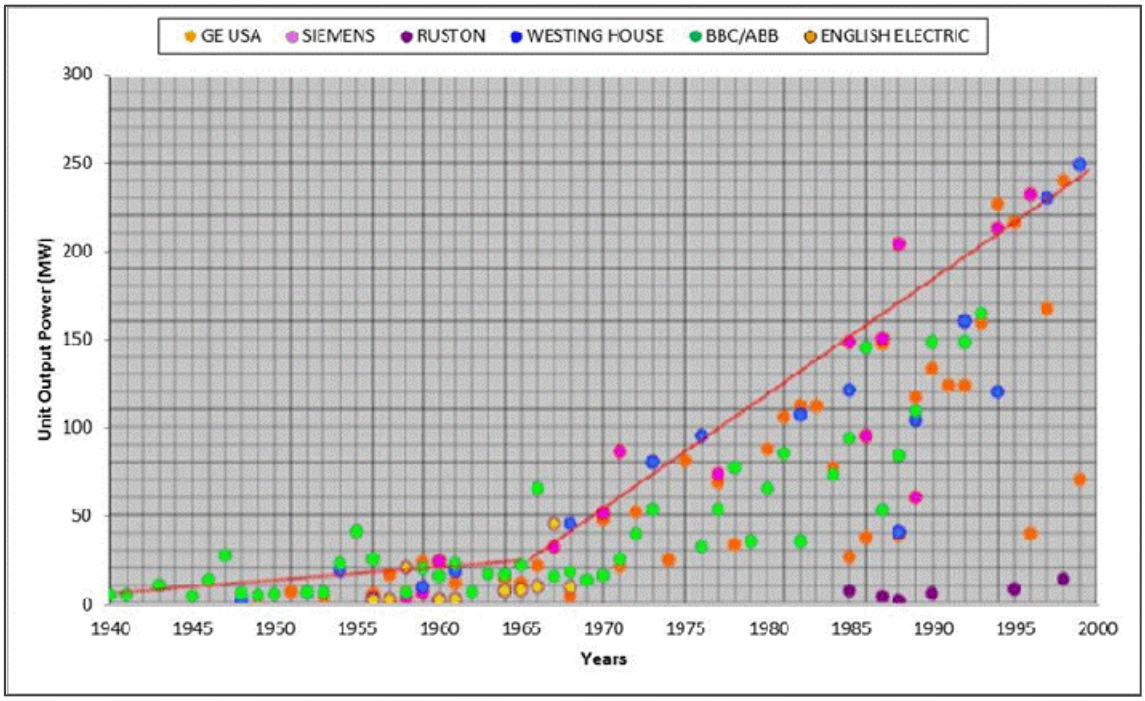

Figure 2-1Historical Trend of Power Output for Some Commercial GT Engines [98]

Some technologies, such as inter-cooling, exhaust heat recovery and recuperation are used in different mechanical gas turbine engine configurations. These technologies are the base of all aforementioned dry cycles. In this project, the focus will be only on dry thermodynamic advanced cycles, and a more detailed review of these cycles is included in the following sections.

2.1.1 Simple Cycle Gas Turbine

The simple cycle type gas turbine has dominated most gas turbine field applications, and the literature shows that the majority of gas turbine engines

are commercially available to operate in simple cycle [74][75]. In many applications the simple cycle cannot satisfy the growing demand made by gas turbine operators for higher thermally efficient and low exhaust emissions, which are mainly considered as the driver of plant economics. Generally, the typical simple cycle gas turbine suffers a reduction in thermal efficiency at part-load operation. This poor thermal efficiency is basically caused by a reduction in turbine inlet temperature and pressure ratio. Achievable thermodynamic performance using the simple Brayton cycle is still limited, despite the advancements made in component design, blade cooling and material technologies [15]. Figure 2-2 demonstrates the average trend of the improvement over time in a simple cycle thermal efficiency of industrial gas turbines owing to improvements in material technologies which lead to improving turbine inlet temperature.

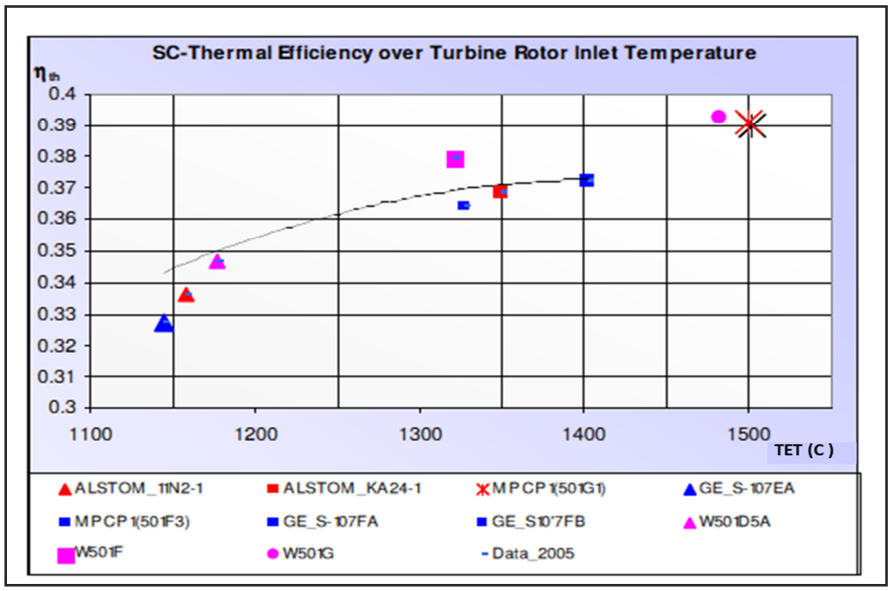

Figure 2-2 Efficiency Trend in Simple Cycle Industrial Gas Turbine vs the improvement in TET [118].

Many attempts to minimise the reduction in engine thermal efficiency have been performed. Exhaust waste heat recovery is one option of improving the reduction in part-load thermal efficiency, which in turn forces the need for further development in more efficient heat exchangers. Highly efficient heat exchangers have been used in two forms of heat recuperating and inter-cooling on the simple gas turbine cycle. Recuperated and inter-cooled recuperated cycles are found within basic open thermodynamic cycles to be the most

thermally efficient cycles, and the second mentioned also has the potential for higher specific power [96].

2.1.2 Heat Exchanger Gas Turbine Cycle

Improving gas turbine plant economics through enhancing gas turbine thermal efficiency and reducing emissions can be gained in different ways. Significant improvements in efficiency and reduction in emission production are achieved by incorporating heat exchanger technology and upgrading simple cycles to recuperated or regenerative cycles. Recuperation technology has been used mainly in small and mid-size gas turbines in order to improve their thermal efficiency, where turbine inlet temperature and pressure ratios are low. Using this technology offers the capability of lowering plant operation costs due to the lower optimum pressure ratio required for a given power output. Hence, it results in lowering the consumed resources and less material stresses [38].

'Recuperated' and 'regenerative' are the terms used to describe the simple cycle gas turbine with heat exchanger installed for heat recovering. They can be distinguished depending on the type of heat exchanger used for recovering. Recuperators transfer heat from hot exhaust heat to air leaving the compressor before entering the combustion chamber. However, development in recuperative gas turbine engines was delayed as a result of early achieved improvements in turbo-machinery efficiency of gas turbine components [22].

Many arrangements are available for the recuperator to be applied or installed on the simple cycle gas turbine plant, which will be covered in detail later. Two shaft engines with heat exchangers in the cycle can have different configurations. Firstly, by locating the heat exchanger after the HP turbine where more concern has to be taken regarding the thermal barriers of the heat exchanger materials [23; 32; 33; 67]. Secondly, there is the commonly used method of installing the heat exchanger at the gas turbine engine exhaust [80]. In this study the terms 'non-conventional' and 'conventional' will be given to the two arrangements respectively. Also, the term 'alternative recuperation' can be used for the non-conventional arrangement.

2.1.2.1 Conventional Recuperated Cycle

The Conventional Recuperated Cycle has been the most commonly used arrangement since the innovation of the heat exchanger technology cycle. Higher thermal efficiency is achieved by recuperating heat from engine exhaust gas and using this heat to preheat air leaving the compression system before entering the combustion chamber. A diagram indicating the construction of a plant of simple cycle regeneration gas turbines is presented in Figure 2-3. Many companies have applied gas turbines with this technology in most of their industrial applications. For example, GE has used the conventional arrangement of recuperation in some gas turbine plants such as PGT5, MS3002, MS5001, MS5002B, MS5002C, MS5002D [43].

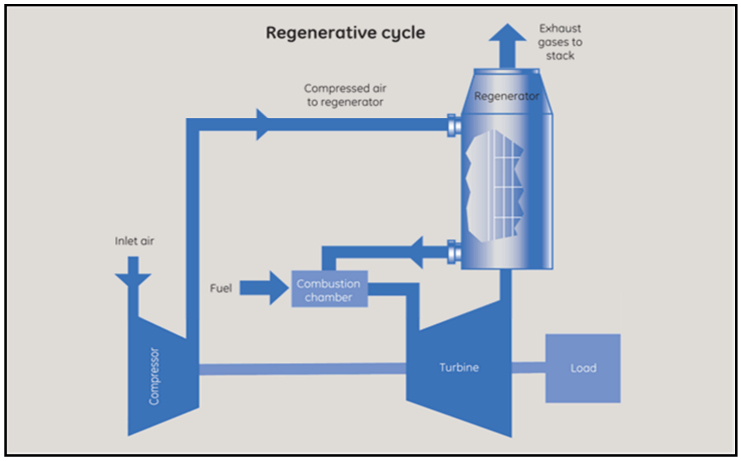

Figure 2-3: Diagram of Gas Turbine Regenerative Cycle [49]

The benefits and advantages of using this technology were addressed and summarised by GE as follows:

- Increasing thermal efficiency
- Lowering heat rate
- Enhanced equipment efficiency in direct coupling design
- Complicated structure
- Lower maintenance

The effectiveness of the utilisation of the heat recovery process is very important and an essential factor from the thermodynamic point of view. More concern should be given to recovery effectiveness at part load operating. In this

respect, similar characteristics were found between the recuperated cycle and steam and gas turbine cycles where both employed heat recovery process at the gas turbine exit. So, the turbine exhaust temperature must be maintained as high as possible in both cases, even at part load operating, in order to achieve full utilisation of heat recovery effect, hence increasing efficiency of the plant.

Considering engine configurations and comparing with direct load coupling arrangement, part load operation behaviour of simple cycle gas turbine engine with free power turbine shows that gas generator exhaust temperature increases at part load operating due to the reduction in air mass flow. So, the free power turbine configuration has the significant advantage of high heat recovery capacity [38; 65; 66]. Figure 2-4 describes the gas turbine engine operating line using the simple method of operating single-shaft gas turbines, considering it as the maximum air flow control method. While other methods of control, such as $VANs$ and $VIGVs$ used a variable air flow control method. In the second method, even during load change, air flow rate is still actively controlled.

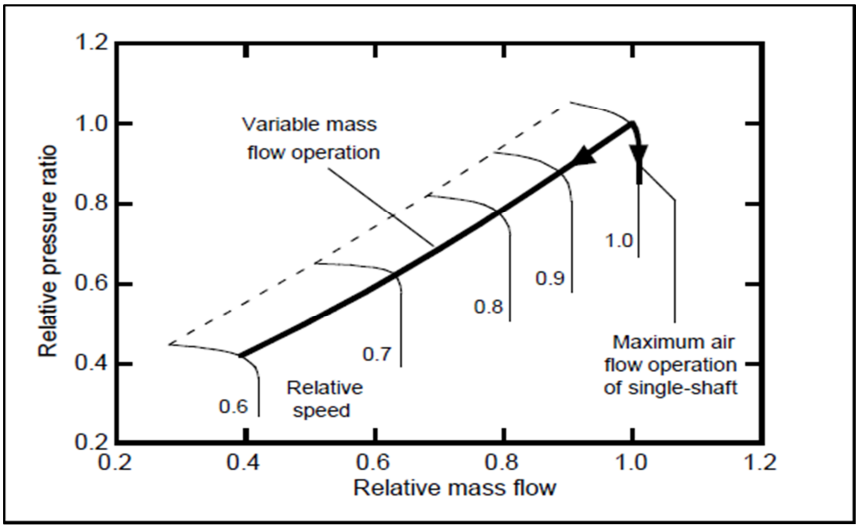

Figure 2-4 Operating Lines Control for both Single Shaft and FPT Gas Turbine Configurations [66]

The efficiency of recovering heat in the recuperator is measured by what is called 'recuperator effectiveness' ($\in$). It refers to the ratio of air temperature difference to the temperature difference between inlet air and gas temperature. If we assume the gas and air flow rates are equal, then the effectiveness can be described in the following equation [32].

$$\in = \frac{T_{aout} - T_{ain}}{T_{gin} - T_{ain}}$$

In practical terms, the recuperator effectiveness changes during off-design operation in accordance with the reduction in mass flow rate of gas and air, hence leading to increasing the effectiveness.

A pressure drop of about 2 psi through the regenerator in the small gas turbine engine on the conventional regenerative cycle makes the performance of simple cycle gas turbines better for the same engine's pressure ratio and design condition.

2.1.2.2 Non-Conventional (Alternative) Recuperated Cycle

Recently, many researchers have demonstrated interest in the alternative recuperative cycle concept, where turbine expansion is divided into two sections, and some independent research studies exist considering this technology. The main objective was to investigate the ability of maintaining higher thermal efficiency at off-design operation using this technology. Generally, the concept involved extracting heat from the hot gas leaving the gas generator in front of the free power turbine configuration as exhibited in Figure 2-5. It is used in order to transfer more heat to the compressed air leaving the compressor and entering the combustor.

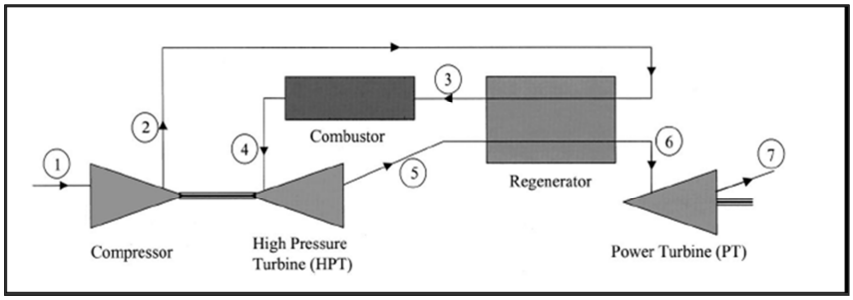

Figure 2-5 Schematic Diagram for non-Conventional Regenerative Cycle Gas Turbine [32]

It is clear that in the conventional regenerative cycle heat is recovered after extraction of as much as maximum work allows. However, in the non-conventional cycle hot gases enter the heat exchanger before they are fully expanded in temperatures much higher than the case in the conventional regenerative scheme. As a result, heat will be added to the combustor at a

relatively higher average temperature leading to improving the cycle thermal efficiency and increasing the cycle optimum pressure ratio at a given operating temperature. However, side effects to be considered include reduction of specific power produced due to enthalpy drop occurring when hot gases enter the free power turbine, which results in less work produced by the PT. Also, the recuperator will suffer from operating at higher pressure ratio, due to the increase in cycle optimum pressure ratio and higher temperature than the conventional regenerative. However, the capability of modern recuperators has improved recently and most of the aforementioned high pressure and temperature are accommodated. In other words, the available improvement in thermal efficiency from the non-conventional regenerative cycle can only be achieved by using pressure ratios higher than those required in conventional regeneration. Figure 2-6 represents the thermodynamic cycles of three cycle configurations (simple cycle, regenerative cycle, and alternative regenerative cycle) on a T-S diagram. According to the stages numbering mentioned and with the assumption of compressor work equal to the first turbine work with un-cooled hot section on ideal cycle, thermal efficiency models can be distinguished using the following formulae [33]:

Simple Cycle Efficiency $\zeta_{th} = \frac{Net\ Out\ Power}{External\ heat\ input} = \frac{W*C_p*(T_5-T_6)}{W*C_p*(T_4-T_2)} = \frac{(h_5-h_6)}{(h_4-h_2)}$

Conventional Regenerative $\zeta_{th} = \frac{Net\ Out\ Power}{External\ heat\ input} = \frac{W*C_p*(T_5-T_6)}{W*C_p*(T_4-T_3)} = \frac{(h_5-h_6)}{(h_4-h_3)}$

Placing the recuperator at the engine exhaust causes no difference in using the previous formula in calculation whether the free power turbine or direct coupling single-shaft configuration is used. However, extracting the heat in between the turbines in non-conventional regenerative arrangements will make a difference in calculation between free power turbines and single shaft configuration and the thermodynamic model used in calculation should be as follows:

Non-Conventional Regenerative $\zeta_{th} = \frac{W*C_p*(T_4-T_5)+W*C_p*(T_6-T_7)-W*C_p*(T_2-T_1)}{W*C_p*(T_4-T_3)}$

$= \frac{(h_4-h_5)+(h_6-h_7)-(h_2-h_1)}{(h_4-h_3)}$

Heat Exchanger Effectiveness $\in = \frac{T_{aout} - T_{ain}}{T_{gin} - T_{ain}}$

Pressure at the inlet of the heat exchanger at stage 5 can be or should be optimised to provide the highest possible cycle thermal efficiency especially in a single-shaft configuration. Heat exchanger effectiveness equations are always useful in calculating outlet temperature at the cold side of the heat exchanger; while the energy balance equation between the hot and cold sides helps in calculating the outlet temperature on the hot side.

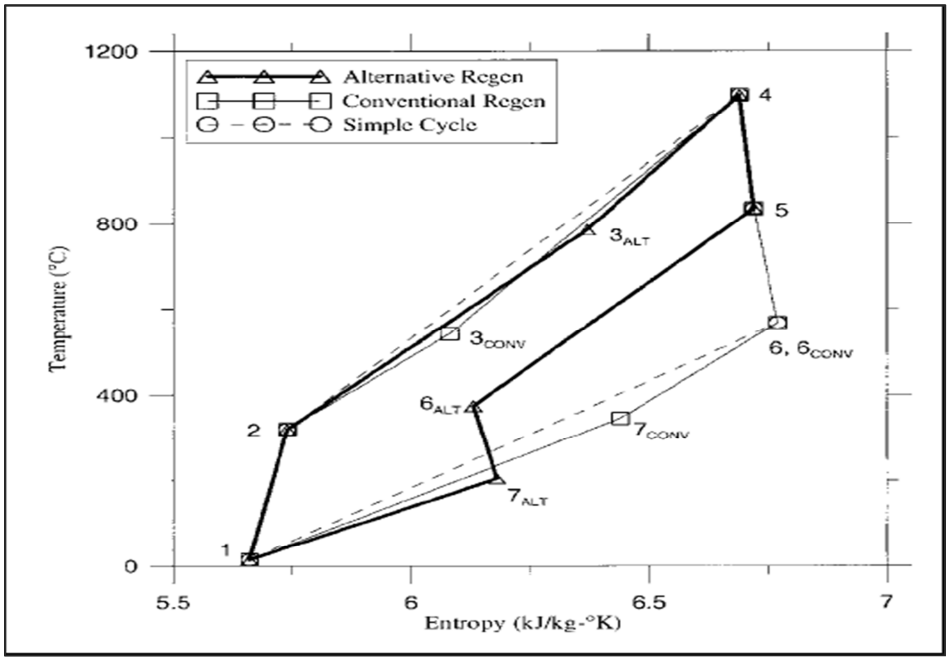

Figure 2-6 Comparison between Conventional, non-conventional and Simple Cycles for $PR = 10,\ TET = 1373\ K^{\circ}, \in = 0.9$

A study conducted by [32][33] observed that using the non-conventional regenerative technology lowered the temperature of gases through the FPT as well as its exit temperature. It also improved cycle thermal efficiency better than the comparable conventional regeneration cycles, providing that high technology applied with the engine operated at high turbine inlet temperatures. On the other hand the improvement in efficiency is limited when relatively low technology gas turbine engines are used. The improvements can only be achieved at lower values of heat exchanger effectiveness in order to keep second turbine inlet temperature high enough for achieving good enthalpy drop. Therefore, divided expansion can be beneficial under certain circumstances,

and for the ability of using them on current, small-size gas turbines with high effectiveness of the modern recuperators, all component efficiencies including the recuperator effectiveness have to be rather high in order to make them competitive in the current market. Non-conventional technology appears to be competitive when severe space limitations are imposed on recuperator size which leads to a reduction in recuperator effectiveness and increased pressure drops. Most literature concluded that it is still possible to achieve the same recuperated cycle thermal efficiency by using simple cycle technology, but with much higher engine's TET and OPR. In addition, all the previous studies conducted for a wide range of turbine inlet temperature and heat exchanger effectiveness, all concluded that the highest values of thermal efficiency were gained with the divided expansion cycle and that it is applicable with relatively high pressure ratios [38].

2.1.3 Intercooled Cycle Gas Turbine

A significant improvement in gas turbine thermal efficiency over the simple cycle gas turbine has been achieved by introducing inter-cooling on the simple cycle, and the improvements rise further with the increase in gas turbine design pressure ratios [30]. Most current gas turbines utilise a ratio of cooled air extracted from the compression processes in order to cool the hot section. By implementing an inter-cooling temperature of cooling air extracted from the compressor, this will be lower than the case in the simple cycle due to the reduction in air temperature entering the HP compressor. As a consequence, the amount of extracted cooling air required to cool the hot gas sections, nozzle guide vans $NGVs$ and turbine blades, will be reduced. In addition, using the inter-cooler results in reducing the amount of turbine work required to drive the compressor in order to compress air between the intermediate and high-pressure compressors, and that leads to increase the cycle's useful work for the given cycle temperature ratio. Lower turbine inlet temperature causes an increase in engine specific fuel consumption SFC, and it has a major positive effect at relatively higher turbine entry temperature TET. Implementing inter-cooler technology allows increasing firing temperature, due to the improvement

in blade cooling effect, to a higher level than that possible on the simple cycle for the same cycle design pressure ratio which leads to a decrease in specific fuel consumption and improves engine performance. Clarifying why IC has higher cycle thermal efficiency than the SC at high pressure ratios for the same TET, it is that the proportional amount of heat added in the combustor is less than the proportional increase in useful work [121]. Also, efficiency increased as a result of the decrease in the compressor losses effect on cycle thermal efficiency due to OPR. On the other hand, at low pressure ratios the engine will be improved in terms of specific power and thermal efficiency will be similar to the simple cycle.

Thermodynamic analysis of the inter-cooled cycle highlighted the need to optimise the cycle owing to the fact that there is always an optimum value of intercooler pressure, of maximum efficiency or specific power, for every given value of overall pressure ratio and TET, as shown in Figure 2-7.

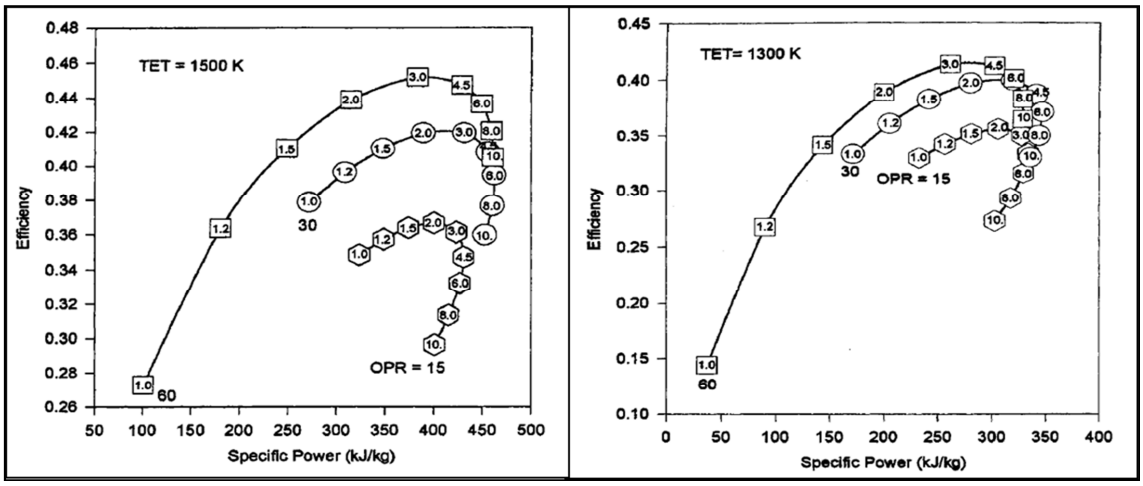

Figure 2-7 Intercooler Optimum Pressure Ratios for Best Compression Splitting [30]

The Figure represents the relationship between cycle specific power and thermal efficiency for different values of overall pressure ratio OPR and turbine inlet temperature TET. Optimising the cycle helps in finding the correct splitting of the compression ratio between low and high pressure compressors. Optimum pressure ratio for maximum efficiency increases with the increase in cycle OPR for given value of turbine inlet temperature, and it also leads to improve thermal efficiency. Furthermore, for every group of constant overall pressure ratio OPR

and turbine inlet temperature TET there is an optimum value of LP compressor pressure ratio which provides either maximum efficiency or maximum specific power as indicated in Figure 2-8. It explores the overall performance curves for optimum pressure ratios obtaining the maximum efficiency for every TET at every group of constant overall pressure ratio.

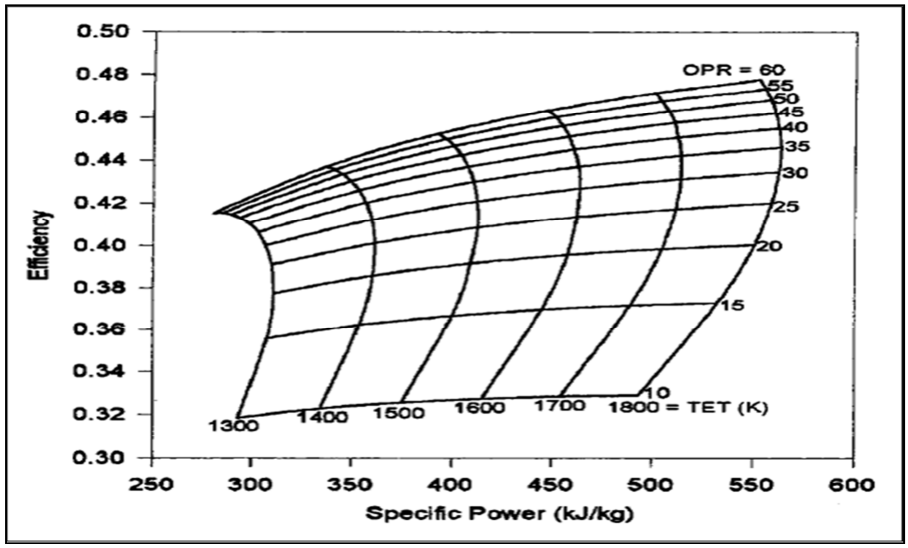

Figure 2-8 Intercooler Thermodynamic Performance for Best Thermodynamic Cycle Efficiency [30]

The curves show that inter-cooling can improve thermal efficiency and its effect on thermal efficiency is major at high values of cycle pressure ratios, which concurs with Figure 2-9. At low pressure ratios also IC has the advantage of increasing specific power compared to the simple cycle. Both previous figures indicate that at low pressure ratio increasing TET has relatively small effect on both inter-cooler optimum pressure and cycle optimum pressure for maximum thermal efficiency relative to the situation of high pressure ratios. The new shape of improved optimum pressure ratio in comparison with the same engine in simple cycle is demonstrated in Figure 2-9.

A calculation of improving performance of simple cycle gas turbines using realistic parameters through applying inter-cooling technology has proved that increasing the turbine inlet temperature no longer means only an increase in cycle efficiency, but also increases the output power. It shows that increasing the pressure ratio and turbine inlet temperature still contributes to improving the performance of the inter-cooled gas turbine cycle [59]. Analysis of inter-cooled

two-shaft gas turbines observed that at part load operation good thermal efficiency can be gained when shaft power is produced at constant rotational speed on the high pressure shaft. The literature mentions that for every degree rise in compressor inlet temperature, there will be losses of 0.1% in simple cycle gas turbine thermal efficiency and about 1.47MW in output power [31].

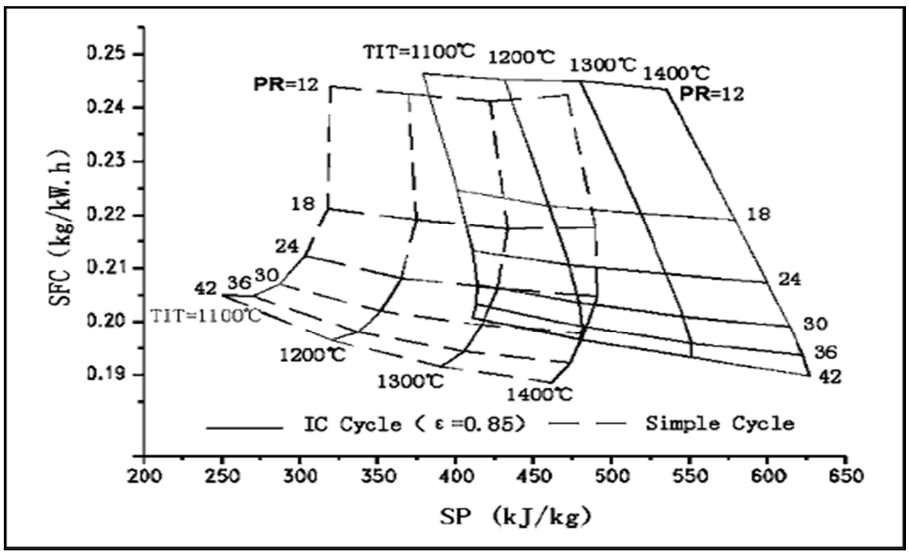

Figure 2-9 Overall Design Performance Comparison between Simple Cycle and Intercooled Cycle [121]

Applying variable geometry turbo-machinery such as $IGVs$ at inlet of HP compressor on inter-cooled gas turbine allows overcoming the problem of exceeding TET the limit at high pressure ratios on simple cycle with fixed geometry turbo-machines. Also, it improved part load performance on a wide range of part load operations. Inter-cooled cycle has advantages over the simple cycle at high pressure ratios, which results in low engine exhaust temperature. It makes high pressure inter-cooled engines inefficient for use in combined cycle application. When availability of water is limited and not cost effective, the inter-cooled gas turbine is found more suitable for peak load operation, due to the massive need for water to operate the inter-cooler in high pressure engines.

A new technology was introduced in [42] focuses on using alternative substances of inter-cooling compressor air by using Methanol and found to have no negative effect on thermal efficiency. In terms of economics however, it

was seen to be not cost effective considering the cost of Methanol and more study is needed to consider life reduction.

2.1.4 Intercooled Recuperated Cycle Gas Turbine

As previously mentioned, the most important process in the recuperated gas turbine is the exhaust heat recovery process at the recuperator and the utilisation of the recovered heat has a major effect on plant efficiency. Introducing inter-cooling technology to the recuperated cycle has further improved thermal efficiency and led to further increases in engine specific power output than the simple cycle, as described in Figure 2-10. Furthermore compared with recuperated cycles for constant rotor inlet temperature RIT and at part load variable shaft rotational speed operation, the two-spool inter-cooled recuperated represents better part load fuel consumption economy than the heat exchanger (recuperated) cycle gas turbine engine [96].

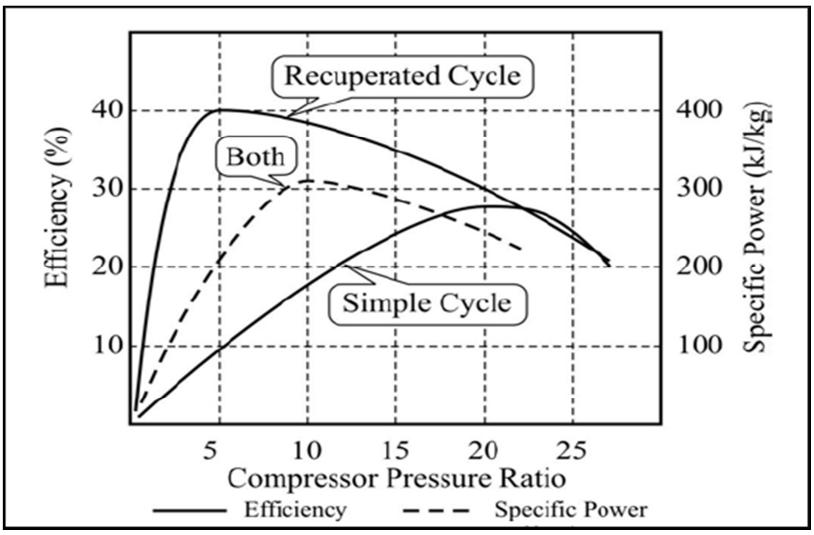

Figure 2-10 Performance Comparison between Simple and ICR Cycle for given Specific Power [115]

Results on the charts indicate constant turbine inlet temperature ($TET = 1200\ C^{\circ}$). The dotted line in the middle represents engine's specific power output for both engines and it is a function of the engine's pressure ratio. It can be noticed that applying ICR technology led to decrease value of optimum pressure ratio for maximum efficiency, and improved values of cycle maximum

thermal efficiency. The ICR technology has demonstrated good thermodynamic performance in electricity generation applications as well as better performance in combined heat and power application [115].

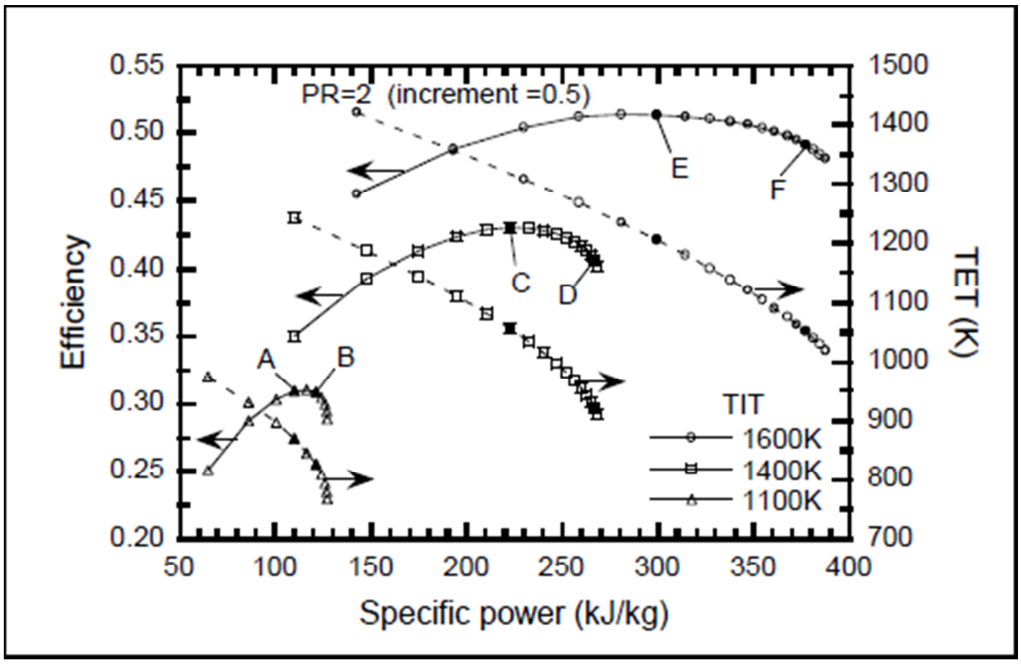

Figure 2-11 Design Point Performance Charts for Different Gas turbine Engines [66]

Significant work was accomplished by [66] in order to compare part-load performance for different gas turbine engines in different configurations and operation strategies including intercooled and recuperated cycle configuration, as shown in Figure 2-12. The study included the feasibility study for investigating further higher engine design parameters than the state-of-the-art engines, and all the design point calculation results are presented in Figure 2-11 in order to compare different inter-cooled recuperated gas turbine engines. It can be noticed from Figure 2-11 that there exist six curves, including three for constant TET and the others for constant OR. Increasing pressure ratio causes an improvement in thermal efficiency until a certain value where any further increase leads to a decrease in thermal efficiency. It has proved that for every given value of TET there will be two different values for optimum pressure ratios, depending on maximum specific work or maximum thermal efficiency, such as point D and point C respectively. Rising turbine inlet

temperature leads to improving engine thermodynamic performance and shifting optimum pressure ratios points to higher values and results in further improvement in thermal efficiency.

From a thermodynamic point of view increasing the difference between turbine exit temperature, or recuperator inlet temperature RIT, and engine exhaust temperature enhances the heat recovery effect at the recuperator. Depending on the engine mechanical configuration ($FPT\ or\ IPT$) there will be several methods available for controlling turbine exit temperature in order to maintain it constant at design value. These methods include using components variable geometry $VIGVs$, $VANs$.

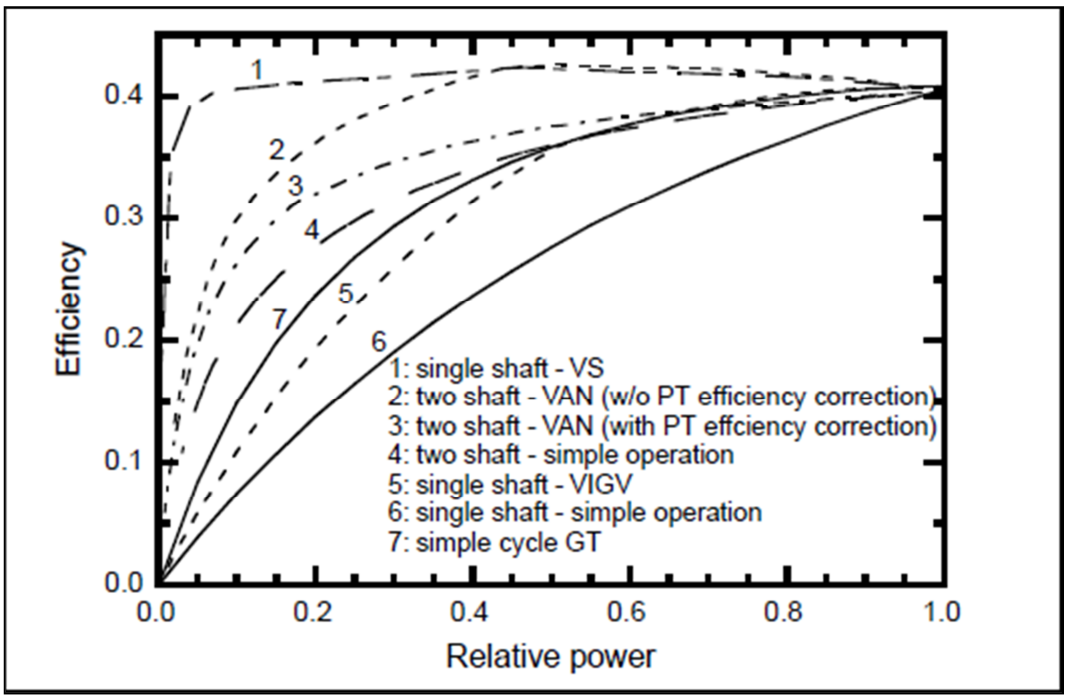

Figure 2-12 Performance Comparison for different Gas Turbine configurations and part-load operation strategies [66]

The basic method used in the early days of recuperated to maintain RIT was by varying engine rotational speed and called Variable Speed VS, which was able to keep turbine exit temperature constant up to values of zero-load, and enhanced the recovery effect through increasing the difference between EGT and RIT. Another simple method called Simple Operation, also used in the early days, is by managing the amount of fuel flow ratio in order to keep RIT as close as possible to the design point value. As noted in Figure 2-12, using fuel control

only results in a reduction in all engine performance parameters and provides lower thermal efficiency than the simple cycle for a given load, despite the fact that it keeps exhaust gas flow W_{ex} constant at design value due to the choking condition in the turbine at design point. Introducing compressor variable inlet guide vans $VIGV_s$ technology for compressor surge control at part load in aero-derivative engines offers another method for maintaining constant turbine exit temperature. It has been observed that using $VIGV_s$ allows keeping rotor inlet temperature constant for up to 30% reduction in engine mass flow rate, and then the simple operation method needs to be applied for any further reduction in mass flow. On the other hand this method demonstrates lower thermal efficiency than the VS method owing to the reduction in compressor efficiency caused by the change in inlet air flow angles. Therefore, variable speed is found as the most efficient method of operation recuperated and inter-cooled recuperated gas turbines and achieves the best part load efficiency [96].

Regarding the VS operation method on points B, D and F in Figure 2-11, they have the optimum PR values for maximum specific power with slightly higher pressure ratio and lower TET than points A, C and E, which have optimum PR for maximum efficiency. It has been discovered that constant RIT operation on these points leads to higher part load efficiency than points A, C and E, due to having lower design TET values. So, at part load it is still possible to increase TET to the design values of the comparative points, and that leads to higher part load efficiency for a wide range of operations than the design point for B,D and F [96][22]. Moreover, choosing a higher design pressure ratio than the optimum provides higher specific power and lowering turbine exit temperature which in turn helps in reducing material cost.

As it is well known that for the same design parameters gas turbines in two-shaft configurations have far higher turbine exit temperature, hence recuperator inlet temperature, than the single-shaft configuration. Two-shaft configuration promised better advantages when operation on fuel control only used. Introducing the variable area nozzles $VANs$ technology in compressor turbines or free power turbine configuration of two-shaft engines enhanced the

capability of further improving thermal efficiency up to the point of a 20% reduction in mass flow rate relative to design value. Then the $VANs$ have to be opened and fuel control only applied. Although closing the $VANs$ in free power turbines reduces turbine swallowing capacity and allows RIT to be maintained as high as possible, it causes a reduction in power turbine efficiency. All the limitations of 30% and 20% flow for $VIGVs$ and $VANs$ respectively, were proven in practical experience of application of gas turbines [66].

It has been concluded that a single shaft configuration engine with $VIGVs$ operation suffers a very rapid drop in its thermal efficiency with the degradation in power at part load than the two-shaft configuration. In addition in variable speed operation, increasing design turbine entry temperature TET decreases degradation in thermal efficiency at part load operation. [67] in his study proved that introducing the alternative (non-conventional) regenerative configuration on inlet air-cooled cycle improves thermal efficiency and increases power output. Also, it lowers the optimum cycle design pressure ratio which provides the maximum thermal efficiency.

2.1.5 Combined Cycle Gas Turbine

Similar to the role applied in combined heat and power applications, a significant improvement in plant thermodynamic performance can be achieved by recovering waste heat from the gas turbine engine exhaust. It has been found that in large gas turbine power generation applications, employing steam turbine cycles provides the best performance in general. The heat-recovery steam generator $HRSG$ is used in recovering the heat of gas turbine exhausts in order to generate steam for the bottoming ST cycle. Gas turbines based combined cycle power plants dominate the present energy sector using natural gas, and it is proposed that output power increases from around 570 GW in 1999 to 2035 GW in 2020; an increase of over 6% annually [102]. Performance of $HRSG$ has a great importance and many gas turbine developers who strongly focus on the gas turbine output are normally unaware of. It has a major effect on the thermodynamic performance of the whole plant. Achieving optimum

steam turbine outputs can be gained as a result of a proper utilisation of exhaust heat of gas turbine engines in the steam cycle. Analysis of a study conducted by [94] for combined cycles with different $HRSG$ configurations concluded that in order to achieve better heat recovery using a dual cycle, high pressure steam turbine pressure must be high, and low pressure steam turbine pressure must be low.

With the assumption of 100% combustion efficiency and neglecting fuel mass flow, combined cycle net plant efficiency can be calculated using the following equation [52].

$$(\zeta_{cc} = \zeta_{GT} + (1 - \zeta_{GT}) * \in_{HRST} * \zeta_{Rankine})$$

One of the commonly used options, offering high efficiency for power production is the combined gas and steam turbines cycle. [52]. Most of the early large combined cycle plants powered by heavy industrial gas turbines utilised the most commonly used control strategy of varying the variable inlet guide vans $VIGVs$ in order to reduce compressor mass flow rate and increase exhaust temperature. The combined cycle gas turbine has mostly been used in base-load electric power generation applications. However, the introduction of aero-derivative gas turbine technology allowed combined gas turbine cycle breaking in the field of other applications for relatively low power capacity less than 50MW. Although most large civilian ships powered by diesel engines, using gas turbines in combined cycles for the propulsion of large ships offers the great advantage of lowering the weight and reducing the required space as well as the amount of produced emission [53]. Also, in some marine applications, such as naval, the combined cycle gas turbine spends a significant time operating at part-load and its performance is of great importance. In this case there is an optimum gas turbine configuration and different specific control strategy $VIGVs$ or/and $VANs$ needed to maximise the plant efficiency at part-load operation.

2.1.6 Gas Turbine Configuration

Gas turbine engines are designed in both single and two-shaft configurations for both generator and mechanical-drive applications. These configurations can be called single-shaft (direct drive) configuration or free turbine configuration. An example of both configurations applied on recuperated gas turbine cycle is presented in schematic diagrams in Figure 2-13. Both types of configurations are available and will be considered in this project. An electricity generator is the driven load in both diagrams.

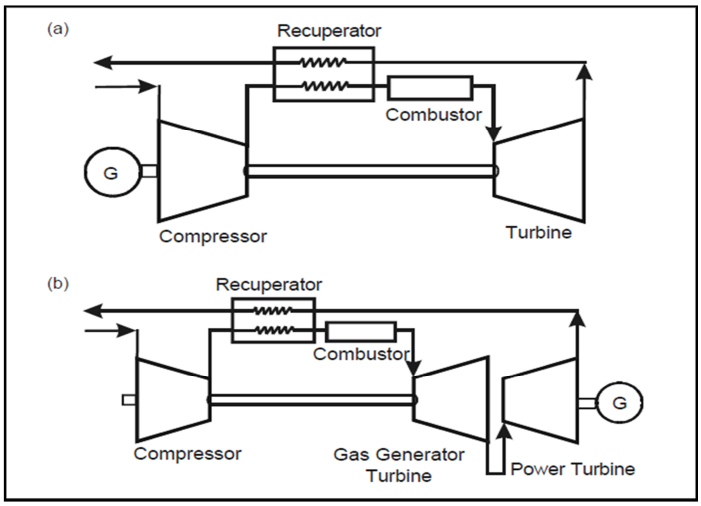

Figure 2-13 Gas Turbine's Single-Shaft and Free Power turbine Configuration [66]

2.1.6.1 Direct Mechanical Coupling Configuration *IPT*

As is clearly seen in Part A of Figure 2-13 the electricity generator will be driven and rotates at the same speed as the engine power shaft. For normal large gas turbines, the major challenge is how to keep the rotating speed of the power shaft of the gas turbine constant in order to produce constant frequency of electricity. However, the digital power controller has solved the issue in the case of small gas turbines (micro turbine). Depending on the power demand the power shaft can operate at different speeds while the output electricity frequency is kept constant [66].

2.1.6.2 Free Power Turbine Configurations FPT

As was mentioned in the literature by [118], “The introduction of the jet engine (turbo-compressor hot gas generators), aero-dynamically coupled to power turbines, was a wakeup call to the industrial single shaft gas turbine industry’’. The first compact split shaft gas turbines were introduced in 1959 free power turbines [35]. Using free power turbine technology made it possible for gas turbine manufactures to break the barrier of $100MW$, and it became possible to have $160\,MW$ power machines with single electric generators offering relatively higher thermal efficiency and lower installation costs. However, it was not possible on single shaft machines to break the barrier of $100MW$ with $60Hz$ until the 1980s with 1250 C° and above, due to improvements in material technology. Free power turbine technology is generally used in power generation and marine application where power turbines have been used. As shown in Part B of Figure 2-13, the engine consists of a gas generator aerodynamically coupled with a free power turbine. The free power turbine can be operated at constant rotational speed with no response to the variation in gas generator rotational speed due to ambient condition change or load variation. Aero-derivative gas turbines represented the multi-shaft gas turbine engines for a long time and found more efficient at part load where variable geometry may be required [65][60].

In the case of having two turbines in series, operating the generator turbine is subject to major restrictions applied by the compressor turbine represented in a mass flow compatibility condition. Choking condition of the power turbine determines the maximum achievable pressure ratio in the compressor turbine, and the pressure ratio will be controlled through the swallowing capacity of the power turbine. The best way to recognise the behaviour of this relationship is by plotting the compressor pressure ratio with the gas generator turbine pressure ratio. It is observed that compressor turbine pressure ratio tends to increase with the increase in compressor pressure ratio until the power turbine becomes choked, and then the turbine pressure ratio remains constant. So, a turbine’s first-row nozzles are always designed to be at

or near the choked condition at maximum power full-load, and at part-load the non-dimensional mass flow starts to decrease due to the fall in both compressor and turbine pressure ratios.

Finally, there are many other competitive technologies, excluded from this project, which have proven their ability of improving thermal efficiency of basic cycles and gaining power augmentations. A study of applying inlet air cooling and after-cooling technologies (absorption inlet cooling, evaporative after cooling, and evaporative inlet cooling) on intercooled recuperated reheat cycle, conducted by [8] promised an improvements in thermal efficiency and power outputs.

2.2 Gas Turbine Applications

2.2.1 Industrial Gas Turbine Applications

Industrial gas turbines can be defined as heavy-duty machines designed especially for stationary applications. Most heavy industrial gas turbines have been designed with 8 to 16 as a compression ratio and were found to be more suitable for combined cycle applications. This result can be justified clearly as a result of the high exhaust temperature which is relatively hot. [78].Figure 2-14 presents some design parameters of a group of less than 50MW gas turbine engines, which are commercially available in different power sizes. It expresses how their exhaust gas temperature and specific power varies according to their power size. The gas turbine has been considered as the most important prime mover in many power generation applications. Its importance was widely realised and became involved in many applications, such as military marine propulsion systems and natural gas pipeline pumping applications. Moreover, in comparison with the other electric power generation technologies which exist today, industrial gas turbines provide significant improvements in plant thermal efficiency providing the lowest capital cost with extremely low emissions [120]. The development of industrial gas turbines with low cost and efficiency 30-38% frame type simple cycle power plants, optimised at their highest power needs.

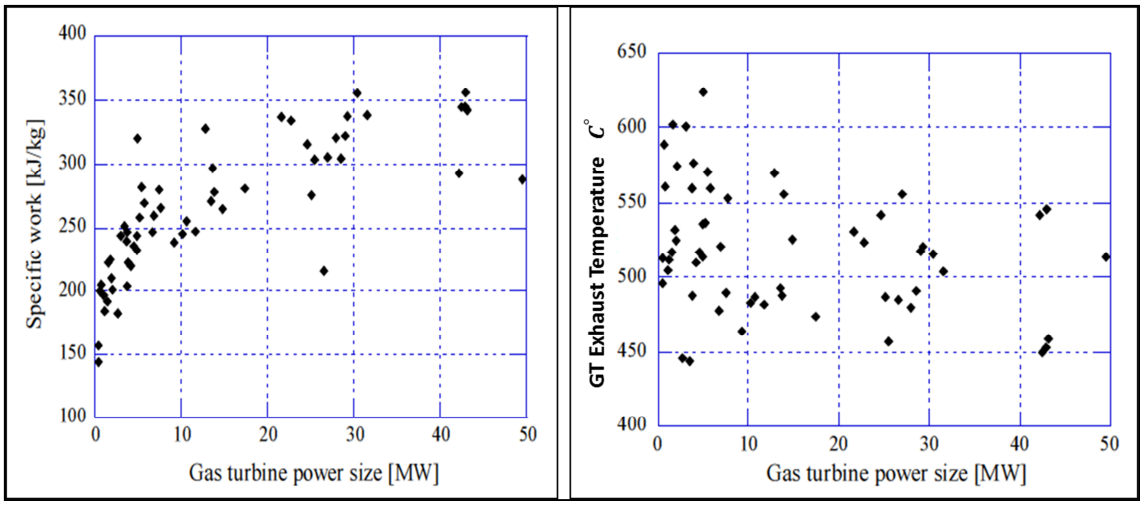

Figure 2-14 Gas Turbine Power Size versus Specific Power and Exhaust Gas temperature [17]

Also, highest cost and efficiency combined cycles in frame type and aero-derivative are optimised for base load needs of 50-60% efficiency. Further improvement in electricity generation cost and efficiency would be expected owing to the never-ending development in gas turbine technologies, specifically with those designed to perform well in intermediate load duty. Estimation of the US market has concluded that in the period 2005-2015 the growth in demand is expected to be between 37000 and 160000MW, accompanied with growth in worldwide natural gas [120]. Also, the International Energy Agency IEA anticipates increase in the electricity demand by 2.4% per year. [62].

2.2.1.1 Electricity Power Generation

The first industrial gas turbine introduced for power generation was in 1937 with 17% of thermal efficiency. Great success in gas turbine technology has been achieved due to the availability of natural gas, which is cheap and rich in hydrogen, leading to lower emissions. In addition, the achievable thermal efficiency of around 60% is a significant factor in that success. Hence, gas turbines dominated the power generation market as result [85].

Despite the poor quality of fuel burning of steam turbines, they can operate and still provide higher thermal efficiency, reliability and capability. The major restrictions applied on them are due to the increased requirements for burning clean fuel. These restrictions force the need to use pure fuel due to

significant rise in environmental costs. Therefore, burning natural gas became relatively cheaper leading to further increase in the research and developments in gas turbines. As result, gas turbine performance has been remarkably increased against steam turbine performance and lower plant prices were achieved [63]**.** Heavy-duty gas turbines are still used in some countries and have more advantages where desert conditions are prevalent. It is the advantage of ability of burning a cheap fuel and the lack of need for cooling water. Gas turbines in electricity power generation can be categorised according to their size and power capacity as follows:

Grid system:

In this system electrical power can be delivered at unchanging frequency, so the shaft power must be operated at constant synchronous speed. Due to the availability of gas turbines in small and large sizes, it is more desirable currently to have a small number of large power stations, used to supply grids, and more flexibly distributed power systems.

***Standby generators*:**

This is a system used in emergency situations where the probability of losing the main power supply is expected. The generated power is normally used for local needs and the unit is not connected to the grid system. In such systems, unit cost is crucial and simple cycle gas turbines have been used to a large extent. In order to reduce unit cost the used gas turbine has to be in single spool rather than with free power turbines as long as part-load speed is not considered. Also, in terms of lower unit cost, a centrifugal compressor with pressure ratio of 5:1 to 10:1 is highly recommend due to the poor thermal efficiency of axial compressors at this range. The selection of this kind of power plant should be following the criteria in the order of unit cost, weight, volume, and start and acceleration time to rated power. Thermal efficiency and emission levels are of secondary importance [85]. It is clear that smaller weight and volume and faster start and acceleration are most effective.

Microturbine:

It can be seen that the turbomachinery of the small size microturbine causes the drop in both pressure ratio and component efficiency. However, the microturbine has been appearing and taking a place in gas turbine market. To recover from the penalty of dropping pressure ratio and component efficiency, these turbines should be used in a recuperated cycle. Microturbines can be used to drive high speed generators directly, and their small size enables them to be installed to supply electricity and heat to a store of a restaurant, for example.

The gas turbine is the candidate in most power generation applications in their different classes and can be briefly illustrated as follows [85]**:**

- Micro-turbines in the class of 0.04-0.25MW, their applications in stores, small office blocks and restaurants.
- Simple cycle standby generator in the class of 0.25-1.5MW, major applications within office blocks and hospitals.
- Small scale combined heat and power CHP in the class of 0.5-10MW, examples of their applications within hospitals and small process factories.
- Large scale CHP within the class range 10-60MW, their application includes electricity and heating for a small town of up to 25000 people, large process factories and exporting electricity.
- Simple cycle peak looping units within the range of 20-60MW, their application is supplying electricity to the grid.
- Simple cycle med merit power stations in the class of 30-60MW, has been used to supply to the grid.
- Combined cycle base load power station within 50-450MW, the applications include supply to grid.

2.2.1.2 Combined Heat and Power Applications

Heating in some industrial applications requires the generation of electricity. The significant development in gas turbine performance during the

last few years has led to increased interest in using gas turbines in combined heat and power applications [112]. In such applications heat is recovered from gas turbine exhaust waste and used either in generating steam using heat recovery steam generator $HRSG$ or as typically utilised in some other industrial process such as desalination and drying processes or absorption air conditioning [83]. Using aero-derivative gas turbines in this form of energy conversion claims an energy saving of about 40% more than the separate power and heat generation. In addition, other advantages of using gas turbine in this combined form are reflected in reduction in losses of distribution and transportation owing to the ability of installing the decentralised energy supply where it is needed. Moreover, aero-derivative gas turbines have recently been more efficient in individual facilities, such as hospitals, in a tri-generation form of energy combining power, heat and cooling. In this form thermal energy can be used for generating steam for cooling systems and heating. Also, generated power can be distributed to the public grid. Lastly, combined heat and power can be sorted according to their capacity and form of outputs into two types as follows:

Small-scale combined heat and power:

Gas turbines in a simple cycle are applied in small-scale combined heat and power units and have the same major effect on unit cost as in the standby electricity generation units. Although the electricity generated in this application is utilised locally, excess electricity might exist which can be exported to the grid. The same level of consideration is given to both thermal efficiency and unit cost in small-scale combined heat and power applications, while emission levels and thermal efficiency are of secondary importance in standby generation units. Most gas turbine engines tend to be in simple cycle configuration, and a centrifugal compressor with a PR of 8:1-15:1 is involved in designing the small gas turbine engines used in such applications. In addition, thermal efficiencies and unit costs must be considered on both simple cycle and combined heat and power cycle. Peak heat demand can be met by using supplementary firing boilers for bridging peak heat demand periods. Also, there is a possibility of

using heat storage media and connecting them to the system for additional increases in operating time and efficiency. Hydraulic equipment is used in the system in order to distribute the heat, while electrical switches and control systems are used to manage the engine and distribute the electricity.

Large-scale combined heat and power:

In this scale of combined heat and power plants, gas turbines have dominated to the extent of being the only technology used. The waste heat is used to increase steam generation. The gas turbine used in these applications can be used for other applications such as marine, oil and gas markets where reducing unit cost is possible. The heavyweight gas turbine is used with axial flow compressors in the size of PR=15 to 35. So, aero-derivative engines demonstrate superiority in this sort of application and range of pressure ratio due to the lighter weight than the heavyweight gas turbines. Moreover, the compromise between CHP and simple cycle thermal efficiency has been applicable by gaining such high pressure ratios.

Performance criteria in combined heat and power include [112]:

Electrical Efficiency= $\frac{GT\ Electricity\ Production}{GT\ Fuel\ Consumption}$

This is dependent on internal parameters within the gas turbine itself and it is related to the process conditions such as process steam pressure.

CHP- Electrical Efficiency = $\frac{Total\ Electricity\ production}{Total\ Fuel\ Consumption}$

Total Efficiency= $\frac{Total\ (Electricity+Heat)Production}{Total\ Fuel\ consumption}$

Power-to-heat Ratio (α):

$\alpha = \frac{Total\ Electricity\ production}{Total\ heat\ Production} = \frac{CHP-Electrical\ Efficiency}{Total\ Efficiency - CHP\ Electrical\ Efficiency}$

Also when the supplementary firing is involved another factor should be included, which is *Supplementary Firing Factor* (SFF)

$$SFF = \frac{Supplementary\ Fuel\ Consumption}{Total\ (GT + Supplement) Fuel\ Consumption}$$

Then,

CHP- Electrical Efficiency = Electrical Efficiency (1-SFF)

The power plant type (cycle and internal efficiency) and the nature of heat demands in the industrial process such as temperature level are the major factors that affect the aforementioned CHP performance parameters.

*CHP plant Size= (Delivered Heat * α)*

Supplementary firing has positive effect on the plant's total efficiency and is normally adopted when there is wide variation in heat loads required. It allows Power-to-heat Ratio (α) value to vary to a great extent. Therefore, the desirable size of CHP plant can be obtained through the ability of adjusting the amount of supplementary firing which provides an opportunity to obtain α value which satisfies the plant's needs.

2.2.1.3 Industrial Mechanical-Drive Applications

The gas turbine in the power range of 5 to 25MW has been widely used in oil compressing and gas pumping stations. Some companies such as Alstom and Nuovo Pignone have been involved in building the units in the range of 5-10MW. At the time of low efficiency simple cycle, the regenerative gas turbines were used in pumping applications and further improvements had been made by replacing the heat exchangers by better efficiency units in the1970s[103].

However, the value of natural gas is much higher than previously when little attention was paid to thermal efficiency due to the cheap cost of natural gas. Hence, pumping units with high efficiency have become more necessary. In addition, most of the pumping units are typically transported and the

simplicity of replacing the gas generator for overhaul is necessary to reduce operating cost. Furthermore, the performance of the simple cycle has been increased remarkably and started to dominate the use in cogeneration and mechanical drive applications. Also, the need has grown for gas turbines to be involved in multi-applications. Therefore, heavy-duty industrial gas turbines became economically undesirable for this application and another more suitable technology must emerge.

2.2.2 Gas Turbine in Civil Aviation

The gas turbine has been used widely in civil aviation and it is still satisfying the growth demand. The demands for better thrust, reliability, weight and cost are still growing and more research concerning these requirements has been taken. These requirements are varied and depend on the applications themselves. For instance, there is particular concern for lower fuel consumption for long range aircraft, less weight and higher thrust for medium-range aircraft and for general aviation aircraft with lower initial cost is now required [99]. Generally in civil aviation, gas turbine engines have been presented in three types of Turbo-Shaft Gas, Turbo-prop Gas Turbine and Turbo-Fan Gas Turbine. Only the turbo-fan engine will be considered in this project and more detailed calculations will be observed in the following sections.

2.3 Aero-Derivative Gas Turbine

Most recent concern about cost and efficiency has led to never-ending attempts to develop and improve gas turbines. Increased availability of natural gas and more sophisticated cooling technologies introduced were the main contributors in early success achieved in improving gas turbine performance. The literature shows that many approaches were introduced in order to further improve gas turbine thermodynamic performance. The first approach, mentioned earlier, was to improve the ability to increase the engine's pressure ratio and firing temperature, through developments aimed at improving cooling technologies and reducing emissions NOx. A further approach is to modify the simple Brayton thermodynamic cycle through the involvement of heat

exchangers technology in designing what are called $IC, ICR, ICRH$, etc. However, the combined cycle gas turbine with its high thermal efficiency and output power has dominated the base-load power generation applications market and became the most popular [16]. A third approach has emerged as a result of increased complexity in deregulation in the power industry, fluctuation in fuel price, and the increase in competition in gas turbine market. So, the need for designing and developing a new gas turbine, which satisfies all the aforementioned requirements, has increased and was expected to take a long time (more than ten years).

Therefore, to reduce the cost of designing and developing new gas turbines, a new, more effective approach found by gas turbine manufacturers is to develop high performance industrial gas turbines modified from the aircraft gas turbine engine [10]. Regarding investment in the gas turbine market, producing sufficient aero gas turbine engines requires much more spending than needed for developing stationary gas turbines based on aero engines for better profitability and more benefits [63].The highly sophisticated technologies used in designing aero engines were the crucial factor involving them in developing land-based industrial gas turbines. The GE LM-6000 gas turbine is an early example of the aero-derivative gas turbine engine. It was developed in the early 1990s by deriving the LP compressor from the CF6-50 aero engine and the HPC from the CF6-80C2 aero engine. The newly developed aero-derivative engine achieved 40% thermal efficiency and reduced the development and designing process to less than 5 years. Due to the advances in material and cooling technology; aerodynamics along with aero-derivative technology, a simple cycle gas turbine has been developed with approximate Turbine Entry Temperature equal to 1500 C° and thermal efficiency of 40 % and more [9][12].

Generally, good part-load efficiencies, higher rate of return and low maintenance downtime have been achieved owing to implementing aero-derivative technology on industrial gas turbines [122]. Also, better flexibility is provided through introducing aero-derivative's removable gas generator, which in turn led to a drastic reduction in maintenance operation and increased the

gas turbine availability in industrial applications [83]. The importance of using aero-derivative technology in power generation, mechanical drive and marine applications was first realised by engineers in the early years of the jet engine. However, high natural gas prices resulted in delays in achieving success in developing the gas turbine until the 1980s when natural gas NG prices dropped [100].

2.3.1 Aero-derivative Verses Industrial Gas Turbine

Aero-derivative technology improved gas turbine thermodynamic performance and the ability of using gas turbine to simultaneously satisfy heat and power demands in different applications, such as CHP and $CCGT$. Compared to old heavy duty industrial gas turbines, aero-derivative gas turbines coped with the increased demand for higher efficiency and better operating flexibility in the intermediate power range [100]. In addition, they were found to be very tough competitors in satisfying the need of operating gas turbine simultaneously in different applications.

Better comparison was made between aero-derivative and old heavy-duty industrial gas turbines relative to their thermal efficiencies, availability and reliability, capital cost, economics and development cost. The aero-derivative gas turbine has gained preference related to its thermal efficiency, start-up time, maintenance and weight [21][83].

The history of technology development in gas turbines shows that early heavy industrial gas turbines had turbine inlet temperatures consistently well below those of aero engines, and their mechanical configuration trend moved towards a simple single-spool arrangement. While the trend of aero-engine configuration however, was to move to multi-spool arrangements which enabled them to operate at relatively higher pressure ratios. As a consequence, aero-derivative gas turbines were derived from the aero engine for land-based power generation applications and operated with relatively higher pressure ratios and turbine inlet temperatures. Based on basic design parameters of the gas turbine, Figure 2-15 exhibits a comparison of some commercially available industrial and aero-derivative gas turbines.

It can be seen clearly in Figure 2-15 that a majority of the industrial gas turbines were designed close to the line where pressure ratio provides maximum specific power output, whilst aero-derivative gas turbines were designed close to lines of maximum available thermal efficiency and pressure ratio. So, the heavy-duty gas turbine is developed and preferred for use where the pressure ratio is relatively low and they tend to demonstrate relatively poor thermal efficiency where the requirements for higher pressure ratio apply.

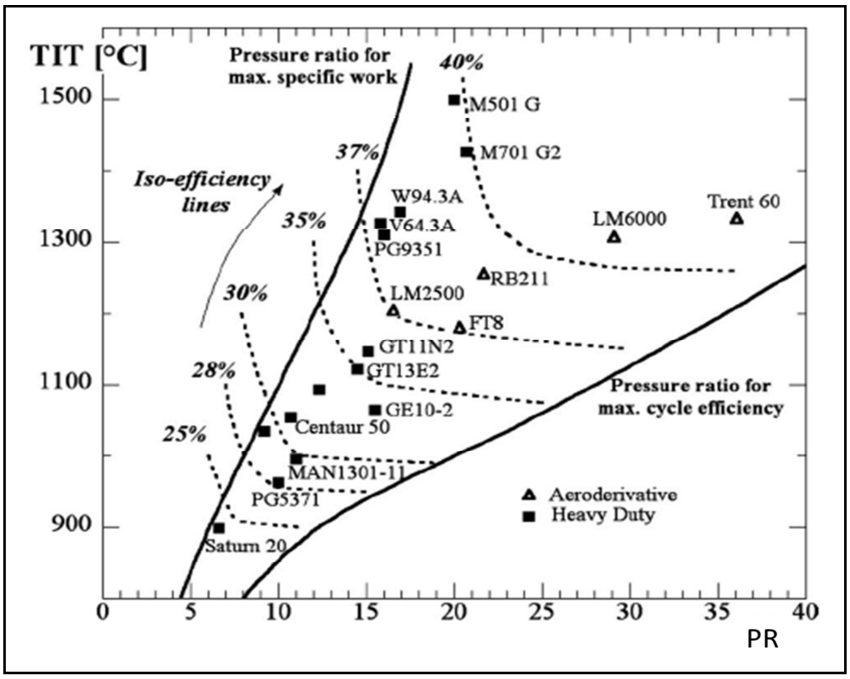

Figure 2-15 Comparative Performance Outputs Using the Basic Gas Turbine Design Parameters[16]

In contrast, the aero-derivative gas turbine has been appointed as the best technology applied with requirements of high pressure ratios, power output and thermal efficiency [63][78]. Inherited aero-engine's technologies helped in increasing reliability, production capacity and flexibility as well as minimising downtime. In addition, inherited aero-engine's performance, which is demonstrated by civil and military aircraft on every flight, made aero-derivative engines economically beneficial and competitive against the same-purpose developed heavy industrial gas turbines [114]. High efficiency and lower operating costs of aero-derivative gas turbines during their life cycle offset the expense of their initial prices [78].

Mechanically, the multi-spool feature of the aero-derivative gas turbine, which was not applicable in early large industrial gas turbine engines, offered aero-derivative engines high compression ratios and gained them priority in multi-purpose application simultaneously. As a result, unit cost was reduced and plant utilisation increased. It was noticed that applying inter-cooling technology to aero-derivative gas turbines with the aforementioned characteristics made them more beneficial [100]. The relative lightweight of aero-derivative gas turbines is vital in some applications, such as off-shore and marine applications, especially where space is very limited. Moreover, the light weight can reduce thermal loads, which in turn enhances heat transfer and quicker cooling and warming of the engine at start-up and shut-down [63]. On the top of that, they proved themselves a strong competitor where installation and mobility cost is more important, in applications such as oil-and-gas. Early aero-derivative gas turbines were originally jet engine-based and the gas generator uses rolling element anti-friction bearing, whilst early industrial gas turbines used hydrodynamic bearing. Considering operating costs in this case, aero-derivative engines will require synthetic lube oil while the industrial engine will operate with mineral oil which is more expensive [21].

2.3.2 Development in Aero-Derivative Gas Turbines

Concern about converting aircraft gas turbines for power generation application was increased alongside the issue of improving electric efficiency and higher specific power, as well as lowering O&M cost with emission in power generation applications [62]. Growing concern about cost, environment and quick availability was expected early from the gas turbine market. This predicted growth had enhanced the need for adapting gas turbines to continually meet the continuing growth in market requirements and load in power generation systems [83]. The end of the Second World War was the starting point for some companies, such as GE and Rolls Royce, to start thinking about using the aircraft-engine components to design aero-derivative engines.

Most aero-derivative technologies (such as cooling technologies, thermal barrier coating advanced high temperature materials) have been applied (for

example by GE, Westinghouse, Kawasaki Heavy Industries) in order to upgrade their turbines in the range of (13-15 MW) applications of simple cycle [122]. The earliest derivation of the aero-derivative gas turbine methodology was the simple substitution of the final nozzle by a power turbine in the jet engine [57].

Some modifications should be applied to the LP compressor due to the removal of the fan on the twin-spool turbofan engine. Hence, other modifications should also be made to the LP turbine as it will not drive the fan. Furthermore, in the case of three shaft turbofan engines the low pressure shaft would be removed completely [105]. The first lightweight derivative industrial gas turbines were introduced in the late 1950s and early 1960s. They were derived directly from aircraft engines and introduced into electric power generation, marine propulsion and pipeline compression applications. They exhibited similar performance characteristics of their steam turbine based cycles with $(PR = 12{:}\,1)$, $(TET = 1200 - 1500\ F^{\circ})$ equal to 922- 1088.7 Kº, and efficiency of 23-27 %. [57]. The GE LM2500 derived from the CF6-6 and Rolls-Royce Avon derived from TF39, are further examples of the early single shaft aero-derivative gas turbine designed with pressure ratio of [18.8]. The new generation of aero-derivative gas turbines were introduced in the late 1970s for industrial service. They were introduced in simple cycle configurations with thermal efficiency in the range of 32-37% and represented a new technological approach of aero-thermo design where the LP turbine drives the low pressure compressor and power generator [57]. Despite the advantages of offering more direct applications of aero-technology and cold-end drive, new generation turbines were suffering from power limitation in low pressure shafts. This issue led to limit power output and chances for their future growth [105]. Later in the 1980s, hybrid designs joined second generation units in keeping the basic structural concept of heavy frames. Applied hybrid designs utilised some of the aero-derivative design advantages, and some hybrid units succeeded in increasing thermal efficiency levels of early simple cycle second-generation aero-derivative units [110].

During development work, increasing gas turbine efficiency and specific power output were the major concern for most of the developed designs, and in

order to improve them firing temperature and pressure ratio had to be increased. So, improvements in component design, materials, cooling and combustion technologies were found necessary [62]. In addition, slight changes to the combustion chamber were needed due to more restricted environmental requirements applied in power generation application. Combustors had to be adapted to burn gas and liquid fuels. As a result of those requirements, the technology of Dry Low Emission combustor was introduced and more research and development investments were provided [120].

The modification of the thermodynamic cycle could be an attractive opportunity to improve the performance of aero-derivative gas turbines [26]. Improving the cycle process condition was considered the most important factor in improving aero-derivative engine performance. Improvements in cycle pressure ratio and operating temperature resulted from using advanced materials and exploring more advanced cooling methods [89]. Turbine inlet temperature has been increased due to improving cooling system effectiveness and using better materials' specification for turbine blades. These improvements led to further improve both specific work and cycle thermal efficiency. Advanced computational fluid dynamics is regarded as a further tool causing major improvements in compressor and turbine efficiencies.

Aero-derivative gas turbines have been used in mixed combined gas-steam cycle power plants and its usage justified by cost effectiveness as the design for the new engine would not be economically feasible. It was also noticed from thermodynamic analysis that better gas turbine thermal efficiencies could be achieved within aero-derivative pressure ratios [25]. Therefore, some thermodynamic modifications were found necessary to be made on simple cycle aero-derivative gas turbine in order to improve the thermodynamic performance. For instance, advanced technologies of mixed air steam ($MAST$), inter and after cooling, recuperated and advanced heat recovery have been used to advance the simple cycle, and improvements to the engine's performance were achieved [89]. Within the retrofitting technologies available, Inlet air cooling (IAC) and steam injection gas turbine ($STIG$) technologies were considered as the most effective ways of modifying the simple cycle gas turbine to increase

output power and thermal efficiency [1]. In addition, compared to the basic gas turbine cycle, combining evaporative after-cooling alongside with inlet air cooling led to an obvious increase in thermal energy efficiency in cogeneration application [64].

Humidifying working fluid of the gas turbine engine can improve engine efficiency and power output [62]. Many different cycles were introduced with steam or water injection injected to the working fluid, and their results led to the following consequences:

- Reducing the negative degradation effect of high ambient temperature or low ambient pressure
- Reducing nitrogen oxides formation
- Improving part-load performance
- Decreasing specific investment cost
- Improving electrical efficiency.

Three of the GE aero-derivative gas turbines have been involved in MAST technology with steam injected, i.e. the LM5000 STIG produces 51.6MWe, LM1600STIG with 17MWe and LM2500 provides 28.1MWe. They also provide 34.5, 22.8 and 13MWe respectively without STIG technology [89]. In the power range of 20-30MW of small and middle power plants, the evaporative cycle aero-derivative GTs have also been found to be a better alternative than the combined cycle. Using this technology on aero-derivative gas turbine engines enhances their thermal efficiency and specific work without the need to use the bottoming steam turbine [58][26]. In addition, as an upgrade to this technology, regenerative water-injected RWI was introduced on aero-derivative GTs through adding more water after the compressor. Hence, power output would increase while the power needed for compressor work remains constant [26][89]. This technology resulted in increasing mass flow entering the turbine and enhanced fuel-to-electricity efficiency. The GE-LM2500 has been used as an upgrade engine for the non-intercooled recuperative water injected cycle [25]. Figure 2-16 shows cycle modifications which included adding economizer (ECO), after-cooler (AC), regenerator (R) and burner (B). The economizer is

used to preheat water before being evaporated in the after-cooler. Also, power turbine PT exhaust gas is utilised to heat the mixture of air-steam into the recuperator. Saturation in the after-cooler could be overcome by adding water in the regenerator and it was approved to achieve better results. As a result compared to the simple cycle aero-derivative GT, a significant increase in thermal efficiency has been gained as well as limited rise in power output owing to the limited ability to improve existing blade cooling systems.

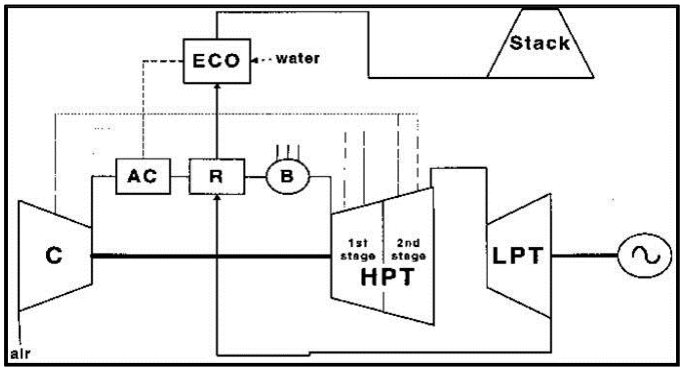

Figure 2-16 Regenerative Water-injected Cycle with GE LM2500 as a Prime Mover [25]

Thermodynamic analysis of the regenerative water-injected RWI cycle observed that aero-derivative gas turbines with pressure ratios from 16 to 20 can reach thermal efficiency of 45% [26].

Intercooled recuperated technology is used widely in aero-derivative gas turbine applications, such as WR-21 ICR. It was justified through the fact that cooling the air makes it easier for compression and results in reducing compressor discharge temperature which in turn enhances recuperator effectiveness [117]. In addition, inter-cooling reduces high pressure compressor work and its inlet temperature, which enhances thermal efficiency due to the increase in both mass flow and pressure ratio. Moreover, parts life consumption and emission will be improved due to providing more cooled air from compression discharge. Therefore, it is found to be more efficient in, for example, marine applications where simplicity is required in certain power classes [120]. Furthermore, in power generation applications where higher efficiency and reduced capital cost are very important, the GE Company in 2004 launched the most powerful aero-derivative intercooled engine. It provides

100MW of power output and achieves 44% of thermal efficiency at high part-load operation. This engine has the advantages of fast start (10 minutes) and low maintenance cost penalty [45]. In comparison with other combined cycle and advanced gas turbine engines, it is very competitive in this class with an unusual, less complex intercooled simple cycle.

Finally it is worth mentioning that, despite the use of advanced cycle technology on aero-derivative gas turbines; simple cycle technology is still dominating the majority of their applications.

2.3.3 Aero-Derivative Gas Turbine Engine Applications

The aero-derivative gas turbine has been involved in many applications including gas and oil transmission pipelines, marine propulsion, off-shore and electricity generation for peak and emergency loads. Some modifications were normally applied on aero-derivative gas turbine usually include combustion systems and strengthening of the bearings. Also, some other components sometimes needed to be added, such as power turbines in the application of electricity generation and a gear box in the direct driven load application. In addition, an increase in the length of the duct between the gas generator and free power turbines must be made to cope with the difference in their diameters in some electric power generation applications, where a free power turbine is connected directly to the gas generator with larger diameter, such as in the Olympus. In contrast, some components need to be removed from the parent aero-engine, such as the fan. The fan is commonly replaced by an LP compressor with lower mass flow and similar PR, as in the Trent (with 50MW and 42% thermal efficiency). In this case the LP turbine will be able to drive the generator due to the excess of power gained through the applied modification. Using the re-staggering technology on the LP compressor allowed the industrial Trent to be able to drive a 60Hz or 50Hz generator running at 3000 rev/min. fixing technology applied on its two stage LP compressor blades, allowing a disc to be added on both applications [103].

2.3.3.1 Aero-Derivative Gas Turbine in Power Generation Applications

As highly advanced research and developments were sponsored by the military, more advanced developed aircraft engines became available, hence higher power outputs. In the early years of aero-derivative GT, the maximum power output provided was 15MW with 25% of thermal efficiency achieved. Procedures utilised in producing these engines were limited to direct replacement of exhaust nozzles with power turbines [103], [85].

Aero-derivative gas turbines have been widely used in power generation applications, and they offer gas turbine engines with relatively higher pressure ratios on different thermodynamic cycles. The advantages of the relatively high pressure ratio and operating temperature in aero-derivative gas turbines including simple cycle configuration resulted in increasing thermal efficiency.

The Rolls Royce Company introduced a derivative in simple cycle with a free power turbine derived from the Turbofan RB-211 model. It was regarded as the best configuration to fit peak-load demand in power generation, providing that a special control system was provided to prevent the sudden over-speed in the power turbine. Integrated power turbine IPT configuration is also introduced in aero-derivative engines, where a new LP turbine is designed to drive the LP compressor and provide the auxiliary work. The three-shaft RR Industrial Trent and GE-Lm6000 derived from CF6-80 C2 are considered as examples of aero-derivative gas turbines with IPT configuration [100].

In comparison with heavy industrial gas turbine, aero-derivatives gas turbine on combined cycle demonstrates around 5% increase in capital cost per installed kilowatt, whilst showing a similar percentage increase in achievable thermal efficiency, making it more beneficial. A case of economic analysis for combined cycle, using aero-derivative as prime mover, shows a reduction in total cost of ownership when compared to other alternative prime movers, considering factors of their viability [105]. Moreover, aero-derivative gas turbines are relatively small and their finance is more simply achievable. Hence, their use is preferred in combined cycle for power output less than 50MW.

Regarding fuel type, the relatively higher cost of fuel used in aero-derivative gas turbines was regarded as the main reason for their use in part-load power generation. However, fuel cost is not always considered and in off-shore application aero-derivative gas turbine is involved in base-load power generation despite of the high cost of its operation. It is an obligation applied to such applications where space and volume are limited and required power in the range of 20-25MW rating. Aero-derivatives with inter-cooled recuperated cycles are widely used in such applications, mostly in the low power range up to 15MW [122].

2.3.3.1.1 Aero-derivative Gas Turbine in Electricity Generations

The gas turbine as an open cycle is considered not to be the most efficient plant system due to losing about 60% of its efficiency as exhaust waste. However, adding a bottoming steam cycle has significantly improved the plant's thermal efficiency, though increasing plant cost and limiting its quick starting capability [3]. It is well recognised that generating electricity is a very complex process, which operates to meet either forecasted or actual power demand required on the grid. The electricity power market shows that power demand varies widely during the day alongside changes in ambient temperature. Therefore, the power generation system in this case has to operate to meet variations in power demand subjected to different ambient conditions (hot and cold waves).

Analysis of gas turbine performance indicates that maximum optimum thermal efficiency is achieved when the generation system operates close to steady state using a steam bottoming cycle. Therefore, with the huge daily variation in power demand the need for additional power generation systems, which can be quickly attached on-line to the grid to provide the additional power, has been increased. At that point the quick start feature of aero-derivative gas turbines gains them the superiority as they are able to be brought online very quickly to provide the additional electrical power required.

Recently, the early vision of producing an open cycle gas turbine which can beat steam turbine has been achieved, with no need for water in some

applications. An example of further advancement for simple cycle aero-derivative gas turbine is the 100MW class introduced by GE that achieves thermal efficiency of around 45% [118]. In addition, the small compacted mobile gas turbine was introduced in the 1950s and has been used for generating electricity and shaft power [35]. Major applications of small and mid-size gas turbine engines are dedicated to electricity generation. Small gas turbine engines of small-size class, providing 4MW of power and can achieve 38.5% of thermal efficiency, have been developed and introduced [66].

2.3.3.1.2 Aero-derivative Gas Turbine in Combined Heat and Power

Cogeneration is an alternative technical term used to express the combined heat and power production plant application. Most of the early heavyweight industrial gas turbines were designed in single spool configurations with few having free power turbines for industrial use only. The majority of heavyweight machines were specifically designed for base-load applications where load demands were higher than 50MW, and on some occasions are designed with optimum pressure ratios (for a given TET) suitable only for combined cycle thermal efficiencies [85]. As a result, these designs limited the options of reducing unit cost and the ability to apply them in multi-purpose applications. One aspect of designing lightweight aero-derivative gas turbines is by directly importing the gas generator of the civil aircraft engine and installing it on the plant for base-load power generation. Aero-derivative engines can in this case be sold as a highly efficient prime mover for base-load combined heat and power or mechanical drive application.

In any cogeneration application project, including the combined cycle, the ratio of power to heat is the base parameter which should be used in selecting the correct prime mover whether steam turbine, heavy industrial gas turbine or aero-derivative engine [73]. Aero-derivative Gas Turbine was found more competitive in CHP application in the less than 50MW of load range, especially where the supplementary firing was not required [105]. Furthermore, the simple cycle aero-derivative promises a superior total efficiency and power-to-heat

ratio, especially when process heat temperature is the lead factor and supplementary firing applied [112].

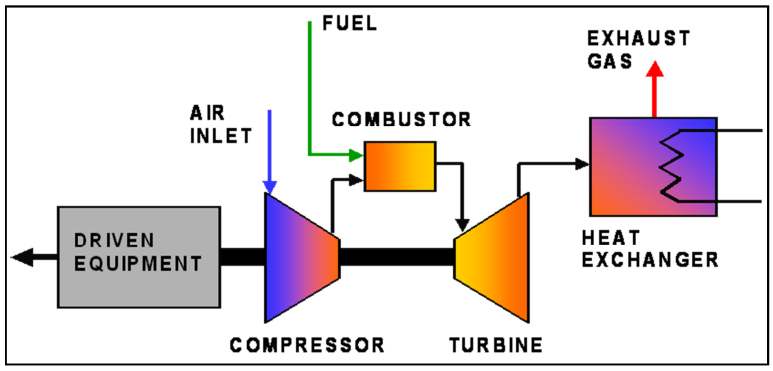

Figure 2-17 Combined Heat and Power Aero-derivative Gas Turbine Engine

Figure 2-17 represents an example of a structure of a small simple cycle CHP plant, where a simple cycle aero-derivative engine combined with a heat exchanger to heat water and generating steam from exhaust waste heat. Many aero-derivative gas turbines have been used on combined electrical power and heat generation application and with different thermodynamic cycles.

The recuperated aero-derivative gas turbine cycle, as seen in Figure 2-18 was used to produce power and generating heat for a small-size application using a small-size aeroderivative gas turbine engine.

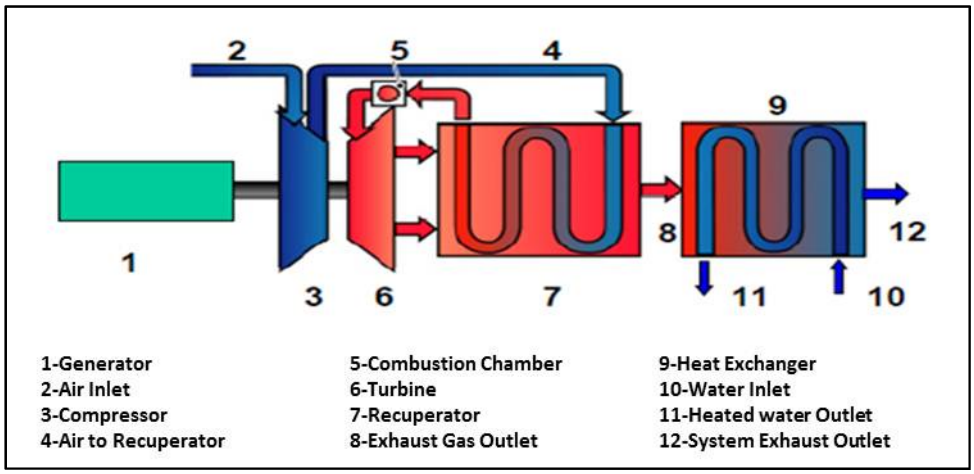

Figure 2-18 Recuperated Gas Turbine plant for CHP Application [70]

Relying on small-size, aero-derivative gas turbine was investigated in a study conducted by [24] for investigating the effect of applying multiple micro-

gas turbine units MTG on CHP plant operation performance. It was proved that splitting plant capacity on several units using multiple small-size gas turbines results in improving plant thermal efficiency at part-load operation. However, it would only be an advantage when a single gas turbine engine would operate at part-load for a significant amount of time. It is clearly owing to the ability of turning off some of the plant units at part-load operation and allows the rest to operate as close as possible to the optimum performance operating point.

Table 2-1 Energetic and Economic Comparison of the Number of MTG Units [24]

No. of MTGs	1	2	3
EE Cogenerated (kWh/m^{3}y)	18.6	18.6	19.5
Cogenerated heat (kWh/m^{3}y)	28.6	30.3	33.1
η_{el} MTG (yearly average)	0.225	0.231	0.239
η_{th} MTG (yearly average)	0.571	0.607	0.643
EES (yearly average)	0.147	0.215	0.232
NPV (€/m^{3}y)	1.45	2.19	2.38
Operating hours MTG #1	3192	2106	988
MTG #2	0	1769	1990
MTG #3	0	0	1265

Analysis of results of the case presented by [24] is observed in Table 2-1, which exhibits outputs and includes all the economic prospects such as NPV, Engine Energy Saving EES. It can be noticed that by splitting plant capacity on many gas turbine units, a substantial increase is achieved in the yearly average of all units' efficiencies and better economics and energetic EES are acquired.

In selecting aero-derivative gas turbines for combined heat and power application, many aspects and factors must be considered such as electric efficiency, utility avoided cost, fuel cost. It is also worth mentioning that from an economic analysis point of view, it is more appropriate to consider the constant value of power-to-heat ratio (α) in order to compare different thermodynamic cycles in cogeneration applications [12].[24].

2.3.3.1.3 Aeroderivative Gas Turbine in Combined Cycle

The majority of proposed methods of recovering gas turbine exhaust heat to be utilised within the plant itself have commercially succeeded in most applications except $CCGT$ in the small and medium plant (up to 50MW) of power generation [19]. However, combined cycle technology is respected as the most efficient utilisation of gas turbines, especially in large-plant power generation. A study of successful simple open bottoming cycles has been introduced in [3], which focuses on peaking power generation with cost effectiveness. The results from this study promised an achievement in greatly reducing emission NOx levels.

It was widely discovered that it is not easy to simultaneously improve both plant electricity efficiency and total efficiency using combined cycle gas turbines. Consequently, supplementary firing was needed and introduced in order to meet variation in heat demand. Assuming that combined cycle aero-derive gas turbine is applied in CHP application and process heat demand allowing for relatively low stack temperature. Then, applying aero-derivative gas turbine with high turbine exit temperature leads to raise (α) value accompanied with relatively unaffected high thermal efficiency relative to simple cycle gas turbine [112]. An aero-derivative engine, derived from the Pratt and Whitney 4000 aero engine, providing 100MW power, has been used as the base engine for the inter-cooled gas turbine cycle in combined cycle applications [104]. It combines the advantages of recovering heat from both exhaust and the inter-cooler up stream at the compressor inlet. In this case, the required power and the desired steam will determine how effective the utilisation from total recovered heat is.

2.3.3.2 Aero-Derivative Gas Turbine in Mechanical-Drive Applications

Aero-derivative gas turbines are widely implemented in some applications where they are required to provide mechanical power in order to drive a propeller in marine crafts, or compressor in oil and gas applications. Nowadays, it has become feasible for large units of 45 to 58MW to be easily

shipped in packages for large power application sites, such as GT10C which provides 30MW and achieves either 36.0% of thermal efficiency in electricity generation or 37.0% in shaft power [55]. They proved their ability to achieve around 40% of thermal efficiency, which cannot be easily achieved without the complexity of combined cycle application.

2.3.3.2.1 Aeroderivative Gas Turbine in Marine Applications

Aero-derivative gas turbines applied in marine application provided a significant challenge for some military-purpose applications. The majority of marine gas turbines with different thermodynamic cycles were derived from aircraft engines and applied in marine propulsion systems of vessels. The late 1960s and early 1970s was the time when GE introduced its first aero-derivative gas turbines in marine application [37]. At that time the GE Company had leveraged their experience of dual-fuel to apply in off-shore electric power generation and LNG carrier propulsion applications. Most of the commercially used aero-derivative gas turbines, which are rated between 40 to 48MW shaft-power for marine propulsion, are under development and some exceeded 60,000Shp Capacity [118]. Recuperated aero-derivative gas turbines were introduced and applied to marine applications with plat-vin type recuperator technology. They have succeeded in achieving +40% thermal efficiency due to their relatively higher turbine inlet temperature than simple gas turbines, regarding which more details can be seen in [117][28][106].

The quantity of fuel consumed and its annual cost are the most important factors which influence selecting the type of propulsion plant installed on merchant ships, such as cruise and cargo ships. So, thermal efficiency is the dominant factor in selecting the type of propulsion plant to be installed on the propulsion system. Although about 96% of maximum power capacity of civilian ships (above 100 gross tons) is produced by diesel engines [52], the aero-derivative gas turbine still has features which make it alternative competitor in marine propulsion. These features can be summarised as its low weight, compactness with relatively high power outputs, high torque, and easy maintenance through rapid on-sight engine change out. Aero-derivative as a

prime mover in marine propulsion is still an economical variant regardless of its relatively higher expenses accounted from the higher initial cost. Overall operating cost of the whole plant is the key factor that must be evaluated, and factors ranging from plant efficiency and performance flexibility to variation in market requirements are significant in this evaluation.

It has been clarified in many studies that the cost of installation is remarkably reduced due to the relative simplicity and physical dimensions of aero-derivative gas turbines. Using diesel engines alone on a cruise ships' propulsion system could not provide the flexibility to meet extreme high power requirements. Therefore, small aero-derivative gas turbines have been used to meet the additional power requirements, also offering the extra advantage of providing more space for accommodation due to its compactness. The same advantage can be obtained from its effective power to weight feature which is provided when aero-derivative gas turbines are combined with diesel engines on fast ferry passenger ship application. Therefore, total ship cost has been reduced with a significant decrease in maintenance cost owing to relatively low requirements for number of crews and avoided down time.

In addition, electrical connection configuration between engine and propulsion systems is a further advantage brought by aero-derivative gas turbines to marine applications. It allows avoiding mechanical drive systems and offers freedom of controlling propeller speed and its rotation direction with no transmission losses and associated lower initial cost. It became possible to have multi-units simultaneously operating and attached to the propeller system. This type of electric propulsion system is also used in some applications where occasionally and during the day there is no need to utilise full output power for the main task (propulsion). Extra power can be utilised in other functions, such as high degree of manoeuvring in ferries or in meeting hotel loads on cruise ships where the load is extremely varied. Although simple cycle dominated the bulk of aero-derivative gas turbine in marine application, the inter-cooled recuperated cycle aero-derivative has gained the attention of marine ship propulsion system designers. The Plat-fin model recuperator is commonly used

in designing inter-cooled recuperated cycle aero-derivative gas turbines for marine propulsion applications. It was confirmed by Kim, T. S. and Hwang, S. H [66], that there is an aero-derivative engine recently developed and able to achieve 40% thermal efficiency with relatively higher turbine inlet temperature than the simple cycle. Figure 2-19 describes an example of power generation plant using aero-derivative gas turbine as a prime mover in inter-cooled recuperated cycle technology.

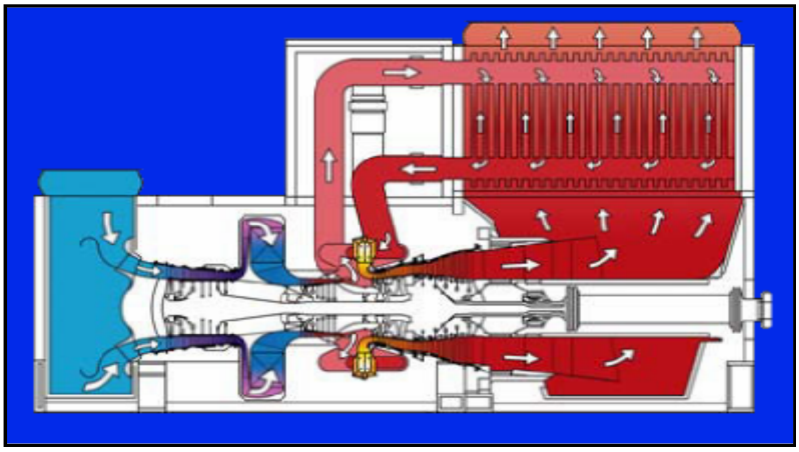

Figure 2-19: Intercooled Recuperated Cycle plant Using Aeroderivative Engine for Marine Application. [28]

Nearly all inter-cooled recuperated aero-derivative involvements in propulsion systems of marine vessels are in the low power range of up to 15MW [122]. Westinghouse and Rolls Royce introduced the WR-21 inter-cooled recuperated aero-derivative gas turbine for naval vessels. It was derived from the 25.2MW family of the Rolls Royce RB211 and Trent700/800, and superseded in providing 27% of fuel savings [97]. Modifications were of course made to the parent engine including removing the fan and accommodating the pressure ratio drop by restaging the first-stage of the LP turbine. Furthermore, a low dry emission combustor was developed from RR Spey and the LP turbine was imported from the RB211-535. The low pressure turbine is a modified version of the aero-engine IP Turbine with different blade angles for meeting the capacity change requirements [117]. Moreover, the power turbine PT derived from Trent 700/800 used with new variable-area nozzle added to maintain high thermal efficiency at off design operation. Closing the variable-area nozzle

reduces engine mass flow, which in turn results in increasing combustor outlet temperature and provides more transferable heat in the recuperator [106].

2.3.3.2.2 Aeroderivative Gas Turbine in Gas Compressing

The first domination of aero-technology in large horse power pipeline applications was achieved in 1963 through applying the jet engine expander. The aero-derivative gas turbine has been used in gas pumping and pipeline compressing application for gas and oil transportation. A unique approach of plant self-fed application is introduced when the aero-derivative gas turbine operates on pipelines of transported natural gas. It is generally observed that "the typical pipeline can consume from 7 to10% of the throughput for compression purpose" [103]. An early example of developed aero-derivative gas turbine engine used in this application was the FT8-55. It is a member of the FT8 family respected as a highly efficient machine, providing 25MW of shaft power in free power turbine arrangement with FPT operating up to 5775 rpm at continuous speed. The FT8-55 engine was developed by Rolls Royce as an industrial derivative gas turbine of the Trent aero-engine [4]. The GG8-1 is another example of aero-derivative gas turbine applied on same applications. It was derived from the civil aviation JT8D aero-engine.

2.4 Gas Turbine Performance Simulation

It is clear that during the design procedures of gas turbine process, performance calculations must be conducted including (design and off-design calculation). The procedures of predicting the off-design performance have been called simulation. The simple analysis of the cycle is not enough to predict the achieved performance of the upgraded aero-derivative engine configurations. So, off-design analysis of the upgraded cycles must be conducted to predict the performance [25]. To achieve the objectives of such calculation there are many different computer software programmes which have been designed to make it easy to complete the calculation in quick time. The advantage of predicting off-design (part-load) gas turbine engine performance is observed in the majority of gas turbine applications including the

aforementioned applications. Many models were developed and improved for the accurate predicting of the gas turbine off-design performance. Although component maps are not easily available from the manufacturer, using them in calculating the engine's part-load performance is still the most commonly known accurate method. [54].

The software code chosen to conduct such calculations in this project is called Turbomatch [101]. It is a flexible in-house developed program code for gas turbine modelling. It has been developed based on experience of tens of years utilised in the gas turbine field [84]. The simulation using this programme requires the determination of certain parameters of the engine. Some of these are available from the manufacturer and others must be assumed [61]. Iterative loops have been made to check many different times for the work compatibility between composers and turbines. Also, flow continuity must be checked between the engine's components. Figure 2-20 represents the flow chart which describe the iterative method of simulation in brief image.

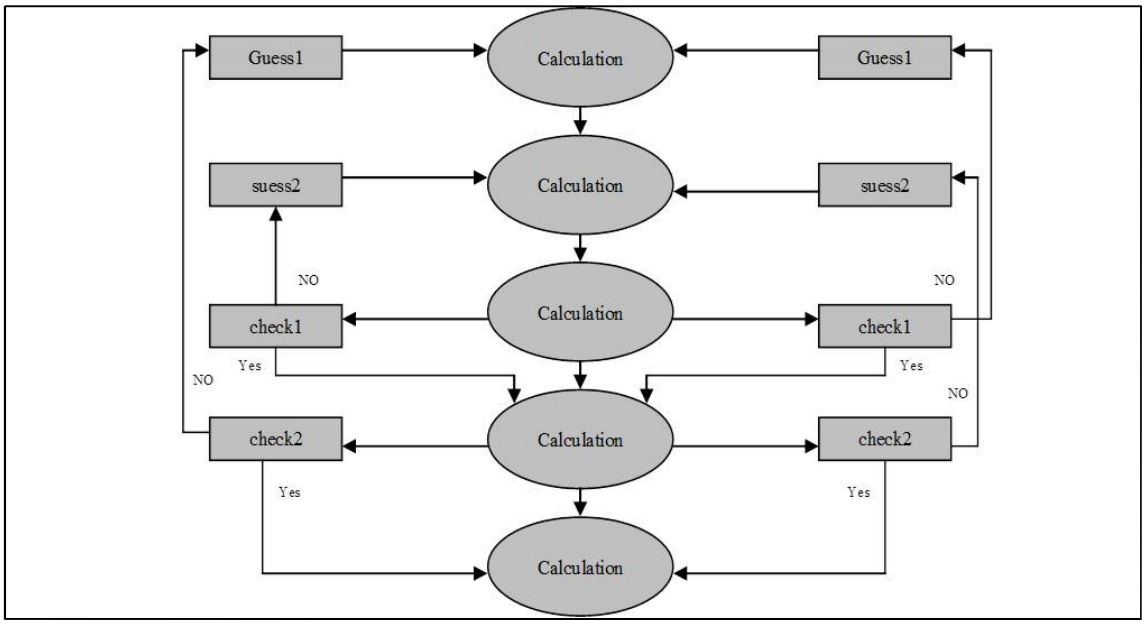

Figure 2-20 Simulation Iterative Method flow chart for Turbomatch Code [84]

Calculation in this code relies on compressor and turbine performance maps which represent their characteristics as functional relationships among four main parameters, i.e.:

- mass flow function
- speed function
- pressure ratio, and
- efficiency

These parameters can be schematically written as follows:

$$F\left(\frac{W\sqrt{T_{in}}}{P_{in}}, \quad \frac{N}{\sqrt{\sqrt{T_{in}}}}, \quad \frac{P_{OUT}}{P_{in}}, \zeta\right) = 0$$

Matching between engine components (compressor and turbine) for operations with fixed gas turbine geometry is carried out based on the aforementioned components' performance maps. Simulation of various operation strategies for different gas turbine engines and configurations using the Turbomatch code will be based on compressor and turbine maps scaled from actual performance maps.

2.4.1 Design Point Simulation

In the case of industrial gas turbine engines, the design point condition presents the point where the engine will operate mostly and is always preferred to cover the base load conditions. The design conditions are always chosen to be at the maximum available power in the industrial application, while to be at the cruise conditions in the aero-engine applications. In this stage, engine configuration must be optimised as well as component performance and cycle parameters.

Typically, engines operating on ($TET > 1200\ K^{\circ}$) need some air extracted from the compressor for NGVs and turbine blade cooling purpose with condition of pressure matching in the stage where it should be injected. Extracted air pressure and temperature will depend on engine size (Pressure Ratio) and the ambient condition. High pressure turbine isentropic efficiency will be affected and it should normally be lower than power turbine efficiency due to the quantity of air extracted from the compressor. Depending on the machine and

combustor configuration, relatively high ratios of air, between 6% and 20% of compressor air-flow, can be extracted from the compressor discharge with some modification needed for the compressor casing, piping and controls. Also, it has been noticed that above 20% of air extraction ratio extensive modification is required for the turbine casing and unit configuration. Up to 5% of the compressor airflow however, can be extracted from the compressor discharge casing without any sort of modification [54]. Figure 2-21 represents the effect of varying the amount of air extracted from the compressor on the gas turbine engine's overall performance. It can be clearly observed that there will be approximately 2% loss in the engine's power for every 1% ration of air extracted.

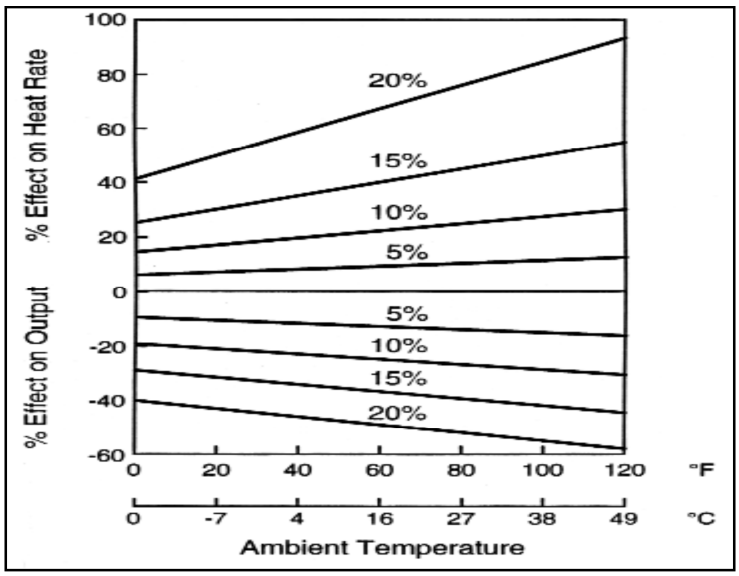

Figure 2-21: Compressor Air Extraction Effect on Engine Performance [54]

Designing a group of engines in different thermodynamic cycles for different applications needs to deal with an indicator showing the optimum combination of cycle parameters (cycle optimisation). Optimisation procedures should be conducted for every given type of engine in order to help the designer to choose the suitable engine for a certain application. The most effective way to present the performance of a group of engines is by plotting the variation of specific work and specific fuel consumption for different turbine inlet temperatures and pressure ratios on a single graph known as Fishhook curve, as shown in

Figure 5-11. As mentioned above, the plots are a useful tool for comparing the performance of different engines in different configurations which may help in considering an engine for already given requirements. Also, each point on the plot must be considered as a different engine cycle.

In order to accommodate a wide range of compressor operating performances for different ambient conditions, compressor performance maps have been used. This presents the relationship between compressor pressure ratio and isentropic efficiency versus corrected mass flow for different lines of non-dimensional rotational speeds. Surge line and constant non-dimensional speed lines, which are presented in percentages corresponding to the design value, are also presented on the compressor map. Corrected mass flow is given by the equations:

$$w = w * \frac{\sqrt{\left({}^{P}/_{P_s}\right)}}{\sqrt{\left({}^{T}/_{T_s}\right)}} \quad \Rightarrow \quad w = w \, \frac{P_{ref}}{P_t} * \sqrt{\frac{T_t}{T_{ref}}}. \text{ [60]}$$

Some factors and parameters have to be known to conduct the engine design point calculations, these variables include:

- Ambient conditions
- Air mass flow
- Component efficiencies
- Specific Heat (C_p) throughout the engine (depending on the chemical composition of the working fluid and to the temperature)
- Cooling air percentage
- Fuel calorific value (FCV)
- Turbine entry temperature (TET), which depends on the thermal durability of the inlet blades of the first turbine row)
- Exhaust pressure

$$Heat\ Rate = (Fuel\ Flow * Fuel\ Heating\ Value)/(Power\ Output)$$

$$(Kg/hr * Kj/Kg)/KW = (m^3/hr * Kj/m^3)/KW = \ KJ/(Kw.hr)$$

$$(Ib/hr * Btu/Ib)/KW \ = \ BTU/(Kw.hr)$$

Maps need some modification when variable geometry technology is applied, such as $VIGVs$ for the single-shaft configuration IPT and $VANs$ for the two-shaft configuration FPT. Modification for the $VIGVs$ operation is carried out as follows:

$$\frac{W\sqrt{T_{in}}}{P_{in}} = a\left(\frac{W\sqrt{T_{in}}}{P_{in}}\right)_n, \qquad \frac{P_{out}}{P_{in}} = b\left(\frac{P_{out}}{P_{in}}\right)_n, \qquad \zeta = C.\zeta_n \quad \Rightarrow a, b, c = f(\Delta\alpha_{IGV})$$

$n : (refers\ to\ nominal\ design\ map)$

$a, b, c : (\ are\ correction\ factors, they\ are\ functions\ of\ IGVs\ \ angle\ change\ )$

Variation in turbine variable area nozzle (VANs) operation angle causes a reduction in the swallowing capacity of the power turbine. This reduction can be modeled according to the following equations:

$$\frac{W\sqrt{T_{in}}}{P_{in}} = \beta\left(\frac{W\sqrt{T_{in}}}{P_{in}}\right)_n, \quad Where \quad \left(\frac{W\sqrt{T_{in}}}{P_{in}}\right)_n = \boldsymbol{f}\left(\frac{N}{\sqrt{T_{IN}}}, \frac{P_{out}}{P_{in}}\right)$$

Different compressor maps can be plotted on the same graph using these equations and the result will be as shown below in Figure 2-22, and tackled in more detail regarding how it can affect the compressor operating line margin from surge.

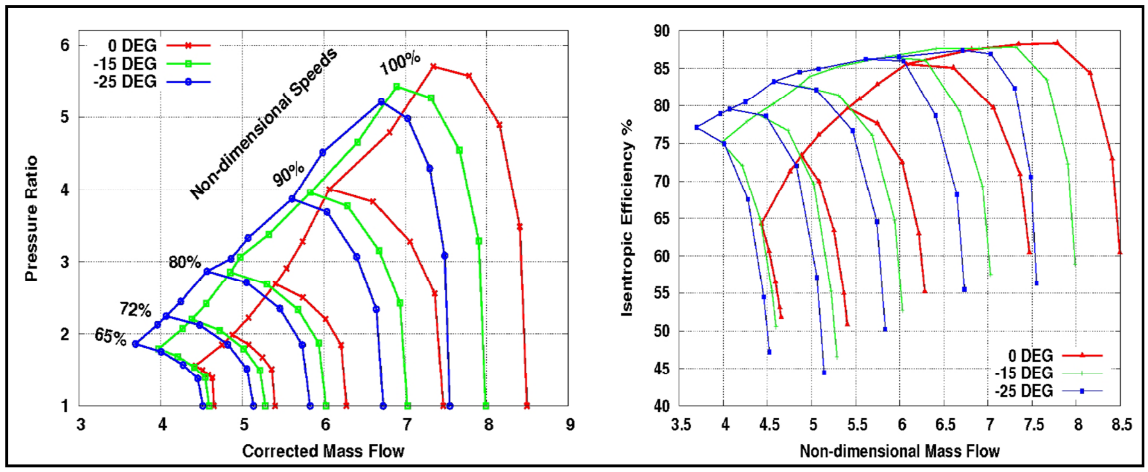

Figure 2-22 Five Stage Axial-Flow Compressor Performance Characteristics with Variable Geometry [60]

It is necessary here to state that modern gas turbines in practice have very complex turbine cooling systems than those modelled in theory. Also, the ratio

of the electrical power output to the mechanical power input can be considered as the definition of electricity generator efficiency.

2.4.2 Off-Design Engine's Performance Simulation

Gas turbines in some applications, such as cogeneration and marine, spend a considerable period of their lifetimes operating at part-load conditions. Therefore, more attention should be given to part-load performance of gas turbine as it is of great importance [54]. Predicting engine performance at off-design conditions provides complete knowledge of an engine's outputs when operating under a variation in environmental conditions. On the one hand, designers must be sure that there are enough margins left between an engine's operating line and compressor surge line at off-design operation. On the other hand, it is crucial as it always affects plant economics especially in cogeneration applications where flexibility in simultaneously generating steam and producing power is required [11]. Also, at part-load operation there will be variation in electric-to-thermal power ratio in cogeneration plants which will have different influences on the economics of the power generation system.

Typically, at off-design operation both thermal efficiency and turbine work are degraded with the increase in ambient temperature (operating in a hotter environment). While the decrease ambient temperature leads to a reduction in required compressor work, which in turn results in linearly increase in thermal efficiency of the gas turbine engine. Specific fuel consumption SFC is another component used to evaluate engine performance and determines the quantity of fuel consumed per unit of power produced with consideration to quality of fuel used. So, the lowest value of SFC is the best engine performance output. It has an opposite behaviour trend to thermal efficiency as it increases with the increase in ambient temperature and decreases in operating temperature. It has been noticed that variation effect of SFC has a noticeable influence on engine performance at relatively high values of ambient temperature (hot areas).

Another general observation of the simple cycle gas turbine is that thermal efficiency is always increased at combinations of low compressor pressure

ratios and high turbine inlet temperatures, until certain value (optimum OPR) when it tends to decrease as result of cooling losses increasing. However, more significant is the variation of thermal efficiency and SFC at high OPR and low operating temperature [90]. It is still possible to enhance engine performance by raising compression ratio even at low values of operating temperature

Regardless of the thermodynamic cycle, gas turbine performance always degrades when it operates at part-load (power demand reduction). So, it is very important to find a way of enhancing its performance in order to improve economic variants of the whole plant [66]. Most aero-derivative gas turbine engines in industrial applications are often provided with several rows of variable stators at the front of the compressor. The stators are designed to achieve large pressure ratio in a single–shaft plant and controlling the surge margin at low power setting in multi-shaft. At a constant rotational speed, varying stators angle from design position results in reducing axial velocity and mass flow. As a result the surge margin will be improved at low rotational speed and stalling and choking are going to be delayed in the front and last stage rows respectively.

In free power turbine configuration, matching non-dimensional mass flow between the two turbines causes the major restrictions on operating compressor turbines. It has been observed in two-shaft engines that compressor turbine is operated in a narrow range of pressure ratio. Design performance specifications of specific power, thermal efficiency and exhaust temperature can be met by adjusting component's isentropic efficiency [54].

Depending on cycle parameters, component efficiencies and air mass flow, each gas turbine engine has its own temperature-effect curve which represents its performance characteristics under effect of ambient condition variation. Altitude change has a major effect on gas turbine output power, and the higher altitude level the more reduction in air density leading to proportional decrease in both mass flow and engine output power. Thermal efficiency however, increases with the increase in altitude.

Humid air is denser than dry air, and increasing humidity in air affects both output power and heat rate. This effect always rises with the increase in quantity of water utilised for NOx control and engine size. The issue of humidity affecting engine performance is mostly found in single-shaft gas turbines where turbine exhaust temperature used to approximate operating temperature. It is so obvious that the increase in air humidity leads to fall in air pressure ratio, and turbine exhaust temperature. This drop will guide the control system to approximate lower firing temperatures. However, in aero-derivative engines where two shaft technologies applied, the control system uses the gas generator outlet temperature to approximate engine firing temperature. The ability to operate gas generators at different speeds than the power turbine allows raising shaft output power due to the increase in its rotational speed resulted from added fuel. Also, increased shaft output power offsets losses generated from the decrease in air density.

Finally, gas turbine performance decreases as time passes during its life operation due to the losses generated in turbomachinery performance. There are two types of gas turbine degradation which can be categorised as:

- Recoverable losses
- Non-recoverable losses

Recoverable loss results from compressor fouling, and this can be partially solved by using on-line washing, or cleaning compressor blades and vans after opening the unit or during the overhaul.

Non-recoverable losses happen due to the increase in turbine and compressor clearances and changes in surface finish and airfoil contour. The only way to deal with these losses is by the replacement of affected parts at recommended inspection intervals. So, it cannot be recovered by operational procedures, external maintenance or compressor cleaning because it exists as a result of the reduction in component efficiencies. It has been indicated from field experience that using off-line water washing frequently is useful in reducing recoverable loss and the rate of the non-recoverable loss.

Generally, using correlation between different sites in quantifying gas turbine engine performance degradation is not a good idea, as it is very difficult to obtain valid field data and can be affected by many other factors such as fuel and diluent injection levels for NOx, air conditions (humidity and contaminants), and mode of operation. In addition, test instruments and procedures vary widely, often with large tolerances. It is been typically found that 24000 hours is the recommended interval for the hot gas inspection. For a corrected to guaranteed field condition and for not replacing degraded part, it has been observed from performance test measurements that during the first interval of operation check performance degradation is 2% to 6%. However, if the degraded part is replaced, performance degradation will be extended and recorded to be 1 to 1.5% [60].

The large variation in turbine inlet temperature at off-design operation may result in compressor surge. There are many actions which can handle this issue, $VIGVs, VANs$, and blow-off valve, which have to be included in the simulation procedures for any computer program used. These actions must be taken to keep the engine operating stably. Figure 2-22 shows the effect of varying the $VIGVs$ setting on a compressor performance map, and represents the compressor maps for the $VIGVs$ angles of $(0^{\circ}, -15^{\circ}, -20^{\circ})$. In addition to controlling surge margin when the engine is subject to variation in ambient condition, some aero-derivative gas turbine engines need to control their compressors surge margins at start-up, during acceleration, and idle operation. Furthermore it is necessary to operate gas turbines at constant recuperator inlet temperature or constant exhaust gas temperature (EGT,T_{ex}) wherever recuperation applied. However, it leads to a reduction in compressor surge margin at part-load operation. Therefore, as a prevention action in two-shaft free power turbine configuration, power turbine variable area nozzles (VANs) have been designed and modulated during the aforementioned operation conditions in order to increase the compressor surge margin.

Finally, it can be concluded that parametric analysis of gas turbine thermodynamic cycle aims to explore relationships between an engine's

performance parameters (specific fuel consumption and specific power) and the following factors:

- Design choices (such as engine size which reflected by OPR)
- Design limitations (such as Turbine inlet temperature)
- Environmental condition variations (Ambient pressure and temperature)

Also, it provides enough knowledge to the designer to decide which of the following criteria best meet the needs of specific applications.

- Engine configuration IPT or FPT
- Engine and component design characteristics (such as compressor and turbine isentropic efficiencies)

3 PERFORMANCE SIMULATION CASE STUDY

At the beginning of the project and in order to verify the procedures of predicting engines' DP and OD performance, two types of aero and aero-derivative industrial engines have been chosen. A two-spool turbofan engine has been chosen to match the output performance of the CFM56-5B5 aero-engine. Also, a two-spool three-shaft inter-cooled engine for power generation is planned to be designed to perform and produce equally the performance outputs of the GE LMS100 engine. The design point and off-design calculations are conducted in greater detail in the following two sections.

3.1 Parent Two-Spool Turbofan Engine

As I began my study with the involvement in a project of designing a 130-seat long-range aircraft engine was running in the Department of Power and Propulsion at Cranfield University in cooperation with the Aviation Industries Corporation of China $AVIC$. The task is conducting the thermodynamic calculations for design and off-design performance of the aircraft engine in order to derive better availability and understanding of performance data for the derivation calculation. The main aim of the project was to design a relatively light weight turbofan engine which can fly a 130-seat aircraft size and be lighter than engines commercially available on the market.

Therefore the design point and off-design calculations are performed to match design point and off-design performance of the CFM56 family, which used as the propulsor of the Airbus 319 and 320. Three groups of MSc students worked on this project as well as three PhD students to coordinate them. The CFM56-5B5 was selected in my project as the base-line aero-engine to match its design and off-design performance. It was developed from the CFM56-5A with some modifications in the LP system (new fan and double annular combustor) leading to improvement in its performance. In addition, HPC was maintained from the CFM56-5C, as illustrated in Figure 3-1. The Easyjet Company has been using the CFM56-5B5 engine since 2002 to power around 120 of its A319s. The design net thrust Fn is about 97.9kN [18].

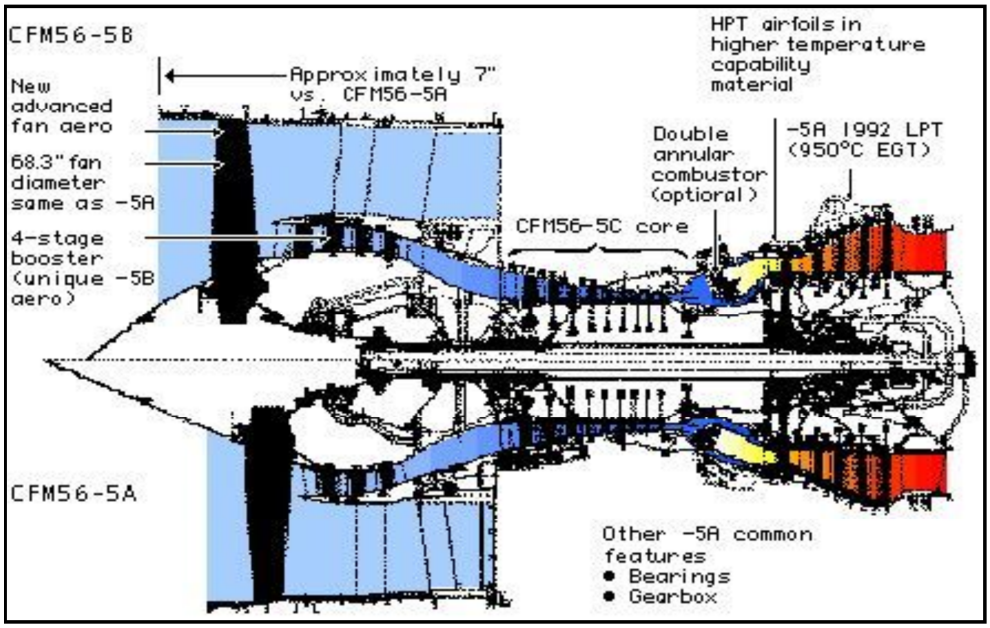

Figure 3-1 The CFM56-5B Turbofan Gas Turbine Aircraft Engine [47]

The engine's schematic structure shown in Figure 3-2 describes the engine components and configuration. It consists of two shafts that drive fan, booster, high pressure compressor, high pressure and low pressure turbines. A model was created using Turbomatch code and stage numbering presented in Figure 3-2, in order to design and simulate a turbofan engine which has the same class of power and performance. Some realistic data was published on the CFM company website and have been used as presented Table 3-1 for the design point calculation.

Table 3-1 The CFM56-5B5 Turbofan Gas Turbine Engine's Practical data [47]

	Altitude(m)	M_n	F_n(N)	$W\ (\frac{Kg}{s})$	BPR	OPR	$SFC\ (\frac{mg}{N.s})$
Take-Off	11000.0	0.8	97860.84	371.03	6		9.064
Max Climb			25043.48			32.6	
Cruise			22330.074				

The remaining design parameters such as compressor and turbine isentropic efficiencies as well as pressure drops, need to be assumed to complete design point calculation and predicting engine off-design performance.

3.1.1 Parent Two-Spool Turbofan Design Point Calculation

Calculating design point parameters of the 100kN turbofan engine is based on some assumptions and realistic data. Component efficiencies, compressors pressure ratios, and pressure drop across the combustor are assumed. Also, ratios of required cooling bleed mass flow are estimated relative to core mass flow value at design point and based on technology dedicated by [85].

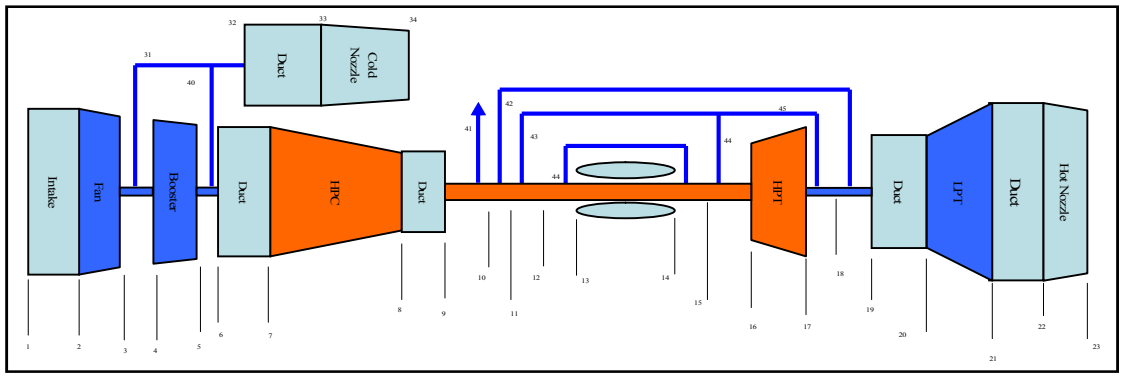

Figure 3-2 Schematic Diagram of The Parent Turbofan Aircraft Engine

All assumed and estimated values are included in Table 3-2. The performance model is created using the Turbomatch code considering stage numbering illustrated in Figure 3-2.

Table 3-2 Parent Turbofan Design Point Performance Characteristics

	FPR	IPC	HPC	η_{isfan}	η_{isIPC}	η_{isHPC}	CPL	HPT η_{ist}	LPT η_{ist}
DP Parameters	1.8	1.404	11.5	89%	89%	89%	5%	90%	91%
	W (kg/s)	OPR	BPR	SFC (mg/N.s)	Fn (KN)	COT (K)	Wf (kg/s)	Mn	Alt (m)
Cruise (DP)	138	29.06	6	17.14	22.341	1500	1.277	0.8	11000
T-O	381.385			12.95	98.649	1748	0.383	0.25	0.0

There are four main design parameters are normally used in designing civil aircraft turbofan engines including bypass ratio BPR, fan pressure ratio FPR,

turbine entry temperature TET or combustor outlet temperature COT, and overall pressure ratio OPR. In this project, combustor outlet temperature is selected as a design parameter instead, and used for all design point and off-design calculations. The engine design point is calculated at cruise conditions and the results are described in Figure 3-3 to Figure 3-6.

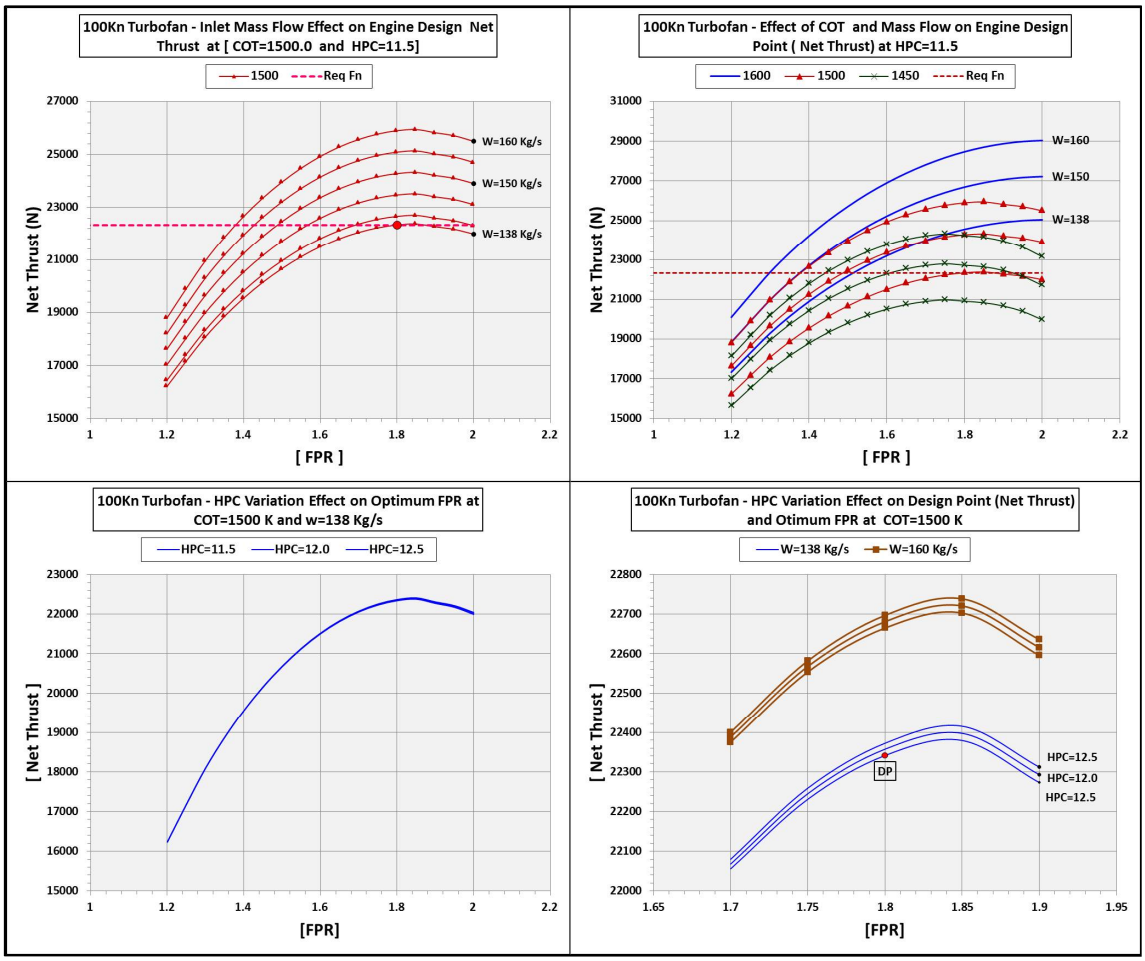

Figure 3-3 : 100kN Turbofan - Effect of Varying inlet Mass flow, HPC and COT on Design Point Net Thrust Fn

In every setting of constant $COT\ and\ OPR$, there is always an optimum value of FPR which achieves either highest net thrust F_n or the lowest SFC as presented in Figure 3-3 and Figure 3-4. The effect of varying design parameters such as mass flow, COT and HPC on optimum fan pressure ratio for maximum thrust has been investigated and results are clarified in Figure 3-3. Although increasing mass flow has no impact on the optimum value of fan pressure ratio, it still has positive effect on engine performance as observed in gaining a

remarkable increase in net thrust at constant value of optimum fan pressure ratio. The second part of Figure 3-3 show results from investigating effect of varying high pressure compressor design on optimum FPR for different given values of inlet mass flow. It can be clearly noticed that for a given engine mass flow value, the optimum fan pressure ratio can still be manipulated by varying operating temperature at constant OPR. Also, varying value of HP pressure ratio applies no significant effect on net thrust along different values of fan pressure ratio as long as the overall pressure ratio and mass flow kept constant. Moreover, optimum FPR for maximum thrust is also not affected with this variation in HP compressor pressure ratios under the aforementioned conditions.

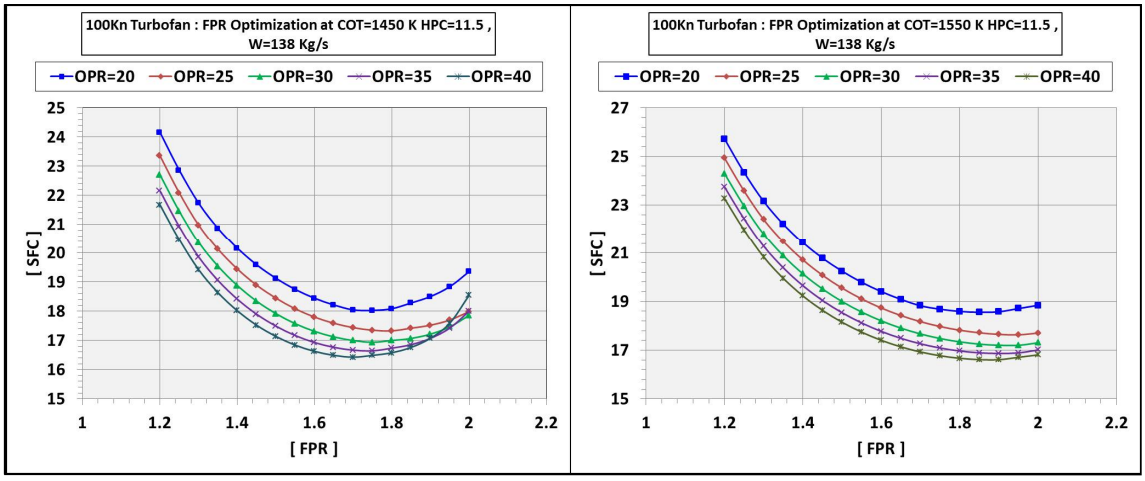

Figure 3-4 : 100kN Turbofan - Fan Pressure Ratio Optimisation for minimum SFC

The investigation as shown in Figure 3-4 has been expanded for a wider range of different cycle overall pressure ratios, including optimum value of fan pressure ratio for minimum specific fuel consumption. It aims to find values of optimum fan pressure ratio which achieves minimum specific fuel consumption at design point for different cycle overall pressure ratios. It is generally observed that increasing an engine's overall pressure ratio (engine size) causes a significant improvement in engine specific fuel consumption and decreasing values of optimum fan pressure ratio which results in smaller fan size. It can also generally be seen from Figure 3-4 that increasing combustor outlet temperature COT at constant overall pressure ratio results in rising specific fuel

consumption and shifts optimum fan pressure ratio to higher values. However, this effect trend is valid for a specific range of OPR, and then the further increase in operating temperature results in improvements in specific fuel consumption. This clarifies the importance of investigating the relationship between specific thrust SF_n and SFC for a wider range of combustor outlet temperature and overall pressure ratio as seen in Figure 3-5 and Figure 3-6.

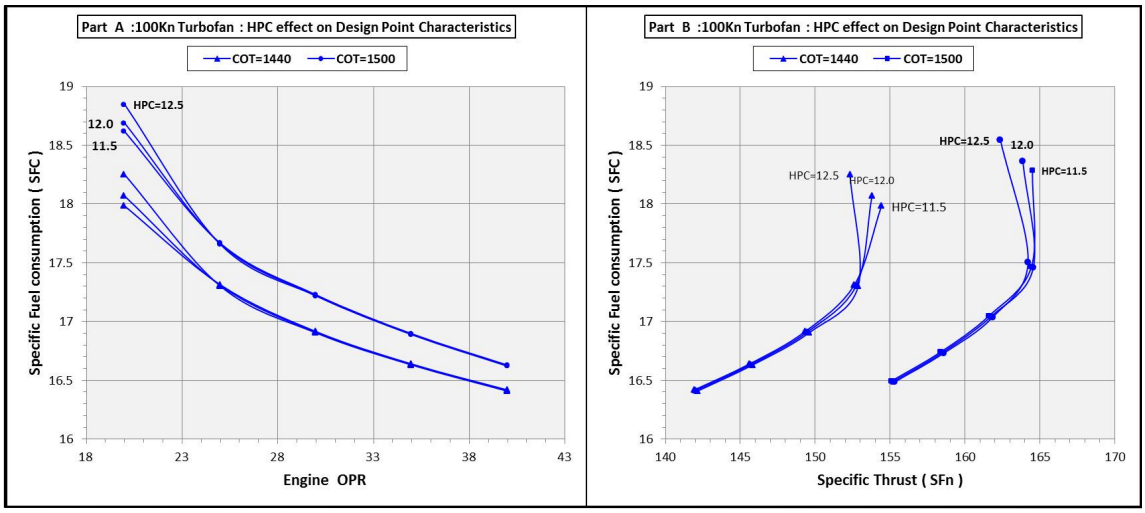

Figure 3-5 : 100kN Turbofan Engine - HPC Combination Effect on engine Design SF_n and SFC at $W = 138Kg/s$ and different COT

It is used to find the best combination of SF_n and SFC, as well as determining the optimum fan pressure ratios. The impact of changing HP compressor pressure ratio is also investigated for variety of OPR and combustor outlet temperature COT, as seen in Figure 3-5. Part A and Part B represent values of SF_n and SFC at the optimum fan pressure ratios for each given value of HP compressor PR and overall pressure ratio. The results express the fact that for every given combination of COT and OPR in the range of $(OPR < 18)$, there is slight impact on engine specific thrust owing to varying high pressure compressor pressure ratio. However, this effect is eliminated at any values of $(OPR > 18)$. Changing in the combination of FPR, IPC and HPC at constant overall pressure ratio will have no significant effect on specific thrust and fuel consumption.

Part B in Figure 3-6 presents an example of clarifying thermodynamic cycle optimisation methodology previously mentioned. It shows the results of a

feasibility study of designing the 100kN-thrust parent Turbofan engine at take-off conditions. Design points on these curves illustrate performance of different engine designs and express their performance at the optimum fan pressure ratio. During design point matching calculation, an optimisation should be performed through repeating all the aforementioned steps of calculation at several values of turbine inlet temperature.

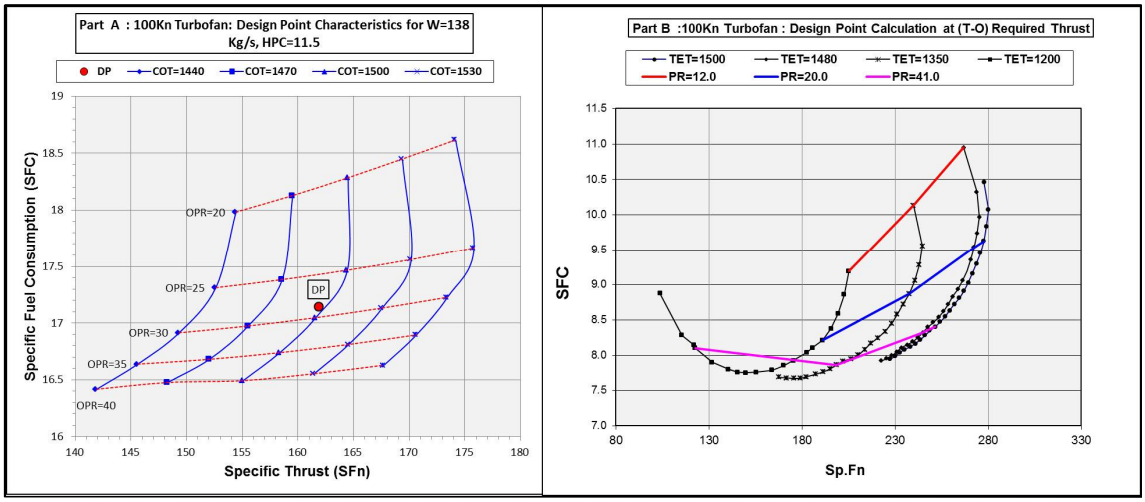

Figure 3-6 : 100kN Turbofan - Design Point Characteristics at Cruise conditions for $W = 138$, and $HPC = 11.5$

Part A on Figure 3-6 includes a plot of all performance characteristics of the optimised design points for a variety of possibly designed engines at cruise conditions. They are all conducted at different values of turbine inlet temperature and cycle overall pressure ratios.

This constitutes a significant tool used in selecting the correct and suitable engine design which suits particular application requirements. Considering engine design points on the line of $(COT = 1500K^{\circ})$ for several OPR, there will be only one optimum engine design for highest SF_n, while there will be another different design (optimum design point) which provides the lowest specific fuel consumption SFC.

3.1.2 Engine's Off-Design Performance Prediction

The final decision of selecting the suitable engine design parameters cannot be taken considering design point calculation results only. Design point

calculation alone is not enough and engine off-design performance must be calculated in order to predict its performed behaviour when operates away from design conditions.

Off-design calculation is conducted for a wide range of operating conditions from cruise altitude down to take-off operation conditions. It involves the effect of ambient temperature, altitude and flight Mach number and the results are presented in Figure 3-7 and Figure 3-9. Also, steady state operating lines for fan, booster and HP Compressor are calculated for different values of turbine inlet temperatures at cruise, and surge margin was investigated on compressors maps as shown in Figure 3-8. It is clearly observed that intermediate pressure compressor (booster) is the most sensitive to variation in combustor outlet temperature COT due to the sever variation occurred in LP shaft non-dimensional speeds ($\frac{N}{\sqrt{T}}$) than happened in the non-dimensional speed of HP shaft. So, booster tends to cross the surge line at low rotational speeds, quicker than the HP compressor does for the same time range. On the other hand, the HP compressor has a flat working line trend, and takes a longer period of time to reach the compressor surge line.

Figure 3-7 illustrates how net thrust and specific fuel consumption can be affected by variations in flight Mach number M_n and altitude for a wide range of operating temperatures COT. Generally, increasing operating temperature leads to improved engine net thrust. It is still possible to increase net thrust while operating at constant COT and flight Mach number by moving the aircraft to lower altitude levels, and this behaviour can be clearly noticed at relatively higher value of flight Mach number. However, there will be a penalty of increasing specific fuel consumption which will have a negative effect on engine performance. Increasing flight Mach number during operating at constant operating temperature and altitude has a negative impact on engine net thrust and specific fuel consumption. It results in thrust degradation and more fuel consumption especially at low levels of flight altitude.

The influence of ambient temperature variation on engine performance has been investigated and the results plotted in Figure 3-9. Results indicate that

engine performance is degraded with the increase in ambient temperature at any altitude and flight Mach number in both cruise and take-off conditions.

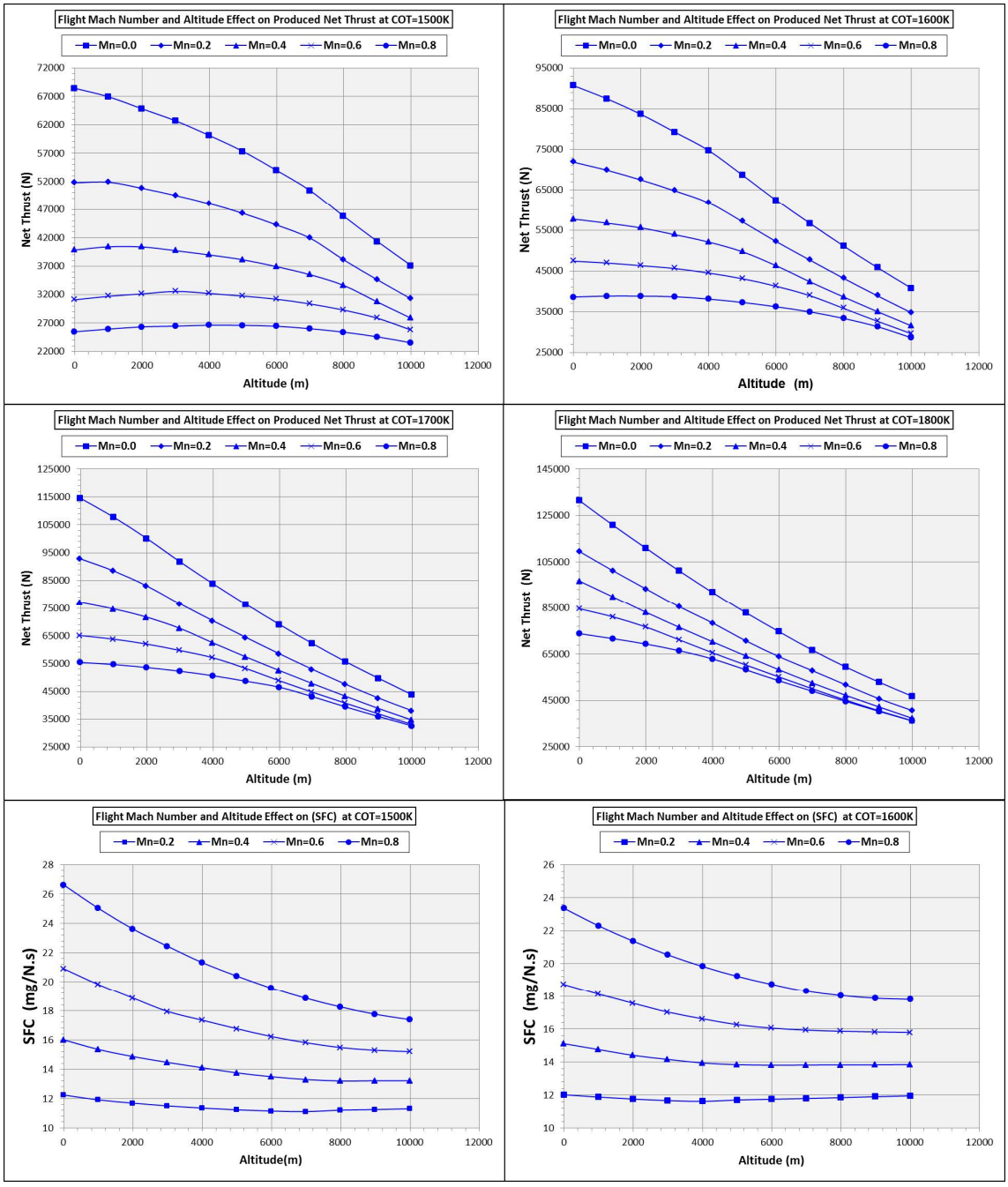

Figure 3-7 : 100kN Turbofan – Effect of Varying Altitude and Mach number on Engine Net thrust and SFC at Off Design Operation

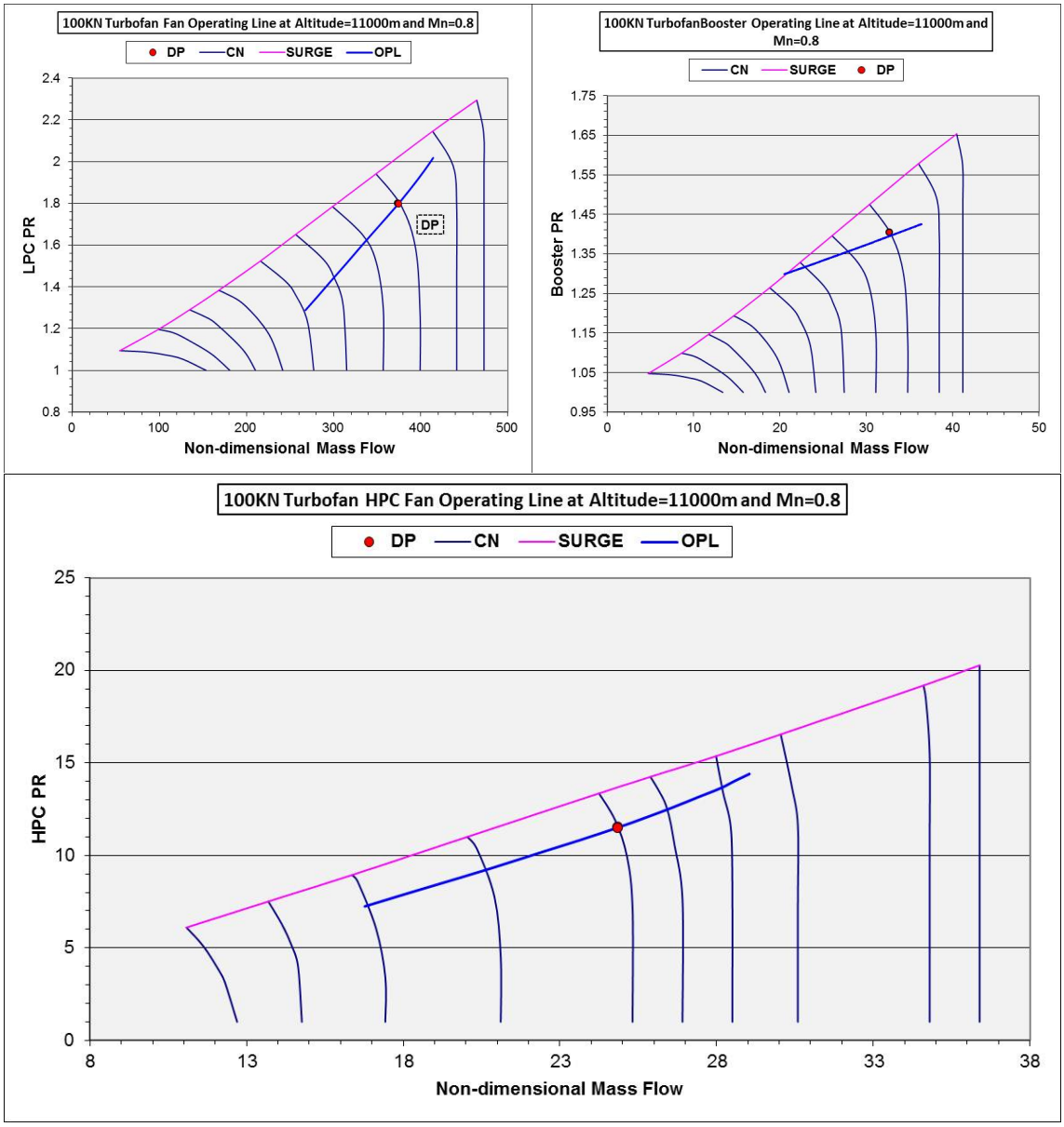

Figure 3-8 : 100kN Turbofan - Compressors Operating Lines

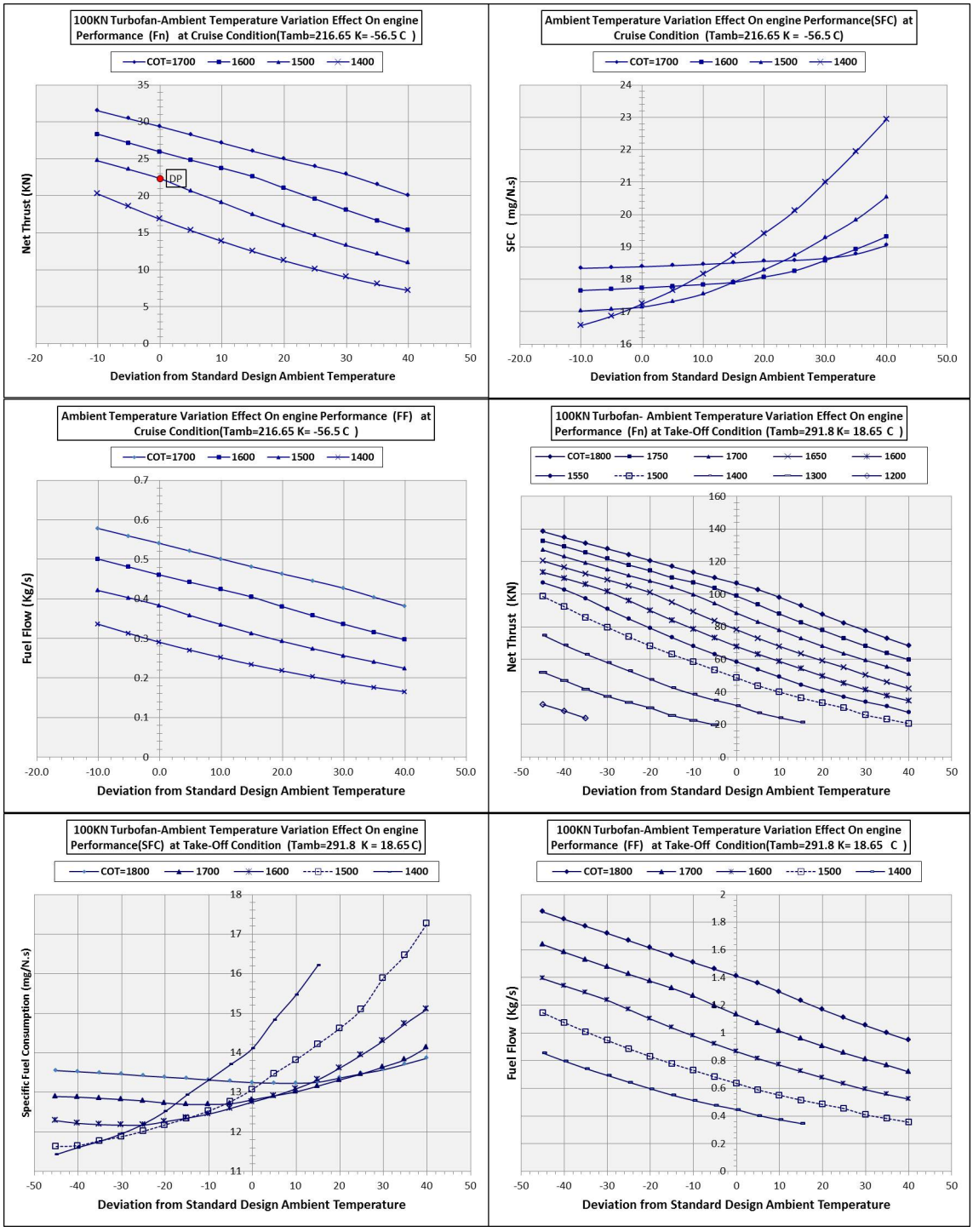

Figure 3-9 : 100kN Turbofan - Ambient Temperature Effect on Engine Performance Outputs at Cruise and T-O Conditions

3.2 100 Mw Intercooled Aero-Derivative Engine

The GE-LMS100 design performance output as well as its thermodynamic cycle has been chosen as a target to be matched in the design of intercooled aero-derivative industrial gas turbine engine. It is an inter-cooled three-shaft simple cycle aero-derivative engine and it is presented in Figure 3-10 and Figure 3-11. The Figures show the engine's configuration and its schematic structure and clearly presents the configuration of its components. The engine consists of a low pressure shaft which contains 6 stages LPC and 2 stages LPT, while the high pressure shaft rotates the HP compressor and 2 stages HPT.

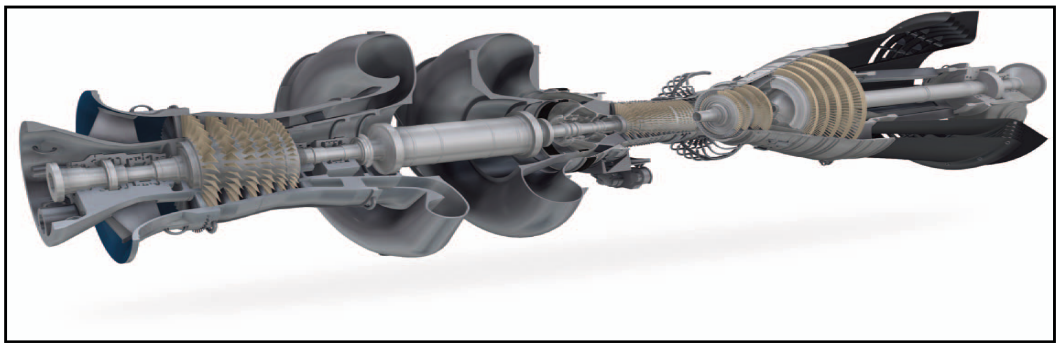

Figure 3-10 GE LMS100 Gas Turbine Engine Configuration [48]

Also, there is a 5-stage free power turbine PT which is indicated as the driver of an electric power generator. The engine was designed to provide a 10% increase in thermal efficiency higher than the highest GE's simple cycle gas turbines at that time.

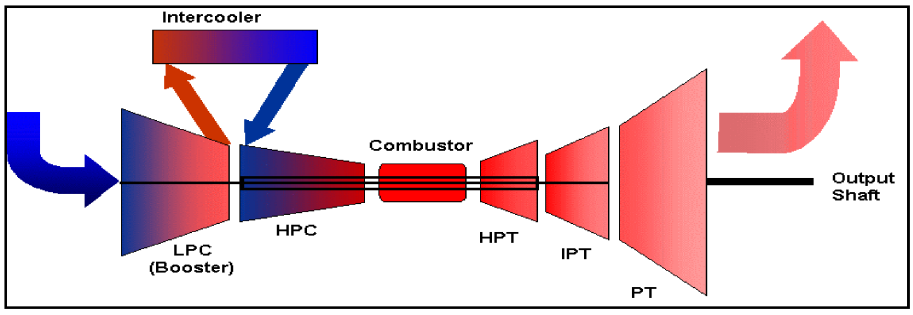

Figure 3-11 Schematic Diagram of GE LMS100 Engine [75]

Some of the engine's design parameters data are included in Table 3-3 and Table 3-4, as they were collected from the public domain.

Table 3-3 The GE LMS100 Published Design Parameters for different Models [46]

LMS100 ISO Performance Data							
Model	ISO Base Rating [KW]	Heat Rate [Btu/Kwh]	Efficiency [%]	Mass Flow [lb/sec]	Turbine Speed [RPM]	Exhaust Temp [F]	Comment
LMS 100 PB	97.718	7592	45.0%	453	3600	783	DLE, 25 ppm NOx
LMS 100 PB	97.878	7579	45.0%	453	3000	784	DLE, 25 ppm NOx
LMS 100 PA	103.112	7773	43.9%	469	3600	770	Water injected to 25 ppm NOx
LMS 100 PA	103.162	7769	43.9%	469	3000	767	Water injected to 25 ppm NOx

Some calculations have been conducted to find engine specific fuel consumption SFC at design point according to the following formula.

$$SFC = \frac{HR}{FCV}$$

Table 3-4 The GE LMS100 Public Domain Design Point Data [75],[27]

ShP(KW)	HR (BTU/Kw.hr)	EGT K°	PT Speed (rpm)	OPR	W $(^{Kg}/_{s})$	ξ_{th}
97718.0	7592	690.372	3600	42.1	205.4	45%

The quantity of heat produced by combustion fuel at constant pressure and under the normal condition is called Fuel Calorific Value FCV.

$$FCV = 43.124\ \frac{MJ}{Kg}\ ,$$

$$SFC = 0.1587\ \frac{K_g}{Kw.hr}$$

Data collected is used in calculating the design point characteristic and predicting the off-design engine performance. All the calculations are introduced in detail in the following sections.

3.2.1 100mw Intercooled Engine's Design Point Matching Calculation

The schematic structure of the engine was made, as shown in Figure 3-12 and it has been used to create a mathematical model (see appendix E.1.6) in

order to calculate engine design parameters and simulate engine performance at off-design operation. Some assumptions have been taken (including cooling bleed flow ratios, components efficiencies) to conduct the design point and Off-design performance prediction calculations. In all design point and off-design calculation, combustor outlet temperature COT, and inter-cooler outlet temperature are used as design parameters.

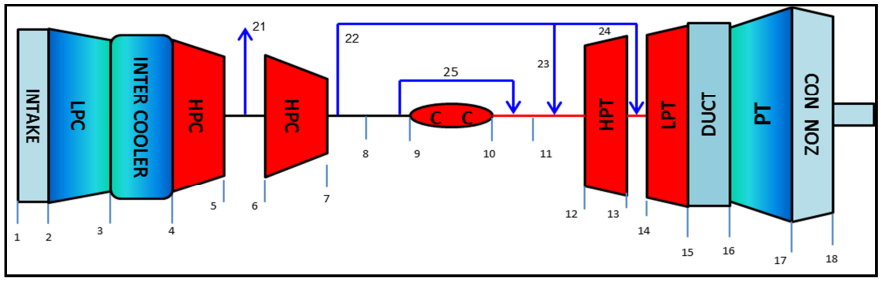

Figure 3-12 The GE-LMS100 Model Schematic Diagram

Apart from fan pressure ratio optimisation and propelling nozzle calculations, the remaining design point calculation steps are identical to the ones taken in aero-engine design point calculations.

Data for design point information are collected from the public domain indicated that the engine overall pressure ratio is equal to $(OPR = 42.1)$. So, the main aim of engine design point calculation is to find the correct design parameters which match published engine design parameters. To conduct the calculation some assumptions were taken to include compressors' isentropic efficiency, turbine isentropic efficiency, combustor efficiency and pressure drop, as well as ratio of air extracted for hot gas section cooling as presented in Table 3-5. It has been confirmed in some studies as in [27], that the variation in inter-cooler outlet temperature has a minor effect on the inter-cooled cycle compared with varying the inter-cooler pressure ratios, as shown in Figure 3-13. Therefore in this calculation, the inter-cooler outlet temperature is assumed to be constant at $10\ C^{\circ}$ higher than the ambient temperature for both design point calculation and off-design performance simulation.

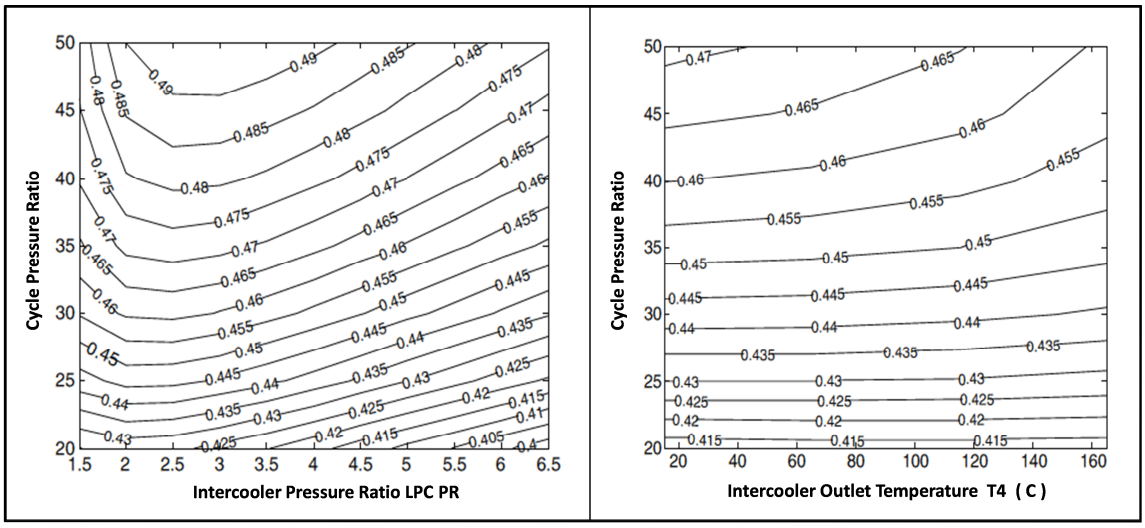

Figure 3-13 The Inter-cooler Pressure and Outlet Temperature Effect on Cycle Thermal Efficiency [27]

It seems a sensible assumption, as [27] has mentioned that most recent machines in the market were designed with inter-cooler outlet temperature equal to ambient temperature. $ISA\ SLS$ conditions assumed for ambient conditions at design point calculations and the results are contained in Table 3-5.Based on the schematic structure and stage numbering in Figure 3-12, The Turbomatch code has been used to create the engine model illustrated in appendix [E.1.6]. All the design point parameters and cycle optimisation results are mapped and plotted in Figure 3-14, Figure 3-15 and Figure 3-16.

Table 3-5 The GE-LMS100 Engine Design Point Parameters

W $(\frac{Kg}{s})$	$LPC\ \ PR$	$HPC\ \ PR$	ζ_{isc}	CPL	$HPT\ \ \zeta_{ist}$	$LPT\ \zeta_{ist}$
205	4.6	9.152	89%	5%	89%	91%
$W_f\ (\frac{Kg}{s})$	$COT\ (K^{\circ})$	ζ_{th} (%)	$SFC\ (\frac{g}{Kw.hr})$	$ShP\ (MW)$	$PT\ \zeta_{ist}$	
5.0389	1570	45.138	185.827	97.568	92%	

The low pressure compressor pressure ratio has been varied for different combustor outlet temperatures, and for every given value of combustor outlet temperature. Pressure ratio of low pressure compressor pressure ratio is varied in the range of (2.0 to 10.0).

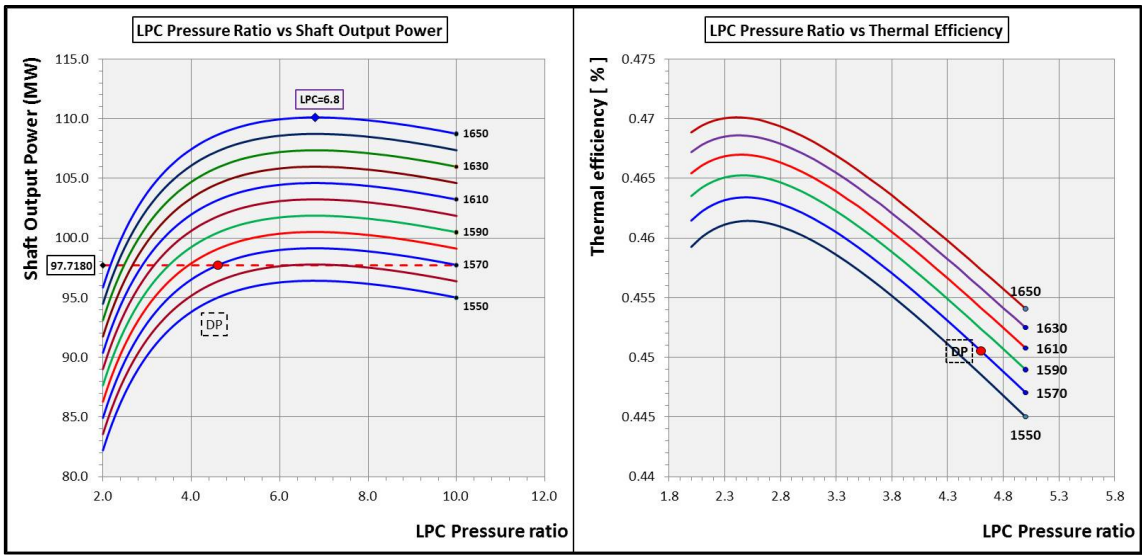

Figure 3-14 100MW 3Shaft Inter-cooled Power Produced at Design Points

These procedures are used for cycle optimisation in order to find the optimum intercooler pressure for maximum efficiency or maximum output power. It can be clearly seen from Figure 3-14, Figure 3-15, Figure 3-16, that increasing combustor outlet temperature causes an increase in output power for a given LPC pressure ratio

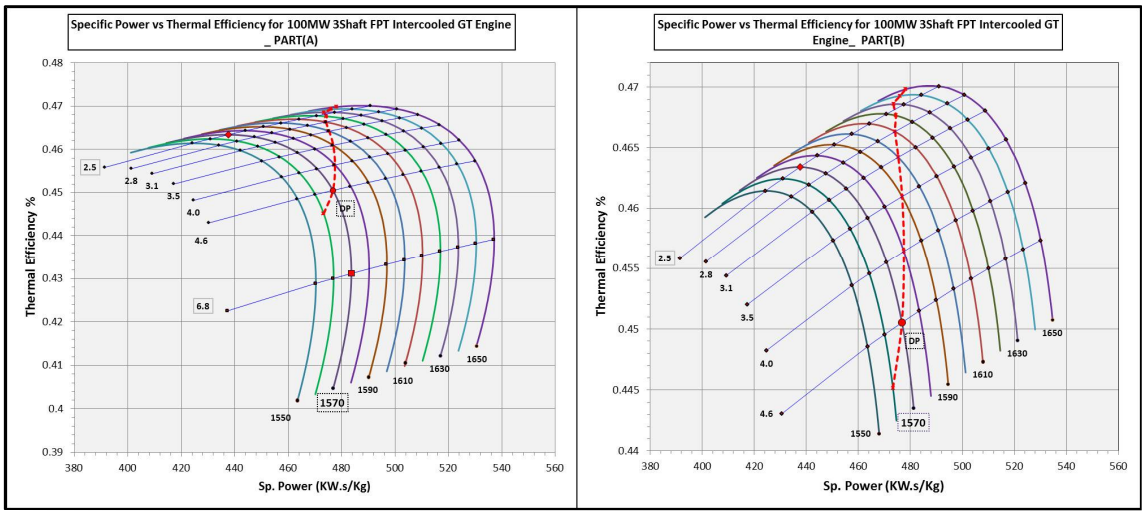

Figure 3-15 Effect of Varying LPC and TET for 100MW Inter-cooled 3Shaft Aeroderivative Gas Turbine on thermal Efficiency at DP

For a constant COT value, the increase in LPC pressure ratio results in a rise in cycle output power and improving thermal efficiency. There is always a certain value of LPC pressure ratio which provides the maximum output power of $LPC = 4.6$ where any further increase leads to a negative effect on thermal

efficiency and positive effect on specific power. The dotted line shows values of COT and LPC pressure ratio which meet the required engine shaft output power.

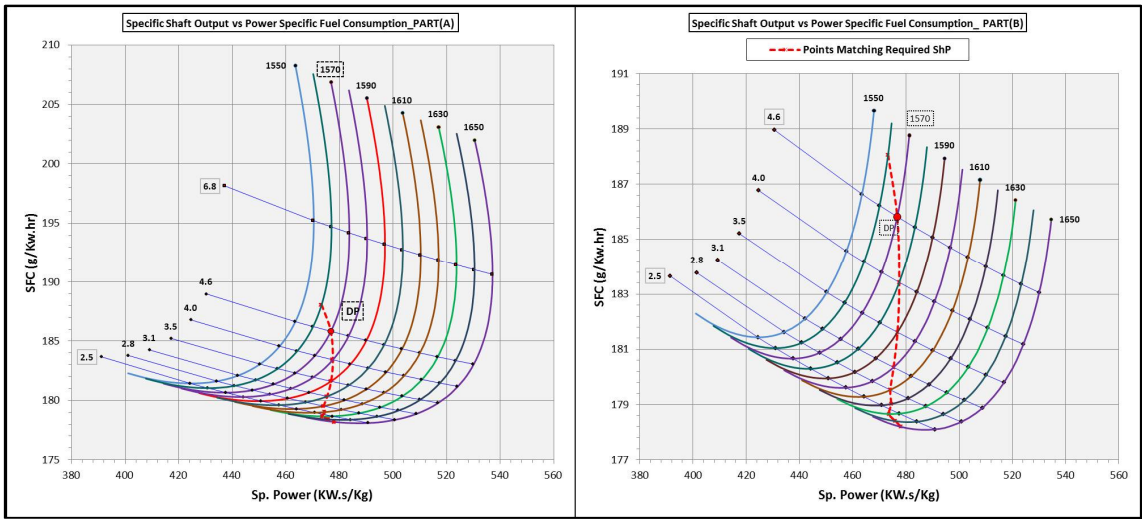

Figure 3-16 Effect of Varying LPC and TET for 100MW Inter-cooled 3Shaft Aeroderivative Gas Turbine on SFC at DP

All values of $COT = 1560\ to\ 1650$ can meet this requirement at different values of LPC pressure ratio. In the same way it can observed from Figure 3-15 and Figure 3-16 that $LPC\ PR = 2.5$ is the optimum value which provide the maximum thermal efficiency and lower specific fuel consumption for all investigated values of COT. The dotted line has showed that no point exists which can simultaneously satisfy the required ζ_{th} and specific power $SpPh$. So, the necessary compromise depends on the application. Design points which are close to maximum $SpPh$ refer to the possible small engine that can be designed, which is of high importance in some applications where space and weight are limited such as off-shore and marine.

In this calculation the compromise has been performed with regard to thermal efficiency ($\zeta_{th} = 45.0\ \%$). The chosen design point has the parameters previously illustrated in Table 3-5.

3.2.2 Engine's Off-Design Performance Prediction

The design point calculation is not enough to allow the design of any gas turbine engine, and the engine performance behaviour when operating away from design conditions must be predicted. It is well known that gas turbine engine performance is degraded in hotter environment with the increased ambient temperature. Simulation of the engine performance is conducted considering $(T_{am} = -15\ C^{\circ}\ to\ 45\ C^{\circ})$ and $(Alt = 0.0\ to\ 3000\ m)$. Off-design performance prediction is calculated and the results are plotted in Figure 3-17, Figure 3-18, and Figure 3-19.

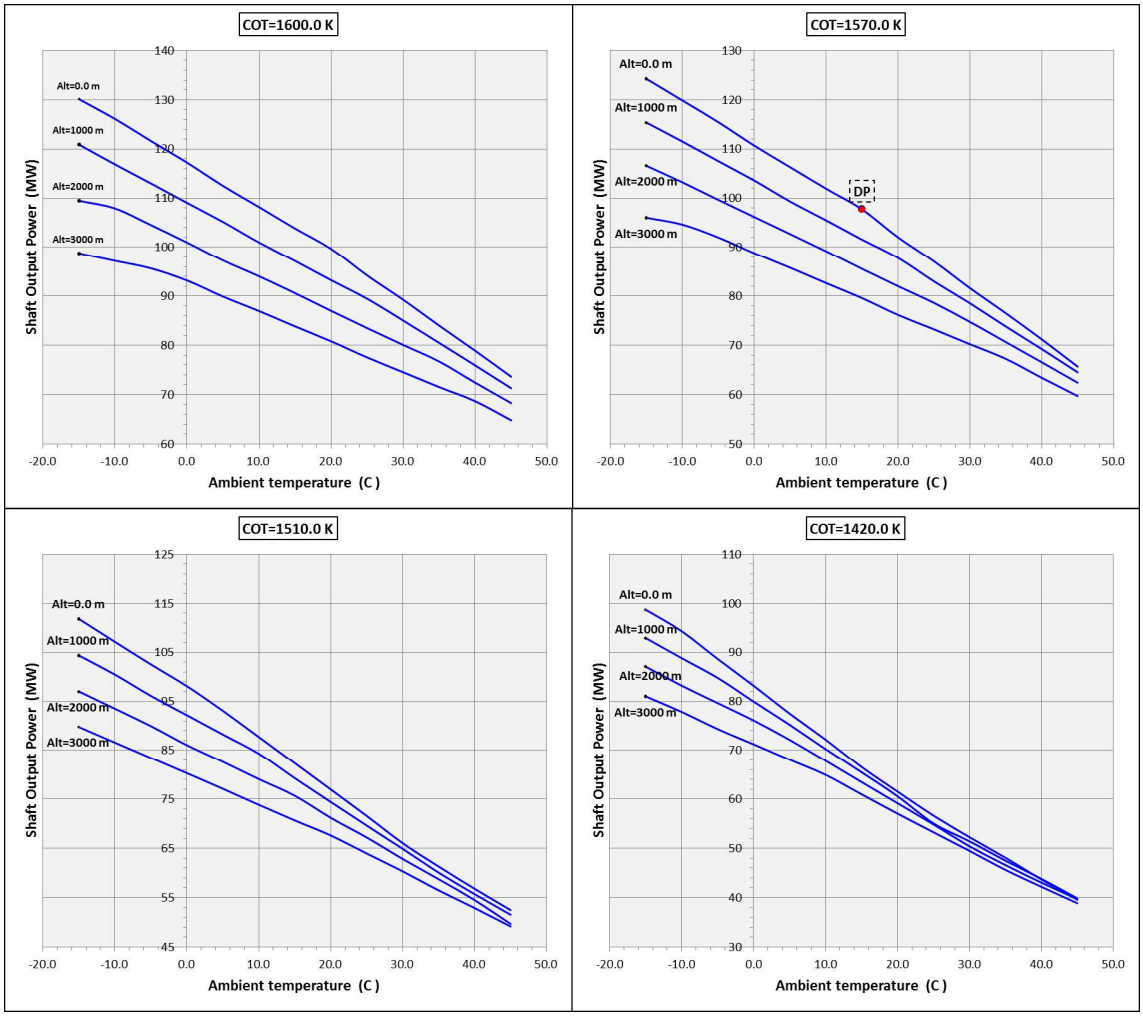

Figure 3-17 100MW 3Shaft IC : Ambient Temperature and Altitude Effect on Shaft output Power for different operating temperature at Off-design

Figure 3-17 demonstrates the effect of ambient temperature variation during engine off-design operation on shaft output power at different levels of altitude.

It can be observed that the engine's output power decreases with the increase in ambient temperature, and degradation rate increases as the combustor outlet temperature COT decreases at a given altitude. In addition, increasing engine altitude has a negative effect on shaft output power. For constant COT operation and the same ambient temperature, lifting the engine to higher altitudes causes a significant reduction in its output power, and this reduction is relatively lower at high values of ambient temperature. Also, the influence of altitude raise has a smaller negative effect at low values of operating temperature COT.

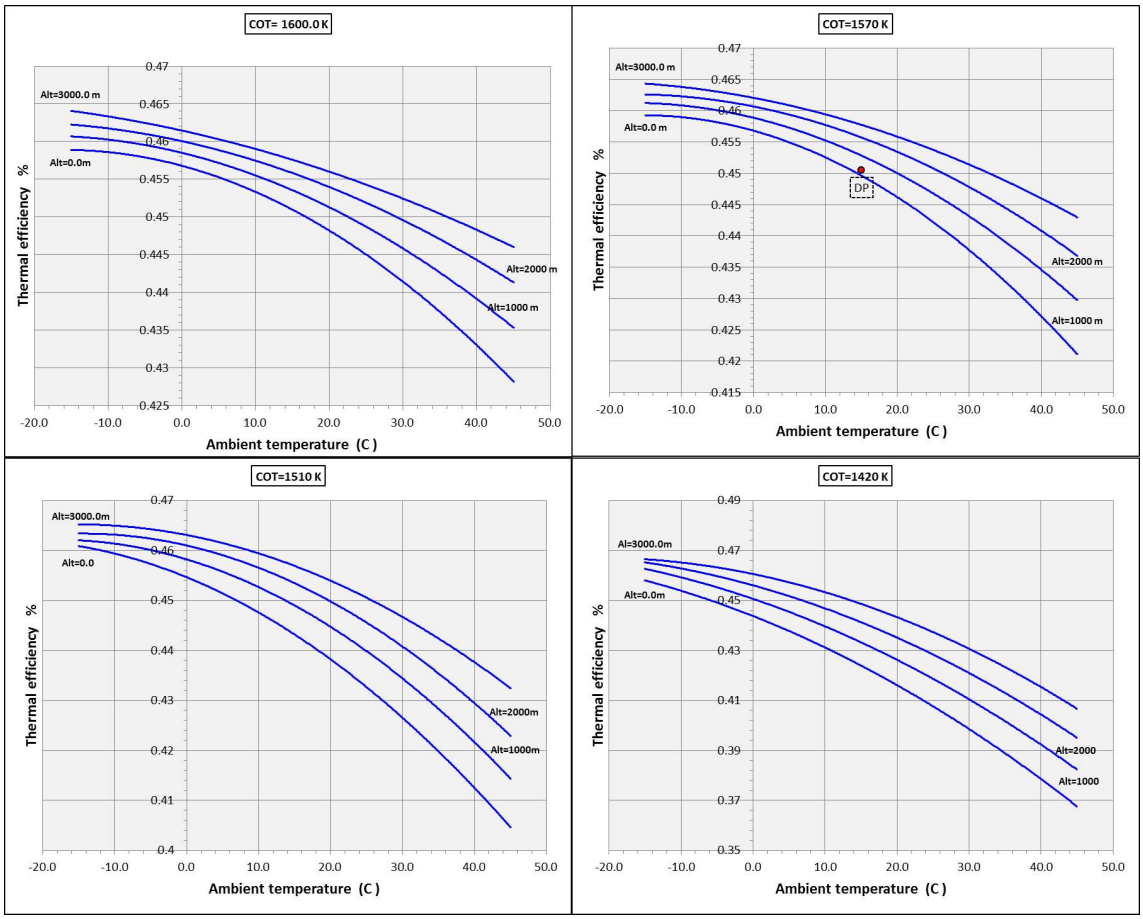

Figure 3-18 100MW 3Shaft IC : Ambient Temperature and Altitude Effect on Thermal Efficiency for Different Operating Temperatures at OD Operation

Increasing ambient temperature in the same way has negative effect on engine thermal efficiency, as clarified in Figure 3-18, and its impact is slightly reduced at lower values of COT. Altitude increase however has the opposite impact on thermal efficiency. There exists a significant improvement in thermal

efficiency owing to raising altitude, and positive impact increases at higher ambient temperature and COT.

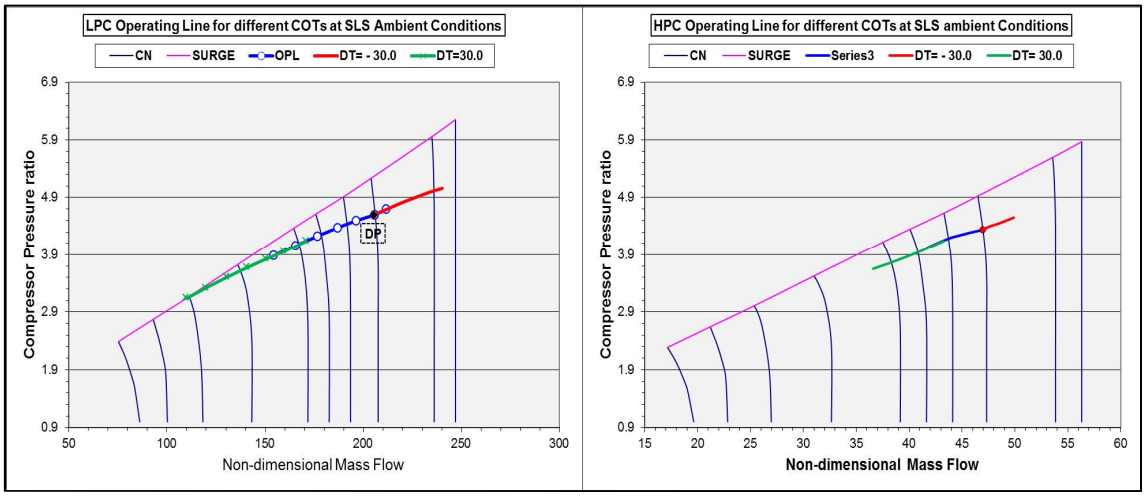

Figure 3-19 Engine Operating Lines on LPC and HPC at Off-Design Performance

High pressure and low pressure compressors operating lines plotted on the compressors maps at $ISA\ SLS$ condition for the investigated range of COT, and the maps are represented in Figure 3-19. Graphs in the figure show that the major effect of off-design operation occurs on the LP compressor operating line. In fact it is the LPC rotational speed CN which rapidly fell more quickly than the HP compressor with the decrease in COT at part-load operation. So, the LPC operating line crosses the surge line quicker than the HP compressor. The HPC operating line seems to have a steady state operating line.

4 AERO-DERIVATIVE ENGINE'S DERIVATION METHODOLOGY

The project objectives will be met through procedures following four main steps. The first step deals with designing different engines in different configurations and thermodynamic cycles. Secondly, re-designing of the engine components which will remain within the further work recommended carrying on. The design of the new enhanced gas turbine engines is carried out under the hypothesis that the high pressure compressor and turbine is unchanged.

4.1 Derivative Engine's Cycles and Applications Selection

Nowadays, the many aspects of the improvements in aero-derivative gas turbines have led to the increase in their output performance. Advanced computational fluid dynamics constitutes a significant factor causing the major improvements in compressor and turbine efficiencies. Also, the success in increasing turbine inlet temperature due to improving cooling system effectiveness and using better materials' specification for turbine blades led to improving specific work and cycle thermal efficiency. Aero-derivative gas turbine engines are produced in different thermodynamic cycles which suit different applications in order to improve their performance characteristic [20]. The demand for engines with better efficiency or higher heat output is the key factor that has to be clarified to choose the best engine for specific applications.

Accordingly, it is concluded from the literature that different combinations of engine configurations in different thermodynamic cycles are chosen in the investigation to suit the variety of selected applications, as shown in Figure 4-1.This table is concluded as a result of the fact that the engine cycle can be chosen depending on the application itself. For example, in power generation for peak-load application a simple cycle and intercooled cycle have been used and found the most efficient in this application. In peak-load application however, combined cycle aero-derivative for low power output

suffers from the penalty of low thermal efficiency. While in contrast, the combined cycle is found to be more efficient in base-load applications.

Cycle	GT Applications				
	P.G Base-Load	P.G Peak-Load	Marine	CHP	Gas Pumping
Core	✓	✓	✓	✓	✓
S.C	×	✓	✓	✓	✓
HE.C	✓	×	×	×	×
I/C	✓	✓	✓	×	×
ICR	✓	×	✓	×	×
CCGT	✓	×	✓	×	×

Figure 4-1 Aero-derivative GT's Cycles and Applications

Applications of aero-derivative gas turbine engines are used widely in base-load applications with different thermodynamic cycles, which made them more efficient than those using a simple cycle.

4.2 Choosing the Parent Aircraft Engine

It was mentioned earlier that the underlying growth in the demand for low weight and cost, better reliability and thrust are still satisfied by using gas turbine engines. In aviation, there is a huge demand for aircraft with less initial cost [99]. Accordingly, this criterion is taken into account in all the further research and the requirements vary depending on the application itself. Great concern exists regarding lower fuel consumption for long range aircraft and higher thrust and less weight for medium-range aircraft. In the aforementioned project of designing the 130-seat aircraft engine, there were another three teams working on the complete engine design of the proposed aircraft. Objective of this engine design is design an engine with relatively lower life cycle cost, long life, fewer parts and further development ability. So, in total there are four engines designed for the same objective, and their design point parameters are expressed in Table 4-1. One of these engines will be chosen as the parent of the newly designed industrial aero-derivative engines.

Table 4-1 100kN Turbofan Engines deigned for 130-Seat Aircraft [7][107][108]

DP Parameter	My Engine	AVIC Group Team1	AVIC Group Team2	AVIC Group Team3
BPR	6	6	7	5
Core mass flowW_c(Kg/s)	19.716	25	22	21.667
OPR	29.06	36	38	33
Fan PR	1.8	1.7	1.74	1.8
Booster PR	1.404	1.4411	1.459	1.6
HPC PR	11.5	14.695	15.0	11.46
Combustor COT (K)	1500.0	1400.0	1492.0	1560.0
Cruise net Thrust Fn (KN)	22.33	26.8	24.02	24.530
Combustor Pressure Loss	5%	4.5%	5%	5%
SFC (mg/ N.s)	17.14	15.9	16.4	18.51
Fan Efficiency %	89%	89.5%	91%	
Booster Efficiency %	89%	87.5%	89%	
HPC Efficiency %	89%	87.5%	89%	88%
HPT Efficiency %	90%	89%	90%	88%
Combustor Efficiency %	99.99%	99.99%	99.99%	
LPT Efficiency %	91%	90%	90%	90%
Bypass Duct Loss	1.0%	1.0%	1.0%	1.2%
HPT NGV Cooling Flow %	8.99% W_c	6	9.55% W_c	10% W3
HPT Blade Cooling Flow %	3.71% W_c	3	4.29% of W_c	3.5% W3
Sealing Flow70% DT to Rear of LPT	1.0% W_c	$1.0\% \, of \, W_c$	$1.5\% \, of \, W_c$	$1.0\% \, of \, W_c$
Off-Design Take-Off ISA COT (K)	1748.0	1500.0	1674.0	1700.0
Off-Design Take-Off ISA net Thrust (Fn) (KN)	97860.84	110.0	120.1	107.682
Off-Design Climb ISA COT (K)	1574.0	1450.0	1538.0	
Off-Design Climb ISA net Thrust (Fn) (KN)	25.043072		26.0	
Number of Shafts	2	2	2	2

In this project the engine designed by the AVIC group team 2 is chosen to be the parent of all the newly designed aero-derivative engines. Figure 4-2 represents the engine's overall structure and dimensions and shows that it consists of Fan, LPC, HPC, Burner, LPT, HPT, and Nozzle.

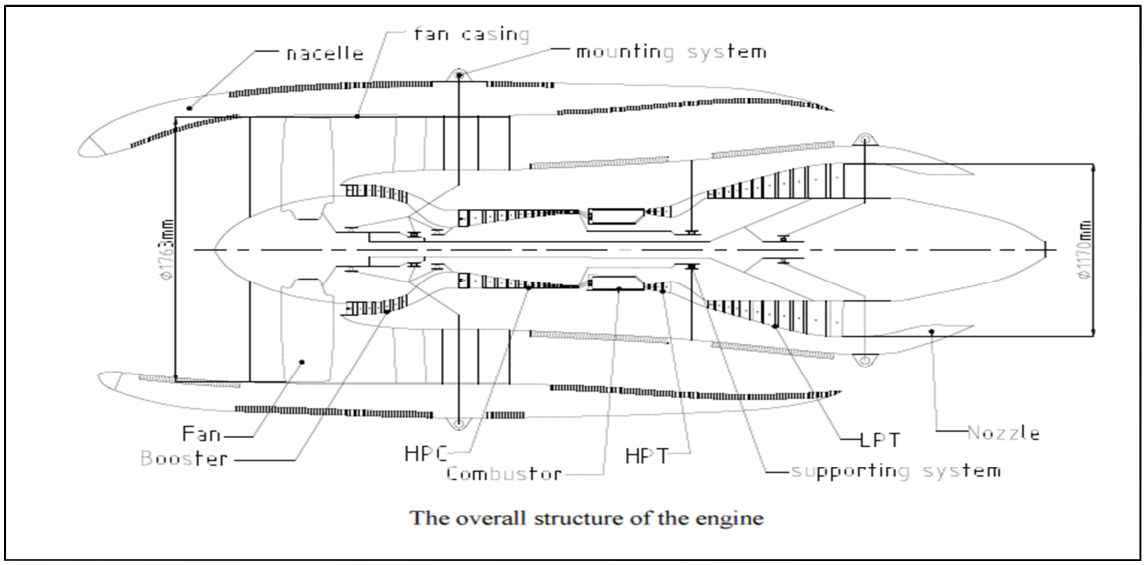

Figure 4-2 The 130-Seat $CUAVA$ Aircraft Turbofan Engine Structure and Dimensions [5]

Based on the schematic structure shown in Figure 4-3, a performance model is created using the Turbomatch code in order to calculate the engine design point and simulate its performance at design conditions away from design point.

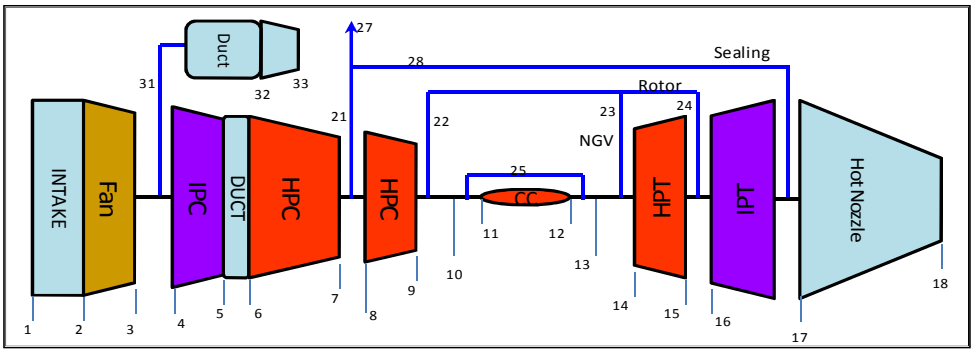

Figure 4-3 The 130-Seat $CUAVA$ Aircraft Turbofan Engine Structure

Cruise requirements and conditions are chosen to be the design point conditions. Calculation is conducted including off-design and maximum climb requirements, the results shown in Table 4-2 and Table 4-3.

Table 4-2 Team2 $CUAVA$ Engine Design Point Parameters at Cruise

BPR	OPR	W_c	$\eta_{isen,comp}$	$\eta_{isen,turb}$	Bypass Duct Loss	Combustor pressure Loss	HPT NGV Cooling	HPT Blade Cooling
7	40	25	90%	90%	0.8%	4.8%	10% of W_{core}	4.5% of W_{core}
OPR	**FP**	**Booster PR**	**HPC PR**	**W (Kg/s)**	**TET (K)**	**Fn (KN)**	**SFC (mg/N/s)**	
38	1.74	1.459	15	176	1492	24.02	16.4	

Engine performance is predicted through the off-design simulation of the engine at take-off and max-climb, and simulation results are presented in Table 4-3 [5].

Table 4-3 $CUAVA$ Engine Performance Parameters at Take-Off & Max-Climb

	BPR	OPR	FPR	Booster	HPC PR	W (Kg/s)	TET (K^o)	Fn (KN)	SFC (mg/N/s)
Take Off	7.46	32	1.591	1.389	14.5	428.12	1674	120.1	8.92
Max.Climb	6.85	40.3	1.782	1.467	15.4	179.85	1538	26	16.52

4.3 Maintaining Only the High Pressure Rotor Components

The main concern regarding the maintenance of aircraft engine components is its very sophisticated technology, especially in the hot section, and reducing the cost of designing and producing new components. By maintaining the LP rotor components both the LP compressor and LP turbine will remain and in some cases new components will be attached to the engine. Both single spool and multi-spool features will be contained and the resulting new engines will be as follows:

- Single-Spool Engines (Direct Derivation).

- Simple Cycle. As in Figure 5-1
- Heat Exchanger Cycle. As in Figure 5-2, Figure 5-3

➢ Two-Spool Engines.

- Simple Cycle. As in Figure 5-4.
- Inter-cooled Cycle. As in Figure 5-8.
- Heat Exchanger Cycle. As in Figure 5-13, Figure 5-16, Figure 5-19.
- Inter-cooled recuperated Cycle. As in Figure 5-22.

4.4 Maintaining the LP and HP Rotor Components

Cycle efficiency and specific work are the most important outputs that need to be improved, increasing the overall pressure ratio and turbine inlet temperature are the factors to improve them [82]. Once the ability to increase TET is applicable, adding a new rotor with both compressor and turbine increases the OPR. On the other hand, the direct derivation to have two-shaft engines allows the same technology to be kept and reduces cost. The following are derivable engines from maintaining the (LP and HP) rotors.

➢ Two-spool engines. (direct derivation).

- Simple cycle

➢ Three-spool engines.

- Simple cycle
- Intercooled cycle

The aero-derivative engine has been used in two different arrangements in designing power turbines. A free power turbine arrangement can be used and it has proved to be better in controlling design performance in some applications such as peak-load and marine [44].

Both configurations chosen in this project will have both arrangements of direct drive DD and free power turbine FPT. Detailed calculation of both design point DP characteristics and Off-Design performance will be dealt with in Chapters 5 and 6 below.

4.5 Derived Engine's Components Design

It is possible for the 60Hz generator to be connected directly to the aircraft engine due to the fact that the rotational speed of the low pressure rotor in the aircraft engine is restricted by the tip speed of the fan. It is around 3000 rev/min. Therefore in some cases the need for a gearbox will be unnecessary and could be avoided [103]. Furthermore, the 50Hz generators running at 3000 rev/min could be coupled to the aircraft engine in the condition of re-staging the LP compressor blades of the aircraft engine. In reality the turbine needs to be modified to offset the change in compression work. Regarding engine configurations of Free Power Turbine FPT or single shaft direct load drive IPT, the aero-derivative engine component modification will be different from one design to another. In the case of two-shaft with a free power turbine in order to absorb removed fan work in direct derivation, the low pressure compressor needs to be modified as well as the low pressure turbine. Similarly, in the case of the two-shaft integrated power turbine, low pressure turbine will have to be completely replaced by new turbine drives in the redesigned compressor and the load. The methodology of designing the new turbines and modifying the compressors will follow the steps described in details in references [92; 93].

4.6 Techno-economic Assessment Calculation

In the majority of investigating and comparison studies, economic assessment is conducted to prove whether or not the project is economically and technically efficient to be carried out. All aspects of lowering emission production (which has minimum global warming impact), legislation and taxation policies are considered in assessing all the proposed new designs of aero-derivative gas turbines.

Assessment methodology used in this project is based on $TERA$, which is a philosophy of technical, economic, environmental and risk assessment analysis used in assessing designs of gas turbine plants. As mentioned this was invented in in Cranfield University, and started as a concept based on the investigation of multi-disciplinary optimisation of power plants as well as the effect of designing and operating power on atmospheric pollution. The aero-engine area $TERA$ software, also created in Cranfield University, is used for modelling gas turbine engine and aircraft performance and it includes different modules integrated with a commercial optimiser [84]. It is capable of optimising more than one goal function; including global warming potential, gaseous emission, engine noise, NO_x and engine direct operating cost.

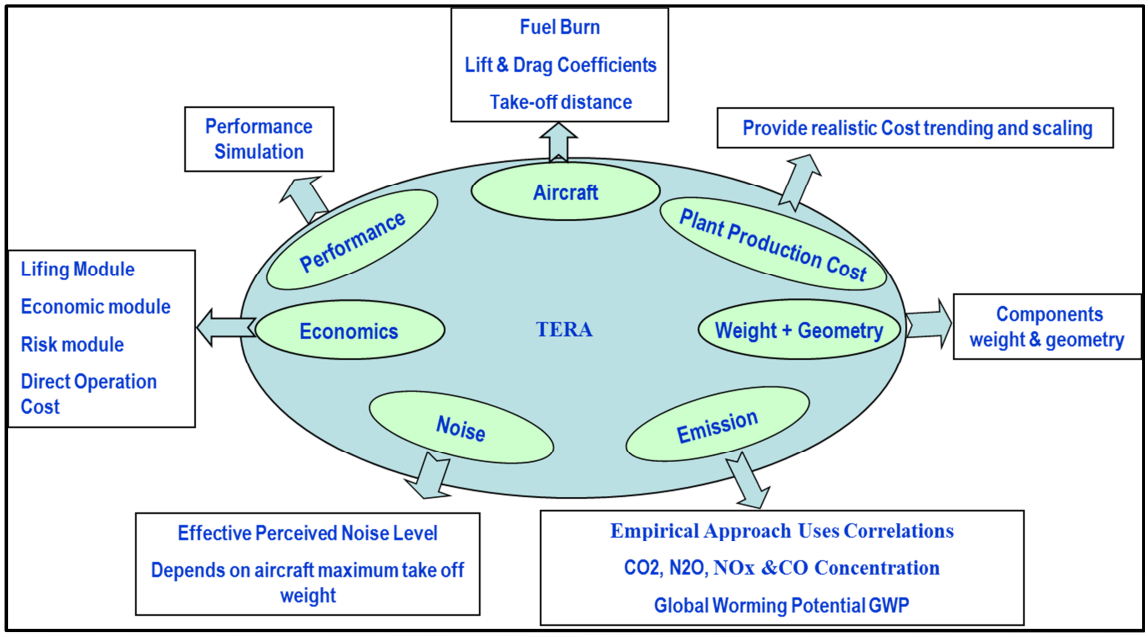

Figure 4-4 $TERA$ Philosophy Software Models for Aero-applications [84]

As it can be seen Figure 4-4 offers a brief and general description of $TERA$ philosophy. An aircraft model using separate software called $HERMES$ can be used to calculate the aircraft performance data such as lift coefficient drag coefficient and take-off distance. Some data such as geometry and aircraft mass must be provided as input data to the optimiser. However, $TERA$ software designed for aero application cannot currently be directly used for aero-derivative turbines on land-based applications without modification. There are

some aspects involved in building aero $TERA$ software, which are not necessarily needed for aero-derivative gas turbine land-based applications. It consists of the following models:

Performance model: or sometimes called engine model. It is a model designed using the Turbomatch Code, which was also designed in Cranfield University for calculating design point characteristics and predicting off-design performance.

Economics: in the case of aero application it considers another four sub-modules as follows:

1. Life module: to estimate HPT disc and blades through analysis creep and fatigue during full working cycle of the engine
2. Environment model: to assess the global warming potential for a given operating scenario. "The model can estimate the GWP indices for (NO_x,CO_2, CO andH_2O) which can be used to assess the climate change impact of an engine solution" [41]. A noise model based on aircraft and engine models will be used to assess the noise level. The assessment method depends on some public methods, which use correlations. In the aircraft, the measurement should be made at three positions of the aircraft; landing, take off and approaching. Then the Effective Perceived Noise Level $EPNL$ will be determined from the total time-integrated noise. Fan, core jet, turbine, and airframe will be involved in the estimation.
3. Economic model: to estimate cost of maintenance. Time between overhaul, labour cost and engine cost including spare parts has to be obtained.
4. Risk module: to study the influence of variation in some parameters on net present cost of operation.

Therefore, in order to use this model on land-based aero-derivative engine applications some parameters can be excluded. Also, it is not necessary to use a noise model $SOPRANO$, used to estimate the aircraft noise [84]) in aero-derivative applications. The emission model should be modified and adapted to

suit aero-derivative land-based applications. Emission model outputs are the source of data provided to the economic model to estimate emission taxes and GWP in aircraft applications [84]. A number of empirical approaches exist based on correlations used to estimate pollutants concentration in the exhaust including NO_x,CO_2,CO and Unburned Hydrocarbon UHC. Minor importance is given to weight and geometry models of aero-application when applied on land-based stationary applications. However, it is very important for aircraft applications to provide important information regarding components' weight and geometry as well as other material required by the other models in the optimiser.

Plant production cost model: which is used in $TERA$ for aircraft application and does not provide the exact value of cost. It is based on a trend of realistic cost imported from manufacturers. In general, there are many different factors which affect the production cost and should be considered and determined through specifying factors such as manufacturing technology level, production cost, wage rates variation [84], etc.

5 DERIVED ENGINES DESIGN POINT CALCULATION

All selected or proposed aero-derivative gas turbine engines' design point performance including exhaust heat output (Q) is calculated in this chapter. Heat is estimated through investigating the possibility of extracting as much as possible from the exhaust heat. The heat exchanger component is assumed to be installed in two proposed configurations, at the exhaust or between divided turbines, in order to recover the engine's waste heat. All heat recovered at the assumption of constant stack temperature of $400K^{\circ}$ or $126.85\mathrm{C}^{\circ}$ for all heat processes. It is estimated from fuel dew-point curves avoiding condensation problems at the exhaust [85][6]. Engine design point calculations are also performed at the standard day temperature and atmospheric pressure at ISA SLS conditions.

Maintaining the same aero-engine's compressor design needs to keep similar, constant values of some non-dimensional parameters at the design point [63]. These parameters include value of non-dimensional mass flows $\left(\frac{w\sqrt{T}}{P}\right)$ at the inlet of compressor and turbine. Cycle temperature ratio of $(\frac{TET}{T})$ should be kept constant in the aero-engine which in turn results in maintaining the same value of turbine inlet non-dimensional mass flow at the inlet of the HP turbine. This concept is applied at the temperature ratio of the combustor outlet temperature to compressor inlet temperature $\left(\frac{COT}{T}\right)$ [78]. The engine model in Figure 4-3 $CUAVA$ was run at design point using the Turbomatch code and all required non-dimensional ratios have been calculated for every component separately. Results of this calculation based on stage numbering in Figure 4-3 are shown in Table 5-1 at all dedicated stages. As previously mentioned, non-dimensional mass flow at the inlet of the high pressure turbine is constant, as long as the ratio of combustor outlet temperature to the HP compressor inlet temperature $\frac{COT}{T}$ remains constant and equal to the design point of aero-engine. However, calculating turbine non-

dimensional mass flow is important in checking whether or not the design point temperature ratio used is correct.

Table 5-1 Non-dimensional Parameters at Design Point for $CUAVA$ engine

$\frac{W2\sqrt{T2}}{P2}$	$\frac{W6\sqrt{T6}}{P6}$	$\frac{W8\sqrt{T8}}{P8}$	$\frac{W14\sqrt{T14}}{P14}$	$\frac{T12}{T2}$	$\frac{T12}{T6}$
1010.26	461.2536	83.0276	62.434	6.103	4.5425

All the design point the procedures have been established based on the assumption of the following parameters.

- Ambient Temperature (T1=288.15 K)
- Ambient pressure (P1=101KPa)
- Inlet Pressure Losses 5%, Duct Losses 2%.
- Intercooler Losses 3%
- Heat Exchanger Cooled Side2%.
- Heat Exchanger Hot side 3% [2]
- $C_{Pc} = 1000\ \frac{J}{K_g.K}$, $C_{PT} = 1150\ \frac{J}{Kg.K}$, $\gamma_C = 1.4$, $\gamma_h = \frac{4}{3}$, $FCV = 43\frac{MJ}{Kg}$

5.1 Maintaining Aero- engine's High Pressure Components

5.1.1 Single Spool Simple Cycle Engine

In this arrangement it is only the HP rotor which will be maintained from the aircraft engine. Following the methodology illustrated previously the design point calculation has been conducted including the value of possible extracted heat from the engine's exhaust. Also, the bleed valve in the HP compressor at stage 21 and cooling bleed at stage 24 have to be kept opened at the design point for the components matching purpose with the parent aero-engine at the design point.

Referring to the schematic draws in Figure 5-1 and Figure 4-3 which show components' configuration and stage numbering for both the single spool

engine and the parent aero-engine respectively. Design point calculations have been conducted using equations illustrated in the following steps:

$$(W_2\sqrt{T_2})/P_2 = \left[(W_6\sqrt{T_6})/P_6\right]_{aero} \quad (5\text{-}1)$$

$$T_8/T_2 = [T_{12}/T_6]_{aero} \quad (5\text{-}2)$$

$W_2 * \sqrt{288.15}/0.995 = 461.2536$ → W_2=27.04 (Kg/s)

$T_8/288.15 = 4.5425$ → T_8=1308.92 (K°)

Intake :(1-2)

$$P_2 = 0.995 * P_1 \quad (5\text{-}3)$$

$$W_2 = W_1 \quad (5\text{-}4)$$

$$T_2 = T_1 \quad (5\text{-}5)$$

Compressor HPC1 (2-3)

$$P_4 = P_2 * PR \quad (5\text{-}6)$$

$$T_3 = {}^{T2}/_{\zeta_{isc}} * \left[PR^{\left({}^{\gamma_c - 1}/_{\gamma_c}\right)} - 1\right] + T_2 \quad (5\text{-}7)$$

$$CW1 = W_3 * C_{P_h} * (T3 - T2) \quad (5\text{-}8)$$

Compressor HPC2 (4-5)

$$W_{21} = 0.04568 * W_3 \quad (5\text{-}9)$$

$$W_4 = W_3 - W_{21} \quad (5\text{-}10)$$

$$T_4 = T_3 \quad (5\text{-}11)$$

$$P_4 = P_3 \quad (5\text{-}12)$$

$$T_5 = {}^{T_4}/_{\zeta_{isc}} * \left[PR^{\left({}^{\gamma_c - 1}/_{\gamma_c}\right)} - 1\right] + T_4 \quad (5\text{-}13)$$

$$CW2 = W_4 * C_{P_h} * (T_5 - T_4) \quad (5\text{-}14)$$

Combustor

$$P_4 = P_3 * (1 - 0.048) \quad (5\text{-}15)$$

$$Q_{cc} = W_3 * C_{P_h} * (T_4 - T_3) \quad (5\text{-}16)$$

$$W_f = Q_{cc}/FCV \quad (5\text{-}17)$$

$$W_4 = W_3 + W_f \quad (5\text{-}18)$$

Turbine (10-11)

$$P_{12} = P_{11} = Pa \quad (5\text{-}19)$$

$$T_{10} - T_{11} = T_{10} * \zeta_{isT}\left[1 - \left(1/(P_{10}/P_{11})^{((\gamma_g - 1)/\gamma_g)}\right)\right] \quad (5\text{-}20)$$

$$TW = W_4 * C_{p_h} * (T_{10} - T_{11}) \quad (5\text{-}21)$$

$$ShP = TW - (CW1 + CW2) \quad (5\text{-}22)$$

Heat Output

$$Q = W_{12} * C_{Ph} * (T_{12} - T_{Stack}) \quad (5\text{-}23)$$

$$\zeta th = (Shp \ / \ HPW) \quad (5\text{-}24)$$

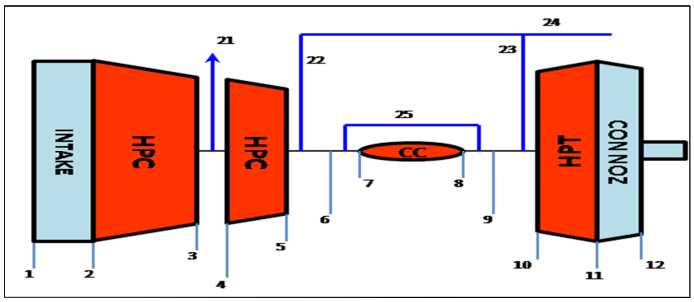

Figure 5-1 Single-Spool Simple Cycle Engine

Turbomatch code is used to calculate design parameters and the Model Input file (see appendix E.1.1) is run. Mass flow and COT from previous calculations have been entered into the input data file and results tabulated in Table 5-2, which represents the engine's design point characteristics.

Table 5-2 Design Point Characteristics of Single-spool Simple Cycle Engine

$W\ (^{K}/_{S})$	$ShP\ (MW)$	ζ_{th}	$Q\ (MW_{he})$	PR	$COT\ (K^{O})$
27.04	5.43	31.05	8.96	15	1308.92

5.1.2 Single-Spool Heat Exchanger Cycle Aeroderivative Engine

Heat exchanger concepts are based on the idea of extracting energy from turbine exhaust gases and utilising it in heating up compressor discharge and increase compressor outlet temperature [2]. Consequently, a reduction in SFC will be experienced due to a decrease in required fuel value to reach the required combustor outlet temperature COT or required output power. Considering the heat exchanger's thermal barriers, the design point is calculated based on the assumption of 2% pressure loss in the cold side of the heat exchanger and 3% on the hot side. Saravanamuttoo and Walsh in [103][85] have mentioned that the highest applicable heat exchanger inlet temperature is in the range of $(T_{15} \leq 900\ K^o)$. However, [76] proved in his study that an annular recuperator has been modified for a micro gas turbine and it was possible to achieve $850\ C^\circ$ which is equal to around $1123\ K^o$. This was recorded using the ceramic type heat exchanger showing that the $1300\ C^\circ$ inlet temperature can be reached at a pressure equal to 4 bar.

Table 5-3 Maximum Operating Condition for Heat Exchanger by Type [76]

HE type	Maximum pressure (bar)	Maximum temperature (°C)	Effectiveness
PHE	40	400	>90
PFHE	120	650	>90
Spiral	30	400	
Flat tube and fin	200	200	
Tubular (profile)	31	750	<85
Tubular (mini)	100	730	
PCHE	500	1000	>97
Ceramic	4	1300	

As it can be observed that Table 5-3 contains some results from the study and shows a list of different heat exchangers sorted by type, and determined the maximum applicable operating temperature and pressure with the effectiveness of each type. Heat exchanger effectiveness has been given an

assumption of $(\epsilon = 0.9)$ for both cold and hot sides at the design point calculation.

5.1.2.1 Single-Spool Conventional HEx Configuration Engines

An arrangement of single-spool configuration exists where the heat exchanger is installed at the exhaust called conventional regenerative cycle. The non-dimensional parameters, which have to be kept equal to the parent aero-engine, are the non-dimensional mass flow, compressor non-dimensional speed, and cycle temperature ratio. That is similar and equal to the calculation of the single-spool simple cycle. Components matching conditions at the design point determine that this engine will have same previous values (see Table 5-2) of mass flow and combustor outlet temperature COT. Referring to the schematic diagram shown in Figure 5-2 and considering the condition of enchasing the cycle thermal efficiency using heat exchangers, heat exchanger inlet temperature has to be higher than the compressor discharge temperature ($T_{15} > T_5$).

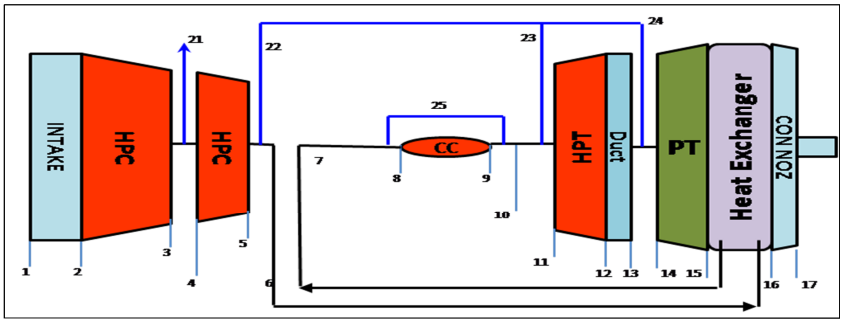

Figure 5-2 Single Spool HEx Conventional Configuration Engine

Values of T_9 and W_2 were fed to the Turbomatch model, (see appendix E.1.7), and the calculation results found as in Table 5-4.

Table 5-4 Design Point Characteristics of Single-Spool HEx Engine

$W\ (^{K}/_{S})$	OPR	$COT\ (K^{O})$	$T_{HEin}\ (K^{\circ})$	$T_{exh}(K^{\circ})$	$ShP\ (MW)$	ζ_{th}	$Q\ (MW)$
27.04	15	1308.92	716.28	673.61	5.242	32.26	7.8731

Comparing with single-spool simple cycle engine, 1.2% increase in thermal efficiency was achieved due to recovering heat from engine's exhaust waste using the heat exchanger. However, there is a slight drop in the engine output power due to the drop in pressure created by heat exchanger losses [79].

5.1.2.2 Single-Spool non-Conventional HEx Configuration FPT

Regardless of the mechanical capability, the core single-spool with free power turbine provides the option of applying an alternative or non-conventional regenerative concept in order to enhance engine thermal efficiency. It can be achieved by installing a recuperator between the compressor turbine and the free power turbine. The arrangement shows that heat exchanger inlet temperature will be higher than it was in the conventional arrangement. The condition of applying the recuperator concept assumes that $(T_{12} > T_5)$.

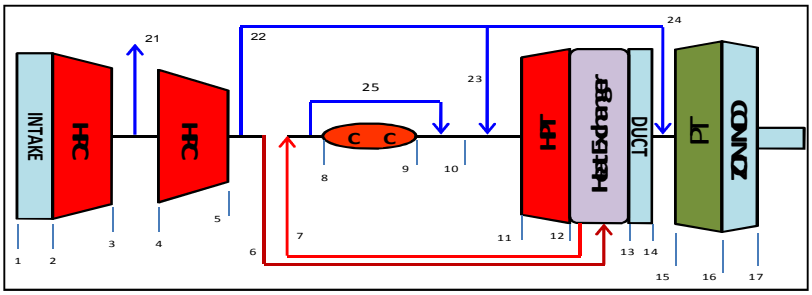

Figure 5-3 Single Spool HEx non-Conventional Configuration Engine

Pressure drops in both the cold and hot side of the heat exchanger remains as assumed at the design point calculation to be 2% and 3% respectively. The engine's mass flow, pressure ratio, and combustor outlet temperature remain equal to the conventional arrangement, as shown in Table 5-5. However, thermal efficiency and output power will vary and their values will be the result from the design point calculation. Referring to the engine arrangement and its components numbering viewed in Figure 5-3, a model has been developed using the Turbomatch code and the engine's performance characteristic recorded in Table 5-5. Heat exchanger inlet temperature is within the acceptable range and further calculation for predicting the engine off design

performance has to be conducted as well as the values of the heat exchanger inlet temperature.

Table 5-5 Design Point Parameters of Single-Spool non-Conventional HEx Engine

$W\ (^{K}/_{S})$	OPR	$COT\ (K^{O})$	$T_{HEin}\ (K^{\circ})$	$T_{exh}(K^{\circ})$	$ShP\ (MW)$	ζ_{th}	$Q\ (MW)$
27.04	15	1308.92	897.87	714.15	4.382563	36.58	4.665

The results in Table 5-5 demonstrate an existence of drop in output power for engines with non-conventional arrangement by 19.2% than the simple cycle and by 16% lower than the conventional recuperative arrangement. Similarly and in the same sequence, recoverable waste heat fell by 47.9% and 40.7% respectively. In contrast however, there was a remarkable increase in thermal efficiency by 5.53% than the simple cycle and 2.77% than the conventional recuperated cycle. So, using the recuperator led to improving the engine's thermal efficiency in reduction of output power. This trend is significantly increased by using the non-conventional cycle arrangement.

5.1.3 Two-Spool Simple Cycle Aeroderivative Engines

In order to improve power output and better engine performance control at off-design, the two-spool engine arrangement has been proposed to produce larger aero-derivative engines for bigger plants and better initial cost. Adding another rotor with a new compressor and turbine improves pressure ratio, which seems to be the only way to increase turbine inlet temperature under the derivation conditions mentioned earlier

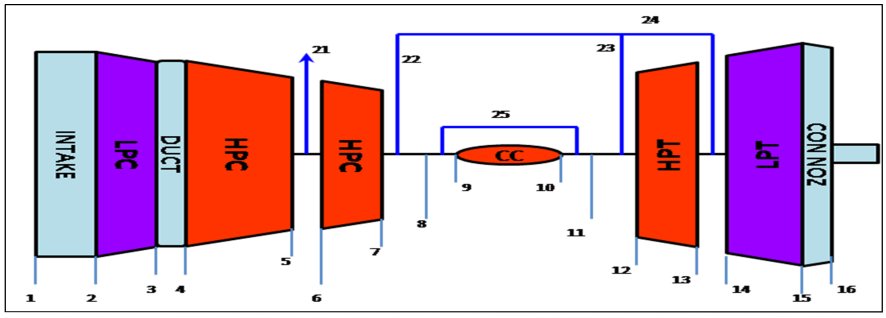

Figure 5-4 Two-Spool Simple Cycle Aeroderivative Engine

The design point calculation matches the calculation procedures previously taken in the single-spool simple cycle engine. However, some other calculations are needed in order to find the proper engine mass flow and turbine inlet temperature relative to component familiarity conditions. As it can be seen from the schematic structure in Figure 5-4, air properties at the inlet of the high pressure compressor are not ambient condition properties and match low pressure compressor outlet properties.

During the design point calculation under derivation conditions, the HP compressor's ambient conditions play a major role in maintaining as much as possible the commonality with the parent aero-engine HP components. Of course there exists a pressure drop resulting from the intake losses which needs to be taken into account. Referring to the stage numbering of the aero-engine in Figure 4-3 and the two spool simple cycle engine in Figure 5-4 and to maintain high pressure shaft components, the HP compressor non-dimensional mass flow and cycle maximum temperature ratio must be kept equal. Accordingly, design point conditions can be written as follows:

$$(W_4\sqrt{T_4}/P_4) = \left(W_6\sqrt{T_6}/P_6\right)_{aero}$$

$$(T_{10}/T_4) = (T_{12}/T_6)_{aero}$$

By keeping the equality and applying different LP compressors, HPC inlet pressure $P4$ will vary and result in different values of inlet mass flow $W4$ and combustor outlet temperature which both met the conditions. The design point calculation is taken in the following steps:

1. Assume LP compressor
2. Calculate$(P_3)\ from\ eq.$(5-6)

   $(P_4\ ) from\ eq$(5-12)

   $(T_3) from\ eq$(5-7)

   $and\ then\ T_4 = T_3$
3. Calculate $T_{10}\ \ for\ a\ given\ T_4\ using\ eq$(5-2)
4. Calculate $W_4\ \ from\ eq$ (5-1)

5. Repeat from step 1 for every given LPC value.

It can be noted in Figure 5-5 that a significant increase in turbine inlet temperature TET, under the aforementioned conditions with constant cycle temperature ratio (T_{10}/T_4), is gained due to the increased cycle overall pressure ratio resulted from increasing the LP compressor pressure ratio. Also, as point 4 moves up to the higher constant pressure line, point 10 also moves up with significant shifting to the left side resulting in an increase in turbine work and decrease in combustor heat input. An Excel spread sheet as shown in appendix [A.2] has been used to conduct all the calculations in order to find the correct values of compressor inlet mass flow W_4 and combustor outlet temperature T_{10}, hence turbine inlet temperatures which satisfy the conditions for every given value of LP compressor pressure ratio in the range of $LPC = 1.2 \ to \ 7.0$.

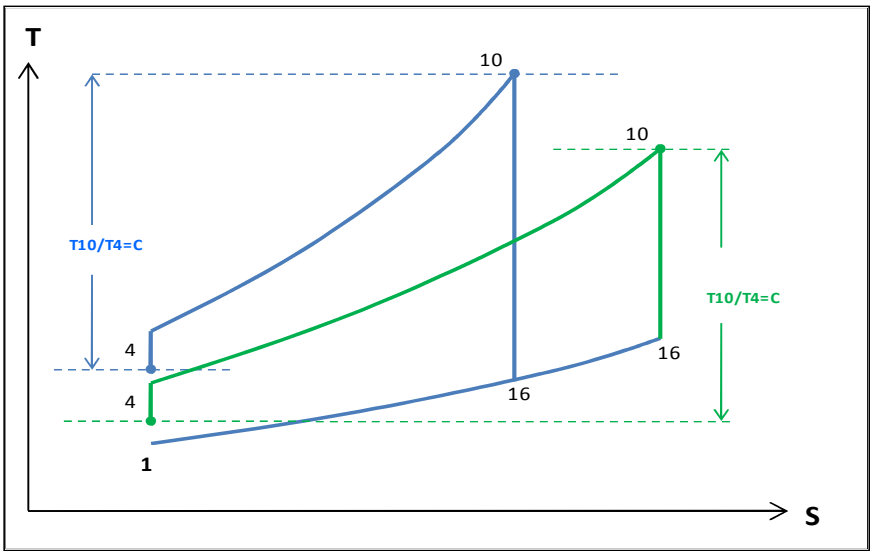

Figure 5-5 Two-spool 2Shaft Cycle on T-S Diagram at DP

Results concluded from the Excel calculations are plotted in Figure 5-6, which represent values of mass flow and combustor outlet temperature relative to given LP compressor pressure ratios that satisfy the design point conditions. It can be observed that conditional mass flow and combustor outlet temperature have significantly increased with the increase in cycle overall pressure ratio through applying higher LP compressor pressure ratio.

Turbomatch has been used in creating a performance model (see appendix E.1.3) for completing proposed design point calculations and predicting engine performance characteristics such as output power, efficiencies and heat output. Results from the calculation are presented in Figure 5-7.

It is obvious that by applying the conditions of maintaining values of high pressure cycle temperature ratio and non-dimensional mass flow, there will be a possibility of designing one engine for every value of combustor outlet temperature COT. That limits the opportunity to design an engine of high pressure ratio and applicable turbine inlet temperature. Based on LP pressure ratio values taken, Charts 1 and 2 in the same figure show the associated values of overall pressure ratio OPR and combustor outlet temperature COT. Considering the assumption of the current state of the art applicable technology of $COT = 1800\, k°$, Charts 2, 4 and 5 clarify that the maximum achievable efficiency is 44.4% of providing output power and exhaust heat of 28.0MW and 29.0MW respectively.

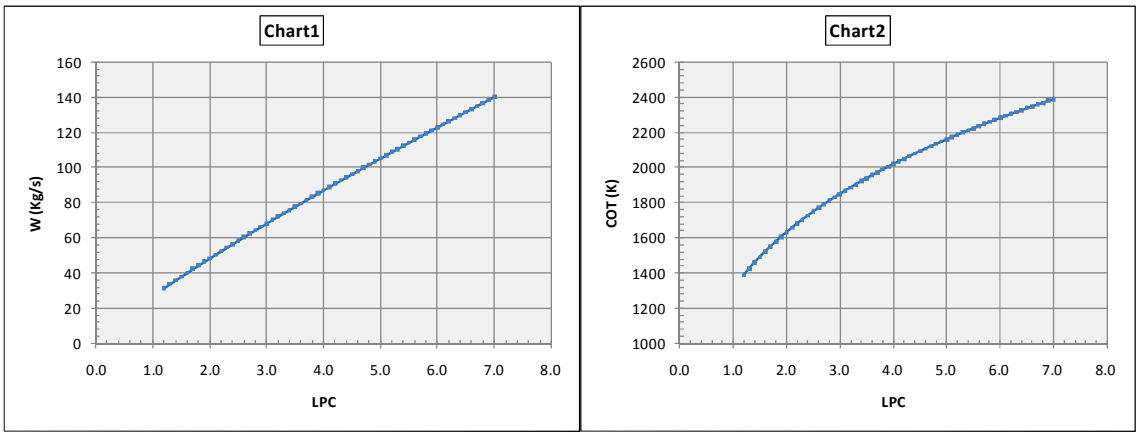

Figure 5-6 Calculated Mass flow and COT values for Two-spool Simple Cycle

To clarify the situation observed in Chart 2, it seems unusual as increasing turbine inlet temperature always causes an increase in cycle thermal efficiency. In simple cycle at the design point with the increasing COT at constant OPR, thermal efficiency increases up to a certain point where any further increase results in falling of thermal efficiency because of the extreme bleed flow required for cooling the hot section. The case in Chart 2 indicates that the

increase in COT always leads to a rise in thermal efficiency; it is only because both combustor outlet temperature and overall pressure ratio are increasing simultaneously. It happens as a result of constant temperature ratio alongside different PR which are imposed in the design point conditions.

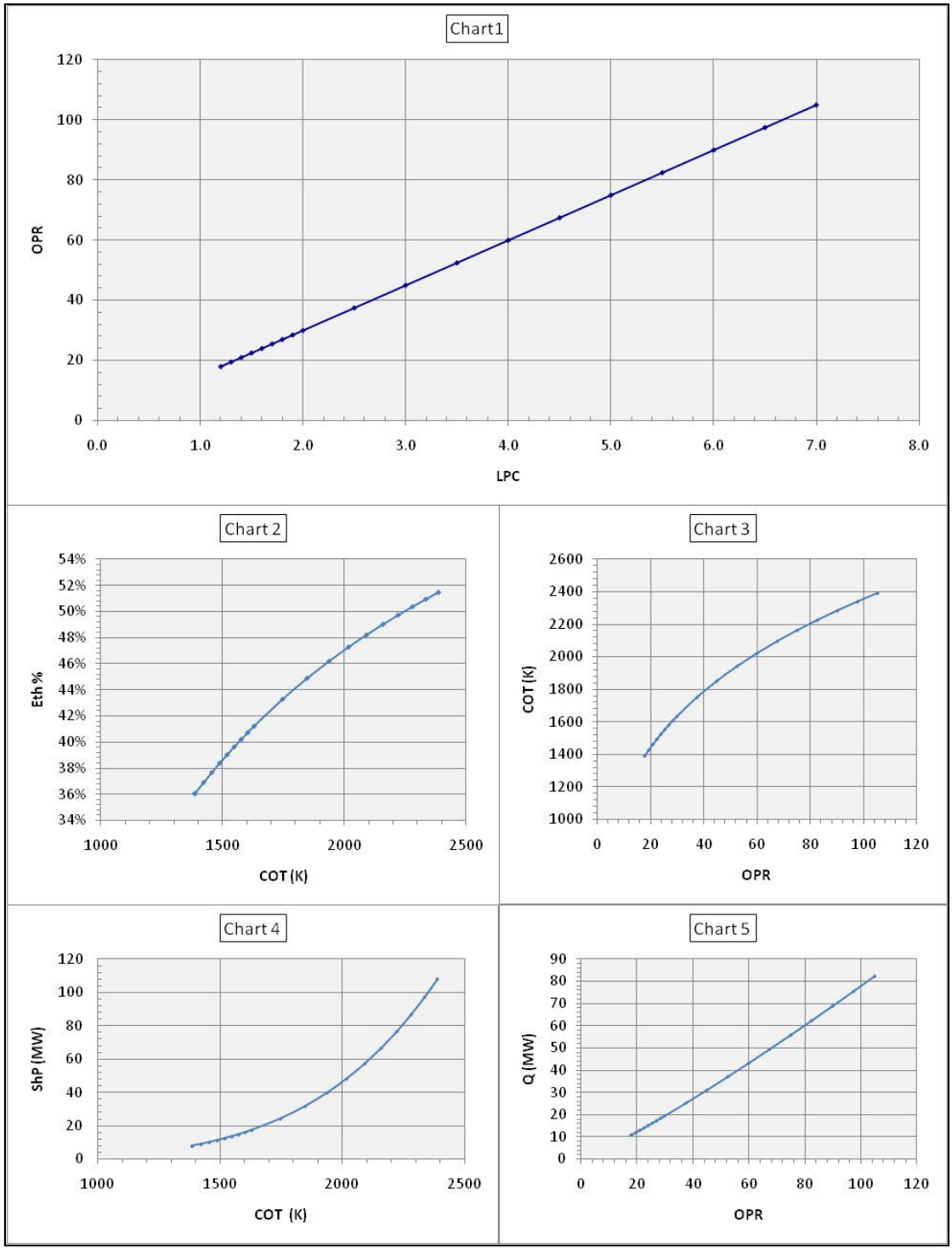

Figure 5-7 Two-Spool Simple Cycle Engines Design Point Characteristics

5.1.4 Two-Spool Intercooled Cycle Aeroderivative Engines

Dividing compression work into two stages and cooling the discharge air exits from the first compressor reduces compression work. Furthermore, inter-cooling results in reducing temperature of the air bleed required to cool turbine bleeds, hence improving the ability to increase TET [95][81]. According to stage numbering in Figure 5-8 and Figure 4-3, the same values of high pressure cycle temperature ratios and non-dimensional mass flow must remain constant for familiarity purposes. Values of combustor outlet temperature have to be calculated relative to intercooler outlet temperature T_4 by applying conditions mentioned in two-spool simple cycle engines. Resulting COT relative to values of T_4 is shown in Figure 5-10, Chart 3.

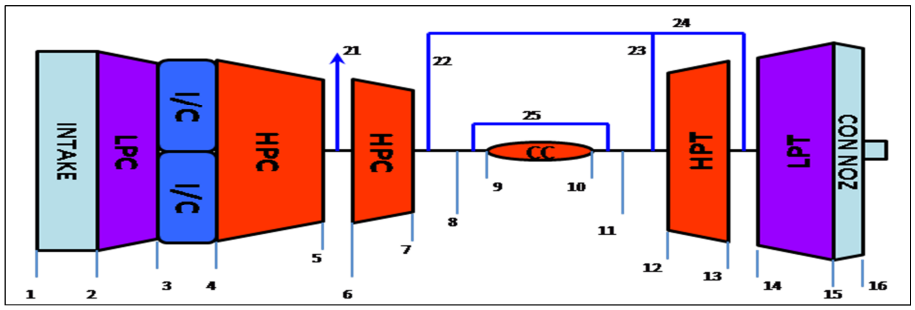

Figure 5-8 Two Spool Intercooled Aeroderivative Engine

Figure 5-9 shows how the ideal cycle process behaves when low pressure compressor PR increases or decreases. Increasing pressure ratio of low pressure compressor at constant temperature ratio ($\frac{T_{10}}{T_4}$) causes that the top part (High Pressure part) of the cycle to move towards the left side for every given value of T_{10}. As a result, point 7 on the cycle moves to a higher isobar line and makes point 16 shifts towards lower temperature value at constant pressure resulting in a significant increase in turbine work. Furthermore, using inter-cooling between the compressors allows the ability to overcome the restrictions previously applied on the simple cycle where there will be only one value of COT for every value of LPC pressure ratio which meet derivation conditions. Cycle optimisation became possible and intercooler optimum pressure can be found by varying low pressure compressor PR for a given value of COT alongside with

controlling T_4 to apply the derivation conditions. Excel (see appendix A3) was used in the calculation to find values of mass flow $W4$ relative to LPC pressure ratio at different given values of COT, and it was conducted according to the following steps:

1. Assume intercooler outlet temperature T_4
2. Calculate T_{10} using equation (5-2).
3. Assume Low Pressure Compressor pressure ratio value (PR_{lc})
4. Calculate W_4 using equation (5-1).
5. Repeat from step 3 to calculate different values of W_4 for a given COT
6. Go to step 1 and repeat from step 1 to step 6

By means of this calculation all values of W_4 and PR_{lc} for every given T_4, hence COT will be found. A performance model was created (see appendix E.1.5) and Excel results were fed into the model. Design point parameters were calculated and all performance characteristics found are shown in Figure 5-10, Figure 5-11, and Figure 5-12.

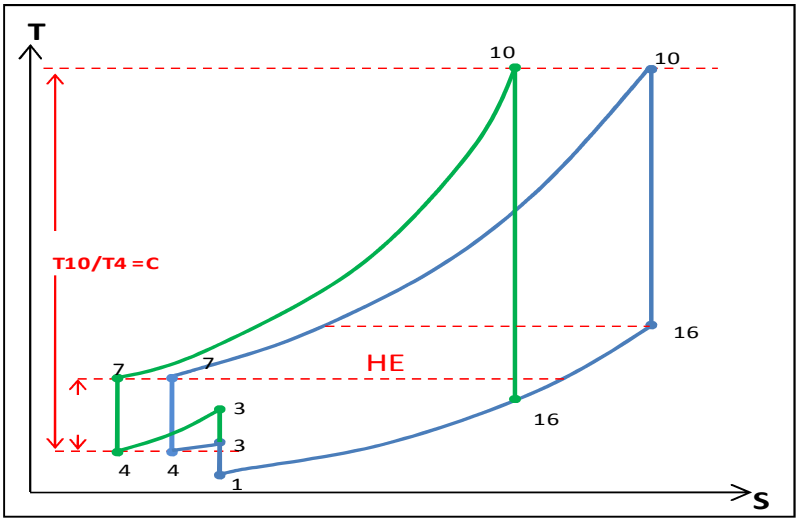

Figure 5-9 Two-spool I/C Cycle on $T-S$ Diagram at DP

Chart 4 in Figure 5-10 represents how the overall pressure ratio can be improved due to either the improvement in the LP compressor stage's pressure ratio (polytrophic efficiency), or increasing stages number contained. Charts 2

and 4 in Figure 5-11 and Figure 5-12 represent performance characteristics which express the effect of varying overall pressure ratio and combustor outlet temperature on performance behaviour of two-spool inter-cooled aeroderivative engines. All possible opportunities of designing inter-cooled derivative engines from the parent aero-engine are investigated by conducting a feasibility study in the ranges of $(T_4 = 300\ to\ 455\ K^o)$ and $(up\ to\ 145.5\ of\ OPR)$ at the design point.

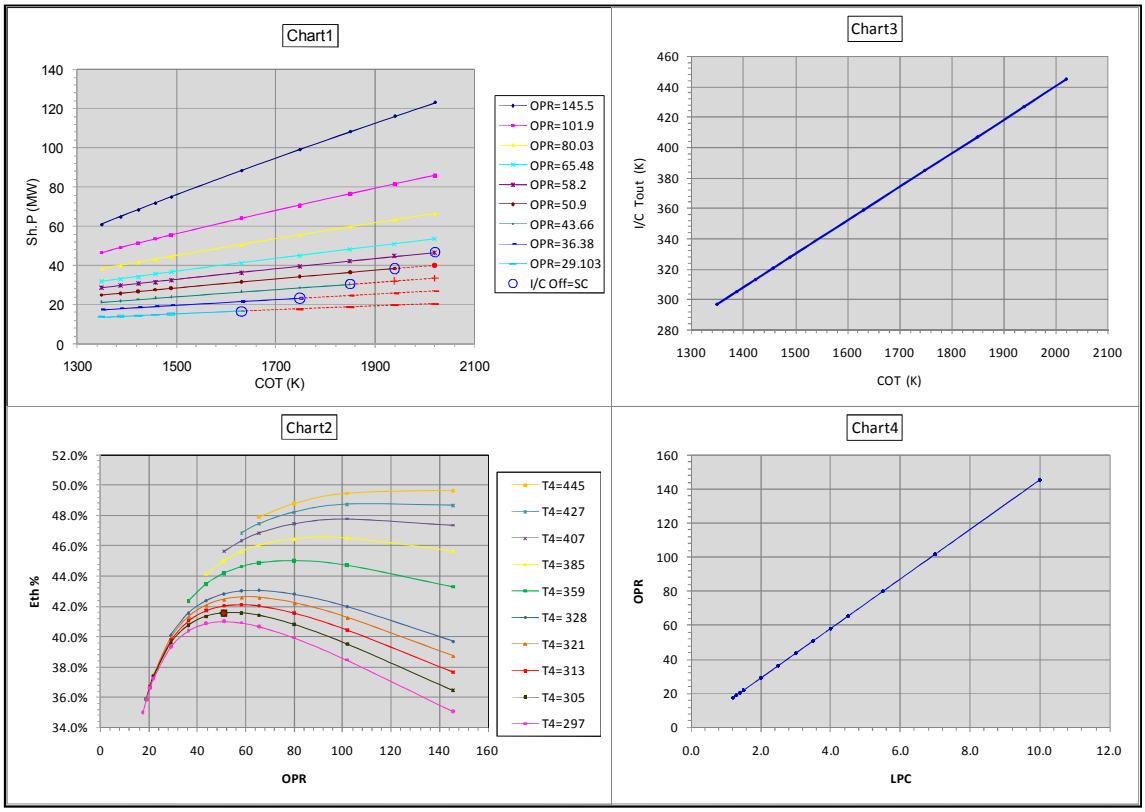

Figure 5-10 Two-Spool Intercooled cycle Engine Design Point Characteristics

In general for a given COT the increase in the engine's OPR leads to increase cycle thermal efficiency ζ_{th} and improves SFC, as shown in Figure 5-11 and Figure 5-12. However, it is obvious from Chart 2 in Figure 5-10 that there is always an optimum value of OPR which achieves the optimum performance characteristic regarding maximum thermal efficiency for a given value of COT. Therefore, this proves the necessity of performing cycle optimisation presented in [95]. Circles on the charts reflect the limitations where the inter-cooler is not applicable for any values of OPR equal or lower than at

these circles where ($T_4 <= T3$) and simple cycle concept would be applied. Because T_4 and $T3$ are limited by the condition of high pressure cycle temperature ratio.

A significant increase in thermal efficiency and output power gained due to the remarkable increase in operating temperature as well as the overall pressure ratio which can be noticed in Figure 5-10 and Figure 5-11. The lower the overall pressure ratio achieved the lower combustor outlet temperature can be applied on the designed engines in this thermodynamic configuration. For instance, an engine with $OPR = 29.1$ cannot be designed with ($COT > 1630.726\ K^o$) for a $T_4 > 359\ K^o$ due to temperature ratio limitations.

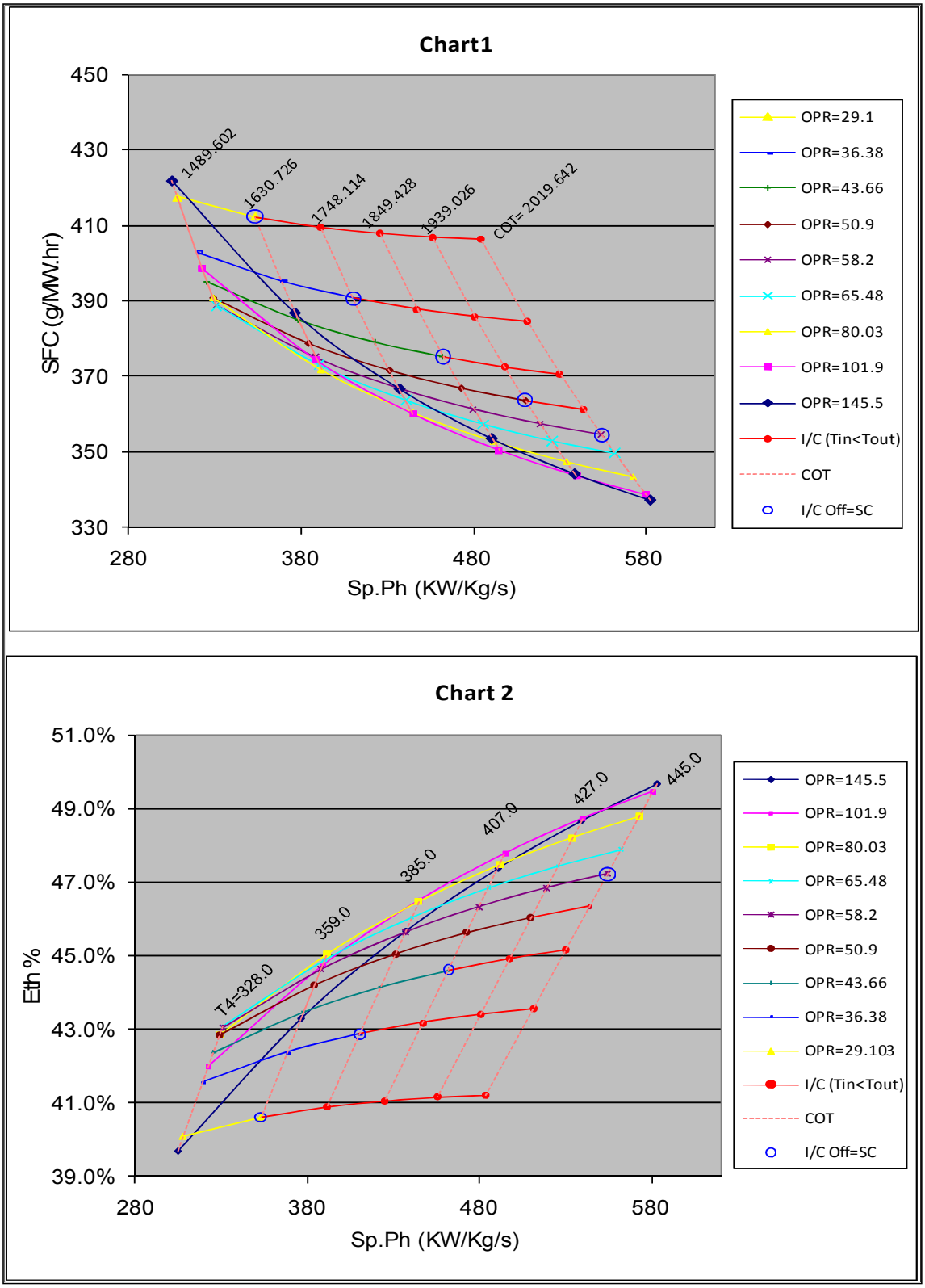

Figure 5-11 Two-Spool Inter-cooled Cycle Design Efficiency and Specific Power (1)

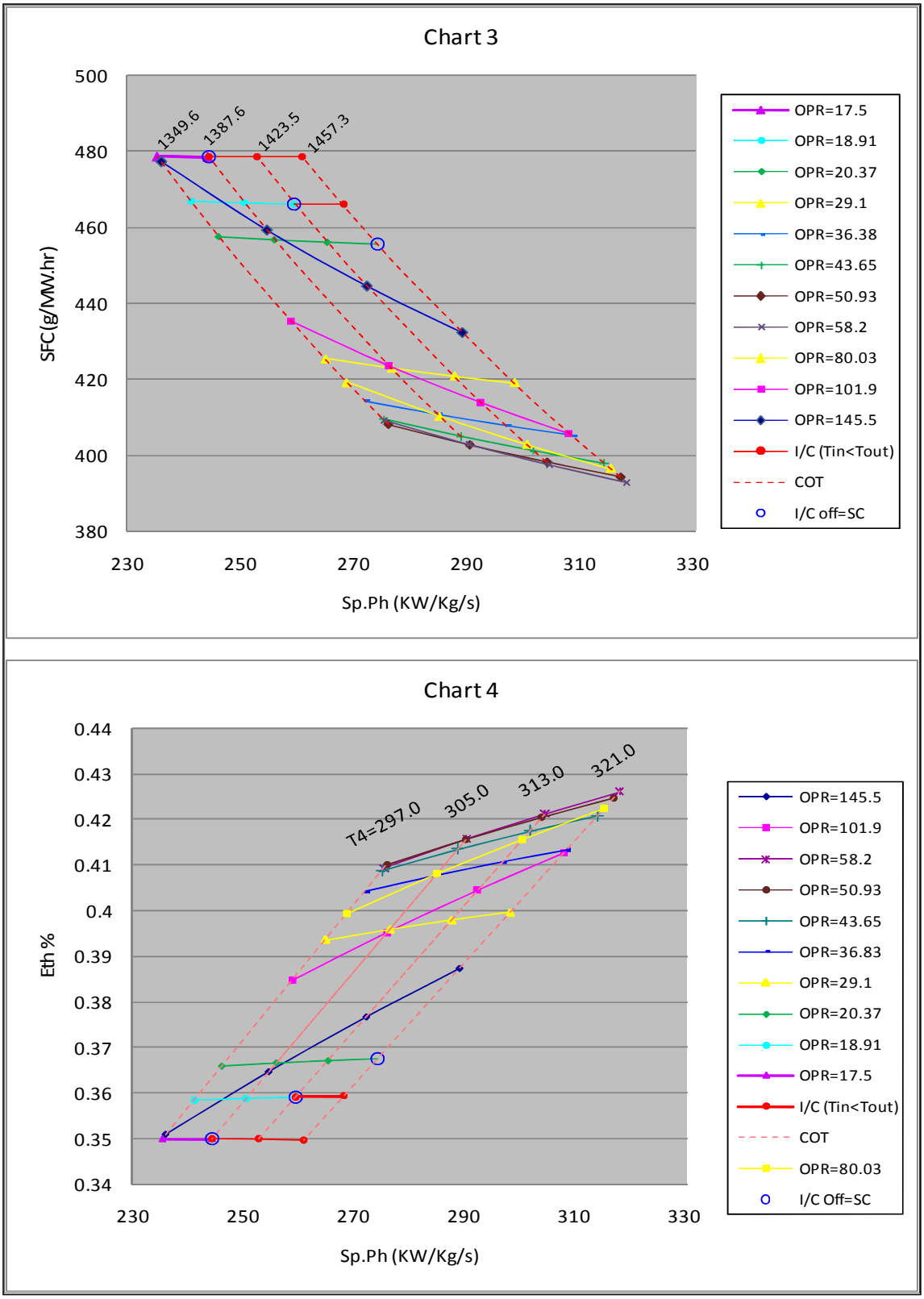

Figure 5-12 Two-Spool Inter-cooled Cycle Design Efficiency and Specific Power (2)

5.1.5 Two-Spool Heat Exchanger Cycle Aeroderivative Engines

As mentioned earlier in the literature review, there are two ways to configure a gas turbine with a heat exchanger in the cycle; either by locating the heat exchanger between turbines in two-shaft arrangement, where more concern has to be given to the thermal barriers of the heat exchanger materials, or by installing it at the engine exhaust which is more commonly used.

5.1.5.1 Two-Spool Conventional HEx Configuration Engines

The conventional arrangement (as shown in the schematic draw in Figure 5-13) is subject to the concept of imposing the heat exchanger at the engine exhaust. It is commonly known that two-spool engine arrangements can be either in the form of two-spool direct drive, where the load driven by the LP shaft, or as two-spool three-shaft where a free power turbine drives the load.

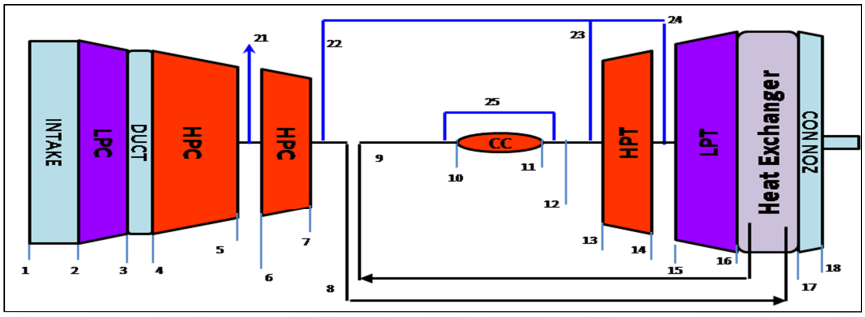

Figure 5-13 Two-Spool Heat Exchanger Aeroderivative Engine

It is clearly seen that the design point calculation will follow the same procedures as taken in the two-shaft simple cycle, except for the additional calculations dealing with the heat exchanger component. Figure 5-14 shows how cycle processes behave when PR_{lc} is increased or decreased. The condition of applying heat exchanger technology on a simple cycle is to always keep the heat exchanger inlet temperature higher than the compression system discharge temperature ($T_{16} > T_7$). Increasing the low pressure compressor pressure ratio PR_{lc} leads to shifting point 7 up and point 16 down as a result of temperature ratio (T_{10}/T_4) condition. This movement will reduce the margin of exchanging heat between the hot and cold side of the heat exchanger.

Moreover, when both points 7 and 16 level off the engine will match the behaviour of simple cycle configuration (with pressure losses because of the heat exchanger component) and no further improvements in efficiency can be achieved. In addition, by moving point 10 further up and shifting it towards the left side more turbine work will be extracted leading to further improvement in thermal efficiency. However, more concern should be given to points 16 and 7 and the increase in PR_{lc} has to be limited by the condition ($T_{16} > T_7$).

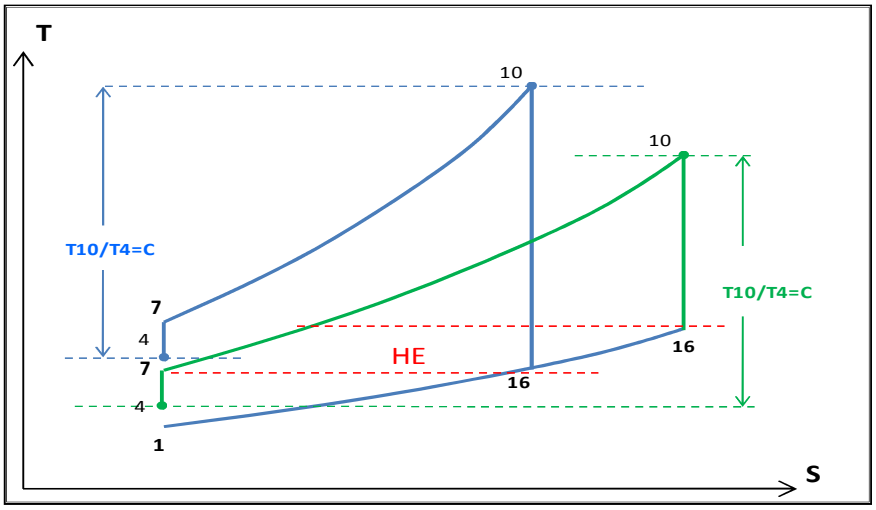

Figure 5-14 Two-spool HEx Cycle on $T-S$ Diagram at DP

The performance input file is made using Turbomatch (see appendix E.1.10) in order to investigate the feasibility study of possibly designed derivatives with a heat exchanger cycle. All design point parameters such as PR_{lc}, W_2 and COT were imported from two-shaft simple cycle Excel sheets (see appendix A.2) and fed to the model, and the results are expressed in Figure 5-15. Considering the schematic draw in Figure 5-13, Charts 1 and 2 in Figure 5-15 show values of PR_{lc} and T_{11} which have negative effect on derivation condition of ($T_{16} > T_7$). It can be seen that the biggest sized engine that can be designed with the conventional recuperative cycle is with ($PR_{lc} = 1.3$), which provides $OPR = 19.5$ and $COT = 1423.5\ K^o$. Furthermore, it is clear from Charts 5 and 6 that the maximum efficiency and power output that can be achieved at design point are 36.2% and 8.75 MW, respectively.

The feasibility study concluded that it is the cycle high pressure temperature ratio condition T_{10}/T_4 which limits the opportunity of designing a derivative engine for higher values of overall pressure ratios OPR. On other words, in order to design the derivative engine with higher LP compressor pressure ratio and keeping ($T_{16} > T_7$), combustor outlet temperature must exceed those values which match the derivation conditions. The drawback observed from these results is that the ability of applying the conventional recuperation concept completely depends on the values of cycle OPR. Also, the higher OPR the higher compressor exit temperature which leads to a lower temperature difference between exhaust gas temperature and compressed air entering the combustor. As a result of that the benefit obtained from the recuperation became too small and this conclusion was proved by June Kee Min [76].

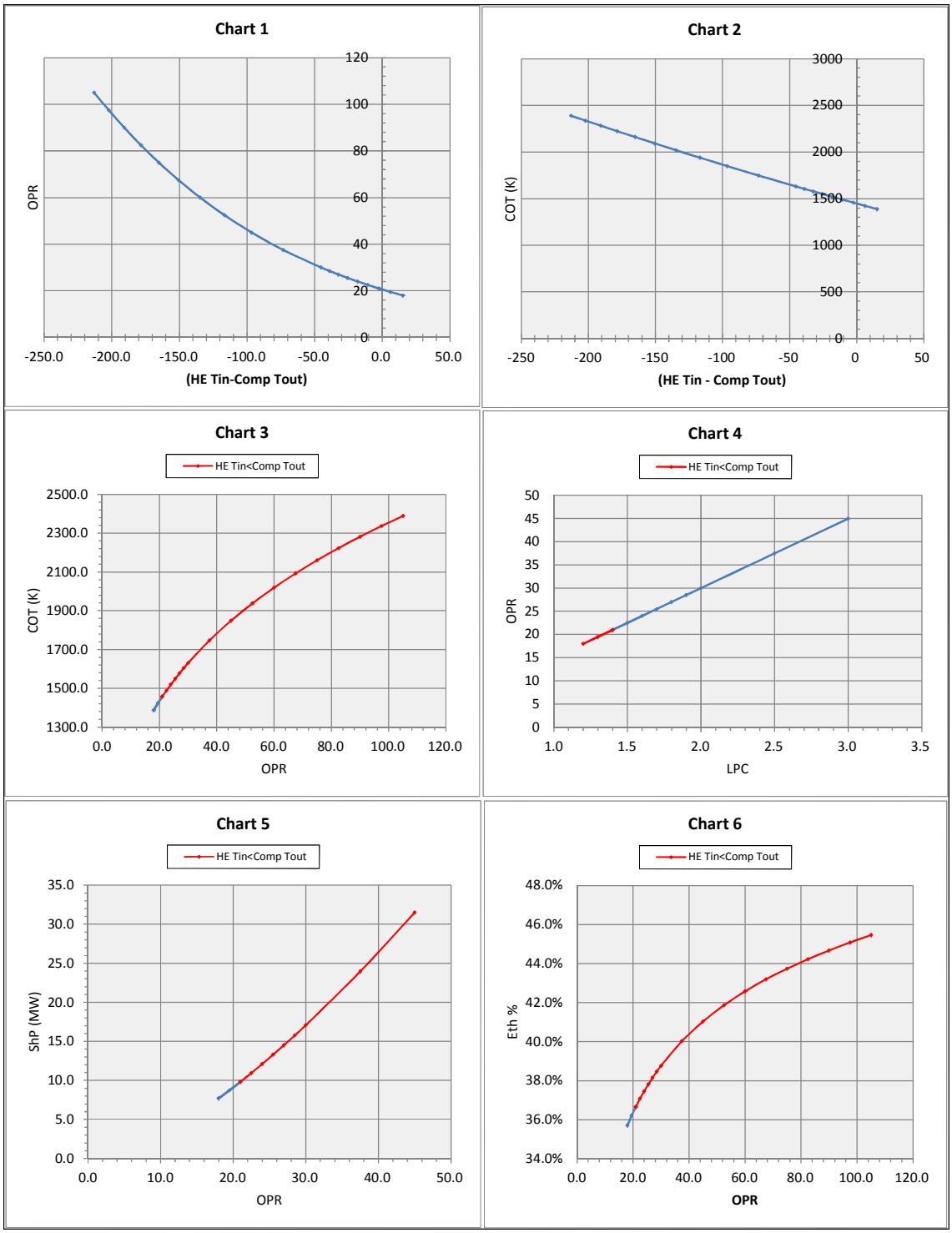

Figure 5-15 Two-Spool Heat Exchanger Cycle Engine Design Point Characteristics

5.1.5.2 Two-Spool non-Conventional HEx Configuration Engines

Installing the heat exchanger between turbines offers a chance of rising heat exchanger inlet temperatures and increasing its temperature difference with the compression discharge temperature which enters the combustor. There are two configurations which need to be investigated and finding which configuration enhances the performance of recuperated derivative engines. This depends on whether free power turbine technology is used or direct drive methods where the load is driven by the LP shaft. Both configurations are considered in detail in the following sections.

5.1.5.2.1 Two-Spool non-Conventional HEx Cycle Engine IPT

Direct drive configuration represents the derivative engine when the heat exchanger is located between HP and LP turbines, and air temperature enters the recuperator is the temperature of air exiting the HP turbine, as described in Figure 5-16.

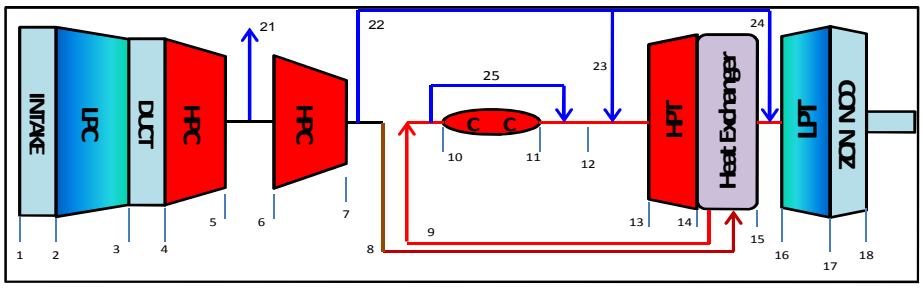

Figure 5-16 Configuration of Two-Spool non-Conventional Regenerative Cycle IPT

Both derivation conditions of mass flow and temperature ratio applied in the two-spool simple cycle are applied here, alongside the heat exchanger condition. Considering the stage numbering in Figure 5-16, the condition can be written as $(T_{14} > T_7)$. Using the performance model (see appendix E.1.11) the design point calculation is conducted and the results presented in Figure 5-17 and Figure 5-18. It can be observed from Chart 1 and 2 in Figure 5-17 that dividing the expansion into two intervals with recuperation between them offers far better recuperation temperature differences and improves recuperation effect on cycle performance. It always provides positive temperature differences

of $(T_{14} > T_7)$ on a wide range of engine overall pressure ratios. In addition, considering heat exchanger material thermal barriers, LPC in the range of 1.2 to 3.4 provides reasonable values of heat exchanger inlet temperature which, according to the literature, can be applicable.

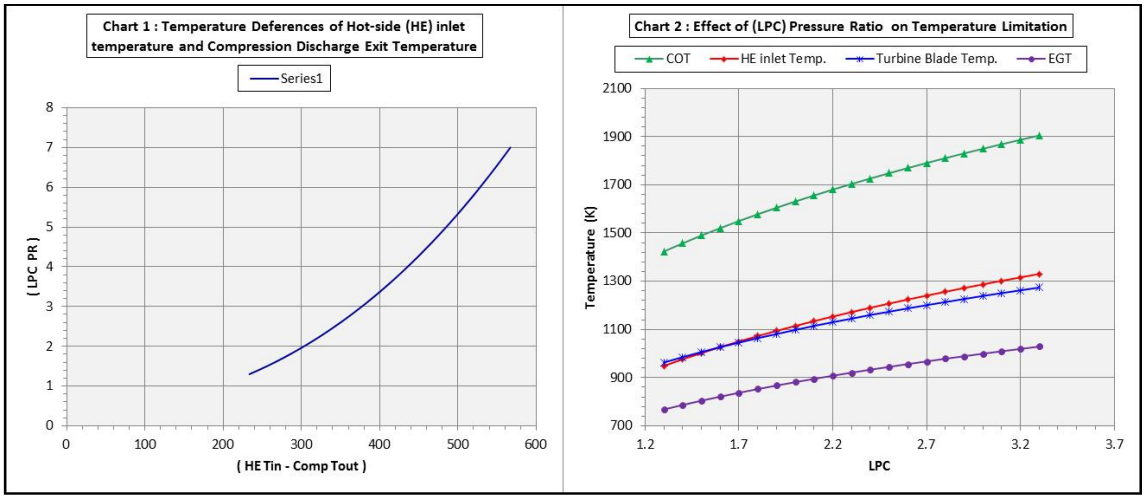

Figure 5-17 Non-Conventional Recuperated LPC Effect on Cycle Temperatures and Recuperation Temperature Differences at Design Point IPT

The overall design point performance characteristics are represented in Figure 5-18. Charts 1 and 2 express how the cycle overall pressure ratio and combustor outlet temperature as well as turbine inlet temperature are influenced by varying the LPC pressure ratio. Also, high pressure turbine blade life estimation at different design points, as shown in Charts 3 and 4, was included in the calculation in the range of $LPC = 2.3\ to\ 2.5$, and found to provide logical values of time to failure. Because of the derivation conditions of cycle temperature ratios which provide one value of COT to each LPC pressure ratio, increasing cycle pressure ratio always improves cycle thermal efficiency as indicated in Chart 5 in Figure 5-18. Also, shaft output power and exhaust heat output is increased with the increase in low pressure compressor pressure ratio and combustor outlet temperature.

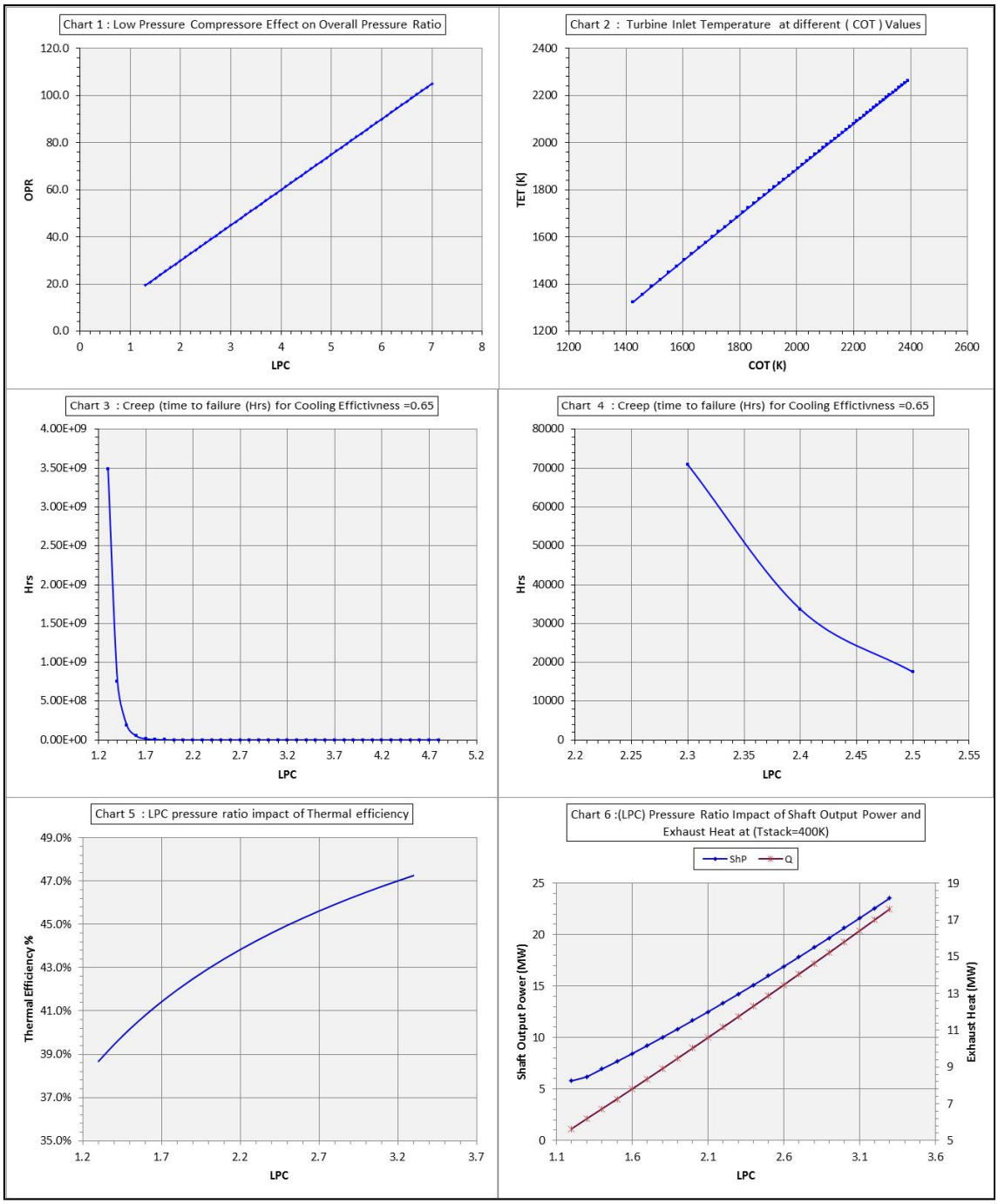

Figure 5-18 Design Point Characteristics for non-Conventional Recuperated Cycle Aero-derivatives with IPT Configuration

5.1.5.2.2 Two-Spool non-Conventional HEx Cycle Engine FPT

The configuration draw which is represented in Figure 5-19 explores how a free power turbine can be aerodynamically coupled to a gas generator with a heat exchanger at the exhaust. It shows that heat is recovered in the

recuperator after full expansion in high and low pressure turbines. In this case, bleed effect at points 23 and 24 takes place before the heat recovery process started. So, it is expected to have a slightly negative impact on heat exchanger performance than in Direct Load Drive configuration as shown in Figure 5-16.

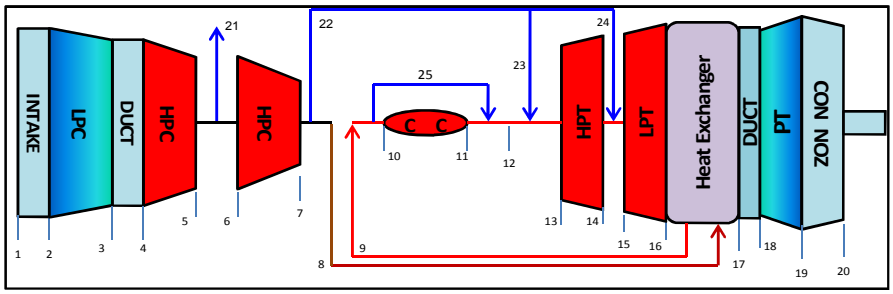

Figure 5-19 Configuration of Two-Spool non-Conventional Regenerative Cycle Engine with FPT Configuration

Following the same calculation process taken in the previous section, the condition of using a heat exchanger in this configuration can be written in the following format ($T_{16} > T_7$). The condition is applied in all calculated design points which have the same mass flow rate and associated low pressure compressor pressure ratio as in the previous section. The performance model used in the direct load drive configuration is modified to suit the recuperated cycle with free power turbine (see appendix E.1.11). Calculation results are included in Figure 5-20 and Figure 5-21.

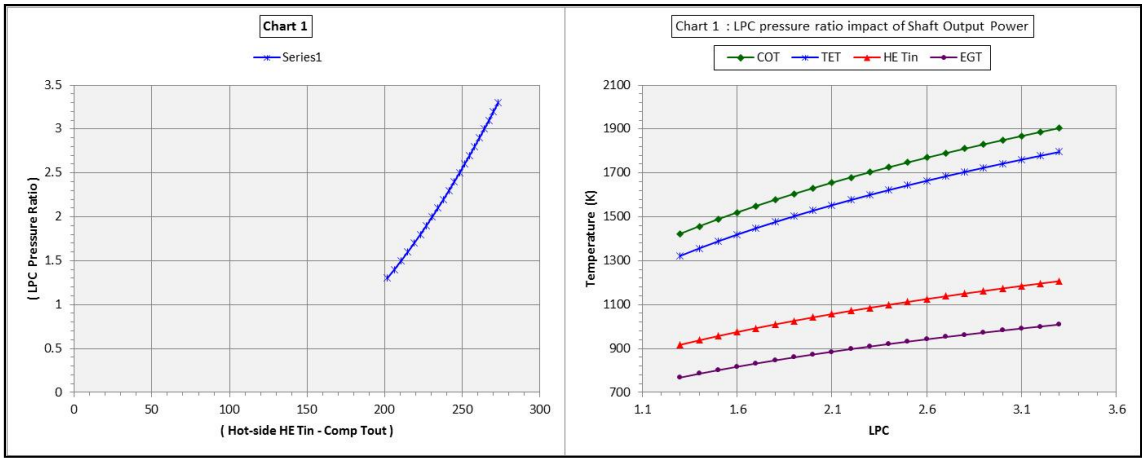

Figure 5-20 Design LPC Effect on Cycle Temperatures and Recuperation Temperature Differences of Non-Conventional Recuperated Engines with FPT

It is obvious that inlet temperature at the hot-side of the heat exchanger will be lower by using the free power turbine configuration, as shown in Chart 1 in Figure 5-20.

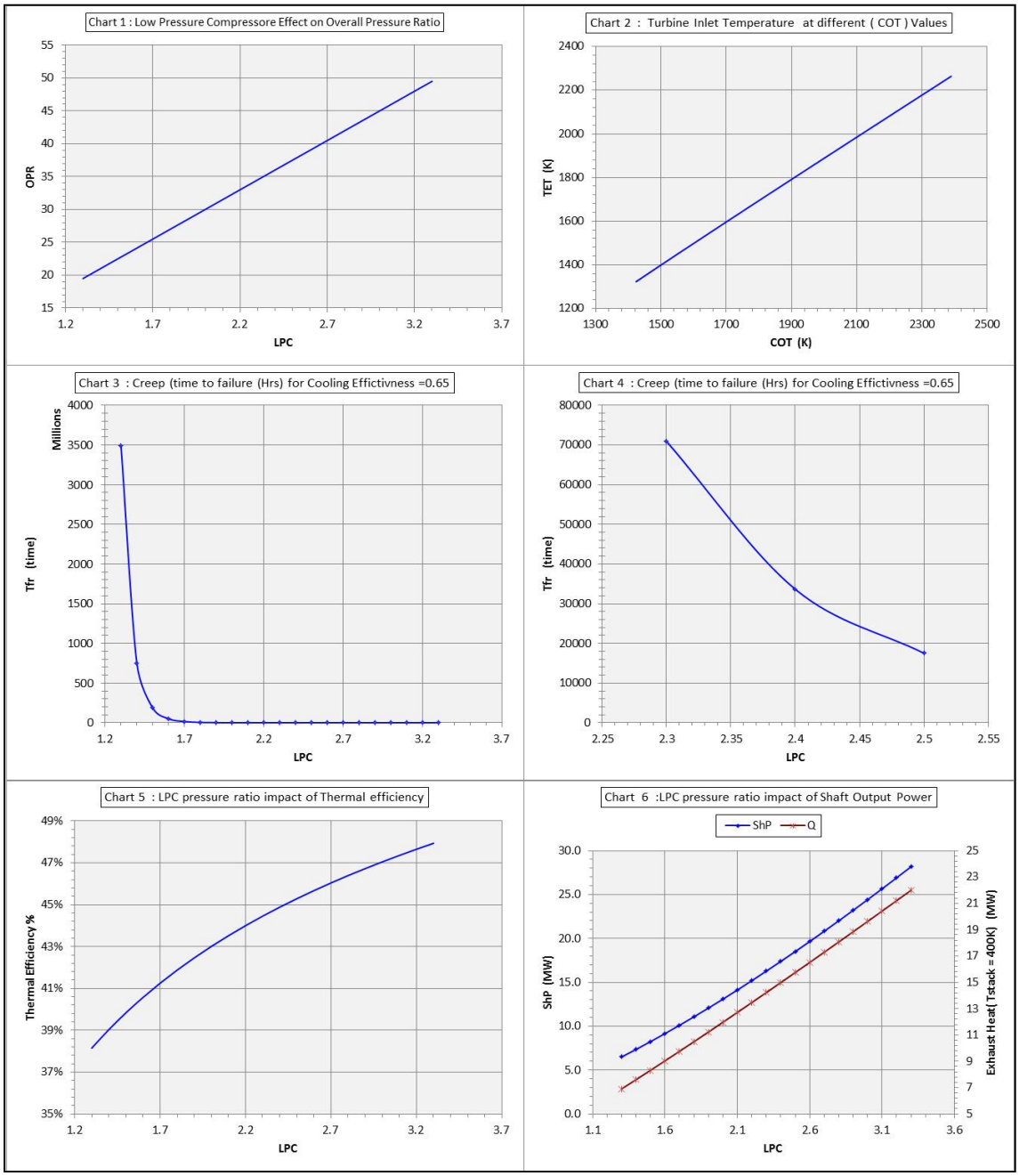

Figure 5-21 Design Point Characteristics for non-Conventional Recuperated Cycle Aero-derivatives Engine with FPT Configuration

Low pressure compressor has the same effect on engine overall pressure ratio and COT, as seen in Figure 5-21. Also, there is no difference to HPT blade life by using FPT. Shaft power and thermal efficiency are always enhanced and

increased by increasing LPC pressure ratio as in Direct Load Driving configuration.

All the calculation results indicated in Figure 5-15, Figure 5-18 and Figure 5-21 demonstrate that applying the recuperation on the two-spool cycle, in conventional and non-conventional configuration, will have the same identical impact trend as the single-spool cycle on engine performance. Non-conventional recuperation on two-spool cycle with FPT promises better engine shaft power and thermal efficiency than on direct load driving. Also, it provides better thermal efficiency than the conventional recuperation regardless of losing in the shaft output power.

5.1.6 Two-Spool Intercooled Recuperated Aeroderivative Engines

It was recognised in previous sections that applying recuperation technology helps in enhancing cycle thermal efficiency especially at low pressure ratio engines (small-sized engines). In addition, despite the fact that applying inter-cooling technology on the simple cycle improved cycle thermodynamic performance at high COT in large-sized engines, it suffers a reduction in thermal efficiency at low values of engine's overall pressure ratio OPR. Therefore, the aim in this section is to investigate the ability of further enhancing simple cycle thermodynamic performance by applying both technologies simultaneously, especially at low values of OPR.

5.1.6.1 Two-Spool Conventional ICR Cycle Configuration Engine

It is clear from previous calculations that the largest engine that can be designed with a conventional recuperated cycle is an engine with ($PR_{lc} = 1.3$) and limited to ($COT = 1423.5\ K^o$). However, it was possible to vary PR_{lc} by adding an inter-cooler between the compressors in a two-shaft simple cycle and it allowed increasing it to slightly higher values for each given amount of COT. Using the inter-cooler increased power output and adding a heat exchanger on the cycle should improve thermal efficiency [52]. The new configuration of adding inter-cooling and recuperation simultaneously to the cycle has been

chosen to be applied in this section. Inter-cooler recuperated cycle technology is already well known, especially in marine application [52].

Although more component losses are applied by adding the inter-cooler and heat exchanger to the cycle, significant improvements in both thermal efficiency and power output are achieved [34]. Considering Figure 5-22, the temperature ratio of the high pressure part of the cycle (T_{11}/T_4) and non-dimensional mass flow $(W_4\sqrt{T_4}/P_4 = \left(W\sqrt{T}/P\right)_{aero})$ still have to be maintained equal to the parent aircraft engine at the design point. Using this equation, mass flow will vary with the change in (PR_{lc}) for every given value of T_4 , $hence\ COT$.

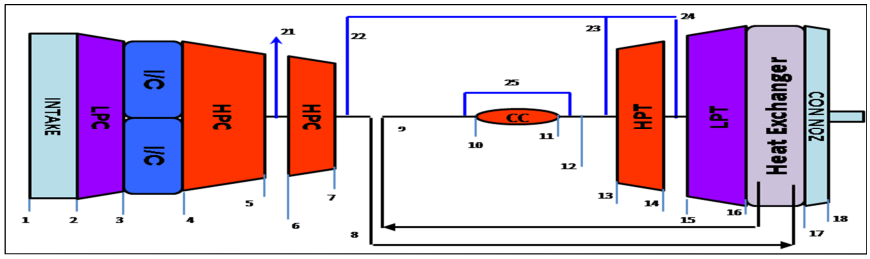

Figure 5-22 Two-Spool Inter-cooled Recuperated Engine

Figure 5-23 illustrates how inter-cooled recuperated cycle processes behave on a T-S diagram with the variation in low pressure compressor pressure ratio. PR_{lc}. More restrictions are applied in order to benefit from the advantages of using inter-cooler and recuperator, by maintaining some temperature differences higher than zero as follows.

$$(T_{16} - T_7) > 0.0\,, \qquad (T_3 - T_4) > 0.0$$

In general, the higher temperature difference the better performance can be gained. However, as was seen earlier, the demand of higher shaft power or best thermal efficiency will be dependent on the kind of recuperation location and engine configuration.

Mass flow rate is calculated at every value of PR_{lc} and for a given COT. This calculation is similar to that performed for the inter-cooled cycle using Excel spread sheets and results can be seen in appendixE.1.12 [A.3]. Input

data file performance model has been created using the Turbomatch code as see appendix [E.1.12].

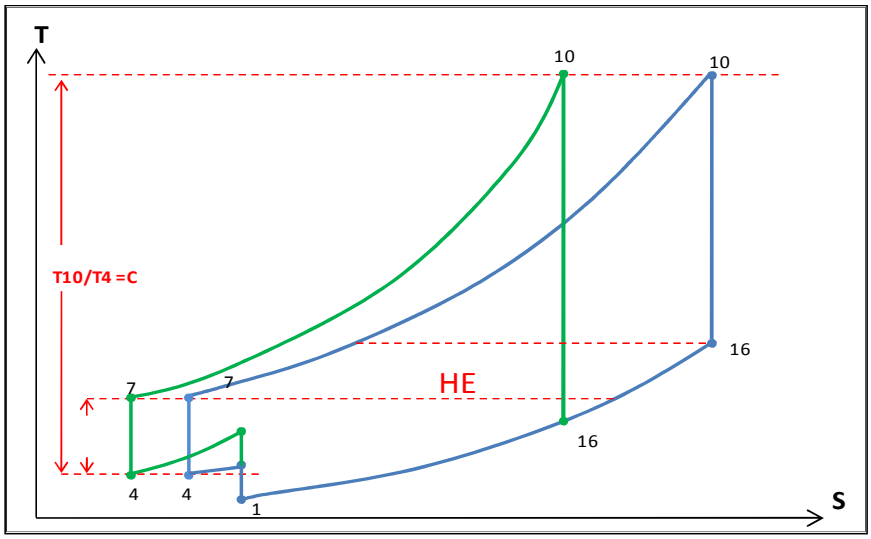

Figure 5-23 Two-spool ICR Engine Cycle on T-S Diagram at DP

Calculated values of mass flow rate for different PR_{lc} and a given COT are used in performing engine design point calculations. The effect of varying low pressure compressor pressure ratio on temperature variations for inter-cooling and recuperation process is described in Figure 5-24 at different values of COT. It can be seen from Chart 1 that increasing LPC in general leads to increasing inter-cooling temperature difference. Rising inter-cooler outlet temperature, subject to derivation cycle temperature ratio conditions, negatively affects inter-cooling temperature difference. As T_4 increased, inter-cooling temperature difference decreased and curves on the chart tend to shift to the negative region regarding temperature difference, which causes a negative effect on cycle performance. On the other hand in Chart 2, increasing inter-cooler outlet temperature under the same conditions has a positive effect on temperature differences between the hot side heat exchanger inlet temperature and compressor discharge temperature. This difference tends to increase with the increase in T_4 for a given PR_{lc} and curves on the chart move towards the region of positive temperature defence.

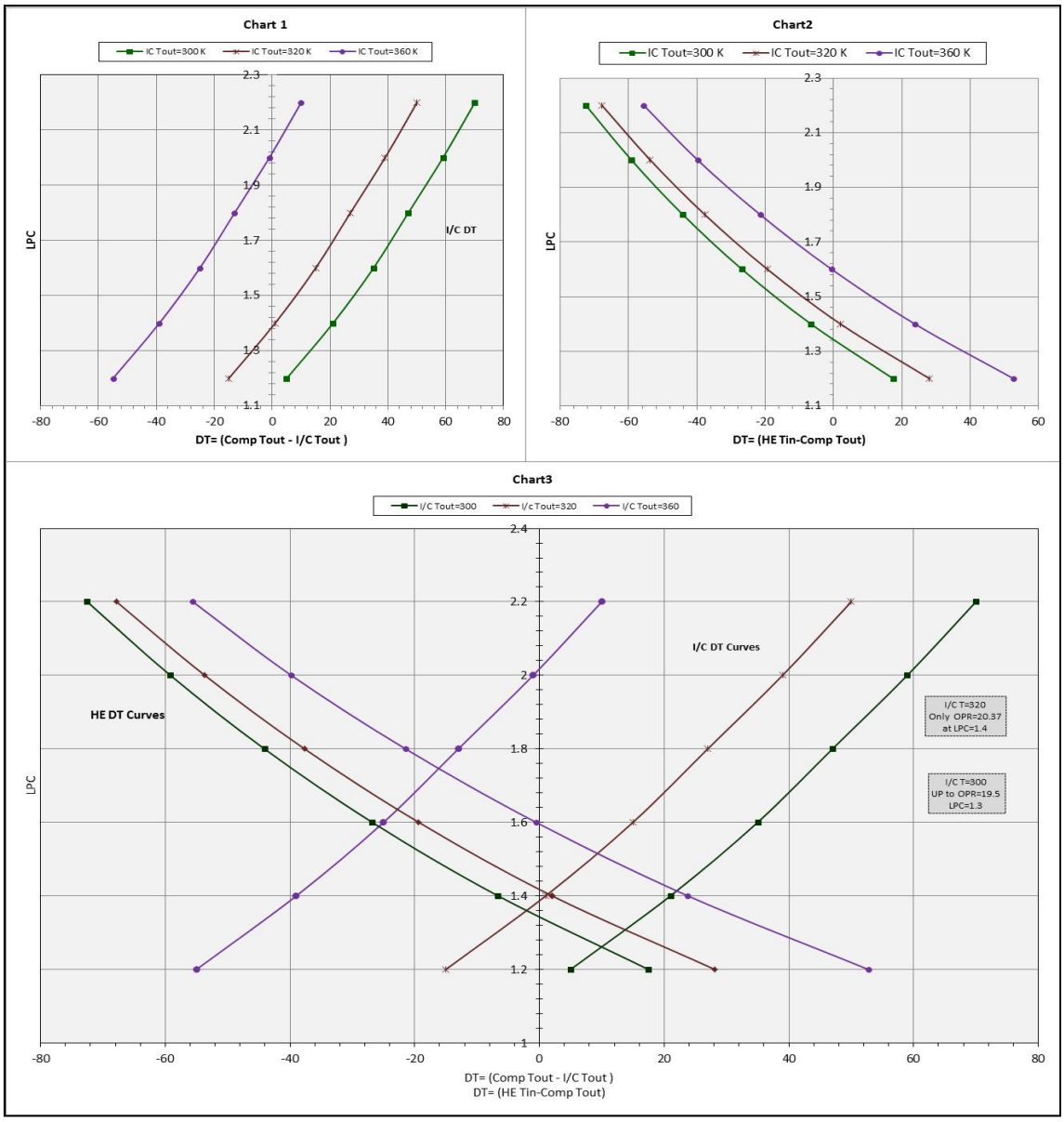

Figure 5-24 LPC Effect on Inter-cooling and Recuperation Temperature Differences for Two-Spool Conventional ICR Aeroderivative Engine

Therefore, a compromise is needed in this case and both groups of inter-cooling and recuperation differences have been plotted on Chart 3. The chart represents values of temperature differences between heat exchanger inlet temperature and high pressure compressor discharge temperature $(T_{16} - T_7)$ combined with values of intercooler temperature differences $(T_3 - T_4)$. While the vertical axis shows values of low pressure compressor pressure ratio LPC . It can be noticed that there exist only few points of LPC pressure ratio which will have simultaneous positive impacts on both inter-cooling and recuperation

efficiencies. So, these values, representing the results of the feasibility study of designing the derivatives with the inter-cooled recuperated cycle. They are the only engines that can be designed for every given value of inter-cooler outlet temperature, hence COT. So, the largest possibly designed engines are with the specifications of ($OPR = 20.37$, $T_4 = 320.0\ K^o$, $COT = 1453.6\ K^o$, $ShP = 9.32MW$, $Q = 11.23(MW)\ and\ \zeta_{th} = 36.1\%$).

Design point performance characteristic and values of overall pressure ratios associated with given LPC pressure ratio are represented in Figure 5-25.

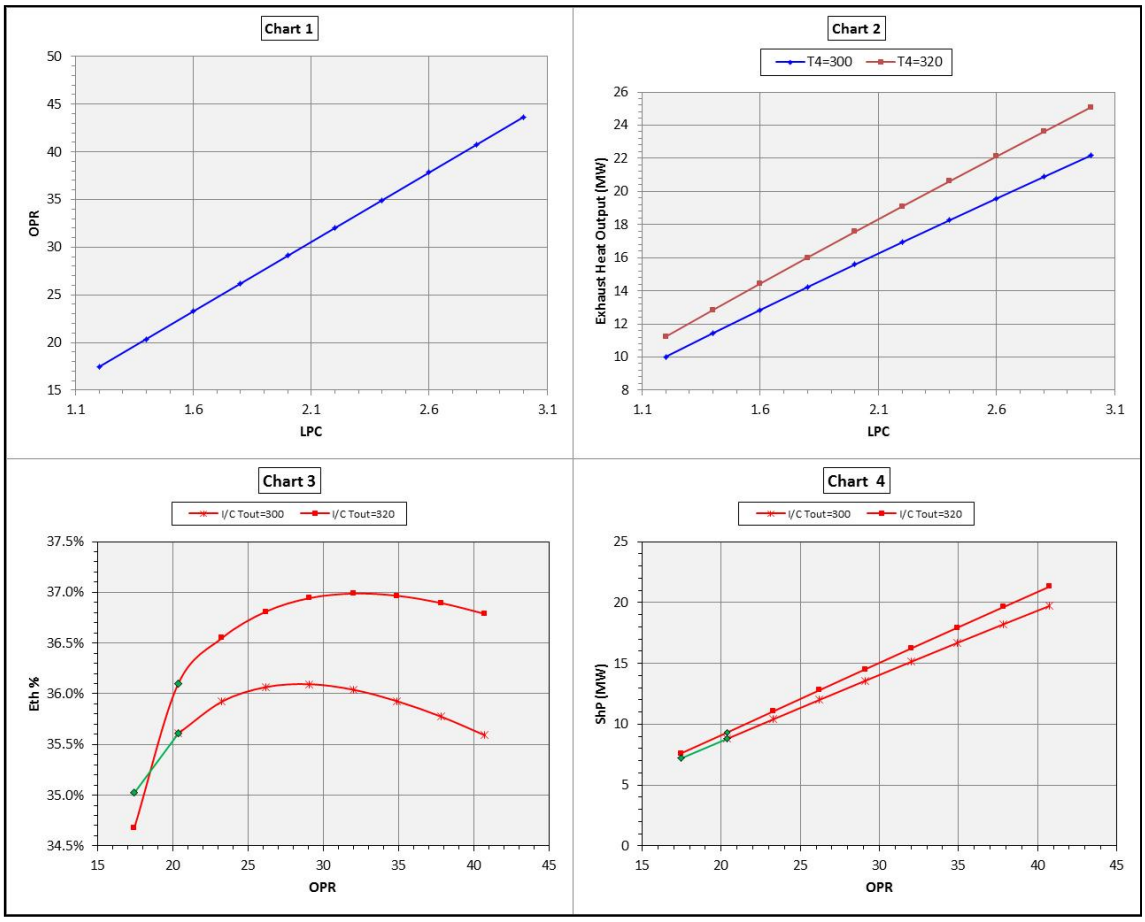

Figure 5-25 Two-Spool Inter-cooled Conventional Recuperated Aeroderivative design Point Characteristics

It is clearly understood that there is an optimum value of low pressure compressor pressure ratio which achieves maximum thermal efficiency. Although, values of ($LPC > 1.4$) have negative effects on recuperation efficiency especially at high values of (T_4) the engine can still achieve higher values of

thermal efficiency. It is owing to the fact that increased turbine work, which is gained by increasing engine's overall pressure ratio, can remarkably offset the decrease in thermal efficiency occurring as a result of $(T_{16} < T_7)$; intercooling effect and pressure losses in the recuperator. Also, the major effect is derivation conditions which limited the possibility to simulate for wider range of mass flow rate and combustor outlet temperature at given T_4.

There will not be significant differences in design point performance calculation results between (direct load drive) and free power turbine configuration, as long as a heat exchanger is installed at the engine exhaust in conventional recuperated configuration.

5.1.6.2 Two-Spool non-Conventional ICR Cycle Configuration Engine

Non-conventional recuperated configurations of gas turbine cycles with inter-cooler has been investigated in this part in both (direct load drive) and free power turbine arrangements. They are covered in detail in the following sections.

5.1.6.2.1 Two-Spool non-Conventional ICR Cycle Engine IPT

It can be seen from Figure 5-26 that the configuration is the way of imposing an inter-cooler device between low and high pressure compressors of a non-conventional recuperated cycle.

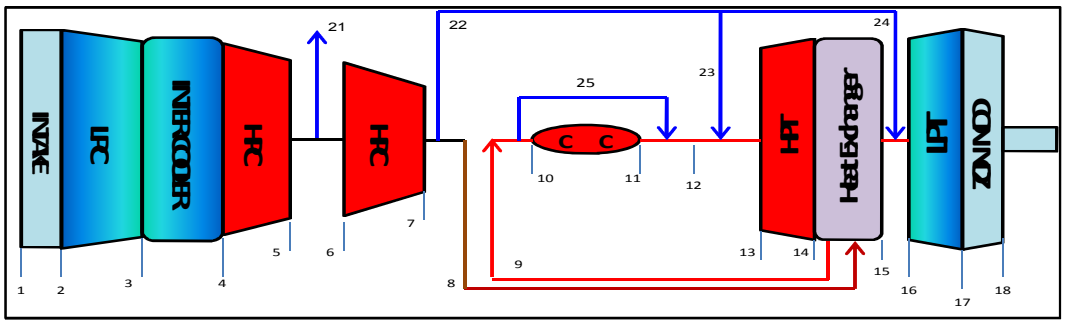

Figure 5-26 Schematic Draw of Two-Spool non-Conv ICR cycle Engine with IPT configuration

This aims to benefit from the advantage of reducing required compression work to drive the compressors and lowering cooling bleed temperature, hence required bleed mass flow. All calculations as will be seen later in this section,

show different behaviour than with the inter-cooled conventional recuperated gas turbine cycle. Figure 5-27 contains a $T-S$ diagram of inter-cooled recuperated gas turbine cycle with the recuperator located between the turbines in a direct load driving arrangement. It can be noticed that for a given value of T_4, changing LP compressor pressure ratio under derivation conditions, of constant non-dimensional mass flow and high pressure cycle temperature ratio, has no effect on recuperation temperature difference ($HE\ T_{in} - HPC\ T_{out}$) and COT values, as will be shown later from results in Charts 2 and 4 in Figure 5-28.

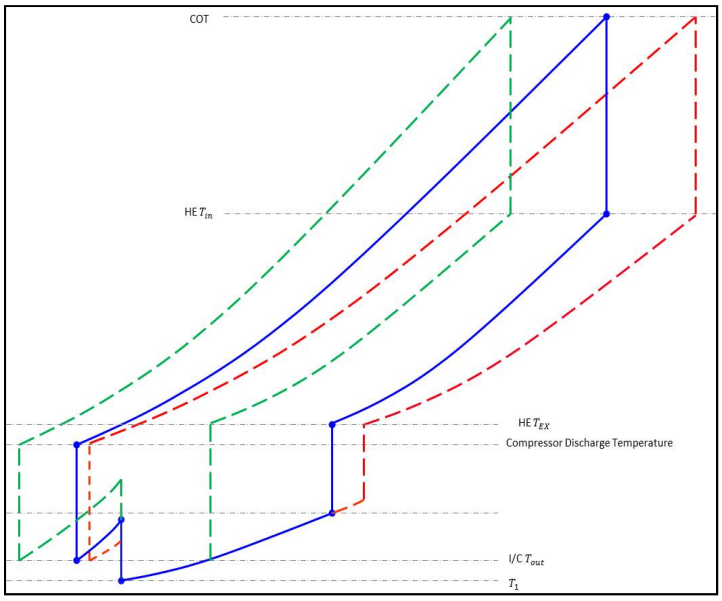

Figure 5-27 Effect of Varying $\boldsymbol{LPC}$ on $\boldsymbol{T-S}$ Diagram for non-conventional $\boldsymbol{ICR}$ with $\boldsymbol{IPT}$

Also, these values of heat exchanger inlet temperature $HE\ T_{in}$ and compressor exit temperature remain constant for different LPC pressure ratios at constant COT. However, inter-cooling temperature difference is affected as well as the value of exhaust gas temperature EGT which leads to varying LP turbine work. Increasing overall pressure ratio results in reduction in exhaust gas temperature and an increase in turbine work.

Applying constant mass flow condition at the inlet of HPC and constant high pressure cycle temperature, the condition can be written as:

$$(W_4\sqrt{T_4})/P_4 = \left[(W_4\sqrt{T_4})/P_4\right]_{aero}$$

$T_{11}/T_4 = [T_{12}/T_4]_{aero}$

The values of W_4 at each LPC which satisfy these conditions are equal to calculated values in the two-spool inter-cooled cycle. It can be calculated using the same steps used in calculating mass flow at different values of combustor outlet temperature.

In the same way the design point simulated in the inter-cooled cycle and heat exchanger cycle, the Turbomatch code is used and input data file created (see appendix E.1.14). Design point simulation results are plotted on the charts in Figure 5-28, Figure 5-29, Figure 5-30. It has been found from previous calculations of the recuperated cycle that applying the recuperation between divided expansion of LP and HP turbines commits to provide heat exchanger inlet temperature $HE\,T_{in}$ always higher than compression discharge temperature. So, in this case it is most important to make sure that T_4 applied at different LPC values is always lower than LP compressor discharge temperature $LPC\,T_{out}$. It can be noticed from Chart 1 in Figure 5-28 that there are some values of LPC pressure ratio which cannot satisfy the condition of applying inter-cooler relative to intercooler outlet temperature. The number of these points is increased as the value of T_4 rises. Charts 2, 4, and 6 indicate that by changing LPC values at a constant inter-cooler temperature, it is only the exhaust gas temperature which changes. However, Charts 3 and 5 indicate that varying T_4 only leads to a deviation in all values of COT, $HE\,T_{in}$, TET and EGT.

Inlet mass flow values, which are calculated to meet the derivation conditions, are presented in Chart 4 in Figure 5-29 at different values of low pressure compressor pressure ratio and inter-cooler outlet temperature. The basic calculation of estimating high pressure turbine blades is conducted and it includes creep calculation only as shown in Charts 1 and 2 in the same Figure.

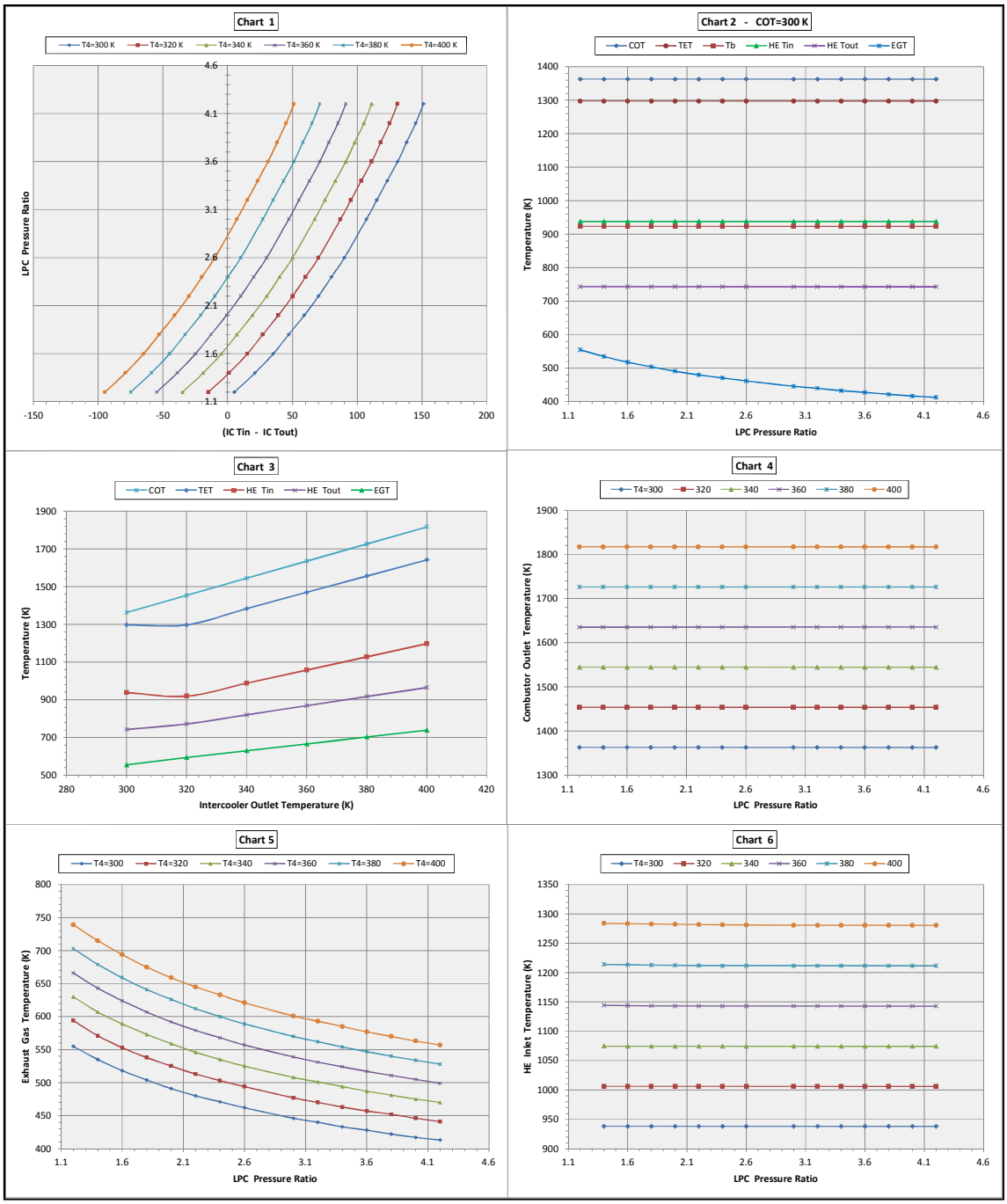

Figure 5-28 $\boldsymbol{LPC}$ Effect on Design Point Characteristics for non-conventional $\boldsymbol{ICR}$ with $\boldsymbol{IPT}$ Configuration

Considering the average of 25000 hrs of engine time to failure, it can be seen that values of inter-cooler outlet temperature in the range of ($T_4 = 360\ to\ 370\ K$) hence combustor outlet temperature ($COT = 1580\ to\ 1700\ K$) provides sensible time to failure at the design point. The effect of varying low pressure compressor pressure ratio and inter-cooler outlet temperature on shaft output power and exhaust output heat is presented in Chart 3 in Figure 5-29. It

can be observed that increasing PR_{lc} and T_4 results in improving shaft output power, because of the constant temperature ratio condition which rises COT as T_4 increases. Exhaust output heat has maximum value at a certain amount of LPC pressure ratio. Optimum values for maximum output heat rise with the increase in inter-cooler outlet temperature and associated combustor outlet temperature.

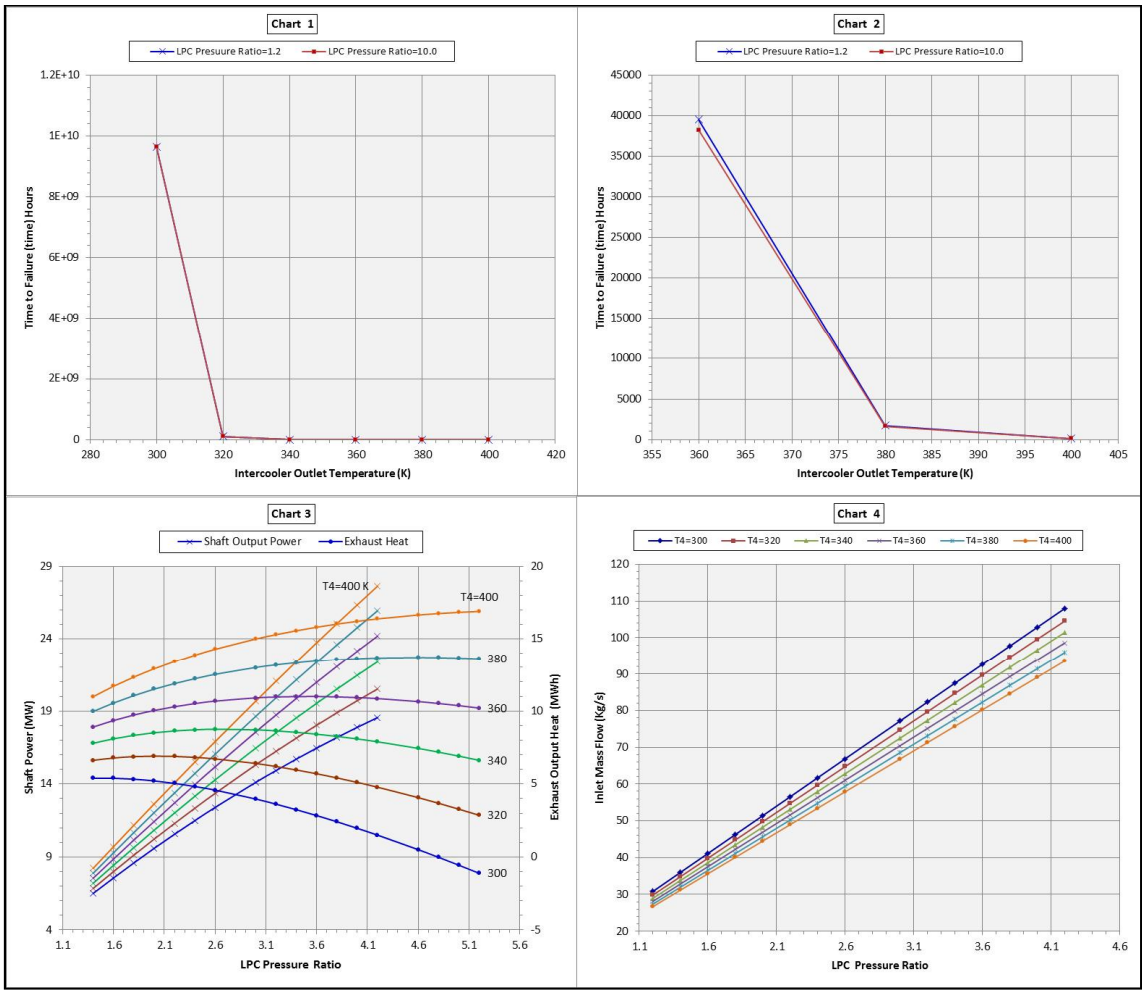

Figure 5-29 Design Point Characteristics of non-Conventional $\boldsymbol{ICR}$ with $\boldsymbol{IPT}$ Configuration

Engine performance characteristics shown in Figure 5-30 indicate that there is always an optimum value of low pressure compressor pressure ratio which achieves maximum thermal efficiency at each T_4, $hence\ COT$. This optimum value of LPC pressure ratio for maximum thermal efficiency is increased when T_4 and associated COT rise.

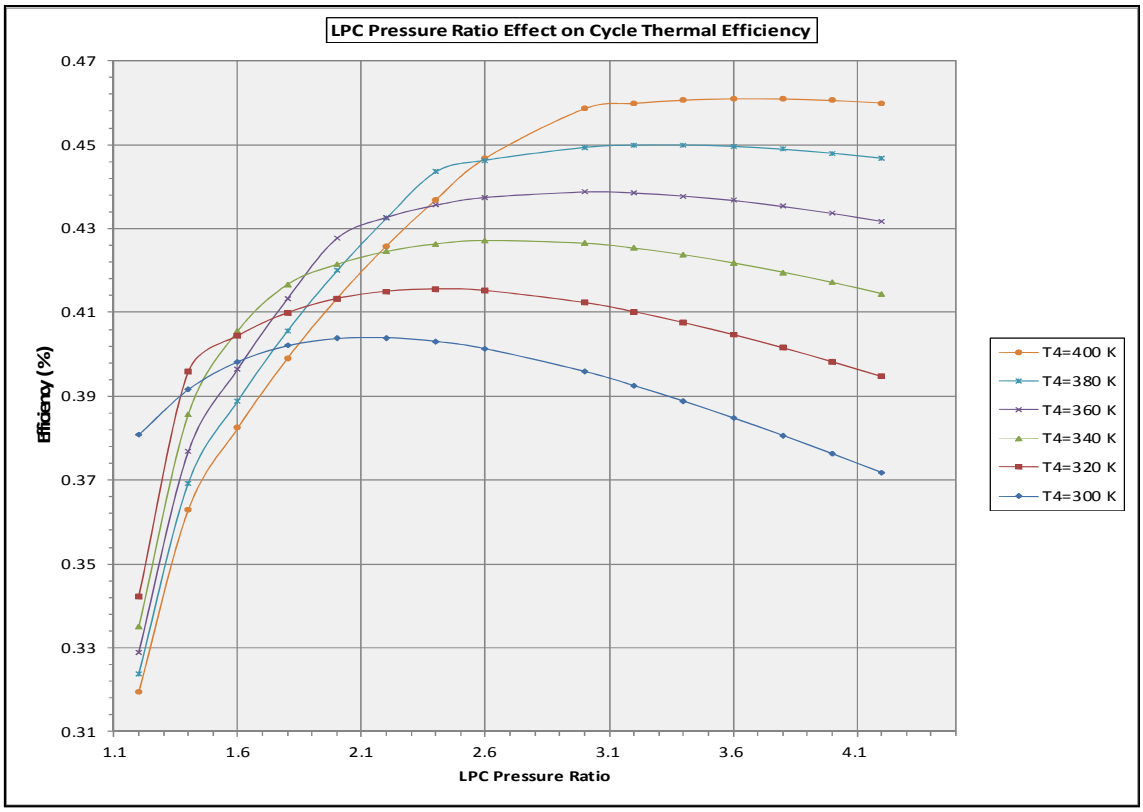

Figure 5-30 Effect of Varying Design $\boldsymbol{LPC}$ on Thermal Efficiency for non-conventional $\boldsymbol{ICR}$ with $\boldsymbol{IPT}$ Configuration

5.1.6.2.2 Two-Spool non-Conventional ICR Cycle Engine FPT

The advantages of recuperation technology between LP turbine and power turbine FPT were concluded and justified in the previous section of Two-Spool non-Conventional HEx Cycle Engine FPT. Figure 5-31 includes a schematic draw of the cycle configuration after applying inter-cooling technology.

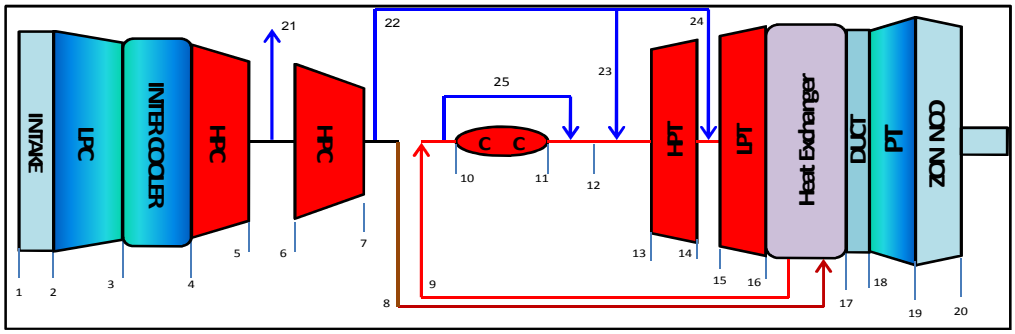

Figure 5-31 Schematic Draw of Two-Spool non-Conventional $\boldsymbol{ICR}$ Aeroderivative Engine with $\boldsymbol{FPT}$

Derivation conditions applied in the previous section is exactly applied on this engine, and there is no difference in the values of calculated mass flow associated with T_4 and COT.

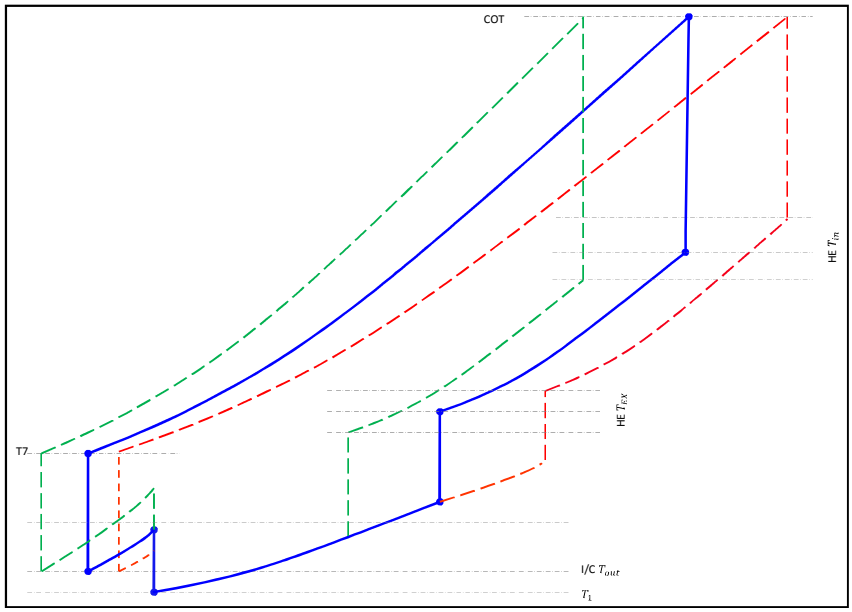

Figure 5-32 Effect of Varying $\boldsymbol{LPC}$ on $\boldsymbol{T-S}$ Diagram for non-conventional $\boldsymbol{ICR}$ with $\boldsymbol{FPT}$

As will be illustrated later regarding design point results, the effect of varying the low pressure compressor pressure ratio on cycle temperatures is presented in the $(T-S)$ diagram in Figure 5-32. Results in Charts 1, 2, 3, 4, 5 and 6 in Figure 5-34 show that subjecting them to the aforementioned derivation condition varying LPC pressure ratio has a major impact on changing hot-side heat exchanger inlet and outlet temperature, cold-side outlet temperature as well as exhaust gas temperature at constant $T_4\ and\ COT$. According to inter-cooling and recuperation technologies, these two temperature differences are very important and the conditions can be written as $(T_3 > T_4)\ \ and\ \ (T_{16} > T_8)$.

Design point simulation is conducted using the Turbomatch code and results are plotted in Figure 5-33, Figure 5-34, Figure 5-35 and Figure 5-36. Recuperation and inter-cooling temperature differences are investigated and their results contained in Charts 1and 2 of Figure 5-33. The general trend of the curves indicate that for given COT increasing LPC pressure ratio has a positive effect on inter-cooler temperature difference, and has a negative effect on

recuperation temperature difference. On the other hand, for a given PR_{LPC} increasing $T_4\ with\ associated\ COT$ has exactly the opposite influence.

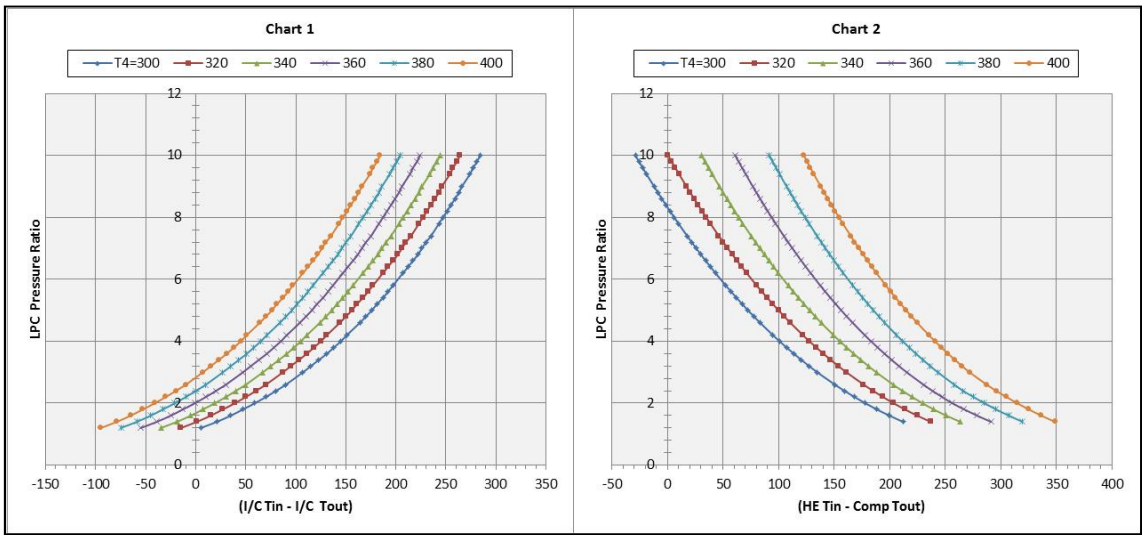

Figure 5-33 ***LPC*** Impact on Recuperation and Inter-cooling Temperature Differences at Design Point for non-conventional ***ICR*** with ***FPT***

Therefore, it is clearly realised that the compromise between these values is crucial and important in order to find the appropriate values of PR_{LPC} and $T_4\ with\ associated\ COT$, which satisfy recuperation and inter-cooling conditions.

Combustor outlet temperature COT values which are associated with chosen values of inter-cooler outlet temperature under the derivation conditions of the constant high pressure cycle temperature ratio with the aircraft engine are plotted on Chart 1 in Figure 5-35. Also in the same Figure, under the same conditions of high pressure compressor constant mass flow, mass flow values have been represented in Chart 2. Increasing inter-cooler outlet temperature $IC\ T_{out}$ under derivation condition causes a decrease in required engine inlet mass flow for given values of low pressure compressor pressure ratio. In addition, basic calculation of estimating engine hot section time to failure is performed and results are plotted on Chart 3 for a wide range of T_4 values. It is considered from the calculation that there is no significant effect on turbine blade life estimation by changing PR_{LPC} only. The range of $T_4 = 360\ to\ 370\ K$ provide logical values of time to failure of 20000-40000 hrs.

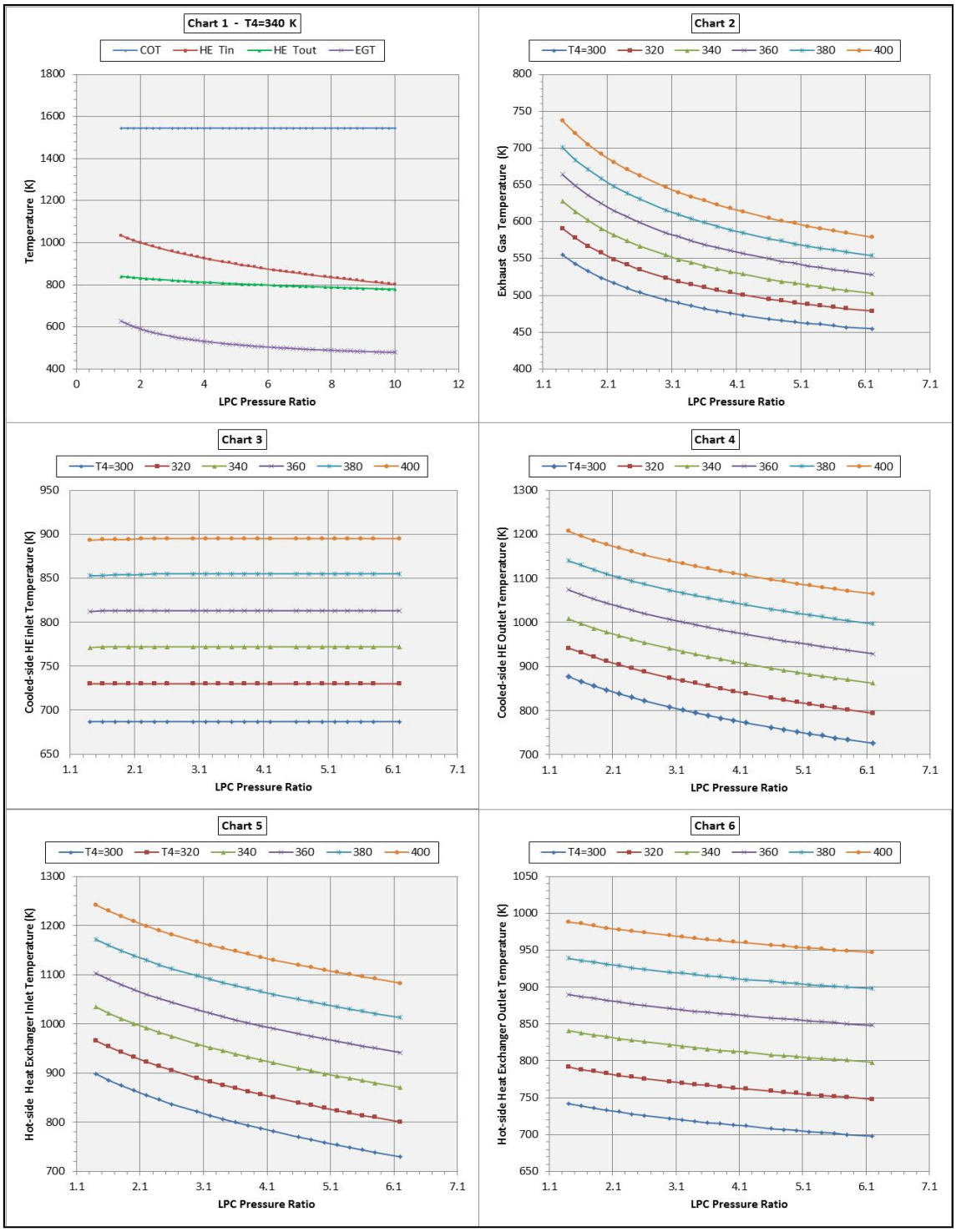

Figure 5-34 Intercooler Outlet Temperature and $\boldsymbol{LPC}$ Effect on Cycle Temperature at design Point for non-conventional $\boldsymbol{ICR}$ with $\boldsymbol{FPT}$

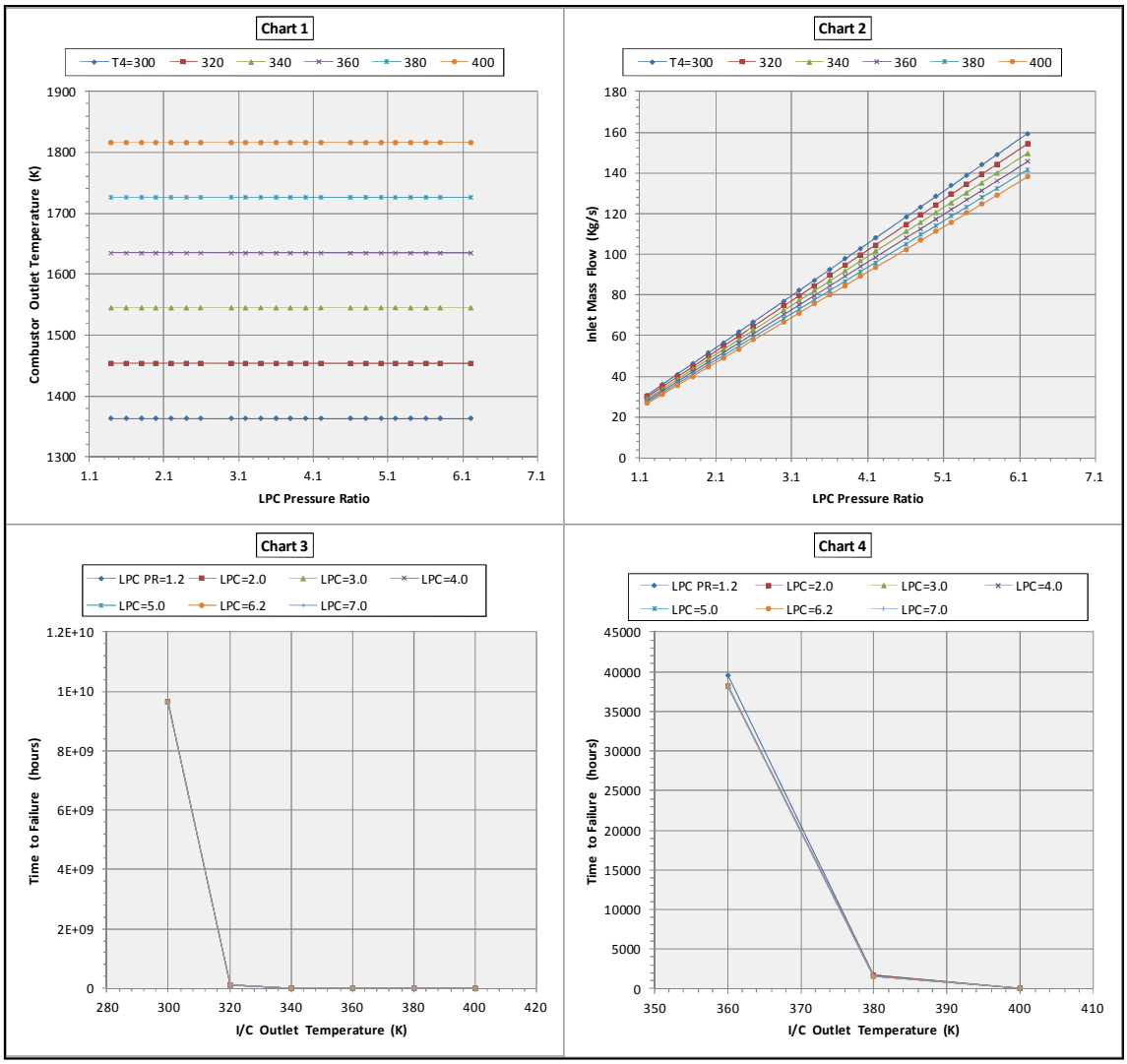

Figure 5-35 Inlet Mass Flow and Turbine Blade Live Estimation at Design Point for non-conventional $\boldsymbol{ICR}$ with $\boldsymbol{FPT}$

In most of the industrial applications thermal efficiency and shaft output power are the most important performance characters to be considered and they express important indicators for choosing the proper engine for specific applications. Figure 5-36 illustrates how engine shaft power and thermal efficiency vary with change in the low pressure compressor pressure ratio and inter-cooled outlet temperature with associated COT. Increasing combustor outlet temperature is subjected to rise inter-cooler outlet temperature, and at constant LPC pressure ratio it leads to enhancing engine cycle thermal efficiency and increasing shaft output power as well as exhaust heat. Shaft output power and exhaust heat are always increased with the increase in cycle temperature ratio (COT/T_4) at a given LP compressor pressure ratio. However,

it can be noticed that there exists an optimum value of PR_{LPC} at constant T_4 and COT which achieves the maximum engine thermal efficiency.

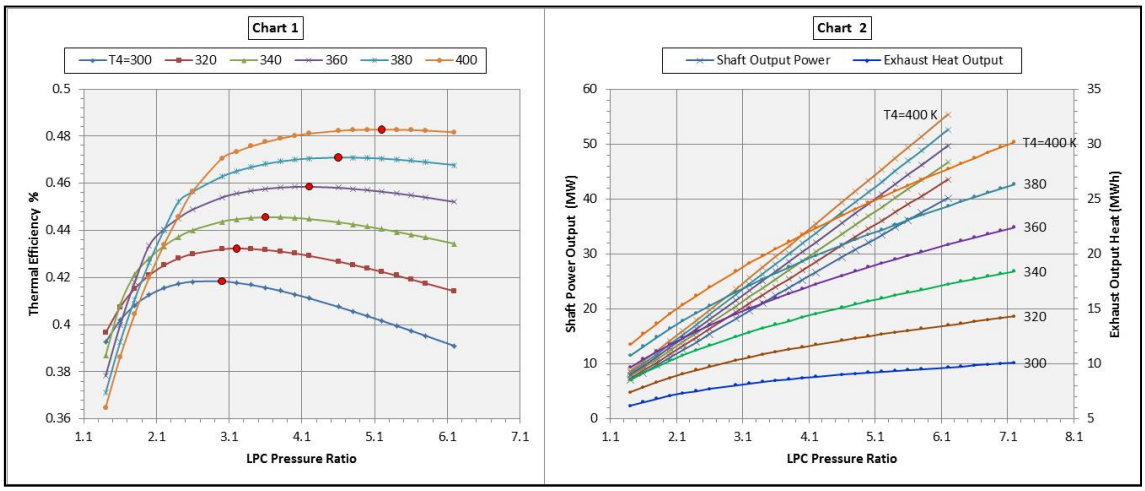

Figure 5-36 Shaft Outlet power and Thermal efficiency Variation for non-conventional $\boldsymbol{ICR}$ with $\boldsymbol{FPT}$ Configuration

Regarding Figure 5-25, Figure 5-30, and Figure 5-36 of the inter-cooled recuperated cycle (conventional and non-conventional recuperation) it can be concluded that Two-Spool non-Conventional ICR Cycle with FPT promises the highest thermal efficiency, while ICR with conventional recuperation offer the highest shaft output power and exhaust heat output.

5.2 Maintaining aero-engine's LP and HP Rotor Components

It has been found from the literature that the multi-spool aero-derivative engine can be derived in different ways. It can be achieved either by maintaining two-shafts and applying modifications to the compressor and/or turbine, or by adding a new compressor and turbine on extra shafts as in the Rolls-Royce MT50 [34]. Accordingly, three engine configurations are proposed to be studied and their design point calculations are conducted and illustrated in the following sections.

5.2.1 Two-Spool Simple Cycle Direct Derivation $\boldsymbol{DDv}$

Removing the propelling nozzle and the fan in addition to adding some stages in front of the compressor constituted one of the early methods of

producing first generation derivative engines [103]. A schematic draw of the proposed engine configuration is illustrated in Figure 5-37 where the objective of maintaining the same aero-engine performance needs slight modifications to the IP compressor in order to accommodate loss in pressure ratio owing to removing the fan. Also, the modifications could be either modifying the IP compressor to increase the pressure ratio or modifying the LP turbine to offset the components' non-dimensional flow and power mismatch.

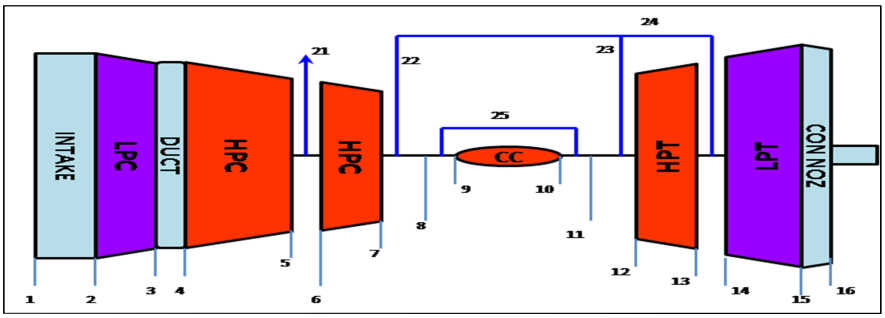

Figure 5-37 Two-Spool Simple Cycle Aeroderivative Engine on $\boldsymbol{DDv}$

Air properties at the inlet of the intermediate pressure compressor will be ambient condition properties at the design point, with pressure drop resulting from intake losses. Derivation conditions of constant non-dimensional mass flow and cycle maximum temperature ratio are applied at the inlet of the IP compressor. Accordingly, by referring to both Figure 4-3 and Figure 5-4 the conditions can be written as follows:

$$(W_2\sqrt{T_2}/P_2) = \left(W_2\sqrt{T_2}/P_2\right)_{aero} = 1010.26$$

$$(T_{10}/T_2) = (T_{12}/T_2)_{aero} = 6.103$$

Using these formulae and applying SLS ambient conditions helps to find values of the engine's inlet mass flow W_2 and combustor outlet temperature COT as follows:

$$W_2 = 59.514\ Kg/s, \quad and \quad COT = 1758.493\ K^o.$$

The Performance Input data file (see appendix E.1.3) was created using the Turbomatch code and used to calculate the value of low pressure

compressor PR_{lc} that maintains temperature ratio and non-dimensional mass flow the same as the aircraft engine. A low pressure compressor pressure ratio which is appropriate to meet derivation conditions ($PR_{lc} = 2.53866$) is suitable. Performance characteristics are calculated and results included in Table 5-6.

Table 5-6 Design Point Parameters of Two-Spool Simple Cycle Engine on DDv

$W\ (^{K}/_{S})$	$ShP\ (MW)$	ζ_{th} %	$Q\ (MW)$	OPR	$COT\ (K^{O})$
59.23	24.86	43.33	25.64	38.08	1758.65

Results show that the direct derivation of the aircraft engine with a simple cycle provides an engine in the rate of 24.86 MW, achieving thermal efficiency of 43.33% and being fired at 1758.49K^{o} at the design point.

5.2.2 Two-Spool Heat Exchanger Cycle Aeroderivative Engines DDv

Applying recuperation to the two-spool simple cycle for the directly derivative engine is within the design point calculations previously calculated for different low pressure compressor pressure ratios. It will be clarified in the following sections.

5.2.2.1 Two-Spool Conventional HEx Configuration Engines DDv

Previous calculations regarding the application of different low pressure compressor pressure ratio showed that the largest PR_{lc} that can be applied on the two-spool conventional heat exchanger is less than ($PR_{lc} < 1.5$).

Therefore, direct derivation of the aero-engine with ($PR_{lc} = 2.53866$) cannot be designed with the two-spool conventional heat exchanger.

5.2.2.2 Two-Spool non-Conventional HEx Configuration Engines DDv

Calculation procedures in non-Conventional configuration are exactly identical to the one conducted in relation to Figure 5-16 and Figure 5-19. In this case however, the objective is to maintain the familiarity with aircraft engine

performance for both LP compressor and turbine, which was not compulsory in the previous calculation when new LP shaft components applied.

Two-Spool non-Conventional HEx Configuration IPT-DDv

Referring to Figure 5-16, Figure 5-17and Figure 5-18, direct derivation of the two-shaft engine provides performance as indicated in Table 5-7.

Table 5-7 DP from Direct Derivation of Two-spool non-Conventional HEx with $\boldsymbol{IPT}$

$W\ (^{K}/_{S})$	$ShP\ (MW)$	ζ_{th}	$Q\ (MW_{he})$	PR	$COT\ (K^{O})$	$HE\ T_{in}\ (K^{\circ})$	$(HE\ T_{in} - Comp\ T_{out})$
59.23	16.6623	45.39	13.1409	38.08	1758.65	1234.44	366.2078

Design point calculations showed that it is necessary to modify the low pressure compressor and redesign the low pressure turbine as a result of imposing the recuperator between high pressure and low pressure turbines. Low pressure turbine non dimensional mass flow is found as $(W\sqrt{T}/P = 226.91)$ and engine specific power and fuel consumption are$SFC = 51.0885\ (g.s/MW)$ and SP=281.192$(KW.s/Kg)$.

Two-Spool non-Conventional HEx Configuration $FPT - DDv$

Using the same method applied in calculating design point for two-spool heat exchanger with free power turbine, the recuperator has been set between FPT and LPT as shown in Figure 5-19. The design point performance characteristic of $LPC = 2.53866$ can be seen from Figure 5-20 and Figure 5-21.

Results are included in Table 5-8. Low pressure turbine non dimensional mass flow is found as $(W\sqrt{T}/P = 248.6674)$ and specific power and fuel consumption are $SFC = 50.6547\ (g.s/MW)$ and SP=326.219 $(KW.s/Kg)$.

Table 5-8 DP from Direct Derivation of Two-Spool non-Conventional HEx with FPT

$W\ (^{K}/_{S})$	$ShP\ (MW)$	ζ_{th}	$Q\ (MW_{he})$	PR	$COT\ (K^{O})$	$HE\ T_{in}\ (K^{\circ})$	$(HE\ T_{in} - Comp\ T_{out})$
59.23	19.33	45.65	16.05	38.08	1758.65	1137.89	269.65

Accordingly, it can be recognised from the results in both Table 5-7 and Table 5-8 that engines with a free power turbine arrangement still promise better performance characteristics at the design point. Higher shaft power and better thermal efficiency enhancement can be gained by locating the recuperator between the low pressure compressor and free power turbine.

5.2.3 Two-Spool Intercooled Cycle Aeroderivative Engine DDv

The engine configuration matches exactly the configuration presented in Figure 5-8, where design point calculation can be assumed as is not affected whether direct load driving configuration or free power turbine is used. An inter-cooler is installed between LP and HP compressors and derivation conditions applied will be exactly as mentioned above regarding simple cycle direct derivation. It appears obvious that there is no need for a controlling temperature ratio between the inter-cooler outlet temperature and combustor outlet temperature at the design point. The whole cycle temperature ratio will be subject to the condition that $(T_{10}/T_2) = (T_{12}/T_2)_{aero} = 6.103$.

The calculation regarding the two-spool simple cycle for the given design point parameters indicates that the low pressure compressor temperature is $(LPC\ T_{out} = 386.67\ K^{\circ})$ at $(LPC = 2.53866)$. The main objective of applying inter-cooling is to reduce this temperature, hence reducing compressor work and cooling bleed temperature.

It has been observed from results in Figure 5-38 that applying inter-cooling to the two-spool simple cycle engine improves the design point characteristics. Charts 1and 2 illustrate how thermal efficiency and specific fuel consumption are improved by reducing HP compressor inlet temperature and required work. Shaft power is also increased and exhaust gas heat decreased

due to the fall in exhaust gas temperature compared to the simple cycle, as shown in Charts 3 and 4. As was mentioned earlier, the inter-cooler helps to cool down cooling flow and reduces its temperature, which leads to improving hot section life time as presented in Charts 5 and 6. Also it decreases the amount of cooling flow needed to cool the hot sections.

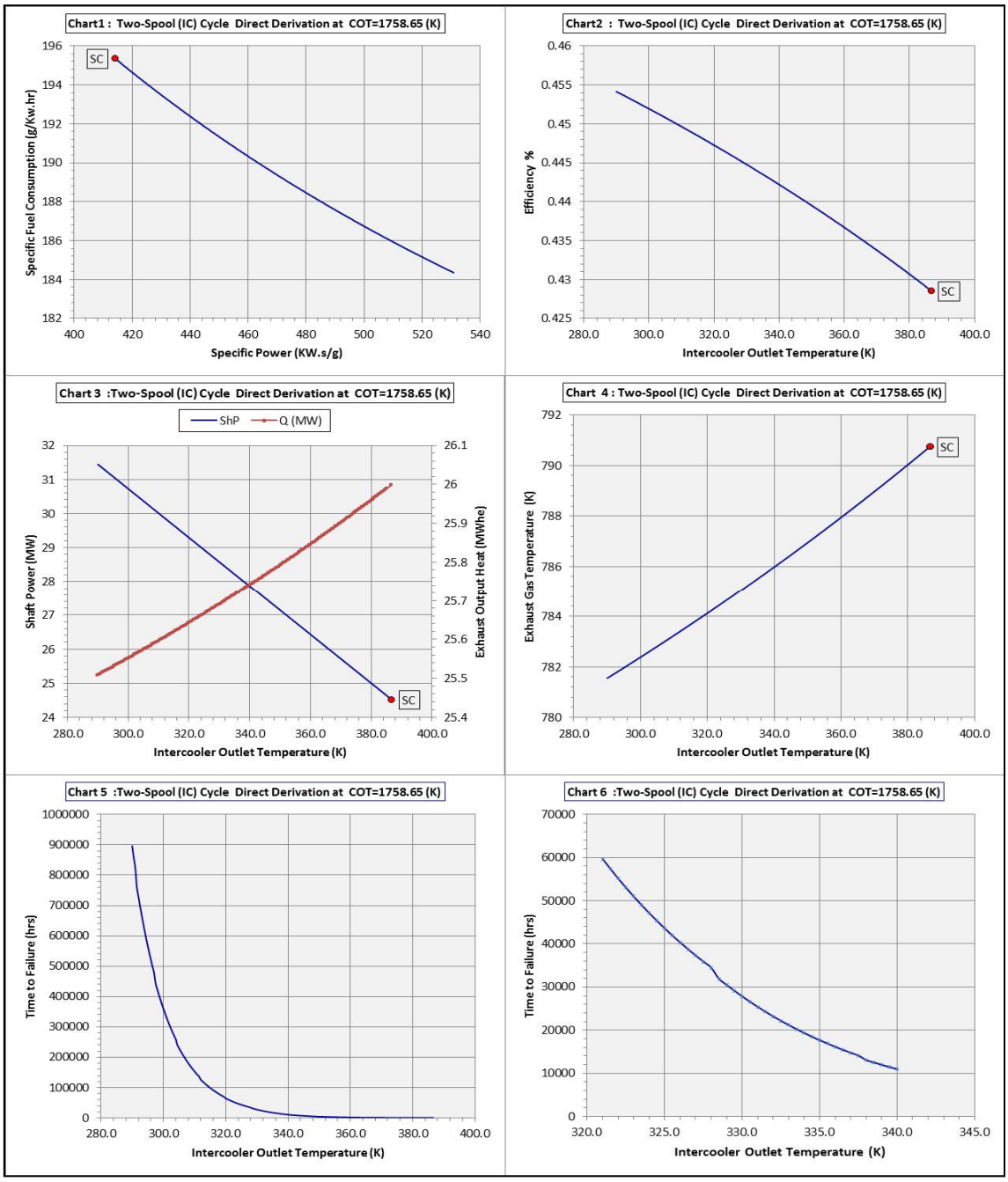

Figure 5-38 Inter-cooler Effect on Design Point Characteristics of Two-Spool Inter-cooled Cycle (Direct Derivation Method $\boldsymbol{DDv}$)

On the other hand however, both values of non-dimensional mass flow at the inlet of the HP compressor and LP turbine will be affected by applying the inter-cooler. It happens to the high pressure compressor as a result of varying the inlet temperature while its inlet pressure and mass flow are kept constant. Also, it becomes necessary to modify the low pressure turbine design in order to cope with the reduction in its inlet non-dimensional mass flow below $\left(W\sqrt{T}/P = 246.0089\right)$ on the aircraft engine at the design point. In fact, all values of $W, P, and\ T$ at the inlet of the low pressure turbine are affected and changed. Therefore, there is no way to apply the inter-cooler without modification to the engine's components when direct derivation concept applied.

5.2.4 Two-Spool Inter-cooled Recuperated Cycle Engines DDv

Applying inter-cooling and recuperation technology to direct derivation two-spool simple cycles is exactly identical to the schematic construction in Figure 5-22, Figure 5-26, and Figure 5-31. As conducted earlier the ability of applying Conventional and non-Conventional recuperation will be investigated in the following sections.

5.2.4.1 Two-Spool ICR Conventional Cycle Configuration DDv

Engine configuration and stage numbering in this case exactly matches the illustration in Figure 5-22. Previous calculations regarding conventional recuperation concluded that the largest LP compressor that can be applied with this technology is equal to $(LPC = 1.5)$. The reason was that LP compressor outlet temperature increases its pressure ratio to a value higher than $LPC = 1.5$. Therefore, in this section the purpose is to apply the inter-cooling technology between the compressors in order to reduce $LPC\ T_{out}$ at $PR_{lc} = 5.3866$ and make it possible to conduct the direct derivation of the two-spool engine with ICR technology.

The design point has been calculated at different $IC\ T_{out}$ values under different scenarios of derivation conditions as follows:

1- Constant inlet mass flow (W_1) and (COT) from conditions$\left(W_1 * \sqrt{T_1}/P_1\right) = \left(W_1 * \sqrt{T_1}/P_1\right)_{aero}and(T_{11}/T_2) = (T_{12}/T_2)_{aero}$.

2- Constant value of combustor outlet temperature (COT) from $(T_{11}/T_2) = (T_{12}/T_2)_{aero}$and different values of (W_1) calculated from the condition that$\left(W_4 * \sqrt{T_4}/P_4\right) = \left(W_6 * \sqrt{T_6}/P_6\right)_{aero}$.

3- Varying both values of (W_1) and (COT) under conditions that $\left(W_4 * \sqrt{T_4}/P_4\right) = \left(W_6 * \sqrt{T_6}/P_6\right)_{aero}$ and $(T_{11}/T_4) = (T_{12}/T_6)_{aero}$.

Design point calculation results of the three scenarios are plotted respectively in Figure 5-39, Figure 5-40 and Figure 5-41.

It is important to notice that two conditions of Scenario 3 are fully applied only on non-conventional ICR configuration, while only $(T_{11}/T_4) = (T_{12}/T_6)_{aero}$ condition which is applied on Conventional ICR configuration.

It can be noted from Charts 1, 2, 3, and 4 that there is consistency in the results of recuperation and inter-cooling temperature differences as well as inlet mass flow, between results in Scenario 1 and Scenario 2. In both scenarios recuperation temperature difference has positive values in the range of $(IC\ T_{out} < 355\ K)$, where heat exchanger is applicable and a condition of $T_{17} > T_7$ is satisfied. On the other hand however, Scenario 3 shows that it is not efficient to apply recuperation technology with inter-cooling for all applied values of $IC\ T_{out}$, and inter-cooling technology alone is most efficient. Also, engine inlet mass flow is constant in this scenario. High pressure turbine blade life is estimated using creep calculation, and its results are compared in Charts 5 and 6. Regarding the practical assumption of 25000 as time to failure, it can be observed that decreasing intercooler outlet temperature improves hot section life time. In addition, values of $(T_4 = 335.2, 340.6,\ and\ 360.8)$ are the highest values to achieve a sensible value of creep time to failure for Scenarios 1, 2, and 3 respectively.

In Figure 5-40, shaft output power, exhaust heat temperature, thermal efficiency and specific fuel consumption are investigated for a wide range of different $(IC\ T_{out})$ in Charts 1, 2, 3, and 4. Shaft power is increased with the

reduction in inter-cooler outlet temperature in Scenarios 1 and 2. Conversely, a reduction in shaft power is experienced in Scenario 3 due to the increase in the negative effect of difference between heat exchanger inlet temperature and compression discharge.

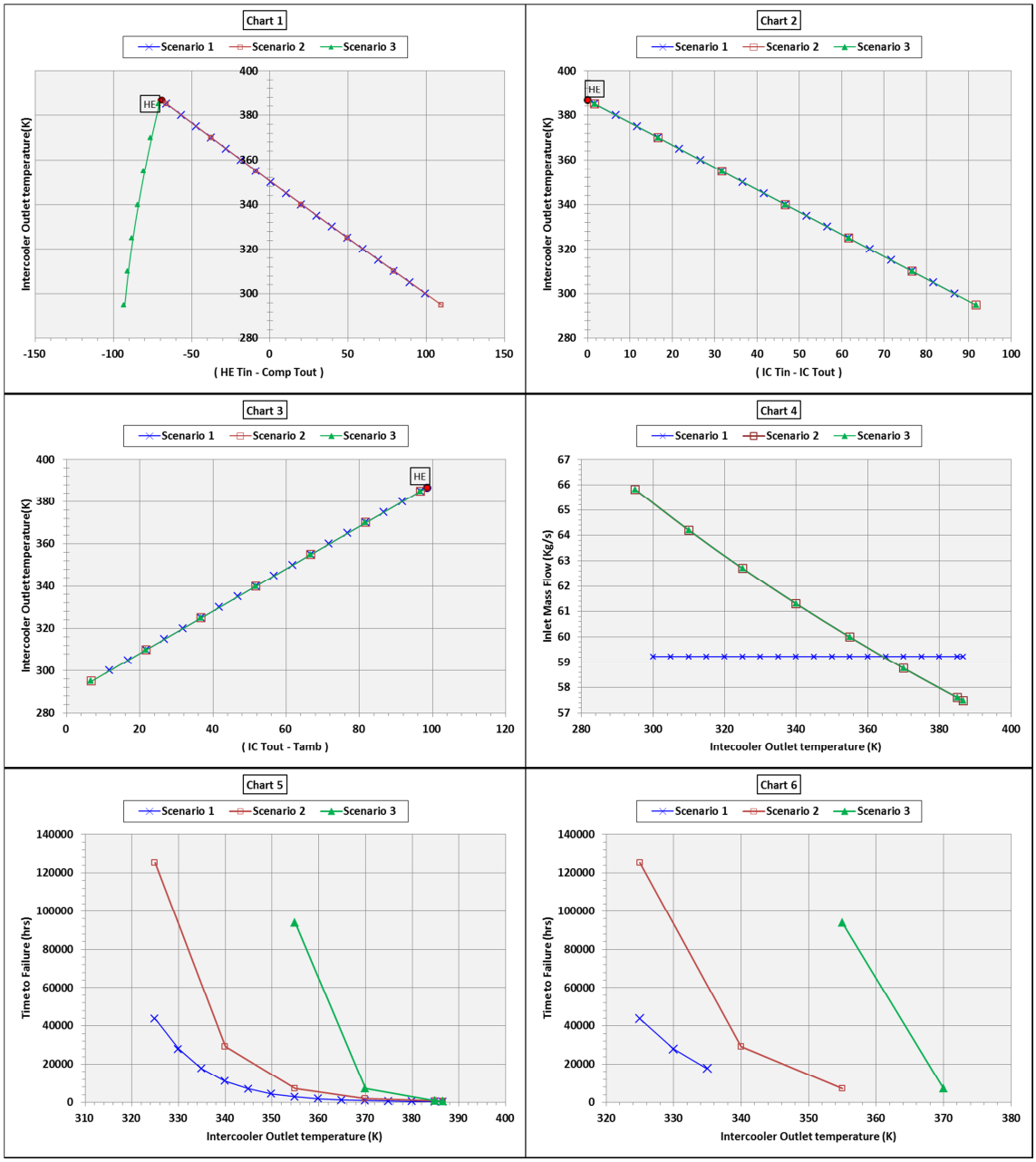

Figure 5-39 Design Point Characteristics for 2-Spool Conventional $\boldsymbol{ICR}$ on Direct Derivation $\boldsymbol{DDv}$ (Group One)

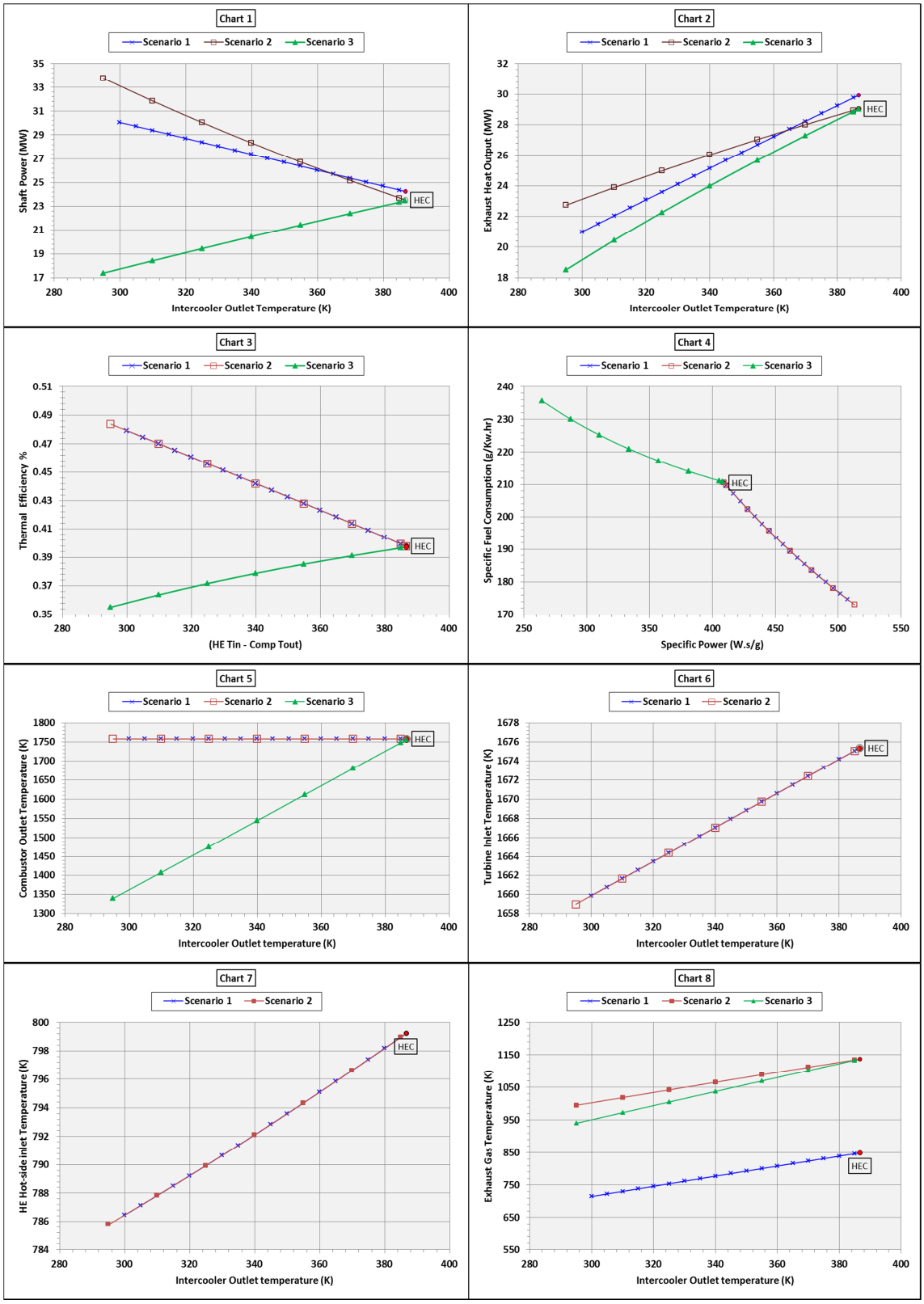

Figure 5-40 Design Point Characteristics for 2-Spool Conventional $\boldsymbol{ICR}$ on Direct Derivation $\boldsymbol{DDv}$ (Group Two)

Scenario 2 is the most superior and promises the highest shaft output power and exhaust heat, despite of the fact that exhaust heat output is decreased with the decrease in intercooler outlet temperature T_4. Furthermore, thermal efficiency and specific fuel consumption are improved and there is no difference in their values between Scenarios 1 and 2, whilst they vary negatively in Scenario 3. The effects of varying design point inter-cooler outlet temperature on combustor outlet temperature, turbine inlet temperature and exhaust gas temperature are shown in Charts (5, 6, 7, and 8). According to the assumptions and derivation conditions applied in Scenarios 1 and 2, combustor outlet temperatures are equal and constant for the whole calculations, whilst it changes in Scenario 3. High pressure turbine inlet temperature is decreased with the reduction in inter-cooler outlet temperature owing to the constant temperature ratio condition. As a result, heat exchanger inlet temperature is reduced and relies within the acceptable thermal barriers of heat exchanger materials.

Observations in Figure 5-41 expose an indicator helps in determining which engine component needs to be modified or redesigned in on each operating scenario. It includes the effect of changing inter-cooling effect at the design point on LP and HP compressors and turbines. It can be noticed that applying the assumptions and derivation conditions of Scenario 1 led to the necessity of implementing modifications or redesigning the high pressure compressor as well as low pressure turbine. Also, non-dimensional mass flow of the LP compressor is not changed and there is no need for any modification apart from the changes needed to accommodating losses in pressure ratio.

It is necessary for some modification to be applied to the low pressure compressor and turbine as well as high pressure turbine on the second design of Scenario 2. The main objective is to design an engine which has high pressure rotor components maintained from the aircraft engine. Although Scenario 3 describes the case which meet this objective, the design cannot meet the recuperation condition of $(T_{17} > T_7)$ and recuperation technology would not be applicable.

Therefore, with inter-cooled conventional recuperated technology, it is not possible to design an aero-derivative engine which maintains HP shaft components with overall pressure ratio $OPR = 38.07$ equal to the aircraft engine.

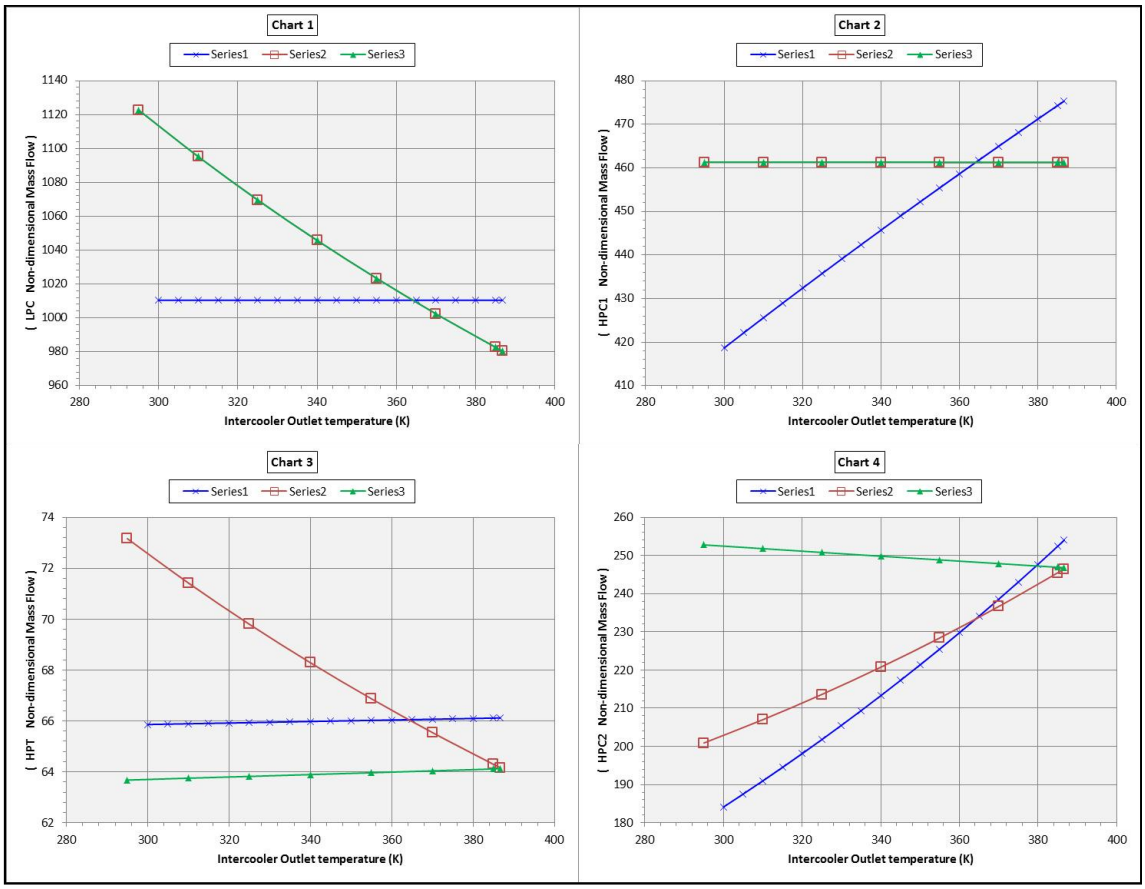

Figure 5-41 Non-dimensional Mass Flow variation of Compressors and $\boldsymbol{HP}$ Turbine at Design Point for 2-Spool Conventional $\boldsymbol{ICR}$ on $\boldsymbol{DDv}$

5.2.4.2 Two-Spool ICR non-Conventional Cycle Configuration DDv

Non-Conventional or alternative recuperation cycle with inter-cooler was presented in two different expansion dividing arrangements in Figure 5-26, and Figure 5-31. Different from calculations conducted in previous section (5.2.4.1), both derivation conditions, which are presented in Scenario 3 of are applied. Inlet mass flow is changed and can be calculated from constant mass flow condition of the HP compressor for every given value of intercooler outlet temperature T_4. Constant temperature ratio condition is also applied and used in calculating combustor outlet temperature.

Two-Spool non-Conventional ICR Cycle Engine $DDv-IPT$

Regarding to engine stage numbering and structure illustrated in Figure 5-26, all the design point calculation was performed and all results of performance characteristics are presented in Figure 5-42 and Figure 5-43. Design inlet mass flow is calculated for each given value of $IC\ T_{out}$ and presented in Figure 5-42. Also, hot section life is estimated and non-dimensional mass flow at the inlet of each component calculated, as shown in Charts 2, 3, and 4.

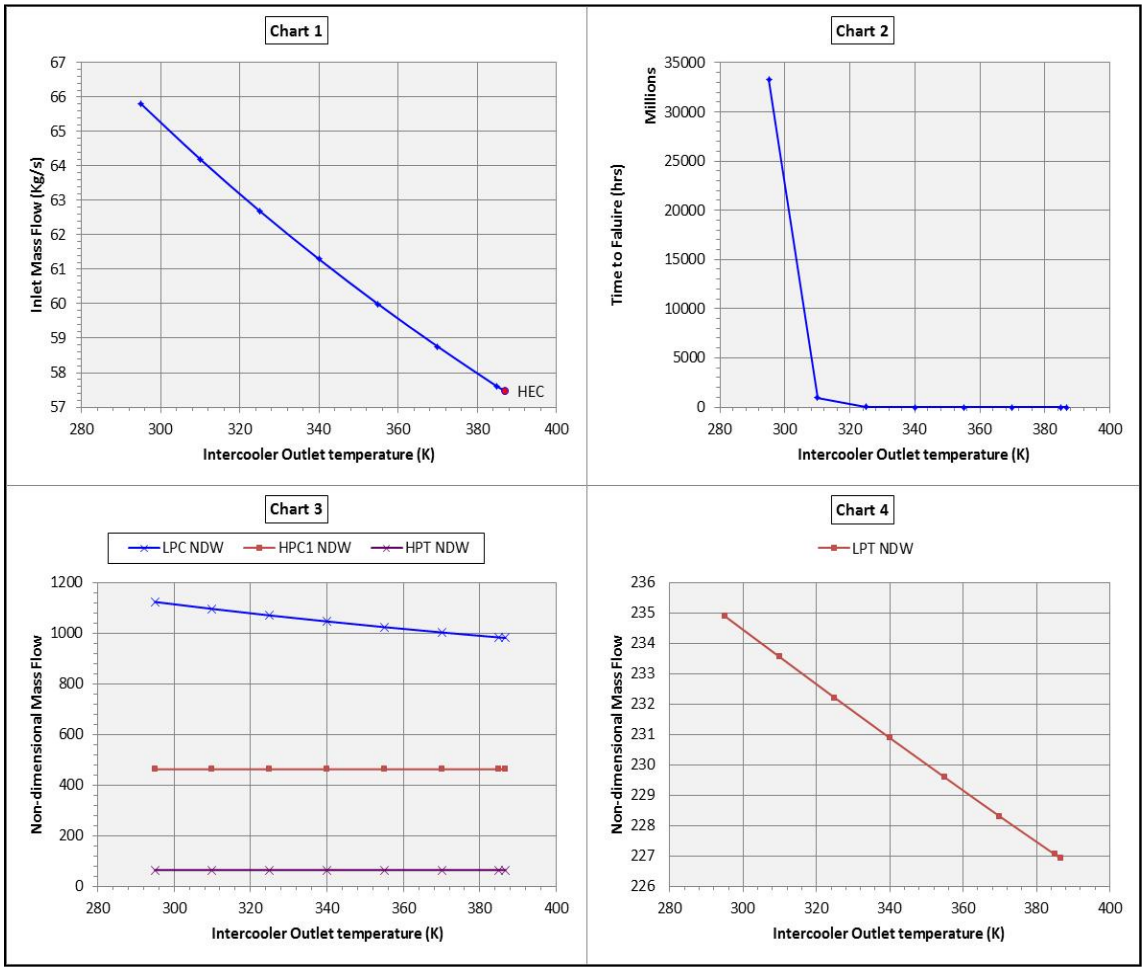

Figure 5-42 Derivation Conditions Variation at Design Point for Two-Spool non-Conventional ICR on Direct Derivation with IPT Configuration

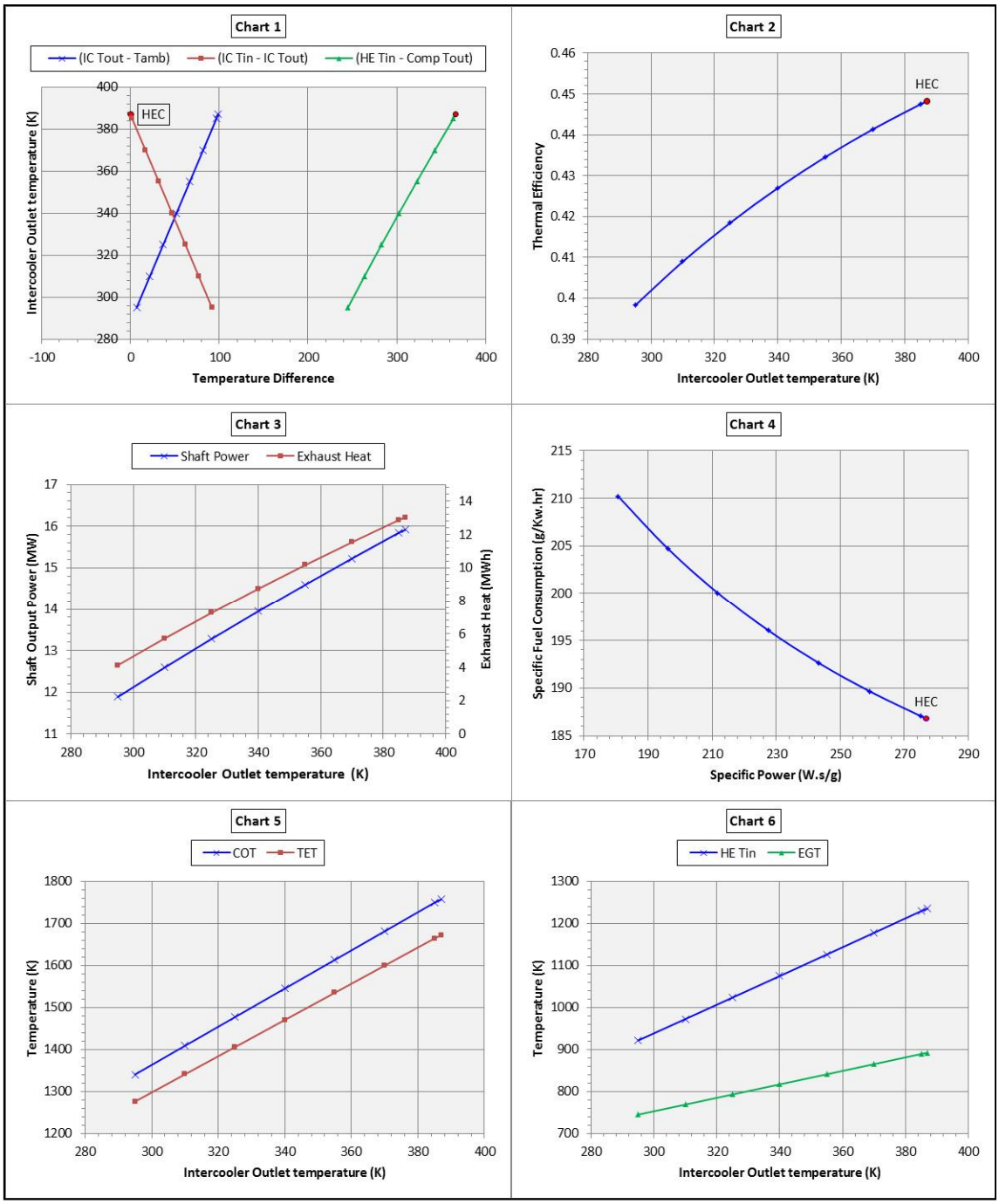

Figure 5-43 Design Point Characteristics of Two-Spool non-Conventional ***ICR*** on Direct Derivation with ***IPT*** Configuration

The effect of varying T_4 on recuperation and inter-cooling temperature differences is indicated in Figure 5-43. It is so obvious from the results that recuperation temperature difference condition of $(HE\ T_{in} - Comp\ T_{out})$ is always positive and satisfied for the all applied intercooler outlet temperature $IC\ T_{out}$ presented in Chart 1. The design point characteristics of thermal efficiency,

specific fuel consumption, shaft power and exhaust heat output are calculated under conditions previously introduced in Scenario 3 and plotted in Charts 2, 3, and 4.

It can be seen from these charts that design point performance characteristics deteriorated as a result of the decreasing in design point intercooler outlet temperature. Therefore applying inter-cooling to non-conventional recuperation technology cannot enhance engine simple cycle performance under the assumptions and derivation conditions applied in Scenario 3. Cycle temperatures are represented in Charts 5 and 6, which show that combustor outlet temperature and HP turbine inlet temperature change with the reduction in inter-cooler outlet temperature. Also, exhaust gas temperature with hot-side HEx inlet temperature both fall with the reduction in (T_4).

Two-Spool non-Conventional ICR Cycle Engine $DDv - FPT$

Investigating direct derivation in the feasibility study was extended to include using recuperation between free power turbines and gas generators. Calculation of the design point characteristic is conducted relative to engine structure and stage numbering, and presented in Figure 5-31.

All design point calculations subject to the assumptions and conditions previously assumed in Scenario 3 and all design point parameters are plotted in Figure 5-44 and Figure 5-45. It can be observed from Chart 5 in Figure 5-44 and Chart 4 in Figure 5-45 that the engine design point characteristics are investigated for the same values of inlet mass flow and combustor outlet temperature used in the direct load driving *(DD)* configuration.

It can be observed from design point characteristics that trends of performance characteristics completely match the design point performance of the engine with recuperator located between low and high pressure turbines. However, all performance outputs have slightly improved by applying recuperation before the free power turbine configuration than locating the recuperation between (LP and HP) turbine.

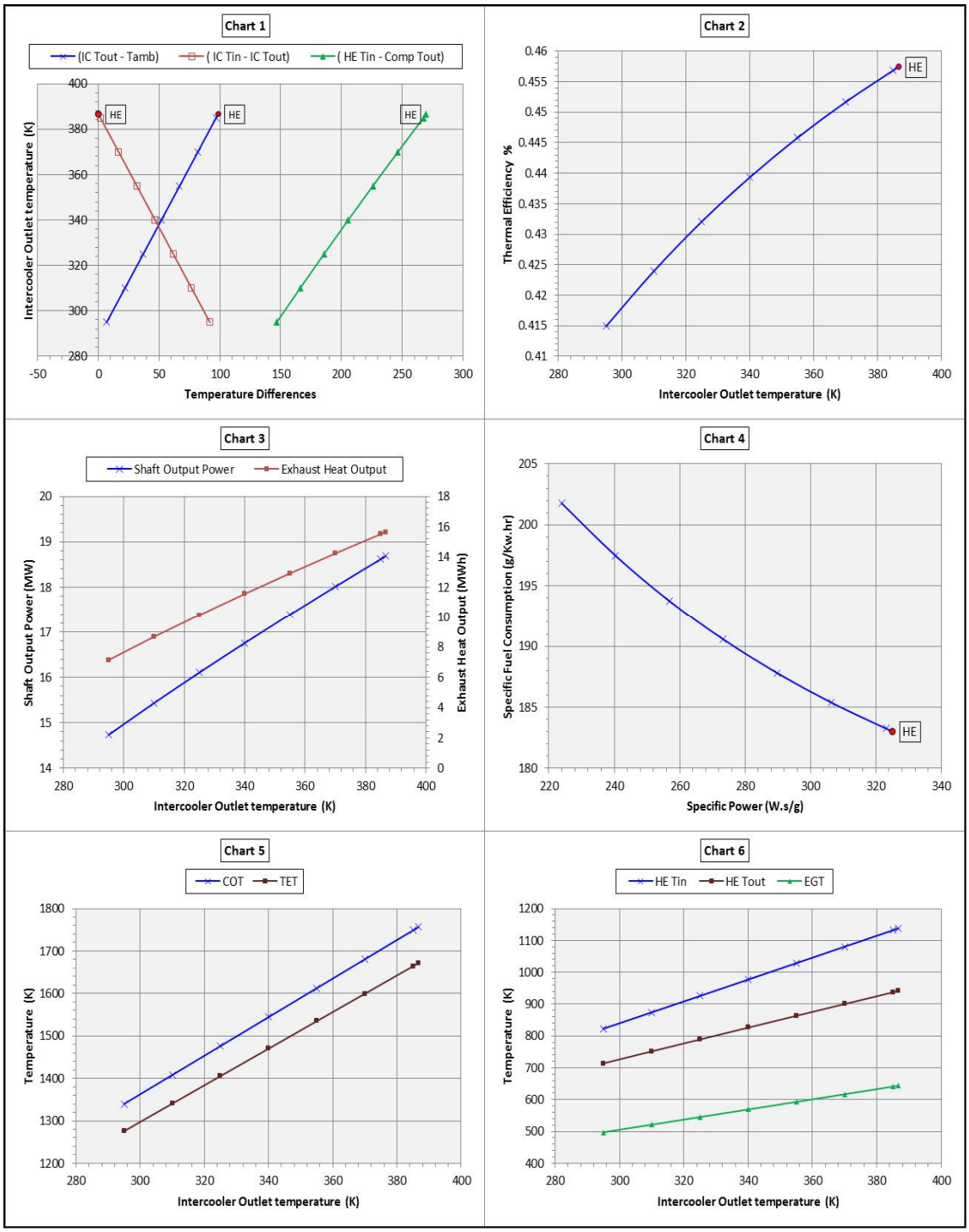

Figure 5-44 Design Point Characteristics of Two-Spool non-Conventional $\boldsymbol{ICR}$ on Direct Derivation with $\boldsymbol{FPT}$ Configuration

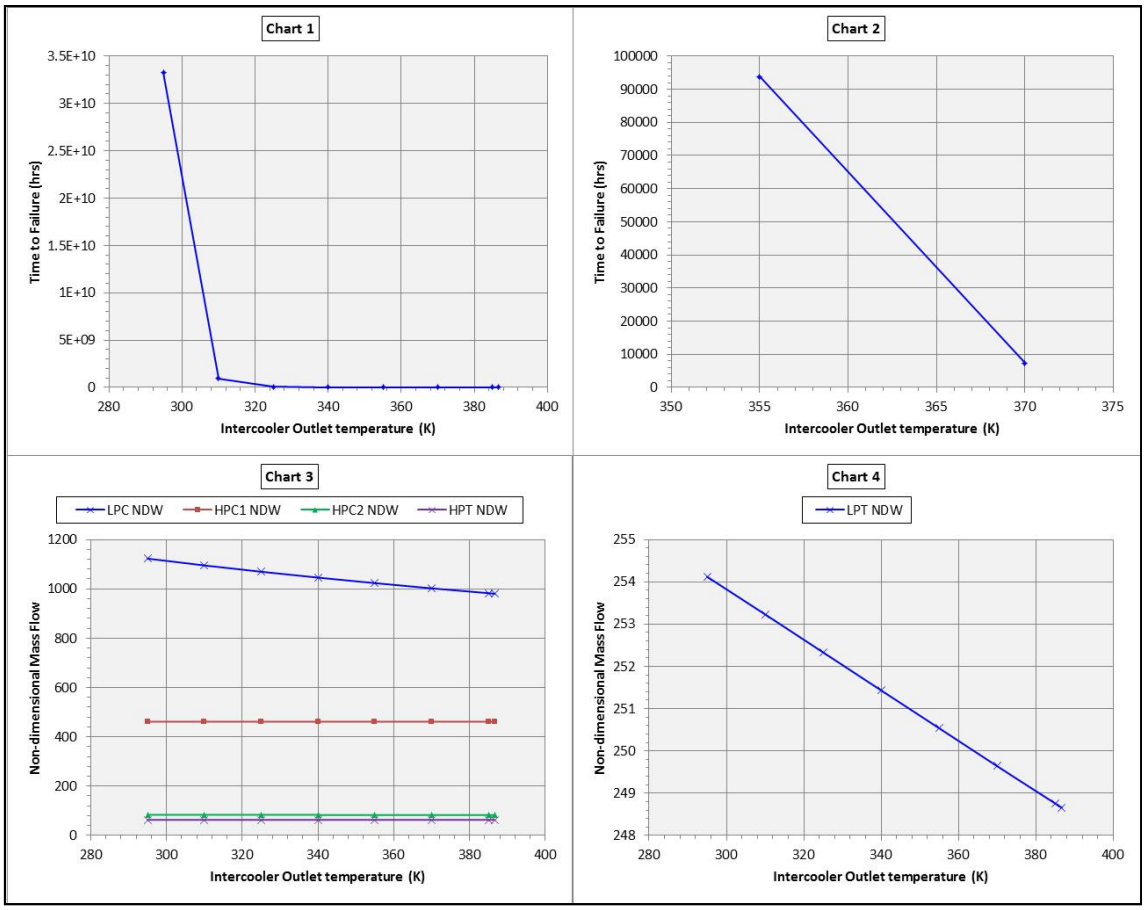

Figure 5-45 Derivation Conditions Variation at Design Point for Two-Spool non-Conventional $\boldsymbol{ICR}$ on Direct Derivation with $\boldsymbol{FPT}$ Configuration

Shaft power, thermal efficiency and exhaust heat has increased and specific fuel consumption decreased. In addition, Charts 4 and 5 in Figure 5-44 indicate that the engine can produce lower exhaust gas temperature, when it is designed with the same values of combustor outlet temperature COT used in designing the engine on FPT arrangement. That leads to further improve both thermal efficiency and exhaust heat.

5.2.5 Three-Spool Simple Cycle Aeroderivative Gas Turbine

Historically, aero-derivative engines have been designed in three-spool configuration, such as the Rolls-Royce MT50 engine for marine application. It is seen from the literature that the larger in size the aeroderivative gas turbine is the better in terms of plant initial cost per the kilowatt power. Improving engine performance, such as specific power, thermal efficiency and heat output is

always at the top priority of customer demand and needs. One way of achieving such is by applying higher engine overall pressure ratio and/or increasing turbine inlet temperature. Therefore, maintaining the LP and HP shaft components of the aircraft engine offers an opportunity to add an extra shaft containing new compressor and turbine in order to increase overall cycle pressure ratio.

In this case there will be three shafts and the derivation conditions of maintaining temperature ratio and non-dimensional mass flow have to be applied at the inlet of the IP compressor of the new designed aeroderivative gas turbine engine. Accordingly, relative to Figure 5-46 and Figure 4-3 therefore, the derivation conditions can be written in the following equations:

$$\left(W_4\sqrt{T_4}/P_4\right) = \left(W_2\sqrt{T_2}/P_2\right)_{aero},\ (T_{12}/T_4) = (T_{12}/T_2)_{aero}.$$

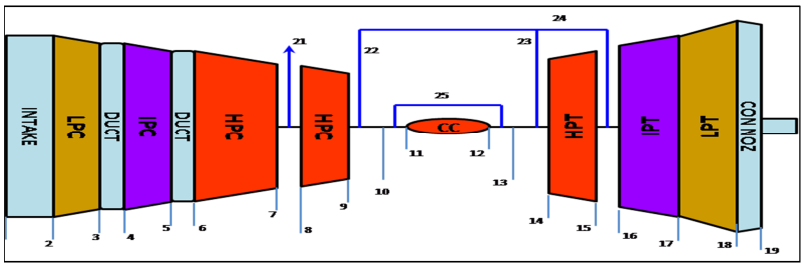

Figure 5-46 Three-Spool Simple Cycle Aeroderivative Engine

An Excel spread sheet (see appendix A.4) is used to calculate engine's mass flow and COT which satisfy these conditions under the given values of low pressure compressors pressure ratios PR_{lc}. It follows the same steps which were taken in the calculation of the two-spool simple cycle engine. Calculated mass flow values, and low pressure compressor PR_{lc} as well as combustor outlet temperature are fed to an input data file (see appendix E.2.2) which is run using the Turbomatch code. Design point calculations are performed and their performance outputs presented in charts contained in Figure 5-47. Low pressure compressor pressure ratio is chosen to be in the range of $(PR_{lc} = 1.2\ to\ 2.8)$ which provide values of overall pressure ratio of $(OPR = 45.54\ to\ 106.26)$.

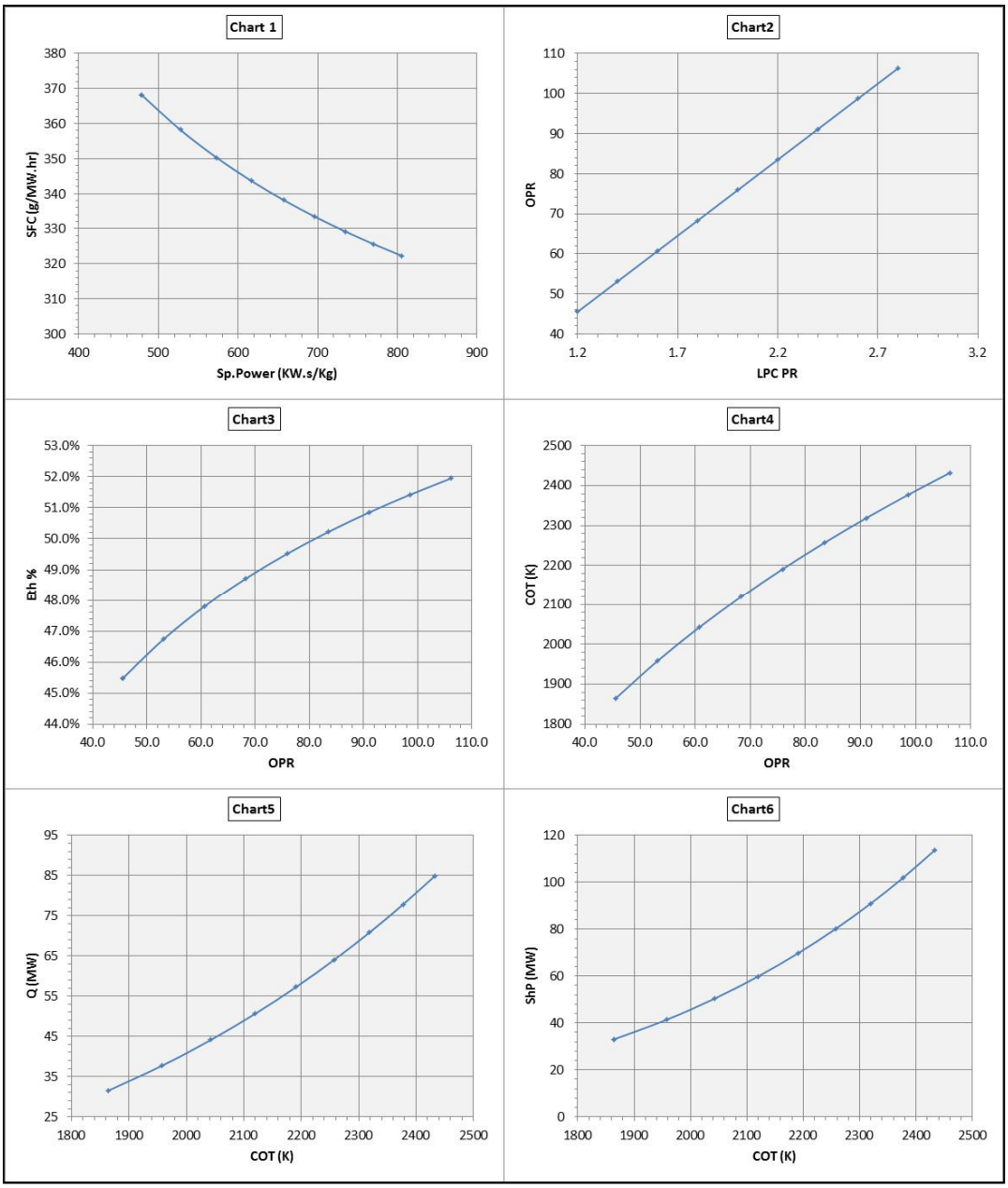

Figure 5-47 Design Point of Three-Spool Simple Cycle Aeroderivative Engines

As seen in Chart 1, the increase in overall pressure ratios leads to a gradual decrease in specific fuel consumption, which results in a major increase in both the engine's specific power and thermal efficiency, as illustrated in Chart 3. Values of combustor outlet temperature associated to the assumed engine OPR are presented in Chart 4. Moreover, as was clarified in previous sections, because of the limitations of maintaining as much as possible from the aircraft engine components, there will be one value of COT for each given value of PR_{lc} to satisfy the derivation objective. Furthermore, Charts 5 and 6 show the

remarkable rise in both engine's output power and heat as a result of the simultaneous increase in OPR and COT. Increasing the pressure ratio from 45.5 to 53.13 combined with COT from 1836.0635 to 1955.75 results in a significant rise in power output from 33.02 to 41.44 MW.

Observation indicates that relative to two-spool simple cycles for the same COT, shaft power has increased by 8.4MW accompanied with around a 1.3% rise in thermal efficiency. Also, exhaust output heat has increased by a measure equal to 6.22MW. However, concern must be given to hot section material thermal barriers, such as for turbine inlet guide vans and rotor blade, which limit the ability to increase cycle pressure ratio under assumed derivation conditions of constant cycle temperature ratio.

5.2.6 Three-Spool Inter-cooled Cycle

It was concluded from the feasibility study for the two-spool heat exchanger cycle engine that adding a heat exchanger to the cycle for recuperation on any $(OPR > 19.5)$ will not be sensible. Hence, the three-spool simple cycle engine cannot be recuperated for the same reason. However, It was found earlier in the same cycle that applying inter-cooling technology helps to increase the chance of the ability of increasing cycle pressure ratio through the ability of decreasing intercooler outlet temperature for a given values of high overall pressure ratio OPR. By applying inter-cooling technology to a large simple cycle engine $(high\ OPR)$ and relatively high turbine inlet temperature, better shaft output and thermal efficiency can be achieved. Therefore, it is only the inter-cooler which needs to be added to the three-spool aero-derivative engine cycle in order to improve its performance outputs.

Inlet mass flow is calculated following the same steps used in the two-spool simple cycle engine at different values of $OPR\ and\ IC\ T_{out}$. Temperature ratios and non-dimensional mass flow at the inlet of the IP compressor remain equal to its design point value on the aircraft engine. Regarding Figure 4-3 and Figure 5-48, derivation conditions equation can be written as follows:

$(W_4\sqrt{T_4}/P_4) = \left(W_2\sqrt{T_2}/P_2\right)_{aero}$, $(T_{12}/T_4) = (T_{12}/T_2)_{aero}$.

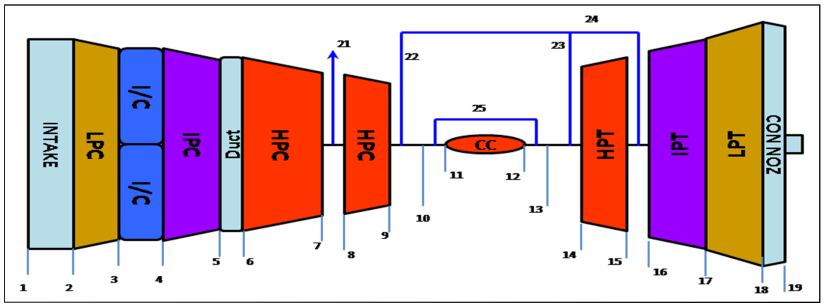

Figure 5-48 Schematic Structure of Three-Spool Inter-cooled Engine

An Excel spread sheet (see appendix A.1) has been used to perform the calculations of inlet mass flow W values at different PR_{lc} for given T_4 or COT, and the results are plotted in Chart 3 in Figure 5-49. The Input data file was created using the Turbomatch code (see appendix E.2.3) and the calculated mass flow values with PR_{lc} and COT are used to calculate design point parameters. All calculated design point parameters are shown in Figure 5-49, Figure 5-50 and Figure 5-51. It can be seen from the results that Chart 1 in Figure 5-49 represents the required COT for each given $IC\ T_{out}$ under cycle temperature ratio conditions. Also, overall pressure ratio associated with each PR_{lc} is illustrated in Chart 2. The condition of applied intercooling condition $(IC\ T_3 - IC\ T_4)$ is investigated and illustrated in Chart 4 in the same Figure 5-49. It shows that rising PR_{lc} and reducing $IC\ T_4$ leads to improve inter-cooling effect and increases its temperature difference.

The impact of varying the inter-cooling effect of shaft output and thermal efficiency, represented in Figure 5-50, illustrates that shaft power is increased with the decrease in $IC\ T_4$ and there is always an optimum value of PR_{lc}, which achieves maximum efficiency, for every COT. This optimum value decreases with the decrease in intercooler outlet temperature.

Figure 5-51 shows values of optimum PR_{lc} which achieves the maximum efficiency or specific work. Moreover, for a given low value of COT, the

optimum value of PR_{lc} which provides the maximum specific power is not the same as the one for maximum thermal efficiency. Blue circles on the curves in both charts indicate points where inter-cooler inlet temperature is equal to intercooler outlet temperature and the engine work under simple cycle regardless of pressure losses. These circles represent the limit of whether or not it is applicable to apply inter-cooling to the cycle and determine the minimum pressure ratio PR which can be applied for a given COT.

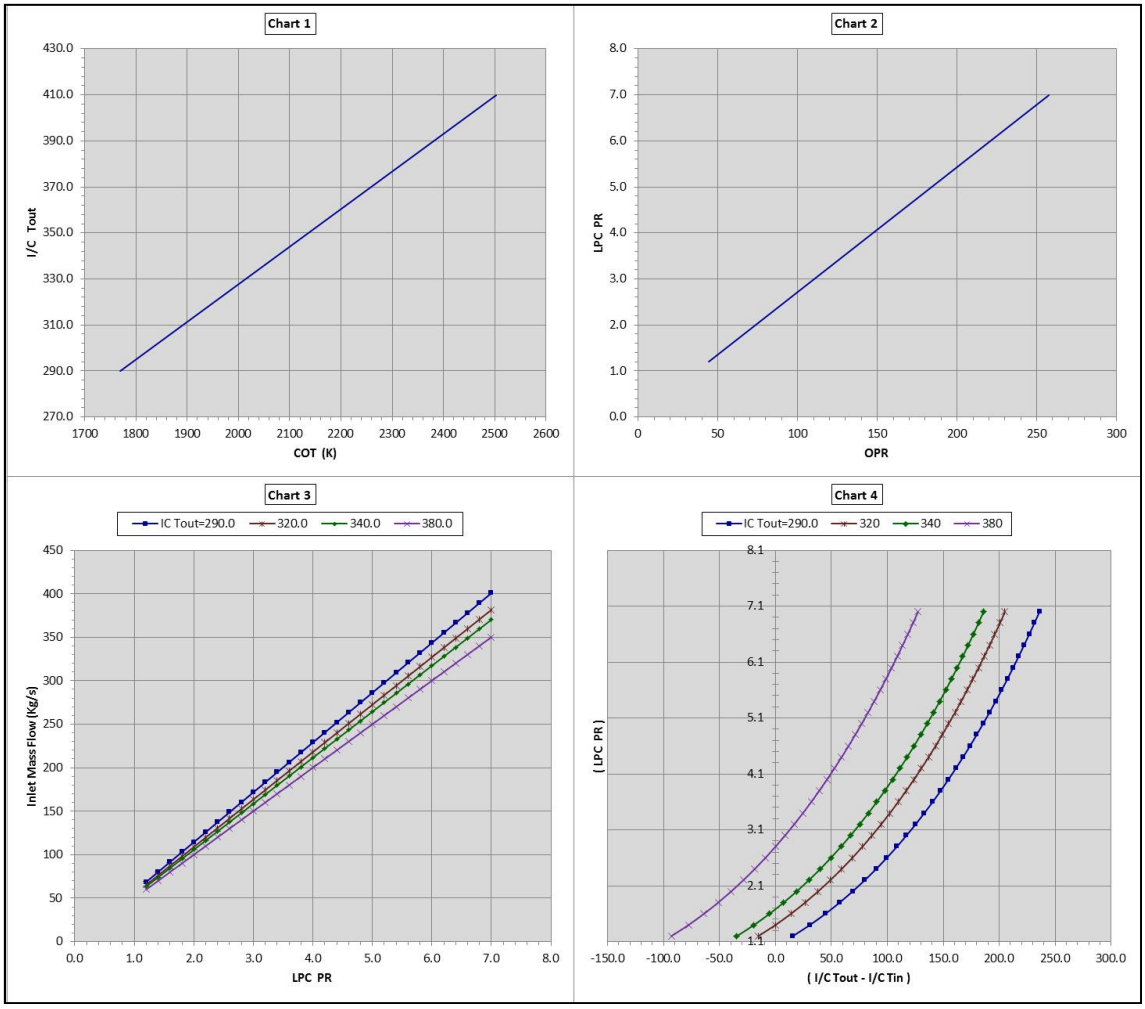

Figure 5-49 Derivation Conditions Effect on Design Point Mass Flow and Temperature Ratios of Three-spool IC engine

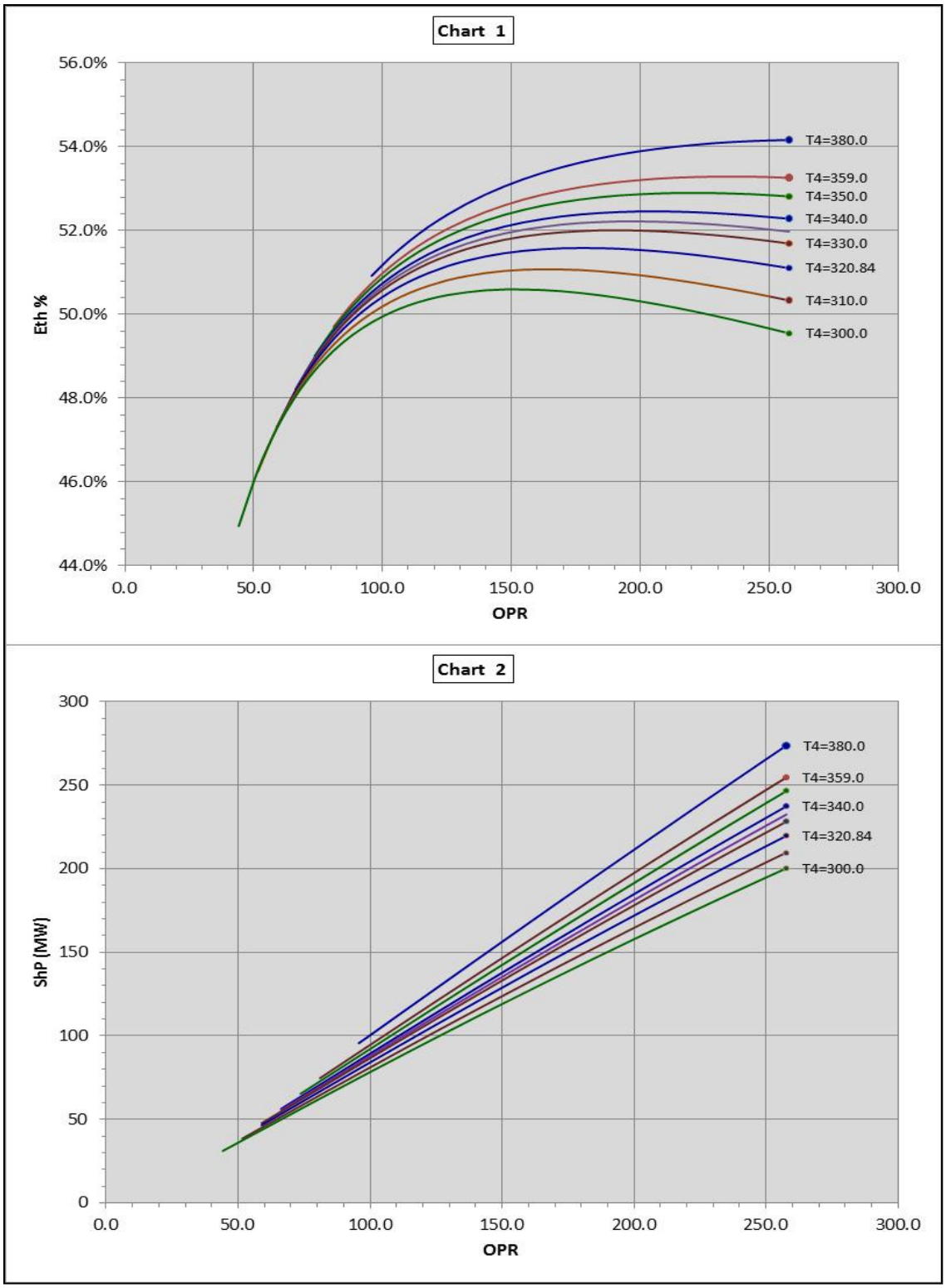

Figure 5-50 Three-spool Inter-cooled Cycle Design Point Thermal Efficiency and Shaft Power

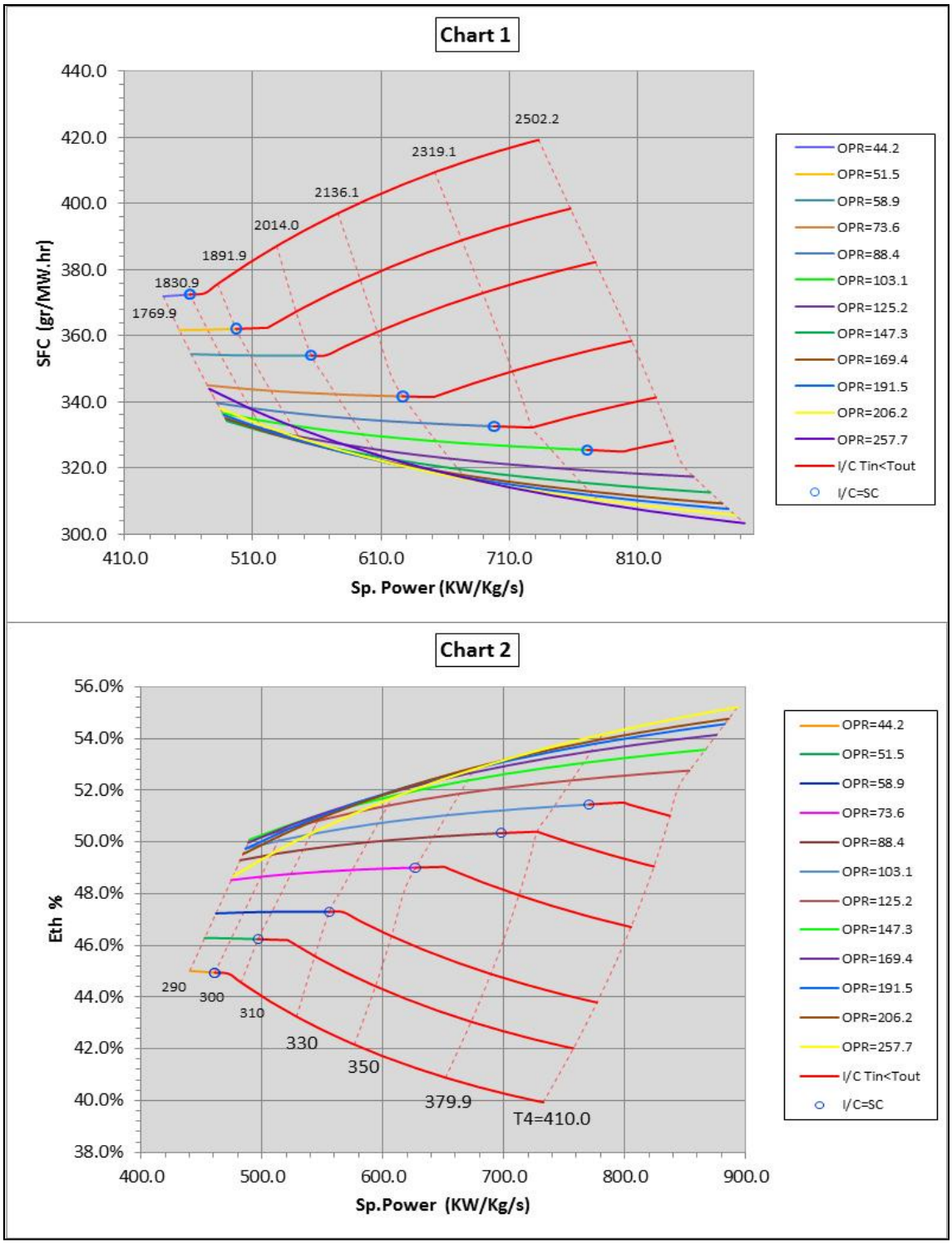

Figure 5-51 Specific Power and SFC of 3-Spool Inter-cooled Cycle Engine

6 OFF-DESIGN PERFORMANCE PREDICTION OF NEW DEVELOPED AERODERIVATIVE ENGINES

Although the design point calculations have been accomplished, it is still not enough to make the decision regarding whether or not the engine will satisfy the demands of its daily operation. Predicting engine operating behaviour during its operating life at different environmental conditions is very important and can be achieved through conducting the off-design calculations. Ambient temperature and pressure are among the most important factors affecting engine performance at off-design operation.

In this chapter engines will be simulated at different values of ambient pressure and temperature and their effect on performance will be calculated. An assumption has been taken of an ambient temperature range of $(45C^o\ to -15\ C^o)$ as the region of engine simulation. Apart from non-conventional recuperation cycles, there is no difference in design point characteristic whether the engine is designed in single direct load driving DD or free power turbine FPT, and they will only be affected by turbine efficiencies [85]. So, component efficiencies are assumed to be constant in design point calculations for both DD and FPT configuration due to the fact that engines with high values of TET reflect high design technology levels. However, these efficiencies will vary during off-design calculation, and methods of controlling engine operation at off-design will vary according to engine configuration and component arrangement.

The following sections include all off-design calculations for the majority of studied engines in both single direct load driving DD and free power turbine FPT arrangements.

6.1 Sustained High Pressure Rotor Components Only

Following the same order as with the design point calculation, the engines will be simulated in both arrangements of direct load driving DD and free power turbine drive FPT.

6.1.1 Single-Spool Simple Cycle Aeroderivative Engine

6.1.1.1 Single-Spool Simple Cycle Aeroderivative Engine IPT

Referring to previous design point calculations (see Table 5-2) of the single-spool simple cycle engine, engine performance characteristics, its power outputs and its components configuration are represented in Figure 5-1. As in Figure 4-3 the parent engine has some air extracted for LP rotor cooling and blow-off valve. Therefore, the same ratios of air have to be extracted at design point operation of the derived engines to maintain the commonality with the aircraft engine. However, when the engine operates at a different point rather than the design point, rotor cooling bleed can certainly be stopped as a result of removing the LP rotor. In addition, the bleed valve will be closed once the referred operating point is away from the surge line. Figure 6-1 illustrates charts of the engine's off-design performance in aforementioned arrangement.

In order to find the best bleed setting, three different scenarios have been chosen for settings of bleed valve and rotor cooling flow. According to engine stages numbering, bleed valve flow and rotor cooling bleed flow are represented by abbreviations $W21$ and $W24$. Investigated scenarios of bleed settings for best engine outputs are manipulated as follows:

1. Booth bleed flow applied $W_{21} = On,\ W_{24} = On$
2. FPT Cooling bleed only applied $W_{21} = Off\ , W_{24} = On$
3. DD Both Bleed flow are closed $W_{21} = Off\ ,\ W_{24} = Off$
4. DD Bleed valve only applied $W_{21} = On\ ,\ W_{24} = Off$

The best thermodynamically efficient choice as observed from Figure 6-1 is Scenario (3), which provides relatively highest efficiency and output power. If the main consideration was given to exhaust heat output however, bleed settings on Scenario (2) can be considered as the best. Scenario (2) must be applied when cooling is needed for free power turbine on two-shaft configuration as clarified in Figure 6-3. It is important to observe from Figure 6-4 that Scenario (3) represents the

best option for achieving highest output power for low values of combustor outlet temperature COT up to 1350 K, then the Scenario(2) later dominates for any ($COT > 1600\ K^o$).

Summing up, Scenario 3 has been chosen as the operating option which provides highest performance outputs of shaft power and thermal efficiency.

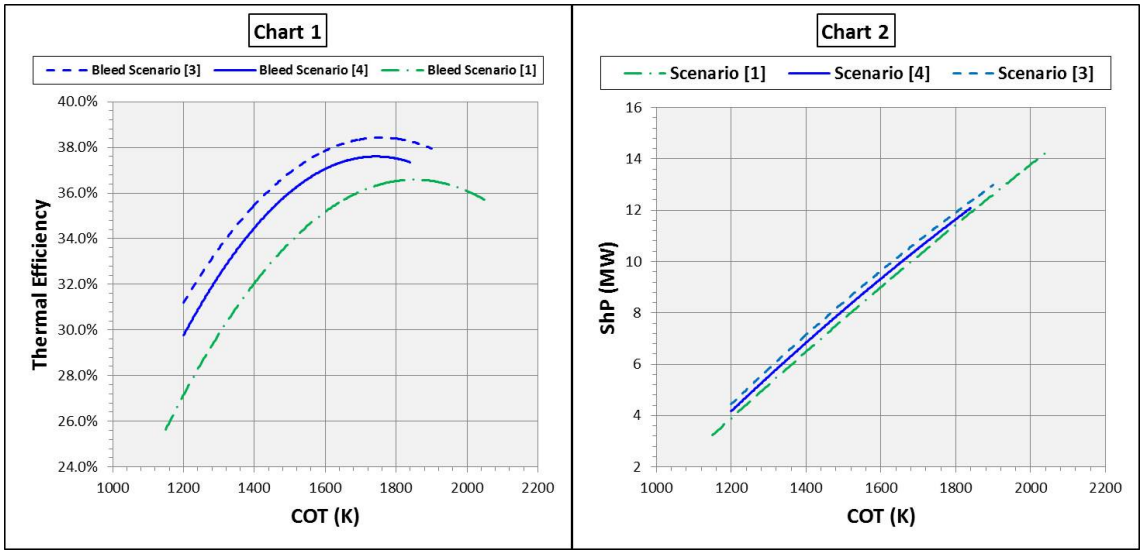

Figure 6-1 Bleed Settings Effect on Thermal Efficiency and Shaft Power for Single-Spool Simple Cycle Aeroderivative Engine with IPT Configuration

As shown in Appendices [E.1.1and E.1.2], two models are created using the Turbomatch code in order to perform the simulation. Bleed is extracted from the middle stages of the HP compressor, and then compression is divided into two pressure ratios of 2.11 and 7.11 which operate on the same shaft.

Simulation analysis of engine at off-design has been conducted under different values of ambient temperature, and its results are presented in Figure 6-2. Engine behaviour at different ambient conditions is represented by operating lines in Chart 4. It can be recognised that as the load varies, for a given day temperature, an engine with IPT configuration operates on a constant speed line on the compressor map. Also, as power demand moves from part-load to full load, engine operating point shifts up due to the increase in operating temperature COT as well as fuel flow. When an engine operates to satisfy base-load demand while day temperature increases, the engine will experience a reduction in non-dimensional speed $(N/\sqrt{T_1})$. As a

result, the engine operating point moves towards lower constant speed line and gets close to the surge line, and vice versa when day temperature decreases. It is clear from the same figure that at standard day ambient temperature the engine tends to surge at values of $(COT < 1150\ K^o)$.

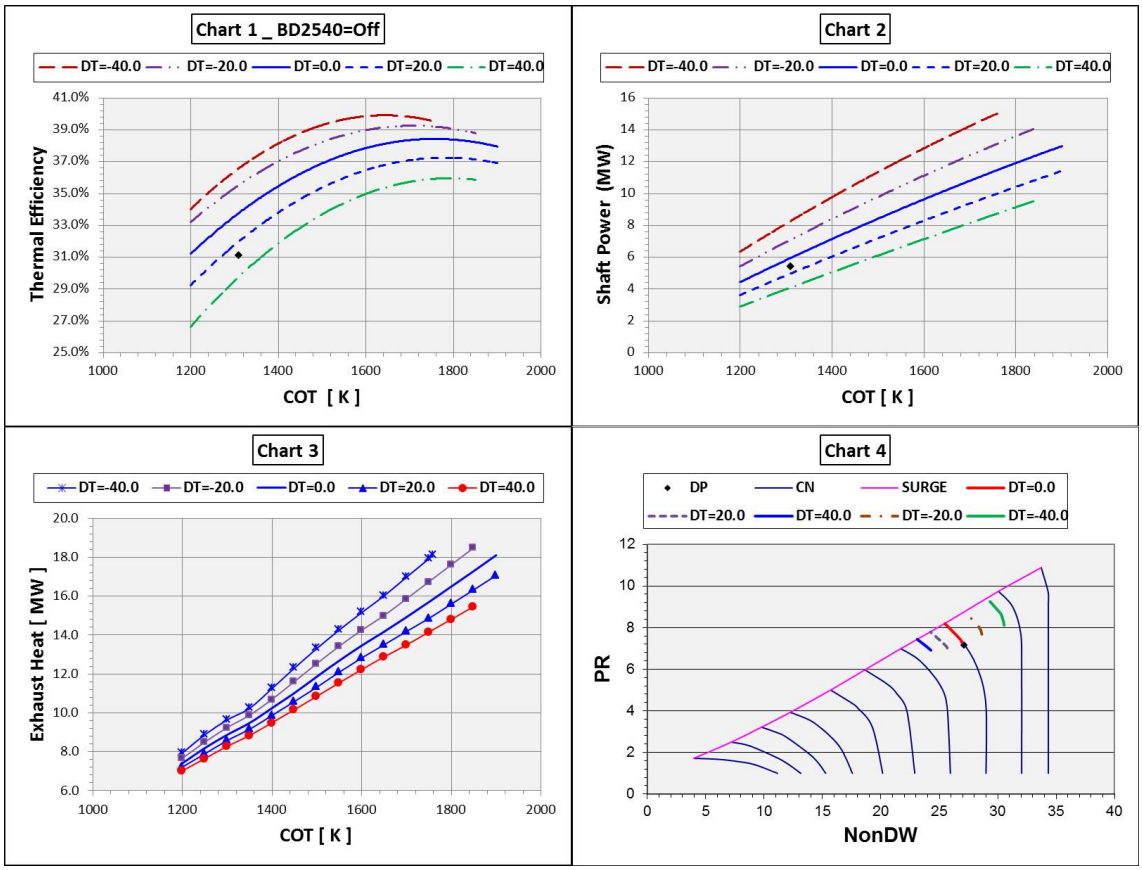

Figure 6-2 Off-Design Performance Features at Different Ambient Temperature of Single-Spool Simple Cycle with IPT Configuration

The effect of variation of ambient temperature on engine performance, regarding thermal efficiency, output power and exhaust heat output, is illustrated in Charts 1, 2 and 3, respectively. For a given operating temperature the decrease in ambient temperature results in an improvement, by the increase in both thermal efficiency and shaft output power. Also, the same impact is experienced on the engine's exhaust heat due to the increase in exhaust temperature. This trend is remarkably observed at high values of operating temperature for both ShP and Q, while it is opposite regarding thermal efficiency where the major effect noticed at low power settings. In addition, for operating on base-load scenario the lower the ambient temperature the lower COT required and hence fuel consumed. On the other

hand, the rise in day temperature leads to reduction in thermal efficiency owing to an increase in fuel consumption.

There will always be an optimum value of pressure ratio for every given ambient temperature, where the engine will operate at maximum efficiency. Furthermore, these optimum values vary with changes in day temperature, and the increase in ambient temperature leads to an increase in optimum pressure ratio and decreases values of maximum thermal efficiencies.

6.1.1.2 Single-Spool 2-Shft Simple Cycle Aeroderivative Engine FPT

Arrangement of the free power turbine, as shown in Figure 6-3 is within the objectives of investigating engines' off-design performance, when the power turbine rotates separately at different speeds. Calculation is performed and results plotted in Figure 6-4, and Figure 6-5.

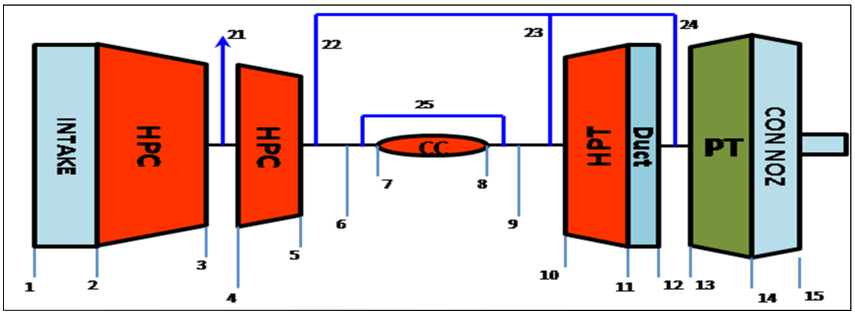

Figure 6-3 Single-Spool Simple Cycle Engine with FPT Configuration

Aforementioned bleed scenarios are investigated and illustrated in Figure 6-4, and it is clearly recognised that Scenario 3 still offers the highest thermal efficiency along with the increase in operating temperature. However, difference in thermal efficiency values between Scenarios 2 and 3 is dramatically lowered with the increase in operating temperature. Also, both scenarios provide similar values of shaft power from $COT = 1400K$ up to $COT = 1600K$, then later Scenario 2 slightly overtakes with higher values. Scenario 2 has been chosen for conducting further calculation of the engine's OD performance.

All off-design performance characteristics are displayed in Figure 6-5, and it can be seen that the engine has different operating lines relative to different ambient

conditions. At standard day temperature, operating at part-load by lowering operating temperature leads to move the operating point to a lower speed line. For every constant speed line, the engine tends to operate as close as possible to the optimum compressor pressure ratio which provides maximum efficiency. Furthermore, the operating line gets closer and closer to the surge line as the engine operates at lower combustor outlet temperature, hence lower power settings.

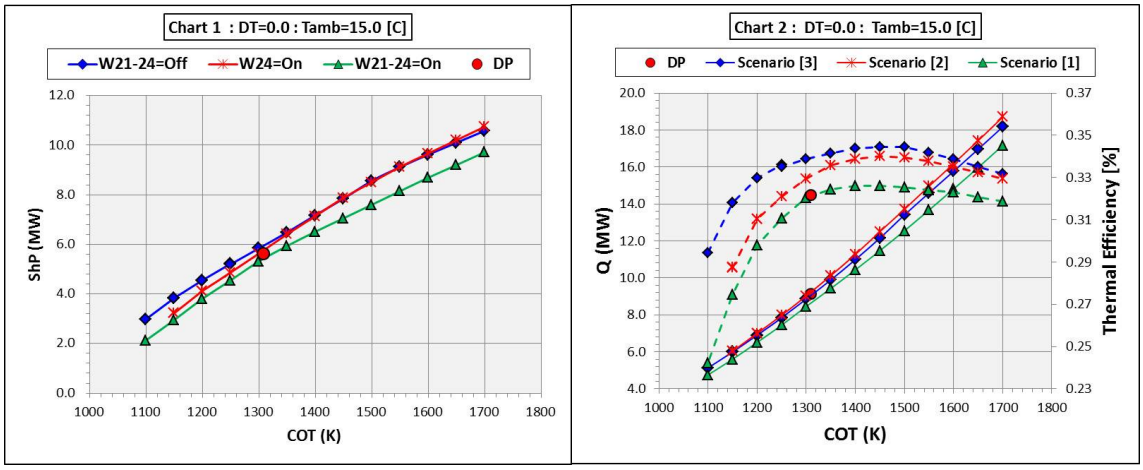

Figure 6-4 Bleed Settings Effect on Performance of Single-Spool Simple Cycle Aeroderivative Engine with FPT Configuration

Unlike the case of IPT arrangement, the power turbine is able to rotate at constant speed while the gas generator operates at different speeds due to the variation in operating or ambient temperatures. There is always an optimum value of gas generator speed, where the gas turbine engine achieves maximum efficiency for every given ambient temperature and power turbine speed [85]. Ambient temperature variation still shows the usual effect on the gas turbine engine operating point. If the ambient temperature decreases the operating point moves to a higher speed line and the whole operating line moves up allowing the gas generator to operate at higher COT. In addition, for a given operating temperature the lower ambient temperature the higher efficiency, heat output and output power achieved.

Calculation helps to determine engine operating limitations in which the engine's operating point crosses the surge line. It is concluded that the compressor bleed valve has to be involved at low power setting for values of ($COT < 1150\ K^o$) at standard day temperature to keep the operating point away from crossing the surge line.

Comparing with Direct Load Driving (IPT) arrangement on single shaft, the FPT engine's operating line seems to be less sensitive to ambient temperature variation. Moreover, thermal efficiency is less variable with changes in gas turbine rotational speed at different power load settings.

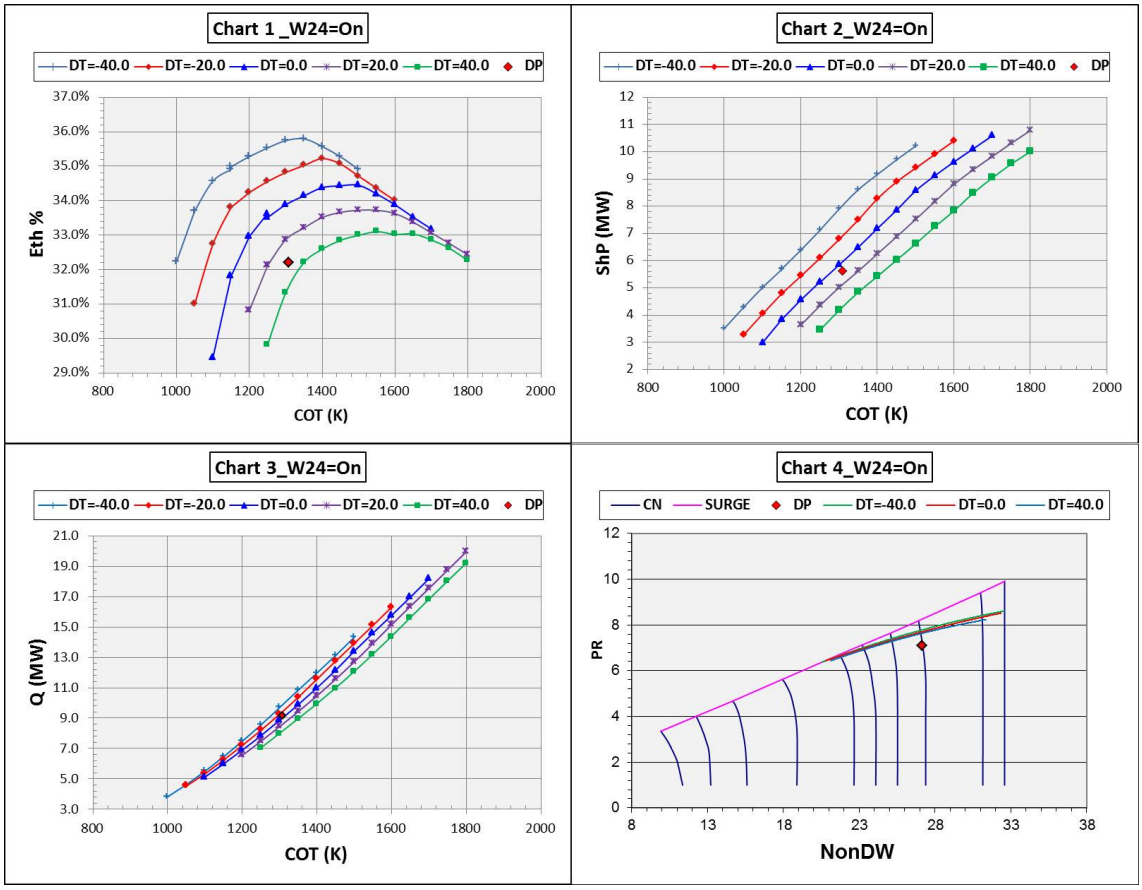

Figure 6-5 Off-Design Performance at Different Ambient Temperatures of Single-Spool Simple Cycle Engine with FPT Configuration

It can be generally observed from off-design calculation for both arrangements of IPT and FPT that increasing COT higher then around $1420\,K^{\circ}$ leads to decreased engine thermal efficiency. This reduction is not desirable and to improve it some modification is proposed to the HP compressor design. The objective is to move the engine design point, for a given value of COT, to lower non-dimensional rotational speed. Investigation of the newly modified engine's performance will be clarified in the following sections.

6.1.1.3 Modified Single-Spool Simple Cycle Aeroderivative Engine IPT

Considering the proposal of modifying the design of HP compressor, engine structures on both turbine arrangements are identical to Figure 5-1 and Figure 6-3 and used to create the Turbomatch model. Changes have been applied to the engine's relative rotational speed at off-design conditions and results are shown in Figure 6-6 and Appendix [B.1]. Thermal efficiency, as displayed in Figure 6-6, improves with the increase in engine operating temperature, and the dilemma of falling thermal efficiency down at the highest applicable operating temperatures in this gas turbine engine design is solved.

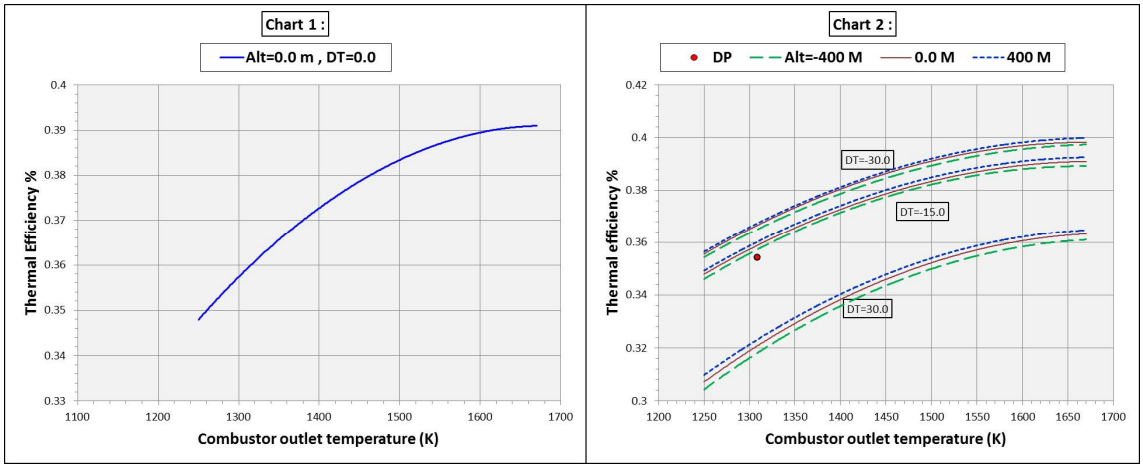

Figure 6-6 Off-Design Performance Features of the Modified Single-Spool Simple Cycle engine with IPT Configuration

Also, ambient temperature and altitude have the same common effect on the engine's OD characteristic. Shape or trend of engine operating line on the compressor map is shown in Appendix [B.1]. In addition, ambient pressure effect on engine performance has been studied through varying the altitude at different values of operating temperature.

6.1.1.4 Modified Single-Spool Simple Cycle Aeroderivative Engine FPT

A free power turbine arrangement is included in studying the proposed modifications in order to change relative rotational speed at off-design operation. Due to the highly sophisticated cooling technology, it is still possible to operate the engine at higher values of COT than the design point. All results in Figure 6-7 and Appendix [B.2] contain off-design characteristics, and it shows a better image of expressing

performance improvement under the proposed modification. Specific fuel consumption is included in the study of off-design performance characteristics and results show that the increase in operating temperature results in an improvement in specific fuel consumption SFC and a rise in thermal efficiency.

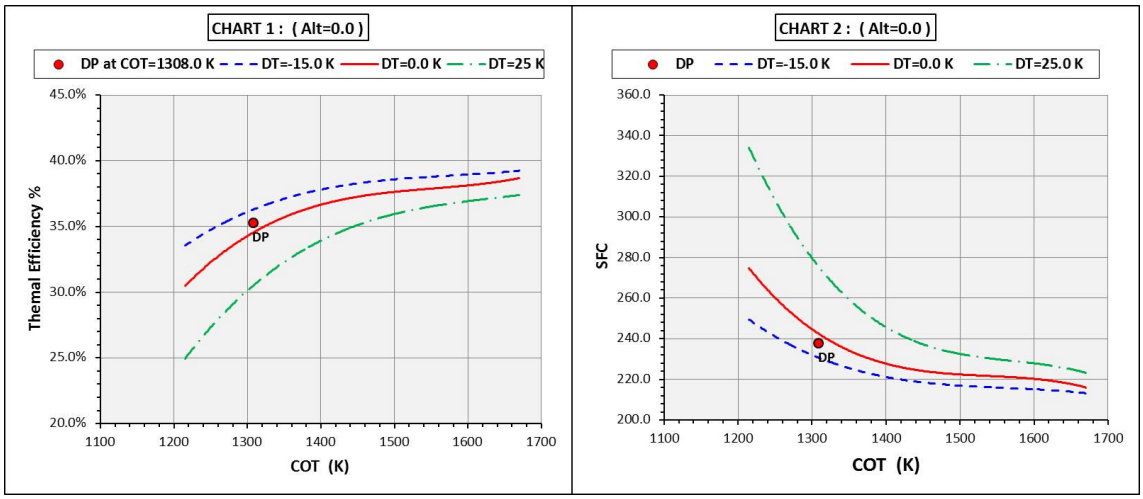

Figure 6-7 Ambient Temperature Effect on Thermal Efficiency of the Modified Single-spool Simple Cycle Aeroderivative Engine with FPT Configuration

Improvements in engine operating line on the compressor map are observed in Chart 2 in Appendix [B.2]. It shows that increasing COT moves operating temperature up to higher rotational speed and thermal efficiency. Engine operating temperature is increased up to the value of $COT = 1670.0\ K$, and its performance at maximum power is plotted on Charts (5, 6, 7 and 8) on appendix [B.2].

6.1.2 Single Spool Heat Exchanger Aeroderivative Gas Turbine

It has been found from the design point calculation that the most important factor in the simple cycle with heat exchanger is the temperature difference between HEx inlet temperature and compression exit temperature ($T_{15} > T_5$). In a free power turbine configuration, Figure 5-2 illustrates an engine sketch which shows the conventional way of locating Heat Exchanger before engine exhaust. In the following sections however, off-design calculation will also include the non-Conventional method of installing the HEx before power turbines on the single spool engine.

6.1.2.1 Single-Spool Conventional HEx Configuration Engines

Locating heat exchanger components at the engine exhaust is the commonly used arrangement in most applications where aero-derivative gas turbine engines are used as a prime mover. Figure 6-8 shows a configuration of single spool simple cycle engine with heat exchanger component installed on an IPT arrangement. Engine design point parameters are previously tabulated in Table 5-4. In order to perform performance simulation, the Turbomatch code is used referring to stage numbering in Figure 6-8 to create a model which presented in appendix [E.1.7]. Also, the engine schematic draw in Figure 5-2 has been used to create a model for FPT configuration which is included in appendix [E.1.8].

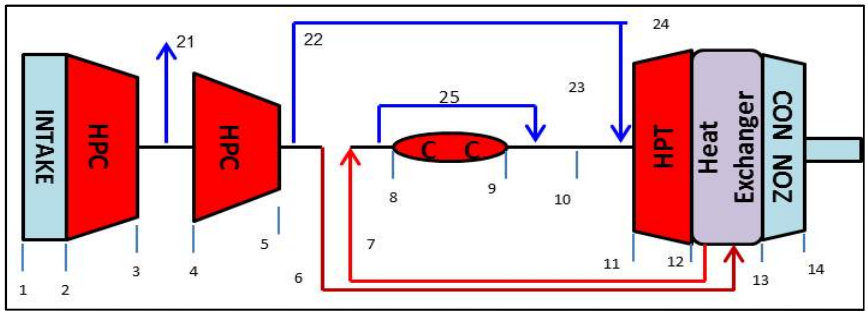

Figure 6-8 Schematic Diagram of Single-Spool Recuperated Cycle Aeroderivative Engine with IPT Configuration

Simulation analysis has been conducted and results for the investigated gas turbine engine in Direct Load Driving IPT arrangement are conveyed in appendix [B.3], while appendix [B.4] represents the off-design results for the free power turbine arrangement FPT.

It can be generally observed from results that operating lines of the HEx engine in both arrangements of IPT and FPT are similar in their trends to those previously plotted for simple cycle calculation. However, more attention should be given here to temperature differences between the heat exchanger inlet temperature and compression outlet temperature, which according to Figure 6-8 can be written as ($T_{12} > T_5$). Variation in recuperation temperature differences with engine operating temperatures COT is presented in Chart 2 in Appendices [B.3 and B.4] for IPT and FPT arrangements respectively.

Off-design performance of the engine on both IPT and FPT arrangement is compared and presented in Figure 6-9, Figure 6-10 and Figure 6-11. It can be seen that the engine with FPT configuration provides slightly better performance characteristics of output power and exhaust heat, while it achieves poor thermal efficiency in $(COT > 1350\ K)$ range. The increase in recuperation temperature difference for IPT at values of $(COT > 1380\ K)$ improves heat exchanger effectiveness and enhances thermal efficiency of gas turbine engine.

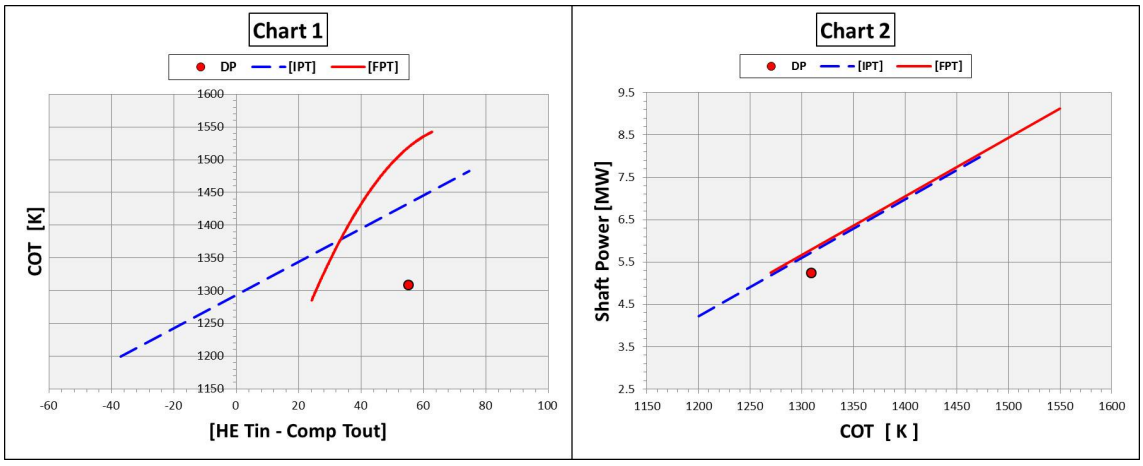

Figure 6-9 Shaft Power and Recuperation Temperature Differences for Single-Spool Recuperated Aeroderivative Engine with IPT and FPT Configurations

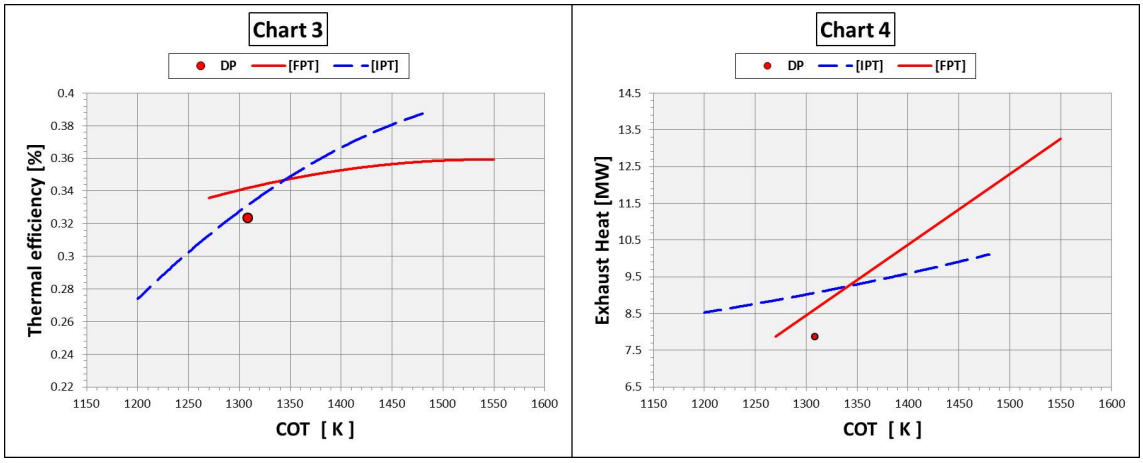

Figure 6-10 Thermal Efficiency and Exhaust Heat Output for Single-Spool Recuperated Aeroderivative Engine with IPT and FPT Configurations

Aeroderivatives with IPT arrangement as shown in Figure 6-10 achieve better efficiency at relatively high operating temperature, while they cannot maintain acceptable values at low operating settings without the need for variable inlet guide

vans $VIGVs$. In addition, similar to simple cycle analysis, FPT arrangement allows the engine to achieve high values of overall pressure ratio and mass flow at high COT which leads to gain higher shaft output power.

Moreover, results in Appendices [B.3 and B.4] highlight that the FPT engine will have better part-load efficiency for relatively higher ambient temperatures (more than the standard) within its nominal operating range line. Therefore, for any values of ($COT < 1250$), the heat exchanger inlet temperature needs to be controlled using $VIGVs$ or $VANs$ and will vary individually and depends on ambient temperature for any ($COT > 1250$).

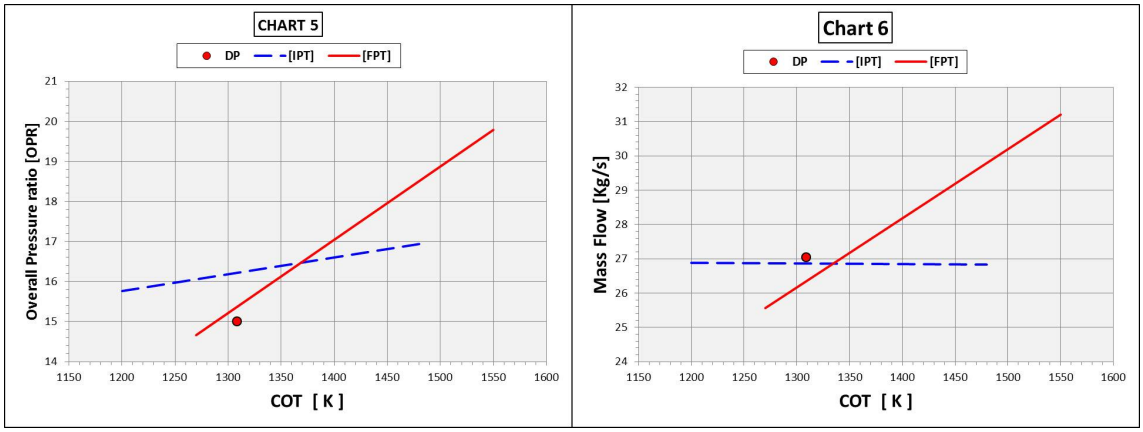

Figure 6-11 Mass Flow and Pressure Ratio Variation of Single-Spool HE_X Aeroderivative Engine with IPT and FPT Configurations

Load reduction in the IPT single-spool engine results in a severe fall in exhaust gas temperature, which in turn leads to low HEx inlet temperature. Compressor variable inlet guide vans $VIGVs$ and Turbine variable area nozzles $VANs$ at the inlet of the turbine have been widely used to maintain T_{15} for a wide range of part-load operations up to 40%. It is very important to understand that closing the $VANs$ decreases mass flow, and there are always certain values where the operating point comes close to the surge line where bleed valves must be used.

6.1.2.2 Single-Spool non-Conventional HEx Configuration FPT

Another arrangement of installing heat exchanger before FPT is also investigated and called 'non-Conventional or Alternative' configuration. According to stage numbering of engine construction presented in Figure 5-3, the Turbomatch

model has been created (see appendix E.1.9) to conduct all off-design simulation. Values of engine off-design parameters are previously shown in Table 5-5, which obtain different values of exhaust heat and output power than conventional HEx configuration. All off-design simulation results at different ambient conditions and load variations are shown in appendix [B.5]. Normal operating limitations of HEx are seen in Chart 2 of appendix [B.5] at different values of ambient temperature. Negative values of $(T_{12} > T_6)$ indicate where $IGVs$ or $VANs$ need to be used in order to raise heat exchanger inlet temperature and enhance gas turbine cycle efficiency.

Results in Appendix [B.5] generally show that increasing operating temperature and fall in ambient temperature lead to an increase in generated power and an improvement in cycle thermal efficiency. However, it can be seen from Charts 4 and 6 that there is always an optimum value of operating temperature for all values of ($T_{amb} < 25\ C^{\circ}$), where highest COT doesn't does not gain the highest thermal efficiency. Despite the increase in HEx inlet temperature with rising ambient temperature (see Charts 7 and 8), recuperation temperature difference is still falling down due to the relatively higher increase in compression system discharge temperature.

A comparison between conventional and non-conventional HEx configuration is conducted through the observations taken from results presented in Figure 6-12 and Figure 6-13. Extra results for engine off-design performance characteristics for this comparison are plotted in Chart 13 to Chart 16 on appendix [B.5]. Recuperation temperature difference is remarkably increased owing to significant rise in heat exchanger inlet temperature occurred from using a non-conventional arrangement (see Chart 13) on appendix [B.5]. As a result thermal efficiency significantly improved for the whole range of operating temperature and the alternative arrangement appears to be the superior in these terms.

In contrast, significant reduction in both shaft power and exhaust heat output is experienced by the engine, which is caused by remarkable relative reduction in engine exhaust temperature as seen in Chart 14 in appendix [B.5].

To summarise, using the alternative arrangement enhances engine cycle thermal efficiency with the extra penalty of loss in engine shaft power and exhaust output heat.

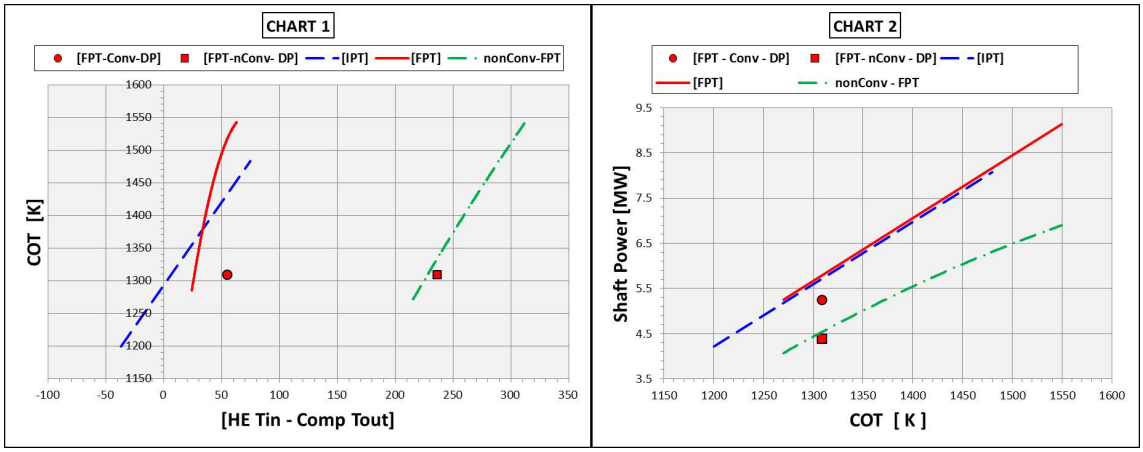

Figure 6-12 Recuperation Temperature Differences and shaft Power of Single-Spool Conventional and non-Conventional Recuperated Engine with FPT

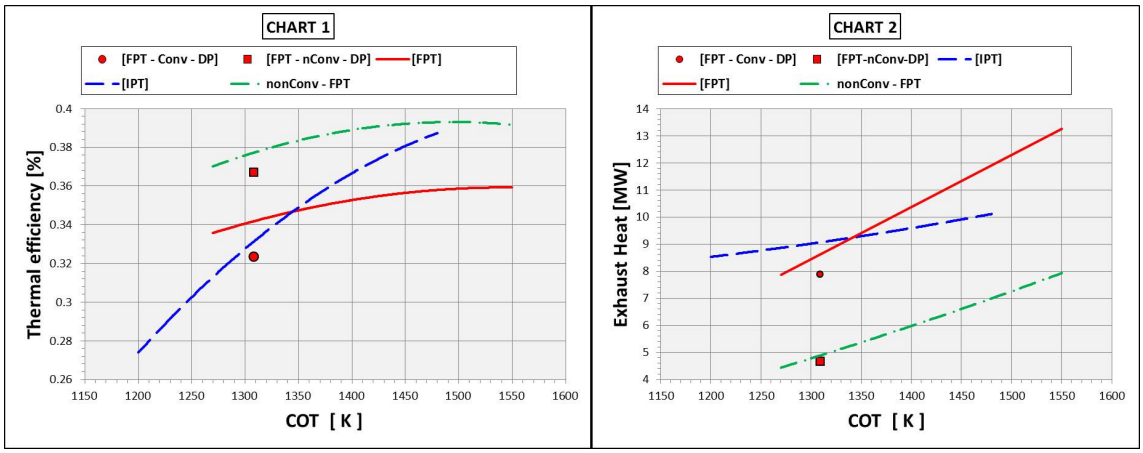

Figure 6-13 Performance Comparison of Single-spool Conventional and non-Conventional Recuperated Aeroderivative with IPT and FPT

6.1.3 Two-Spool Simple Cycle Aeroderivative Engines

In this section, the two-spool simple cycle derivative gas turbine engine will be simulated at off-design operation on both IPT and FPT configuration. The schematic draw of engine structures illustrated in Figure 5-4 and Figure 6-14, which is associated with direct load driving IPT and free power turbine FPT configurations respectively, are used to create two Turbomatch models, as observed in appendices

[E.1.5 and E.1.6]. By looking back at cooling bleed and bleed valve scenarios, Scenario 2 has been chosen in order to conduct the simulation analysis for the two-spool simple cycle engine with IPT and FPT arrangements. It was previously seen in design point calculation that depending on value of new LP pressure ratio, there will be many options for designing aeroderivative gas turbine engine.

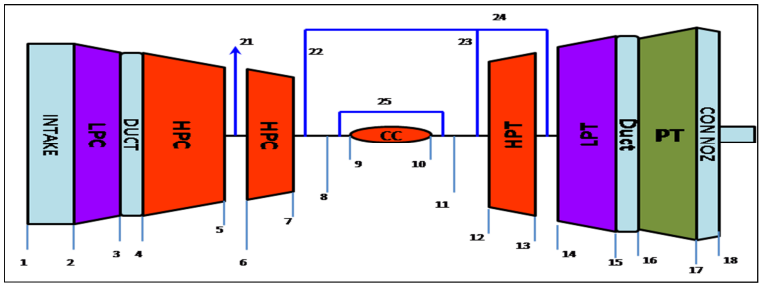

Figure 6-14 Two-Spool Simple Cycle Engine with FPT

Therefore, according to design point calculation in Section [5.1.3], an engine with $(PR_{lc} = 3.5)$ has been chosen to be simulated and rest of its design point characteristics are illustrated in Table 6-1.

Table 6-1 Design Point Characeristics of Two-spool Simple Cycle Engine(1)

$W\ (^{K}/_{s})$	$ShP\ (MW)$	ζ_{th}	$Q\ (MW)$	PR	$COT\ (K^{O})$
77.755	39.7	46.06	37.01	52.5	1939.0

Results are generated from the off-design performance simulation of the engine with IPT configuration and considered in Appendix [B.6] and Figure 6-15, while performance simulation results of the engine with FPT arrangement are presented in Appendix [B.7] and Figure 6-16.

Starting with results of the IPT arrangement in Figure 6-15, it is observed that for a given day temperature the LP compressor operates on a constant speed line and the operating point moves vertically, which seems to have the same operating line as the single-spool single-shaft in IPT arrangement. However, the operating point takes the opposite direction on the line when the load varies. It means that when the engine operates at part-load, the operating point moves towards the surge line. It is a unique behaviour relative to the IPT single-spool simple cycle, and the reason is that

values of constant temperature ratio lines of two-spool simple cycle IPT normally decrease towards the surge line. Therefore, at part-load operating temperature COT falls down and the value of temperature ratio is reduced, which leads the operating point to shift vertically close to the surge line. Conversely, the HP compressor operates in the same way as the single-spool two-shaft simple cycle engine. The operating point moves from one speed line to another when the load increases or decreases.

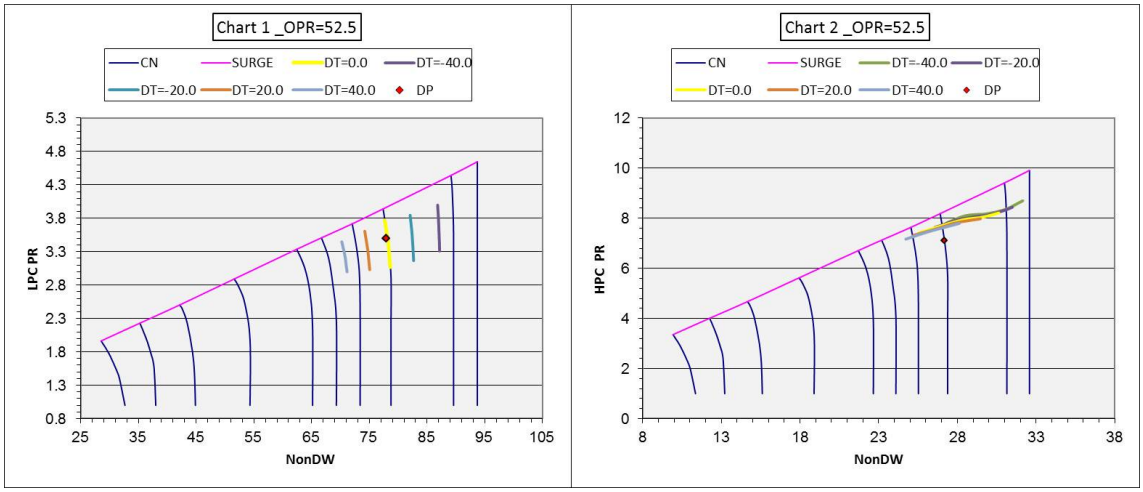

Figure 6-15 Operating Line on Compressor Maps of Two-spool Simple Cycle Aeroderivative Engine with IPT Configuration

A further observation is that with the change in load, the operating temperature on the LP compressor tends to cross surge line faster than the HP compressor. In other words, the low pressure compressor seems to be more sensitive to variation in rotational speed at off-design conditions. It is important to mention that the design point on the HP compressor is below the operating line at the standard temperature due to keeping the bleed valve opened at the design point to maintain features of the parent aero-engine's components at the design point.

The effect of ambient temperature on engine performance was included in the simulation, and it shows its common effect on operating points in both HP and LP compressors. In both engine arrangements, increase in ambient temperature results in a decrease in both thermal efficiency and shaft power, as shown in Charts 1, 2, and 3 in appendices [B.6 and B.7]. Moreover, the operating point on the LP compressor moves to a lower constant speed line when ambient temperature

increases due to a reduction in the non-dimensional speed of ($\frac{N}{\sqrt{T}}$). There is always an optimum value of engine operating temperature for maximum thermal efficiency. As day temperature falls down the optimum operating temperature COT decreases with an increase in cycle thermal efficiency.

Referring to performance results of the engine with FPT arrangement presented in Figure 6-16, the LP compressor has a different operating line than the IPT arrangement. It has a relatively horizontal operating line which is similar to the operating line of the single-spool single-shaft with FPT. However, the HP compressor seems to have a shorter operating line and it tends to move towards the surge line faster than the LP compressor. So, at part-load operation it is the HP compressor which needs to be controlled using the bleed valve to keep its operating line away from surge.

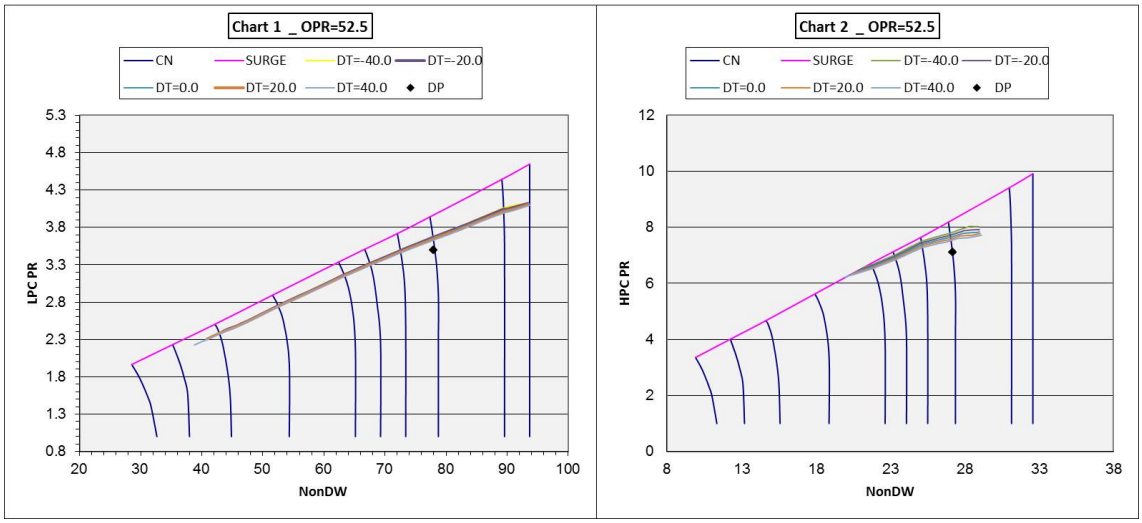

Figure 6-16 Operating Line on Compressor Maps of Two-spool Simple Cycle Aeroderivative Engine with FPT Configuration

Comparing with the engine in direct load driving arrangement, the engine with FPT is recognised as relatively less sensitive to variation in ambient temperature. Variation in thermal efficiency with speed is remarkably smaller. Moreover, surge problems can be prevented by the ability to operate the gas generator at different speeds than the power turbine. It is also observed that the engine can operate at relatively lower power settings up to ($COT = 1500\ K^o$) using free power turbine without additional control method, while the lowest it can go is down to ($COT =$

$1940\ K^o$) on integrated power turbine arrangement IPT where bleed valve should be involved.

Results generated from creep life estimation are presented in Chart 5 on both appendices [B.6 and B.7]. Results highlight the drawback of unacceptable life time cycle of the designed gas turbine engine. Therefore, smaller engines with lower pressure ratios of ($OPR = 30$) are assumed to be investigated where ($PR_{lc} = 2.0$). Engine design point characteristics and parameters are presented in Table 6-2.

Table 6-2 Design Point Characeristics of Two-spool Simple Cycle Engine(2)

$W\ (^{K}/_{s})$	$ShP\ (MW)$	ζ_{th}	$Q\ (MW)$	PR	$COT\ (K^O)$
48.45	17.257	40.97	19.5708	30.0	1630.7

Less output power and lower thermal efficiency will be generated and achieved from the new derivative owing to the reduction in design point pressure ratio. All off-design simulation analysis has been conducted for the FPT arrangement and results are plotted in Figure 6-17 and appendix [B.7].

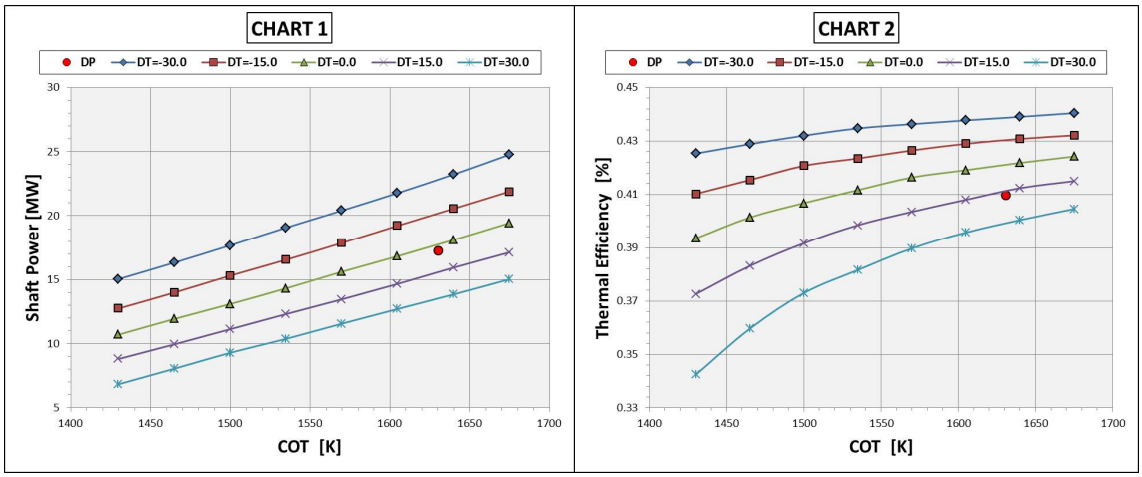

Figure 6-17 Shaft Output Power and Thermal Efficiency of Two-Spool Simple Cycle Aeroderivative Engine with FPT Configuration

Operating temperature at the design point is among the state of the art technology and creep calculation (see appendix B.7) shows clearly the life time cycle of the designed derivative engine with $OPR = 30$. The thermal efficiency trend is improved as engines always achieve higher thermal efficiency with the increase in operating temperature up to the design point. In other words, there is not an optimum

value of COT for maximum efficiency along the operating range and the highest combustor outlet temperature applied up to $1675\ K^{\circ}$ is the highest thermal efficiency achieved. For more details regarding all engine off-design performance at maximum operating temperature, for different values of ambient temperature and altitudes, see appendix [B.7].

6.1.4 Two-Spool Inter-cooled Cycle Aeroderivative Engines

Design point analysis concluded that in order to maintain turbine inlet non-dimensional mass flow equal at design point, HP cycle temperature ratio (T_{12}/T_4) on Figure 6-18] must be kept constant. Also, installing the inter-cooler provides the ability to control temperature ratio through controlling the inter-cooler outlet temperature (T_4) at the design point. Engine structures in Figure 5-8 and Figure 6-18 used in creating performance models (see appendices E.1.5 and E.1.6) for both IPT and FPT arrangements, respectively.

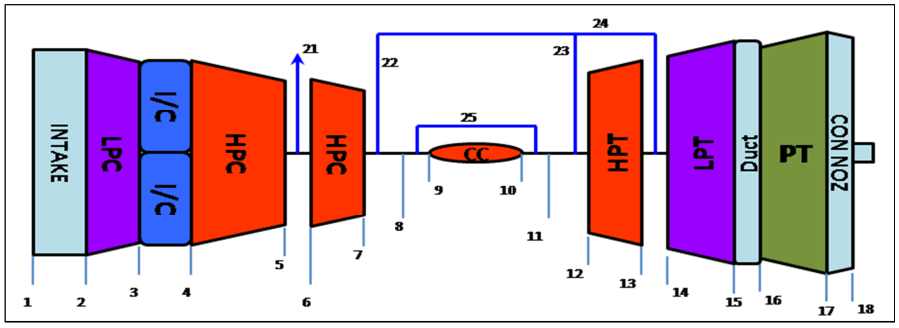

Figure 6-18 Two-Spool Inter-cooled Cycle Engine with FPT

The installed inter-cooler is operated at off-design subject to the assumption of keeping the inter-cooler outlet temperature roughly higher than ambient temperature by about $10.0\ C^{\circ}$. This means $(T_4 = 10.0 + T_{am})$ throughout all off-design simulation calculation. The improved ability to control intercooler outlet temperature T_4 at the design point allows us to design more than one engine at the same value of OPR. It has been found that one designed engine can operate at $(COT = 1387.63\ K^o)$ and must have $(T_4 = 305.4\ K^o)$, while another one can be designed with $(COT = 1630.72\ K^o\ and\ T_4 = 358.993\ K^o)$ for the same OPR. Table 6-3 contains design point characteristics of two selected inter-cooler engines to be compared through their performance simulation analysis.

Firstly, considering the engine arrangement illustrated in Figure 6-18, the performance of the two selected engines has been compared and the results illustrated in Figure 6-19 and Figure 6-20. The aim is to discover whether or not designing the engine at low turbine entry temperature and operating it at higher possible values of COT at off-design provides the best performance outputs.

Table 6-3 Design Point Characeristics of Two-spool Intercooled Cycle Engine

	$W\ (^{K}/_{S})$	I/C $T_{out}(K^{o})$	$ShP\ (MW)$	ζ_{th}	$Q\ (MW)$	OPR	$COT\ (K^{O})$
Eng. 1	89.16	305.4781	25.54	46.06	15.73	52.5	1387.63
Eng. 2	82.244	358.993	31.268678	43.61	25.3306	52.5	1630.7256

Secondly, a comparative study of engine (Eng.2) is conducted based on its performance characteristics on IPT and FPT arrangements and results are shown in the aforementioned Figures. More details on performance characteristics for both engines are included in Appendices [B.8 and B.9] for FPT and IPT configurations, respectively.

Generally, the results in Appendices [B.8 and B.9] show that operating lines for both intercooled engines matches behaviour or trends of simple cycle gas turbine engines for both configurations. The free power turbine design provides the ability to operate the engine at low power settings up to 15 MW without the need to use the blow-off valve or $VIGVs$ in hotter environments. Although engines with the FPT arrangement has better surge control at off-design, engines designed with IPT has better optimum thermal efficiency at high operating temperatures. It is owing to the fact that the operating point moves away from surge when operating temperature increase and it will be shifted towards higher constant efficiency line.

It can be seen from Chart 2 in Figure 6-19 that there is an optimum value of operating temperature which provides the maximum thermal efficiency. Gas turbine engines which are designed with relatively higher operating temperature of $1630.72\ K^{o}$ are able to enhance engine thermal efficiency, and shifts optimum operating point to higher values of operating temperature. That means that it is better

to design the engine at the highest possible firing temperature than to design it at low COT and operate at higher possible value at off-design. However, engine designed at relatively low COT for the same OPR is able to provide better shaft power and output heat when operated at higher values of combustor outlet temperature at off-design operation.

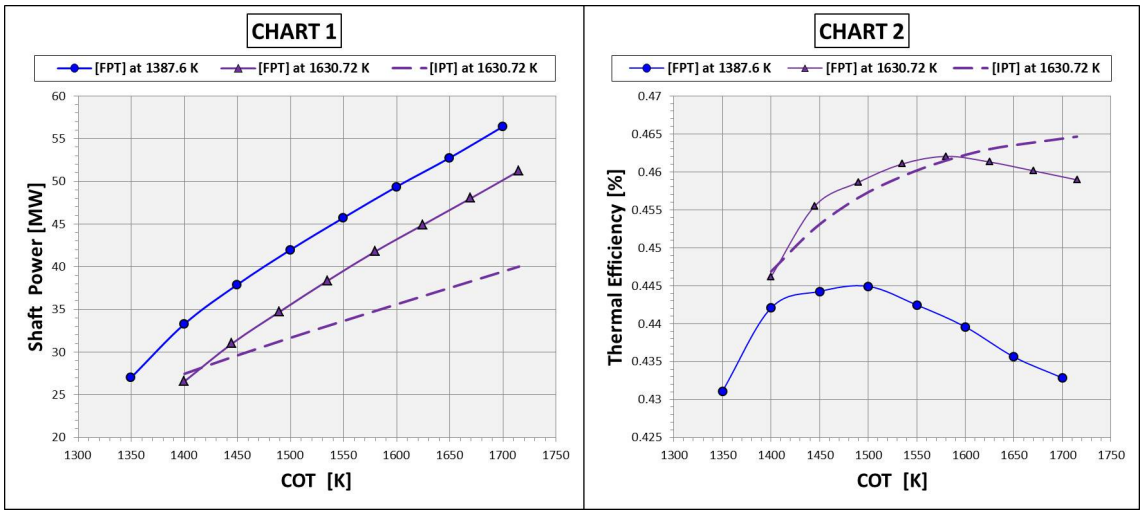

Figure 6-19 Thermal Efficiency and Shaft Power Comparison of Two-spool Intercooled Aeroderivative Engines with IPT and FPT Configurations

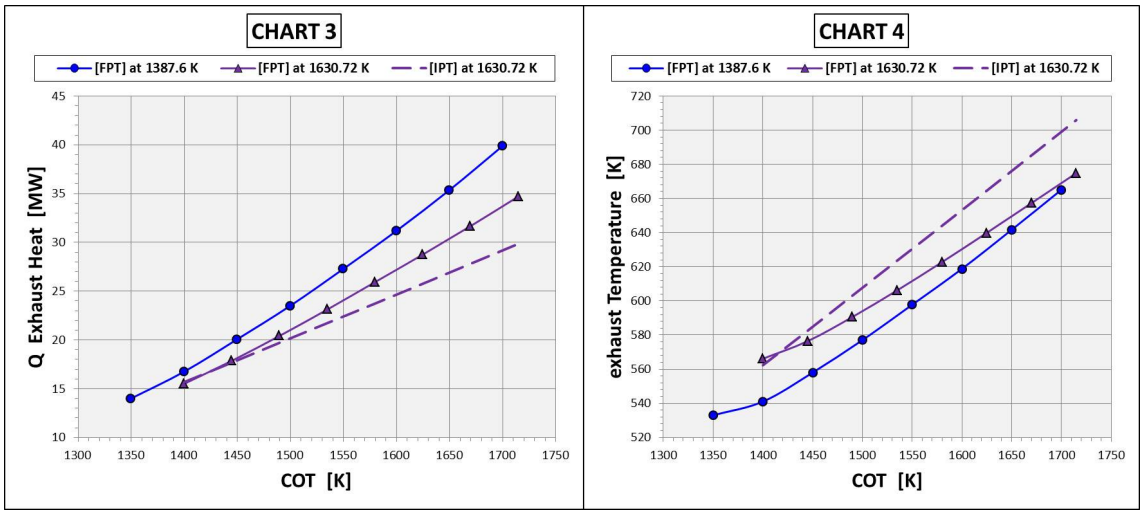

Figure 6-20 Exhaust Temperature and Heat Output Variation of Two-Spool Intercooled Aeroderivative Engine with IPT and FPT Configuration

As it is previously concluded, it can be noticed that designing the engine with a free power turbine allows the engine to achieve better off-design control and enhances the thermal efficiency at part-load operation. In addition, as seen in Figure 6-20, an engine on IPT design provides poor exhaust heat output and exhaust

flow leaves at higher temperature values than the FPT design. As seen from Chart 7 on appendix [B.8], it is the negative effect of the relatively low exhaust gas mass flow. Exhaust gas flow leaves the engine with IPT configuration at much lower values than in the engine with free power turbine configuration.

6.1.5 Two-Spool Heat Exchanger Cycle Gas Turbine Engines

Increasing pressure ratio or/and turbine entry temperature are well known as the key factors enhancing an engine's cycle thermal efficiency and output power. In addition, applying the heat exchanger concept will further improve cycle thermal efficiency. In this section, two concepts of conventional and alternative recuperation are investigated regarding free power turbine configuration.

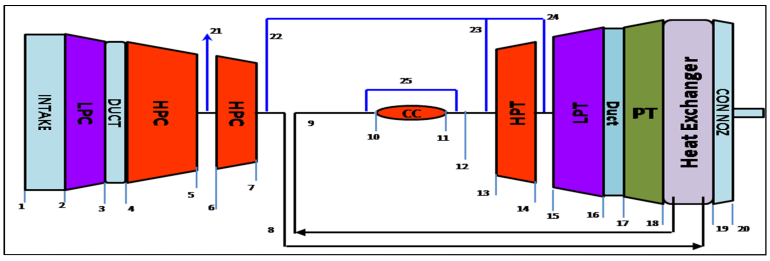

Figure 6-21 Schematic Diagram of Two-Spool HEx Engine with FPT Configuration

6.1.5.1 Two-Spool Conventional HEx Configuration Engines

The engine is simulated on FPT configuration, which is shown in Figure 6-21 with a heat exchanger component located at the engine exhaust. Aforementioned Scenario number 2 of bleed settings is selected throughout the off-design performance simulation. The design point characteristics of the selected engine for simulation are tabulated in Table 6-4 below.

Table 6-4 Design Point Characteristics of Two-spool HEx Cycle Engine

$W\ (^{K}/_{S})$	$ShP\ (MW)$	ζ_{th}	$Q\ (MW)$	PR	$COT\ (K^{O})$
33.7	8.75	36.11	11.92	19.5	1423.5

According to stage numbering in Figure 6-21, a model of input data file, created using Turbomatch as seen in appendix [E.1.10], was used to perform the simulation.

First of all, the engine has been simulated at standard $VIGVs$ and $VANs$ for compressors and turbines and off-design characteristics are plotted on Charts 1 and 2 in appendix [B.10]. Investigation determines limitations of operating the heat exchanger which considered recuperation temperature differences of ($T_{18} > T_7$). It became possible to determine positions where $VIGVs$ and $VANs$ are needed to be used at different values of ambient temperatures to maintain enough HEx inlet temperature to satisfy the recuperation condition. It can be observed that the engine can be operated at any ($COT > 1550$) for any ambient temperature without the need for controlling HEx inlet temperature. However, it is necessary to use $VIGVs$ or/and $VANs$ as COT gradually decreases.

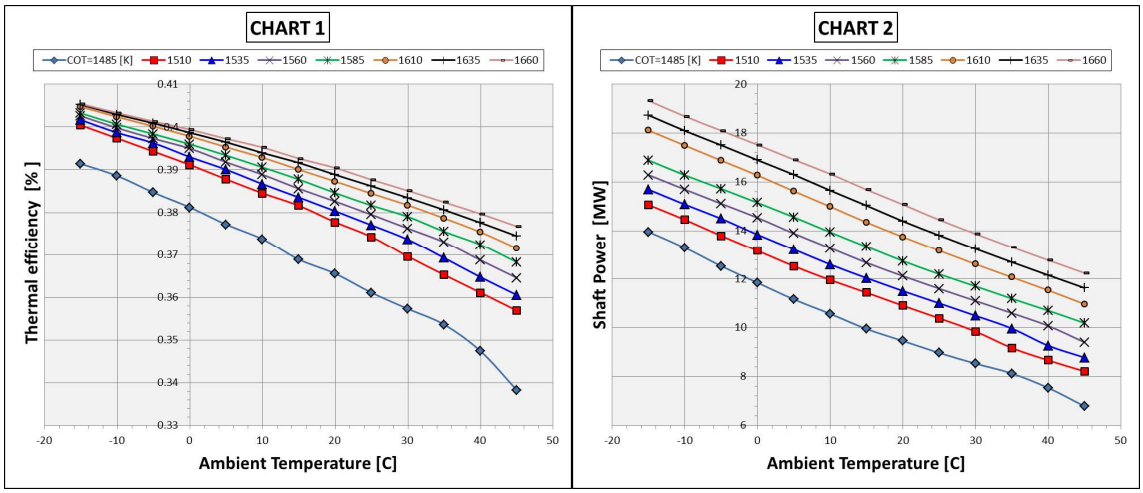

Figure 6-22 Shaft Power and Thermal efficiency of Two-Spool Conventional HEx Aeroderivative Gas Turbine Engine with FPT Configuration

Using $VANs$ to control the exhaust temperature is very important and it has been emphasized that it should be used for part-load up to 40% from full power. Turbine variable area nozzles are used in order to increase heat exchanger inlet temperature and keeping ($T_{18} > T_7$). Results of all off-design performance calculations are presented in Figure 6-22 and Charts 3, 4, 5, and 6 in appendixes [B.10]. Compared to the single-spool HEx cycle, the increased pressure ratio helped in enhancing engine thermal efficiency achieved. As shown in Charts 3 and 4 in appendix [B.10] different values of turbine $VANs$ angles were used according to values of COT and ambient temperature. Also, it shows the ability of matching the condition of maintaining ($T_{18} > T_7$) throughout the investigated operation range. The effect of ambient conditions on engine performance outputs of thermal efficiency and shaft

power is explored in Figure 6-22. In addition, variation of exhaust heat output and heat exchanger inlet temperatures are highlighted in Charts 5 and 6 in appendix [B.10]. Maximum HEx inlet temperature was reached at the worst operating scenario of maximum power and ambient temperature is still lower than the aforementioned limitations of thermal barrier of heat exchanger.

6.1.5.2 Two-Spool non-Conventional HEx Configuration Engines FPT

The engine's off-design performance investigation of two-spool recuperated gas turbine engine also considers the other option of locating the HEx component between turbines, as illustrated earlier in Figure 5-19 regarding the FPT arrangement. Stage numbering shown in Figure 5-19 is used for the Turbomatch model as illustrated in appendix [E.1.11] in order to conduct the off-design simulation. It is very important to understand that the HEx inlet temperature will be significantly increased and needs to be investigated and monitored especially at high values of operating temperature. As was seen previously in Section 5.1.5.2.2, using non-Conventional helped to satisfy recuperation condition ($T_{16} > T_7$) at a higher value than in the conventional recuperation cycle. Therefore, the engine providing ($OPR = 30.0$) has been selected for off-design simulation and its design point characteristics are included in Table 6-5.

Table 6-5 Design point Characteristics of Two-spool non-Conventional HEx Engine with FPT

$W\ (^{K}/_{S})$	$ShP\ (MW)$	ζ_{th}	$Q\ (MW)$	PR	$COT\ (K^{O})$
48.45	13.08	42.36	12.3602	30.0	1630.73

It can be seen that a recuperation condition of maintaining ($T_{16} > T_7$) is satisfied for all investigated off-design operating ranges (see Figure 6-23) without the need for varying $VANs$ angle from the design point. Of course, increasing engine pressure ratio and operating temperature results in rising output power and enhancing thermal efficiency, as seen in Figure 6-24. More detailed results for engine off-design performance characteristics are presented in appendix [B.11]. The engine's operating lines on both compressor maps are displayed and show similar trends to all two-spool FPT engines with simple or intercooled cycles. Heat exchanger inlet

temperature is calculated at maximum operating temperature of 1640 K° and for maximum ambient temperature of 45 C° and found to be around 1080 K° which is still acceptable within the proposed material thermal barriers.

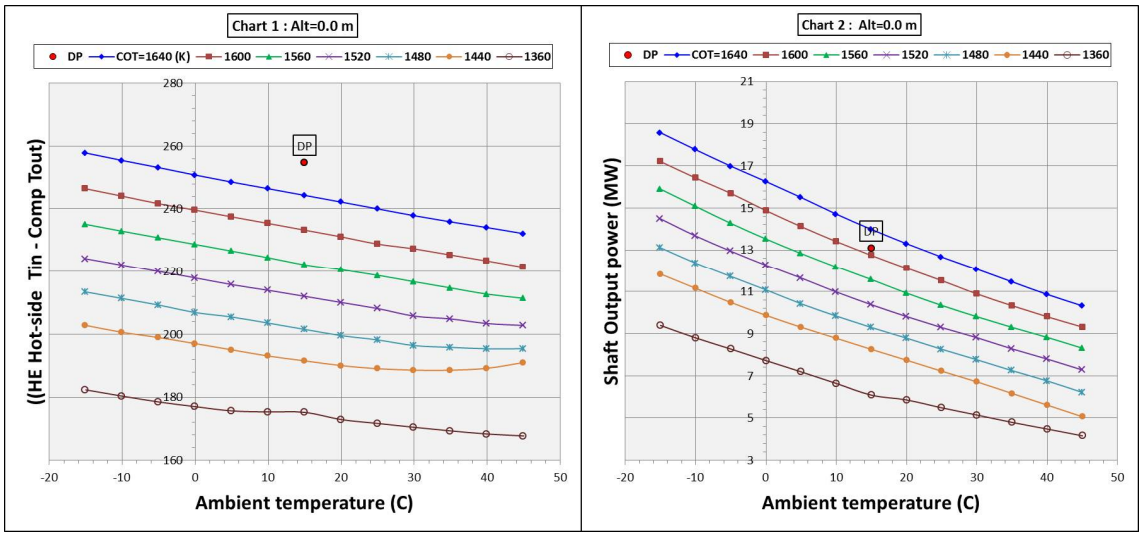

Figure 6-23 Shaft power and Recuperation Temperature Differences of Two-spool non-Conventional HEx Engine with FPT Configuration

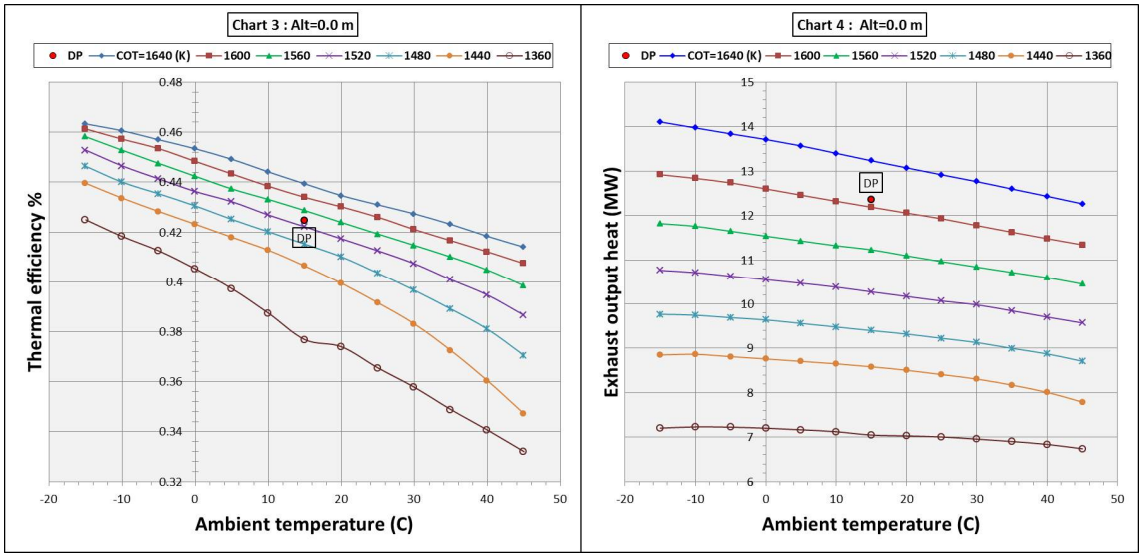

Figure 6-24 Thermal Efficiency and Exhaust Heat Output of Two-spool non-Conventional HEx Engine with FPT Configuration

In addition, results include the effect of varying altitude, and hence ambient pressure on engine off-design performance. Engine hot section creep time to failure is also estimated using a model created by the author using both Excel and FORTRAN languages and will be later explained in details in Section [7.1].

6.1.6 Two-Spool Intercooled Recuperated Cycle Aeroderivative Engine.

In this section engine performance will be investigated focusing on the concept of imposing an intercooler component on the two-spool recuperated cycle engine between its compressors. In the same way, both conventional and alternative recuperation are included in the investigation.

6.1.6.1 Two-Spool 2Shaft Conventional-ICR Cycle Aeroderivative Engine IPT

Referring to the design point calculations of two-spool intercooled conventional recuperated cycle engine in Section [5.1.6.1], an engine with ($OPR = 18$) is chosen for off-design simulation for the IPT arrangement. The configurations structure represented in Figure 5-22 is used in creating the Turbomatch input data file model (see Appendices E.1.12) for the IPT configuration.

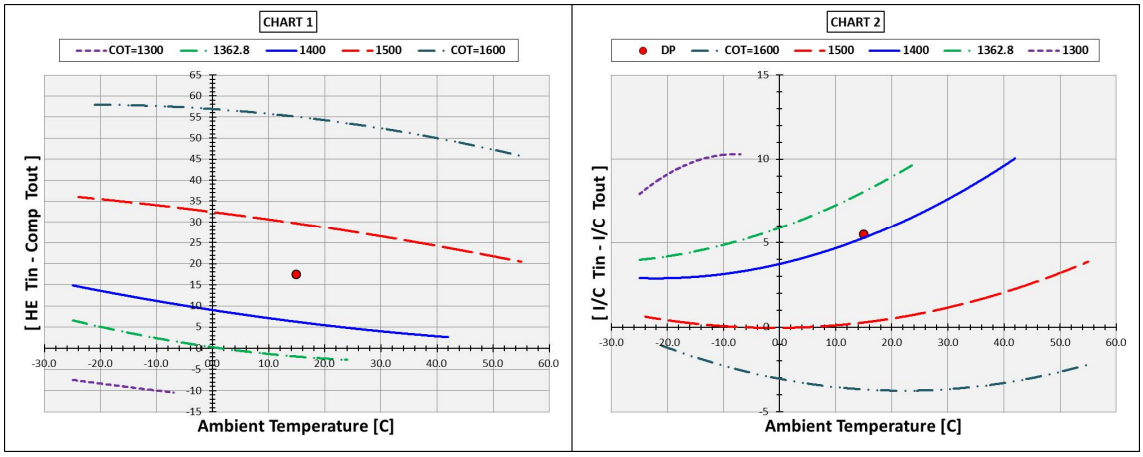

Figure 6-25 Off-design Operating Limitations of Intercooler and recuperator of Two-Spool Conventional ICR Cycle Engine with IPT Configuration

It has been found from design point calculations that attention should be paid to two conditions of controlling temperature differences in both heat exchanger and the recuperator ($T_{18} > T_5$) and ($T_4 < T_3$). For inter-cooler off-design operation an assumption of maintaining ($T_4 = 11.85 + T_{am}$) has been considered throughout off-design operation. Scenario 2 of bleed valve and cooling flow settings is used in simulation and all off-design performance results of the engine with IPT are illustrated in Figure 6-25 and Appendix [B.12]. Results show the operating line of the engine on both compressor maps. Also, it includes variation of engine shaft power

and thermal efficiency with changes in ambient temperature at different values of operating temperature. The importance of the results illustrated in Figure 6-25 lies in determining limitations of operating the Intercooler and recuperator at off-design at standard $VIGVs$ and $VANs$ angles. It specifies positions where conditions of $(T_{18} > T_5)\ and\ (T_4 < T_3)$ are not matched and varying $VIGVs$ or/and $VANs$ for compressor and/or turbine is required. Although using turbine $VANs$ for values of $(COT \leq 1300\ K^o)$ is dependent on the value of ambient temperature applied, it is still needed for any given value of ambient temperature when operating at any $(COT \leq 1350\ K^o)$.

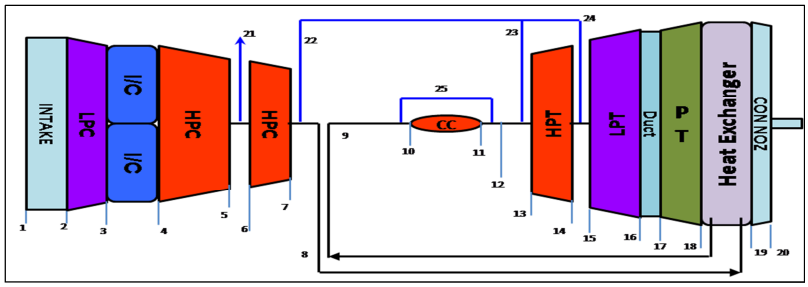

Figure 6-26 Two-Spool Inter-cooled Recuperated Cycle Aeroderivative Engine with FPT Configuration

Figure 6-26 represents the construction of the engine with FPT arrangement with stage numbering considered in the input data file model used in appendix [E.1.13]. The engine selected for FPT simulation has $(OPR = 19.5)$ and its design point characteristics are collected in Table 6-6.

Table 6-6 Design Point Characteristics of Two-spool ICR Cycle Engine

$W\ (^{K}/_{s})$	I/C Tout	$ShP\ (MW)$	ζ_{th}	$Q\ (MW)$	PR	$COT\ (K^O)$
32.969	308.2003	8.18	35.42%	11.2814	19.5	1400.0

Results from off-design simulation of the engine with FPT are presented in Figure 6-27 and Figure 6-28, and further detailed graphs are displayed in appendix [B.13]. An inter-cooler has been operated at off-design subject to the assumption of keeping its outlet temperature 10 degrees higher than ambient $(T_4 = 10.0 + T_{am})$. Starting with the curves in Figure 6-27, differences between the inter-cooler inlet and outlet temperatures are seen in Chart 2 which it shows that the condition of

maintaining ($T_4 < T_3$) is satisfied for all investigated operating temperatures and ambient temperature.

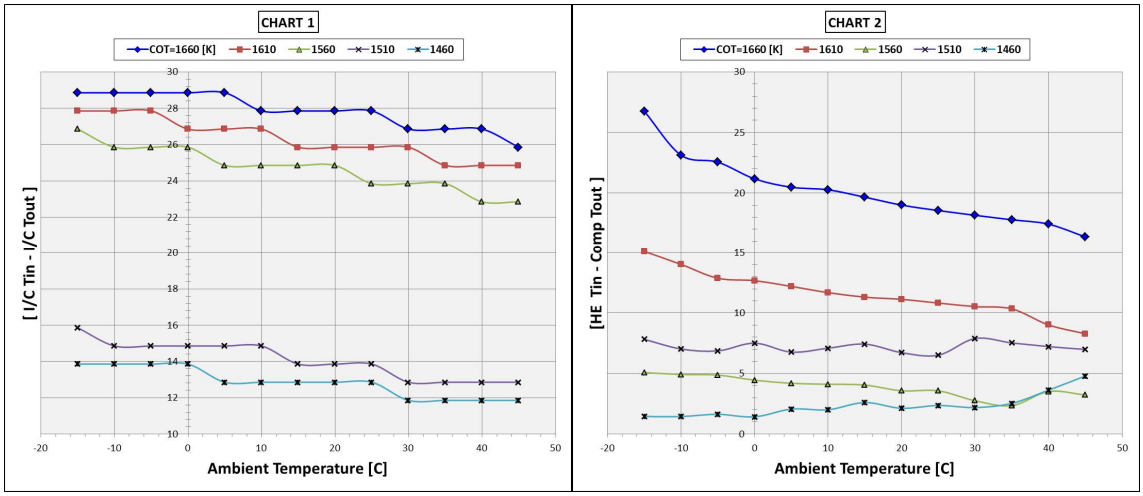

Figure 6-27 Off-design Operating Limitations of Intercooler and recuperator of Two-Spool Conventional ICR Cycle Engine with FPT Configuration

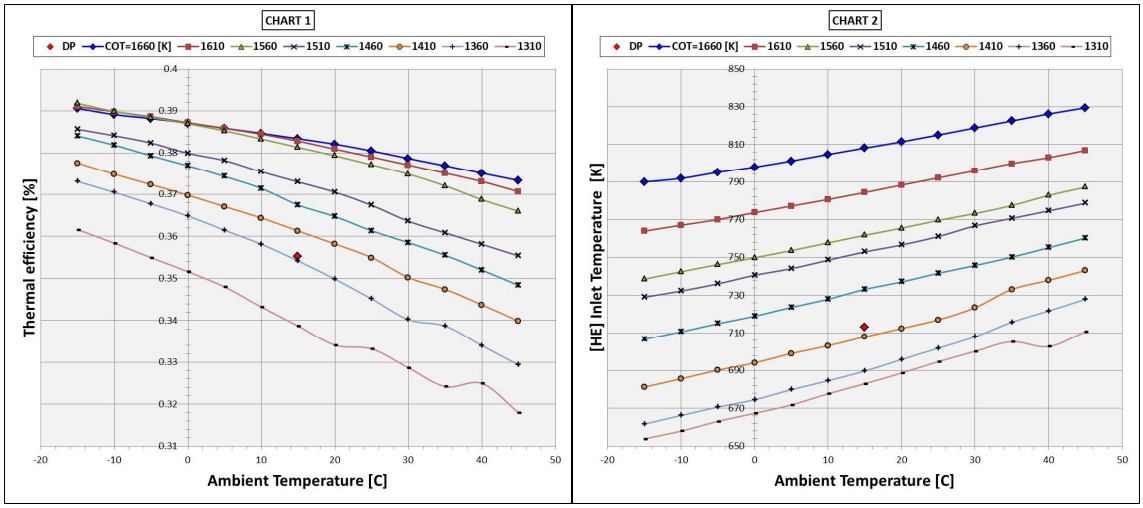

Figure 6-28 Thermal Efficiency and HEx Inlet Temperature of Two-spool Conventional ICR Cycle Aeroderivative Engine with FPT Configuration

Turbine Vans is closed by 5 degrees when needed and it can be seen from Chart 2 that it succeeded in keeping the heat exchanger inlet temperature always higher than the compression outlet temperature for any given COT and ambient temperature. In addition, the bleed valve is also used at low power settings ($COT < 1400$) for some high ambient temperatures to protect engine operating line from crossing the HP compressor surge line.

Engine's operating lines on both compressors are included in Charts 1 and 2 in appendix [B.13], and extra results of engine shaft power and exhaust heat output for the whole investigated operating range are considered on the remaining charts.

It can be seen from Figure 6-28 that the effect of varying engine operating temperature on the heat exchanger inlet temperature is considered in this investigation for a wide range of different ambient temperatures. Considering material thermal barriers of the heat exchanger, results observe positive values (below limitations) for all considered values of operating and ambient temperature including maximum values. It can be observed that there is a fluctuation in the curves of low values of combustor outlet temperature, resulting from applying a blow-off valve at these power settings at relatively high ambient temperatures. Values of thermal efficiency show an optimum value of operating temperature when operate on different values of low ambient temperature (less than zero). It is found that most efficient to operate the engine at ($COT = 1560\ k$) in the range of (Tamb= -5 to -15) than operating at any higher operating temperature.

6.1.6.2 Two-Spool non-Conventional ICR Cycle Aeroderivative Engines FPT

Inter-cooling technology is also applied to non-conventional recuperated two-spool gas turbine engine, and its configuration, as seen in Figure 5-31 for the FPT arrangement. Table 6-7 includes all design point characteristics of the selected gas turbine engine for simulation under a non-Conventional recuperation concept.

Table 6-7 Design Point Characteristics of Two-spool non-Conventional ICR Engine with FPT

$W\ (^{K}/_{s})$	I/C Tout	$ShP\ (MW)$	ζ_{th}	$Q\ (MW)$	PR	$COT\ (K^{O})$
70.4	360.0	21.6	45.26%	14.5620	45	1635.3

The Turbomatch model used for off-design simulation is seen in appendix [E.1.14] and has been built according to stage numbering shown in Figure 5-31 . All off-design calculation is performed for different ambient temperatures and altitude under the assumption that the inter-cooler outlet temperature is always around $10\ C^{\circ}$ higher than ambient temperature. The engine has been operated at different values

of operating temperature and at a wide range of ambient pressure and temperature, and all results from the simulation are shown in appendix [B.14] and Figure 6-29.

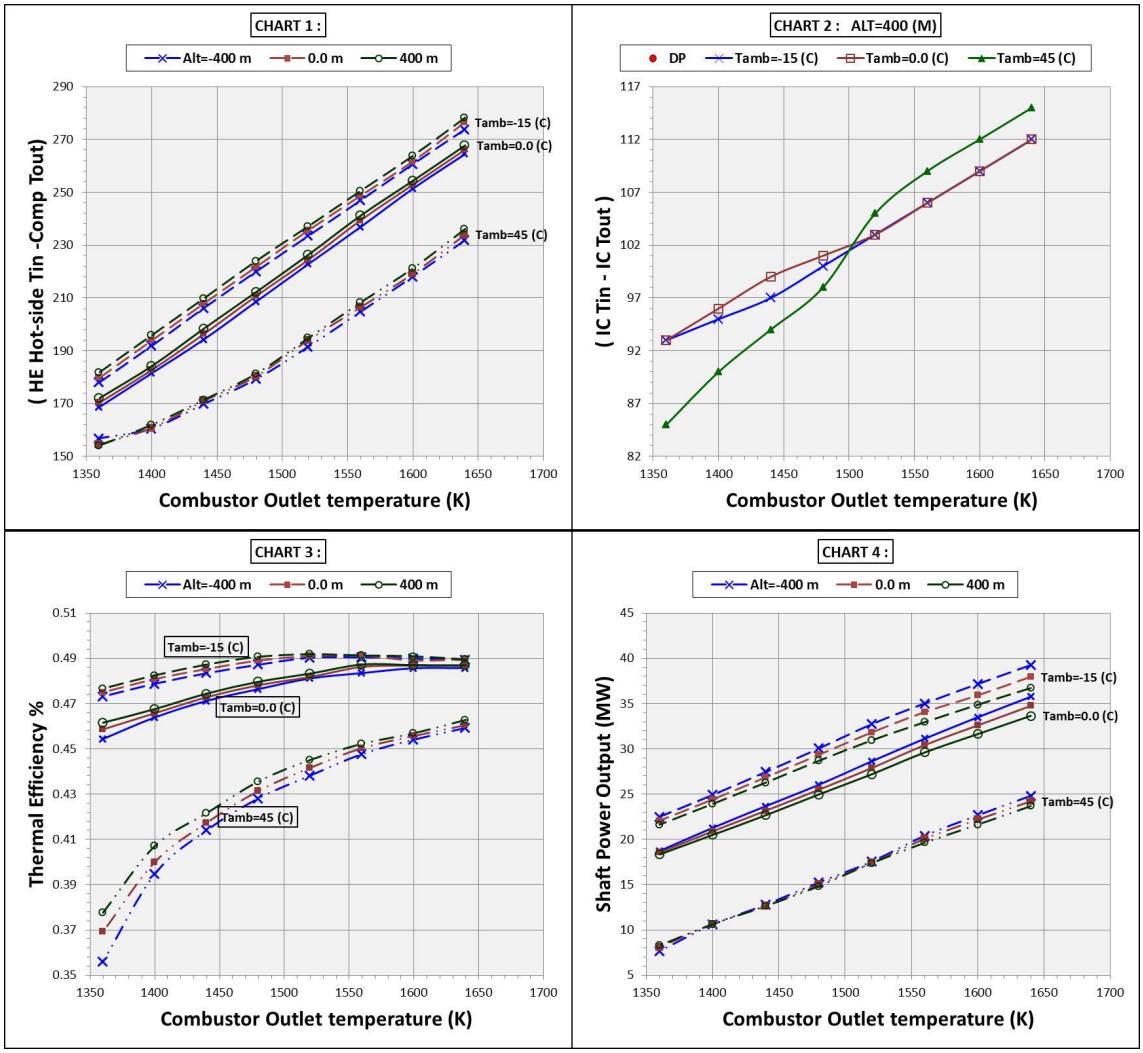

Figure 6-29 Off-design Performance Features of Two-spool non-Conventional ICR Cycle Aeroderivative Engine with FPT Configuration

As was mentioned earlier, locating the HEx between turbines leads to increasing its inlet temperature which enhances the satisfying recuperation condition of maintaining ($T_{16} > T_7$). Generally, it can be seen that an increase in ambient temperature has a negative effect on engine performance of thermal efficiency and shaft power. Charts 1, 2, 3 and 4 in appendix [B.14] illustrate the operating lines of the engine on compressor maps including efficiency maps. Results in Chart 2 in Figure 6-29 indicate that operating the inter-cooler at outlet temperature of 10 C° degrees higher than ambient temperature results in a good enough margin which

keeps ($T_4 < T_3$) throughout the investigated values of operating temperature for all given ambient temperature and altitude.

Similar to the conventional concept, thermal efficiency curves show an optimum operating temperature of about $1520\,K$ for a given value of ambient temperature equal to $15\,C^{\circ}$. Acceptable time to failure for the hot section of the HP turbine is observed from results in appendix [B.14], and it allows the engine to be operated at maximum up ($COT = 1640\,K$) . Moreover, the heat exchanger inlet temperature has been investigated at maximum operating temperature and ambient temperature and been found within material thermal barrier of modern HEx components.

6.2 Sustained Components of Low and High Pressure Rotors

In this section, off-design performance of engines designed under the simple direct derivation method is investigated. Starting with what was mentioned in the literature, the traditional method taken at early production of multi-spool aero-derivative engine was by removing the fan and modifying the LP compressor to accommodate the change in pressure ratio [20]. Another method is to add new (third) rotor with new components of compressor and turbine in the IPT arrangement.

6.2.1 Two-Spool Simple Cycle DDv Aeroderivative Engine

Direct derivation of the two-spool gas turbine engine is chosen as an example of applying the straight forward derivation method to the aircraft engine. The designed engine is simulated at off-design with different methods of controlling performance. Design point characteristics of the simulated engine are previously shown in Table 5-6. The Turbomatch code was used and models are presented in appendix [E.2.1] for the engine on free power turbine configuration. It is clear that an operating temperature of $1758.65\ K^{\circ}$ is slightly high, and it is important to estimate creep effect on hot section life.

The engine has been simulated at a wide range of operating and ambient temperatures and all off-design performance is presented in appendix [B.15] and Figure 6-30. Engine shaft power always increases with the increase in engine operating temperature, while there is an optimum value for maximum thermal

efficiency at every given value of ambient temperature. In addition, the reduction in ambient temperature results in shifting the optimum value to lower operating temperature and enhancing engine thermal efficiency.

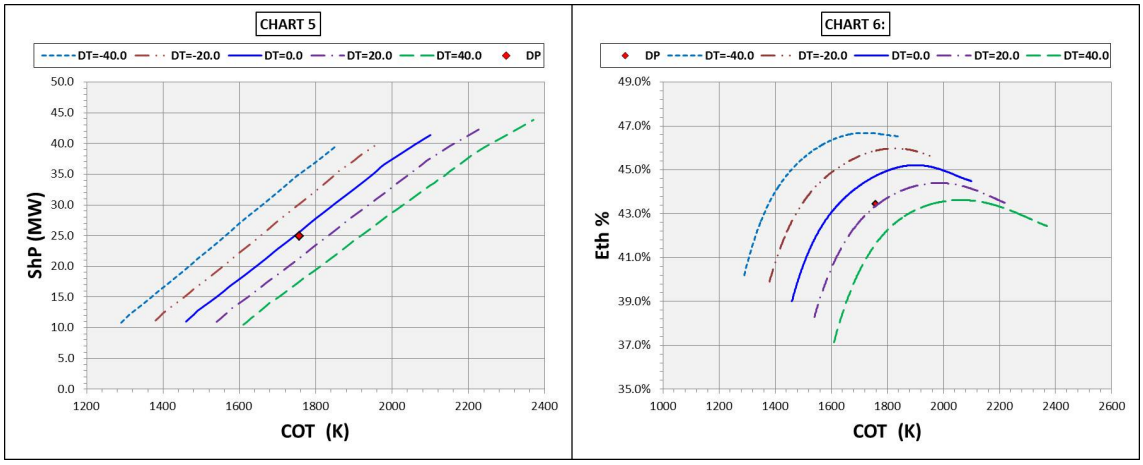

Figure 6-30 Performance Outputs from Direct Derivation of Two-Spool Simple Cycle Aeroderivative Engine with FPT Configuration

The engine has been simulated twice using two different methods of controlling the operating line at low power settings. One method is by using low pressure compressor $VIGVs$ with a blow-off valve, and the second is by assuming installation of $VIGVs$ at the inlet of the HP compressor. Results in appendix [B.15] show that because of losses in the blow-off valve, using the second method provides better shaft power and thermal efficiency at low power settings. Also, creep life estimation results indicated in Chart 5 indicate that it is still possible to operate the engine at a relatively high operating temperature of $1675.0\,K^{\circ}$ and achieve good engine performance outputs.

6.2.2 Three-Spool Intercooled Cycle Derivative Aeroderivative Engine

Investigation performance and behaviour of the three-spool gas turbine engine at off-design has been implemented in two stages. It starts with simulating the engine on simple cycle configuration, which was clarified earlier in Figure 5-46. Then, investigating changes happened in engine performance when inter-cooling technology is applied in order to explore the advantages and disadvantages. Stage numbering used in creating the Turbomatch model is considered in Figure 5-46 and

Figure 5-48 for SC and I/C respectively, and developed Turbomatch models can be seen in Appendices [E.2.2 and E.2.3].

Starting with the three-spool simple cycle, this design configuration is similar to the MT50 gas turbine engine designed by Rolls-Royce [34]. It is noticed from previous calculations of engine design point (see Section 5.2.5) that both shaft power and thermal efficiency are always improved with the increase in the engine's overall pressure ratio. This unusual behaviour happened only because of limitations imposed on the design point calculations by derivation conditions. It is the objective of maintaining non-dimensional mass flow constant at inlet of the LP compressor and turbine and equal to their values on aero-engine at design point. Design point parameters presented in Table 6-8 are dedicated for the selected three-spool simple cycle gas turbine engine.

Table 6-8 Design Point Characteristics of the Three-spool Simple Cycle Engine with IPT

$W\ (^{K}/_{S})$	$ShP\ (MW)$	ζ_{th}	$Q\ (MW)$	PR	$COT\ (K^{O})$
69.02	33.026	45.34	31.53	45.54	1864.33

Engine off-design performance is predicted in order to know how operating line of the three-spool engine will behave on compressor maps and determining limitations associated with compressor surge problems.

The curves on Figure 6-31 proved that the LP compressor operating line has the same shape as the two-spool simple cycle with Direct Load Driving configuration IPT. Also, results in appendix [B.16] illustrate the identical effect of ambient temperature on engine performance of the two-spool engine has been experienced. However, there are difficulties in operating the engine at temperatures lower than design point without the need for a controlling method to keep the compressor away from surge.

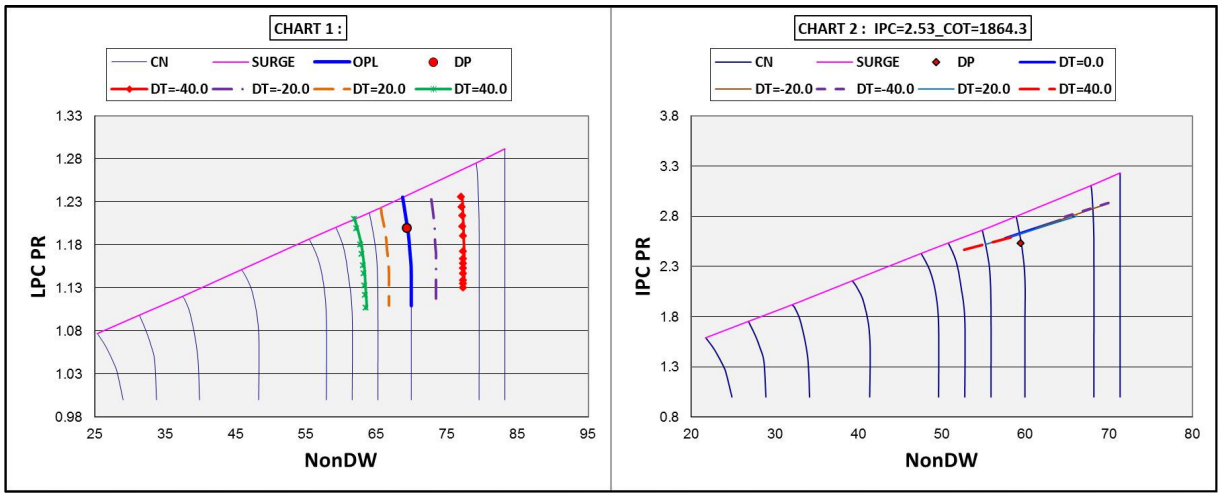

Figure 6-31 Operating Line on compressor Maps of Three-Spool Simple Cycle Aeroderivative Engine

Three-Spool Inter-cooled Cycle Engine

Considering engine structure in Figure 5-48 and design point results in Section [5.2.6], the engine with design $(OPR = 75.0)$ has been selected to conduct off-design simulation for three-spool inter-cooled IPT gas turbine engine. Design point performance characteristic and outputs for chosen engine are indicated in Table 6-9. It provides shaft output power of $57.2\ MW$ with thermal efficiency of around 48.58% as well as 40.99 MW of output heat. Off-design calculations have been performed and the results are shown in appendix [B.17] and Figure 6-32.

Table 6-9 Design Point Characteristics of Three-Spool Intercooled Cycle Engine with IPT

$W\ (^{K}/_{s})$	I/C $T_{out}(K^o)$	$ShP\ (MW)$	ζ_{th}	$Q\ (MW)$	OPR	$COT\ (K^O)$
111.59	305.4781	57.2	48.58	40.99	75.9	1864.3

The assumption of maintaining $(T_4 = 17.33 + T_a)$ is applied during off-design performance predication. Charts in both figures show that the engine exhibits normal behaviour, similar to the two-spool simple cycle engine.

Applying the inter-cooler allows us to increase engine overall pressure ratio at relatively low values of engine operating temperature at the design point. Thermal efficiency and shaft power are enhanced significantly by applying inter-cooling

technology on the large-sized engine with high COT and OPR. It is a result from the fact that the increase in shaft power due to the higher overall pressure ratio applied offsets the thermal losses caused by applying inter-cooling technology. Furthermore, it becomes easy to control and operate the engine at low power settings to meet part-load demand. However, exhaust heat output is still not much improved compared to smaller engines with simple and recuperated cycles.

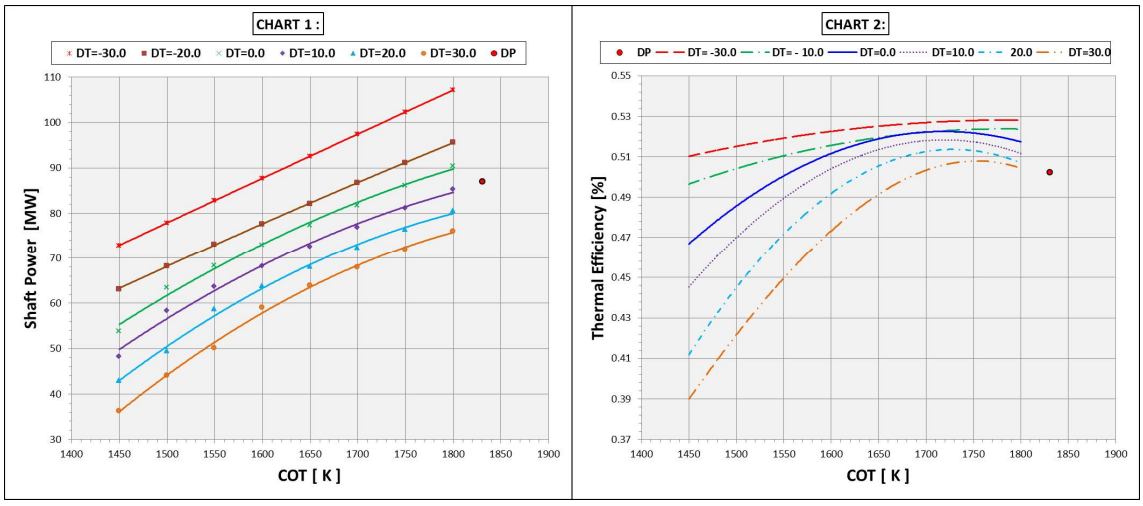

Figure 6-32 Off-Design Performance Features of Three-Spool Inter-cooled Cycle Aeroderivative Engine with IPT Configuration

It has been noticed from previous calculations that selecting gas turbines for any application cannot be fulfilled by the theoretical design point thermodynamic analysis or determining compressor surge margin at off-design operations. Additional design factors must be considered and included to complete the selection.

Engine's size and weight are crucial and play a major factor in selecting gas turbine engine in some applications, such as marine and off-shore applications. Other important factors such as economic, emission production, manufacturing cost as well as direct operating cost are found to dominate, as more than 50% of the annual cost depends on used fuel price. In addition to these mentioned factors, there are significant other factors such as engine durability and whether it is mechanical drive or turbo-generator [96].

It can be concluded from all previous off-design operation for selected engines that the free power turbine arrangement demonstrates better control on engine performance throughout the different investigated ambient conditions. Also, it shows

that the gas turbine engine on this configuration tends to operate with less sensitivity to variation in driven load factor.

6.3 Aeroderivative Engines Selected for Assessment

All engine performance parameters and characteristics previously calculated will be numerically arranged in specific format which can be later used for models built using FORTRAN language. Also in this section, budget and specific prices of designed derivative gas turbine engines will be calculated.

6.3.1 Text Files Creator Model

Matlap Code has been used to build a model which has been used in creating (TXT) format files containing values of all engines off-design performance parameters such as: -

- Output power
- Thermal Efficiency
- Fuel Flow
- Pressure ratio
- Intercooler Outlet Temperature
- Cooling Bleed Temperature
- $CO, CO2, NOx, UHC$
- Heat Exchanger Inlet Temperature
- Compressors $VIGVs$ Angles
- Turbines $VANs$ Angles
- Mass Flow Rate
- Exhaust Heat Power
- High Pressure Shaft Relative Rotational speed
- Exhaust Temperature
- Exhaust Flow

All these off-design characteristics are calculated and recorded at different ambient temperatures and different altitudes (for inlet pressure variation investigation). Therefore, it makes it possible for other models created in FORTRAN to read performance parameters from these (TXT) files.

6.3.2 Performance Limitations and Prices of [GT] Engines Selected for Techno-economic Assessment

Some of the newly designed engines, which satisfy power demand in the chosen industrial applications, have been selected for the techno-economic assessment. They will be applied in three different applications marine, power generation, and CHP depending on their installed capacity. Considering the methodology mentioned in calculating the engine's design point, by keeping constant non-dimensional mass flow and rotational speed for a given pressure ratio the nominal design point of some engines is calculated by design at relatively low TET values. So, considering the level of technology involved in designing the aircraft engine, it is still possible for those engines to operate at relatively high values of turbine entry temperatures. Therefore, some of designed aero-derivative gas turbine engines are operated at maximum possible power, as shown in Table 6-12. While Table 6-11 contains design point performance characteristics of the same selected derivative engines.

Also, for later economic considerations the unit cost of all selected gas turbine engines has been estimated using the assumptions of applying 30% of unit cost on inter-cooler and heat exchangers, as shown in Table 6-10. The specific unit prices were taken from 'Gas Turbine World 2008' magazine [50; 51].

Table 6-10 Cost of Selected Aeroderivative Gas Turbine Engines

Eng. Model		Shaft. Power (MW)	Unit SC Specific Price (£/MW)	IC Cost% of Unit Cost	HEx Cost % of Unit Cost	Specific Price (£/MW)
DvGT*1	1Sp-SC-IPT	5.437943	325317.3248	-	-	325317.3248
DvGT*2	1Sp-SC-FPT	5.619688	318049.5987	-	-	318049.5987
DvGT*3	Mod-1Sp-SC-IPT	6.2316155	297283.7261	-	-	297283.7261
DvGT*4	Mod-1Sp-SC-FPT	6.1915865	298023.6815	-	-	298023.6815
DvGT*5	2Sp-SC-FPT_DDV (LPC IGVs & Bleed)	24.8645546	268306.758	-	-	268306.758
DvGT*51	2Sp-SC-FPT_DDV (HPC IGVs)	24.864546	268306.758	-	-	268306.758
DvGT*52	2Sp-SC-FPT (HPC IGVs)	17.256648	317251.3376	-	-	317251.3376
DvGT*6	IC-2Sp-IPT	31.268678	178635.1529	30%	-	232225.6987
DvGT*7	IC-2Sp-FPT	31.596822	191423.0764	30%	-	248849.9994
DvGT*8	IC-3Sp_IPT	87.01308	144467.879	30%	-	187808.2427
DvGT*9	HE-1Sp-Conv-IPT	5.242601	333318.3949	-	30%	433313.9134
DvGT*10	HE-1Sp-Conv_FPT	5.6076	318472.879	-	30%	414014.7427
DvGT*11	HE-1Sp-nConv-FPT	4.384399	278293.4076	-	30%	361781.4299
DvGT*12	HE-2Sp-Conv-FPT	8.751524	309402.5223	-	30%	402223.279
DvGT*13	HE-2Sp-nConv-FPT	13.086652	304500.6624	-	30%	395850.8611
DvGT*14	ICR-2Sp-Conv-FPT	8.184656	306676.3312	30%	30%	490682.1299
DvGT*15	ICR-2Sp-nConv-FPT	21.600906	264849.5032	30%	30%	423759.2051

Table 6-11 Nominal Design Point Characteristics of Selected Aeroderivative Gas Turbine Engines

Engine Models	ShP (MW)	ζ_{th} %	Q (MW)	W $(\frac{Kg}{s})$	COT_{DP} (K°)	OPR	T_{HEin}	T_{ex}	IC T_{out}	$(T_{HEin}-T_{Comp\ out})$	F.F $(\frac{Kg}{s})$	RPM	COT_{min}
DvGT*1	5.437943	31.05	8.9634	27.04	1308.92	15.0	-	711.0	-	-	0.4061	13300.0	1135
DvGT*2	5.619688	32.09	9.1258	27.04	1308.92	15.0	-	702.0	-	-	0.4061	13300.0	1185
DvGT*3	6.2316155	35.33	9.0332	24.691	1308.92	15.0	-	712.0	-	-	0.3932	13300.0	1250
DvGT*4	6.1915865	35.0	9.0111	24.691	1308.92	15.0	-	698.0	-	-	0.4102	13300.0	1250
DvGT*5	24.8645546	43.32	25.6528	59.23	1758.58	38.0	-	785.56	-	-	1.3308	15410.32	1430
DvGT*51	24.864546	43.32	25.6528	59.23	1758.58	38.0	-	785.56	-	-	1.3308	15410.82	1430
DvGT*52	17.256648	40.85	19.5708	48.45	1630.73	30.0	-	760.43	-	-	0.9795	15410.82	1430
DvGT*6	31.268678	43.61	25.3306	82.244	1630.73	52.5	-	674.82	358.99	-	1.6627	14848.98	1400
DvGT*7	31.596822	44.07	24.9895	82.244	1630.73	52.5	-	671.12	358.99	-	1.6627	14848.98	1400
DvGT*8	87.013080	50.0	47.7013	168.9	1830.9	113.85	-	651.07	300.0	-	4.0291	15691.43	1450
DvGT*9	5.242601	32.26	7.8731	27.04	1308.92	15.0	716.28	673.61	-	54.95	0.3768	13300.0	1200
DvGT*10	5.607600	33.82	8.1834	27.04	1308.92	15.0	701.79	671.71	-	40.46	0.3845	13300.0	1270
DvGT*11	4.384399	36.6	4.663	27.04	1308.92	15.0	897.86	555.46	-	236.54	0.2778	13300.0	1270
DvGT*12	8.751524	36.11	11.9275	33.7071	1423.5	19.5	721.58	715.47	-	6.1138	0.5621	13873.43	1485
DvGT*13	13.086652	42.36	12.3602	48.45	1630.73	30.0	1066.07	628.91	-	254.78	0.7164	13873.43	1360
DvGT*14	8.184656	35.42	11.2814	32.969	1400	19.5	713.21	706.57	308.2	8.77	0.5358	13758.51	1310
DvGT*15	21.600906	45.26	14.5620	70.4	1635.3	45.0	1028.56	585.42	360.0	215.17	1.1066	14869.85	1360

Table 6-12 Maximum Power Performance of Selected Aeroderivative Gas Turbine Engines

Engine	COT_{max} (K°)	ShP (MW)	ζ_{th} %	Q (MW)	W ($\frac{Kg}{s}$)	OPR	T_{HEin}	T_{ex}	$IC\ T_{out}$	(T_{HEin}- $T_{Comp\ out}$)	F.F ($\frac{Kg}{s}$)	RPM	Time to Creep failure
DvGT*1	1485.0	9.061	37.0	12.242	28.671	18.16	-	764.075	-	-	0.569	13300.0	VL
DvGT*2	1535.0	9.638	34.1	15.067	32.343	20.353	-	797.028	-	-	0.657	14483.7	833044.2
DvGT*3	1670.0	11.456	39.2	15.308	26.614	17.605	-	892.905	-	-	0.679	13300	689564.061
DvGT*4	1670.0	12.886	35.3	19.55	35.379	23.328	-	869.279	-	-	0.848	13406.4	78363.428
DvGT*5	1675.0	24.801	45.1	23.551	59.143	38.897	-	738.906	-	-	1.28	14655.2	29910.913
DvGT*51	1675.0	24.801	45.1	23.551	59.143	38.987	-	738.906	-	-	1.28	14655.6	29910.913
DvGT*52	1675.0	21.902	43.2	22.741	53.693	35.32	-	760.373	-	-	1.179	15518.6	28731.329
DvGT*6	1715.0	43.563	46.9	30.878	88.337	59.44	-	696.696	283.15	-	2.162	13497.7	11034.82
DvGT*7	1715.0	55.865	46.1	36.029	114.89	77.357	-	666.159	283.15	-	2.817	13438.3	12038.809
DvGT*8	1800.0	98.392	52.6	47.486	179.97	122.43	-	624.021	283.15	-	4.353	15330.5	9482.69
DvGT*9	1480.0	8.689	38.9	10.479	28.674	18.13	767.747	712.156	-	767.747	0.519	13300.0	VL
DvGT*10	1550.0	9.708	36.3	13.53	32.476	20.554	804.158	755.45	-	66.342	0.622	14536.9	VL
DvGT*11	1550.0	7.351	39.4	7.88	32.593	20.54	1061.178	607.487	-	322.134	0.434	14590.1	VL
DvGT*12	1660.0	17.52	39.9	21.2095	46.051	30.393	808.17	791.85	-	22.4402	1.02	13027.1	52440.09
DvGT*13	1640.0	16.254	45.3	13.7137	53.703	34.894	1070.38	618.654	-	250.7984	0.834	13776.3	40002.81
DvGT*14	1660.0	17.502	38.7	21.109	46.942	30.66	797.872	782.48	283.15	19.66	1.052	14969.2	36263.33
DvGT*15	1640.0	34.747	48.7	13.685	99.742	64.594	1025.026	517.377	283.15	266.1541	1.661	14706.2	51496.11

7 TECHNICAL AND ECONOMIC ASSESSMENT FOR THE NEW DERIVED ENGINES

Technical and economic assessments are the major aspects used for any newly designed gas turbine assessment. In the technical assessment there are many factors to be considered which deal with gas turbine parts life. Creep, thermal fatigue, corrosion and erosion are the major factors to be considered in technical assessment of the gas turbine life cycle. Market demand and gas turbine equipment price have significantly increased due to improved manufacturing technology and raised material cost, which has resulted in increased manufacturing cost. In fact the economic assessment is the complement of technical assessment and separating them is not possible in order to achieve sensible assessment. Economic assessment has some factors which vary depending on the gas turbine application itself.

7.1 Creep Model

Estimating the life of the gas turbine engine can be specified by estimating the life of the hot section (high pressure turbine blade and disc) through creep and fatigue analysis, which are the most limiting factors to the life of gas turbine engines [86]. Creep is one of the most important criteria used in assessing life of gas turbine hot section parts such as HPT blades. It has been chosen in this project to be the only measurement used in accounting engine life. Hot sections of gas turbine are stretched owing to creep effect, and the consequence will be metal deformation. Time plays a remarkable role in creep deformation, because it is a consequence of operating under prolonged high temperature companied to mechanical load (stress).

Creep impact on turbine blade leads to changed blade shape and its aerofoil which results in the blade not functioning as designed. Figure 7-1 represents an example of turbine blades affected by creep. It can be seen that physical dimensions of the blade have been changed which might affect tip clearance and cause it to touch the engine case. Regardless of the kind of

materials used, it has been found that creep is very important when ratio between the material temperature and its melting temperature is more than 0.5 but it can be in the range of 0.4 to 0.6 [77].

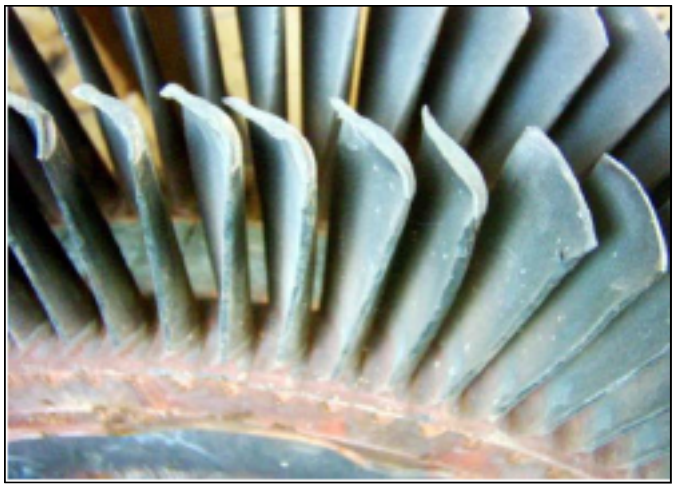

Figure 7-1 Creep attack Impact on
Turbine Blades [77]

A simple method used to evaluate high pressure turbine blade is based on the assumption that the blade is untwisted and is uniform across the section area along its height. According to designed HP turbine dimensions provided by the designer (Team 2 AVIC), the HP turbine consists of two stages and its dimensions are presented in Figure 7-2. One method used in calculating creep is used (Larson Millar Parameter) and will be examined in detail. This method is approved and used in references [40], [77], [109], and [116].

Larson Millar Parameter

This is one of the simplest methods used in estimating the life of hot section of the HP turbine. The method is used widely in engineering and it depends on time and temperature with some assumptions that has provided a significant level of accuracy which was validated by experimental data [36]. It focuses on function in high pressure turbine blade metal temperature as well as stress, and the output is 'time to rupture', as shown in the following equation:

$LMP = T_b\left(20 + log\ t_f\right) * 10^{-3}$[109]

$$log\ t_f = LMP/T_b - C_{LMP}[77] \quad (7\text{-}1)$$

$$T_b = T_g - \in_b (T_g - T_c)[40] \quad (7\text{-}2)$$

$$C_{st} = (K * H_b * Dens * \left(2\pi * \frac{N_{HT}}{60}\right)^2 * \left(\frac{D_m}{2}\right))/1000000[40] \quad (7\text{-}3)$$

$$K = constant = 1.2$$

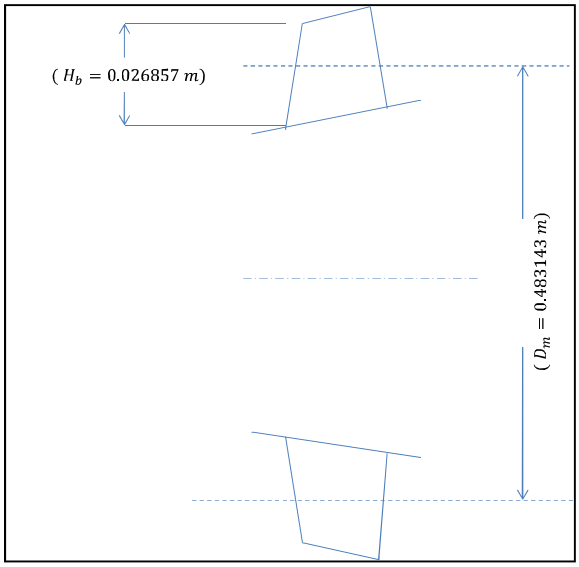

Figure 7-2 High Pressure Turbine
Blade and Shaft Diameters

The challenge in calculating (LMP) from the graph presented in appendix [A.5]. It contains imperial data from industrial present values of LMP as functioning in metal centrifugal stress, as shown. Centrifugal stress can be calculated based on dimensions presented in Figure 7-2 and on values of $(Dens = 7850\ Kg/m^3)$ and $(\mu = 3.14)$. In addition, values of shaft rotational speed will vary according to engines of design operation conditions.

Excel is used to create a simple model to calculate time to failure values at different values of centrifugal stress based on different shaft rotational speeds. Blade metal temperature is calculated from formula, representing it as a function of cooling bleed temperature, combustor outlet temperature COT, and blade cooling effectiveness.

7.2 Emission Model

Nowadays, the main objective in developing and improving gas turbine engines is producing engines which are environmental friendly, with higher specific fuel consumption and lower emissions [76]. Gas turbine manufacturers have been developing some combustion technologies in order to reduce or minimise formation rate of pollutants such as Nitrogen Oxides NO_x, Carbon Monoxides CO and Dioxide CO_2 which have a negative effect on the environment. Generally, in gas turbine operations it has been found that low combustor operation temperature results in a reduction in NO_x and an increase in CO formation. Mixing a large amount of air with fuel before combustion lowers combustion temperature. So, a higher air to fuel ratio in the primary combustion zone is recommended to reduce NO_x levels at full-load operation due to achieving what is called Lean-premix combustion. In addition, a relatively large physical volume of primary-zone in the combustor helps to retain the mixture of air and fuel in the combustion zone for a longer period of time. That leads to an increase combustion residence time which helps to achieve complete combustion.

Emission model developed and created using FORTRAN code by [29], which was modified in joint work conducted with Raja (EngD student) [91] to be adapted to serve both projects and matches the format of outputs generated from different performance models. All mathematical equations used in the model based on work introduced by [71], [86]. The adapted model has been used in estimating all emission indices in this project, and it calculates specific values of $CO2, CO, UHC, and\ NOx$ per unit kilogram of fuel burned.

It has been observed from the literature that one of the most important factors affecting emission formation is the kind of fuel used. In most experimental work it was found that CO_2 formation has constant level of concentration at a wide range of engine operation. However, CO_2 and SO_2 levels vary with the kind of fuel used. Liquid fuel (such as diesel) has relative higher level of concentration of Carbon Dioxide emission due to the fact that it contains

higher carbon levels. Sulphur Dioxide SO_2 has an important concern for large scale gas turbine plants for power generation. Carbon price was expected to have remarkable impact on generation cost due to legislation and deregulation. How carbon price affects running cost is directly dependent on fuel quality, electric efficiency of power technology, fuel carbon content and carbon price. The following formula illustrates the effect of these factors.

$$(Production\ Cost = (Running\ Cost + Emmission\ Cost) + Deficit\ Cost) \quad (7\text{-}4)$$

$$(PrCst_t = (RunCst_t + EmsTax_t) + (DefCst_t))$$

$$CO2Tax_t = 3600 * \delta t * CO2TaxR * (2.75 * CO2EmsM_t) * CO2Al \quad (7\text{-}5)$$

$$CO2EmsM_t = CO2SM_t * MFC_t \quad (7\text{-}6)$$

$$CO2SM_t = \left({}^{44}/_{12}\right) * CMCF_t \quad (7\text{-}7)$$

As was mentioned previously, carbon price has been the key for a long time and EU emission Trade Scheme (EU ETS) is a commonly used scheme implemented in Europe in order to include emission cost in generation cost of power plants. Fuel type, heat value, and quantity are the major factors that affect the concentration of Carbon Dioxide emission. Emission cost can be added to the production cost, especially Running Cost, and the formulae which can be used to calculate additional generation emission cost can be written as follows [36]:

$$AdGC = \frac{(3.6 * CO2TaxR * CO2SM * CO2Al)}{\zeta_e * LHV} \quad (7\text{-}8)$$

ζ_e : $Electrical\ Efficiency$

This equation is widely used in medium-term generation for one year optimization calculations. It is worth mentioning that variation in gaseous emissions was observed in most gas turbine emission studies affected by quantity of fuel consumed, which in turn affects plant operating cost.

7.3 Economic Considerations and Assessment

There are many methods utilised in the financial assessment of technical ideas and projects. Net Present Value NPV is one of the most well-known techniques used to compare the financial benefits, especially for long term projects [124]. By using NPV it becomes possible to estimate the present value of the future net cash flow on the whole economic life of the project. Although [124] has proved that the Real Option Approach ROA is better than standard NPV in considering the uncertainty of market development, the simplicity of NPV made it preferable and it can be combined with other commercial software such as Monte Carlo (MC) to conduct sensitivity analysis of the ability to include market uncertainty in the assessment. NPV is based on cumulative net cash flow calculation, which is the sum of annual net cash flow for the whole period of economic life time of investment [123][111].

It has been used widely in the economic assessment of power generation projects and approved as the most popular method used in investment evaluation. So, all the economic assessment of this project investigation will be based on the NPV technique.

The following important factors must be calculated in order to conduct the economic assessment of power generation project using NPV techniques:

Cash Flow

Cash in-flow=Cash income (sale, loans, grants, etc.)

Cash out-flow=cash outgoings (supplier payments, salaries, etc.)

$$[Initial\ Cash\ Flow(ICF) = Loan - investment\ Capital\ Cost] \quad (7\text{-}9)$$

$$[Net\ Cash\ Flow = Cash\ inFlow - Cash\ outflow] \quad (7\text{-}10)$$

Internal Rate of Return (IRR)

It is the project interest rate which makes that total cumulative net cash flow equal zero.

***Time value of money**:*

Calculating net cash flow and payback period is not enough to decide the economic viability of the project. It is very important to calculate the internal rate of return IRR which helps to represent figures of the economic viability of the project. Also, future and present value of money invested should be determined at each period of the project especially when bank loans are involved in the investment. Time value of money is influenced by rate of return of the investment ROI [56; 119].

$$[Present\ Value(PV) = Future\ Value\ (FV)/(1 + {ROI}/{_{100}})] \quad (7\text{-}11)$$

Assuming $variable\ (ROI)$over the life time of the project then,

$$\left[PV = FV/\left[\left(1 + \frac{ROI_1}{100}\right)\left(1 + \frac{ROI_2}{100}\right),.,\left(1 + \frac{ROI_n}{100}\right)\right]\right] \quad (7\text{-}12)$$

Assuming $fixed\ (ROI)$ is over the life time of the project then,

$$\left[PV = FV/\left(1 + \frac{ROI_1}{100}\right)^n\right] \quad (7\text{-}13)$$

Therefore the value of annual net present value $ANPV$ of the project can be estimated using the following equation:

$$[ANPV = Initial\ Cash\ Flow\ ICF + Annual\ Present\ Valueof\ money\ (APV)]$$

$$\left[ANPV = ICF + \frac{FV}{\left(1 + \frac{ROI}{100}\right)}\right] \quad (7\text{-}14)$$

Then the total net present value of the project over its economic life time period with variable interest rate(ROI)can be calculated from the following equation:

$$\left[NPV = ICF + \sum_{t=1}^{T} \frac{FV_t}{\left(1 + \frac{ROI_1}{100}\right)\left(1 + \frac{ROI_2}{100}\right),.,\left(1 + \frac{ROI_n}{100}\right)}\right] \quad (7\text{-}15)$$

$(T)\ is\ the\ economic\ time\ period\ of\ the\ project$

Assuming $fixed\ interest\ rate\ ROI$, the Net Present Value can be written as follows:

$$\left[NPV = ICF + \sum_{t=1}^{T} \frac{FV_t}{\left(1 + \frac{ROI}{100}\right)^T}\right] \quad (7\text{-}16)$$

Using this equation the Internal Rate of Return IRR can be calculated at the condition($NPV = 0.0$), and the equation can be modified as follows:

$$\left[0.0 = ICF + \sum_{t=1}^{T} \frac{FV_t}{\left(1 + \frac{IRR}{100}\right)^t}\right] \quad (7\text{-}17)$$

Payback Period of Time (DPB)

This refers to the minimum period of time necessary for the project to break even (it implies that total cumulative net cash flow NPV equal or greater than zero). It can be calculated from the following equation:

$$0.0 \leq \left[ICF + \sum_{t=1}^{DPB} \frac{FV_t}{\left(1 + \frac{ROI_1}{100}\right)\left(1 + \frac{ROI_2}{100}\right),.,\left(1 + \frac{ROI_{DPB}}{100}\right)}\right] \quad (7\text{-}18)$$

$Assuming\ fixed\ interest\ rate\ (ROI), then$

$$0.0 \leq \left[ICF + \sum_{t=1}^{DPB} \frac{FV_t}{\left(1 + \frac{ROI}{100}\right)^t}\right] \quad (7\text{-}19)$$

There is a fourth factor which is important in assessing power generation application projects, i.e.:

Generation Cost (GC):

This is the ratio of total production cost of the plant to the total electricity or power produced.

$$(GC)_t = \frac{Annual\ Total\ Production\ Costs}{Annual\ Power\ or\ Electricity\ Produced} \quad (7\text{-}20)$$

Project duration is very important and should be taken into consideration when the comparison is made between two different projects. It is possible for two different projects to generate the same amount of cash at a different economic period of time. However, the cash generated after the break-even

point should be considered. It is clearly noticed that projects with longer payback period can generate more relatively profit over the total project duration.

The advantages of using NPV can be illustrated briefly in the fact that it deals with cash flow over the time period of the project rather than the profits, and it helps to recognise the time value of money which offers the ability to compare projects based on benefits and costs. Also, it allows the investigator to adjust both expected cash flow and discount rates in order to include the risk in the assessment investigation. Finally, the accepted project based on NPV technique will increase the value of invested money.

7.4 Techno-economic Assessing of Designed Derivative GT Engine Models on Power Generation Application

Most of the economic planning of power generation projects is established based on long-term investment projection. Economic assessment or estimation of long-term investment projects is conducted on yearly based calculations. Considering the methodology previously explained in equations (7-9) to (7-20), the NPV method can be applied, starting with cash flow and ending with calculating the annual NPV as follows:

Cash in-flow: It includes

Loans

Annual Electricity Produced Cost ($A_{vo}C_{st}E_l$)

Annual Sell of Power Surplus ($R_{ev}S_eS_uE_l$),

Cash out-flow:

Capitation Cost (C_aC_{st})

$$\text{GT Unit Cost} = \text{Specific GT Price}\left(S_pGTC_{st}\right) * Power\ Capacity(P_{iso})$$

$$\text{Installation Contingency Cost}(I_{ns}C_{on}C_{st}R_a) = 0.26 * (C_aC_{st})$$

Cost of Power Deficit ($A_nP_{wr}D_fC_{st}$)

Cost of Fuel Consumed ($A_nF_uC_{st}$)

Operating and Maintenance Cost ($O_pM_aC_{st}$)

Cost of Emission produced (E_mC_{st})

Annual Operating Profit ($A_nO_pP_{rft}$) = (Cash inflow-Cash outflow)

There are aspects of gas turbine costs which are considered as contents of direct operating cost, such as:

- Fuel cost
- Maintenance cost
- Taxation cost (including emission)
- Investment's Insurance and payable interest

This can be numerically modelled as follows:

$A_{vo}C_{st}E_l = (A_nE_lP_{rod}) * (C_oE_lP_r)$

$(C_oE_lP_r)$: Contract Electricity Price

$(A_nE_lP_{rod}) = \sum_m^{PEL}(P_{wr} * N_uD_{ays} * 24) * A_{va}$

$A_{va} = (MTBF)/(MTBF + D_wT_m)$

$A_nF_uC_{st} = (A_nF_uM_aF_l * F_uT_{rf}R_a)$

$(F_uT_{rf}R_a)$: Fuel Tariff Rate

$(A_nF_uM_aF_l) = \sum_m^{PEL}(F_uM_aC_{ns} * N_uD_{ays} * 24 * 3600) * A_{va}$

$O_pM_aC_{st} = S_pOMC_{st} * A_nE_lP_{rod}$

(S_pOMC_{st}): Specific Operating and Maintenance Cost

$A_nE_lP_{rod} = \sum_m^{PEL}(P_{wr} * N_uD_{ays} * 24) * A_{va}$

$R_{ev}S_eS_uE_l = (A_nS_uE_l * A_nS_uP_r)$

$(A_nS_uE_l)$: Annual Surplus of Electricity

$(A_nS_uP_r)$: Annual Surplus Sell Price

$A_nP_{wr}D_fC_{st} = (A_nP_{wr}D_f * E_lB_uP_r)$

$(A_nP_{wr}D_f)$: Annual power Deficit

$(E_lB_uP_r)$: Electricity Buy Price

$E_{mis}G_{st} = A_nC_{o2}M_a * C_{o2}T_{ax}R_a$

$(C_{o2}T_{ax}R_a)$: Carbon Dioxide Emission Tax rate

$(A_nC_{o2}M_a)$: Annual Carbon Dioxide Produced Mass

$[A_nO_pP_{rft} = (A_{vo}C_{st}E_l + R_{ev}S_eS_uE_l - A_nF_uC_{st} - O_pM_aC_{st} - A_nP_{wr}D_fC_{st} - E_{mis}C_{st})]$

Annual Net Cash Flow

$[A_n N_e C_a F_l$ = $((A_n O_p P_{rft})$ - ($A_n loanR_{ep}$) - ($A_n T_{ax} P_y$)]

For last year and when Residual Value ($R_e V_{lu}$) applied

$[A_n N_e C_a F_l$ = $(A_n O_p P_{rft})$ - ($A_n loanR_{ep}$) - ($A_n T_{ax} P_y$)+($R_e V_{lu}$)]

($R_e V_{lu}$): Residual Value

($A_n LoanR_{ep}$): Annual Loan Repayment

$[A_n LoanR_{ep} = Loan * C_a R_{ec} F_{act}]$

($C_a R_{ec} F_{act}$): Capital Recovery Factor

$$C_a R_{ec} F_{act} = \frac{LoanIOR * (1 - LoanIOR) ** (T_m P_e loanR_{ep})}{\left((1 - LoanIOR) ** \left(T_m P_e loanR_{ep}\right)\right) - 1}$$

($LoanIOR$): Loan Annual Rate of Loan Repayment

($T_m P_e loanR_{ep}$): Time Period of Loan Repayment

($A_n T_{ax} P_y$): Annual Tax Payment

$[A_n T_{ax} P_y = T_{axb} I_{ncm} * A_n T_{ax} R_a]$

($A_n T_{ax} R_a$): Annual tax Rate

($T_{axb} I_{ncm}$): Taxable Income

$$T_{axb} I_{ncm} = A_n O_p P_{rft} - A_{cc} D_p C_{hrg} - loanI_{nt} C_{hrg}$$

($A_{cc} D_p C_{hrg}$): Accounted Depreciation Charge Cost

$$A_{cc} D_p C_{hrg} = \frac{C_a C_{st}}{T_m P_e D_{ep}}$$

($T_m P_e D_{ep}$): Time Period of Depreciation

($loanI_{nt} C_{hrg}$): Loan Interest Charged

Net Present Value [NPV]:

From equation (7-14) and (7-15)

Initial Cash Flow$[I_n C_a F_l = Loan - C_a C_{st}]$

$C_a C_{st} = (S_p GTC_{st} * P_{iso})/(1 - (I_{ns} C_{on} C_{st} R_a))$

$$[NPV = I_n C_a F_l + \sum_{m}^{PEL} \frac{A_n N_e C_a F_l}{(1 + loanIOR)}]$$

In this project FORTRAN95 language is used to build an economic model used for all the calculations required to evaluate the economic factors, which can be used to determine economic viability of the project through calculating

the Internal Rate of Return and time of starting generating money by knowing the Discounted Payback Period, and calculate NPV as well as Generation Cost.

Energy and Power Demand

Three sites in Greece have been chosen to represent three magnitudes of power demands. In all three sites power, heat and energy demands are included and represented in Figure 7-3 and Figure 7-4 [88].

Rhodes Island: -This lies within a group of islands located in the south-eastern part of the Aegean Sea.

Lemnos Island: - This is also a Greek island located in the northern Aegean Sea. It has wide area of 476km^2, and is considered as the second largest island in Lesvos County.

International Airport: - This airport is placed in the second-largest city in Greece, Thessaloniki. It is the capital of Central Macedonia region. The airport is established with 8,000,000 passengers per year capacity, and estimated total peak load of 3500 passengers hourly. More details about the three locations (sites) are available in [88].

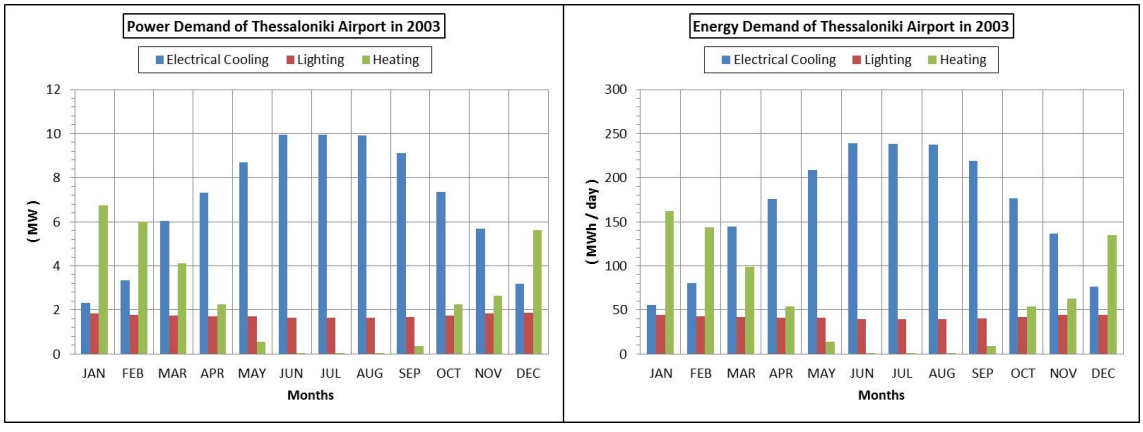

Figure 7-3 Energy and Power demand for Thessaloniki Airport

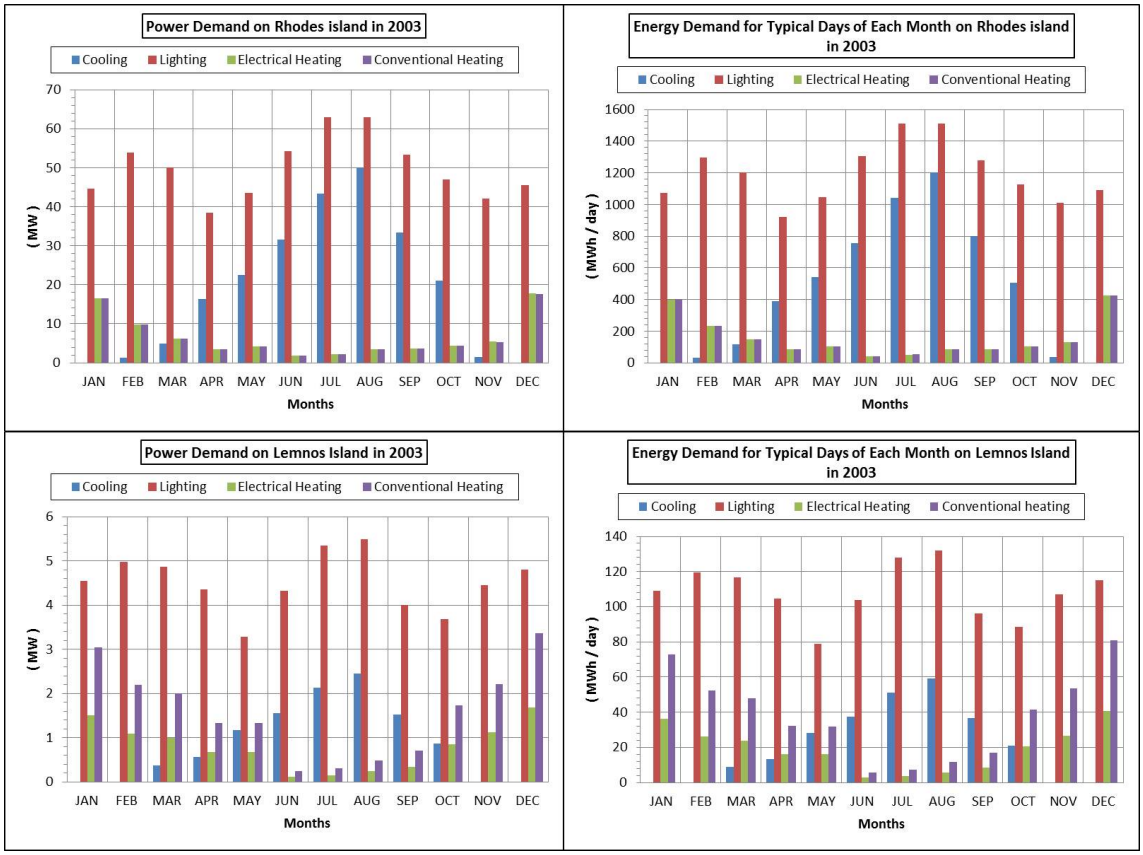

Figure 7-4 Energy and Power demand for Rhodes and Lemnos Islands

Hourly variation of Power Demand and Ambient Temperature

Hourly demand of power given in Figure 7-3 and Figure 7-4 is the average of a typical day. So, the hourly demand profile changes with ambient temperature are analysed and manipulated in order to apply the newly designed derivative gas turbine engines on power generation application. The ambient temperature change profile is calculated based on climate change history records published in Weather Underground [87]. As was mentioned, three typical seasonal days have been chosen to cover the whole year. Dotted lines on Figure 7-5 and Figure 7-6 represent the ambient temperature of the determined three typical seasonal days, whilst other lines show values of power demand. It can be clearly observed from Figure 7-4 that demand curves show that Rhodes Island has the largest power and energy demand with average maximum total of magnitude 110MW. Lemnos Island exhibits the smallest demand of the three sites.

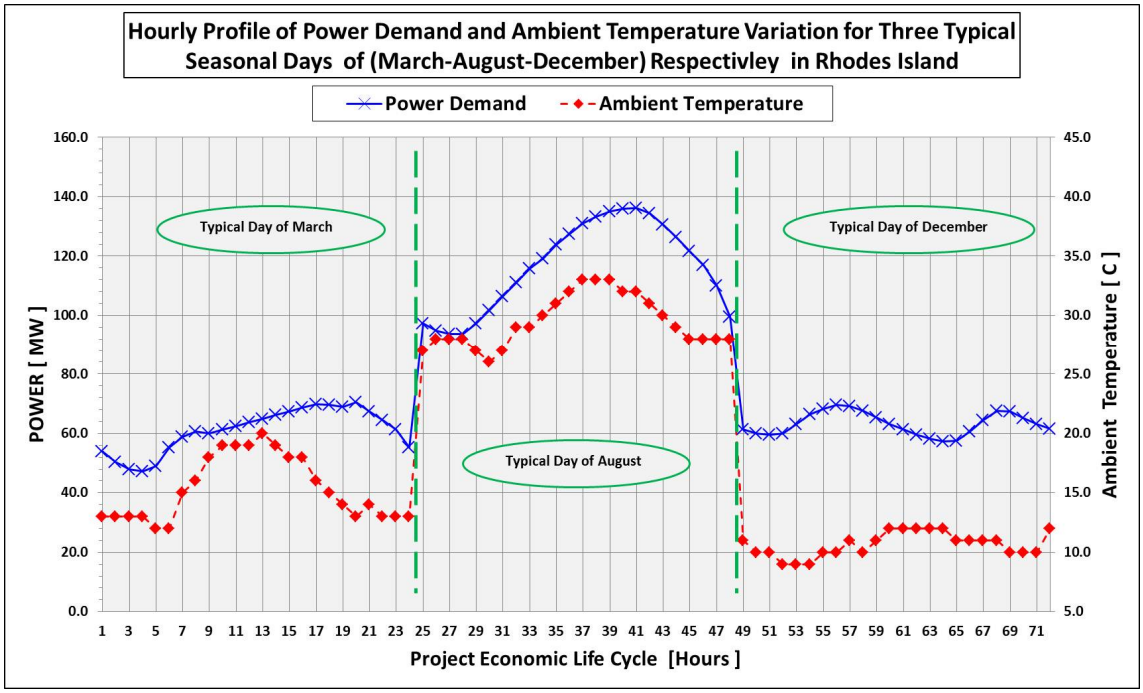

Figure 7-5 Daily Power Demand and Ambient Temperature Profiles of Typical (Winter-Fall-Summer) Days in Rhodes Island, Greece

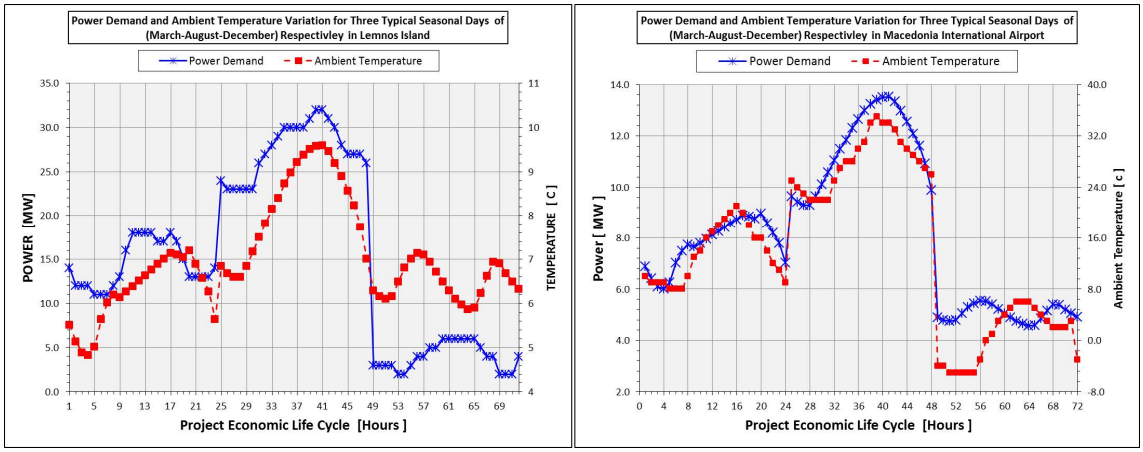

Figure 7-6 Daily Power Demand and Ambient Temperature Profiles of Typical (Winter-Fall-Summer) Days in Lemnos Island and Macedonia Airport (Thessaloniki)

Power demand hourly variation profiles were estimated according to the average values previously given. The estimation is based on methods for estimating load variation adapted from ERCOT [39]. In this project, an Excel worksheet is used to create correlations from energy and power demand curves provided by (2010 ERCOT) planning reports for three different seasons of the year. These correlations are used to form the demand curves for Rhodes, Lemnos Islands and the Airport based on the given hourly average demand.

The results of three seasonal days are shown in Figure 7-5 and Figure 7-6. The line curves represent power demand while dotted curves are allotted to ambient temperature for March, August, and December of each site. Electricity power demand is based on the assumption of adding the demand of lighting, cooling, and electric heating in total to represent the electricity power demand required by all sectors to form the demand curves.

Emission Prediction

The emission model was already used in estimating emission contents of $CO_2, CO, NO_X, and\ UHC$ for a wide range of the engine's off-design performance under variation of ambient temperature and pressure. The emission model used predicts the quantity of each factor relative to unit of kilogram of burned fuel, and all these values are already provided within the engine's performance TXT files.

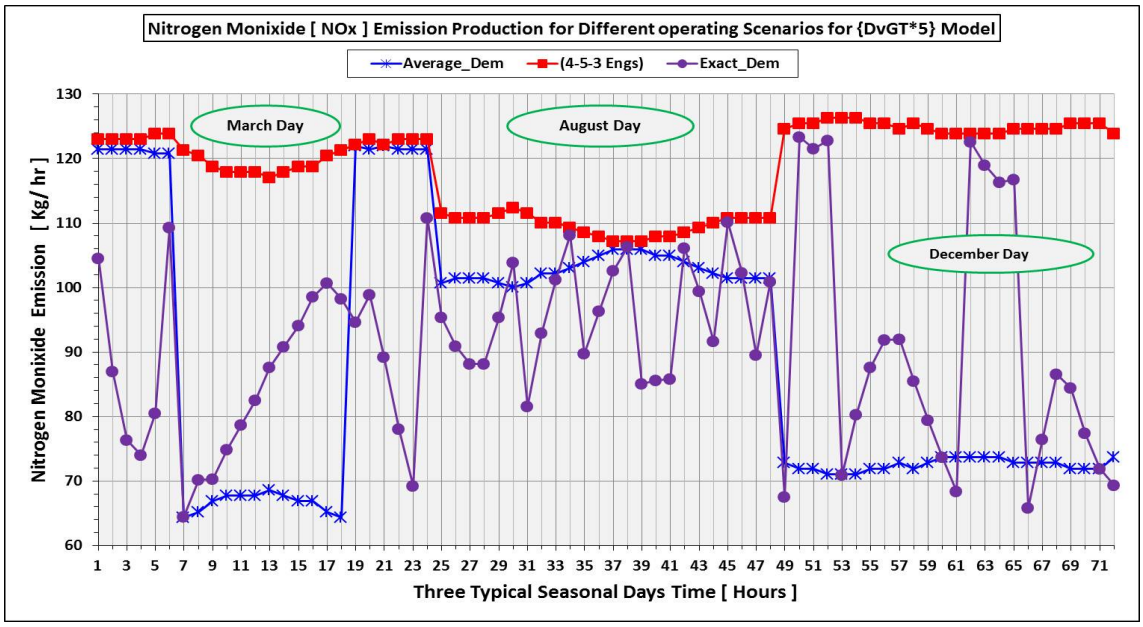

Figure 7-7 Hourly Production of NOx Emission for Typical Three Seasonal Days for DvGT*5 Aeroderivative Engine Model

The economic model interpolates values of emission contents at each hour and then sums up the total produced in each season and per year and the results are plotted as shown in the example in Figure 7-7. It shows an example of hourly production of NOx emission for three chosen typical seasonal days.

It is worth to mention that three curves on Figure 7-7 are representatives of three operating scenarios [Averge_Dem, (4-5-3), Exact_Dem] of gas turbine engine model applied on power generation application. Hourly production of NOx emission is varying depends on number of units engaged and their operating temperature. More details are shown later in Figure 7-8.

Other aspects or factors of emission pollutant, such as $CO, CO2, and\ UHC$ are calculated and presented in figures included in appendix [C.2]. In fact, these values are influenced and affected by changes in power demand and operating ambient conditions, which are considered as the main factors affecting the engine's fuel consumption and emission of pollutants.

Economic Factors Evaluation

Calculations in the economic model start with finding and matching the exact engine's operating point, which either exactly matches power demand or provides maximum power at specific ambient temperature and altitude. Also, it figures out engines-number configuration which satisfies the demand at determined conditions. All the economic factors (Cash flow-in and Cash flow-out) are calculated based on NPV methodology over the whole proposed project economic life cycle.

A project's economic life time period of investment is represented by yearly time intervals, and each year is assumed to be divided into three segments of three seasons (Winter, Spring & Autumn, and Summer). One typical day has been chosen for each season to represent the whole season period of time and multiplied by the number of days in each season. Therefore, the one typical seasonal day used to represent Spring season weather has also been chosen to represent Autumn season. Therefore, these typical days will be multiplied in the dedicated number of days of the month, then in the number of months of each season. So, the total will be 365 days which is equal to a year.

An optimisation study is needed to find the best economic hourly operating scenarios for the engines for the three typical selected seasonal days of the year. Optimisation analysis will be based on different Engine-Number

configurations throughout the year. Four different operating scenarios have been determined for conducting the optimisation analysis, and an assumption of selling surplus and buying for deficiency when proposed is applied. Operating scenarios are summarised as follows:

1. Matching the exact demand curve profile for the three seasons
2. Matching constant average demand curve profile
3. Operating on constant number of engine operating all over the year
4. Operating randomly on different engine-number configurations

Economic variants required for economic calculation are assumed as follows:

- Economic Life Cycle time= 25 Years
- Loan = Capital cost
- Loan Interest Rate= 11.5%
- Time Period of Loan repayment=11 Years
- Annual Tax Rate =20.0 [%]
- CO2 Tax Rate= 17 [£/Tone]
- Contract Electricity Price= 33.5 [£/MWe]
- Electricity Surplus Price= 13.77 [£/MWe]
- Electricity Buy Price= 26.22 [£/MWe]
- Fuel tariff Rate= 0.058282 [£/Kg]
- Interest Rate is Fixed along the Investment and equal=6.0 [%]

All selected gas turbine engine models are implemented in the optimisation study and their results are clarified in Figure 7-8 and appendix [C.3]. An example of optimisation calculation results is plotted in Figure 7-8, which represents engine model DvGT*1. It can be seen that operating a constant number of engines throughout the year leads to the shortest payback period and the highest NPV at the end of the project. Similar conclusions resulted from the optimisation process for most investigated engine models. In addition, a huge variation in the number of engines from 6 to 19 engines was required to exactly match the demand variation profile of the three proposed typical seasonal days of the year. Moreover, the maximum number of engines required has been reduced by two-engines when the power generation plant operated on

Scenario 2 of matching the average of power demand profile. The second most efficient and economic option is when the plant operated on Scenario 4 when the engines operate at maximum output power of eight engines in winter and fall seasons, while twelve engines required for operating in summer.

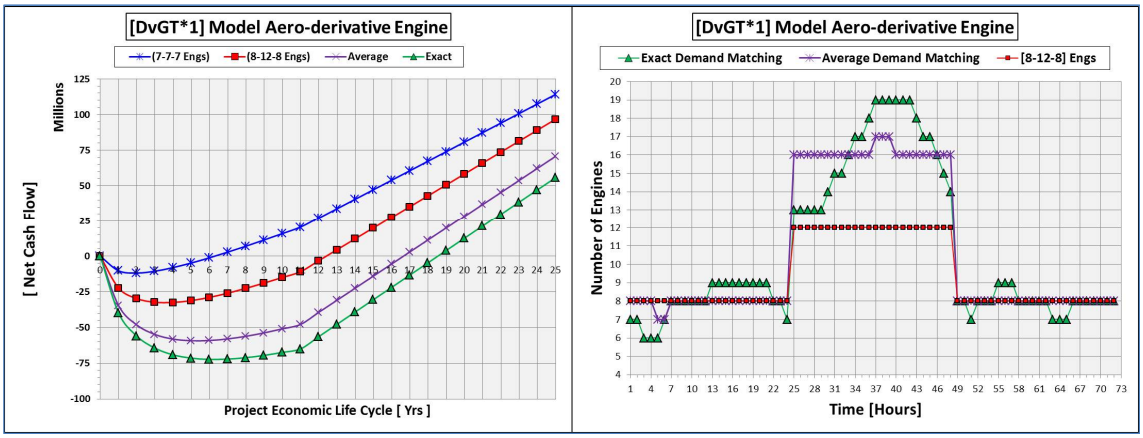

Figure 7-8 Techno-economic Optimization of Different Operating Scenarios for Selected DvGT*1 Engine Model on PG Plant in Rhodes Island

However, it is important to remember that assessing the newly designed derivative gas turbine engines are the main objective of performing the comparative techno-economic analysis in this chapter. Therefore, conclusions from optimisation analysis are dependent on the proposed estimation of the values of economic variants as well as the assumption of their fixed value throughout the economic life time of investment.

In fact, these days economic variants such as surplus selling price, deficient buying price and interest rate are variable along the life time of investment. In the comparison, whether the economic variants are constant or variable, results of comparative investigation study will not affect this application.

Therefore, the engine's operating (Scenario 1) is chosen to represent the comparative assessment between selected gas turbine engine models using NPV, and its results illustrated from Figure 7-9 to Figure 7-12, while results from the comparative analysis under Scenarios (2, 3, and 4) are conveyed in Appendices [C.4 to C.8]. It can be seen in Figure 7-9 that cash-flow curves help

to determine break-even points, which specify payback periods on investment for the project for each applied model.

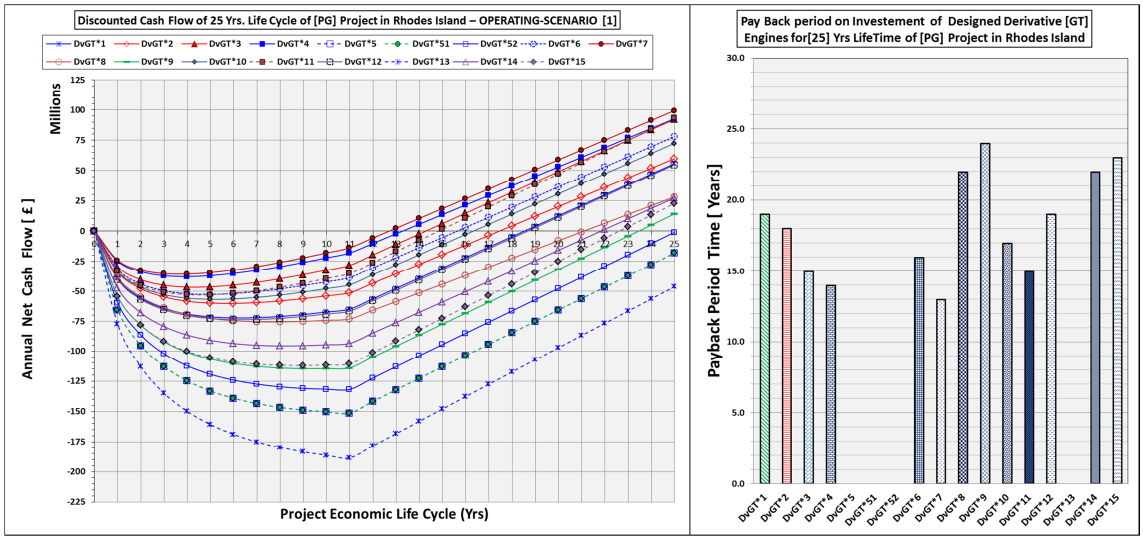

Figure 7-9 Discounted Cash Flow of all Applied Aeroderivative Models on Operation Scenario (1) for Power Generation Application in Rhodes Island

It becomes also easier to notice which engine provides the highest or lowest values of accumulative annual net profit at each year of investment. The shortest payback period is achieved on project investment when gas turbine engine models DvGT*7 and DvGT*4 are used in turn, which is followed by engines DvGT*(3, 11, 6, 10, 2, 1) respectively. In contrast, the longest payback period gained on operating engine model DvGT*9, and in turn followed by engines DvGT*(15, 14, 8, and 12). Payback period PBP is not obvious on operating engine models (DvGT*5, 51, 52, and 13), because project cash-flow does not break-even along 25 years of the project life.

As can be seen from results plotted in Appendices [C.4 and C.5], when the plant operated on Scenario3 and Scenario3 it shows the fact that the shortest payback period does not reflect the most economical selection on investment. Although the shortest payback period is achieved by selecting engine model DvGT*4, the highest net present value is attained by attaching engine model DvGT*3. So, engines DvGT*3 are considered as the most economic selection for investment on the proposed operating scenario. However, results from Scenario 1 which illustrated in Figure 7-10 shows that engine DvGT*7 achieves the shortest payback period and highest net present value, and is considered as

the most economic selection when operating in Scenario 1. It is very important to notice that if the condition of not modifying the design of aero HP compressor is applied and engines DvGT*3 and DvGT*4 are excluded, then engines DvGT*(11, 6, 10) become respectively the most efficient variants. Engine models DvGT*(5, 51) are similar variants in providing almost the same value of NPV.

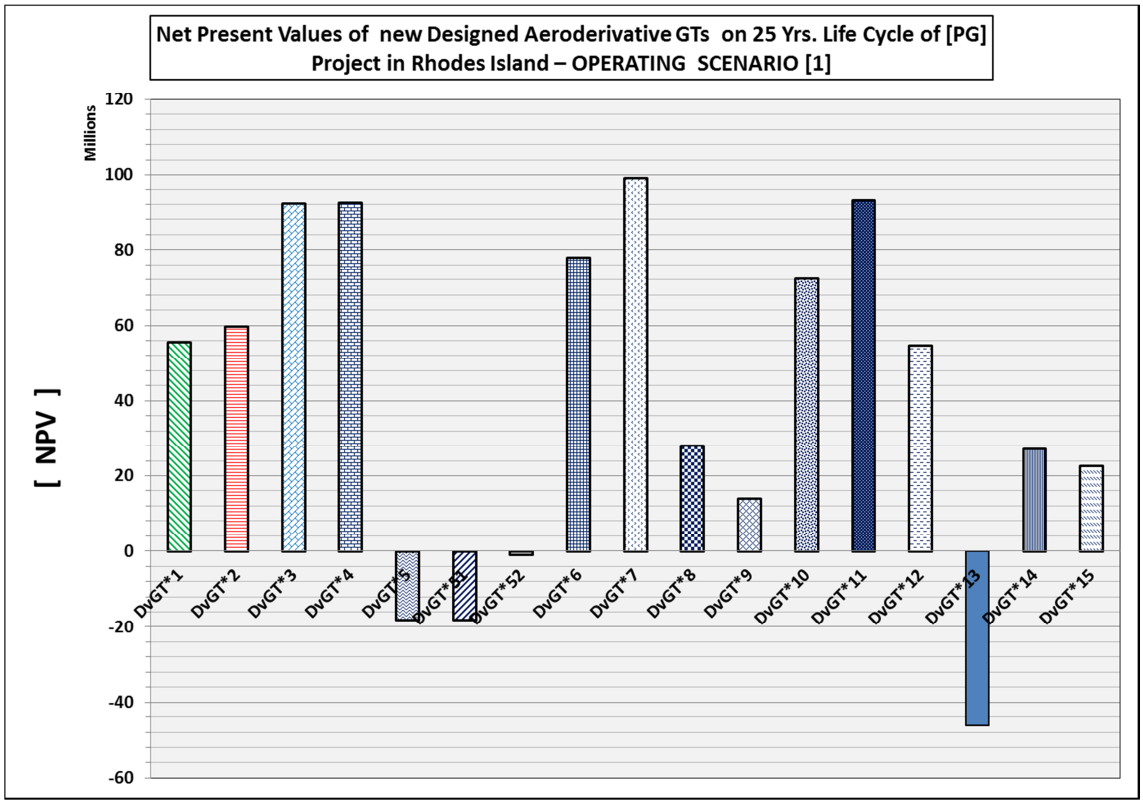

Figure 7-10 Techno-economic Comparison of Investigated Aeroderivative Engine Models on Scenario (1) Using Net Present Value Method

The definition of internal rate of return informs us that the value of Interest Rate which leads to $NPV = 0.0$ is the value of internal rate of return. An example can be seen in Figure 7-9, where an Interest Rate of 6.0% is equal to IRR on investment for engine model DvGT*52 and NPV at the end of the investment life time equals zero.

Fuel cost, as remarkably observed in Figure 7-11, dominates more than 50% (up to 72%) of running cost of most of the investigated engines. The exception is engine model DvGT*8 where fuel cost is equivalent to 46% of running cost, but it is still the highest among aspects of total operating cost. In

addition, 17.5% to 20.8% of total running cost is dedicated to O&M cost of aeroderivative gas turbine engines, while the lowest percentage of 2.5% to 6.5% is a share of deficient power cost. As shown in Figure 7-12, a huge variation in $CO2$ taxation cost of about 5.5% to 33.25% is recognised for applied derivative gas turbine engines. Also, the highest percentage is relatively generated by model DvGT*8 and the lowest related to engine DvGT*11.

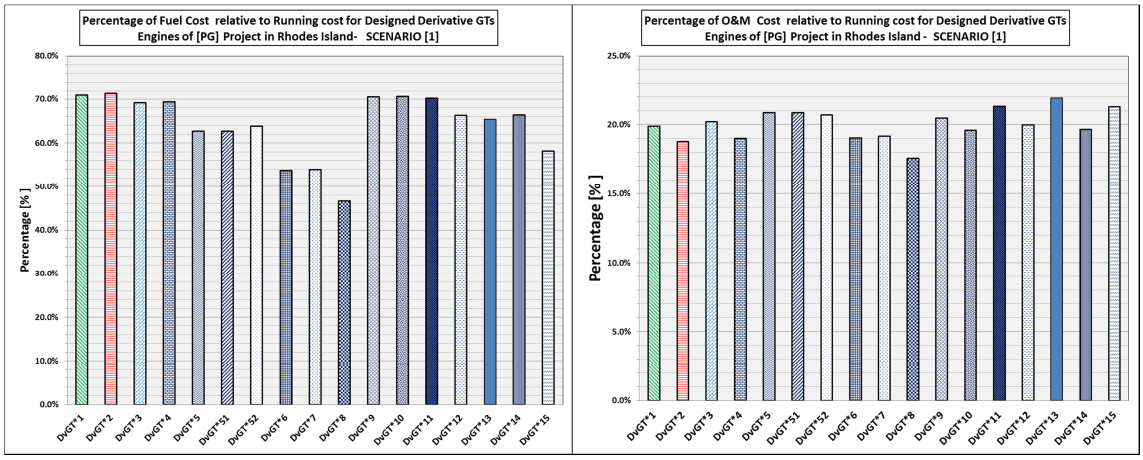

Figure 7-11 Percentage of Fuel and O&M Costs Relative to Running Cost of all Selected Aeroderivative Models on PG Application in Rhodes Island

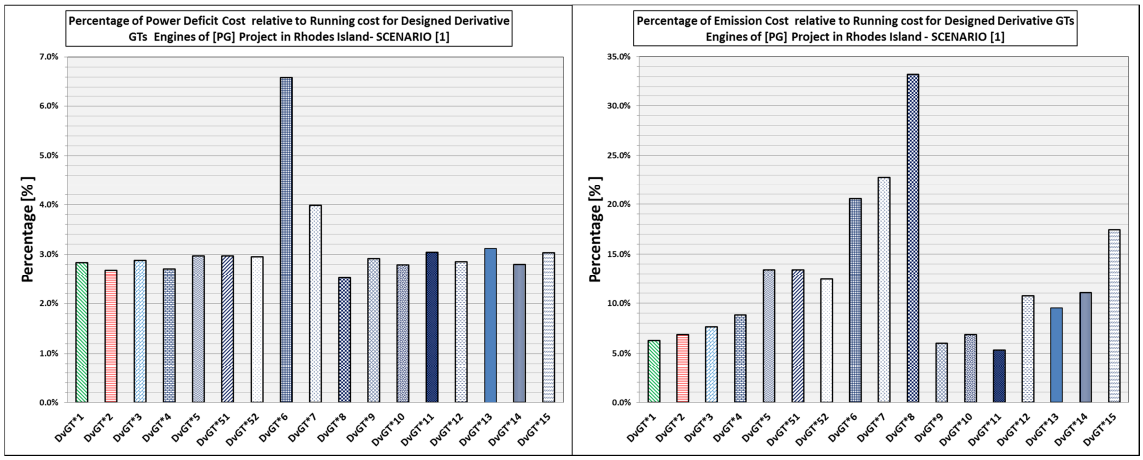

Figure 7-12 Accumulative Annual Profit and Generation Cost of all Selected Aeroderivative Models on PG Application in Rhodes Island

The results shown in appendix [C.8] indicate that the lowest accumulative annual profit can be gained on operating engine model DvGT*8, while obtaining the largest amount varies between engine models DvGT*11 and DvGT*13.

To summarise, variations and differences in results exist between investigated gas turbine engines in all operating scenarios. Observation shows that selection of a certain engine model in one scenario can be the best economical choice, whilst it is not the best in a different scenario of operation such as engine DvGT*(7, 11 and 3). In general, models of DvGT*(2, 3, 7, and 11) represent the most economic selections on all investigated scenarios, with more than 50% of running cost dedicated to fuel cost.

7.5 Techno-economic Assessing of Designed Derived GT Engine Models on Marine Propulsion Application

Diesel engine and steam turbines have dominated the propulsion of merchant ships owing to their ability of operating with crude and low quality fuel. When time restriction on delivery of passengers and food applied however, aero-derivative gas turbines offer better advantages in relatively short time such as in fast ferries and cruise ships. Aero-derivative's advantages include simplicity in installation and maintenance, achieving higher sea speed as well as lower emission. However, operating them needs higher operating cost which was overcome recently by combining two small and large gas turbines or one small gas turbine and large diesel engine to satisfy part-load operation requirements at higher thermal efficiency.

One project aiming to develop a model of investigating the performance of several aero-derivative marine gas turbines currently exists [72]. The investigation includes several models of aero-derivative gas turbine engines applied as the prime movers of propulsion system of merchant vessels. The effect of environmental variation on the voyages is included in the aero-derivative gas turbine engines evaluation. The project was first introduced by [40], and it is an integrated simulation platform for marine propulsion called Poseidon, which consists of numerical models used to evaluate the performance of ship propulsion systems using gas turbine as the prime mover. Also, the platform is capable of assessing the techno-economic potentials and environmental impacts of the gas turbine propulsion system. The assessment is

conducted through investigating the effect of environment on propulsion system performance as well as the environmental impact of marine gas turbine exhaust pollutants on the environment.

Further research work taken by [72] on the same project was based on the drawback that the initial development and implementations show that the voyage scenarios could not go beyond twenty four hours. This problem limited the applicability of the model on longer haul ocean-going voyages where the ship is expected to face diversity of rough and smooth sea and weather conditions through the manoeuvring from one ocean to another. So, in the project the aim was to further develop this simulation platform to overcome these constraints. It was conducted through investigating the performance of a variety of ship prime mover aero-derivative gas turbine propulsion systems, implemented on different ship types and configurations. Their performance investigation was conducted as a comparative analysis to evaluate the effect of varying the voyage environmental conditions. The aim could be fulfilled through the following:

- Further develop Poseidon to include the simulation for longer haul voyages.
- Evaluate the operating cost of any ocean-going merchant vessels through predicting marine aero-derivative gas turbine performance and their exhaust pollutant emissions of(CO, CO_2, UHC, NO_x).
- Finding how sea environment conditions can affect the performance of aero-derivative gas turbine engines as well as discovering how gas turbine's exhaust pollutant emission can have impact on the environment.

The last contributor introduced four merchant vessel models which represented four trade routes in order to cover long ocean to ocean distances for longer duration and transit times. The simulation based on fixed voyage road for each type of ships (cruise, fast speed ferry, cargo ship), and takes into account all possible hydrodynamic and environmental factors which ships can experience during their ocean-going movement, as shown in Table 7-1. Three

different seasonal days are taken into account for weather variation consideration as well as different sea status with three different levels of ship haul fouling roughness=120 to 360 μm. Taking into account Beaufort as the scale of sea status, the scenarios can be briefly summarised as follows:

Table 7-1 Routes Data Profiles of the Vessels [72]

Type of vessel	Port of Loading	Port of discharge	Range [nm]	Ship speed [knots]	Trip duration [hrs]
LNG Carrier	Algiers	Portsmouth	1619	19.5	84
Cargo ship	Cape Town	Rotterdam	6342	25	254
Cruise ship	Lagos	Jeddah	5687	22	259
Fast Ferry	Malta	Marseille	639	30	22

- Calm Weather (IWC): sea status less than or equal 2.0 Beaufort with wave height equal to 1.0 metre, and wind speed from 0.0 to 2.0 knots. Also, the ship hull is clean with no more than 30μm roughness.

- Rough Weather (AWC): sea status is above 3.0 on the Beaufort scale and clean surface roughness roughly equal 30μm. Also, wind speed is supposed as higher than 4 Knots.

A further two scenarios are generated based on the previous two, to apply or varying sea status (sea waves) hourly along the routes. In addition, ship hull fouling was the other parameter which has been varied for the sake of including different scenarios, also based on the conditions of the aforementioned scenarios.

To date the work has only included four gas turbine engines of simple cycle in single-spool and two-spool, and inter-cooled recuperated, all in the magnitude of 19MW to 36MW.

Relating to this project the relevance of the studies is in the aim of investigating and evaluating the performance of a variety of ship prime mover aero-derivative gas turbine propulsion systems, which are implemented on different ship types and configuration. It has been conducted through implementing the newly designed aero-derivative engines on the simulation

platform in order to increase investigated power magnitude to include the range from 5 to 87 MW. Also, implementing the designed aero-derivative engines on the ship model contributes to further improving the level of techno-economic assessment of these newly designed engines to include economic potentials in marine applications. Two routes and voyages have been chosen for assessment as presented in Figure 7-13. On the one hand it presents the journey requirements of a cruise ship when it encounters different weather conditions whilst moving from Lagos on the ocean to Jeddah in the Gulf Sea, passing through Mediterranean Sea conditions. On the other hand it expresses the effects of ambient condition changes at relatively higher speed required on a ferry moves from Malta towards Marseille. The cruise ship passenger journey from Lagos to Jeddah is proposed with ship speed equal to 40.74Km/hr equal to 22 Knots for a distance of 5687 nautical miles, which can be covered in 11 days. Required propulsion power is 42MW added to ship service requests of 34MW, which in total sums up total installed power equal to 76MW. The ferry carries passengers and their luggage at speeds of 30 knots to across 639 nm per voyage in 22 hours between Malta and Marseille.

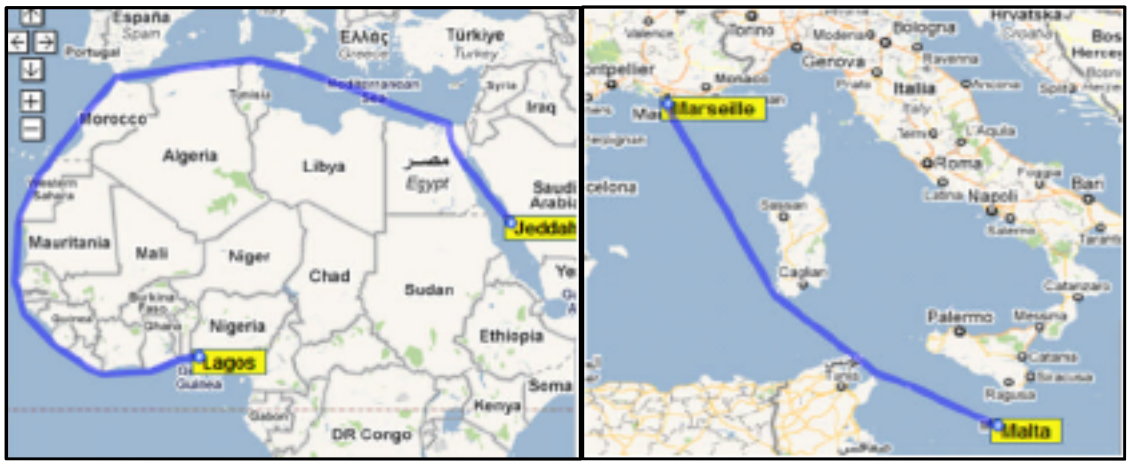

Figure 7-13 Routes Selected for Ferry and Cruise Liner Ship [72]

In this study, as illustrated in Figure 7-14 and Figure 7-15, only one operating scenario is chosen for this investigation, where calm weather IWC has been assumed on a clean ship hull journey (zero fouling). Also, sea status varies on the fast ferry ship route, while it is assumed to be calm on the cruise ship journey. So, the effect of ambient pressure and temperature change will be

investigated in order to evaluate the economic potential and technically assessing the newly designed aeroderivative engines in marine application.

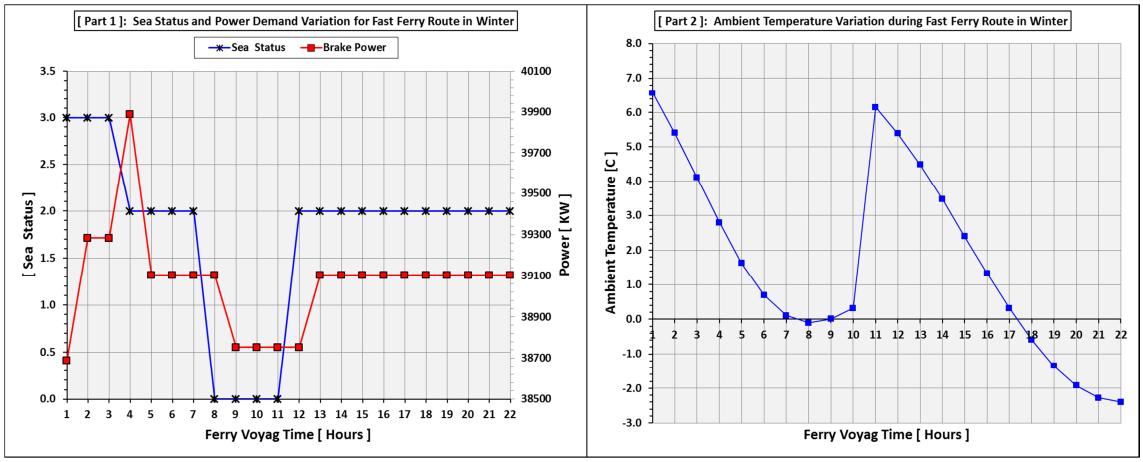

Figure 7-14 Ferry Vessel Route Conditions and Power Requirements in winter Season and Calm Weather

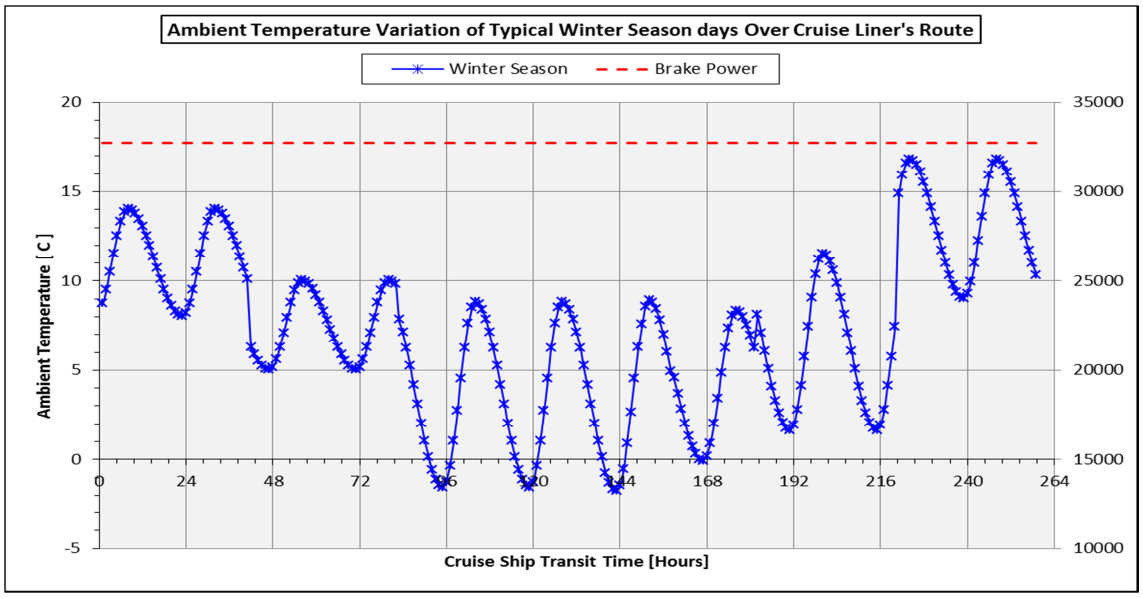

Figure 7-15 Ambient Temperature Variation of Typical Winter days Over Cruise Ship Route

7.5.1 Aeroderivative Model's Performance and Techno-economic Factors Evaluation on Ship Voyage's

Technical considerations in selecting the aero-derivative gas turbine as a prime mover of ship propulsion system on marine plant were mentioned earlier as including power capacity, weight, dimensions, ambient conditions and sea

conditions. However, economic considerations are very important factors in selecting aero-derivative gas turbine engines for marine propulsion. In addition to operating cost, which is considered as the dominator factor in selecting the gas turbine engine, reliability and durability as well as initial cost are also included. Of course environmental friendliness is another issue which must be considered amongst criteria of gas turbine selection engine these days.

Economic estimation in this work is limited to include fuel consumed on the vessel's voyage and quantities of $CO2, CO, NOx, UHC$ produced during operation along the voyage's routes. In addition, the percentage of the engine's hot section life consumed is counted as a criterion of the engine's technical evaluation.

Emission Prediction

The previous contributor has integrated the simulation platform with the emission prediction model called APPEM. It is created based on the same methodology used in the emission model previously used for power generation application, and it uses efficiency correlations with semi-empirical models in order to estimate emission pollutants at part-load operation. However, applying this model on the newly designed derivative engine faced problems of technology limitation applied on applicable combustor inlet pressure and temperature. Therefore, the emission model used in power generation application has been modified in its outputs to fit the input format of the Poseidon model, and has been used for all emission prediction calculation in marine application, an example being illustrated in Figure 7-19. It displays how emission of Carbon Monoxide mass varies with the change in propulsion power required and ambient pressure and temperature during the ferry voyage route in the winter season.

Engine Hot Section Life Estimation

All hot section life estimation is based on calculating creep, and this calculation is conducted using a model integrated in the simulation platform using the same method previously used in the power generation application

model. The outputs from the creep life calculation model are used as input data to the simulation platform. Results will be in the form of a percentage of engine life consumed, shown in Figure 7-21 and later tackled in the comparison between the newly designed derivative models.

In the next sections the gas turbine engine's performance will be investigated in both cruise and fast ferry vessel routes for different ship speeds under the assumptions of clean hull surface in calm sea status.

It can be clearly noted from Figure 7-16 that in both ships brake power varies with changes in requested ship speed. Ship brake power increases with the rise in requested ship's cruise speed. All selected models of derivative gas turbine engines have been implemented on both ship plants in order to determine their operating limitations. It is a preliminary evaluation of the variation of engine's combustor outlet temperature, thermal efficiency and emission contents when cruise speed slowly increases till the maximum possible limits of speed.

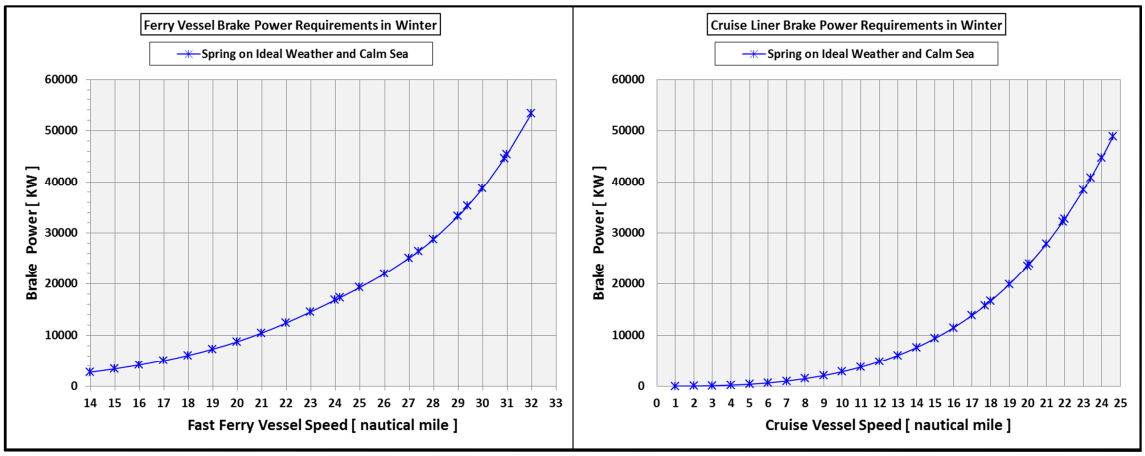

Figure 7-16 Brake Power Variation Over Different Vessel's Speed for Both Ferry and Cruise Liner

7.5.1.1 Cruise Ship Engine Performance Evaluation and Voyage Analysis

Engine's Performance Preliminary Evaluation:-

All selected derivative gas turbine engines are implemented on the cruise ship plant and operated at standard weather conditions as previously mentioned. Results from the engine's performance preliminary evaluation are

represented, some in Figure 7-17 to Figure 7-19 and the remaining in Appendices [D.1.1 to D.1.5]. For the purpose of simplifying the graphic's complexity, Figure 7-19 contains a sample of engine's performance evaluation of DvGT*1, DvGT*2, DvGT*3 and DvGT*4 while the rest are represented in the aforementioned appendices.

It can be observed in Figure 7-17 that thermal efficiency varies along with the changes in cruise ship speed on all selected gas turbine models with different configurations (number of engines required) required to satisfy these speeds.

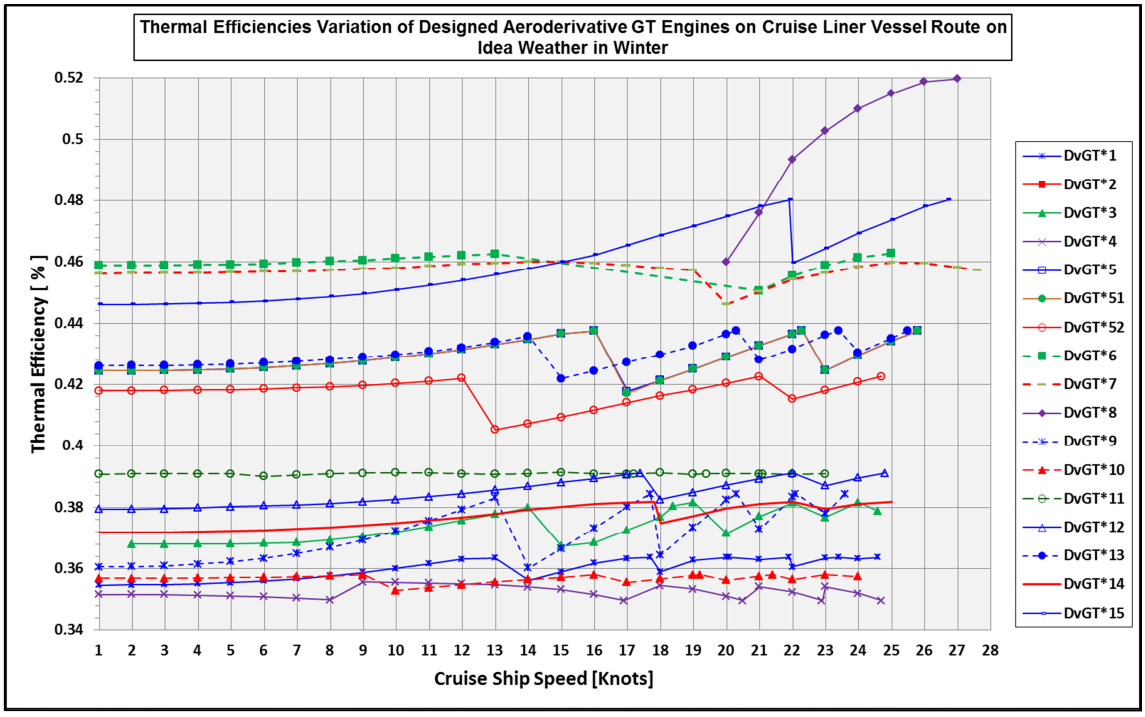

Figure 7-17 Thermal Efficiency Variation of Applied Aeroderivative Engines on Different Cruise Ship Speeds at SLS Conditions

Although the model of DvGT*8 represents the highest values of thermal efficiency on one required engine, as shown in appendix [D.1.4], it is still limited to a minimum speed of 20 knots and cannot be applied for lower ship speeds. It is important to mention that when more than one engine is engaged in propulsion system, all engines are equally sharing the load of power required to meet the requested ship's speeds. Therefore, it can be indicated that thermal efficiency profile fluctuates in intervals along changes in vessel speed due to

the differences in number of engines operating and sharing the load at each speed.

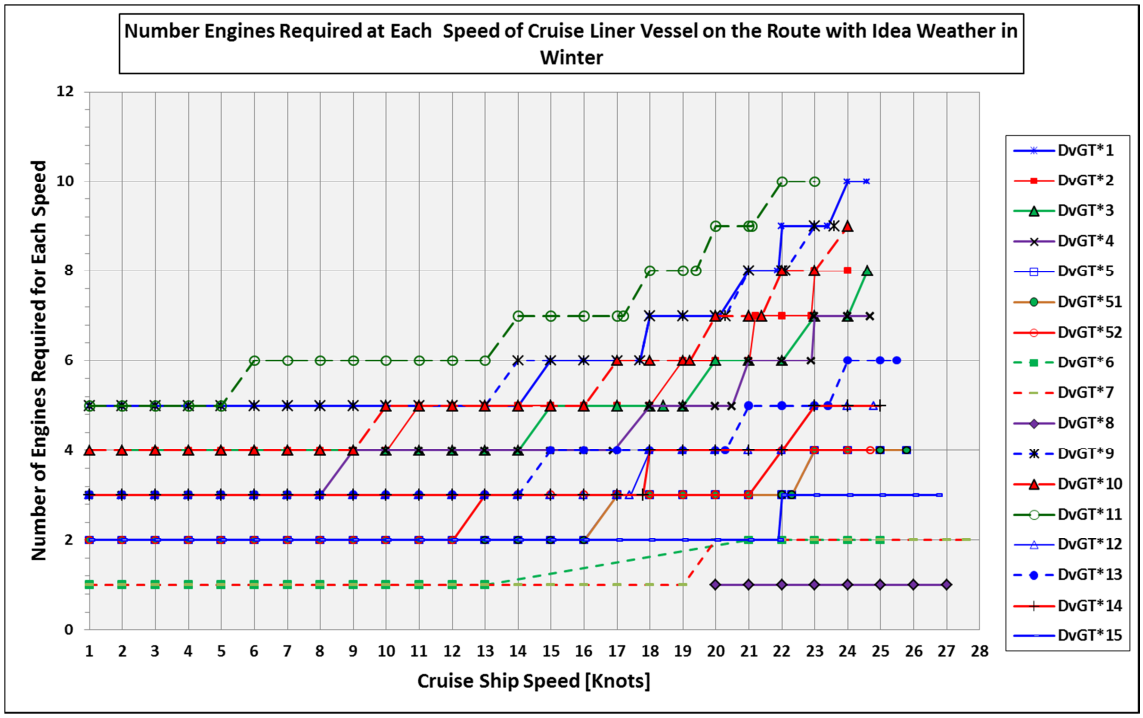

Figure 7-18 Number of Aeroderivative Engines Required for Different Cruise Liner's Vessel Speeds at SLS Conditions

Furthermore, the same trend of fluctuation is observed in profiles of combustor outlet temperature, shaft power and emission production, which are included in Appendices [D.1.1, D.1.3, D.1.5] on all cruise ship performance figures. In addition, the number of engines required to match ship brake power at each speed is plotted on appendix [D.1.4] on all performance figures and for every selected gas turbine model. The highest number of engines required at most ship speeds is dominated by engine model DvGT*11, which represents the smallest variation in thermal efficiency in the average of 39% over a wide range of ship speeds. Models DvGT*1 and DvGT*9 come second regarding the highest number of engines required with lower thermal efficiency. Most of the selected engines prove their ability of operating at low operating limits and satisfy low ship speeds with different engine configurations.

Results also indicate that engine models DvGT*6 and DvGT*7 represent the best highest thermal efficiency on a wide range of low ship speeds up to 15

knots with the lowest number of engines engaged to match these speeds. Then, engine model DvGT*15 overtakes the priority with slightly higher thermal efficiency until approaching 21knots but with a higher number of required engines. However, results on the other hand express an issue that engine DvGT*6 cannot be used in the speed range of 14 to 20knots. The reason is that the engine's maximum operating limits able to satisfy ship power demand for 13knots speed, while the minimum operating barriers of two attached engines can only meet the minimum speed of 21knots at ideal weather and sea conditions. This is justified by the fact that the two attached engines have to equally share the ship's brake power load.

Regardless of the significant loss in engine thermal efficiency however, a method of control engine mass flow can be used in order to reduce the generated output power for each engine. Then be able to operate two attached engines of DvGT*6 in the range of 14 to 20knots speed.

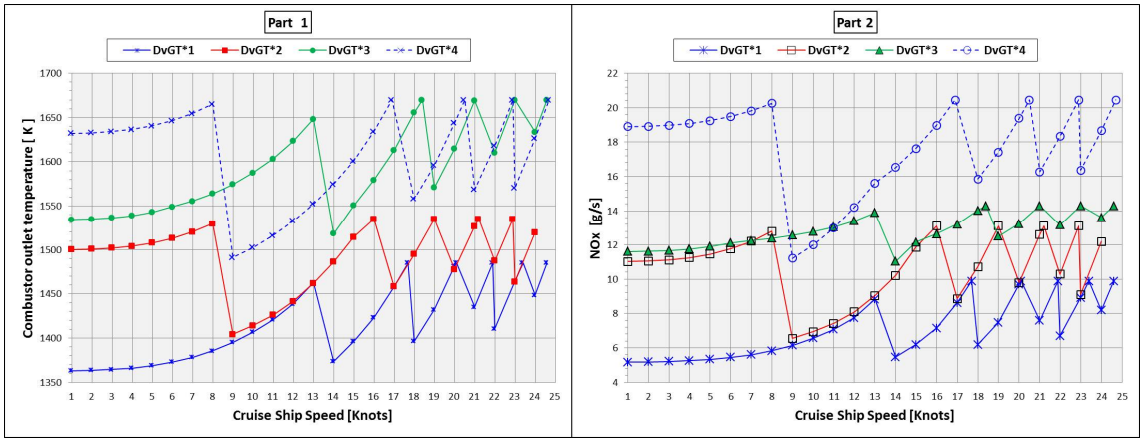

Figure 7-19 Combustor Outlet Temperature and NOx Production of a sample of Aeroderivative Engines Applied on Cruise Ship Route at SLS Conditions

The NOx emission production and combustor outlet temperature profiles are clarified in Figure 7-19 and Appendices [D.1D.1.1 and D.1.5]. Severe drop or losses occurred in performance parameters when an extra engine was attached due to the fact that all engines share equally share the load and operate at lower operating temperature. A magnitude of this drop is gradually reduced at relatively high values of ship speed where the variation in operating temperatures becomes relatively minor.

Voyage Analysis:-

Gas turbine power output is matched to the required cruise ship's brake power along the voyage route conditions with the purpose of discovering which engine's model can best fit the requirements of the vessel. The investigation is conducted subjected to the aforementioned weather conditions and sea status represented in Figure 7-15. The economic ship speed is dedicated as equal to 22knots. According to the gas turbine model's performance evaluation, there will be a variety of engine configurations used and required to satisfy power required to boost the cruise ship at this speed in ideal sea and weather conditions. Power availability and number of required installed gas turbine engines is stated in Table 7-2. It is worth mentioning that these values are calculated considering ideal weather conditions and calm sea status.

Table 7-2 Number of Installed Engines on Cruise Ship Vessel

GT Model	Ship Brake Power (KW)	Ship Economic Speed	Installed Engines Number	Min Eng Power (MW)	Min Ship Speed	Min Brake Power (KW)	Max Eng Power (MW)	Max Ship Speed	Max Brake Power (KW)
DvGT*1	32740.612	22	9	7.416	22	32740.612	8.042	23	38376.073
DvGT*2	32740.612	22	8	8.343	22	32740.612	8.932	22.9	37779.556
DvGT*3	32740.612	22	7	9.534	22	32740.612	10.311	23	38376.073
DvGT*4	32740.612	22	6	10.303	21	27815.63	11.896	22.9	37779.556
DvGT*5	32740.612	22	3	15.401	17	12203.76	21.511	22.3	30579.366
DvGT*51	32740.612	22	3	15.401	17	12203.786	21.511	22.3	30579.366
DvGT*52	32740.612	22	4	15.78	22	29120.048	19.445	24.7	44411.307
DvGT*6	32740.612	22	2	29.341	21	24681.159	40.024	25	46445.512
DvGT*7	32740.612	22	2	27.422	20	20844.45	51.23	27.6	69111.869
DvGT*8	32740.612	22	1	54.844	20	20844.45	90.44	27	56504.125
DvGT*9	32740.612	22	8	7.335	21	24681.159	7.948	22.1	29602.089
DvGT*10	32740.612	22	8	8.343	22	32740.612	9.041	23	38376.073
DvGT*11	32740.612	22	10	6.674	22	32740.312	6.901	23	35469.259
DvGT*12	32740.612	22	4	12.167	18	14666.235	15.686	22	29120.048
DvGT*13	32740.612	22	5	11.736	21	24681.159	13.979	23.4	36438.818
DvGT*14	32740.612	22	4	12.167	18	14666.235	15.78	22	29120.048
DvGT*15	32740.612	22	3	21.04	22	29120.048	31.217	26.7	60092.803

With the assumption of calm sea status and clean ship hull, ambient temperature is the only factor considered to affect the performance of the cruise ship and gas turbine engines. As a result, ship brake power required is almost constant along the cruise ship voyage route and only the gas turbine engine performance will be affected. Results of the techno-economic evaluation and

effects of ambient temperature variation on gas turbine engine performance along the cruise ship's route are conveyed on Figure 7-20 to Figure 7-22 as well as appendix [D.1.6]. It highlights the performance characteristic and economic factors of a one-way trip of 11 days from Nigeria to Jeddah, as mentioned above.

The target speed for the whole journey is 22knots and Figure 7-20 profiles the engine's operating temperature across the route. As is common, all applied gas turbine engines behave normally as they tend to operate at lower firing temperature when a reduction experienced in ambient temperature and vice versa when it increases.

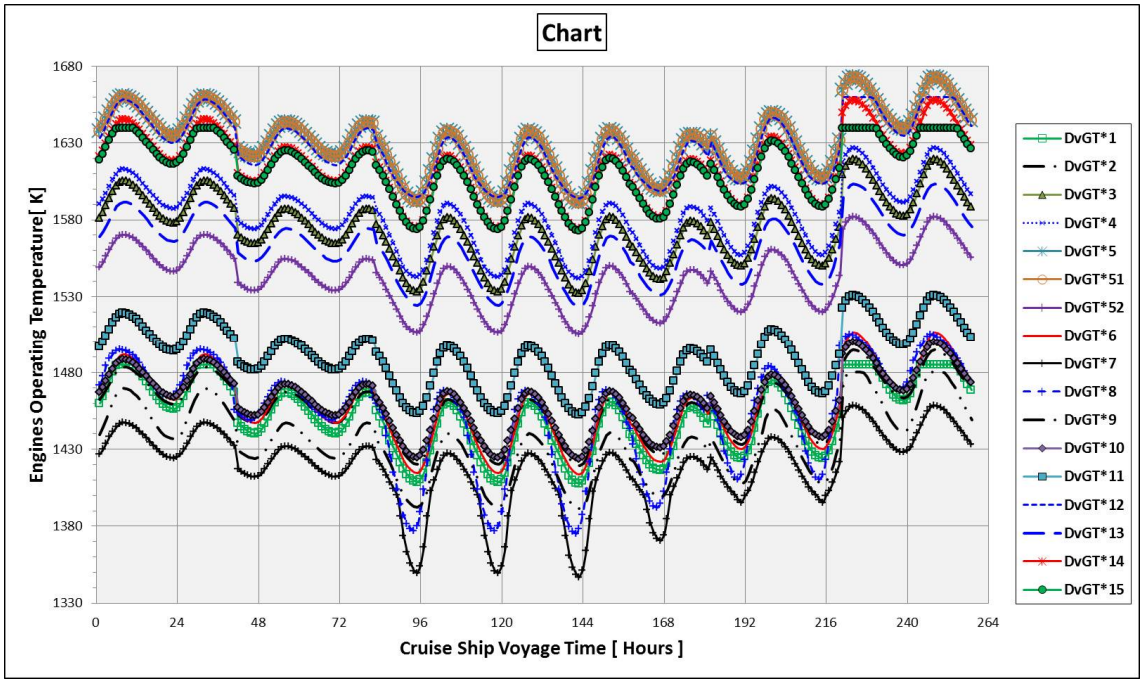

Figure 7-20 Operating Temperature Variation of Aeroderivative Engines during Changes in Cruise Ship Voyage Route Conditions

It can be highlighted from Chart 4 in appendix [D.1.6] that under assumed conditions and power availability all investigated engines are able to satisfy required propulsion power with a constant number of operating engines from the start. In other words, minimum and maximum operating limitations of each selected engine's configurations can offset variation occurring in ambient temperatures. However, the case will be expected to be different where higher propulsion power is required when sea status changes and ship hull degraded.

Economic evaluation is limited to the amount of fuel consumed and quantity of emission produced from each engine model. Also, the life of the engine hot section parts is considered. It is concluded from evaluation of economic factors, as illustrated in Figure 7-21 and Figure 7-22 that engine model DvGT*11 appears to be the most economic option.

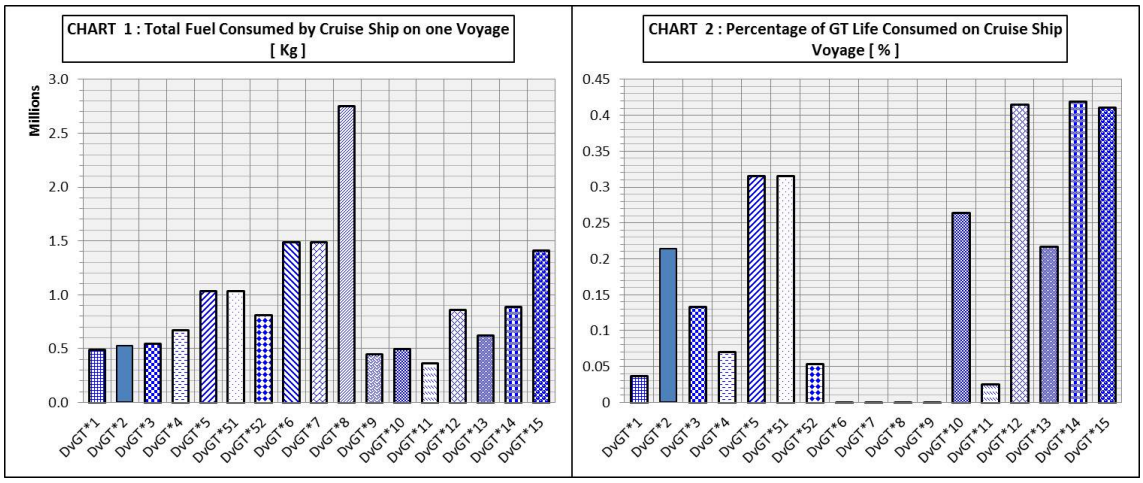

Figure 7-21 Total Fuel and Hot Section Life Consumed by Cruise Ship on One-Way Voyage Route

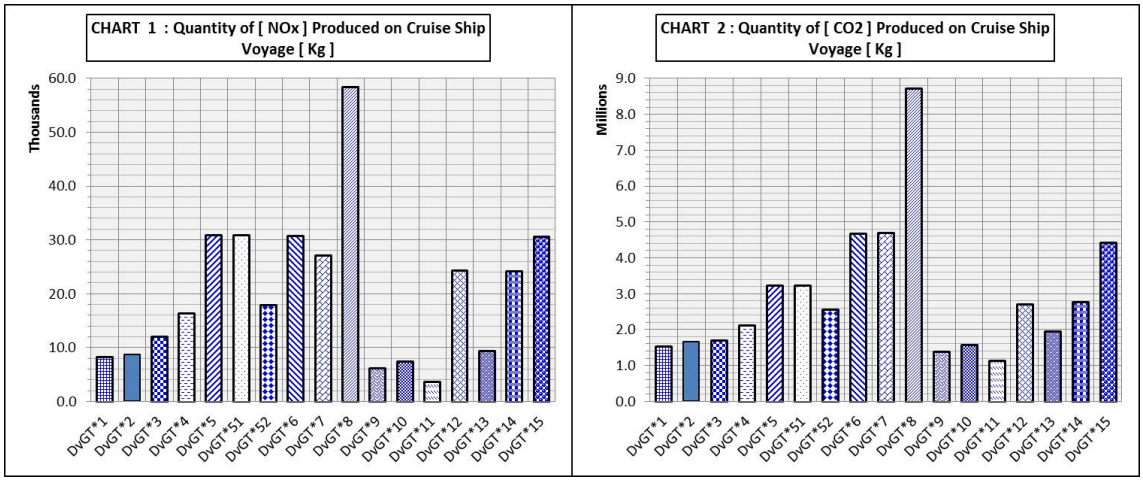

Figure 7-22 Quantity of $CO2$ and NOx Produced by Aeroderivative Engine Model's Applied on One-way Cruise Ship Voyage Route

The lowest amount of fuel consumed was recorded for this engine with acceptable percentage of life consumption. Considering taxation and toxicity, Nitrogen Monoxide and Carbon Dioxide are the most important of emission components, and engine model DvGT*11 has recorded the smallest produced

quantity of them. However, it does not compete in producing UHC and CO and there are other engines which produce less. Another option is the second competitor engine model DvGT*9 which needs a slightly higher amount of fuel consumed and gains a much better percentage of life consumed. The engine models of DvGT*1, DvGT*2, DvGT*3 and DvGT*10 represent a good third option for choice, while the relatively worst case selection will be engine model DvGT*8 with a massive quantity of fuel consumed as well as emission produced.

7.5.1.2 Fast Ferry Engine Performance Evaluation and Voyage Analysis

Fast ferry is the second marine application chosen in order to fulfil the techno-economic assessment of the designed derivative gas turbine engines. Accordingly, all derivative gas turbine engine models previously applied in the cruise ship plant are being implemented and investigated in ferry application. Referring to Figure 7-14 the ferry vessel will encounter variation in sea status along with a change in ambient temperature.

Engine's Performance Preliminary Evaluation:-

First of all, performance of all investigated engines will be evaluated on the ferry ship route at different ship speeds in ideal weather conditions and (0.0 $\mathcal{C}$) ambient temperature. All engine performance preliminary evaluation is contained in Figure 7-23 and Figure 7-24 as well as Appendices [D.2.1D.2.5].

Unlike the case of cruise ships, the ferry relatively requires much less brake power, as previously illustrated in Figure 7-16, to reach the same cruise speeds. Thermal efficiency variation profiles of each investigated engine are plotted in Figure 7-23. It can be seen that the trend is similar to cruise ship application. For each specific engine configuration thermal efficiency rises with the increase in ship speeds. However, the whole engine's performance experiences severe drop at each point where extra engines are engaged owing to operating all engines in the configuration at lower operating temperature.

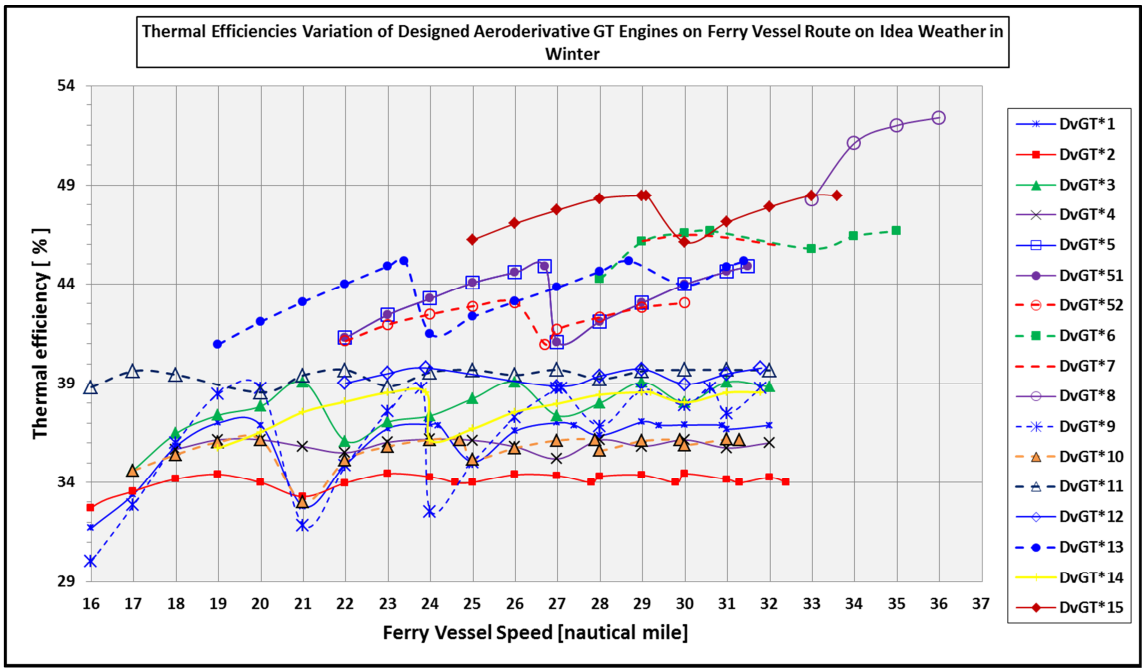

Figure 7-23 Thermal Efficiency Variation of Aeroderivative Engines Applied on Different Fast Ferry Vessel Speeds at SLS Conditions

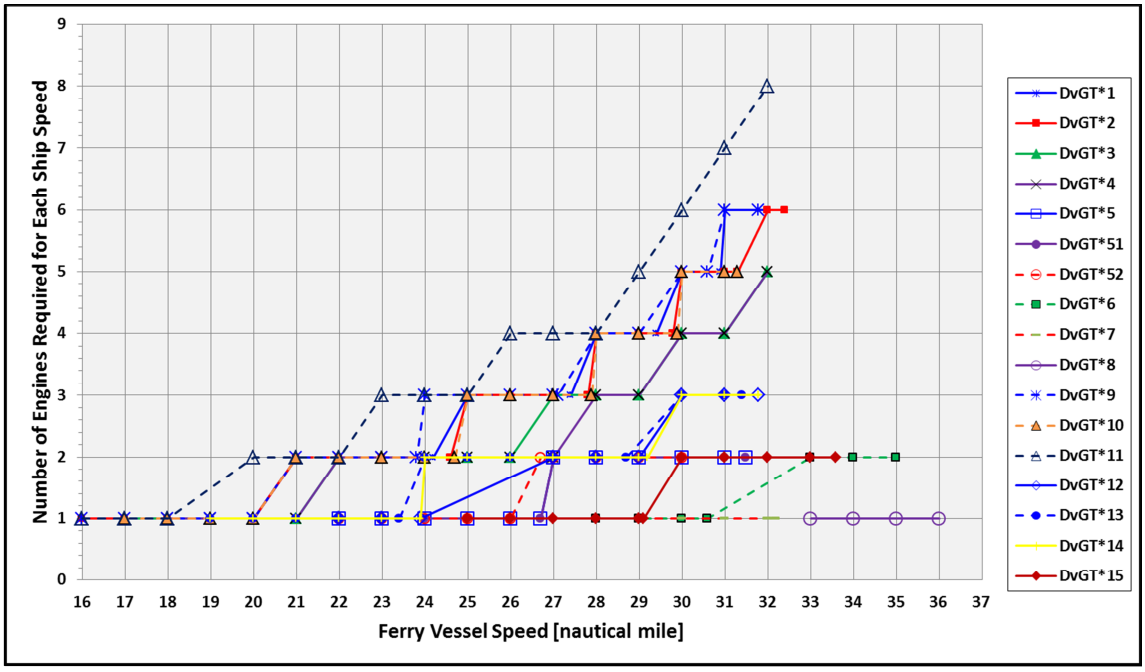

Figure 7-24 Performance Evaluation of a sample of the new Designed Aero-derivative Engines Applied on Ferry Route at ISA Conditions

The designed economic speed of the ferry ship is determined at 30knots, and the investigations are conducted including values far beyond this speed (as in Figure 7-24) in order to accommodate extra load encountered due to sea

status variation. Also, the lowest speed chosen on this investigation is 16knots. According to power availability and limitations, it is only engine models DvGT*(1, 2, 3, 4, 9, 11) which can normally operate at the low speed limit of 20knots. If it is necessary for the rest of the engines to operate at this level, a method of mass flow control such as $VIGVs$ can be used. The highest value of efficiency is gained by engine DvGT*11 at low speeds of up to 19knots, which is then dominated by engine DvGT*13, where it in turn hands over to engine DvGT*15 at a speed of 24knots which competes up to 25knots. In addition, the range of 25 to 29.8knots speed is predominated by engine DvGT*15 with highest efficiency as well as speeds from 31 to 33 knots. While, DvGT*6 achieves superior efficiency in between in the speed interval of (30 to 30.9) knots.

Considering the dedicated economic speed of 30 knots all required engine configurations and their power availability are listed in Table 7-3 and summarised in Appendices [D.2.3 and D.2.4].

Table 7-3 Engine-Number and Configurations of Installed Engines on Fast Ferry Ship

GT Model	Ship Brake Power (KW)	Ship Economic Speed	Installed Engines Number	Min Eng Power (MW)	Min Ship Speed	Min Brake Power (KW)	Max Eng Power (MW)	Max Ship Speed	Max Brake Power (KW)
DvGT*1	38753.46	30	5	7.951	30	38753.46	9.0601	30.9	44691.717
DvGT*2	38753.46	30	5	7.951	30	38753.46	9.638	31.3	47658.976
DvGT*3	38753.46	30	4	9.938	30	38753.46	11.456	31	45413.183
DvGT*4	38753.46	30	4	9.938	30	38753.46	11.603	31	45413.183
DvGT*5	38753.46	30	2	13.029	27	25058.906	24.801	31.5	49222.831
DvGT*51	38753.46	30	2	13.029	27	25058.906	24.801	31.5	49222.831
DvGT*52	38753.46	30	2	13.029	27	25058.906	21.902	30.7	43285.233
DvGT*6	38753.46	30	1	29.759	28	28759.446	43.563	30.6	42600.122
DvGT*7	38753.46	30	1	34.259	29	33259.156	55.865	32.2	55110.948
DvGT*8	38753.46	30	1	63.634	33	62634.098	98.392	36	98016.766
DvGT*9	38753.46	30	5	7.951	30	38753.46	8.689	30.6	42600.122
DvGT*10	38753.46	30	5	7.951	30	38753.46	9.708	31.3	47658.976
DvGT*11	38753.46	30	6	6.626	30	38753.46	6.626	30	38753.46
DvGT*12	38753.46	30	3	13.251	30	38753.46	17.52	31.8	51666.409
DvGT*13	38753.46	30	3	13.251	30	38753.46	16.254	31.4	48433.504
DvGT*14	38753.46	30	3	13.251	30	38753.46	17.502	31.8	51666.409
DvGT*15	38753.46	30	2	19.877	30	38753.46	34.747	33.6	65523.014

It can be clearly observed that the most efficient engines operate at this speed are, in ascending order, DvGT*(6, 15, 13, 5 and 51), while the most inefficient models are respectively DvGT*(2, 10, 4, 9). But it is important to

understand that these best and worst orders are only valid specifically under current operational conditions. It means that it is not necessary for the competitor engine under current sea status conditions to be so for the whole voyage route, even at the same speed.

Voyage Analysis:-

Analysing the voyage helps in finding the best suitable gas turbine engine model and its configuration (thermodynamic cycle and engine configuration) for the determined ferry voyage route and under weather and sea status, indicated in Figure 7-14. Similar procedures to those taken in Section 7.5.1.1 are followed to perform the techno-economic evaluation for all investigated derivative gas turbine models. Unlike the case of cruise ships, engines on the fast ferry ship route come across variation of both sea status and weather ambient temperature. All selected models have been exercised and results of all techno-economic evaluation are summarised in Figure 7-25 and Figure 7-26 as well as appendix [D.2.6].

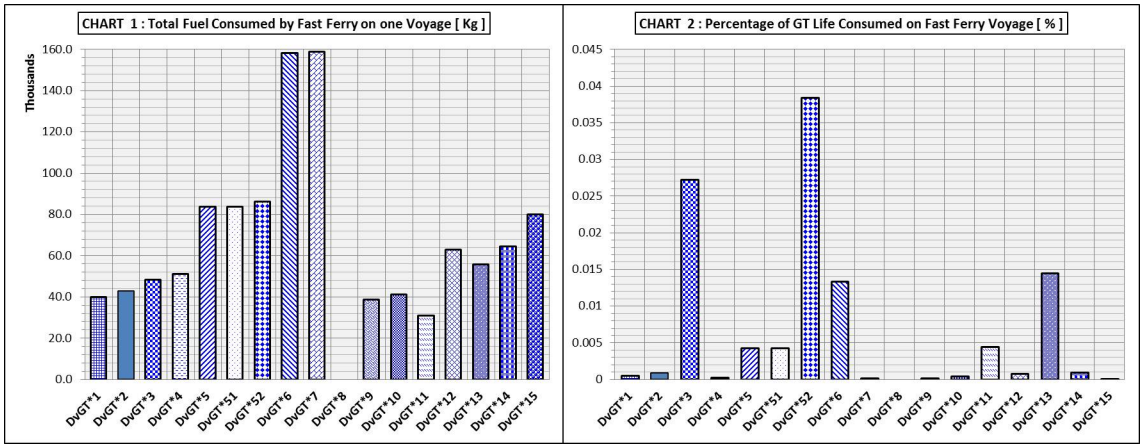

Figure 7-25 Percentage of Hot section Life and Quantity of Fuel Consumed on One-way Journey of Fast Ferry Ship Voyage

It can be clearly highlighted that DvGT*8 cannot be applied to the application as its lowest operating limit is still over or far above the maximum economic speed. Also, the negative effect of sea irritation can be illustrated in Charts 1, 2, 3 and 7 in appendix [D.2.6]. Engine performance trends indicate

that the more the sea irritated, the higher brake power was demanded by the propulsion system owing to the increase in ship resistance.

Considering fuel consumption, engine model DvGT*11 proved the best competitor consuming the relatively lowest amount of fuel along the ship's voyage. Also, the percentage of engine life consumed and quantity of emission produced NOx and CO2 are still acceptable among the investigated models. In addition, next to the most efficient choice, engine models DvGT*(1, 2, 9, and 10) provide acceptable competitors, almost demanding the same amount of fuel and producing a comparable quantity of emission contents. On the other hand, engine models DvGT*6 and DvGT*7 produce the highest quantities of emissions as well as consume the highest amount of fuel along the voyage.

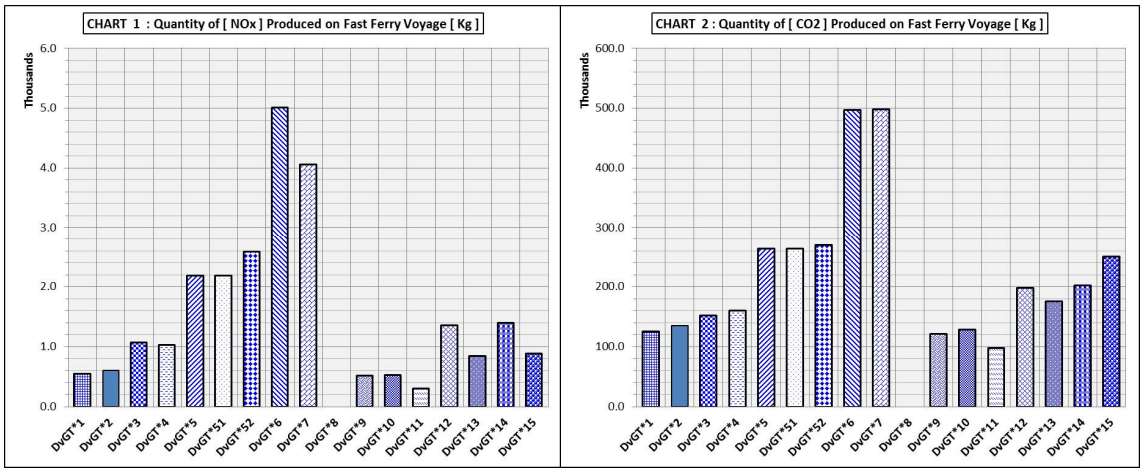

Figure 7-26 Emission Production of NOx and $CO2$ by Aeroderivative Engines along One-way Voyage Route of Fast Ferry ship

Although DvGT*11 is the most efficient, the ferry ship requires the highest number of engines from this model relative to others in order to satisfy the economic ship speed. In contrast, the simplest engine-number configuration of two engines is provided by engine models DvGT*6 and DvGT*7. Therefore, the compromise is very important and more detailed economic factors such as initial cost and maintenance cost should be included in the evaluation in order to perform plant economic optimisation on the determined voyage route.

Moreover, preliminary evaluation of gas turbine engines' performance suggested that engine-number configurations of five engines and six engines

for both DvGT*10 and DvGT*11 respectively satisfy the demand needed for 30knots speed. It can be seen in appendix [D.2.7] however, that a configuration of four and five engines respectively is still able to cover the distance at the determined time at slightly lower speeds at the average of 29.5knots. It is important to indicate the disadvantages of operating at this configuration. Both models will operate at their maximum operating temperature which leads to an increase in the percentage of their life consumed. Referring to an engine's off-design performance in Charts 11 and 12 in appendix D.2.7, engines on four and five configuration operate at relatively lower thermal efficiency. So, as shown in Chart 10 more fuel will be consumed on these engine-number configurations.

8 CONCLUSION AND FURTHER WORK

It is well-known that the access to experimental data for research and development in the turbo-machinery community is very limited and restricted by original equipment manufacturers. This fact constrains conducting validation for computer programs built and used in this project. However, comparative assessment showed that trends of results and outputs from these models are in agreement with those published in the literature. Also, the methodology and models used in this work are fully described which allow validation and verification possible at a later date when experimental data does become available.

8.1 Conclusion

The conclusion will be based on the observations taken from design and off-design calculations of all the aeroderivative industrial gas turbine engines investigated in this study. All the investigation was performed subject to derivation conditions of maintaining constant non-dimensional mas flow, rotational speed and temperature ratio equal to the design values of the two-spool turbofan engine. The conclusion will also include observations from comparing technologies of different thermodynamic cycle including simple cycle, intercooled, recuperated, intercooled and recuperated cycles.

A comprehensive literature work including nearly all gas turbine thermodynamic cycles and applications showed that the demand for better efficiency or higher heat output is a key factor in selecting certain gas turbine cycle for specific application. Although it has been concluded that the simple cycle is suitable for all the proposed applications, small size simple cycle engines are avoided on base-load applications. Aeroderivatives with intercooled cycle are among the best economic variants when applied on marine and power generation on base and part-load, while they respectively show poor performance and economics when applied on combined heat and power, as well as gas compressing applications. In addition, the recuperated aeroderivative gas turbine is observed to be among the worst options for peak-

load power generation, marine and combined heat and power applications. It is only economically applicable for base-load power generation application. Moreover, intercooled recuperated and combined cycle aeroderivative are both suitable for base-load power generation and marine application.

Considering the core of the aircraft engine, the design point calculation concluded that there is only one engine design of aeroderivative gas turbine in single spool simple cycle which meets the applied derivation conditions of constant non-dimensional mas flow, rotational speed and temperature ratio. Based on the design point assumption of 1300 C° as the maximum applicable heat exchanger inlet temperature, with 2% and 3% pressure loss in the cold and hot side respectively, applying the heat exchanger technology on the simple cycle led to a reduction in specific fuel consumption due to a decrease in the required fuel value to reach the required combustor outlet temperature or output power. A 1.2% increase in thermal efficiency was achieved due to exhaust waste heat recovery with a slight drop in the engine output power resulted from the drop in pressure created by pressure losses. Keeping the recuperator inlet temperature higher than the compression discharge temperature is the main condition to apply heat exchanger component. However, it was observed that under the constant temperature ratio of derivation condition, increasing the low pressure compressor pressure ratio led to an increasing compressor discharge temperature and decrease in heat exchanger inlet temperature. This movement has reduced the margin between the hot and cold side of the heat exchanger temperatures, which led to negative effect on the recuperation effectiveness. Therefore, it is concluded that it is the cycle high pressure temperature ratio condition which limits the opportunity of designing the recuperated aeroderivative gas turbine engine with relatively high values of cycle pressure ratios. The drawback observed from these results is that the ability of applying the conventional recuperation concept is completely dependent on the values of cycle overall pressure ratio. Also, the benefit obtained from the recuperation became too small and this conclusion was previously approved by June Kee Min in [76].

Free power turbine provides an option of applying an alternative or non-conventional recuperation concept which contributed in further enhancing thermal efficiency for all investigated engines within the thermal barrier of the heat exchanger material. There was a remarkable increase in thermal efficiency by 5.5% over the simple cycle and by 2.77% over the conventional recuperation cycle. While a 19.2% drop in output power experienced by the non-conventional recuperation compared to the simple cycle, and 16% lower than the conventional recuperation. Similarly and in the same sequence, recoverable waste output heat fell by 47% and 40% respectively. This method has overcome the drawback of the limited ability to design recuperated aeroderivative gas turbine under derivation conditions observed in the conventional method. However, by locating the heat exchanger between turbines in two-shaft arrangement more concern must be given to the material thermal barriers of the heat exchanger during design and off-design operation, because the heat exchanger inlet temperature in this case is much higher than in the conventional recuperation.

It was also observed that the inlet air conditions of the high pressure compressor played the major role in maintaining the design conditions for the parent aircraft engine when two-spool mechanical configuration was applied on the aircraft engine core. To satisfy the derivation conditions in the two spool simple cycle configuration, the design mass flow and operating temperature have significantly increased with the rise in cycle overall pressure ratio. This is achieved by applying a higher pressure ratio in the low pressure compressor. As a result, there will only be one designed engine for every value of combustor outlet temperature, which limits the opportunity to design an engine with high pressure ratio for an applicable turbine inlet temperature. Unlike the nature of simple cycle, increasing the turbine inlet temperature always causes an infinite increase in cycle design thermal efficiency, which is justified by the simultaneous increase in both operating temperature and overall pressure ratio. The same observation was also concluded when recuperation technology was applied on these gas turbine engines.

By dividing compression work into two stages and cooling the discharge air that leaves the first compressor in both simple and recuperated cycles, the shaft power increases, offsetting the pressure losses occurred by applying the recuperation. In addition to reducing compressor work, applying the intercooling enables higher increase in turbine inlet temperature over both the simple and recuperated cycles. Furthermore, using inter-cooling technology overcomes the restrictions of designing only one engine for each operating temperature to meet derivation conditions, as was previously the case in the simple cycle. Cycle optimisation now becomes feasible, because the intercooler optimum pressure for the highest efficiency can be found by varying the low pressure compressor pressure ratio for a given value of operating temperature. However, the intercooler outlet temperature needs to be controlled for every given operating temperature in order to meet the derivation condition for a constant high cycle temperature ratio.

In the design calculation of the intercooled recuperated aeroderivative engine, a compromise was needed to find the appropriate combination of the intercooler outlet temperature and low pressure compressor pressure ratio which simultaneously satisfies both recuperation and inter-cooling conditions. It was also observed that the inlet mass flow was reduced by increasing inter-cooler outlet temperature at low pressure ratios under the applied derivation conditions.

Applying the non-conventional recuperation technology on two-spool aeroderivative engine with free power turbine configuration promises the highest achievable thermal efficiency. On the other hand the conventional recuperation offers the highest shaft output power and exhaust heat output. The lowest pressure ratio that can be applied on the intercooled recuperated engines was limited due to the applied derivation conditions at design point. These limitations resulted from the condition of always maintaining a lower value of intercooler outlet temperature than the intercooler inlet temperature.

All the developed and investigated engines expressed better part-load performance when they were designed with free power turbine configurations.

In addition, the decrease in ambient temperature during engine operation led to a decrease in the required operating temperature and fuel consumed to satisfy the needed power load. However, when ambient temperature rises during the day, the designed gas turbine engines needed to operate at higher operating temperature in order to meet the demand. This increase in operating temperature was followed by a reduction in thermal efficiency due to the additional amount of fuel consumed.

For power generation application, it was observed from the results that the engines responded differently when operating under different environmental profiles. This also depended on the number of units engaged and their thermodynamic cycle, as well as mechanical configurations. It was also noticed that one selected gas turbine engine can be the best economic choice for operating on a specific operating scenario, while it fails to be superior when operating in different scenarios.

The assessment of the developed gas turbine engines on the investigated marine application showed that the lowest specific cost (small engine size) can sometimes be a very important criterion in selecting the gas turbine engine as was confirmed by [24]. On the other hand, fuel cost over the investment life time for both applications represented higher than 50% of the operating cost. This emphasizes the importance of cycle thermal efficiency as a selecting criterion in those applications.

To briefly conclude the work, the methodology of evaluating the potential to produce aeroderivative industrial gas turbines from a parent 130-seat aircraft engine was successfully developed and applied. The investigated techno-economic and environmental risk assessment method $TERA$ has been successfully adapted and used in the assessment. The $TERA$ method has proved its ability to assessing all the investigated aero-derivative industrial gas turbines on different thermodynamic cycles for different applications.

8.2 Future Work

It is obvious that all the calculations were made depending on some assumptions which should be considered. Future work should consider the following aspects which will further improve the models.

- The Off-design performance calculations must include compressor, combustor, and turbine degradation for better off-design performance prediction. Component degradation has major effect on compressor operating point as well as engine operating parameters. Also, it affects the performance characteristic of gas turbine at both full load and part load modes of operating.[68; 69]
- The amount of heat recovered which falls by time as a result of the increased fouling, quantifies the performance of heat exchanger. A remarkable economic penalty is paid as a result of heat exchanger fouling, such as increase in consumed energy cost, shot down cost for cleaning, and the treatment fluid used [113]. Therefore, the economic inducement of heat exchanger cleaning should be involved and evaluated in the economic calculation.
- Humidity was not taken into account among the ambient condition factors which were involved in the calculation of predicting the gas turbine performance. As is well-known from the literature, output power and heat rate are affected by the increase in air humidity. So, it is recommended for the humidity to be included in gas turbine performance prediction.
- An important point observed from literature is that the ability of extracting more air from compression systems must be evaluated and must be considered among factors contained in the overall heat and material balance.
- Combined heat and power (CHP) is an application included as part of methodology followed in this investigation. However, with time constraints on the investigation it was not possible to investigate the developed derivative gas turbine engines on this application. Significant research work on aero-derivative in CHP application is accomplished and

recommendation for further investigation of the engines on this application should be done. Some work of 60% has been conducted on the mathematical model of CHP using FORTRAN language, and it is able to quantify the amount of annual fuel and life consumed. Further work on including economic parameters must be conducted on the current model.

- The ambient temperature profile on the fast Ferry ship trip was taken as a hypostatical profile in order to conduct the comparison study between the new designed aeroderivative gas turbine engines. So, it must be corrected to a real match with temperature profile change during winter a cross the Mediterranean from Malta to Marseille.

REFERENCES

[1] *Agarwal, S., Kachhwaha, S. S. and Mishra, R. S. (2011), "Performance improvement of a simple gas turbine cycle through integration of inlet air evaporative cooling and steam injection", Journal of Scientific and Industrial Research, vol. 70, no. 7, pp. 544-553.*

[2] *Al-Hinai, A. H. H. (2005), Gas Turbine Heat Exchanger Analysis (MSc thesis), Cranfield University, Cranfield University, Library.*

[3] *Anderson, R. O. (2005), "Dual open cycle peaking gas turbine power plant", 2005 ASME Power Conference, Vol. PART B, 5 April 2005 through 7 April 2005, Chicago, IL, pp. 1243.*

[4] *Aschenbruck, E., Blessing, R. and Turanskyj, L. (1994), "FT8-55 mechanical drive aeroderivative gas turbine: design of power turbine and full-load test results", pp. 1.*

[5] *AVIC Team2 (2008), Preliminary Engine Design for 130 Seats Aircraft, 2, Cranfield University, UK.*

[6] *Avila, S., Benito, A., Berro, C., Blanco, S. T., Otín, S. and Velasco, I. (2006), "Dew-point curves of natural gas. Measurement and modeling", Industrial and Engineering Chemistry Research, vol. 45, no. 14, pp. 5179-5184.*

[7] *BaoHua, L. (2008), Preliminary Design of an Engine for the Approximate 130 Seats Civil Aircraft: Cycle Selection and Performance Simulation.(Team3), Part B-Volume I, Cranfield University, UK.*

[8] *Bassily, A. M. (2004), "Performance improvements of the intercooled reheat recuperated gas-turbine cycle using absorption inlet-cooling and evaporative after-cooling", Applied Energy, vol. 77, no. 3, pp. 249-272.*

[9] *Bhargava, R., Bianchi, M., Negri di Montenegro, G. and Peretto, A. (2002), "Thermo-economic analysis of an intercooled, reheat and recuperated gas turbine for cogeneration applications - Part I: Base load operation", Journal of Engineering for Gas Turbines and Power, vol. 124, no. 1, pp. 147-154.*

[10] *Bhargava, R., Blanchi, M., Peretto, A. and Spina, P. R. (2004), "A feasibility study of existing gas turbines for recuperated, intercooled, and reheat cycle", Journal of Engineering for Gas Turbines and Power, vol. 126, no. 3, pp. 531-544.*

[11] *Bhargava, R., Negri di Montenegro, G. and Peretto, A. (2002), "Thermoeconomic analysis of an intercooled, reheat, and recuperated gas turbine for cogeneration applications - Part II: Part-load operation", Journal of Engineering for Gas Turbines and Power, vol. 124, no. 4, pp. 892-903.*

[12] *Bhargava, R. and Peretto, A. (2002), "A unique approach for Thermoeconomic optimization of an intercooled, reheat, and recuperated gas turbine for cogeneration applications", Journal of Engineering for Gas Turbines and Power, vol. 124, no. 4, pp. 881-891.*

[13] *Bhargava, R. K. (2007), "Gas Turbine based Power Cycles - A state-of-the-Art Review", Gas Turbine Based Power Cycles-A State-of-the-Art Review, 2007, China, .*

[14] *Bhargava, R. K., Bianchi, M., Campanari, S., De Pascale, A., Di Montenegro, G. N. and Peretto, A. (2008), "High efficiency gas turbine based power cycles - A*

study of the most promising solutions: Part 1 -A review of the technology", Vol. 7, pp. 305.

[15] Bhargava, R. K., Bianchi, M., Campanari, S., De Pascale, A., Di Montenegro, G. N. and Peretto, A. (2008), "High efficiency gas turbine based power cycles - A study of the most promising solutions: Part 2 - A parametric performance evaluation", Vol. 7, pp. 315.

[16] Bhargava, R. K., Bianchi, M., Campanari, S., de Pascale, A., di Montenegro, G. N. and Peretto, A. (2010), "A parametric thermodynamic evaluation of high performance gas turbine based power cycles", Journal of Engineering for Gas Turbines and Power, vol. 132, no. 2.

[17] Bianchi, M., Negri di Montenegro, G., Peretto, A. and Spina, P. R. (2005), "A feasibility study of inverted Brayton cycle gas turbine repowering", Journal of Engineering for Gas Turbines and Power, vol. 127, no. 3, pp. 599-605.

[18] Bill Gunston OBE, F. (2006), Jane's, Twenty ed, Jane's Information Group Limited, UK.

[19] Bolland, O. and Stadaas, J. F. (1995), "Comparative evaluation of combined cycles and gas turbine systems with water injection, steam injection, and recuperation", Journal of Engineering for Gas Turbines and Power, vol. 117, no. 1, pp. 138-145.

[20] Boyce, M. P. (ed.) (2006), Gas Turbine Engineering Handbook, 3rd ed, Elsavier Inc, UK.

[21] Brun, K. and Kurz, R. (2006), "The truth about gas turbines", Turbomachinery International, vol. 47, no. 7, pp. 28.

[22] Cai, R. (1998), "A new analysis of recuperative gas turbine cycles", Proceedings of the Institution of Mechanical Engineers, Part A: Journal of Power and Energy, vol. 212, no. 4, pp. 289-296.

[23] Cai, R. and Jiang, L. (2006), "Analysis of the recuperative gas turbine cycle with a recuperator located between turbines", Applied Thermal Engineering, vol. 26, no. 1, pp. 89-96.

[24] Campanari, S., Boncompagni and Macchi, E. (2004), "Microturbines and trigeneration: Optimization strategies and multiple engine configuration effects", Journal of Engineering for Gas Turbines and Power, vol. 126, no. 1, pp. 92-101.

[25] Camporeale, S. M. and Fortunato, B. (1998), "Performance of a mixed gas-steam cycle power plant obtained upgrading an aero-derivative gas turbine ", Energy Conversion and Management, vol. 39, no. 16-18, pp. 1683-1692.

[26] Camporeale, S. M. and Fortunato, B. (2000), "Performance of evaporative cycle gas turbines derived from aeroengines ", Journal of Propulsion and Power, vol. 16, no. 6, pp. 1011-1021.

[27] Canière, H., Willockx, A., Dick, E. and De Paepe, M. (2006), "Raising cycle efficiency by intercooling in air-cooled gas turbines", Applied Thermal Engineering, vol. 26, no. 16, pp. 1780-1787.

[28] Commander Colin R English Royal Navy (2003), "The WR-21 Intercooled Recuperated Gas Turbine Engine-Integration Into Future Warships", International Gas Turbine Congress, November 2-7, 2003, Tokyo, GTSJ, UK, .

[29] Courtinho, A. (2009), Preliminary Universal Emission Model (MSc thesis), Cranfield University, UK.

[30] Da Cunha Alves, M. A., De Franca Mendes Carneiro, H. F., Barbosa, J. R., Travieso, L. E., Pilidis, P. and Ramsden, K. W. (2001), "An insight on intercooling and reheat gas turbine cycles", Proceedings of the Institution of Mechanical Engineers, Part A: Journal of Power and Energy, vol. 215, no. 2, pp. 163-172.

[31] De Sa, A. and Al Zubaidy, S. (2011), "Gas turbine performance at varying ambient temperature", Applied Thermal Engineering, vol. 31, no. 14-15, pp. 2735-2739.

[32] Dellenback, P. A. (2002), "Improved gas turbine efficiency through alternative regenerator configuration", Journal of Engineering for Gas Turbines and Power, vol. 124, no. 3, pp. 441-446.

[33] Dellenback, P. A. (2006), "A reassessment of the alternative regeneration cycle", Journal of Engineering for Gas Turbines and Power, vol. 128, no. 4, pp. 783-788.

[34] Doug, W. (ed.) (2004), Pounder's Marine Diesel Engines and Gas Turbines, Eighth ed, Elsevier, UK.

[35] Eckardt, D. and Rufli, P. (2002), "Advanced gas turbine technology: ABB/BCC historical firsts", Journal of Engineering for Gas Turbines and Power, vol. 124, no. 3, pp. 542-549.

[36] Eli Eber Batista Gomes (2007), Operational Optimization of Gas Turbine Distributed Generation Systems in Comparative Electricity Market (PhD thesis), Cranfield University, UK.

[37] Ellington, L., McAndrews, G., Harsema-Mensonides, A. and Tanwar, R. (2006), "Gas turbine propulsion for LNG transports", Vol. 5 PART A, pp. 65.

[38] Elmegaard, B. and Qvale, B. (2004), "Regenerative gas turbines with divided expansion", 2004 ASME Turbo Expo, Vol. 7, 14 June 2004 through 17 June 2004, Vienna, pp. 675.

[39] ERCOT (2010), Long-Term Hourly Peak demand and energy Forecast, June25, Electric Reliability Council of Texas, Inc., US.

[40] Evangelos Tsoudis (2008), Techno-economic Environmental and Risk Analysis of Marine Gas Turbine Plants (PhD thesis), Cranfield University, UK.

[41] Fernando, C., Daniele, P., Stephen, O. and Pericles, P. (2008), "Future Aero-Engine' Optimization for Minimal operating Cost", June 9-13, 2008, Germany, ASME Turbo Expo: Power for Land, Sea and Air, .

[42] Fortin, J. A. C. and Bardon, M. F. (1983), "GAS Turbine Compressor Inter-stage Cooling Using Methanol."

[43] Frank J. Brooks, GE Power Systems Schenectady, NY GE Gas Turbine Performance Characteristic, .

[44] Gamez, R. (1996), Combined Heat and power from A Military Turbojet (MSc thesis), Cranfield University, Cranfield University, Library.

[45] GE Energy (2008), GE 100 Flexible Power, .

[46] GE, E. (2006), LMS100 Flexible Power, GEA-14355 A(09/06), GE Energy, US.

[47] General Electric, www.geae.com/engines/commercial/cfm56/index.html.

[48] General-Electric (2007),**www.gepower.com/corporate/ecomagination_home/lms100.htm**.

[49] General Electric Company and GE Oil & Gas (2012), Heat Recuperators, available at: http://www.ge-energy.com/products_and_services/products/petroleum_reactors_and_steam_condensers/heat_recuperators.jsp (accessed 08/23).

[50] GTW (2008), Gas Turbine World 2007-08 GTW Handbook, Vol 26, Pequot Publishing Inc., USA.

[51] GTW (ed.) (2009), Gas Turbine World 2009 GTW Handbook, Vol 27 ed, Pequot Publishing Inc, USA.

[52] Haglind, F. (2010), "Variable geometry gas turbines for improving the part-load performance of marine combined cycles - Gas turbine performance", Energy, vol. 35, no. 2, pp. 562-570.

[53] Haglind, F. (2011), "Variable geometry gas turbines for improving the part-load performance of marine combined cycles - Combined cycle performance", Applied Thermal Engineering, vol. 31, no. 4, pp. 467-476.

[54] Haglind, F. and Elmegaard, B. (2009), "Methodologies for predicting the part-load performance of aero-derivative gas turbines", Energy, vol. 34, no. 10, pp. 1484-1492.

[55] Hellberg, A., Norden, G. and Shukin, S. (2002), "GT10C - 30 MW gas turbine for mechanical drive and power generation", Vol. 4 A, pp. 235.

[56] Hisham Katib (2003), "Economic Evaluation of Projects in the Electricity Supply Industry", in A.T.Johns, D. F. Warne, Hisham Katib, (ed.) Power and Energy Series44, Series 44 ed, Institute of Energy and Technology, London, UK, pp. 31-41.

[57] Horlock, J. H. (1997), "Aero-engine derivative gas turbines for power generation: Thermodynamic and economic perspectives ", Journal of Engineering for Gas Turbines and Power, vol. 119, no. 1, pp. 119-123.

[58] Horlock, J. H. (1998), "The evaporative gas turbine [EGT] cycle ", J.Eng.Gas Turbines Power, vol. 120, no. 2, pp. 336-343.

[59] Ibrahim, T. K., Rahman, M. M. and Abd Alla, A. N. (2010), "Study on the effective parameter of gas turbine model with intercooled compression process", Scientific Research and Essays, vol. 5, no. 23, pp. 3760-3770.

[60] Jo˜ ao Roberto Barbosa (2011), "Influence of Variable Geometry Transients On Gas Turbine Performance",.

[61] Jon Ariza De Miguel (2003), An Aeroderivative Gas turbine for Turboelectronic Locomoive (MSc thesis), Cranfield University, UK, Cranfield University Library.

[62] Jonsson, M. and Yan, J. (2005), "Humidified gas turbines - A review of proposed and implemented cycles ", Energy, vol. 30, no. 7, pp. 1013-1078.

[63] Jose` Pedro Neto (1999), Aeroderivative Gas Turbine Engine With Inlet Air Cooling (MSc thesis), Cranfield University, UK, Cranfield University Library.

[64] Khaliq, A. and Dincer, I. (2011), "Energetic and exergetic performance analyses of a combined heat and power plant with absorption inlet cooling and evaporative aftercooling", Energy, vol. 36, no. 5, pp. 2662-2670.

[65] Kim, J. H., Kim, T. S., Sohn, J. L. and Ro, S. T. (2002), "Comparative analysis of off-design performance characteristics of single and two shaft industrial gas turbines", Proceedings of the ASME TURBO Expo 2002:Controls, Diagnostics, and Instrumentation, Cycle Innovations, Marine, Oil and Gas Applications, Vol. 2 A, 3 June 2002 through 6 June 2002, Amsterdam, pp. 509.

[66] Kim, T. S. and Hwang, S. H. (2006), "Part load performance analysis of recuperated gas turbines considering engine configuration and operation strategy", Energy, vol. 31, no. 2-3, pp. 260-277.

[67] Kumar, N., Krishna, K. and Sita Rama Raju, A. V. (2007), "Performance improvement and exergy analysis of gas turbine power plant with alternative regenerator and intake air cooling", Energy Engineering: Journal of the Association of Energy Engineering, vol. 104, no. 3, pp. 36-53.

[68] Kurz, R., Brun, K. and Wollie, M. (2008), "Degradation effects on industrial gas turbines", 2008 ASME Turbo Expo, Vol. 7, 9 June 2008 through 13 June 2008, Berlin, pp. 493.

[69] Kurz, R., Brun, K. and Wollie, M. (2009), "Degradation effects on industrial gas turbines", Journal of Engineering for Gas Turbines and Power, vol. 131, no. 6.

[70] Lagerström, G. and Xie, M. (2002), "High performance & cost effective recuperator for micro-gas turbines", Proceedings of the ASME Turbo Expo 2002; Aircraft Engine, Coal, Biomass and Alternative Fuels, Combustion and Fuels, Education, Electric Power, Vehicular and Small Turbomachines, Vol. 1, 3 June 2002 through 6 June 2002, Amsterdam, pp. 1003.

[71] Lefebvre, A. H. (1984), "Fuel effects on gas turbine combustion-liner temperature, pattern factor, and pollutant emissions", Journal of Aircraft, vol. 21, no. 11, pp. 887-898.

[72] Mathias Usman Bonet (2012), Techno-Environmental Assessment of Marine gas Turbine for the Propulsion of Merchant Ships (PhD thesis), Cranfield University, UK.

[73] McCann, D. (2001), "A review of the application of gas turbine generators to the pulp and paper industry", Vol. C, pp. C17.

[74] McDonald, C. F. and Wilson, D. G. (1996), "The utilization of recuperated and regenerated engine cycles for high-efficiency gas turbines in the 21st century", Applied Thermal Engineering, vol. 16, no. 8-9, pp. 635-653.

[75] Michael J. Reale (2004 General Electric Company), "New High Efficiency Simple Cycle Gas Turbine - GE's LMS100™", in General Electric Company (ed.), GER-4222A (06/04),

[76] Min, J. K., Jeong, J. H., Ha, M. Y. and Kim, K. S. (2009), "High temperature heat exchanger studies for applications to gas turbines", Heat and Mass Transfer/Waerme- und Stoffuebertragung, vol. 46, no. 2, pp. 175-186.

[77] MOHAMMAD, FAHMI BIN ABDUL GHAFIR. (2011): Performance Based Creep Life Estimation for Gas Turbines Applications (PhD thesis), Cranfield University, UK.

[78] N Ortun Perez (1999), Intercooled Aeroderivative Industrial Gas Turbine (MSc thesis), Cranfield University, UK, Cranfield University Library.

[79] Najjar, Y. S. H. (1996), "Relative effect of pressure losses and inefficiencies of turbomachines on the performance of the heat-exchange gas turbine cycle", Applied Thermal Engineering, vol. 16, no. 8-9, pp. 769-776.

[80] Najjar, Y. S. H. and Aldoss, T. K. (1986), "Waste energy utilization in heat-exchange gas turbine cycles", Journal of Heat Recovery Systems, vol. 6, no. 4, pp. 323-334.

[81] Najjar, Y. S. H. and Nahas, M. N. (1994), "Intercooled low-pressure turbo steam-injection gas turbine with cogeneration", Journal of the Institute of Energy, vol. 67, no. 470, pp. 30-36.

[82] Najjar, Y. S. H. (1987), "OPTIMIZATION OF SHAFT GAS TURBINE CYCLES.", International Journal of Mechanical Engineering Education, vol. 15, no. 4, pp. 267-276.

[83] Najjar, Y. S. H. (2000), "Gas turbine cogeneration systems: a review of some novel cycles ", Applied Thermal Engineering, vol. 20, no. 2, pp. 179-197.

[84] Ogaji, S.O.T., Pilidis, P., and Hales, R (2007), "TERA - A Tool for Aero-engine Modelling and Management", Second World Congress on Engineering Asset Management and the Fourth International Conference on Condition, 11-14 June2007, Harrogate, UK, UK, .

[85] P.P. Walsh, P. F. (2004), Gas Turbine performance Second Ed, Blackwell science Ltd, Oxford, UK.

[86] Pascovici, D. S., Colmenares, F., Ogaji, S. O. T. and Pilidis, P. (2007), "An economic and risk analysis model for aircrafts and engines", 2007 ASME Turbo Expo, Vol. 3, 14 May 2007 through 17 May 2007, Montreal, Que., pp. 103.

[87] Perry Samson, Jeff Ferguso, Alan Steremberg and Chris Schwerzler (2008), Weather Underground, available at: http://www.wunderground.com/ (accessed 1995).

[88] Polyzakis, A. L. (2006), Techno-economic Evaluation of Tri-generation Plant: gas turbine performance, absorption cooling and district heating (PhD thesis), Cranfield University, Cranfield University, Library.

[89] Poullikkas, A. (2005), "An overview of current and future sustainable gas turbine technologies ", Renewable and Sustainable Energy Reviews, vol. 9, no. 5, pp. 409-443.

[90] Rahman, M.M., Ibrahim, T.K., Kadirgama, K., Mamat, R. and Bakar, R.A., (2011), Influence of operation conditions and ambient temperature on performance of gas turbine power plant, Guilin Ed.

[91] Raja Khan (2012), TERA for Rotating Equipment Selection (EngD thesis), Cranfield University, UK.

[92] Ramsden, K. W. (2008), Axial Compressor Design Manual, Cranfield University, UK.

[93] Ramsden, K. W. (2008), Axial Turbine Design Manual, Cranfield University, UK.

[94] Ravi Kumar, N., Rama Krishna, K. and Sita Rama Raju, A. V. (2007), "Thermodynamic analysis of heat recovery steam generator in combined cycle power plant", Thermal Science, vol. 11, no. 4, pp. 143-156.

[95] Razak, A. M. Y. (ed.) (2007), Industrial Gas Turbines , Performance and Operability, First ed, CRC Press LLC, 6000 Broken Sound Parkway, NY, Boca Raton, FL 33a87, USA.

[96] Rodgers, C., Stone, A. and White, D. (2007), "A gas turbine cycle selection issue - Recuperated or ICR", Vol. 3, pp. 373.

[97] Rolls-Royce,www.rolls-royce.com/marine/downloads/gas_diesel/wr21_fact.pdf.

[98] Ronald, J.H., (2011), The History of the Industrial Gas Turbine (Part 1 The First Fifty Years 1940-1990), Version 2 ed., (idgtE) Institution of Diesel and Gas Turbine Engineers, UK.

[99] ROSEN, G. (1971), "Trends in aircraft propulsion", Anglo-Am Aeronaut Conf, 12th, PP.,

[100] S. Rodriguez Falla (1999), Study of An Aeroderivative Solution Of A Twin-Spool High Bypass Ratio Turbofan For Power Generation (MSc thesis), Cranfield University, UK, Cranfield University Library.

[101] S.M.E Cranfield, (1999), The Turbomatch Scheme For Aero/Industrial Gas Turbine Engine Design point/Off Design Performance Calculation, Cranfield University, UK.

[102] Sanjay (2011), "Investigation of effect of variation of cycle parameters on thermodynamic performance of gas-steam combined cycle", Energy, vol. 36, no. 1, pp. 157-167.

[103] Saravanamuttoo, H. I. H., Rogers, G. F. C. and Cohen, H. (2001), Gas Turbine Theory, Fifth Edition ed, Pearson Education, Essex UK.

[104] Seery, D. J., Sangiovanni, J. J., Robson, F. L. and Ruby, J. (1996), "Engineering development of a coal-fired high performance power generating system", Vol. 30, pp. 295.

[105] Sheard, A. G. and Raine, M. J. (1998), "The combined cycle application of aeroderivative gas turbines ", ASME Fuels Combust Technol Div Publ FACT, vol. 22, pp. 701-712.

[106] Shepard, S. B., Bowen, T. L. and Chiprich, J. M. (1994), "Design and development of the WR-21 intercooled recuperated (ICR) marine gas turbine ", pp. 1.

[107] SHU, T. (2008), Preliminary Gas Turbine Overall structure Design for 130-Seat Aircraft. (Team2) Cranfield University, UK.

[108] Song, J. (2008), Preliminary Design Technical Report of Engine of “130-seat” series Aircrafts (Team1), Report 2, Cranfield University, UK.

[109] Special Metals (2008), Special Metals (NIMONIC alloy 115), available at: http://www.specialmetals.com (accessed 2004).

[110] Spector, R. B. (1989), "Method of evaluating life cycle costs of industrial gas turbines ", Journal of Engineering for Gas Turbines and Power, vol. 111, no. 4, pp. 637-641.

[111] Stoiljkovic, V. (2010), "Net present value analysis comparing engineering projects by financial return", IEEE Potentials, vol. 29, no. 3, pp. 17-21.

[112] Strömberg, J., Franck, P. -. and Berntsson, T. (1993), "Consequences of recent gas turbine developments for industrial CHP applications", Heat Recovery Systems and CHP, vol. 13, no. 3, pp. 219-231.

[113] Tavares, V.B.G., Costa, A.L.H., Queiroz, E.M., Pessoa, F.L.P., Liporace, F.S. and Oliveira, S.G., (2009), Thermohydraulic simulation of heat exchanger networks subjected to fouling.

[114] Tayo, M., GE Industrial Aeroderivative Gas Turbines and Evendale, O. (2001), "Aeroderivative gas turbine provides efficient power for LNG processing ", Pipeline and Gas Journal, vol. 228, no. 10, pp. 54.

[115] Touchton, G. L., Senkevych, M., Belokon, A. and Belyaev, V. (2004), "A novel gas turbine product line for onsite generationand combined heat and power between 400 kWe and 1.6 MWe", Vol. 6, pp. 159.

[116] Vaezi, M. and Soleymani, M. (2009), "Creep life prediction of Inconel 738 gas turbine blade", Journal of Applied Sciences, vol. 9, no. 10, pp. 1950-1955.

[117] Valenti, M. (1995), "Turbine for tomorrow's navy ", Mechanical Engineering, vol. 117, no. 9, pp. 70-73.

[118] Van Der Linden, S. and Von Rappard, A. (2005), "Gas turbine development, more than 50 years ago", Vol. 5, pp. 483.

[119] Walter Short, Daniel J. Packey, Thomas Holt (1995), A Manual for the Economic Evaluation of Energy Efficiency and Renewable Energy Technology, AS026100, National Renewable Energy Laboratory, US.

[120] William, H. D. (2002), "Pratt & Whitney's Next Generation Turbine Program ", DOE Turbine Power systems Conference and Condition Monitoring Workshop, Feb 25-27, Glaveston, Google Scholar, .

[121] Xue-You, W. and Dong-Ming, X. (2008), "Feasibility study of an intercooled-cycle marine gas turbine", Journal of Engineering for Gas Turbines and Power, vol. 132, no. 2.

[122] Yang, W. -. (1997), "Reduction of specific fuel consumption in gas turbine power plants ", Energy Conversion and Management, vol. 38, no. 13-10, pp. 1219-1224.

[123] Zhang, X., Sugishita, H., Ni, W. and Li, Z. (2005), "Economics and performance forecast of gas turbine combined cycle", Tsinghua Science and Technology, vol. 10, no. 5, pp. 633-636.

[124] Zhe, L., Liebman, A. and Zhao, Y. D. (2006), "Power generation investment opportunities evaluation: A comparison between net present value and real options approach", 2006 IEEE Power Engineering Society General Meeting, PES, 18 June 2006 through 22 June 2006, Montreal, QC,

APPENDICES

Following sections include some examples of excel spread sheets and engine models which have been made used Turbomatch.

Appendix A Excel Models for Creep and DP Mass flow Calculations

A.1 Three-Spool I/C Engine

I/C Tout (T4)	TET	LPC PR	P1	T1	P2	P2 (atm)	T2	P3	P3 (atm)	ζ	γ	T3	P4	P4(atm)	W
305.48	1864.3444	1.2	101.0000	288.1500	100.4950	0.9950	288.1500	120.5940	1.1940	0.9000	1.4000	305.2701	120.2322	1.1904	68.8084
305.48	1864.3444	1.2	101.0000	288.1500	100.4950	0.9950	288.1500	120.5940	1.1940	0.9000	1.4000	305.2701	120.2322	1.1904	68.8084
305.48	1864.3444	1.4	101.0000	288.1500	100.4950	0.9950	288.1500	140.6930	1.3930	0.9000	1.4000	320.4572	140.2709	1.3888	80.2764
305.48	1864.3444	1.6	101.0000	288.1500	100.4950	0.9950	288.1500	160.7920	1.5920	0.9000	1.4000	334.1646	160.3096	1.5872	91.7445
305.48	1864.3444	1.8	101.0000	288.1500	100.4950	0.9950	288.1500	180.8910	1.7910	0.9000	1.4000	346.6971	180.3483	1.7856	103.2126
305.48	1864.3444	2.0	101.0000	288.1500	100.4950	0.9950	288.1500	200.9900	1.9900	0.9000	1.4000	358.2709	200.3870	1.9840	114.6806
305.48	1864.3444	2.2	101.0000	288.1500	100.4950	0.9950	288.1500	221.0890	2.1890	0.9000	1.4000	369.0450	220.4257	2.1824	126.1487
305.48	1864.3444	2.4	101.0000	288.1500	100.4950	0.9950	288.1500	241.1880	2.3880	0.9000	1.4000	379.1405	240.4644	2.3808	137.6167
305.48	1864.3444	2.6	101.0000	288.1500	100.4950	0.9950	288.1500	261.2870	2.5870	0.9000	1.4000	388.6518	260.5031	2.5792	149.0848
305.48	1864.3444	2.8	101.0000	288.1500	100.4950	0.9950	288.1500	281.3860	2.7860	0.9000	1.4000	397.6538	280.5418	2.7776	160.5529
305.48	1864.3444	3.0	101.0000	288.1500	100.4950	0.9950	288.1500	301.4850	2.9850	0.9000	1.4000	406.2077	300.5805	2.9760	172.0209
305.48	1864.3444	3.2	101.0000	288.1500	100.4950	0.9950	288.1500	321.5840	3.1840	0.9000	1.4000	414.3633	320.6192	3.1744	183.4890
305.48	1864.3444	3.4	101.0000	288.1500	100.4950	0.9950	288.1500	341.6830	3.3830	0.9000	1.4000	422.1625	340.6580	3.3729	194.9570
305.48	1864.3444	3.6	101.0000	288.1500	100.4950	0.9950	288.1500	361.7820	3.5820	0.9000	1.4000	429.6406	360.6967	3.5713	206.4251
305.48	1864.3444	3.8	101.0000	288.1500	100.4950	0.9950	288.1500	381.8810	3.7810	0.9000	1.4000	436.8276	380.7354	3.7697	217.8932
305.48	1864.3444	4.0	101.0000	288.1500	100.4950	0.9950	288.1500	401.9800	3.9800	0.9000	1.4000	443.7492	400.7741	3.9681	229.3612
305.48	1864.3444	4.2	101.0000	288.1500	100.4950	0.9950	288.1500	422.0790	4.1790	0.9000	1.4000	450.4278	420.8128	4.1665	240.8293
305.48	1864.3444	4.4	101.0000	288.1500	100.4950	0.9950	288.1500	442.1780	4.3780	0.9000	1.4000	456.8830	440.8515	4.3649	252.2973
305.48	1864.3444	4.6	101.0000	288.1500	100.4950	0.9950	288.1500	462.2770	4.5770	0.9000	1.4000	463.1319	460.8902	4.5633	263.7654
305.48	1864.3444	4.8	101.0000	288.1500	100.4950	0.9950	288.1500	482.3760	4.7760	0.9000	1.4000	469.1896	480.9289	4.7617	275.2335
305.48	1864.3444	5.0	101.0000	288.1500	100.4950	0.9950	288.1500	502.4750	4.9750	0.9000	1.4000	475.0696	500.9676	4.9601	286.7015
305.48	1864.3444	5.2	101.0000	288.1500	100.4950	0.9950	288.1500	522.5740	5.1740	0.9000	1.4000	480.7839	521.0063	5.1585	298.1696
305.48	1864.3444	5.4	101.0000	288.1500	100.4950	0.9950	288.1500	542.6730	5.3730	0.9000	1.4000	486.3433	541.0450	5.3569	309.6377
305.48	1864.3444	5.6	101.0000	288.1500	100.4950	0.9950	288.1500	562.7720	5.5720	0.9000	1.4000	491.7576	561.0837	5.5553	321.1057
305.48	1864.3444	5.8	101.0000	288.1500	100.4950	0.9950	288.1500	582.8710	5.7710	0.9000	1.4000	497.0354	581.1224	5.7537	332.5738
305.48	1864.3444	6.0	101.0000	288.1500	100.4950	0.9950	288.1500	602.9700	5.9700	0.9000	1.4000	502.1848	601.1611	5.9521	344.0418
305.48	1864.3444	6.2	101.0000	288.1500	100.4950	0.9950	288.1500	623.0690	6.1690	0.9000	1.4000	507.2130	621.1998	6.1505	355.5099
305.48	1864.3444	6.4	101.0000	288.1500	100.4950	0.9950	288.1500	643.1680	6.3680	0.9000	1.4000	512.1266	641.2385	6.3489	366.9780
305.48	1864.3444	6.6	101.0000	288.1500	100.4950	0.9950	288.1500	663.2670	6.5670	0.9000	1.4000	516.9317	661.2772	6.5473	378.4460
305.48	1864.3444	6.8	101.0000	288.1500	100.4950	0.9950	288.1500	683.3660	6.7660	0.9000	1.4000	521.6340	681.3159	6.7457	389.9141
305.48	1864.3444	7.0	101.0000	288.1500	100.4950	0.9950	288.1500	703.4650	6.9650	0.9000	1.4000	526.2384	701.3546	6.9441	401.3821
320.84	1958.0865	1.2	101.0000	288.1500	100.4950	0.9950	288.1500	120.5940	1.1940	0.9000	1.4000	305.2701	120.2322	1.1904	67.1411
320.84	1958.0865	1.4	101.0000	288.1500	100.4950	0.9950	288.1500	140.6930	1.3930	0.9000	1.4000	320.4572	140.2709	1.3888	78.3313
320.84	1958.0865	1.6	101.0000	288.1500	100.4950	0.9950	288.1500	160.7920	1.5920	0.9000	1.4000	334.1646	160.3096	1.5872	89.5215
320.84	1958.0865	1.8	101.0000	288.1500	100.4950	0.9950	288.1500	180.8910	1.7910	0.9000	1.4000	346.6971	180.3483	1.7856	100.7116
320.84	1958.0865	2.0	101.0000	288.1500	100.4950	0.9950	288.1500	200.9900	1.9900	0.9000	1.4000	358.2709	200.3870	1.9840	111.9018
320.84	1958.0865	2.2	101.0000	288.1500	100.4950	0.9950	288.1500	221.0890	2.1890	0.9000	1.4000	369.0450	220.4257	2.1824	123.0920
320.84	1958.0865	2.4	101.0000	288.1500	100.4950	0.9950	288.1500	241.1880	2.3880	0.9000	1.4000	379.1405	240.4644	2.3808	134.2822
320.84	1958.0865	2.6	101.0000	288.1500	100.4950	0.9950	288.1500	261.2870	2.5870	0.9000	1.4000	388.6518	260.5031	2.5792	145.4724
320.84	1958.0865	2.8	101.0000	288.1500	100.4950	0.9950	288.1500	281.3860	2.7860	0.9000	1.4000	397.6538	280.5418	2.7776	156.6625
320.84	1958.0865	3.0	101.0000	288.1500	100.4950	0.9950	288.1500	301.4850	2.9850	0.9000	1.4000	406.2077	300.5805	2.9760	167.8527
320.84	1958.0865	3.2	101.0000	288.1500	100.4950	0.9950	288.1500	321.5840	3.1840	0.9000	1.4000	414.3633	320.6192	3.1744	179.0429
320.84	1958.0865	3.4	101.0000	288.1500	100.4950	0.9950	288.1500	341.6830	3.3830	0.9000	1.4000	422.1625	340.6580	3.3729	190.2331
320.84	1958.0865	3.6	101.0000	288.1500	100.4950	0.9950	288.1500	361.7820	3.5820	0.9000	1.4000	429.6406	360.6967	3.5713	201.4233
320.84	1958.0865	3.8	101.0000	288.1500	100.4950	0.9950	288.1500	381.8810	3.7810	0.9000	1.4000	436.8276	380.7354	3.7697	212.6135
320.84	1958.0865	4.0	101.0000	288.1500	100.4950	0.9950	288.1500	401.9800	3.9800	0.9000	1.4000	443.7492	400.7741	3.9681	223.8036
320.84	1958.0865	4.2	101.0000	288.1500	100.4950	0.9950	288.1500	422.0790	4.1790	0.9000	1.4000	450.4278	420.8128	4.1665	234.9938
320.84	1958.0865	4.4	101.0000	288.1500	100.4950	0.9950	288.1500	442.1780	4.3780	0.9000	1.4000	456.8830	440.8515	4.3649	246.1840
320.84	1958.0865	4.6	101.0000	288.1500	100.4950	0.9950	288.1500	462.2770	4.5770	0.9000	1.4000	463.1319	460.8902	4.5633	257.3742
320.84	1958.0865	4.8	101.0000	288.1500	100.4950	0.9950	288.1500	482.3760	4.7760	0.9000	1.4000	469.1896	480.9289	4.7617	268.5644
320.84	1958.0865	5.0	101.0000	288.1500	100.4950	0.9950	288.1500	502.4750	4.9750	0.9000	1.4000	475.0696	500.9676	4.9601	279.7545
320.84	1958.0865	5.2	101.0000	288.1500	100.4950	0.9950	288.1500	522.5740	5.1740	0.9000	1.4000	480.7839	521.0063	5.1585	290.9447
320.84	1958.0865	5.4	101.0000	288.1500	100.4950	0.9950	288.1500	542.6730	5.3730	0.9000	1.4000	486.3433	541.0450	5.3569	302.1349
320.84	1958.0865	5.6	101.0000	288.1500	100.4950	0.9950	288.1500	562.7720	5.5720	0.9000	1.4000	491.7576	561.0837	5.5553	313.3251
320.84	1958.0865	5.8	101.0000	288.1500	100.4950	0.9950	288.1500	582.8710	5.7710	0.9000	1.4000	497.0354	581.1224	5.7537	324.5153
320.84	1958.0865	6.0	101.0000	288.1500	100.4950	0.9950	288.1500	602.9700	5.9700	0.9000	1.4000	502.1848	601.1611	5.9521	335.7055
320.84	1958.0865	6.2	101.0000	288.1500	100.4950	0.9950	288.1500	623.0690	6.1690	0.9000	1.4000	507.2130	621.1998	6.1505	346.8956
320.84	1958.0865	6.4	101.0000	288.1500	100.4950	0.9950	288.1500	643.1680	6.3680	0.9000	1.4000	512.1266	641.2385	6.3489	358.0858
320.84	1958.0865	6.6	101.0000	288.1500	100.4950	0.9950	288.1500	663.2670	6.5670	0.9000	1.4000	516.9317	661.2772	6.5473	369.2760
320.84	1958.0865	6.8	101.0000	288.1500	100.4950	0.9950	288.1500	683.3660	6.7660	0.9000	1.4000	521.6340	681.3159	6.7457	380.4662
320.84	1958.0865	7.0	101.0000	288.1500	100.4950	0.9950	288.1500	703.4650	6.9650	0.9000	1.4000	526.2384	701.3546	6.9441	391.6564

A.2 Two-Spool two Shaft Simple Cycle Engine

LPC PR	HPC PR	OPR	P1	T1	P2	P2 (atm)	T2	P3	P3 (atm)			T3	COT	W
1.2000	15.0000	18.0000	101.0000	288.1500	100.4950	0.9950	288.1500	120.5940	1.1940	0.9000	1.4000	305.2701	1386.6895	31.5211
1.2000	15.0000	18.0000	101.0000	288.1500	100.4950	0.9950	288.1500	120.5940	1.1940	0.9000	1.4000	305.2701	1386.6895	31.5211
1.3000	15.0000	19.5000	101.0000	288.1500	100.4950	0.9950	288.1500	130.6435	1.2935	0.9000	1.4000	313.0725	1422.1319	33.7197
1.4000	15.0000	21.0000	101.0000	288.1500	100.4950	0.9950	288.1500	140.6930	1.3930	0.9000	1.4000	320.4572	1455.6770	35.8927
1.5000	15.0000	22.5000	101.0000	288.1500	100.4950	0.9950	288.1500	150.7425	1.4925	0.9000	1.4000	327.4742	1487.5517	38.0422
1.6000	15.0000	24.0000	101.0000	288.1500	100.4950	0.9950	288.1500	160.7920	1.5920	0.9000	1.4000	334.1646	1517.9426	40.1701
1.7000	15.0000	25.5000	101.0000	288.1500	100.4950	0.9950	288.1500	170.8415	1.6915	0.9000	1.4000	340.5626	1547.0055	42.2779
1.8000	15.0000	27.0000	101.0000	288.1500	100.4950	0.9950	288.1500	180.8910	1.7910	0.9000	1.4000	346.6971	1574.8717	44.3670
1.9000	15.0000	28.5000	101.0000	288.1500	100.4950	0.9950	288.1500	190.9405	1.8905	0.9000	1.4000	352.5928	1601.6529	46.4387
2.0000	15.0000	30.0000	101.0000	288.1500	100.4950	0.9950	288.1500	200.9900	1.9900	0.9000	1.4000	358.2709	1627.4454	48.4939
2.1000	15.0000	31.5000	101.0000	288.1500	100.4950	0.9950	288.1500	211.0395	2.0895	0.9000	1.4000	363.7496	1652.3325	50.5337
2.2000	15.0000	33.0000	101.0000	288.1500	100.4950	0.9950	288.1500	221.0890	2.1890	0.9000	1.4000	369.0450	1676.3870	52.5588
2.3000	15.0000	34.5000	101.0000	288.1500	100.4950	0.9950	288.1500	231.1385	2.2885	0.9000	1.4000	374.1712	1699.6726	54.5702
2.4000	15.0000	36.0000	101.0000	288.1500	100.4950	0.9950	288.1500	241.1880	2.3880	0.9000	1.4000	379.1405	1722.2459	56.5684
2.5000	15.0000	37.5000	101.0000	288.1500	100.4950	0.9950	288.1500	251.2375	2.4875	0.9000	1.4000	383.9641	1744.1570	58.5541
2.6000	15.0000	39.0000	101.0000	288.1500	100.4950	0.9950	288.1500	261.2870	2.5870	0.9000	1.4000	388.6518	1765.4507	60.5279
2.7000	15.0000	40.5000	101.0000	288.1500	100.4950	0.9950	288.1500	271.3365	2.6865	0.9000	1.4000	393.2124	1786.1672	62.4903
2.8000	15.0000	42.0000	101.0000	288.1500	100.4950	0.9950	288.1500	281.3860	2.7860	0.9000	1.4000	397.6538	1806.3426	64.4419
2.9000	15.0000	43.5000	101.0000	288.1500	100.4950	0.9950	288.1500	291.4355	2.8855	0.9000	1.4000	401.9834	1826.0097	66.3830
3.0000	15.0000	45.0000	101.0000	288.1500	100.4950	0.9950	288.1500	301.4850	2.9850	0.9000	1.4000	406.2077	1845.1983	68.3140
3.1000	15.0000	46.5000	101.0000	288.1500	100.4950	0.9950	288.1500	311.5345	3.0845	0.9000	1.4000	410.3325	1863.9352	70.2355
3.2000	15.0000	48.0000	101.0000	288.1500	100.4950	0.9950	288.1500	321.5840	3.1840	0.9000	1.4000	414.3633	1882.2452	72.1476
3.3000	15.0000	49.5000	101.0000	288.1500	100.4950	0.9950	288.1500	331.6335	3.2835	0.9000	1.4000	418.3051	1900.1510	74.0509
3.4000	15.0000	51.0000	101.0000	288.1500	100.4950	0.9950	288.1500	341.6830	3.3830	0.9000	1.4000	422.1625	1917.6733	75.9455
3.5000	15.0000	52.5000	101.0000	288.1500	100.4950	0.9950	288.1500	351.7325	3.4825	0.9000	1.4000	425.9397	1934.8312	77.8317
3.6000	15.0000	54.0000	101.0000	288.1500	100.4950	0.9950	288.1500	361.7820	3.5820	0.9000	1.4000	429.6406	1951.6425	79.7100
3.7000	15.0000	55.5000	101.0000	288.1500	100.4950	0.9950	288.1500	371.8315	3.6815	0.9000	1.4000	433.2688	1968.1234	81.5804
3.8000	15.0000	57.0000	101.0000	288.1500	100.4950	0.9950	288.1500	381.8810	3.7810	0.9000	1.4000	436.8276	1984.2892	83.4433
3.9000	15.0000	58.5000	101.0000	288.1500	100.4950	0.9950	288.1500	391.9305	3.8805	0.9000	1.4000	440.3201	2000.1539	85.2988
4.0000	15.0000	60.0000	101.0000	288.1500	100.4950	0.9950	288.1500	401.9800	3.9800	0.9000	1.4000	443.7492	2015.7306	87.1473
4.1000	15.0000	61.5000	101.0000	288.1500	100.4950	0.9950	288.1500	412.0295	4.0795	0.9000	1.4000	447.1176	2031.0316	88.9889
4.2000	15.0000	63.0000	101.0000	288.1500	100.4950	0.9950	288.1500	422.0790	4.1790	0.9000	1.4000	450.4278	2046.0683	90.8238
4.3000	15.0000	64.5000	101.0000	288.1500	100.4950	0.9950	288.1500	432.1285	4.2785	0.9000	1.4000	453.6822	2060.8515	92.6521
4.4000	15.0000	66.0000	101.0000	288.1500	100.4950	0.9950	288.1500	442.1780	4.3780	0.9000	1.4000	456.8830	2075.3910	94.4741
4.5000	15.0000	67.5000	101.0000	288.1500	100.4950	0.9950	288.1500	452.2275	4.4775	0.9000	1.4000	460.0322	2089.6964	96.2900
4.6000	15.0000	69.0000	101.0000	288.1500	100.4950	0.9950	288.1500	462.2770	4.5770	0.9000	1.4000	463.1319	2103.7765	98.0998
4.7000	15.0000	70.5000	101.0000	288.1500	100.4950	0.9950	288.1500	472.3265	4.6765	0.9000	1.4000	466.1837	2117.6396	99.9038
4.8000	15.0000	72.0000	101.0000	288.1500	100.4950	0.9950	288.1500	482.3760	4.7760	0.9000	1.4000	469.1896	2131.2936	101.7021
4.9000	15.0000	73.5000	101.0000	288.1500	100.4950	0.9950	288.1500	492.4255	4.8755	0.9000	1.4000	472.1510	2144.7459	103.4948
5.0000	15.0000	75.0000	101.0000	288.1500	100.4950	0.9950	288.1500	502.4750	4.9750	0.9000	1.4000	475.0696	2158.0036	105.2820
5.1000	15.0000	76.5000	101.0000	288.1500	100.4950	0.9950	288.1500	512.5245	5.0745	0.9000	1.4000	477.9467	2171.0731	107.0639
5.2000	15.0000	78.0000	101.0000	288.1500	100.4950	0.9950	288.1500	522.5740	5.1740	0.9000	1.4000	480.7839	2183.9609	108.8407
5.3000	15.0000	79.5000	101.0000	288.1500	100.4950	0.9950	288.1500	532.6235	5.2735	0.9000	1.4000	483.5823	2196.6728	110.6123
5.4000	15.0000	81.0000	101.0000	288.1500	100.4950	0.9950	288.1500	542.6730	5.3730	0.9000	1.4000	486.3433	2209.2146	112.3790
5.5000	15.0000	82.5000	101.0000	288.1500	100.4950	0.9950	288.1500	552.7225	5.4725	0.9000	1.4000	489.0680	2221.5915	114.1408
5.6000	15.0000	84.0000	101.0000	288.1500	100.4950	0.9950	288.1500	562.7720	5.5720	0.9000	1.4000	491.7576	2233.8087	115.8978
5.7000	15.0000	85.5000	101.0000	288.1500	100.4950	0.9950	288.1500	572.8215	5.6715	0.9000	1.4000	494.4130	2245.8711	117.6502
5.8000	15.0000	87.0000	101.0000	288.1500	100.4950	0.9950	288.1500	582.8710	5.7710	0.9000	1.4000	497.0354	2257.7832	119.3980
5.9000	15.0000	88.5000	101.0000	288.1500	100.4950	0.9950	288.1500	592.9205	5.8705	0.9000	1.4000	499.6257	2269.5495	121.1413
6.0000	15.0000	90.0000	101.0000	288.1500	100.4950	0.9950	288.1500	602.9700	5.9700	0.9000	1.4000	502.1848	2281.1743	122.8803
6.1000	15.0000	91.5000	101.0000	288.1500	100.4950	0.9950	288.1500	613.0195	6.0695	0.9000	1.4000	504.7136	2292.6614	124.6149
6.2000	15.0000	93.0000	101.0000	288.1500	100.4950	0.9950	288.1500	623.0690	6.1690	0.9000	1.4000	507.2130	2304.0148	126.3454
6.3000	15.0000	94.5000	101.0000	288.1500	100.4950	0.9950	288.1500	633.1185	6.2685	0.9000	1.4000	509.6837	2315.2382	128.0716
6.4000	15.0000	96.0000	101.0000	288.1500	100.4950	0.9950	288.1500	643.1680	6.3680	0.9000	1.4000	512.1266	2326.3350	129.7938
6.5000	15.0000	97.5000	101.0000	288.1500	100.4950	0.9950	288.1500	653.2175	6.4675	0.9000	1.4000	514.5424	2337.3087	131.5120
6.6000	15.0000	99.0000	101.0000	288.1500	100.4950	0.9950	288.1500	663.2670	6.5670	0.9000	1.4000	516.9317	2348.1624	133.2263
6.7000	15.0000	100.5000	101.0000	288.1500	100.4950	0.9950	288.1500	673.3165	6.6665	0.9000	1.4000	519.2954	2358.8993	134.9368
6.8000	15.0000	102.0000	101.0000	288.1500	100.4950	0.9950	288.1500	683.3660	6.7660	0.9000	1.4000	521.6340	2369.5223	136.6434
6.9000	15.0000	103.5000	101.0000	288.1500	100.4950	0.9950	288.1500	693.4155	6.8655	0.9000	1.4000	523.9481	2380.0343	138.3463
7.0000	15.0000	105.0000	101.0000	288.1500	100.4950	0.9950	288.1500	703.4650	6.9650	0.9000	1.4000	526.2384	2390.4381	140.0456

A.3 Two-Spool Two-Shaft I/C cycle Engine

T4	COT	LPC PR	P1	T1	P2	P2 (atm)	T2	P3	P3 (atm)	ε	γ	T3	P4	P4(atm)	T4	W
305.4781	1387.6344	1.2	101.0000	288.1500	100.4950	0.9950	288.1500	120.5940	1.1940	0.9000	1.4000	305.2701	120.2322	1.1904	305.4781	31.4159
305.4781	1387.6344	1.2	101.0000	288.1500	100.4950	0.9950	288.1500	120.5940	1.1940	0.9000	1.4000	305.2701	120.2322	1.1904	305.4781	31.4159
305.4781	1387.6344	1.3	101.0000	288.1500	100.4950	0.9950	288.1500	130.6435	1.2935	0.9000	1.4000	313.0725	130.2516	1.2896	305.4781	34.0339
305.4781	1387.6344	1.4	101.0000	288.1500	100.4950	0.9950	288.1500	140.6930	1.3930	0.9000	1.4000	320.4572	140.2709	1.3888	305.4781	36.6518
305.4781	1387.6344	1.5	101.0000	288.1500	100.4950	0.9950	288.1500	150.7425	1.4925	0.9000	1.4000	327.4742	150.2903	1.4880	305.4781	39.2698
305.4781	1387.6344	1.6	101.0000	288.1500	100.4950	0.9950	288.1500	160.7920	1.5920	0.9000	1.4000	334.1646	160.3096	1.5872	305.4781	41.8878
305.4781	1387.6344	1.7	101.0000	288.1500	100.4950	0.9950	288.1500	170.8415	1.6915	0.9000	1.4000	340.5626	170.3290	1.6864	305.4781	44.5058
305.4781	1387.6344	1.8	101.0000	288.1500	100.4950	0.9950	288.1500	180.8910	1.7910	0.9000	1.4000	346.6971	180.3483	1.7856	305.4781	47.1238
305.4781	1387.6344	1.9	101.0000	288.1500	100.4950	0.9950	288.1500	190.9405	1.8905	0.9000	1.4000	352.5928	190.3677	1.8848	305.4781	49.7418
305.4781	1387.6344	2.0	101.0000	288.1500	100.4950	0.9950	288.1500	200.9900	1.9900	0.9000	1.4000	358.2709	200.3870	1.9840	305.4781	52.3598
305.4781	1387.6344	2.1	101.0000	288.1500	100.4950	0.9950	288.1500	211.0395	2.0895	0.9000	1.4000	363.7496	210.4064	2.0832	305.4781	54.9778
305.4781	1387.6344	2.2	101.0000	288.1500	100.4950	0.9950	288.1500	221.0890	2.1890	0.9000	1.4000	369.0450	220.4257	2.1824	305.4781	57.5958
305.4781	1387.6344	2.3	101.0000	288.1500	100.4950	0.9950	288.1500	231.1385	2.2885	0.9000	1.4000	374.1712	230.4451	2.2816	305.4781	60.2138
305.4781	1387.6344	2.4	101.0000	288.1500	100.4950	0.9950	288.1500	241.1880	2.3880	0.9000	1.4000	379.1405	240.4644	2.3808	305.4781	62.8317
305.4781	1387.6344	2.5	101.0000	288.1500	100.4950	0.9950	288.1500	251.2375	2.4875	0.9000	1.4000	383.9641	250.4838	2.4800	305.4781	65.4497
305.4781	1387.6344	2.6	101.0000	288.1500	100.4950	0.9950	288.1500	261.2870	2.5870	0.9000	1.4000	388.6518	260.5031	2.5792	305.4781	68.0677
305.4781	1387.6344	2.7	101.0000	288.1500	100.4950	0.9950	288.1500	271.3365	2.6865	0.9000	1.4000	393.2124	270.5225	2.6784	305.4781	70.6857
305.4781	1387.6344	2.8	101.0000	288.1500	100.4950	0.9950	288.1500	281.3860	2.7860	0.9000	1.4000	397.6538	280.5418	2.7776	305.4781	73.3037
305.4781	1387.6344	2.9	101.0000	288.1500	100.4950	0.9950	288.1500	291.4355	2.8855	0.9000	1.4000	401.9834	290.5612	2.8768	305.4781	75.9217
305.4781	1387.6344	3.0	101.0000	288.1500	100.4950	0.9950	288.1500	301.4850	2.9850	0.9000	1.4000	406.2077	300.5805	2.9760	305.4781	78.5397
305.4781	1387.6344	3.1	101.0000	288.1500	100.4950	0.9950	288.1500	311.5345	3.0845	0.9000	1.4000	410.3325	310.5999	3.0752	305.4781	81.1577
305.4781	1387.6344	3.2	101.0000	288.1500	100.4950	0.9950	288.1500	321.5840	3.1840	0.9000	1.4000	414.3633	320.6192	3.1744	305.4781	83.7757
305.4781	1387.6344	3.3	101.0000	288.1500	100.4950	0.9950	288.1500	331.6335	3.2835	0.9000	1.4000	418.3051	330.6386	3.2736	305.4781	86.3936
305.4781	1387.6344	3.4	101.0000	288.1500	100.4950	0.9950	288.1500	341.6830	3.3830	0.9000	1.4000	422.1625	340.6580	3.3729	305.4781	89.0116
305.4781	1387.6344	3.5	101.0000	288.1500	100.4950	0.9950	288.1500	351.7325	3.4825	0.9000	1.4000	425.9397	350.6773	3.4721	305.4781	91.6296
305.4781	1387.6344	3.6	101.0000	288.1500	100.4950	0.9950	288.1500	361.7820	3.5820	0.9000	1.4000	429.6406	360.6967	3.5713	305.4781	94.2476
305.4781	1387.6344	3.7	101.0000	288.1500	100.4950	0.9950	288.1500	371.8315	3.6815	0.9000	1.4000	433.2688	370.7160	3.6705	305.4781	96.8656
305.4781	1387.6344	3.8	101.0000	288.1500	100.4950	0.9950	288.1500	381.8810	3.7810	0.9000	1.4000	436.8276	380.7354	3.7697	305.4781	99.4836
305.4781	1387.6344	3.9	101.0000	288.1500	100.4950	0.9950	288.1500	391.9305	3.8805	0.9000	1.4000	440.3201	390.7547	3.8689	305.4781	102.1016
305.4781	1387.6344	4.0	101.0000	288.1500	100.4950	0.9950	288.1500	401.9800	3.9800	0.9000	1.4000	443.7492	400.7741	3.9681	305.4781	104.7196
305.4781	1387.6344	4.1	101.0000	288.1500	100.4950	0.9950	288.1500	412.0295	4.0795	0.9000	1.4000	447.1176	410.7934	4.0673	305.4781	107.3376
305.4781	1387.6344	4.2	101.0000	288.1500	100.4950	0.9950	288.1500	422.0790	4.1790	0.9000	1.4000	450.4278	420.8128	4.1665	305.4781	109.9555
305.4781	1387.6344	4.3	101.0000	288.1500	100.4950	0.9950	288.1500	432.1285	4.2785	0.9000	1.4000	453.6822	430.8321	4.2657	305.4781	112.5735
305.4781	1387.6344	4.4	101.0000	288.1500	100.4950	0.9950	288.1500	442.1780	4.3780	0.9000	1.4000	456.8830	440.8515	4.3649	305.4781	115.1915
305.4781	1387.6344	4.5	101.0000	288.1500	100.4950	0.9950	288.1500	452.2275	4.4775	0.9000	1.4000	460.0322	450.8708	4.4641	305.4781	117.8095
305.4781	1387.6344	4.6	101.0000	288.1500	100.4950	0.9950	288.1500	462.2770	4.5770	0.9000	1.4000	463.1319	460.8902	4.5633	305.4781	120.4275
305.4781	1387.6344	4.7	101.0000	288.1500	100.4950	0.9950	288.1500	472.3265	4.6765	0.9000	1.4000	466.1837	470.9095	4.6625	305.4781	123.0455
305.4781	1387.6344	4.8	101.0000	288.1500	100.4950	0.9950	288.1500	482.3760	4.7760	0.9000	1.4000	469.1896	480.9289	4.7617	305.4781	125.6635
305.4781	1387.6344	4.9	101.0000	288.1500	100.4950	0.9950	288.1500	492.4255	4.8755	0.9000	1.4000	472.1510	490.9482	4.8609	305.4781	128.2815
305.4781	1387.6344	5.0	101.0000	288.1500	100.4950	0.9950	288.1500	502.4750	4.9750	0.9000	1.4000	475.0696	500.9676	4.9601	305.4781	130.8995
305.4781	1387.6344	5.1	101.0000	288.1500	100.4950	0.9950	288.1500	512.5245	5.0745	0.9000	1.4000	477.9467	510.9869	5.0593	305.4781	133.5174
305.4781	1387.6344	5.2	101.0000	288.1500	100.4950	0.9950	288.1500	522.5740	5.1740	0.9000	1.4000	480.7839	521.0063	5.1585	305.4781	136.1354
305.4781	1387.6344	5.3	101.0000	288.1500	100.4950	0.9950	288.1500	532.6235	5.2735	0.9000	1.4000	483.5823	531.0256	5.2577	305.4781	138.7534
305.4781	1387.6344	5.4	101.0000	288.1500	100.4950	0.9950	288.1500	542.6730	5.3730	0.9000	1.4000	486.3433	541.0450	5.3569	305.4781	141.3714
305.4781	1387.6344	5.5	101.0000	288.1500	100.4950	0.9950	288.1500	552.7225	5.4725	0.9000	1.4000	489.0680	551.0643	5.4561	305.4781	143.9894
305.4781	1387.6344	5.6	101.0000	288.1500	100.4950	0.9950	288.1500	562.7720	5.5720	0.9000	1.4000	491.7576	561.0837	5.5553	305.4781	146.6074
305.4781	1387.6344	5.7	101.0000	288.1500	100.4950	0.9950	288.1500	572.8215	5.6715	0.9000	1.4000	494.4130	571.1030	5.6545	305.4781	149.2254
305.4781	1387.6344	5.8	101.0000	288.1500	100.4950	0.9950	288.1500	582.8710	5.7710	0.9000	1.4000	497.0354	581.1224	5.7537	305.4781	151.8434
305.4781	1387.6344	5.9	101.0000	288.1500	100.4950	0.9950	288.1500	592.9205	5.8705	0.9000	1.4000	499.6257	591.1417	5.8529	305.4781	154.4614
305.4781	1387.6344	6.0	101.0000	288.1500	100.4950	0.9950	288.1500	602.9700	5.9700	0.9000	1.4000	502.1848	601.1611	5.9521	305.4781	157.0794
305.4781	1387.6344	6.1	101.0000	288.1500	100.4950	0.9950	288.1500	613.0195	6.0695	0.9000	1.4000	504.7136	611.1804	6.0513	305.4781	159.6973
305.4781	1387.6344	6.2	101.0000	288.1500	100.4950	0.9950	288.1500	623.0690	6.1690	0.9000	1.4000	507.2130	621.1998	6.1505	305.4781	162.3153
305.4781	1387.6344	6.3	101.0000	288.1500	100.4950	0.9950	288.1500	633.1185	6.2685	0.9000	1.4000	509.6837	631.2191	6.2497	305.4781	164.9333
305.4781	1387.6344	6.4	101.0000	288.1500	100.4950	0.9950	288.1500	643.1680	6.3680	0.9000	1.4000	512.1266	641.2385	6.3489	305.4781	167.5513
305.4781	1387.6344	6.5	101.0000	288.1500	100.4950	0.9950	288.1500	653.2175	6.4675	0.9000	1.4000	514.5424	651.2578	6.4481	305.4781	170.1693
305.4781	1387.6344	6.6	101.0000	288.1500	100.4950	0.9950	288.1500	663.2670	6.5670	0.9000	1.4000	516.9317	661.2772	6.5473	305.4781	172.7873
305.4781	1387.6344	6.7	101.0000	288.1500	100.4950	0.9950	288.1500	673.3165	6.6665	0.9000	1.4000	519.2954	671.2966	6.6465	305.4781	175.4053
305.4781	1387.6344	6.8	101.0000	288.1500	100.4950	0.9950	288.1500	683.3660	6.7660	0.9000	1.4000	521.6340	681.3159	6.7457	305.4781	178.0233
305.4781	1387.6344	6.9	101.0000	288.1500	100.4950	0.9950	288.1500	693.4155	6.8655	0.9000	1.4000	523.9481	691.3353	6.8449	305.4781	180.6413
305.4781	1387.6344	7.0	101.0000	288.1500	100.4950	0.9950	288.1500	703.4650	6.9650	0.9000	1.4000	526.2384	701.3546	6.9441	305.4781	183.2592
305.4781	1387.6344	7.1	101.0000	288.1500	100.4950	0.9950	288.1500	713.5145	7.0645	0.9000	1.4000	528.5055	711.3740	7.0433	305.4781	185.8772
305.4781	1387.6344	7.2	101.0000	288.1500	100.4950	0.9950	288.1500	723.5640	7.1640	0.9000	1.4000	530.7499	721.3933	7.1425	305.4781	188.4952
305.4781	1387.6344	7.3	101.0000	288.1500	100.4950	0.9950	288.1500	733.6135	7.2635	0.9000	1.4000	532.9721	731.4127	7.2417	305.4781	191.1132
305.4781	1387.6344	7.4	101.0000	288.1500	100.4950	0.9950	288.1500	743.6630	7.3630	0.9000	1.4000	535.1726	741.4320	7.3409	305.4781	193.7312
305.4781	1387.6344	7.5	101.0000	288.1500	100.4950	0.9950	288.1500	753.7125	7.4625	0.9000	1.4000	537.3521	751.4514	7.4401	305.4781	196.3492
305.4781	1387.6344	7.6	101.0000	288.1500	100.4950	0.9950	288.1500	763.7620	7.5620	0.9000	1.4000	539.5108	761.4707	7.5393	305.4781	198.9672
305.4781	1387.6344	7.7	101.0000	288.1500	100.4950	0.9950	288.1500	773.8115	7.6615	0.9000	1.4000	541.6494	771.4901	7.6385	305.4781	201.5852
305.4781	1387.6344	7.8	101.0000	288.1500	100.4950	0.9950	288.1500	783.8610	7.7610	0.9000	1.4000	543.7683	781.5094	7.7377	305.4781	204.2032
305.4781	1387.6344	7.9	101.0000	288.1500	100.4950	0.9950	288.1500	793.9105	7.8605	0.9000	1.4000	545.8678	791.5288	7.8369	305.4781	206.8211
305.4781	1387.6344	8.0	101.0000	288.1500	100.4950	0.9950	288.1500	803.9600	7.9600	0.9000	1.4000	547.9484	801.5481	7.9361	305.4781	209.4391
305.4781	1387.6344	8.1	101.0000	288.1500	100.4950	0.9950	288.1500	814.0095	8.0595	0.9000	1.4000	550.0105	811.5675	8.0353	305.4781	212.0571
305.4781	1387.6344	8.2	101.0000	288.1500	100.4950	0.9950	288.1500	824.0590	8.1590	0.9000	1.4000	552.0545	821.5868	8.1345	305.4781	214.6751
305.4781	1387.6344	8.3	101.0000	288.1500	100.4950	0.9950	288.1500	834.1085	8.2585	0.9000	1.4000	554.0808	831.6062	8.2337	305.4781	217.2931
305.4781	1387.6344	8.4	101.0000	288.1500	100.4950	0.9950	288.1500	844.1580	8.3580	0.9000	1.4000	556.0897	841.6255	8.3329	305.4781	219.9111
305.4781	1387.6344	8.5	101.0000	288.1500	100.4950	0.9950	288.1500	854.2075	8.4575	0.9000	1.4000	558.0817	851.6449	8.4321	305.4781	222.5291
305.4781	1387.6344	8.6	101.0000	288.1500	100.4950	0.9950	288.1500	864.2570	8.5570	0.9000	1.4000	560.0569	861.6642	8.5313	305.4781	225.1471
305.4781	1387.6344	8.7	101.0000	288.1500	100.4950	0.9950	288.1500	874.3065	8.6565	0.9000	1.4000	562.0158	871.6836	8.6305	305.4781	227.7651
305.4781	1387.6344	8.8	101.0000	288.1500	100.4950	0.9950	288.1500	884.3560	8.7560	0.9000	1.4000	563.9587	881.7029	8.7297	305.4781	230.3831
305.4781	1387.6344	8.9	101.0000	288.1500	100.4950	0.9950	288.1500	894.4055	8.8555	0.9000	1.4000	565.8859	891.7223	8.8289	305.4781	233.0010
305.4781	1387.6344	9.0	101.0000	288.1500	100.4950	0.9950	288.1500	904.4550	8.9550	0.9000	1.4000	567.7977	901.7416	8.9281	305.4781	235.6190
305.4781	1387.6344	9.1	101.0000	288.1500	100.4950	0.9950	288.1500	914.5045	9.0545	0.9000	1.4000	569.6943	911.7610	9.0273	305.4781	238.2370
305.4781	1387.6344	9.2	101.0000	288.1500	100.4950	0.9950	288.1500	924.5540	9.1540	0.9000	1.4000	571.5762	921.7803	9.1265	305.4781	240.8550
305.4781	1387.6344	9.3	101.0000	288.1500	100.4950	0.9950	288.1500	934.6035	9.2535	0.9000	1.4000	573.4434	931.7997	9.2257	305.4781	243.4730
305.4781	1387.6344	9.4	101.0000	288.1500	100.4950	0.9950	288.1500	944.6530	9.3530	0.9000	1.4000	575.2964	941.8190	9.3249	305.4781	246.0910
305.4781	1387.6344	9.5	101.0000	288.1500	100.4950	0.9950	288.1500	954.7025	9.4525	0.9000	1.4000	577.1354	951.8384	9.4241	305.4781	248.7090
305.4781	1387.6344	9.6	101.0000	288.1500	100.4950	0.9950	288.1500	964.7520	9.5520	0.9000	1.4000	578.9606	961.8577	9.5233	305.4781	251.3270
305.4781	1387.6344	9.7	101.0000	288.1500	100.4950	0.9950	288.1500	974.8015	9.6515	0.9000	1.4000	580.7722	971.8771	9.6225	305.4781	253.9450
305.4781	1387.6344	9.8	101.0000	288.1500	100.4950	0.9950	288.1500	984.8510	9.7510	0.9000	1.4000	582.5706	981.8964	9.7217	305.4781	256.5629
305.4781	1387.6344	9.9	101.0000	288.1500	100.4950	0.9950	288.1500	994.9005	9.8505	0.9000	1.4000	584.3559	991.9158	9.8209	305.4781	259.1809
305.4781	1387.6344	10.0	101.0000	288.1500	100.4950	0.9950	288.1500	1004.9500	9.9500	0.9000	1.4000	586.1284	1001.9352	9.9202	305.4781	261.7989

A.4 Three-Spool SC Engine

LPC PR	IPC	HPC PR	OPR	P1	T1	P2	P2 (atm)	T2	P3	P3 (atm)	ζ	γ	T3	COT	W
1.2000	2.5300	15.0000	45.5400	101.0000	288.1500	100.4950	0.9950	288.1500	120.5940	1.1940	0.9000	1.4000	305.2701	1863.0635	69.0391
1.2000	2.5300	15.0000	45.5400	101.0000	288.1500	100.4950	0.9950	288.1500	120.5940	1.1940	0.9000	1.4000	305.2701	1863.0635	69.0391
1.4000	2.5300	15.0000	53.1300	101.0000	288.1500	100.4950	0.9950	288.1500	140.6930	1.3930	0.9000	1.4000	320.4572	1955.7506	78.6139
1.6000	2.5300	15.0000	60.7200	101.0000	288.1500	100.4950	0.9950	288.1500	160.7920	1.5920	0.9000	1.4000	334.1646	2039.4065	87.9824
1.8000	2.5300	15.0000	68.3100	101.0000	288.1500	100.4950	0.9950	288.1500	180.8910	1.7910	0.9000	1.4000	346.6971	2115.8925	97.1748
2.0000	2.5300	15.0000	75.9000	101.0000	288.1500	100.4950	0.9950	288.1500	200.9900	1.9900	0.9000	1.4000	358.2709	2186.5271	106.2137
2.2000	2.5300	15.0000	83.4900	101.0000	288.1500	100.4950	0.9950	288.1500	221.0890	2.1890	0.9000	1.4000	369.0450	2252.2817	115.1169
2.4000	2.5300	15.0000	91.0800	101.0000	288.1500	100.4950	0.9950	288.1500	241.1880	2.3880	0.9000	1.4000	379.1405	2313.8947	123.8989
2.6000	2.5300	15.0000	98.6700	101.0000	288.1500	100.4950	0.9950	288.1500	261.2870	2.5870	0.9000	1.4000	388.6518	2371.9418	132.5712
2.8000	2.5300	15.0000	106.2600	101.0000	288.1500	100.4950	0.9950	288.1500	281.3860	2.7860	0.9000	1.4000	397.6538	2426.8814	141.1438
3.0000	2.5300	15.0000	113.8500	101.0000	288.1500	100.4950	0.9950	288.1500	301.4850	2.9850	0.9000	1.4000	406.2077	2479.0853	149.6248

A.5 Creep Calculation Model

K	1.2
H	0.026857
Den	7850
Dm	0.483143
Pi	3.141592654
Ndp	14848.978
Cooling effectivness	0.63

LMP	CSt (Mpa)
28.5	80
28.0	105
27.5	135
27.0	150
26.5	191
26.0	225
25.5	270
25.0	300
24.5	360
24.0	410
23.5	480

PCN	Nod (rpm)	CSt (Mpa)	Tg (K)	Tc (K)	Tb (K)	LMP	tf (hrs)
1	14848.978	147.77619	1308.9	661	900.723	26.6131	3518645569
0.95719	14213.293	135.39442	1250	644	868.22	26.7988	73514037384
0.94841	14082.919	132.92195	1250	647	870.11	26.8359	69496432374
0.94255	13995.904	131.28444	1250	651	872.63	26.8604	60391033583
0.94175	13984.025	131.06168	1250	655	875.15	26.8638	49684795262
0.94019	13960.861	130.62783	1250	659	877.67	26.8703	41256586729
0.93841	13934.429	130.13368	1250	663	880.19	26.8777	34375407532
0.93284	13851.721	128.59343	1250	666	882.08	26.9008	31405598498
0.92613	13752.084	126.75012	1250	669	883.97	26.9284	29041882453
0.91011	13514.203	122.40305	1250	671	885.23	26.9936	31139965044
0.91011	13514.203	122.40305	1250	671	885.23	26.9936	31139965044
0.92448	13727.583	126.29888	1250	669	883.97	26.9352	29560878201
0.93223	13842.663	128.42531	1250	666	882.08	26.9033	31611221962
0.93796	13927.747	130.0089	1250	662	879.56	26.8796	36331233250
0.9402	13961.009	130.63061	1250	659	877.67	26.8702	41245764399
0.94179	13984.619	131.07281	1250	655	875.15	26.8636	49658657257
0.94357	14011.05	131.56874	1250	651	872.63	26.8562	59725449379
0.94856	14085.147	132.964	1250	648	870.74	26.8352	65893676905
0.955	14180.774	134.77558	1250	644	868.22	26.8081	75349755186
0.95677	14207.057	135.27563	1250	643	867.59	26.8006	77778324846
0.95014	14108.608	133.40732	1250	647	870.11	26.8286	68166777957
0.94405	14018.178	131.70263	1250	650	872	26.8542	62531798164
0.94219	13990.559	131.18417	1250	654	874.52	26.8619	52019275092
0.94057	13966.503	130.73345	1250	658	877.04	26.8687	43217621264
0.93917	13945.715	130.34455	1250	662	879.56	26.8745	35849391327
0.93416	13871.321	128.95762	1250	665	881.45	26.8953	32551014187
0.92766	13774.803	127.16925	1250	668	883.34	26.9221	30034405284
0.91596	13601.07	123.98167	1250	671	885.23	26.9699	29278270412
0.91596	13601.07	123.98167	1250	671	885.23	26.9699	29278270412
0.92757	13773.467	127.14458	1250	668	883.34	26.9225	30065737655
0.93397	13868.5	128.90516	1250	665	881.45	26.8961	32619110939
0.93775	13924.629	129.9507	1250	661	878.93	26.8804	38290880632
0.94059	13966.8	130.73901	1250	658	877.04	26.8686	43206276378
0.94222	13991.004	131.19253	1250	654	874.52	26.8618	52005580374
0.94409	14018.772	131.71379	1250	650	872	26.854	62498782849
0.95017	14109.053	133.41575	1250	647	870.11	26.8285	68148741267
0.95682	14207.799	135.28977	1250	643	867.59	26.8004	77737051044
0.95859	14234.082	135.79077	1250	642	866.96	26.7928	80224923326
0.95182	14133.554	133.87951	1250	646	869.48	26.8215	70428441702
0.94557	14040.748	132.12708	1250	649	871.37	26.8478	64717498812
0.94266	13997.538	131.31509	1250	653	873.89	26.86	54467048037
0.94098	13972.591	130.84745	1250	657	876.41	26.867	45262998038
0.93951	13950.763	130.43894	1250	661	878.93	26.8731	37565554280
0.93559	13892.555	129.35273	1250	664	880.82	26.8894	33704672142
0.92945	13801.383	127.6605	1250	668	883.34	26.9148	29468290891
0.92361	13714.665	126.06128	1250	671	885.23	26.9388	27003080121
0.92361	13714.665	126.06128	1250	671	885.23	26.9388	27003080121
0.92967	13804.649	127.72094	1250	668	883.34	26.9139	29399238945
0.93574	13894.783	129.39421	1250	664	880.82	26.8888	33651848379
0.93808	13929.529	130.04217	1250	660	878.3	26.8791	40137684693
0.94099	13972.74	130.85023	1250	657	876.41	26.8669	45251107688
0.94269	13997.983	131.32344	1250	653	873.89	26.8598	54438352898
0.94568	14042.382	132.15782	1250	649	871.37	26.8473	64632047657

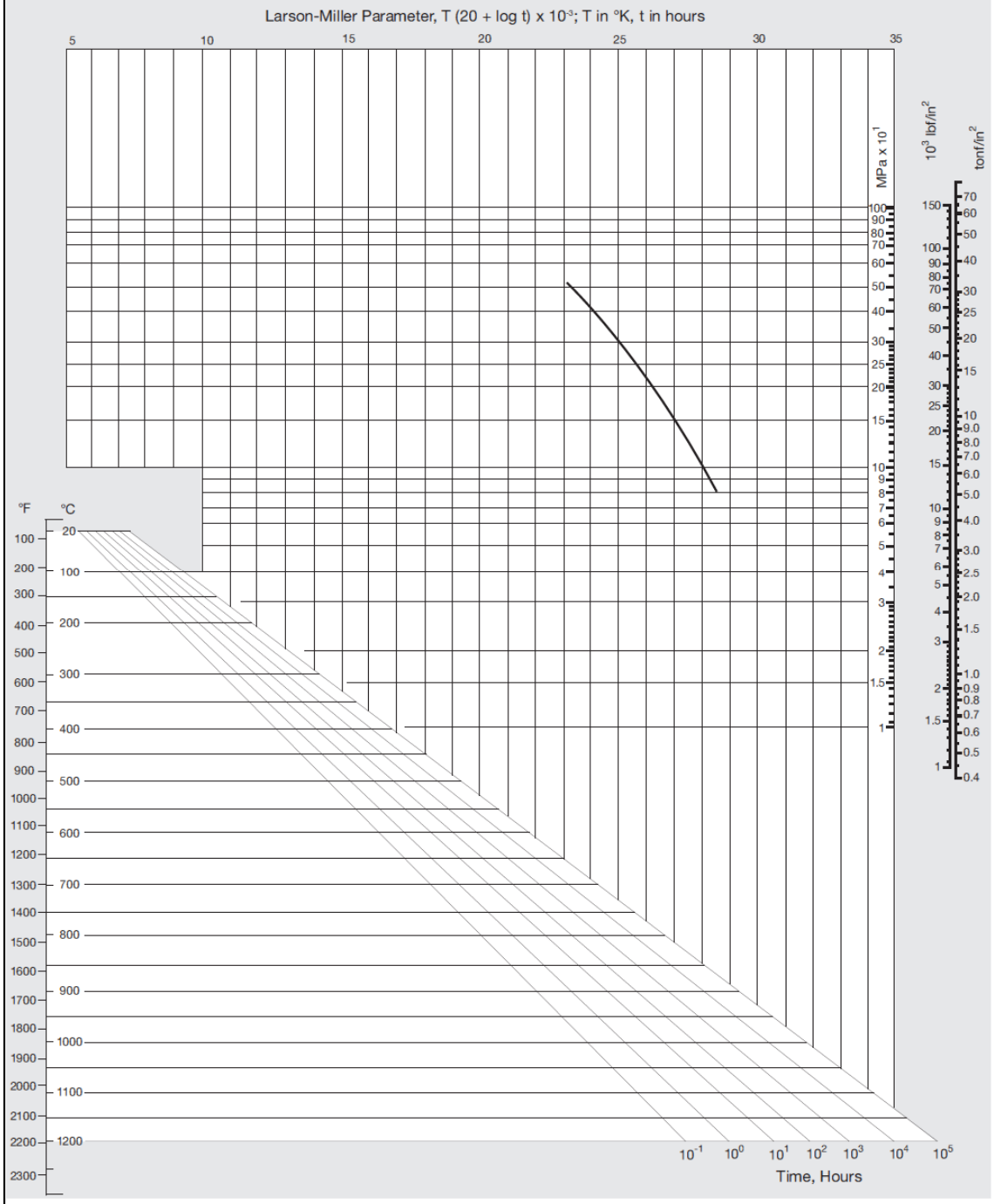

Figure 2. Creep-rupture properties of NIMONIC alloy 115 forged bar. Heat treatment 1.5 h/1190°C/AC+6h/1100°C/AC

Appendix B Off-Design Derivative [GT] Engines

B.1 (SC) Modified Single-Spool [IPT]

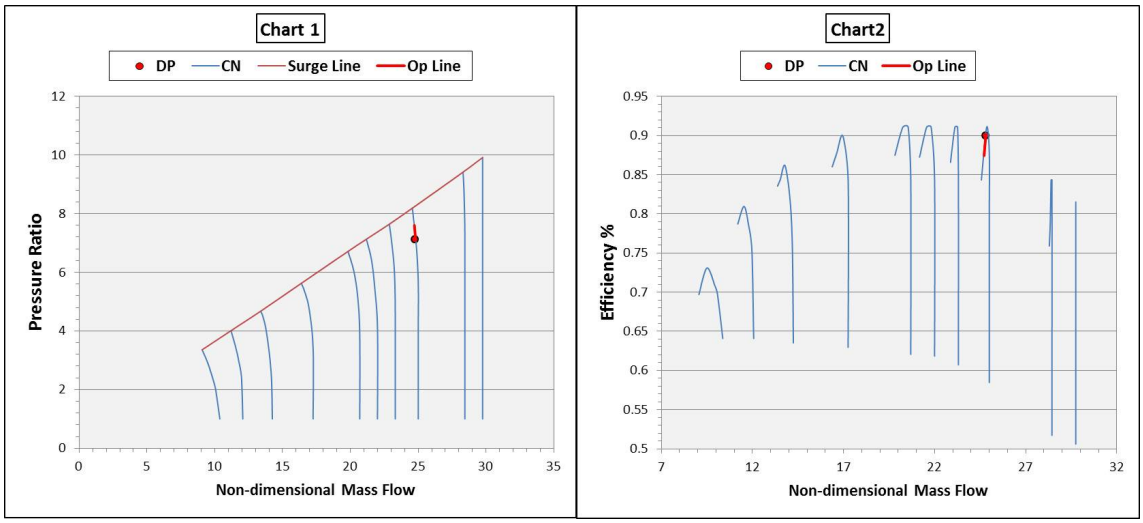

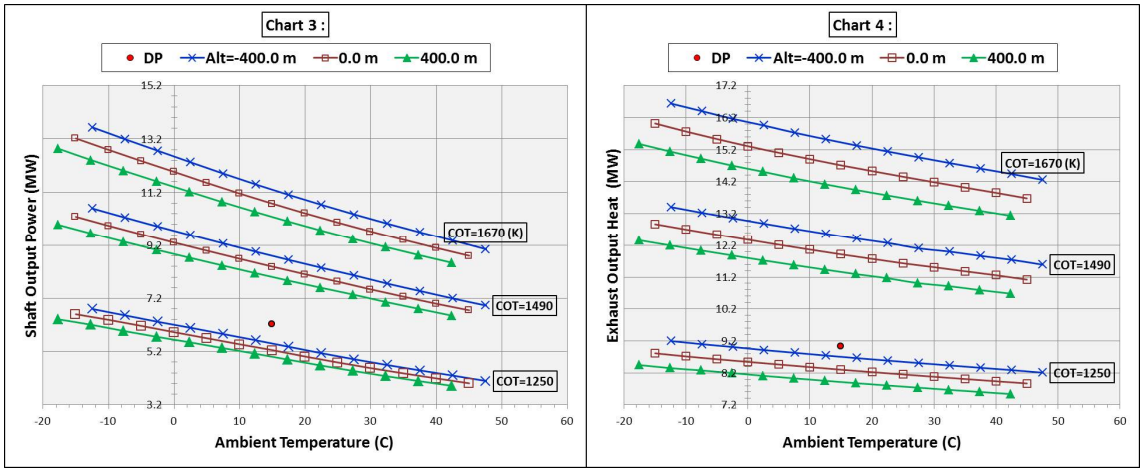

B.2 (SC) Modified Single-Spool [FPT]

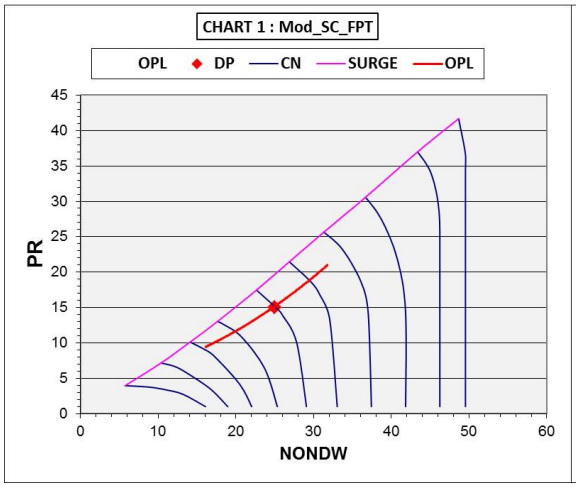

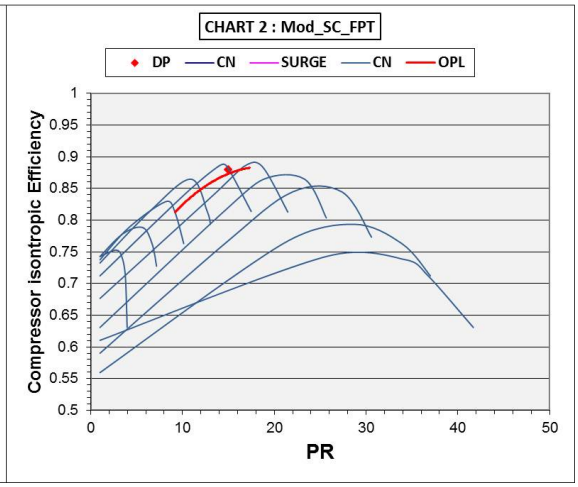

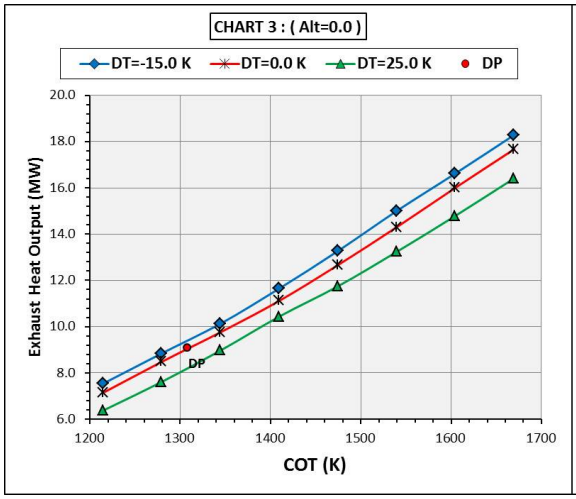

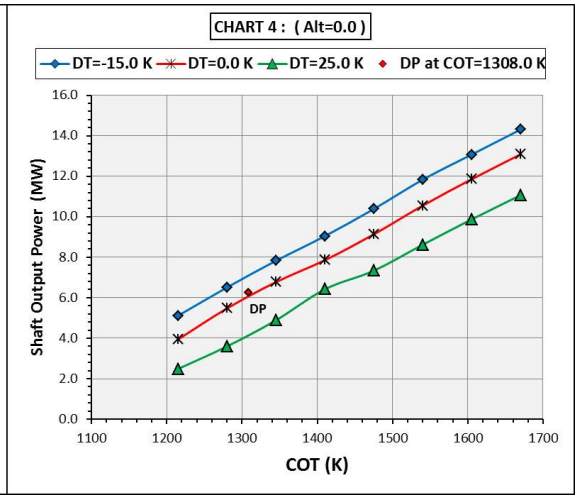

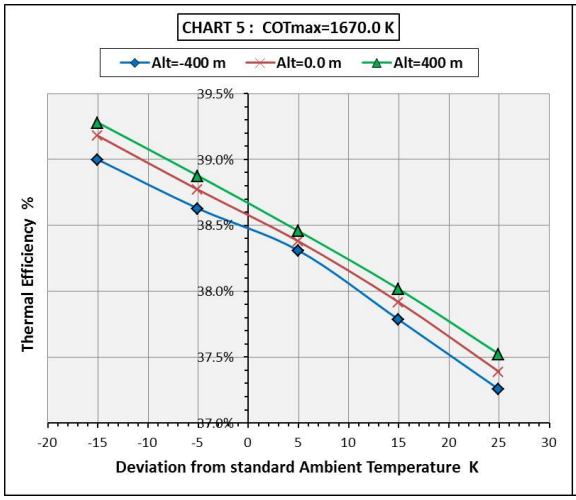

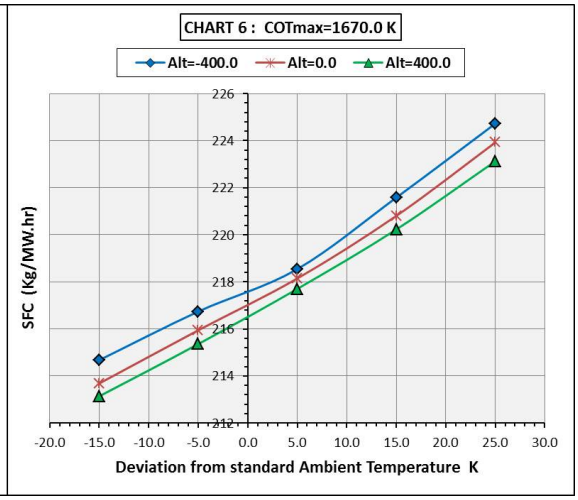

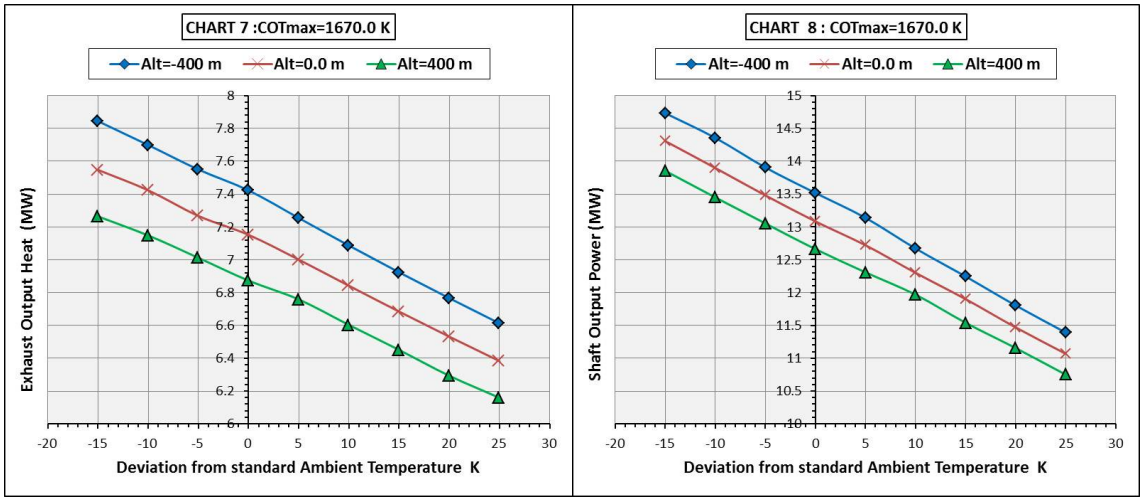

B.3 (HEC) Single Spool (Conv)-[IPT]

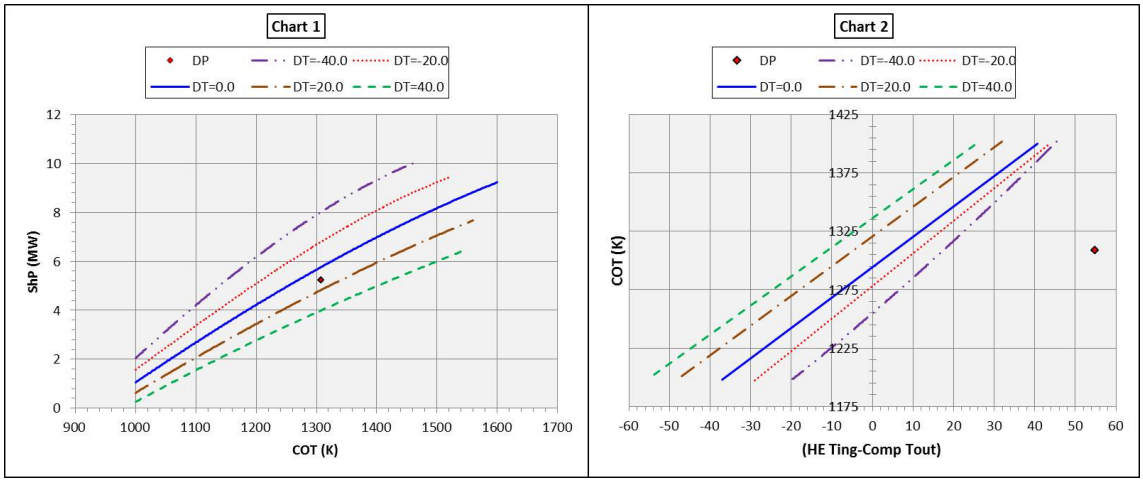

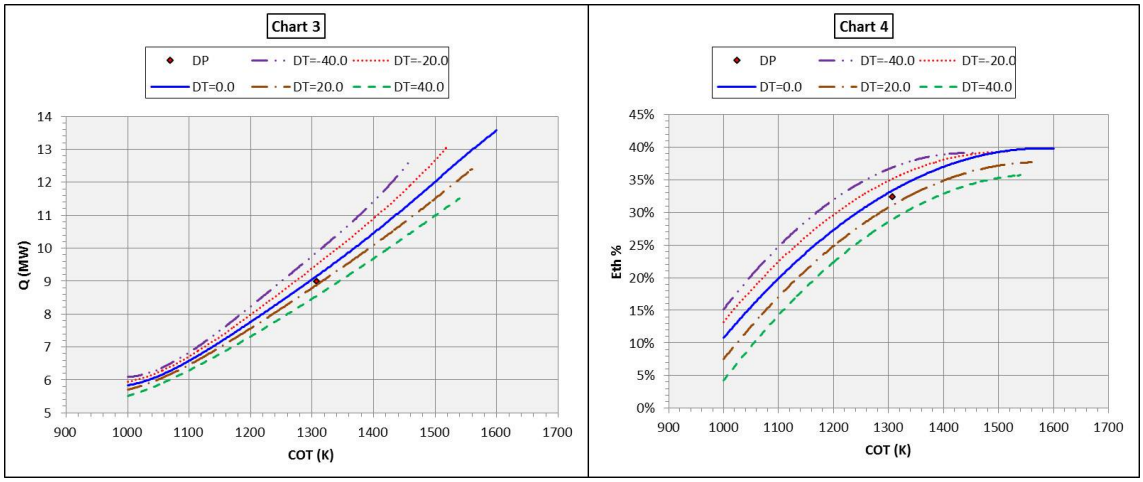

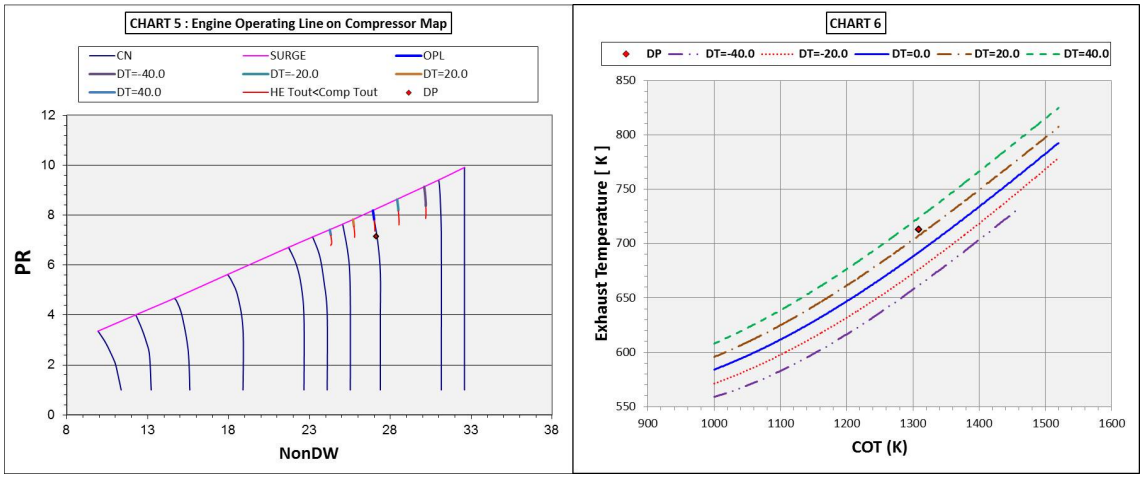

B.4 (HEC) Single Spool (Conv)-[FPT]

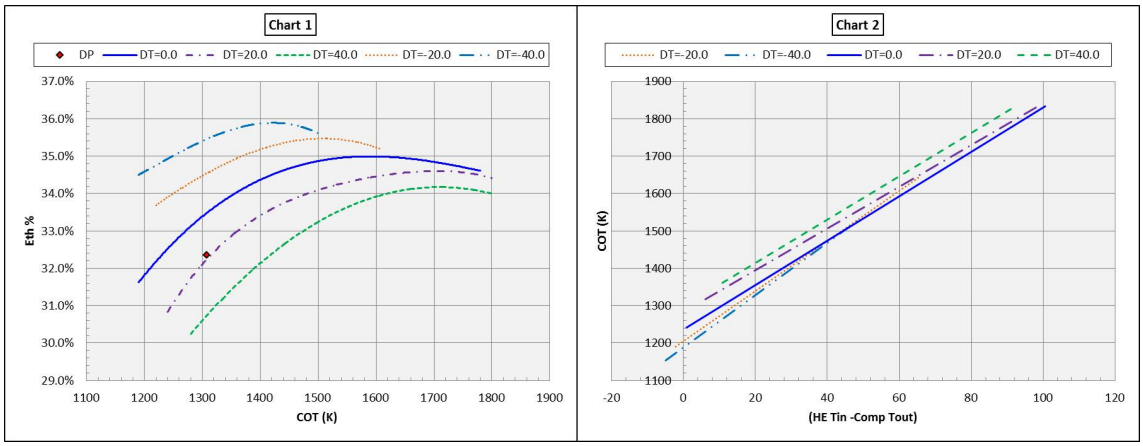

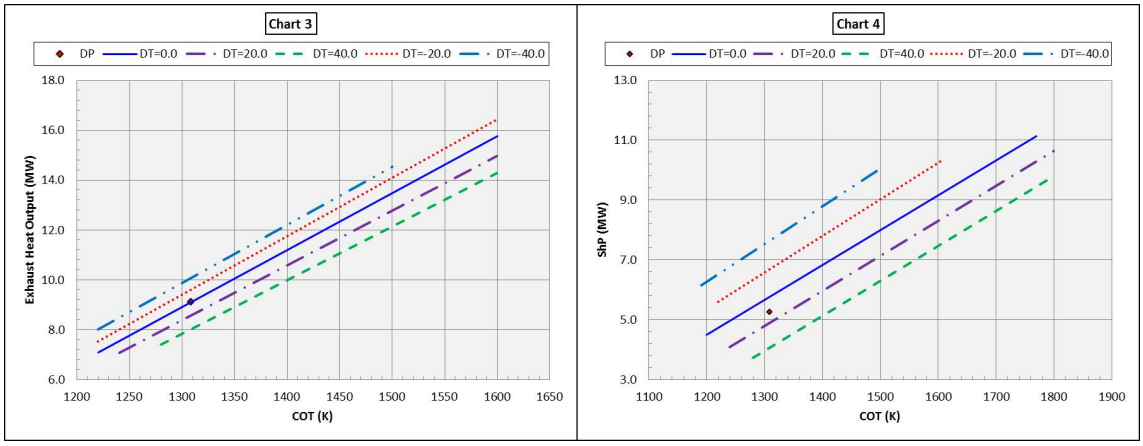

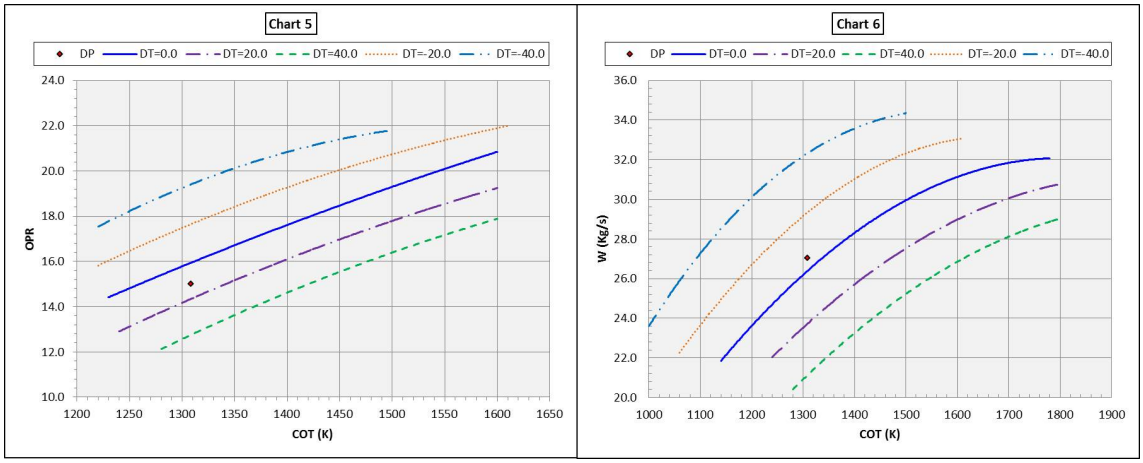

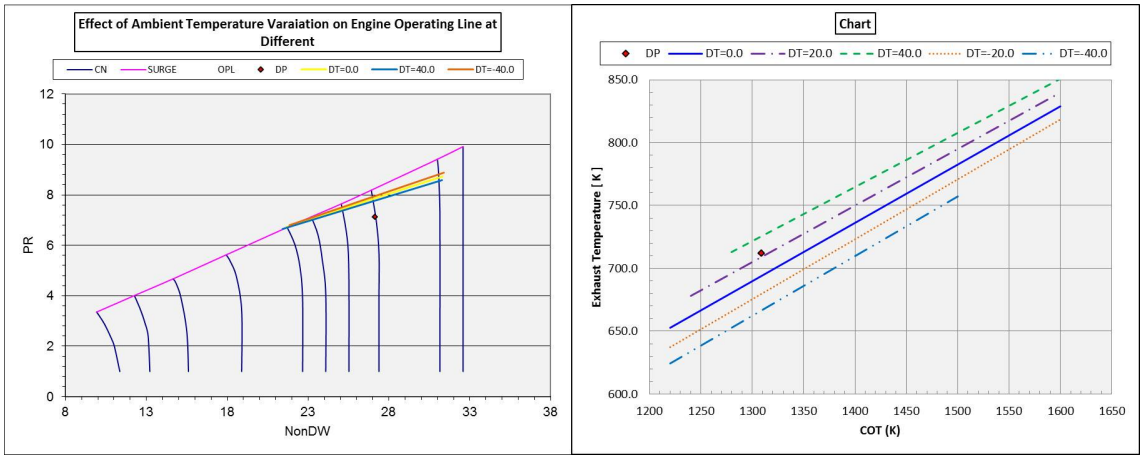

B.5 (HEC) Single Spool (non-Conv)-[FPT]

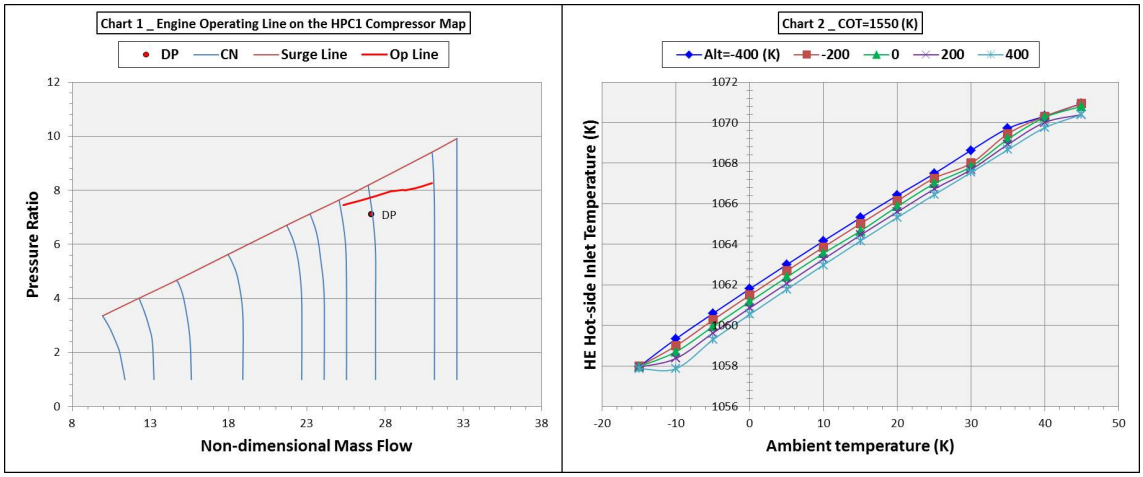

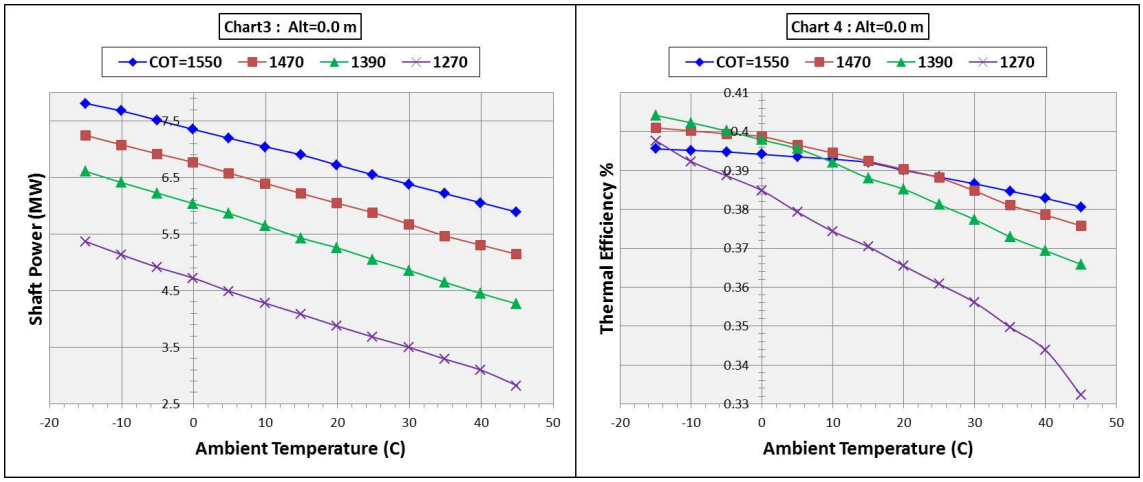
Chart3 : Alt=0.0 m
COT=1550
1470
1390
1270
Shaft Power (MW)
Ambient Temperature (C)
Chart 4 : Alt=0.0 m
Thermal Efficiency %
Ambient Temperature (C)

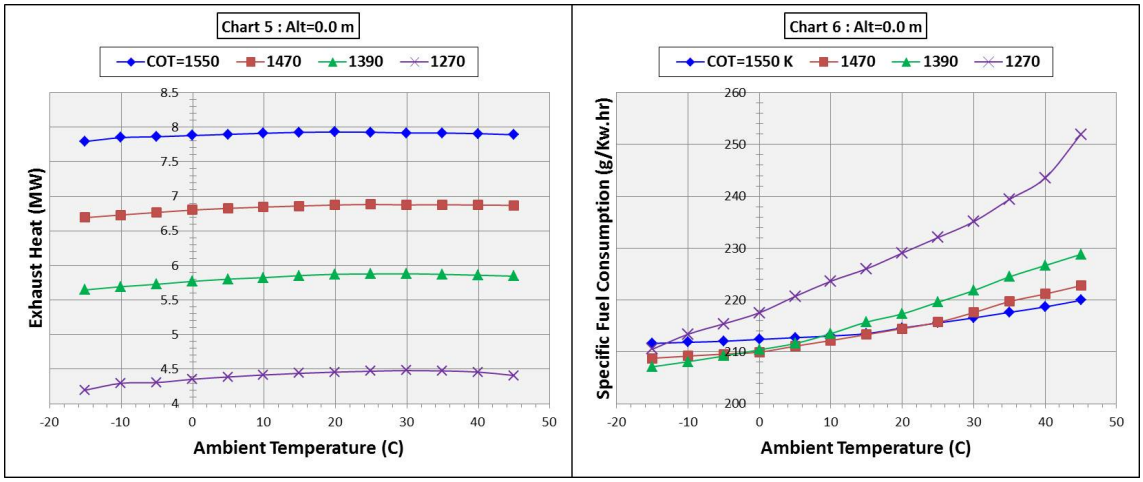
Chart 5 : Alt=0.0 m
COT=1550
1470
1390
1270
Exhaust Heat (MW)
Ambient Temperature (C)
Chart 6 : Alt=0.0 m
COT=1550 K
Specific Fuel Consumption (g/Kw.hr)
Ambient Temperature (C)

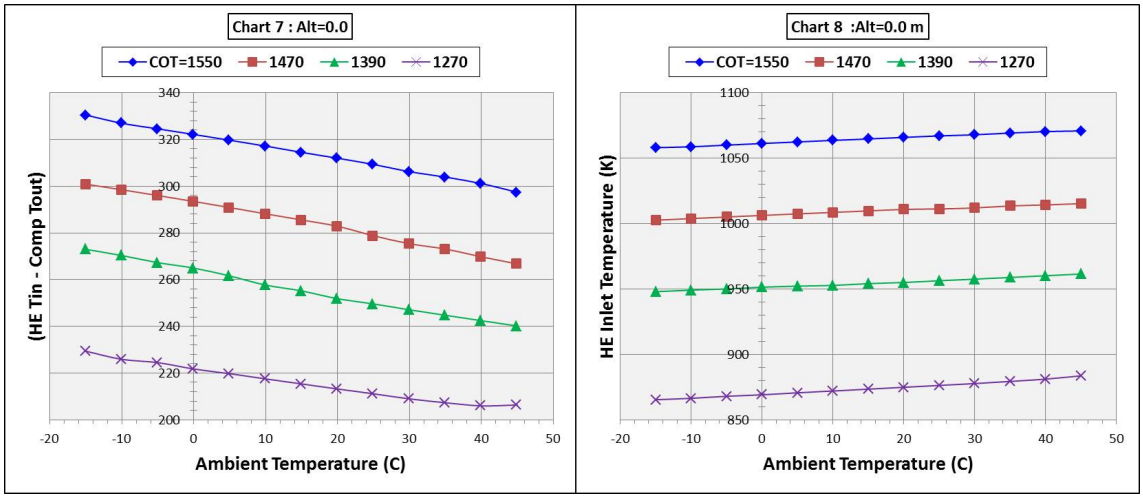
Chart 7 : Alt=0.0
COT=1550
1470
1390
1270
(HE Tin - Comp Tout)
Ambient Temperature (C)
Chart 8 :Alt=0.0 m
HE Inlet Temperature (K)
Ambient Temperature (C)

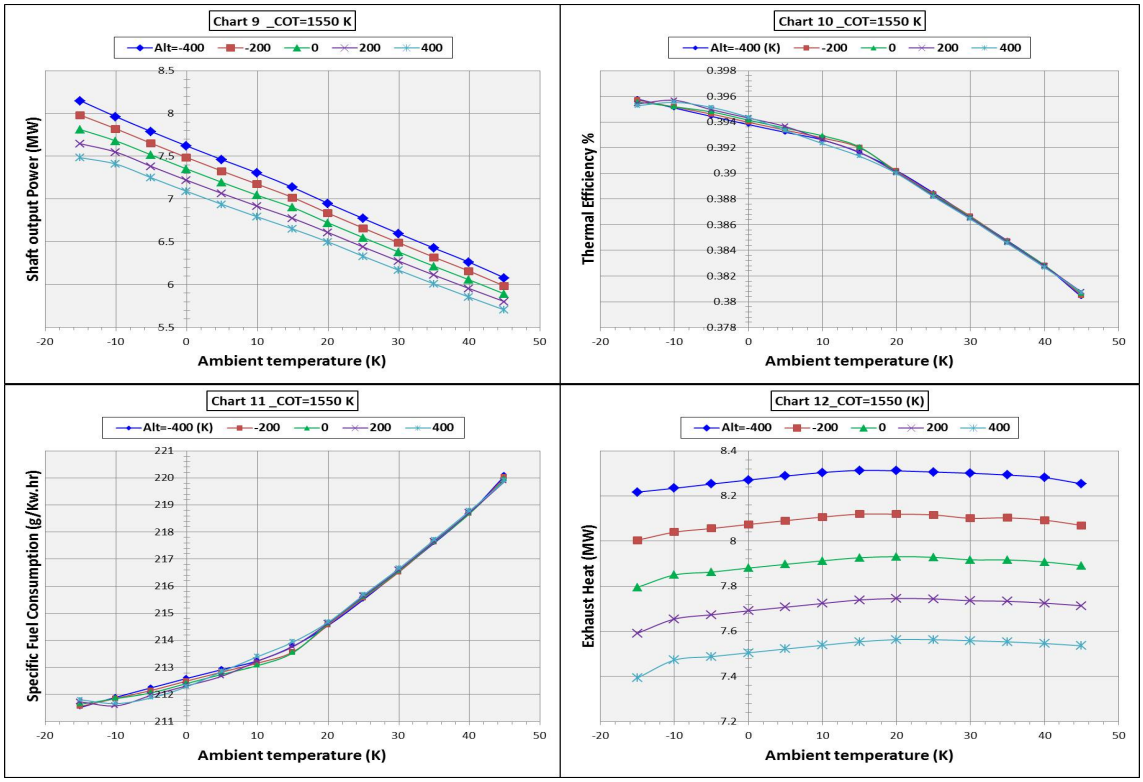
Chart 9 _COT=1550 K
Alt=-400
-200
0
200
400
Shaft output Power (MW)
Ambient temperature (K)
Chart 10 _COT=1550 K
Alt=-400 (K)
-200
0
200
400
Thermal Efficiency %
Ambient temperature (K)
Chart 11 _COT=1550 K
Alt=-400 (K)
-200
0
200
400
Specific Fuel Consumption (g/Kw.hr)
Ambient temperature (K)
Chart 12_COT=1550 (K)
Alt=-400
-200
0
200
400
Exhaust Heat (MW)
Ambient temperature (K)

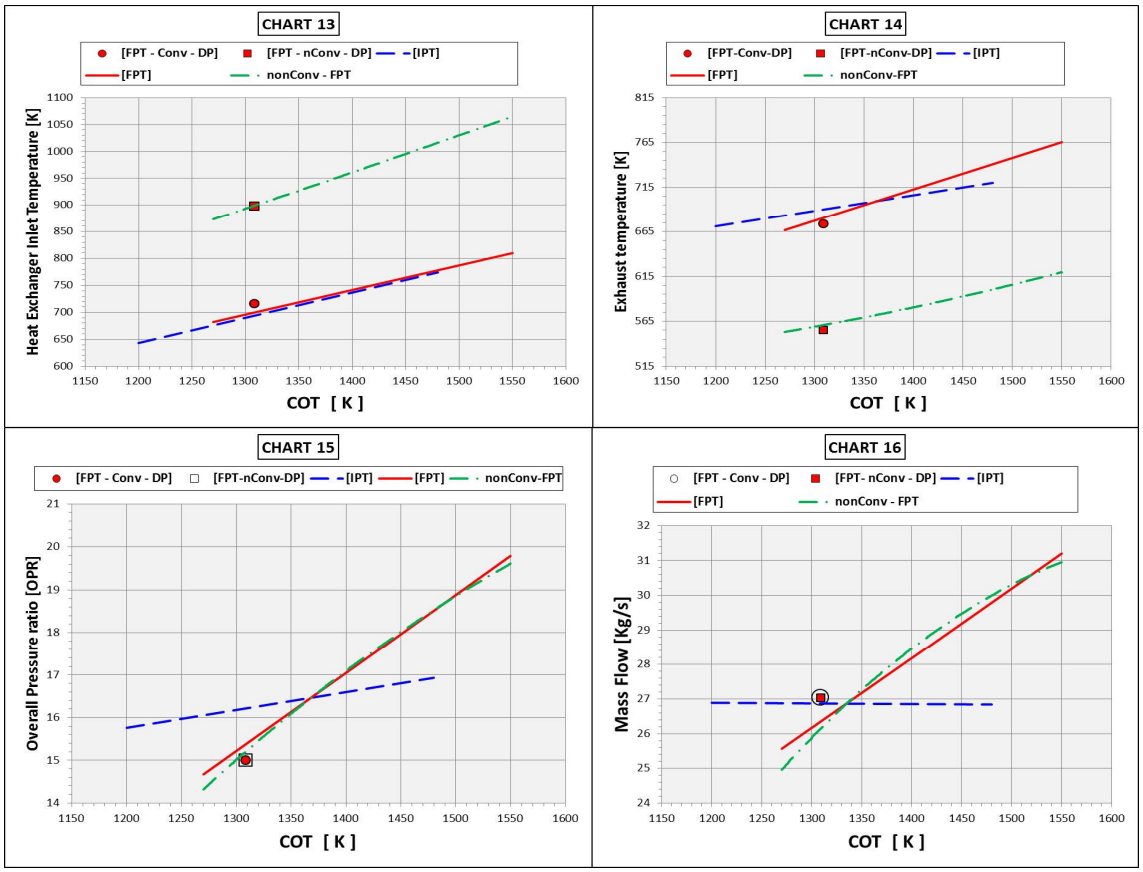
CHART 13
[FPT - Conv - DP]
[FPT - nConv - DP]
[IPT]
[FPT]
nonConv - FPT
Heat Exchanger Inlet Temperature [K]
COT [K]
CHART 14
[FPT-Conv-DP]
[FPT-nConv-DP]
[IPT]
[FPT]
nonConv-FPT
Exhaust temperature [K]
COT [K]
CHART 15
[FPT - Conv - DP]
[FPT-nConv-DP]
[IPT]
[FPT]
nonConv-FPT
Overall Pressure ratio [OPR]
COT [K]
CHART 16
[FPT - Conv - DP]
[FPT- nConv - DP]
[IPT]
[FPT]
nonConv - FPT
Mass Flow [Kg/s]
COT [K]

B.6 (SC) Two-Spool 2Shaft-[IPT] Engine

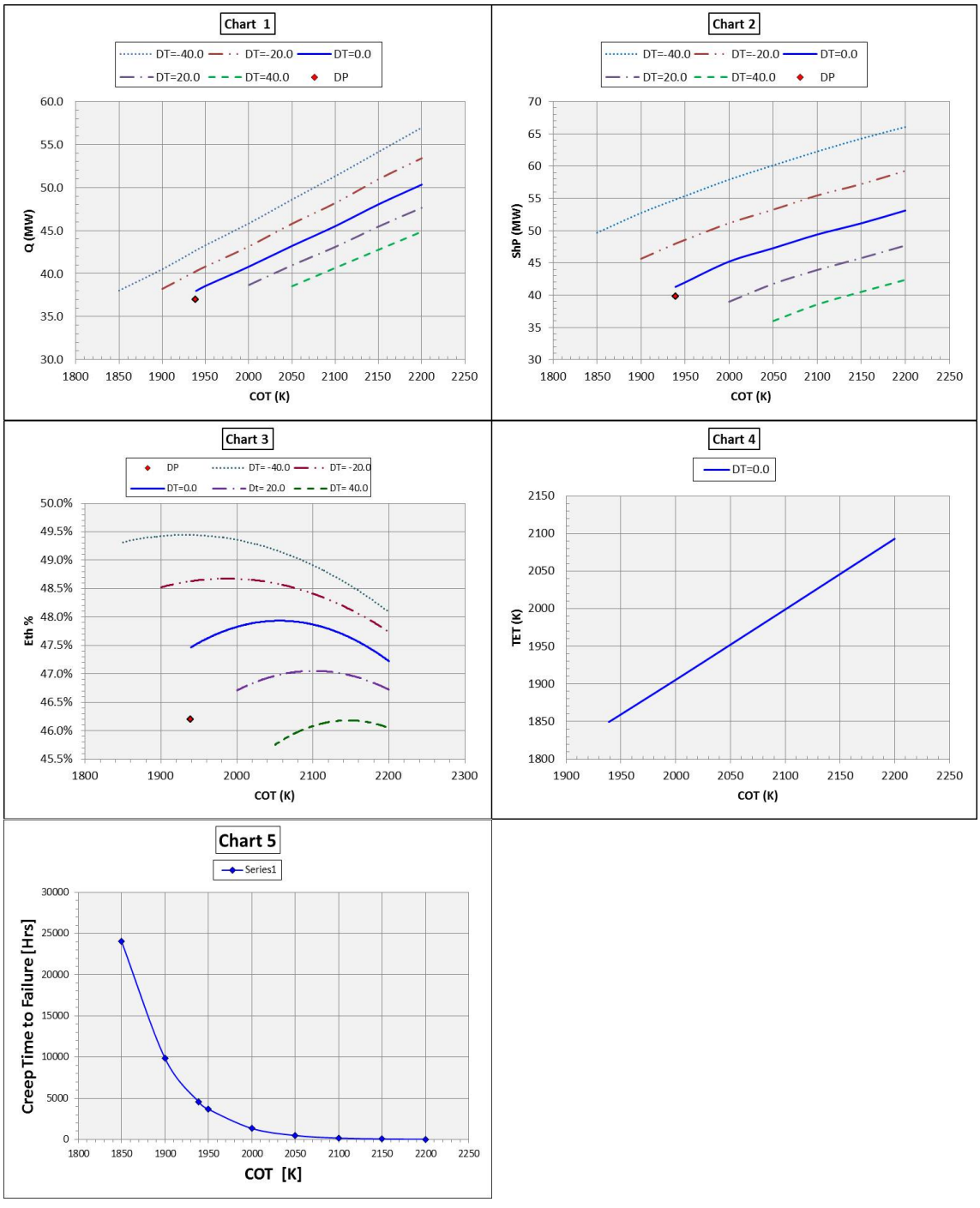

B.7 (SC) Two-Spool 3Shaft-[FPT] Engine

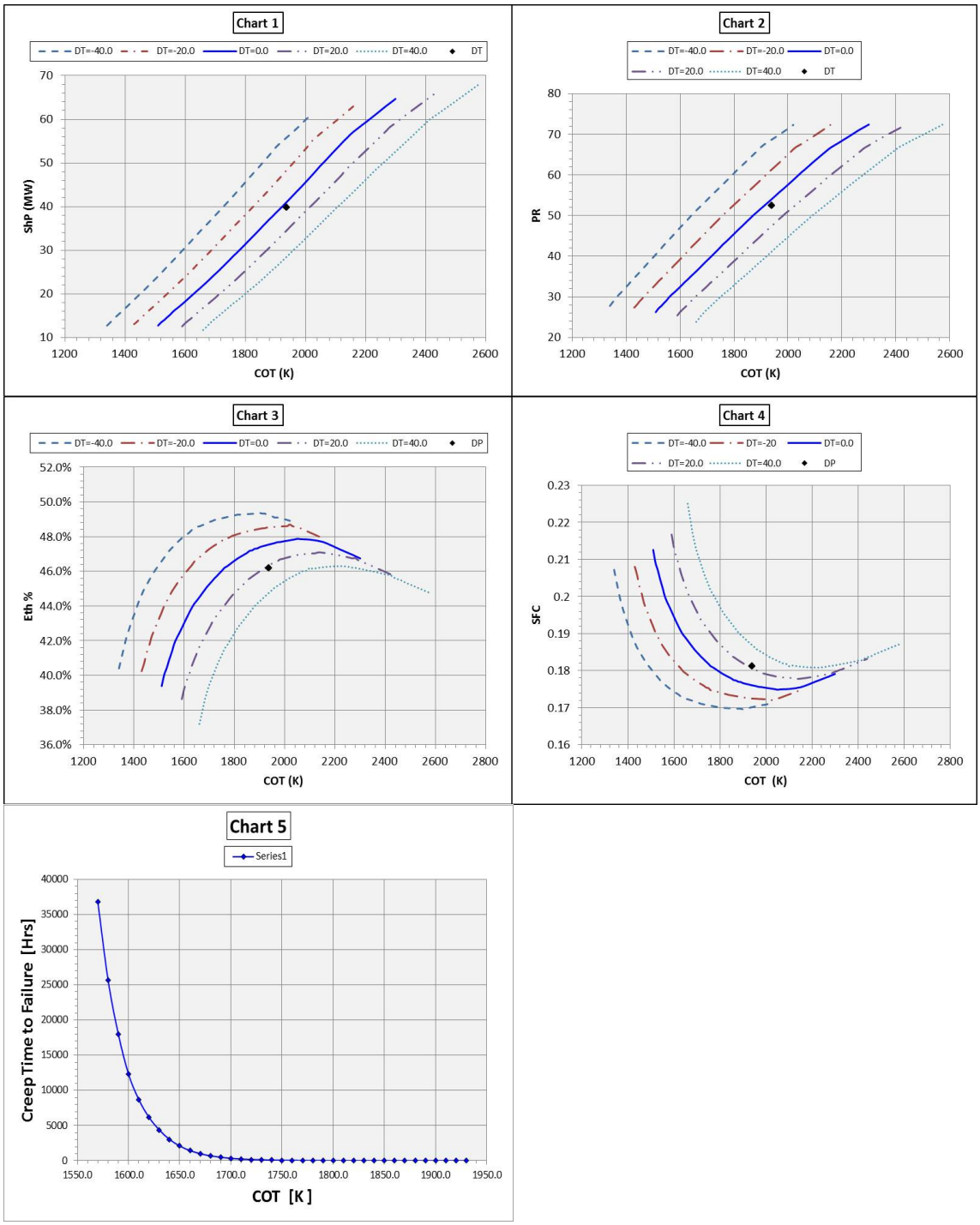

Performance Characteristic of Two-Spool [FPT] with [$PR_{lc} = 2.0$]

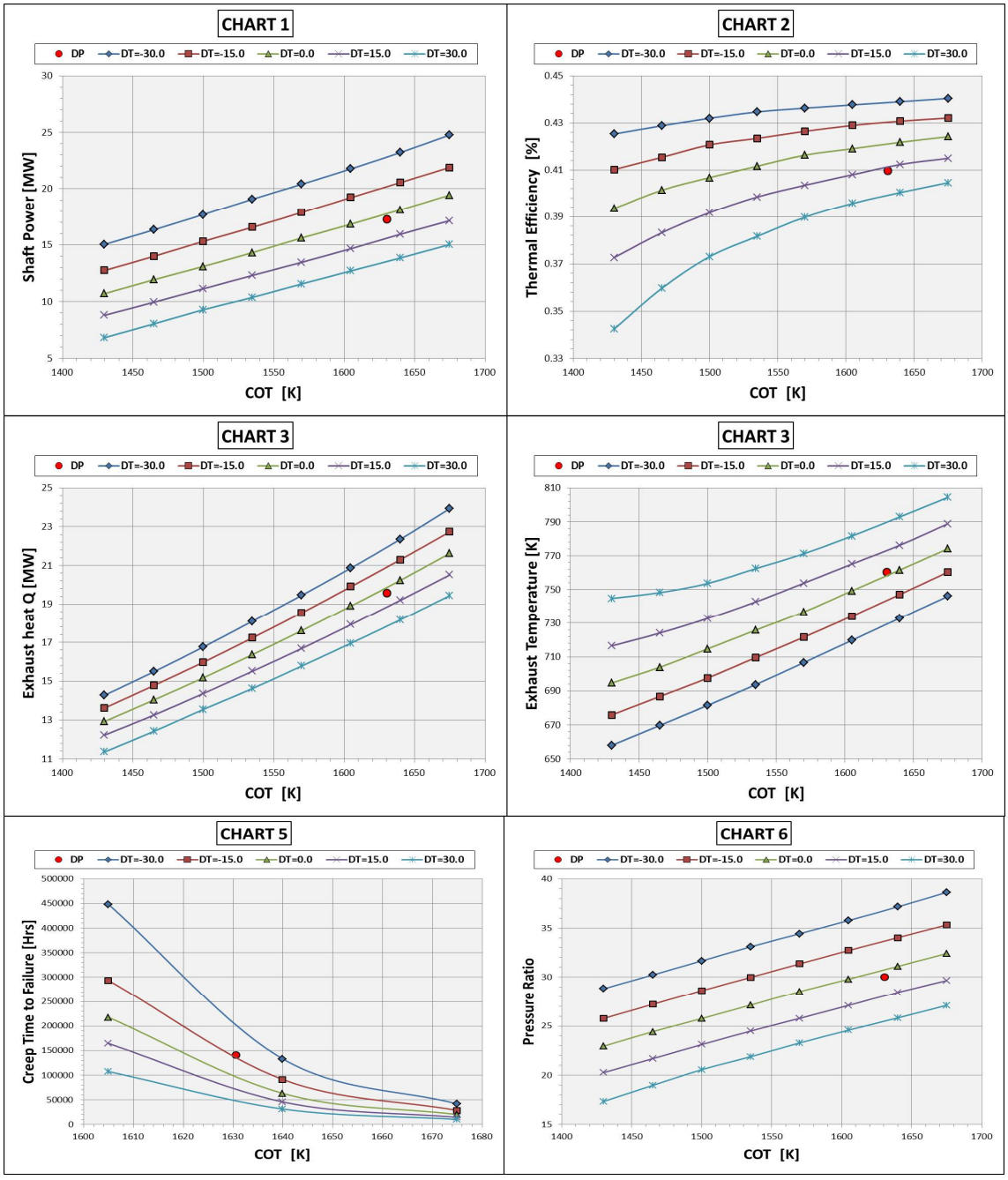

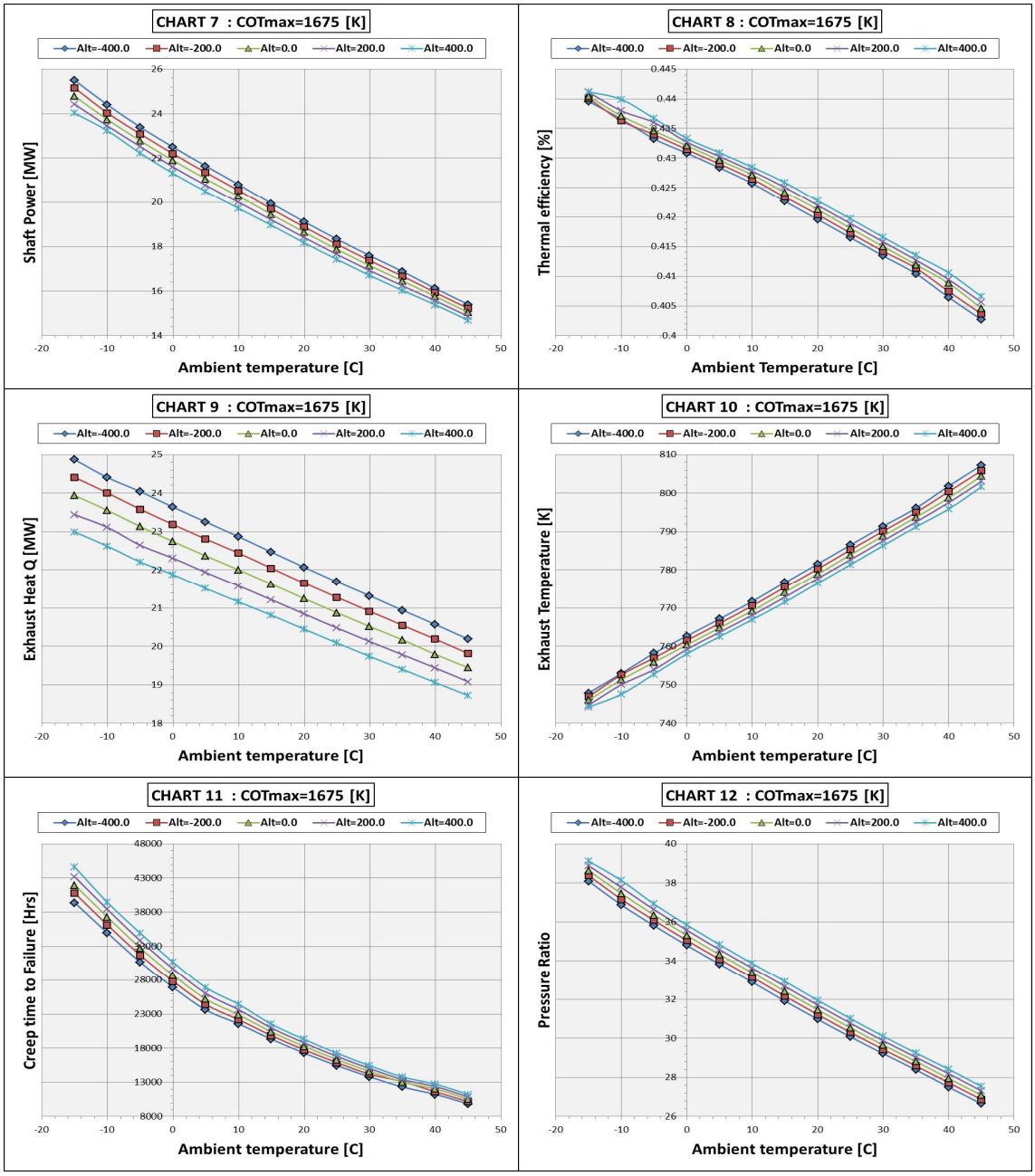
CHART 7 : COTmax=1675 [K]
Alt=-400.0
Alt=-200.0
Alt=0.0
Alt=200.0
Alt=400.0
Shaft Power [MW]
Ambient temperature [C]
CHART 8 : COTmax=1675 [K]
Thermal efficiency [%]
Ambient Temperature [C]
CHART 9 : COTmax=1675 [K]
Exhaust Heat Q [MW]
Ambient temperature [C]
CHART 10 : COTmax=1675 [K]
Exhaust Temperature [K]
Ambient temperature [C]
CHART 11 : COTmax=1675 [K]
Creep time to Failure [Hrs]
Ambient temperature [C]
CHART 12 : COTmax=1675 [K]
Pressure Ratio
Ambient temperature [C]

B.8 (I/C) Two-Spool 3Shaft-[FPT] Engine

[A]: COT=1387.63 [K]

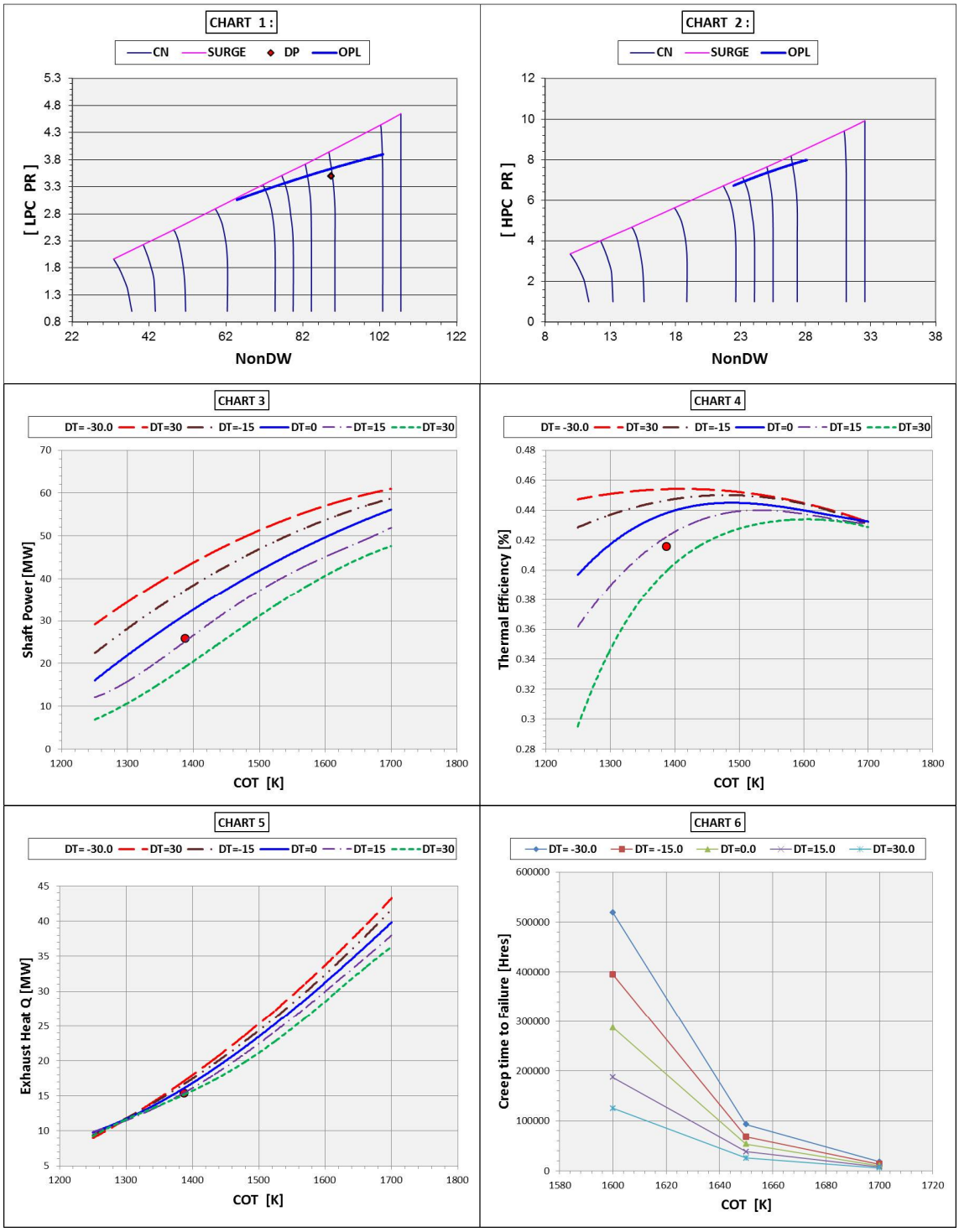

[B]: COT=1630.72 [K]

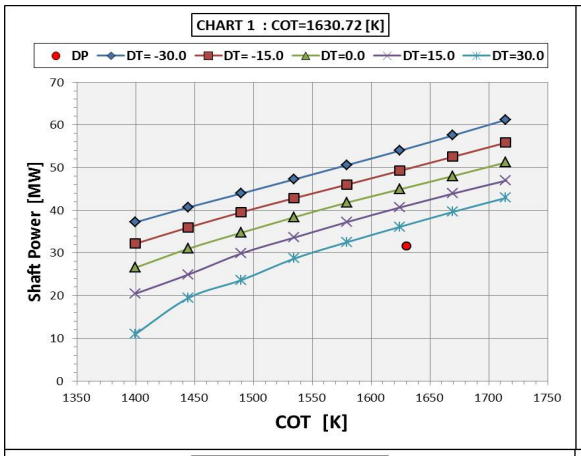

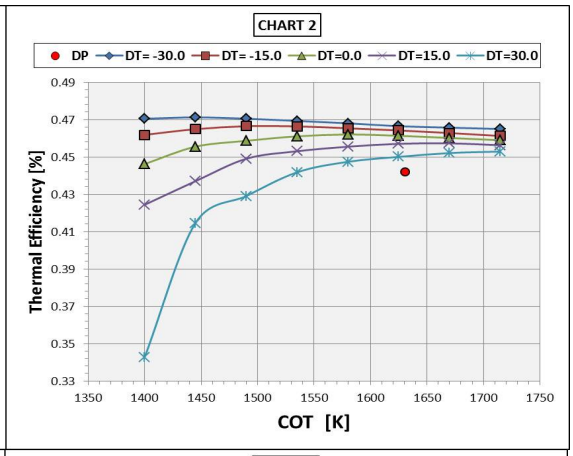

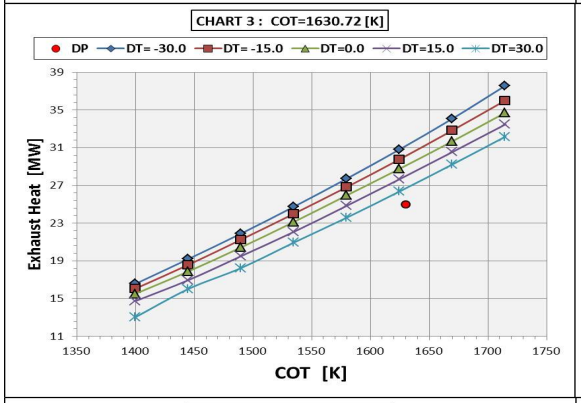

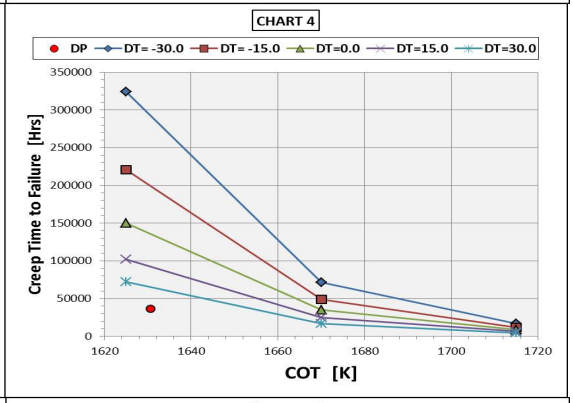

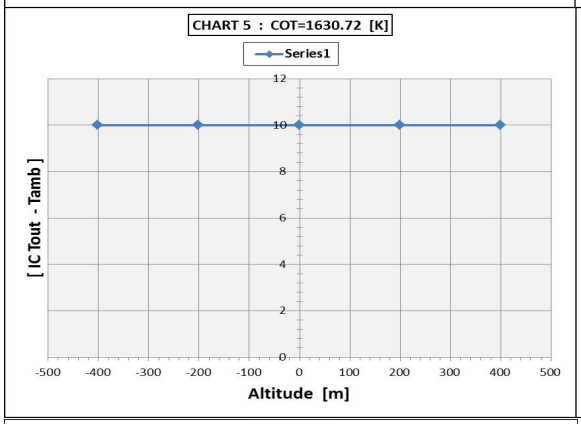

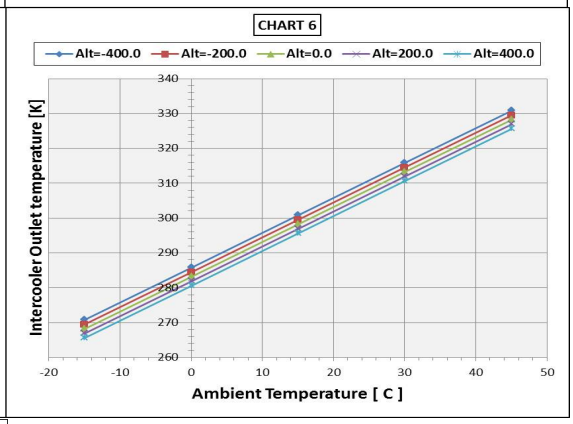

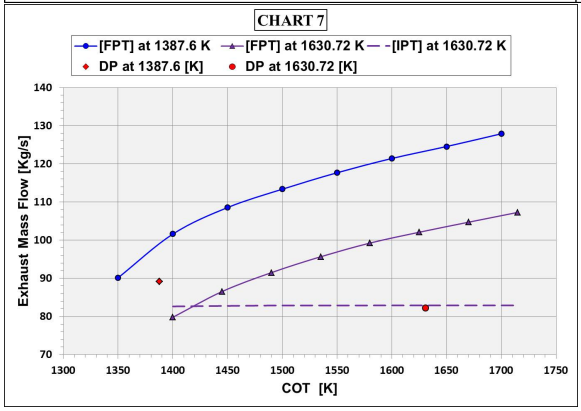

B.9 (I/C) Two-Spool 2Shaft-[IPT] Engine

COT=1630.72 [K]

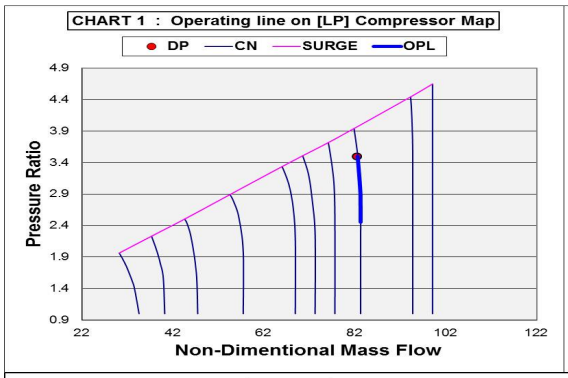

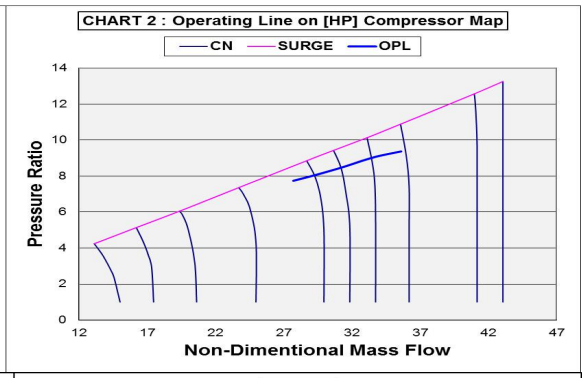

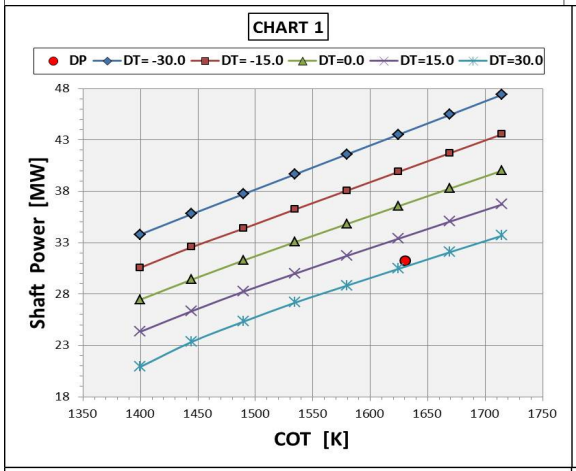

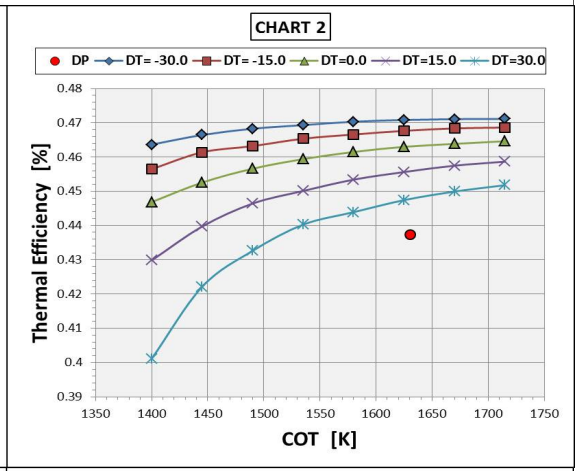

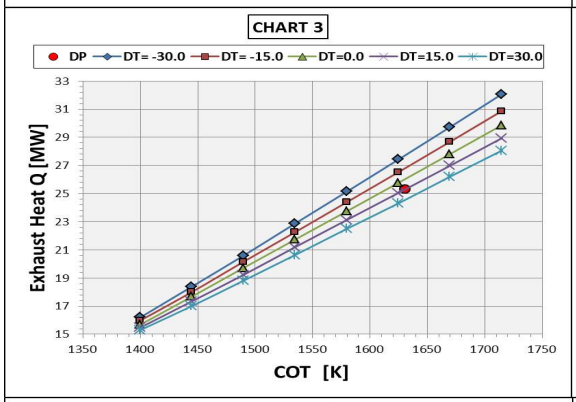

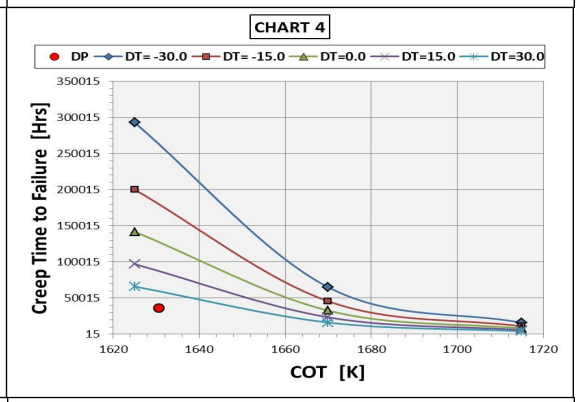

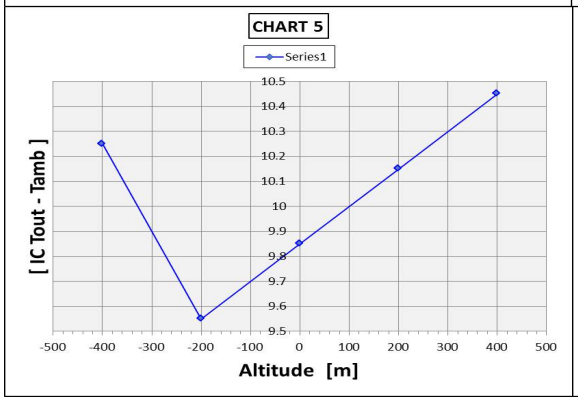

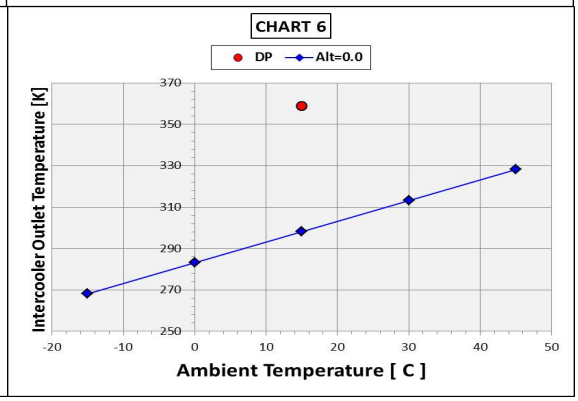

B.10 (HEC) Two-Spool 3Shaft (Conv)-[FPT]

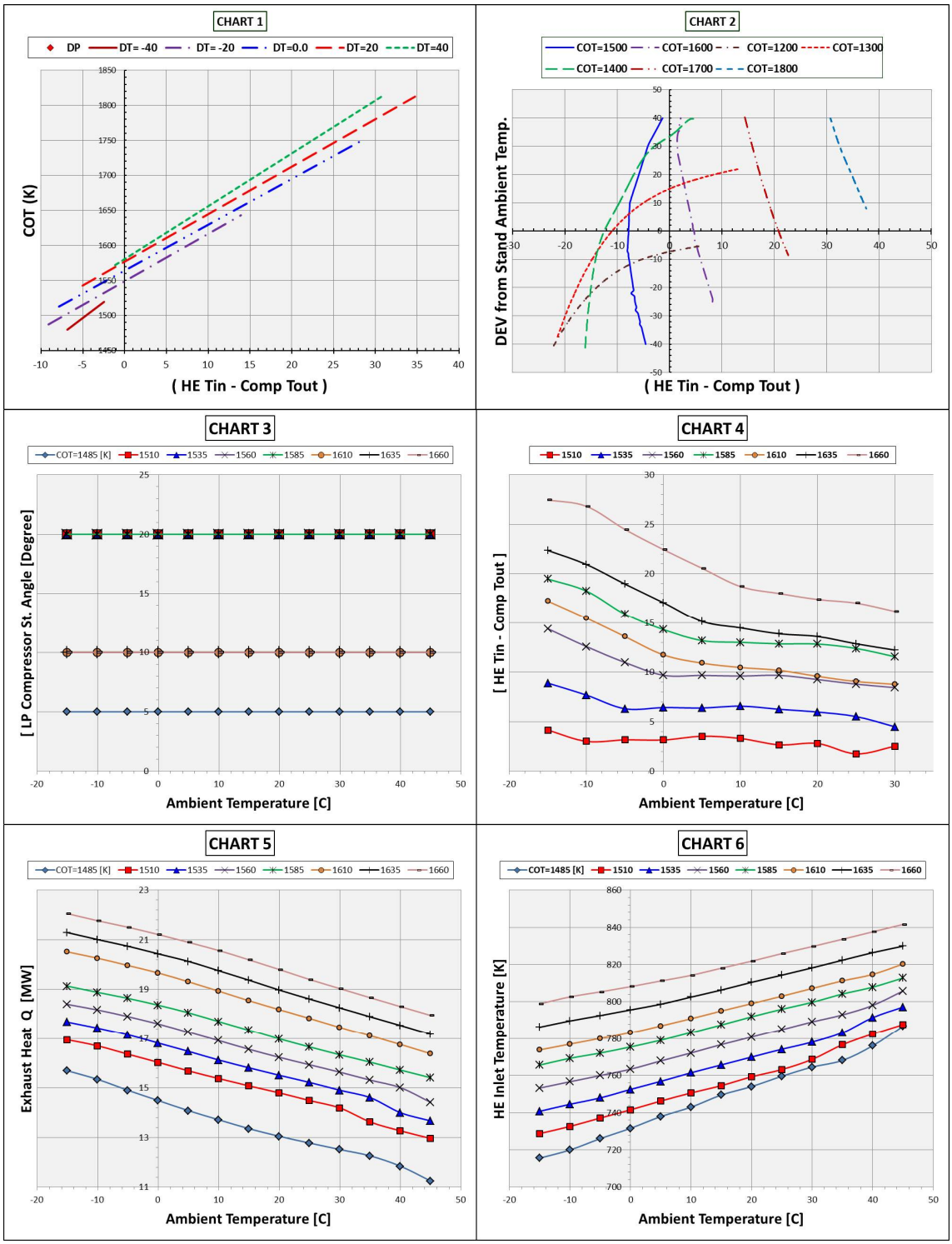

B.11 (HEC) Two-Spool 3Shaft (non-Conv)-[FPT]

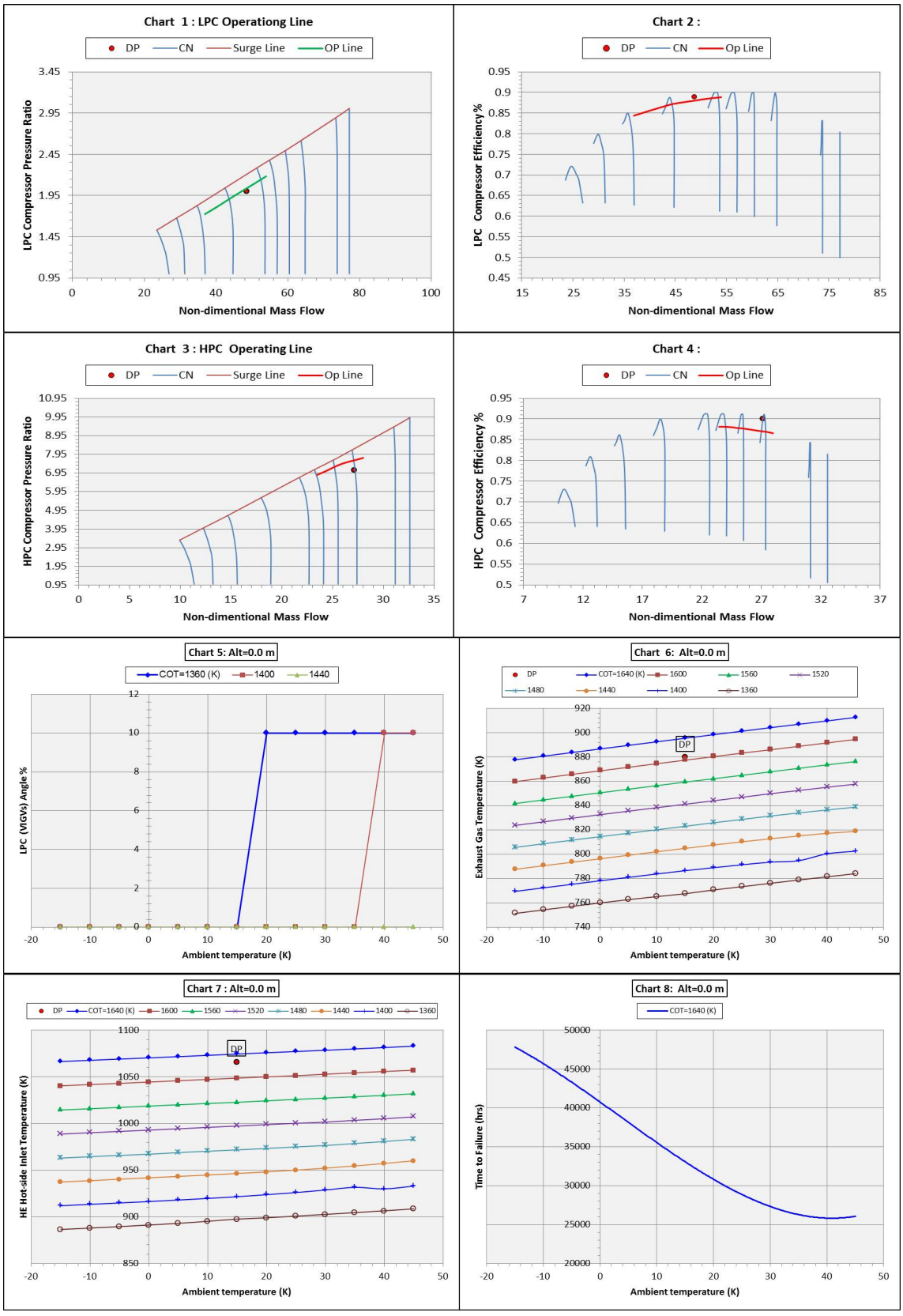

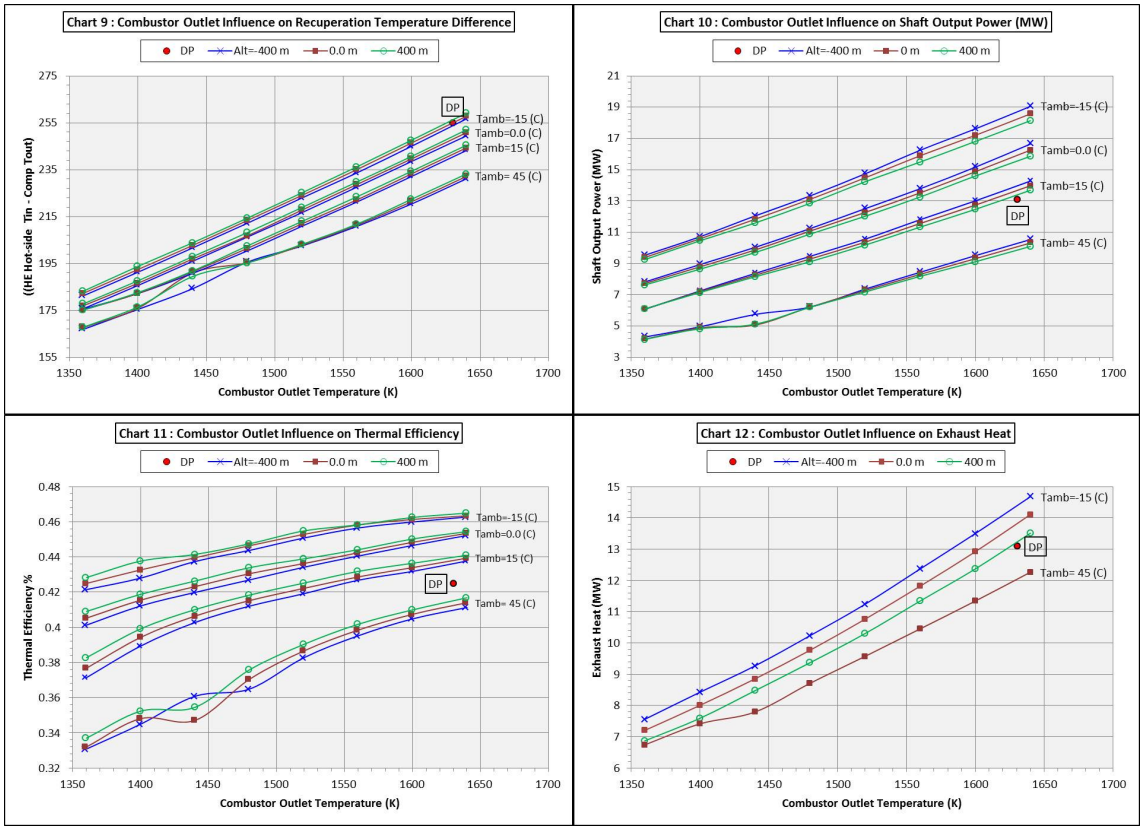
Chart 9 : Combustor Outlet Influence on Recuperation Temperature Difference
DP
Alt=-400 m
0.0 m
400 m
(HE Hot-side Tin - Comp Tout)
Combustor Outlet Temperature (K)
Tamb=-15 (C)
Tamb=0.0 (C)
Tamb=15 (C)
Tamb= 45 (C)
Chart 10 : Combustor Outlet Influence on Shaft Output Power (MW)
Shaft Output Power (MW)
Chart 11 : Combustor Outlet Influence on Thermal Efficiency
Thermal Efficiency %
Chart 12 : Combustor Outlet Influence on Exhaust Heat
Exhaust Heat (MW)

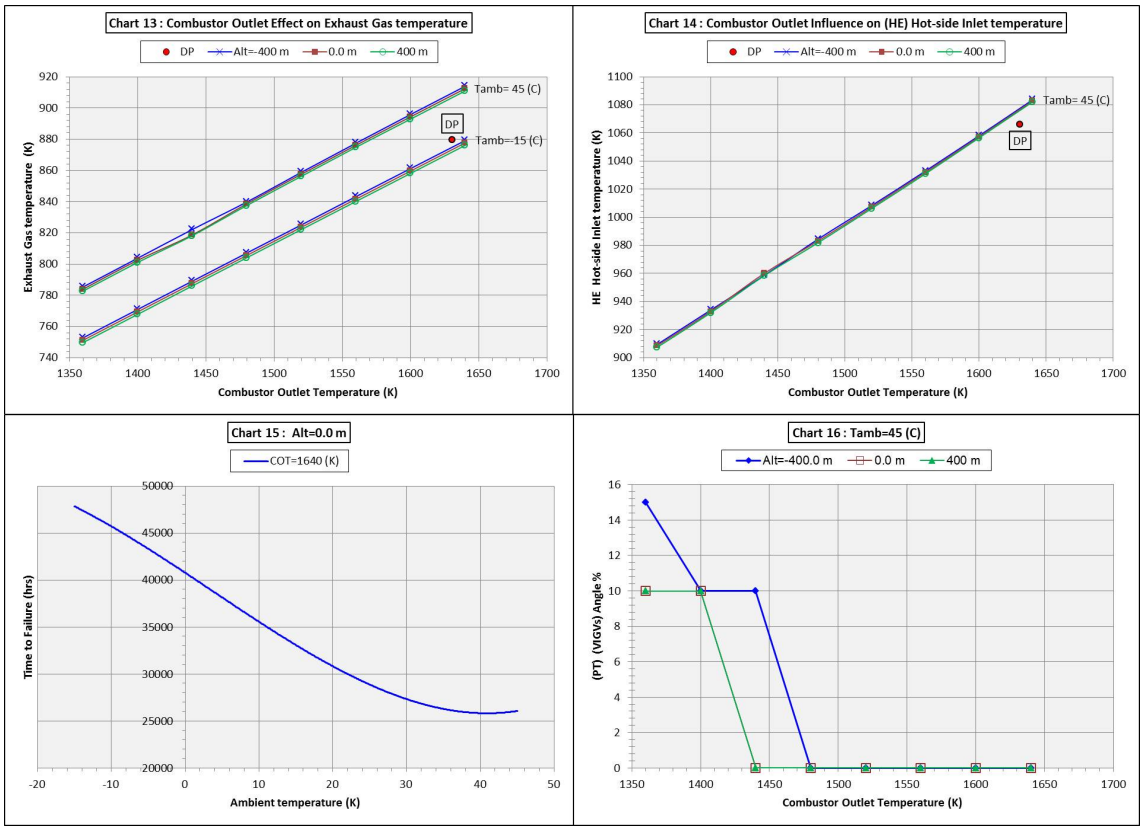
Chart 13 : Combustor Outlet Effect on Exhaust Gas temperature
Exhaust Gas temperature (K)
Chart 14 : Combustor Outlet Influence on (HE) Hot-side Inlet temperature
HE Hot-side Inlet temperature (K)
Chart 15 : Alt=0.0 m
COT=1640 (K)
Time to Failure (hrs)
Ambient temperature (K)
Chart 16 : Tamb=45 (C)
Alt=-400.0 m
(PT) (VIGVs) Angle %

B.12 (ICR) Two-Spool 2Shaft (Conv) [IPT]

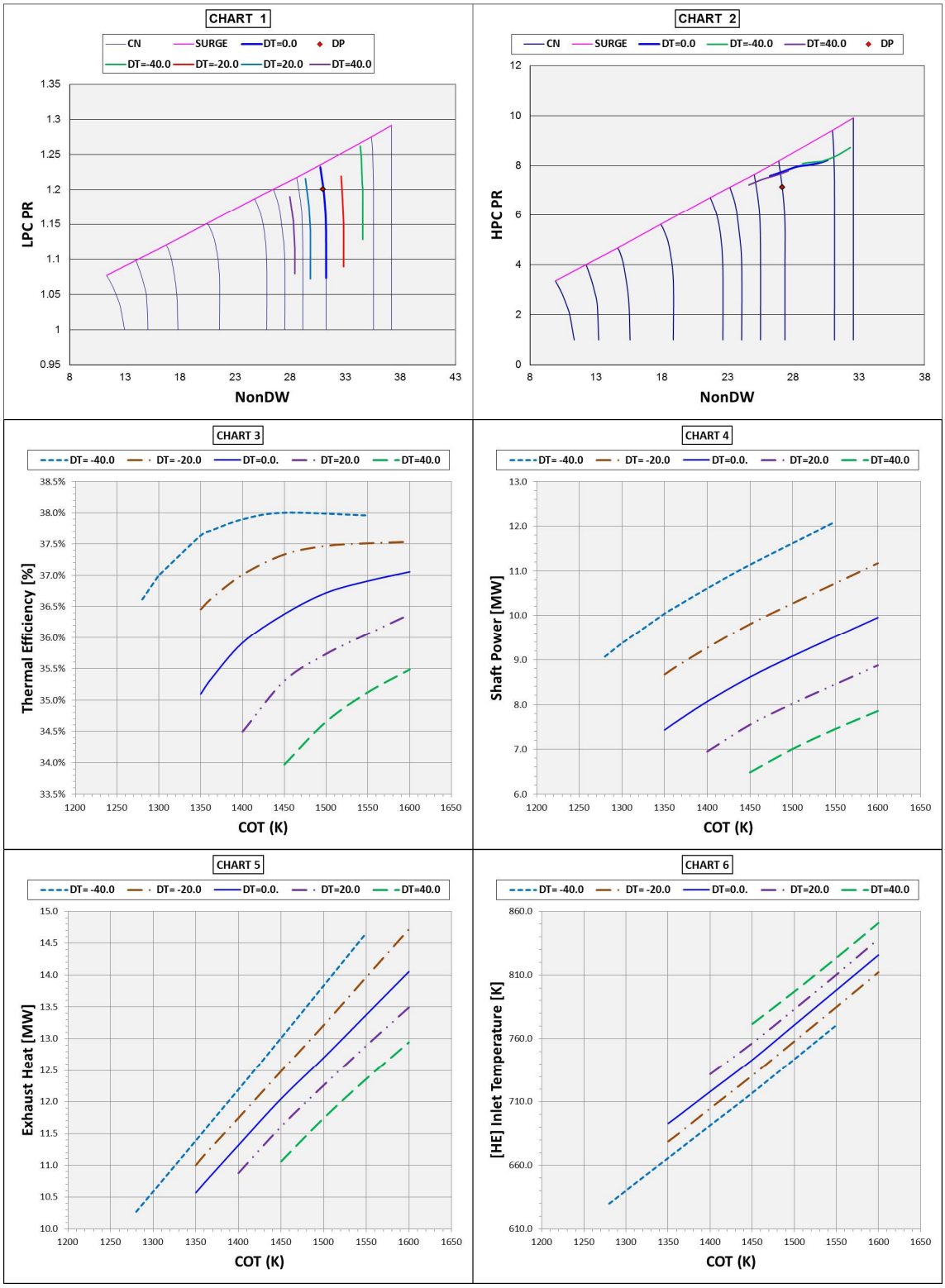

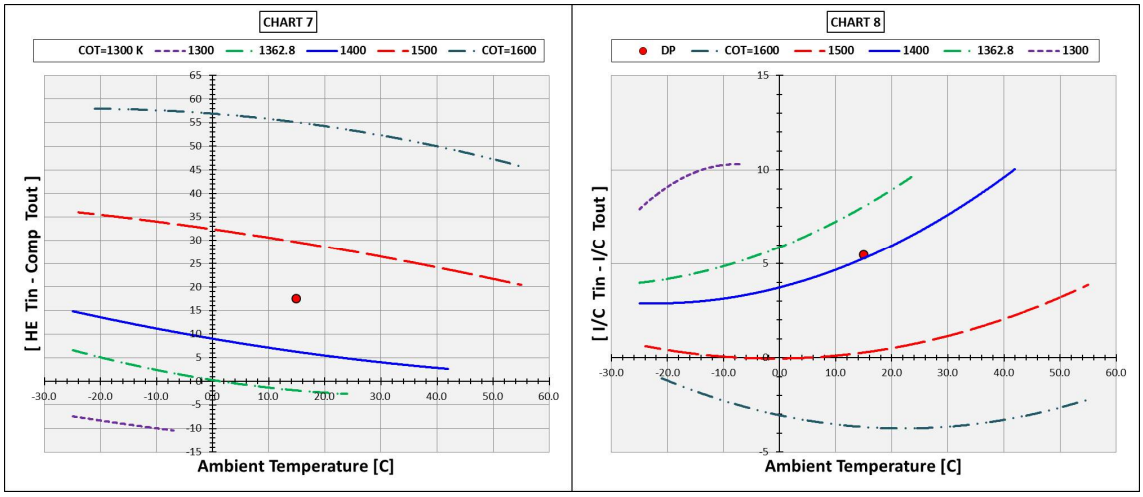

B.13 (ICR) Two-Spool 3Shaft (Conv) [FPT]

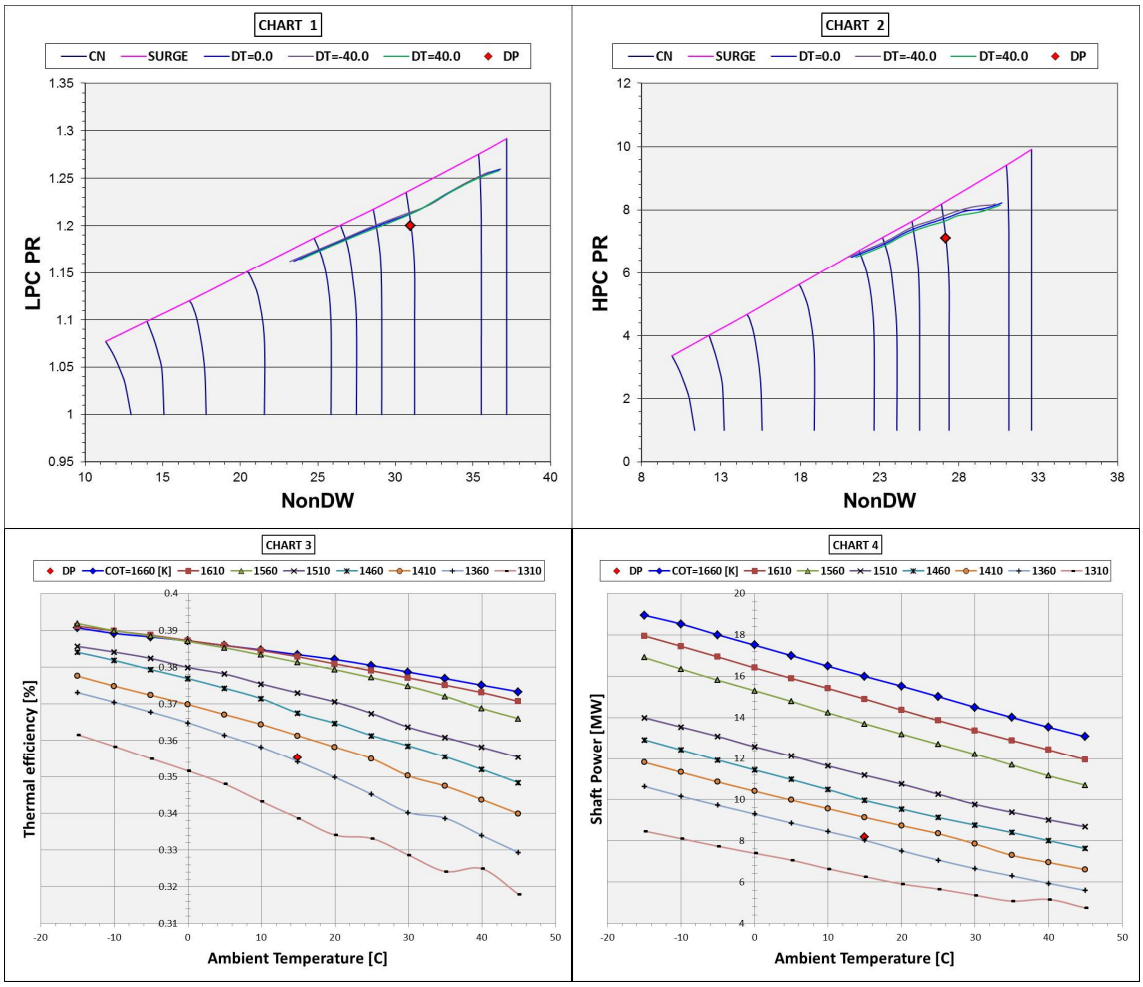

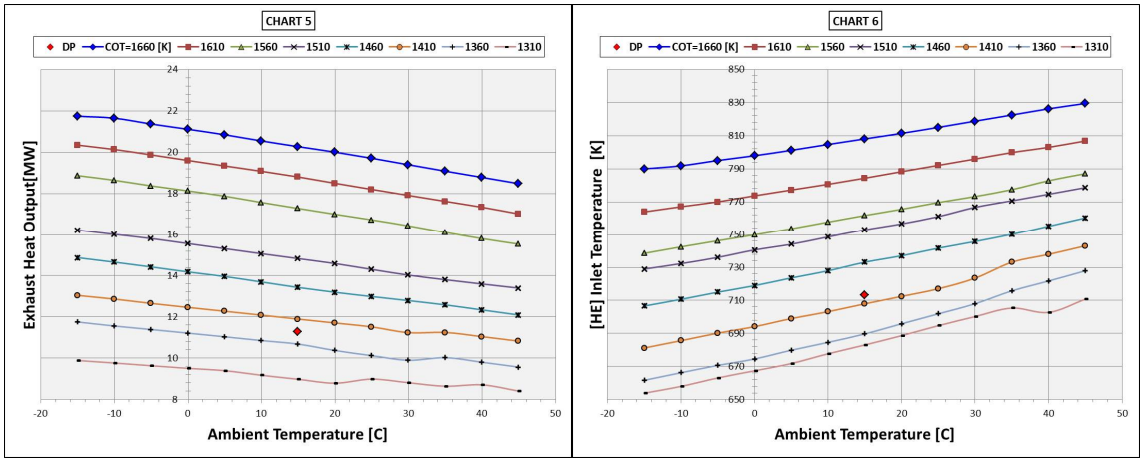

B.14 (ICR) Two-Spool 3Shaft (non-Conv) [FPT]

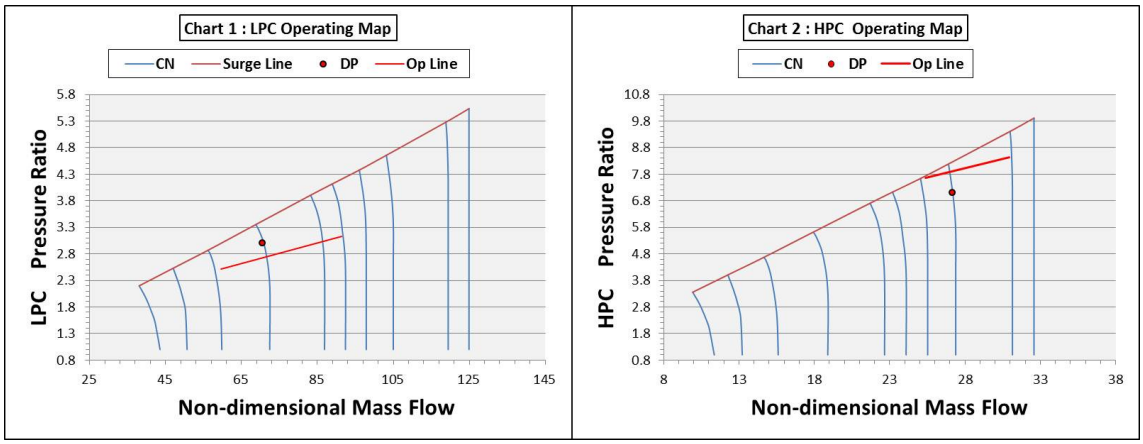

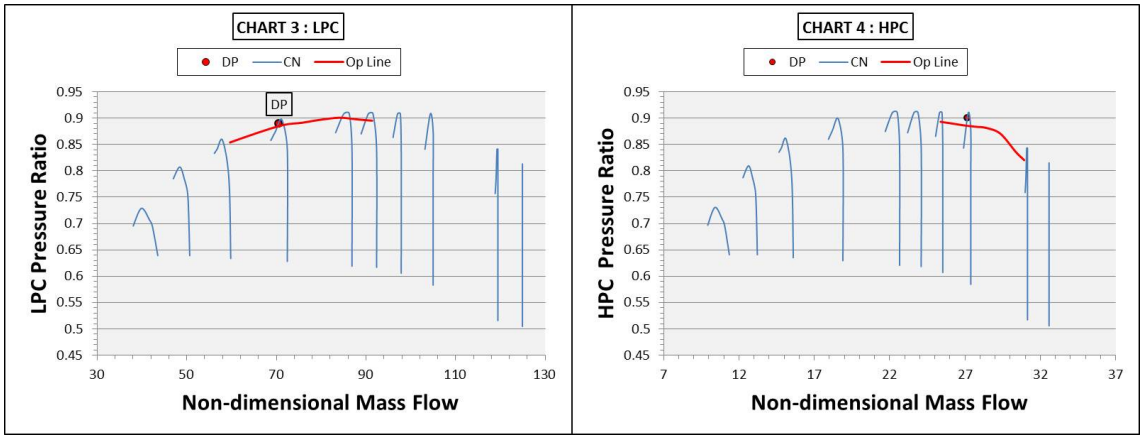

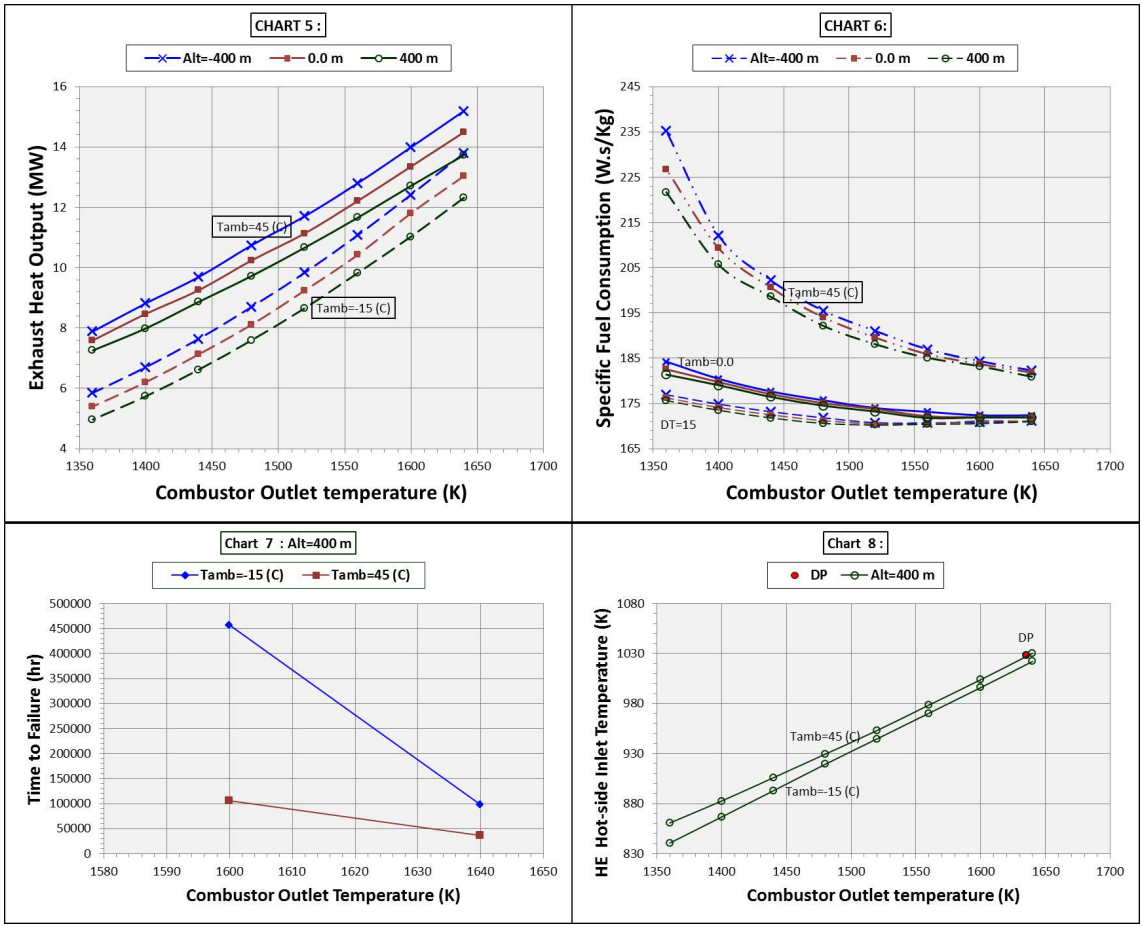

B.15 (SC) Two-Spool 3Shaft-[FPT] Direct Derivation

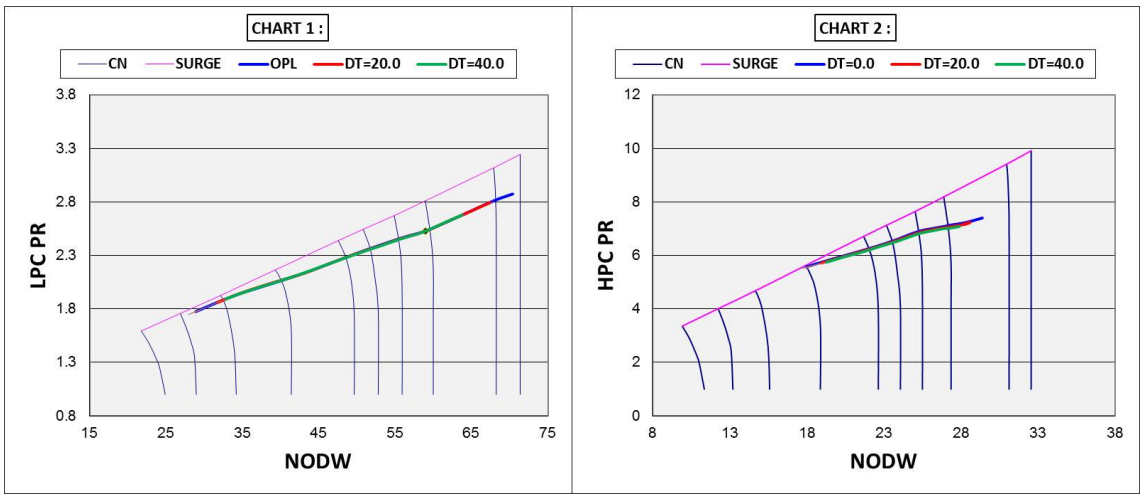

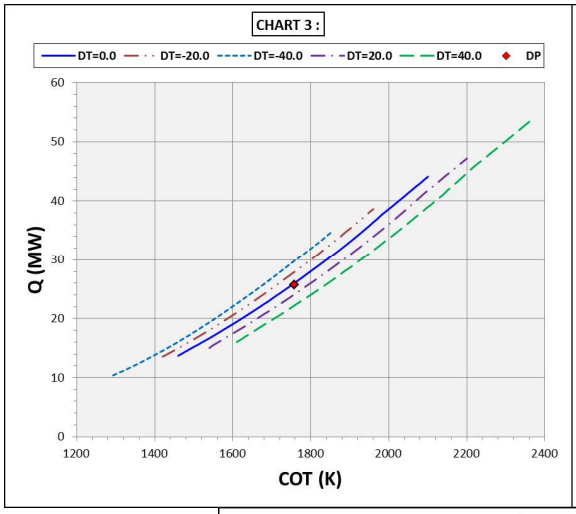
CHART 3 :
DT=0.0
DT=-20.0
DT=-40.0
DT=20.0
DT=40.0
DP
Q (MW)
COT (K)

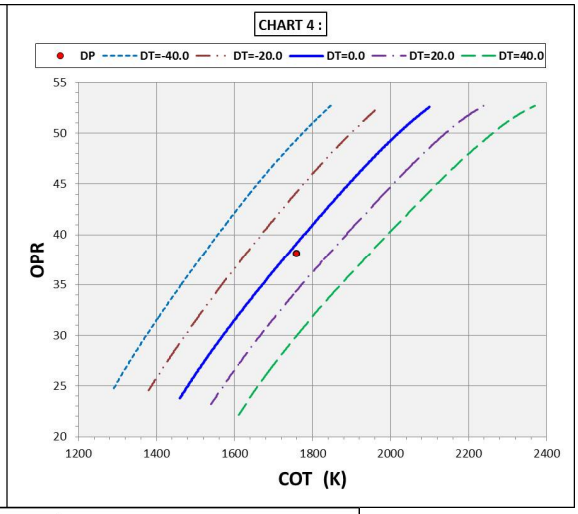
CHART 4 :
DP
DT=-40.0
DT=-20.0
DT=0.0
DT=20.0
DT=40.0
OPR
COT (K)

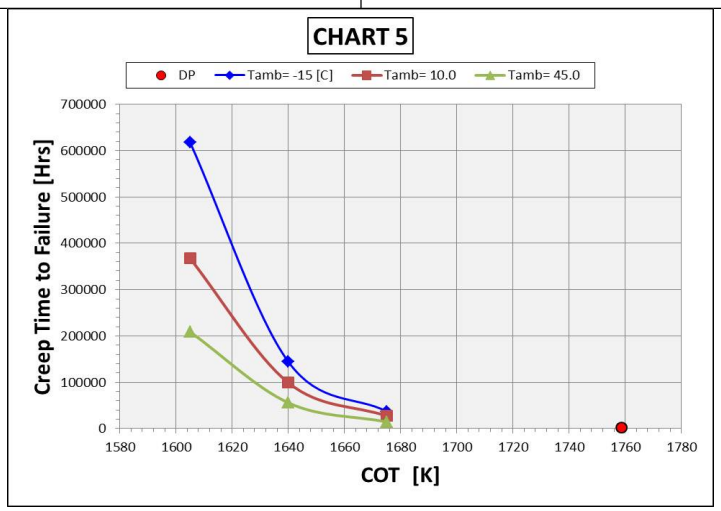
CHART 5
DP
Tamb= -15 [C]
Tamb= 10.0
Tamb= 45.0
Creep Time to Failure [Hrs]
COT [K]

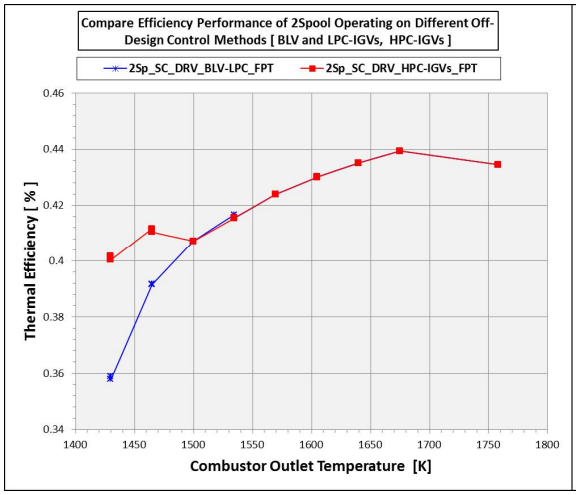
Compare Efficiency Performance of 2Spool Operating on Different Off-Design Control Methods [BLV and LPC-IGVs, HPC-IGVs]
2Sp_SC_DRV_BLV-LPC_FPT
2Sp_SC_DRV_HPC-IGVs_FPT
Thermal Efficiency [%]
Combustor Outlet Temperature [K]

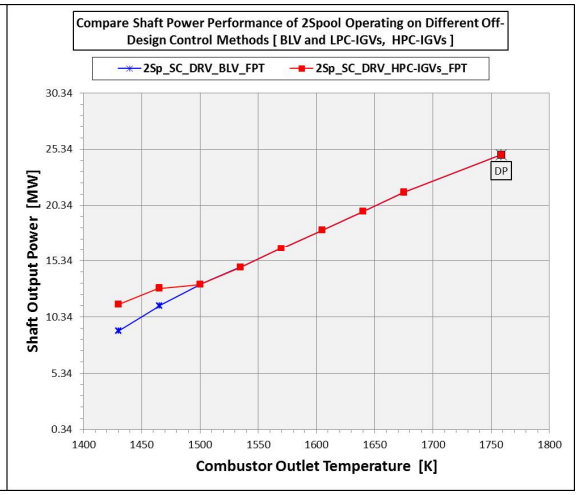
Compare Shaft Power Performance of 2Spool Operating on Different Off-Design Control Methods [BLV and LPC-IGVs, HPC-IGVs]
2Sp_SC_DRV_BLV_FPT
2Sp_SC_DRV_HPC-IGVs_FPT
Shaft Output Power [MW]
DP
Combustor Outlet Temperature [K]

B.16 (SC) Three-Spool [IPT]

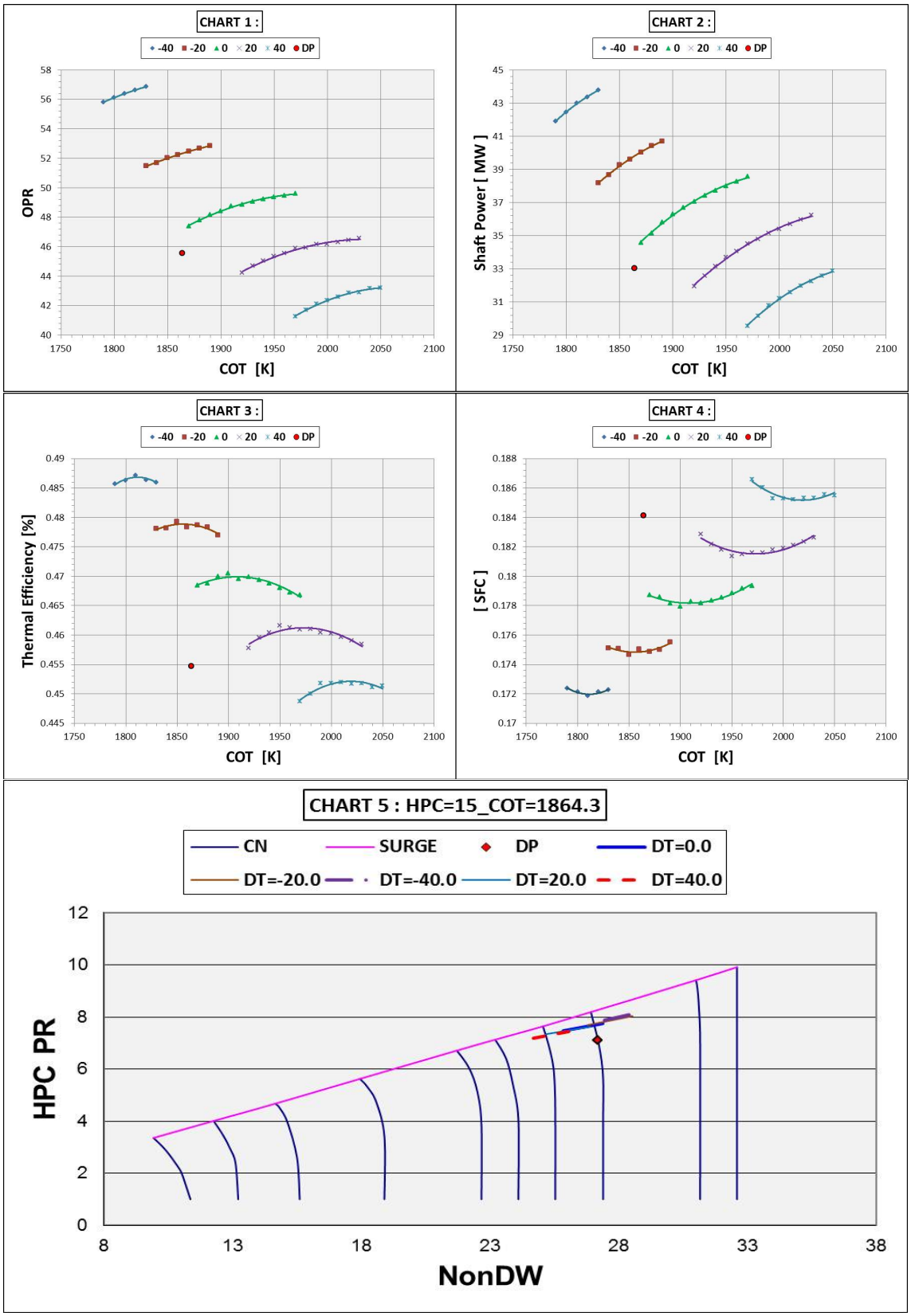

B.17 (I/C) Three-Spool [IPT]

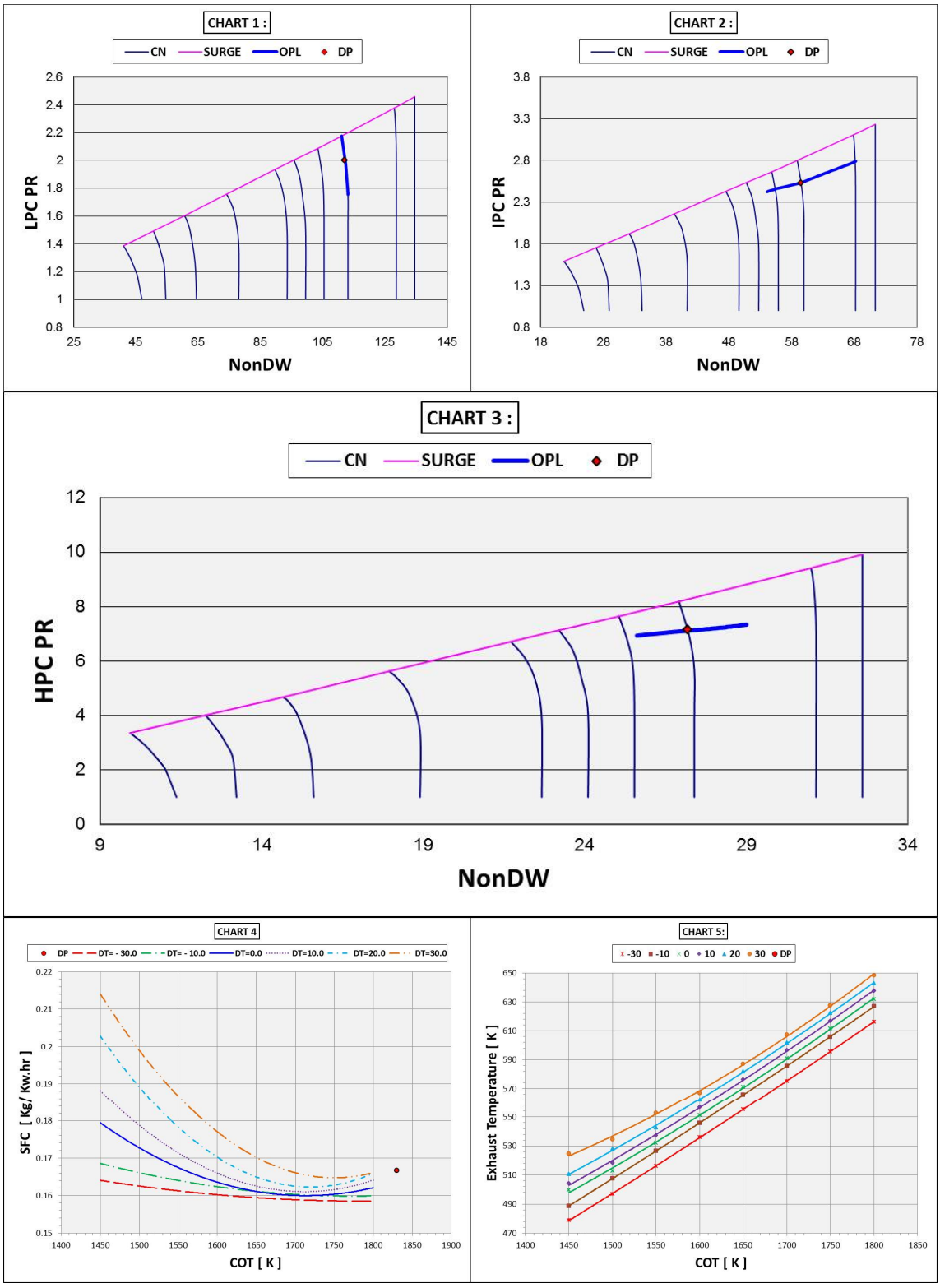

Appendix C GT Assessment on [PG] Application

C.1 Energy and Power Demand

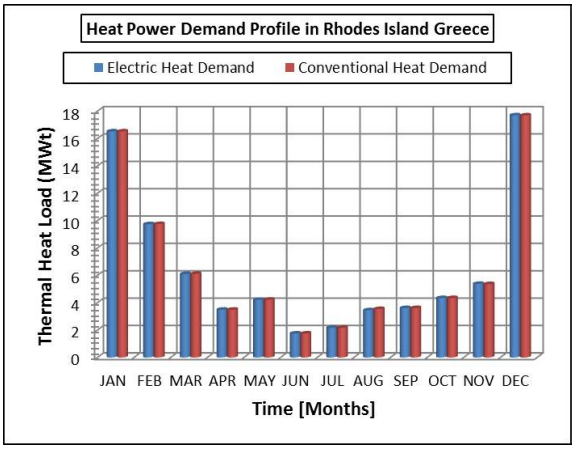

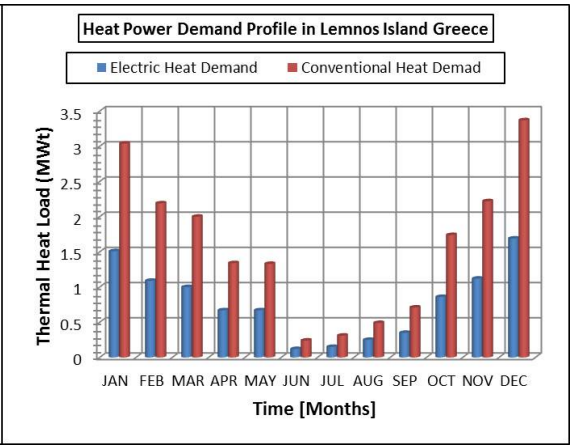

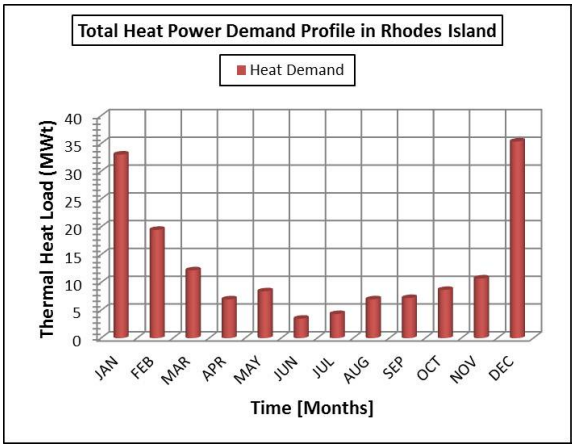

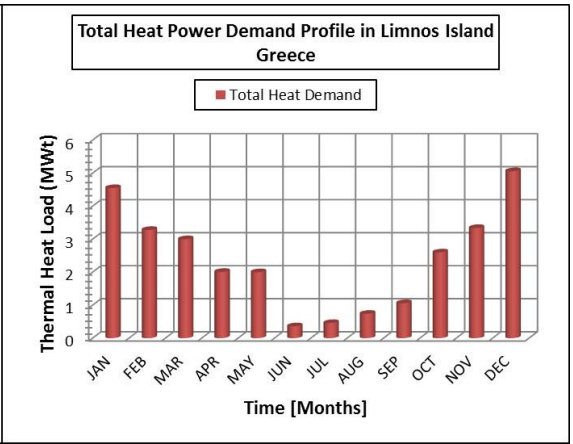

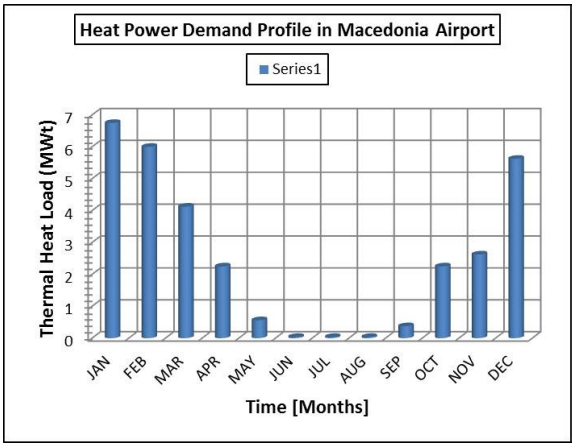

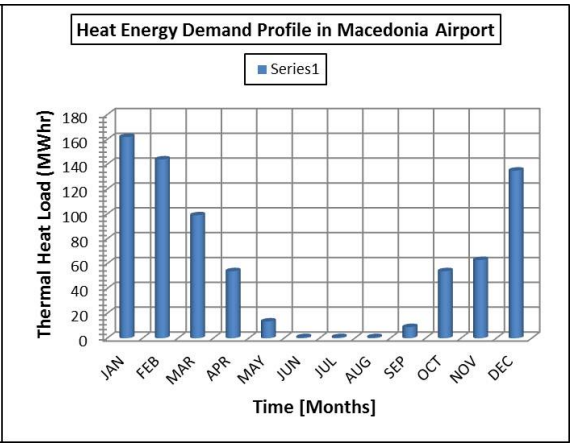

C.2 Different GT Engine Scenarios for Optimization

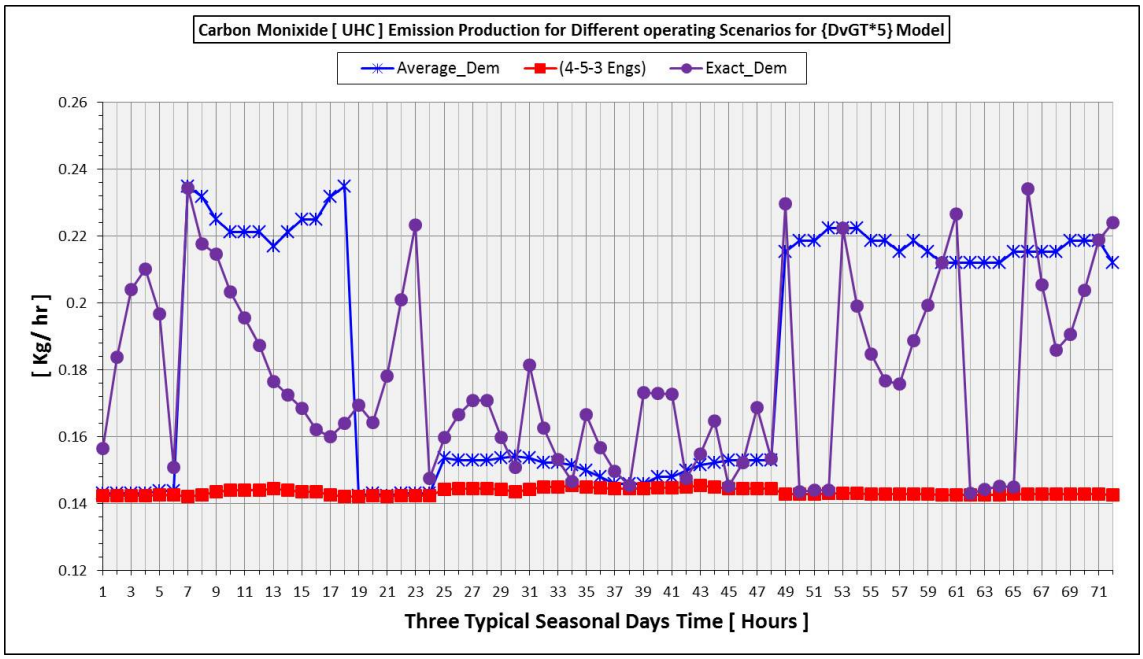

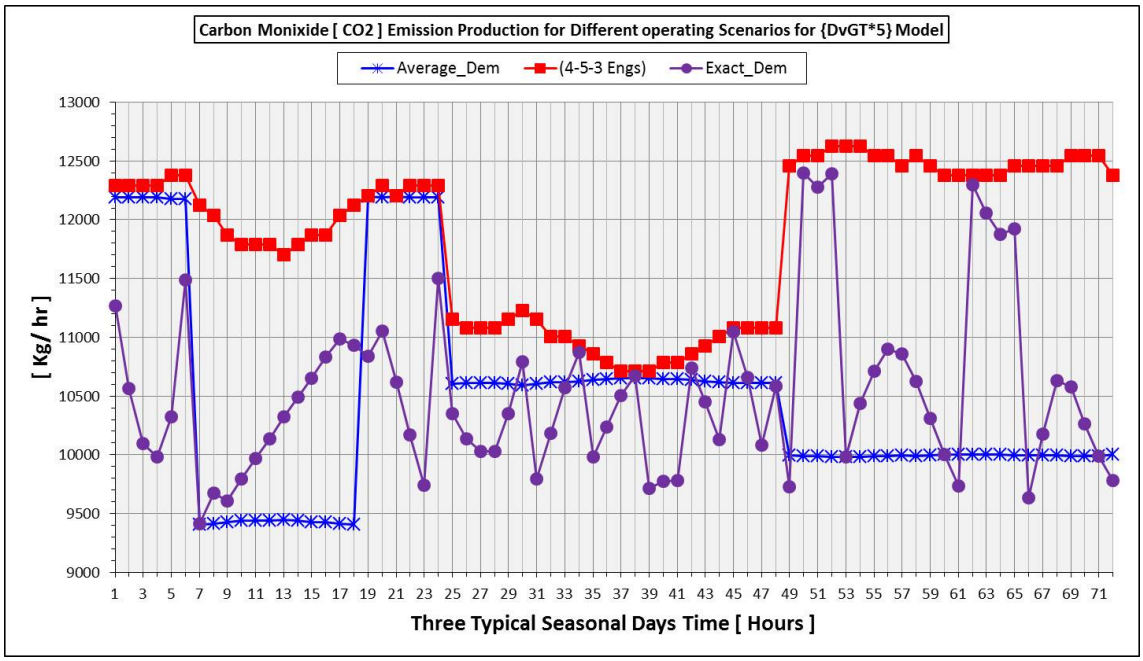

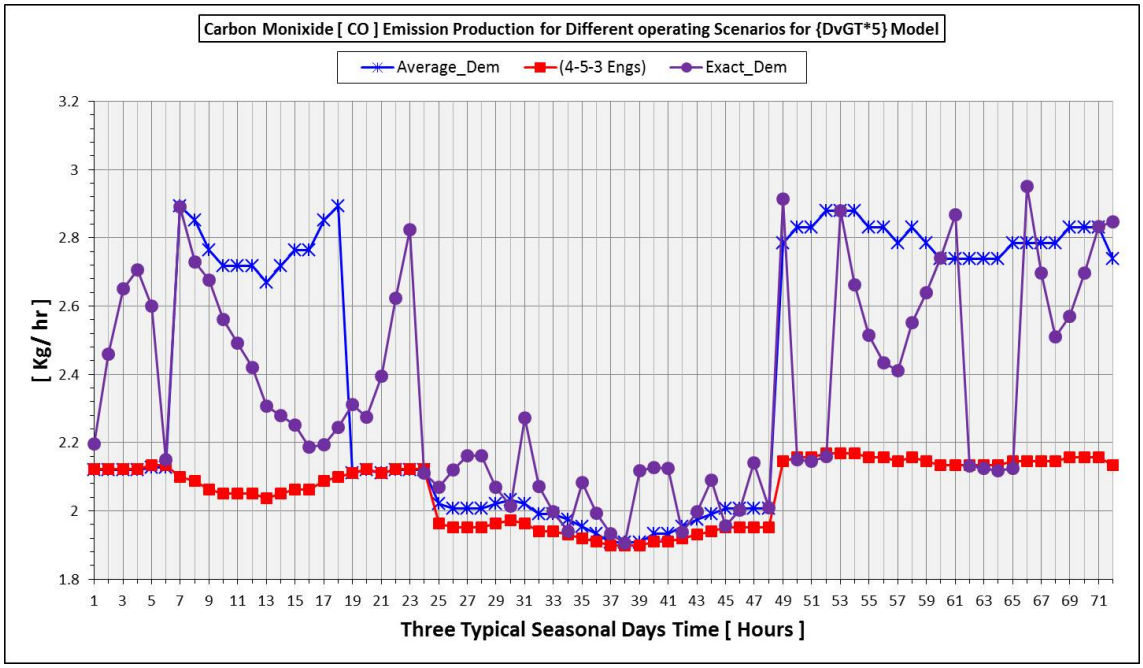

C.3 Different GT Engine Scenarios for Optimization

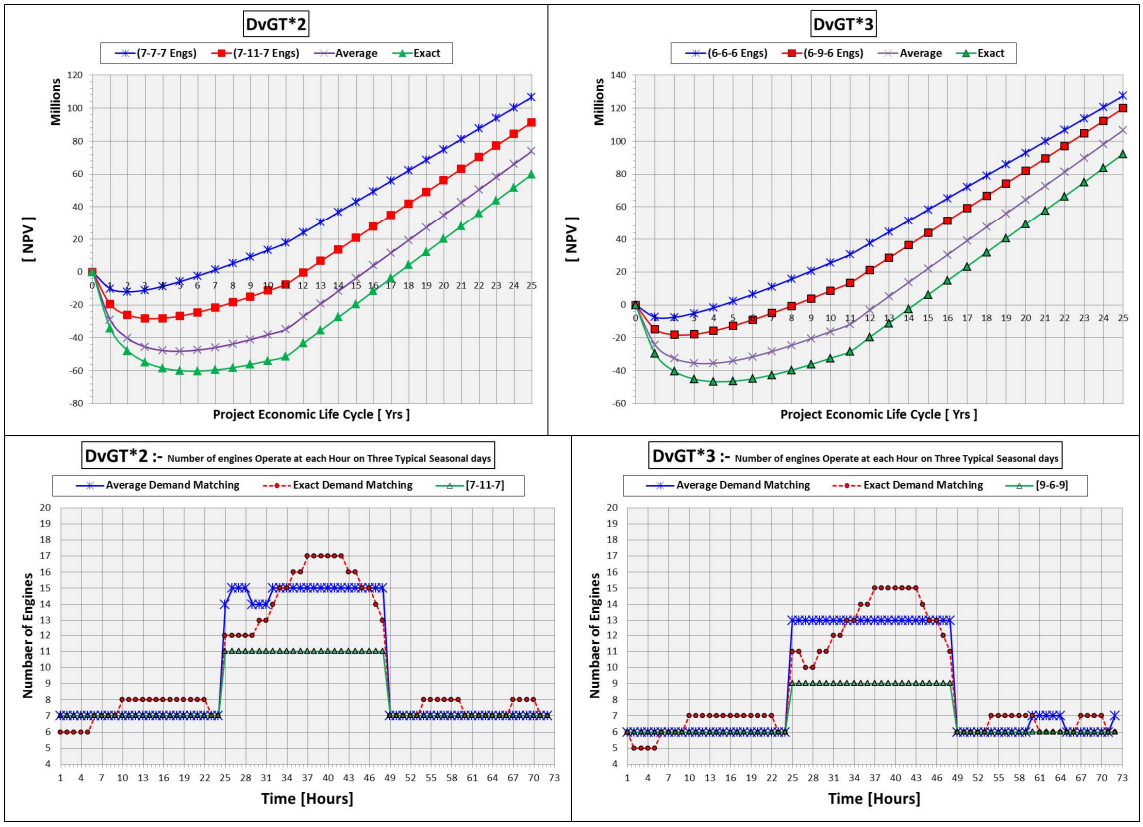

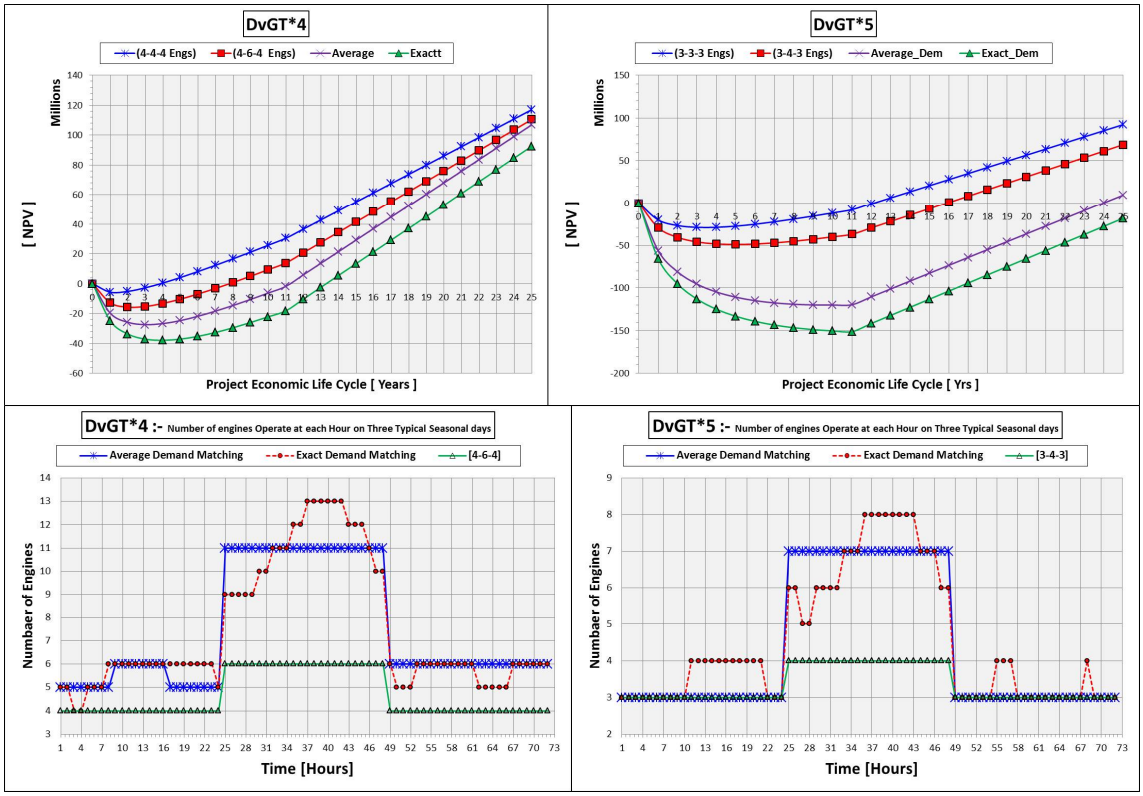
DvGT*4
(4-4-4 Engs)
(4-6-4 Engs)
Average
Exactt
Millions
[NPV]
Project Economic Life Cycle [Years]
DvGT*5
(3-3-3 Engs)
(3-4-3 Engs)
Average_Dem
Exact_Dem
Millions
[NPV]
Project Economic Life Cycle [Yrs]
DvGT*4 :- Number of engines Operate at each Hour on Three Typical Seasonal days
Average Demand Matching
Exact Demand Matching
[4-6-4]
Numbaer of Engines
Time [Hours]
DvGT*5 :- Number of engines Operate at each Hour on Three Typical Seasonal days
Average Demand Matching
Exact Demand Matching
[3-4-3]
Numbaer of Engines
Time [Hours]

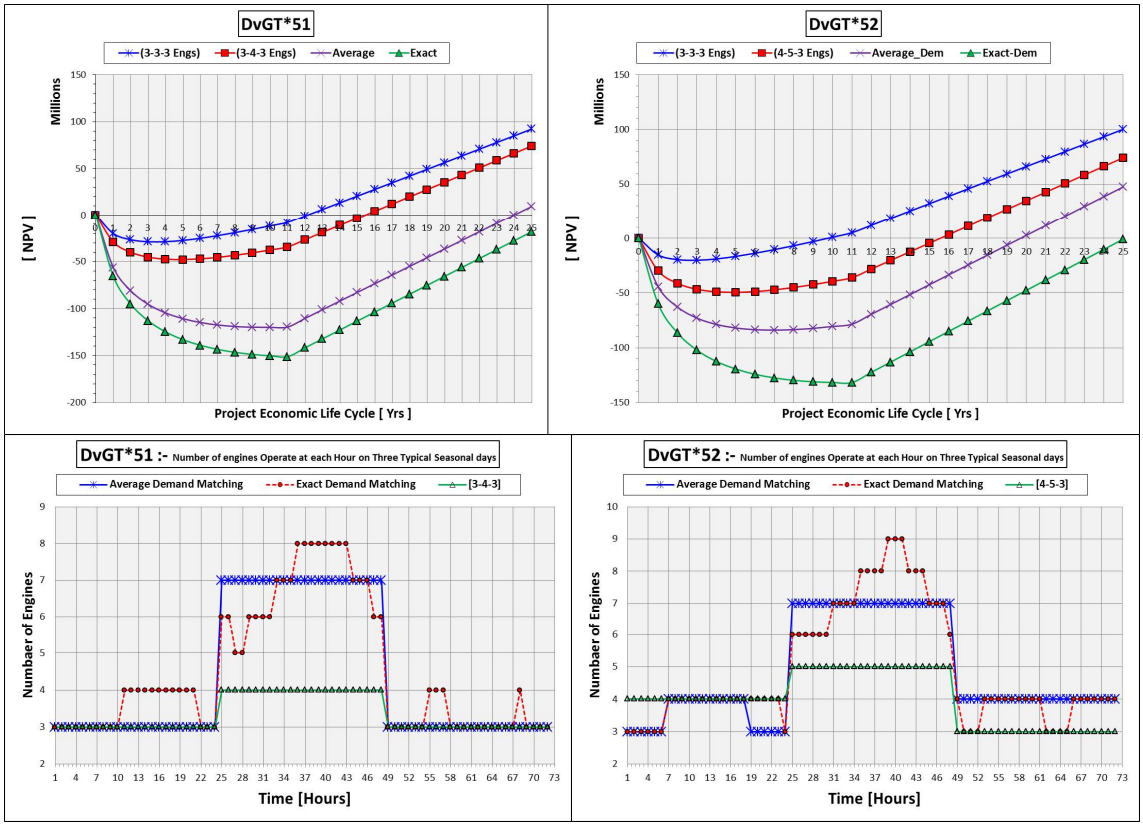
DvGT*51
(3-3-3 Engs)
(3-4-3 Engs)
Average
Exact
Millions
[NPV]
Project Economic Life Cycle [Yrs]
DvGT*52
(3-3-3 Engs)
(4-5-3 Engs)
Average_Dem
Exact-Dem
Millions
[NPV]
Project Economic Life Cycle [Yrs]
DvGT*51 :- Number of engines Operate at each Hour on Three Typical Seasonal days
Average Demand Matching
Exact Demand Matching
[3-4-3]
Numbaer of Engines
Time [Hours]
DvGT*52 :- Number of engines Operate at each Hour on Three Typical Seasonal days
Average Demand Matching
Exact Demand Matching
[4-5-3]
Numbaer of Engines
Time [Hours]

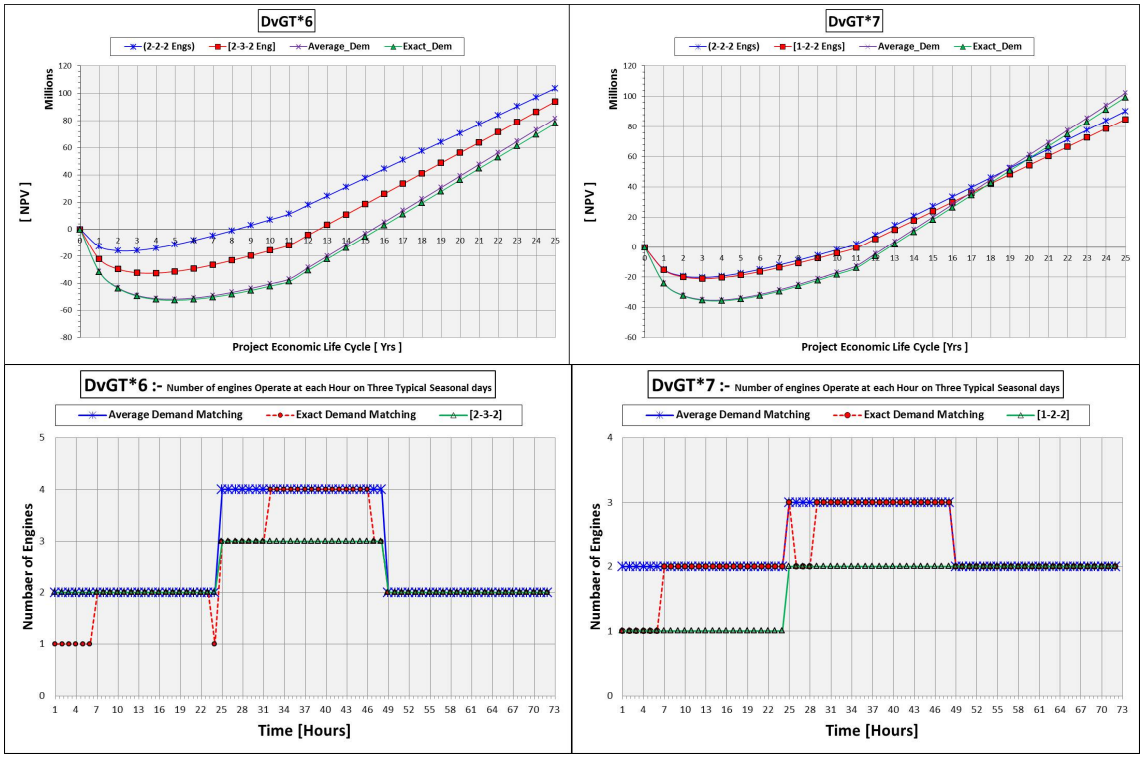
DvGT*6
(2-2-2 Engs)
[2-3-2 Eng]
Average_Dem
Exact_Dem
Millions
[NPV]
Project Economic Life Cycle [Yrs]
DvGT*7
(2-2-2 Engs)
[1-2-2 Engs]
Average_Dem
Exact_Dem
Millions
[NPV]
Project Economic Life Cycle [Yrs]
DvGT*6 :- Number of engines Operate at each Hour on Three Typical Seasonal days
Average Demand Matching
Exact Demand Matching
[2-3-2]
Numbaer of Engines
Time [Hours]
DvGT*7 :- Number of engines Operate at each Hour on Three Typical Seasonal days
Average Demand Matching
Exact Demand Matching
[1-2-2]
Numbaer of Engines
Time [Hours]

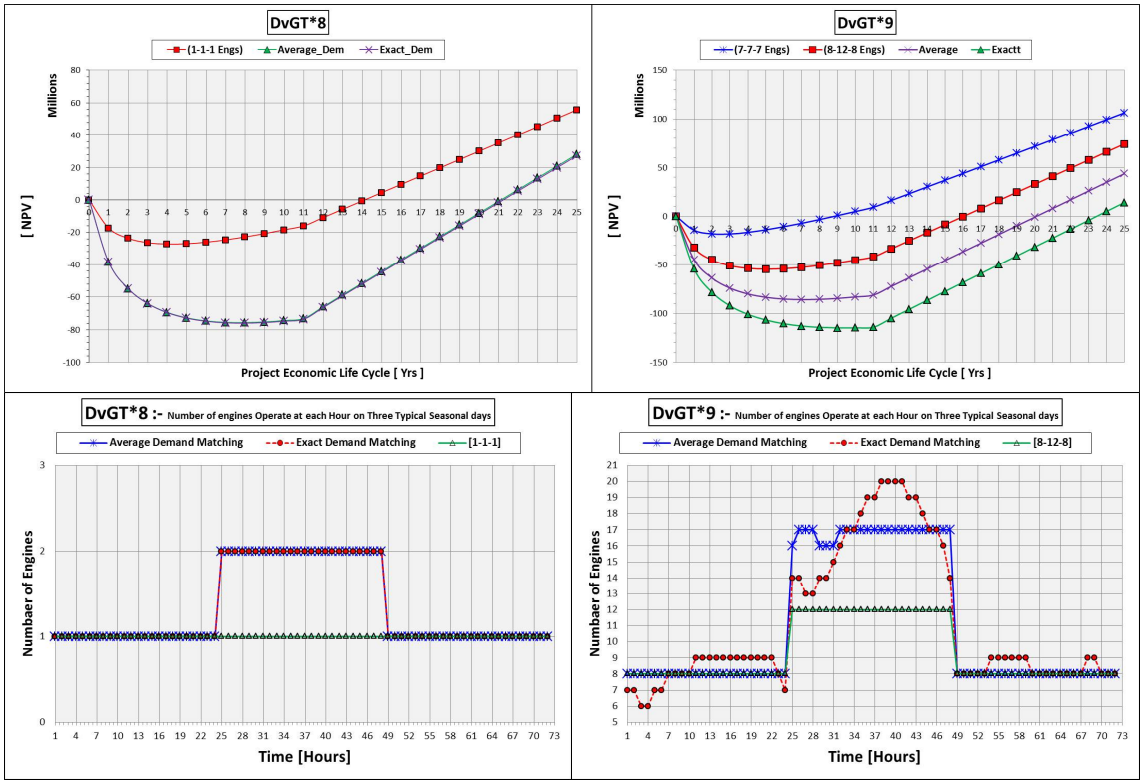
DvGT*8
(1-1-1 Engs)
Average_Dem
Exact_Dem
Millions
[NPV]
Project Economic Life Cycle [Yrs]
DvGT*9
(7-7-7 Engs)
(8-12-8 Engs)
Average
Exactt
Millions
[NPV]
Project Economic Life Cycle [Yrs]
DvGT*8 :- Number of engines Operate at each Hour on Three Typical Seasonal days
Average Demand Matching
Exact Demand Matching
[1-1-1]
Numbaer of Engines
Time [Hours]
DvGT*9 :- Number of engines Operate at each Hour on Three Typical Seasonal days
Average Demand Matching
Exact Demand Matching
[8-12-8]
Numbaer of Engines
Time [Hours]

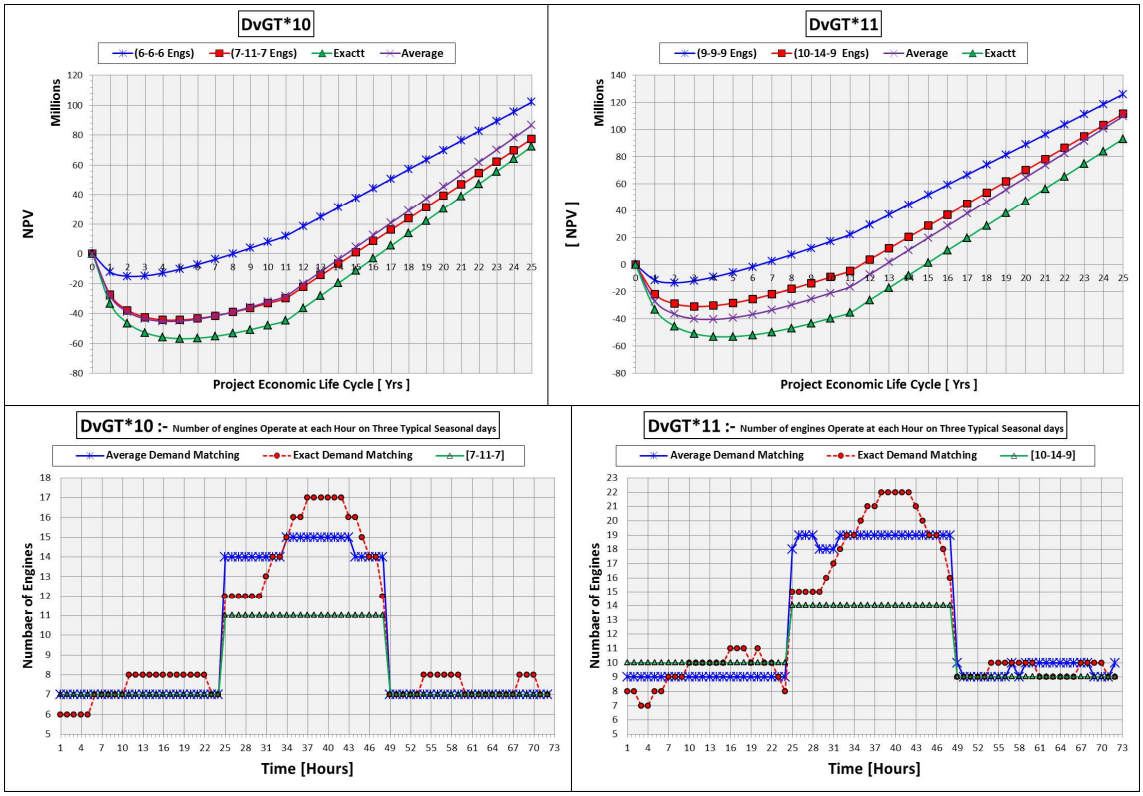
DvGT*10
(6-6-6 Engs)
(7-11-7 Engs)
Exactt
Average
Millions
NPV
Project Economic Life Cycle [Yrs]
DvGT*11
(9-9-9 Engs)
(10-14-9 Engs)
Average
Exactt
Millions
[NPV]
Project Economic Life Cycle [Yrs]
DvGT*10 :- Number of engines Operate at each Hour on Three Typical Seasonal days
Average Demand Matching
Exact Demand Matching
[7-11-7]
Numbaer of Engines
Time [Hours]
DvGT*11 :- Number of engines Operate at each Hour on Three Typical Seasonal days
Average Demand Matching
Exact Demand Matching
[10-14-9]
Numbaer of Engines
Time [Hours]

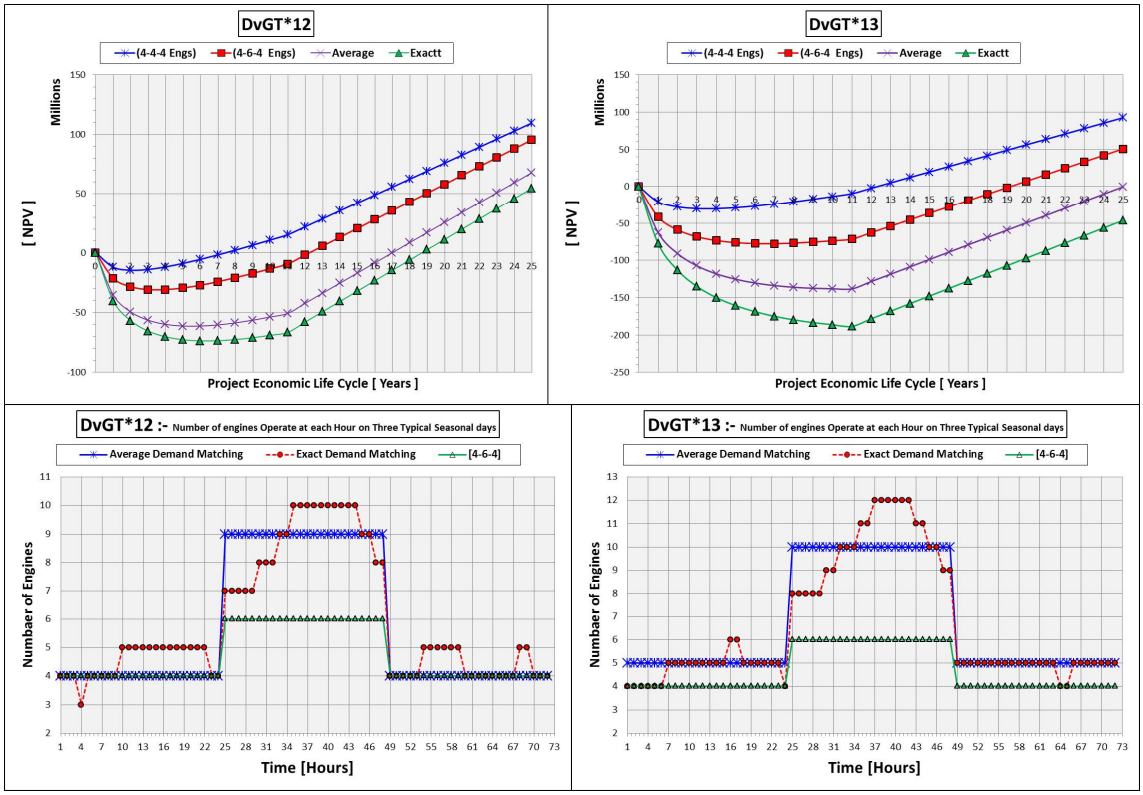
DvGT*12
(4-4-4 Engs)
(4-6-4 Engs)
Average
Exactt
Millions
[NPV]
Project Economic Life Cycle [Years]
DvGT*13
(4-4-4 Engs)
(4-6-4 Engs)
Average
Exactt
Millions
[NPV]
Project Economic Life Cycle [Years]
DvGT*12 :- Number of engines Operate at each Hour on Three Typical Seasonal days
Average Demand Matching
Exact Demand Matching
[4-6-4]
Numbaer of Engines
Time [Hours]
DvGT*13 :- Number of engines Operate at each Hour on Three Typical Seasonal days
Average Demand Matching
Exact Demand Matching
[4-6-4]
Numbaer of Engines
Time [Hours]

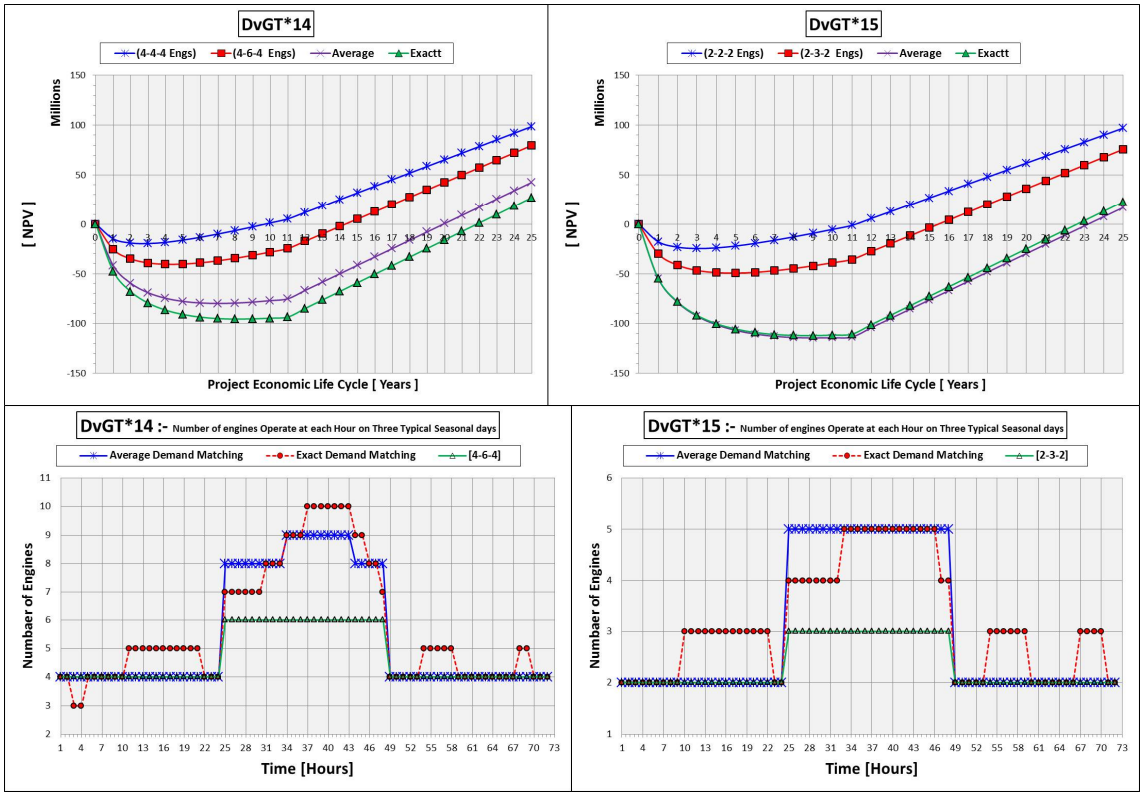

C.4 NPV of [PG] Application on Operating 4 Scenario

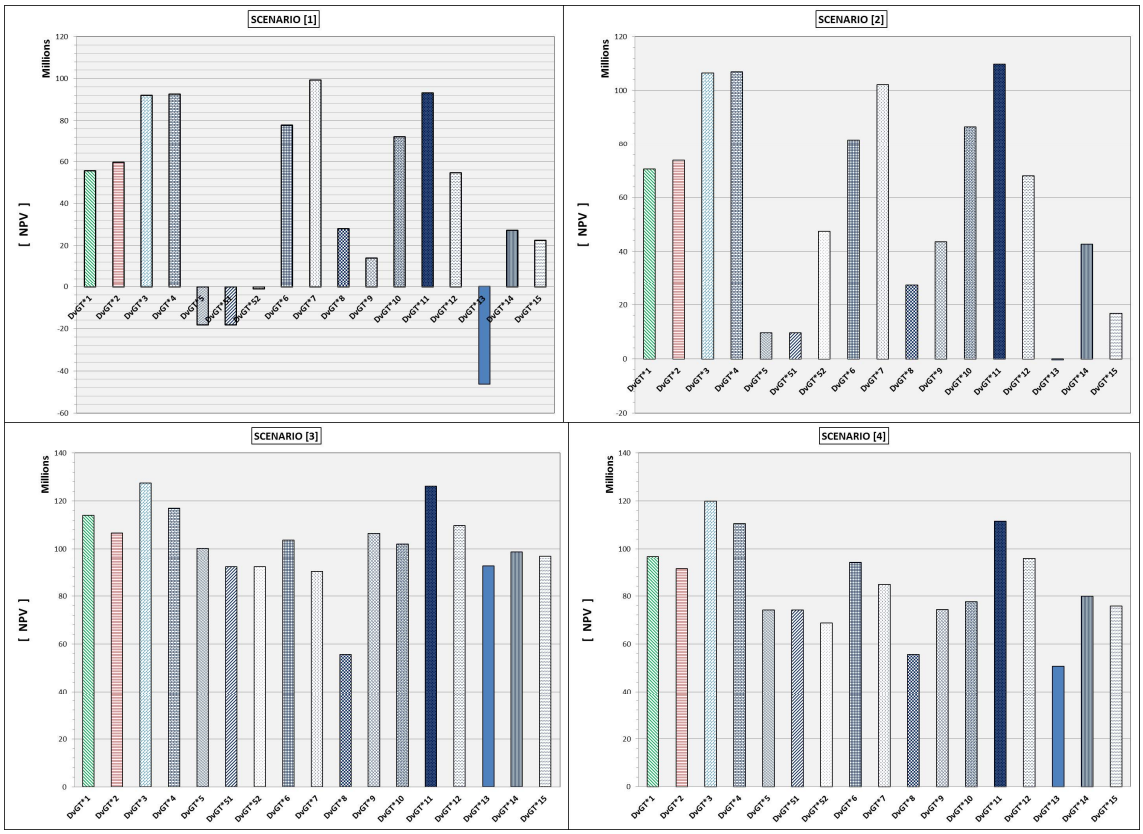

C.5 Annual Net Cash-Flow and [PBP] of [PG] App. on 4 Scenarios

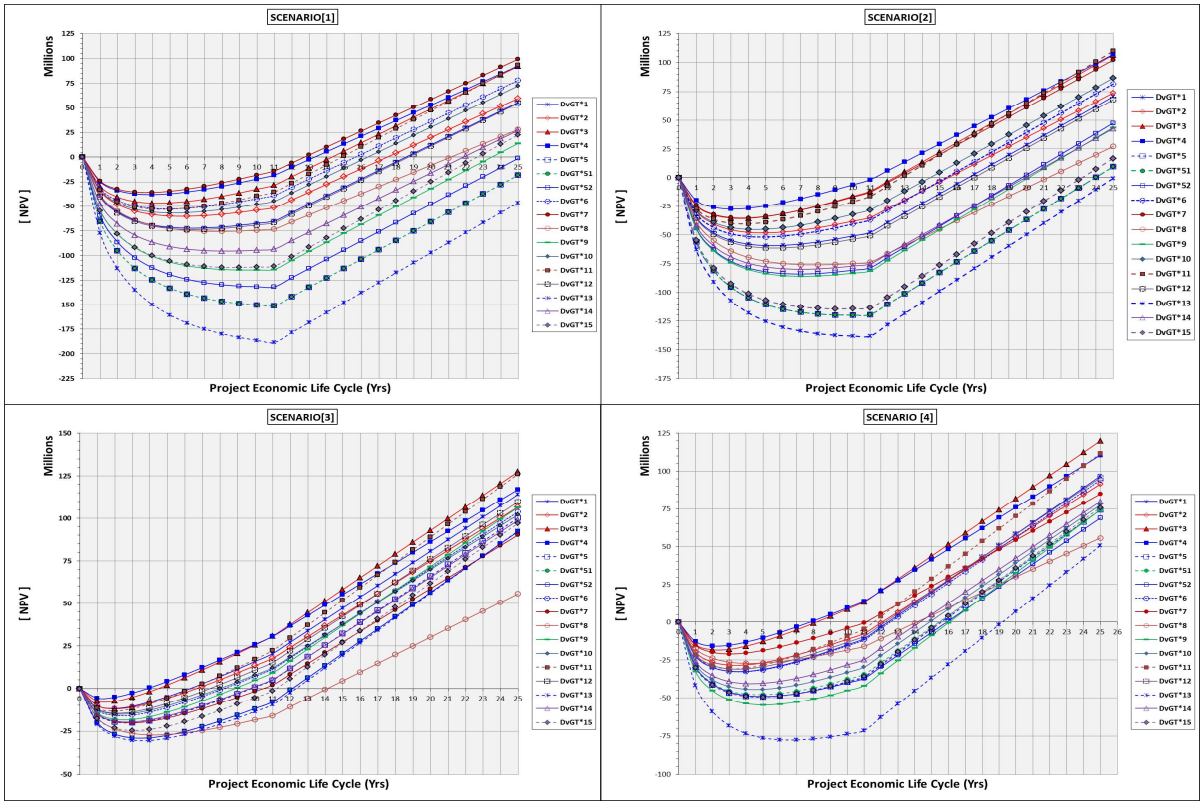

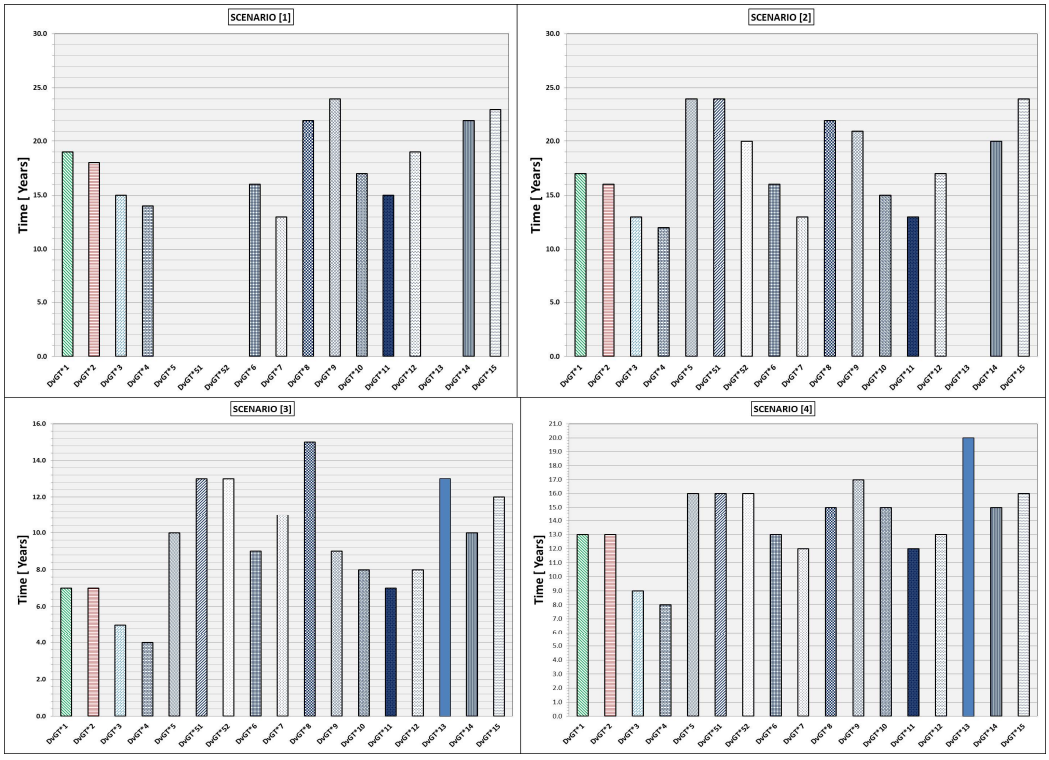

C.6 Relative Fuel Cost of [PG] Application

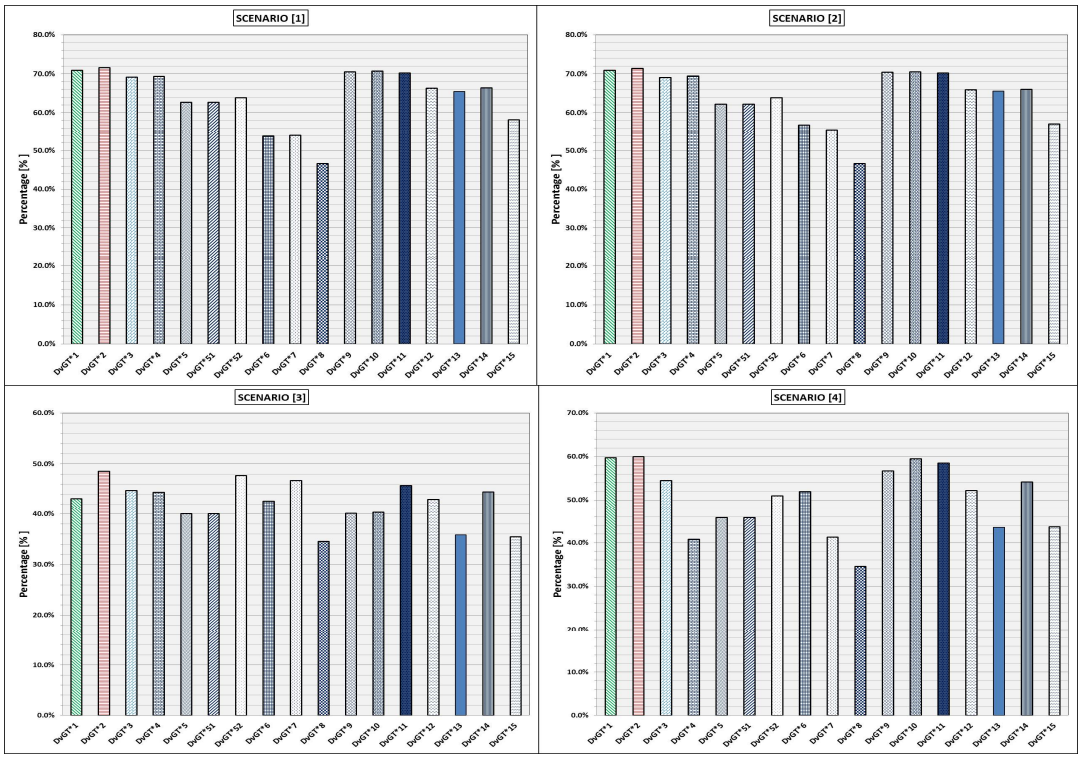

C.7 Relative O&M Cost of [PG] Application

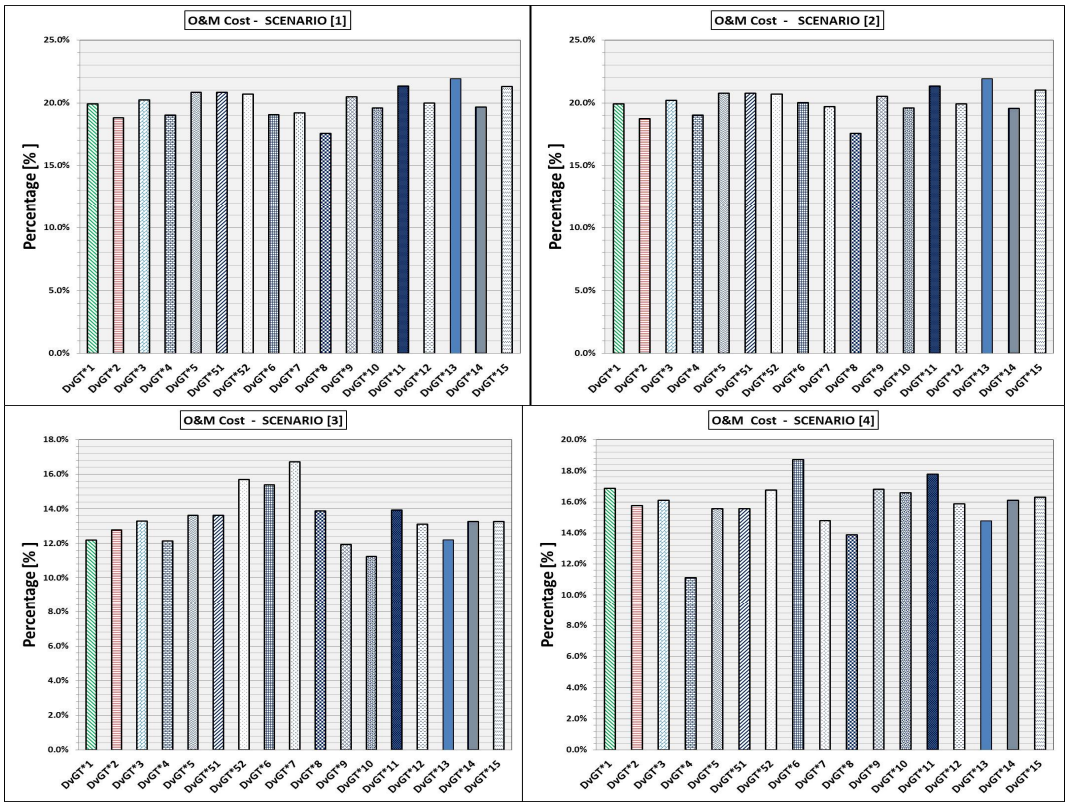

C.8 Relative Running Costs of [PG] Application

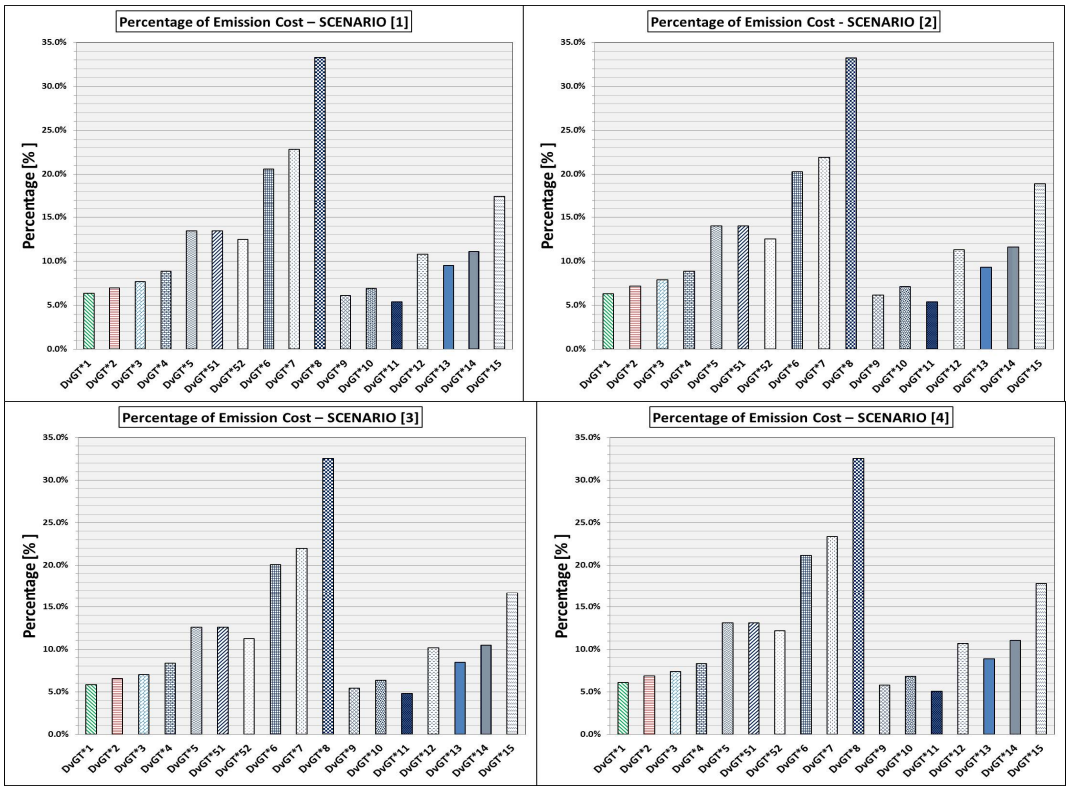

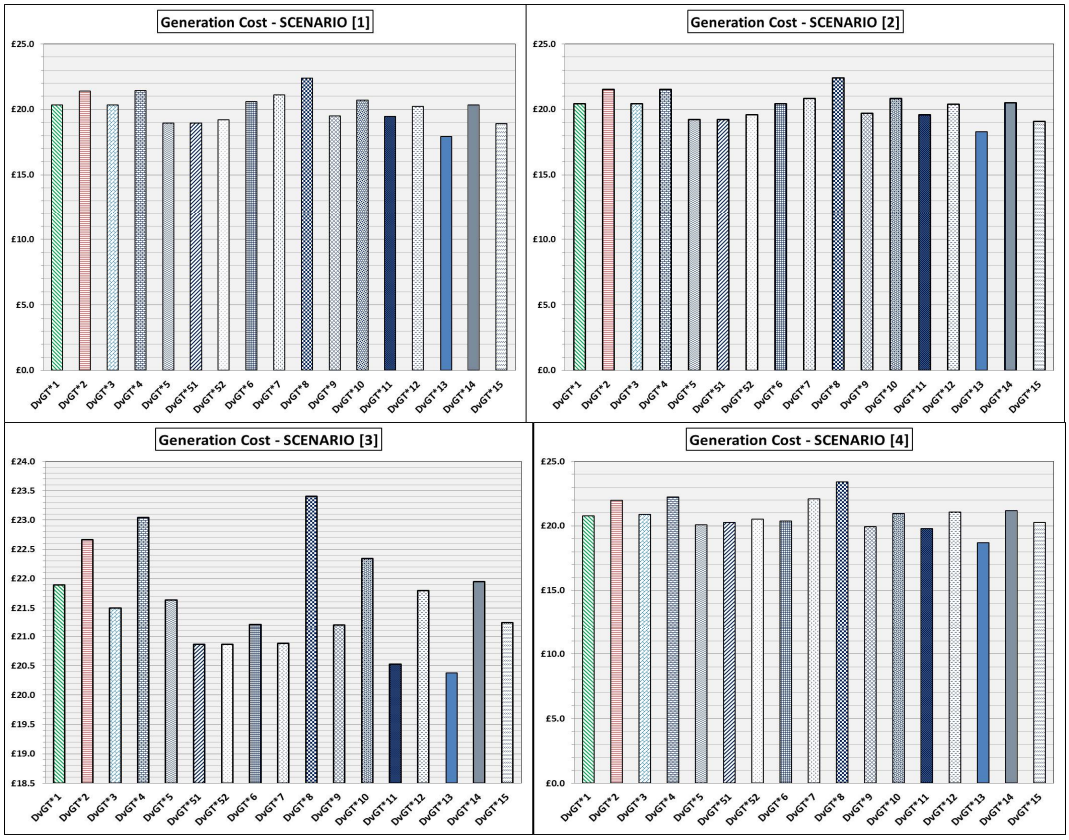

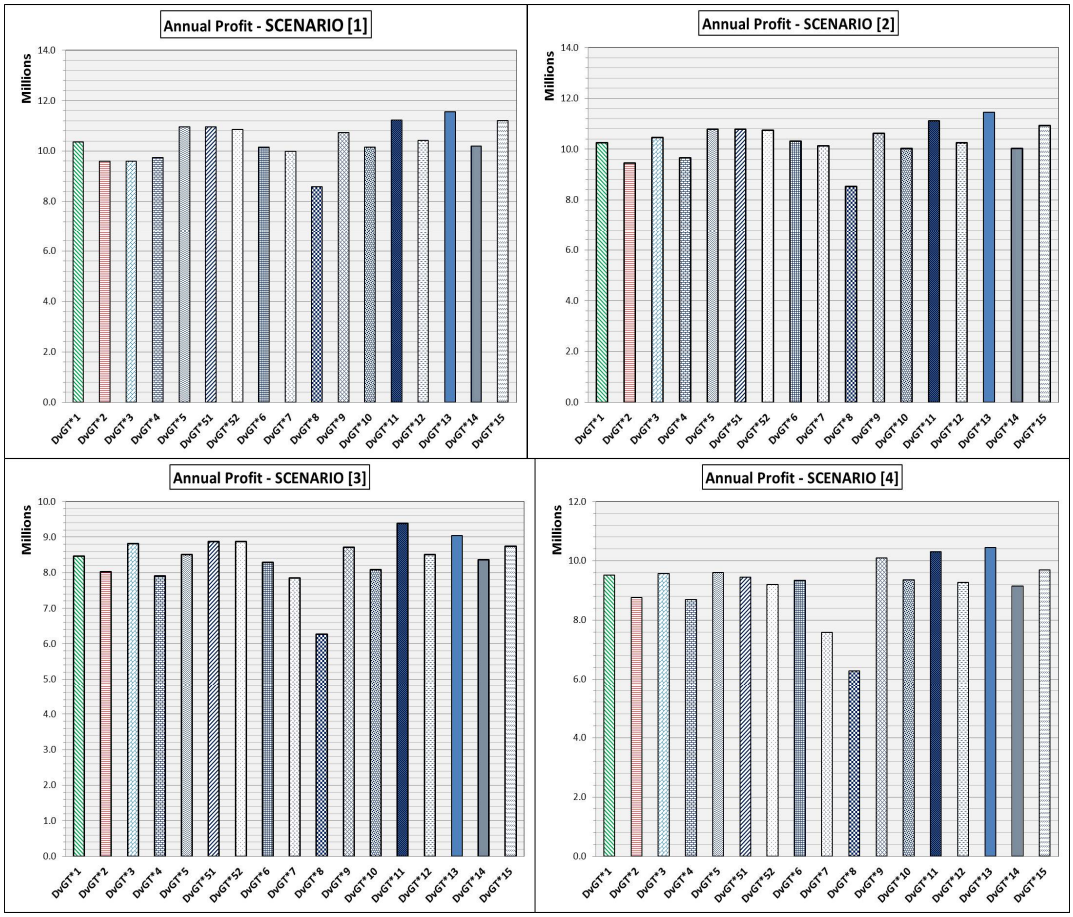
Annual Profit - SCENARIO [1]
Millions
14.0
12.0
10.0
8.0
6.0
4.0
2.0
0.0
DvGT*1 DvGT*2 DvGT*3 DvGT*4 DvGT*5 DvGT*51 DvGT*52 DvGT*6 DvGT*7 DvGT*8 DvGT*9 DvGT*10 DvGT*11 DvGT*12 DvGT*13 DvGT*14 DvGT*15
Annual Profit - SCENARIO [2]
Millions
14.0
12.0
10.0
8.0
6.0
4.0
2.0
0.0
DvGT*1 DvGT*2 DvGT*3 DvGT*4 DvGT*5 DvGT*51 DvGT*52 DvGT*6 DvGT*7 DvGT*8 DvGT*9 DvGT*10 DvGT*11 DvGT*12 DvGT*13 DvGT*14 DvGT*15
Annual Profit - SCENARIO [3]
Millions
10.0
9.0
8.0
7.0
6.0
5.0
4.0
3.0
2.0
1.0
0.0
DvGT*1 DvGT*2 DvGT*3 DvGT*4 DvGT*5 DvGT*51 DvGT*52 DvGT*6 DvGT*7 DvGT*8 DvGT*9 DvGT*10 DvGT*11 DvGT*12 DvGT*13 DvGT*14 DvGT*15
Annual Profit - SCENARIO [4]
Millions
12.0
10.0
8.0
6.0
4.0
2.0
0.0
DvGT*1 DvGT*2 DvGT*3 DvGT*4 DvGT*5 DvGT*51 DvGT*52 DvGT*6 DvGT*7 DvGT*8 DvGT*9 DvGT*10 DvGT*11 DvGT*12 DvGT*13 DvGT*14 DvGT*15

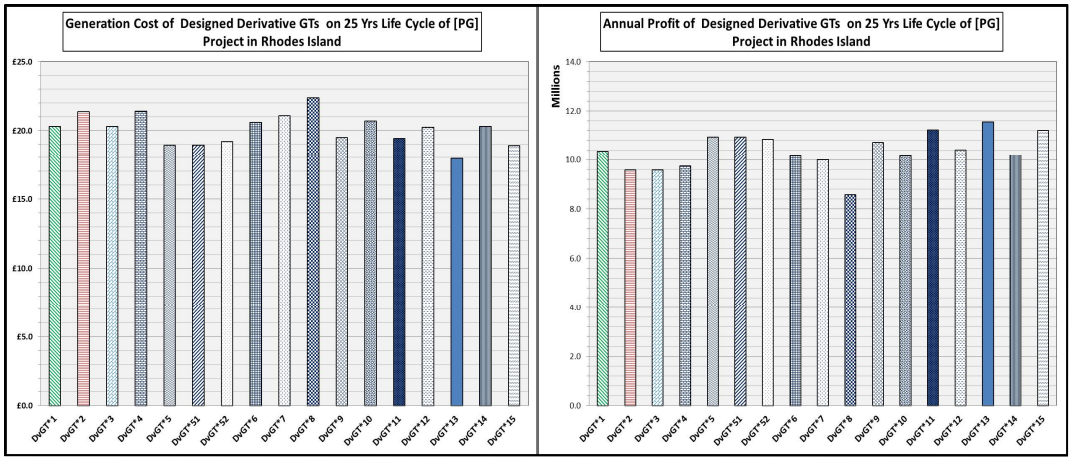
Generation Cost of Designed Derivative GTs on 25 Yrs Life Cycle of [PG] Project in Rhodes Island
£25.0
£20.0
£15.0
£10.0
£5.0
£0.0
DvGT*1 DvGT*2 DvGT*3 DvGT*4 DvGT*5 DvGT*51 DvGT*52 DvGT*6 DvGT*7 DvGT*8 DvGT*9 DvGT*10 DvGT*11 DvGT*12 DvGT*13 DvGT*14 DvGT*15
Annual Profit of Designed Derivative GTs on 25 Yrs Life Cycle of [PG] Project in Rhodes Island
Millions
14.0
12.0
10.0
8.0
6.0
4.0
2.0
0.0
DvGT*1 DvGT*2 DvGT*3 DvGT*4 DvGT*5 DvGT*51 DvGT*52 DvGT*6 DvGT*7 DvGT*8 DvGT*9 DvGT*10 DvGT*11 DvGT*12 DvGT*13 DvGT*14 DvGT*15

Appendix D GT Assessment on Marine Applications

D.1 Performance of Selected Derivative GT Engines on Cruise Liner Route

D.1.1 COT Variation for Different Cruise Liner's Ship Speeds on the Rout at ISA Condition

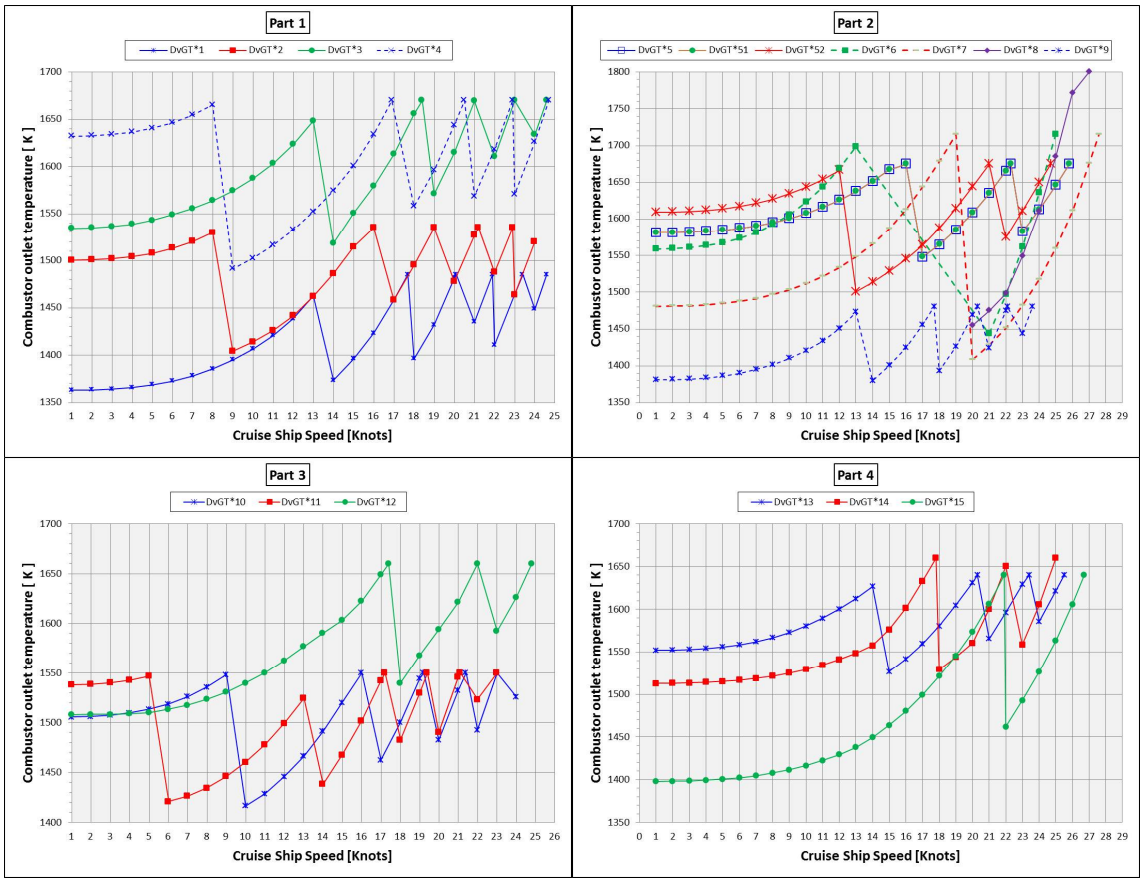

D.1.2 Thermal Efficiency Variation for Different Cruise Liner's Ship Speeds on the Rout at ISA Condition

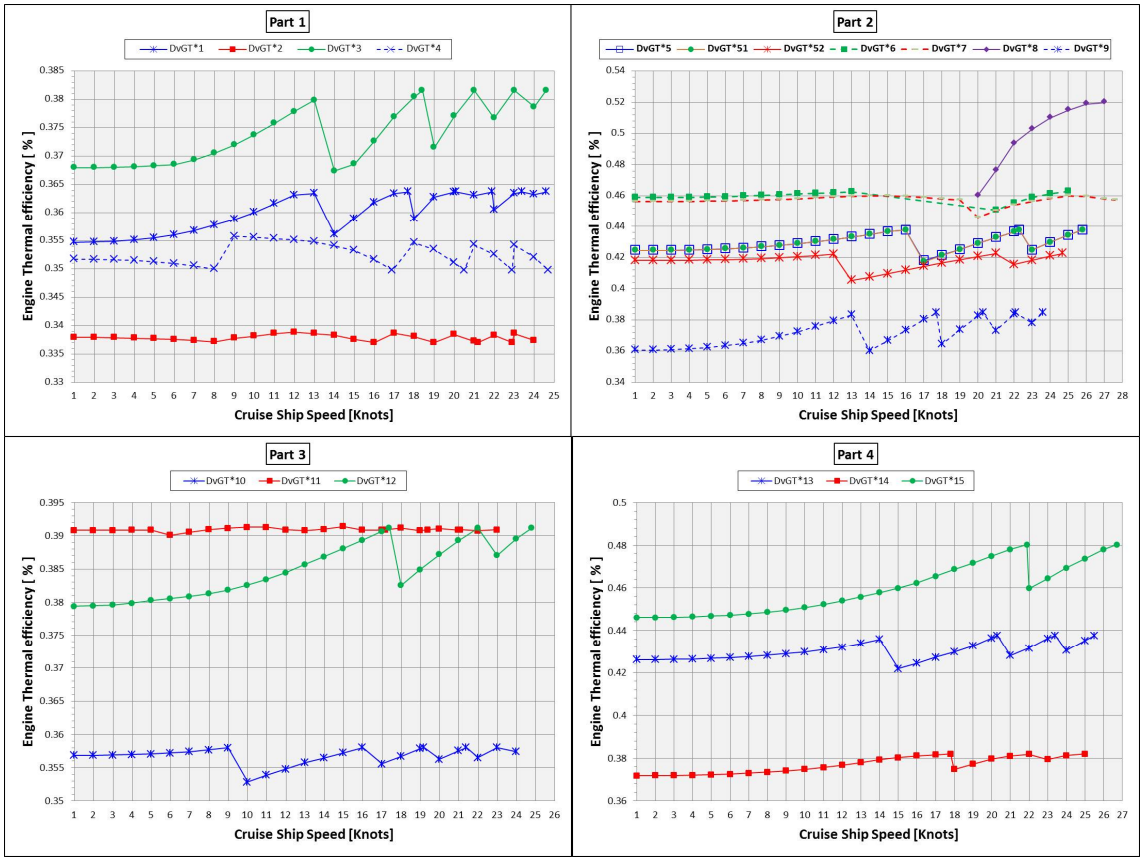

D.1.3 Shaft Power Variation for Different Cruise Liner's Ship Speeds on the Rout at ISA Condition

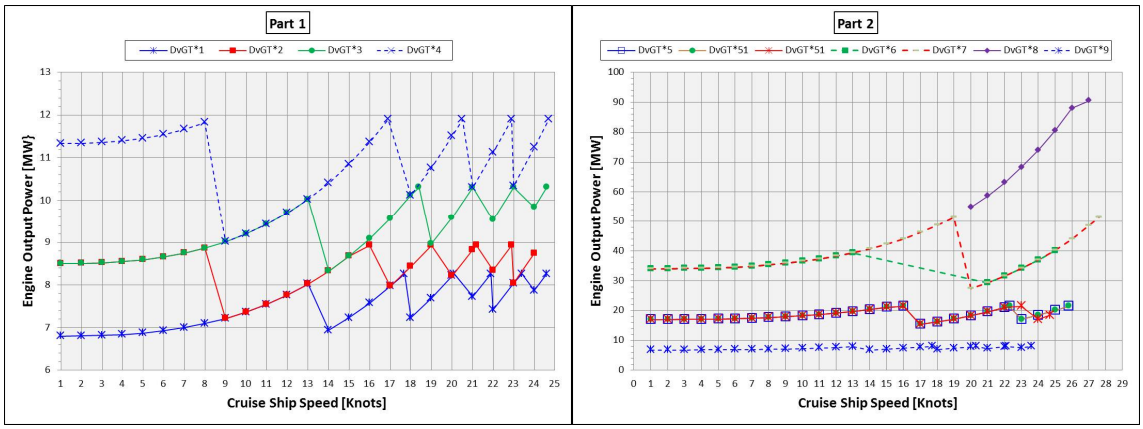

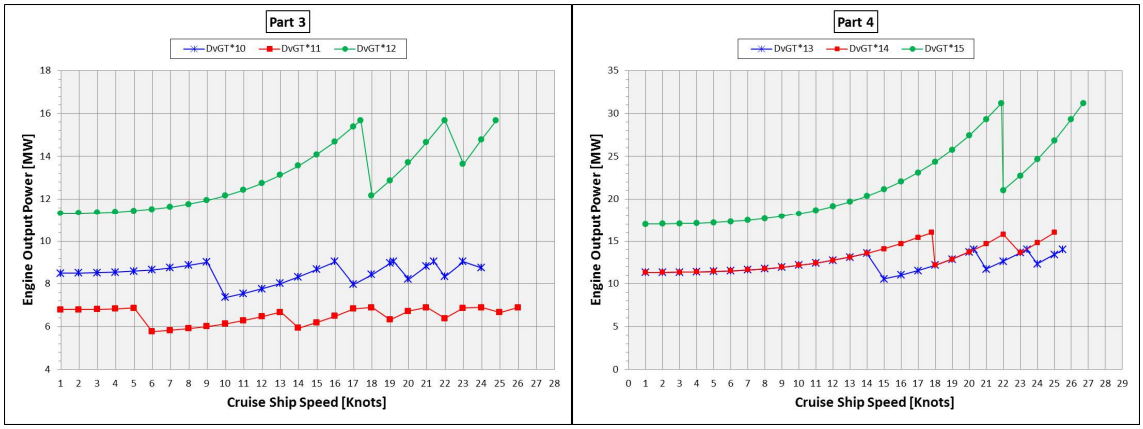

D.1.4 Number of GT Engines Required for Different Cruise Liner's Ship Speeds on the Rout at ISA Condition

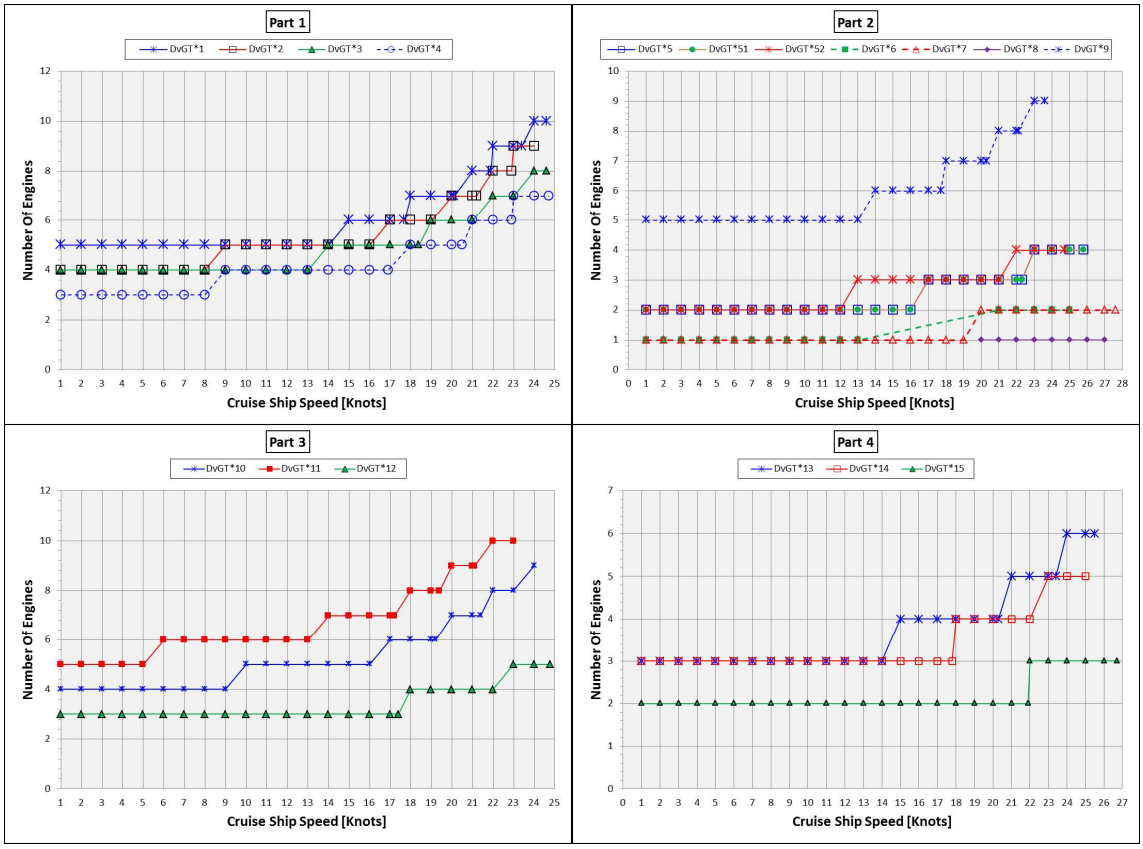

D.1.5 NOx Production Variation for Different Cruise Liner's Ship Speeds on the Rout at ISA Condition

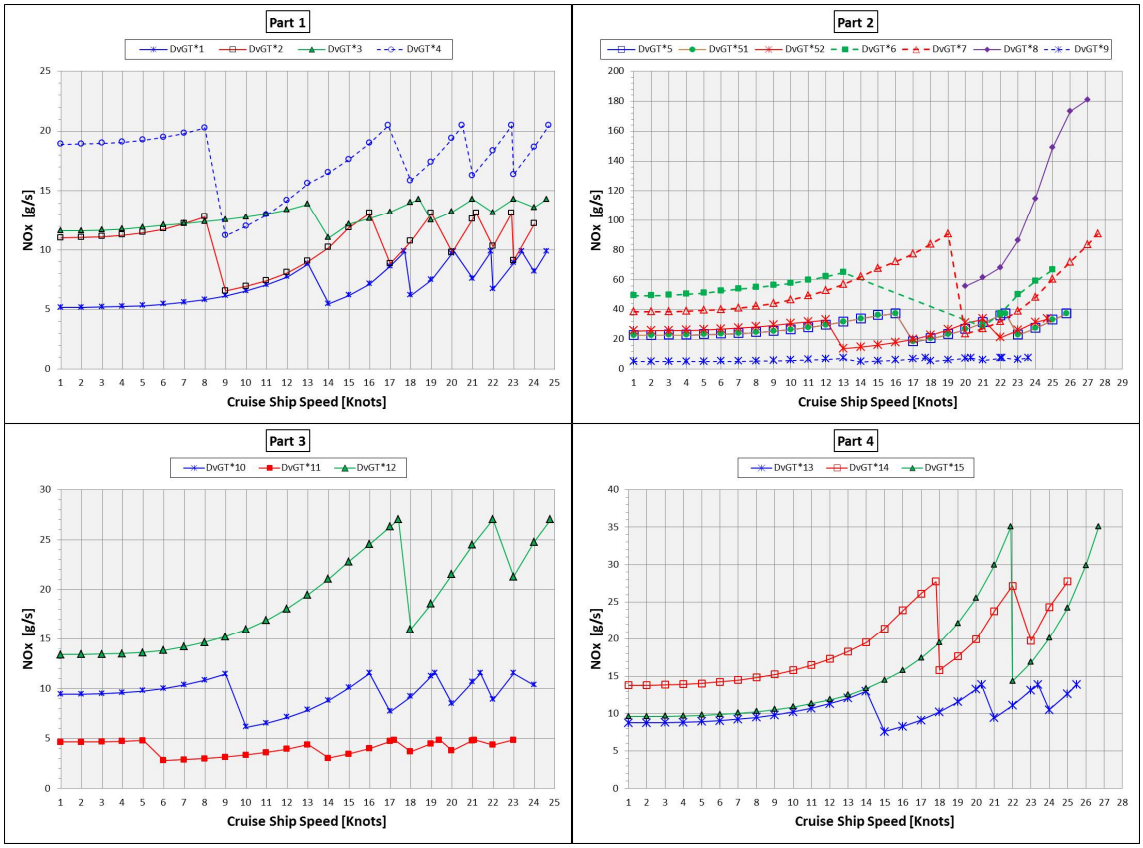

D.1.6 Selected Derivative GT Performance Variation along one way Cruise Ship Voyage Route on Different Sea and Weather Conditions

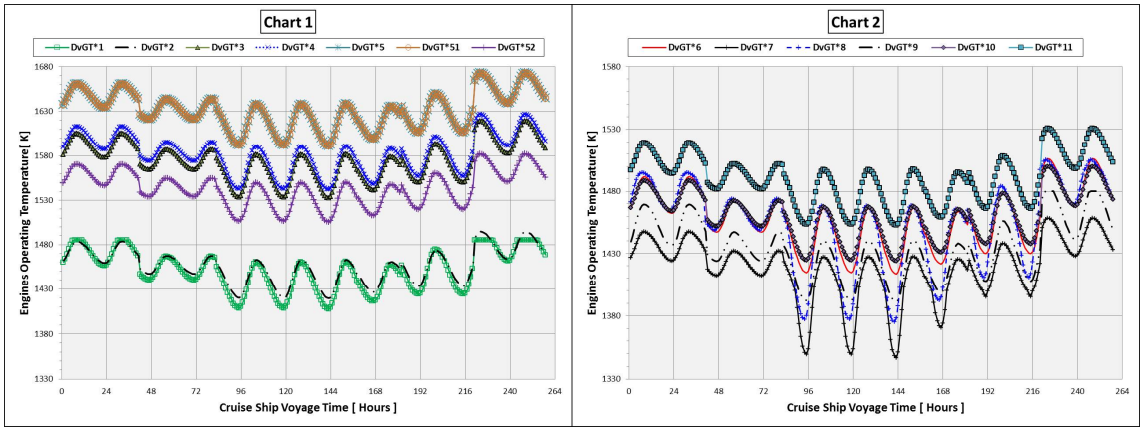

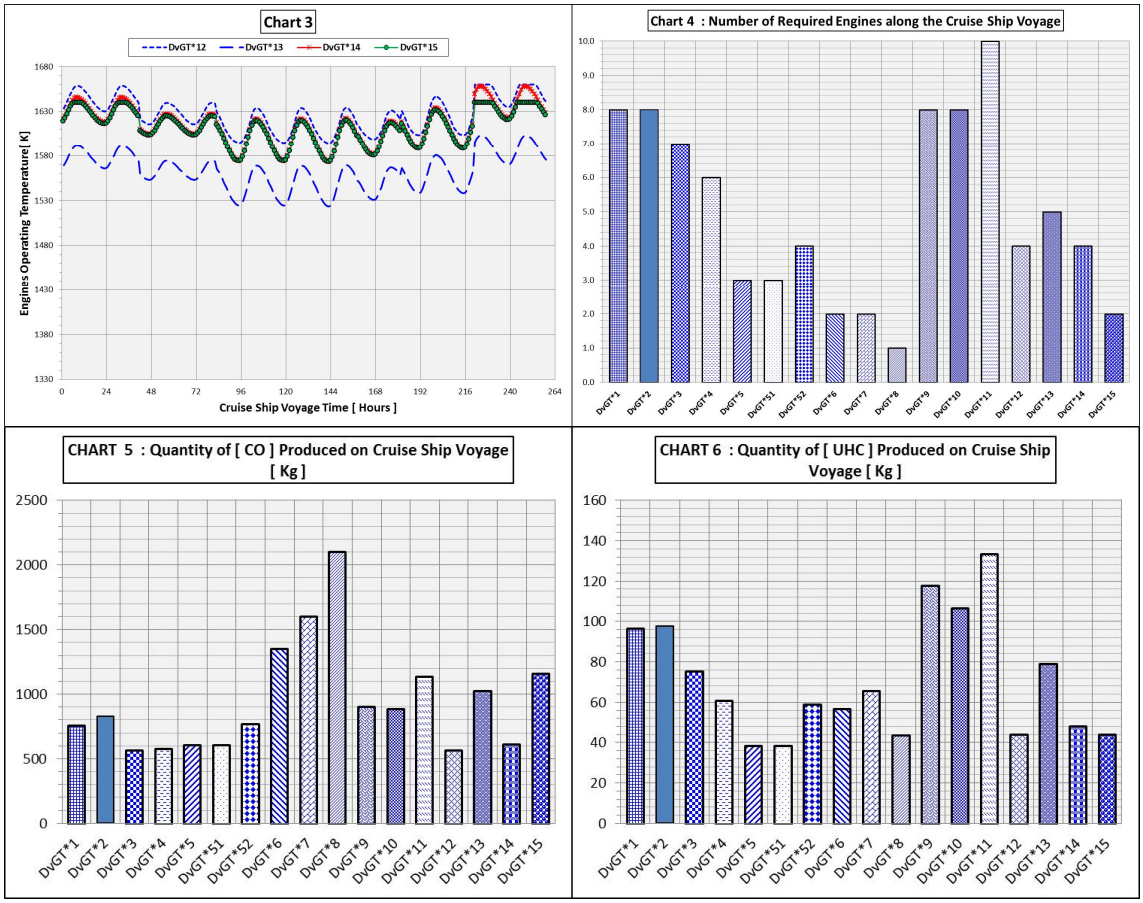
Chart 3
DvGT*12
DvGT*13
DvGT*14
DvGT*15
Engines Operating Temperature[K]
Cruise Ship Voyage Time [Hours]
Chart 4 : Number of Required Engines along the Cruise Ship Voyage
CHART 5 : Quantity of [CO] Produced on Cruise Ship Voyage [Kg]
CHART 6 : Quantity of [UHC] Produced on Cruise Ship Voyage [Kg]

D.2 Performance of Selected GT Models on Ferry Route

D.2.1 Ferry Route COT Variation for Different Speeds at ISA Condition

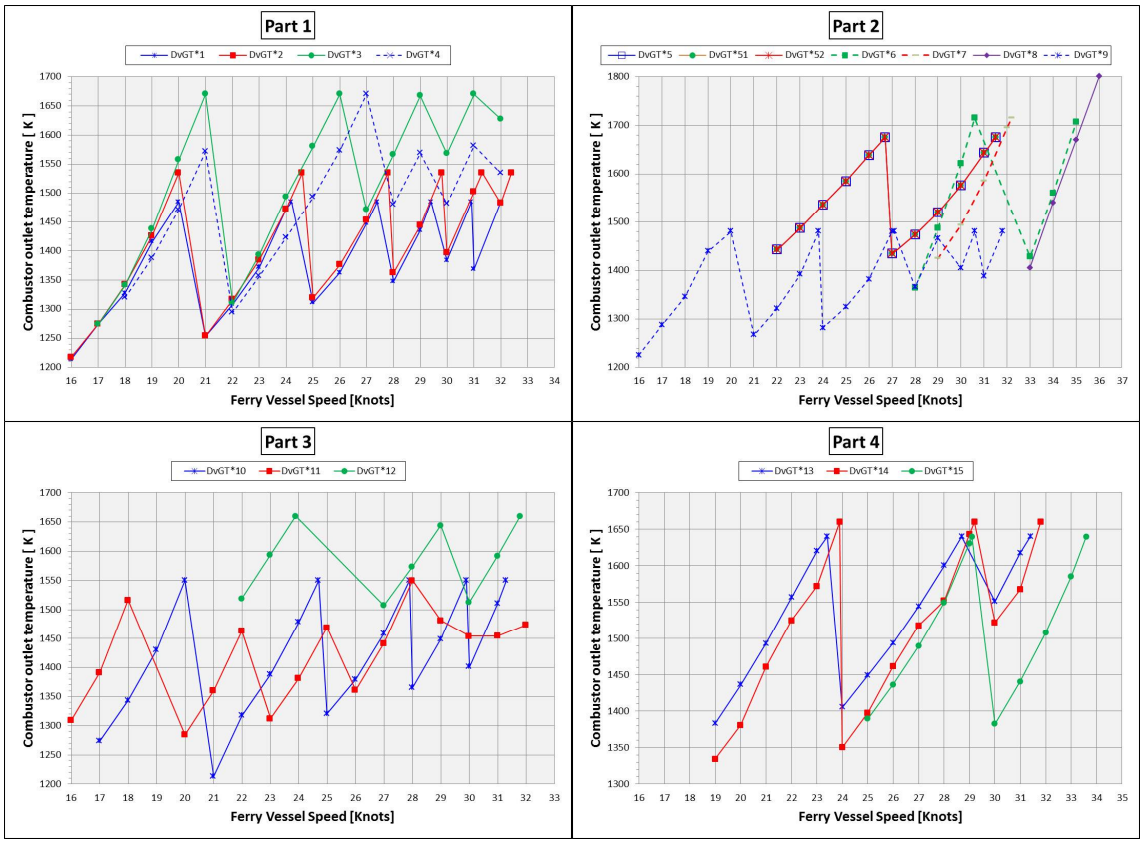

D.2.2 Ferry Route Thermal Efficiency Variation for Different Speeds at ISA Condition

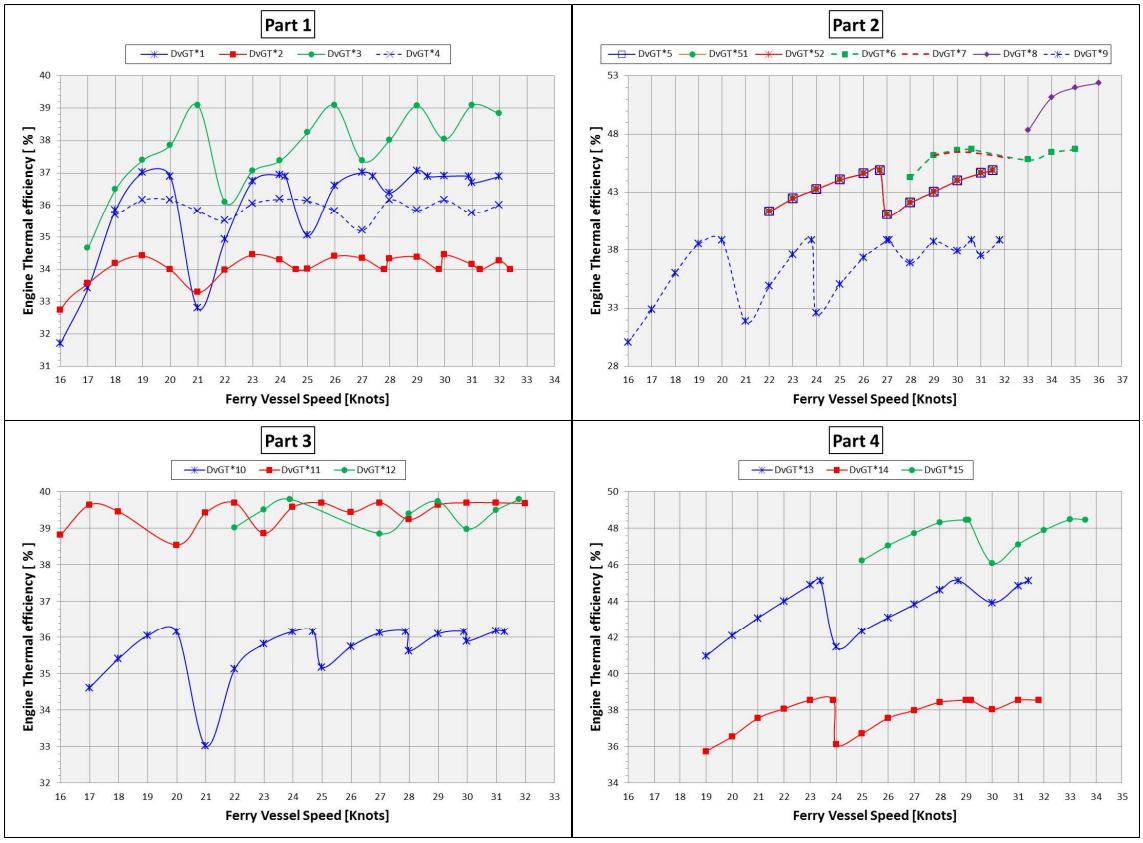

D.2.3 Ferry Route Shaft Power Variation for Different Speeds at ISA Condition

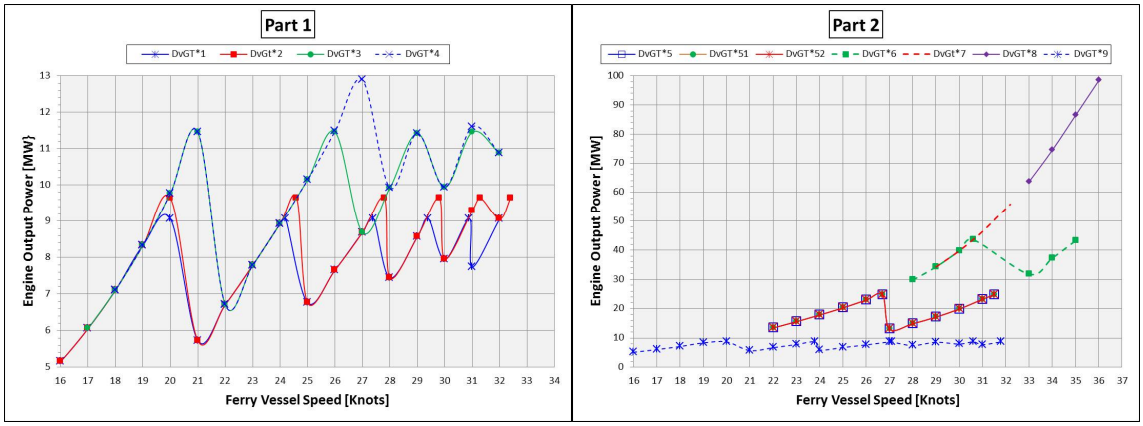

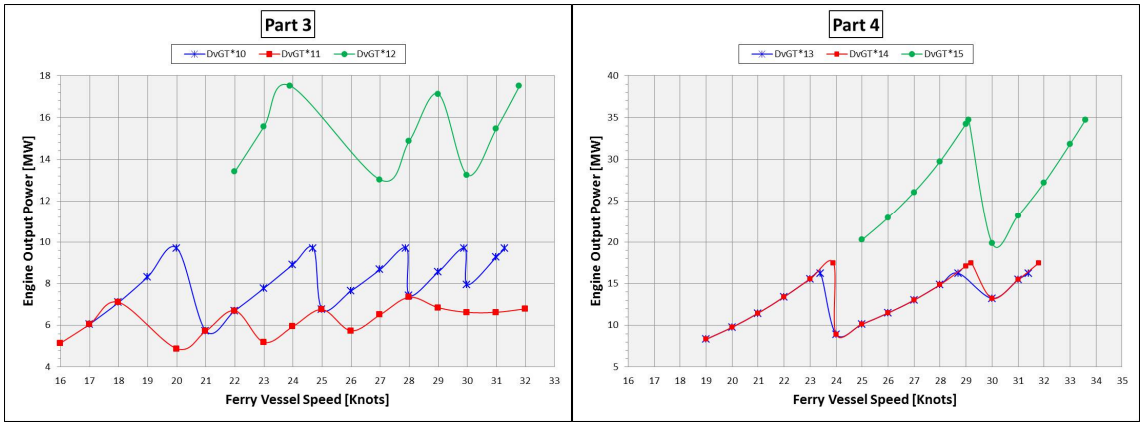

D.2.4 Ferry Route Number of Engines Variation for Different Speeds at ISA Condition

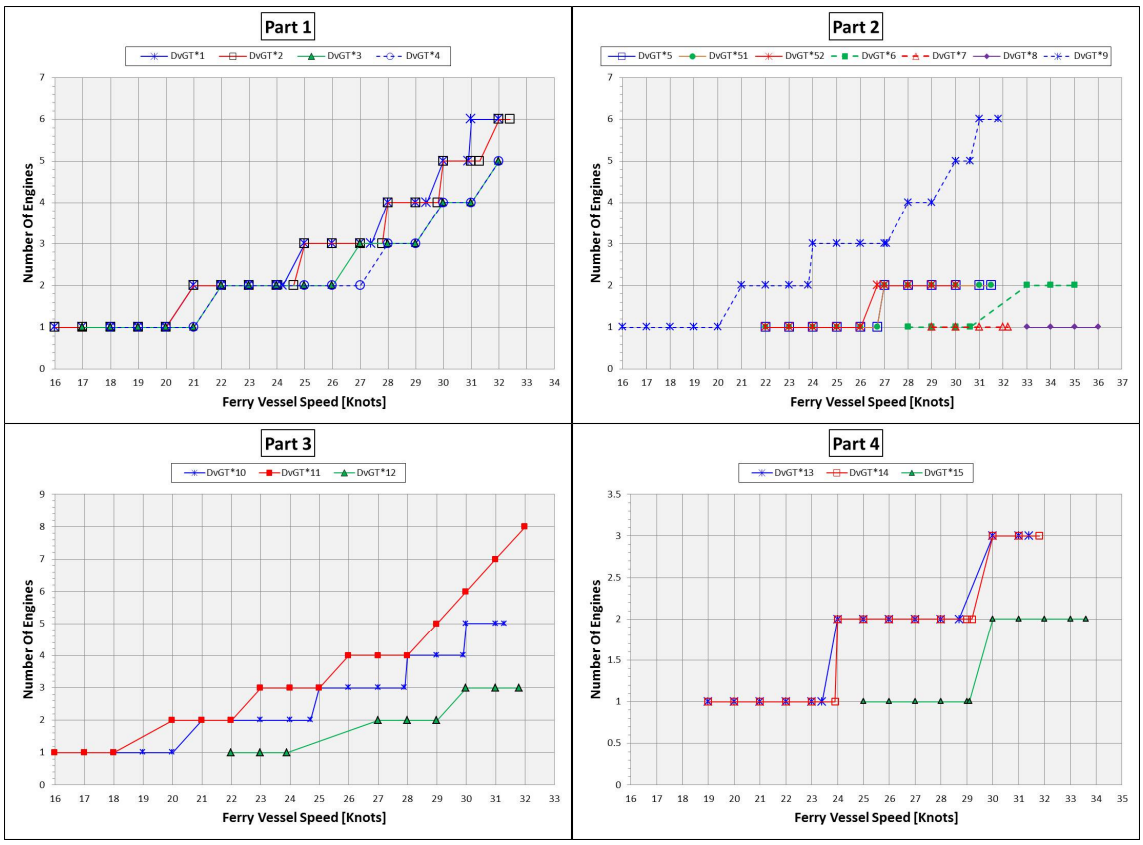

D.2.5 Ferry Route NOx Production at ISA Condition

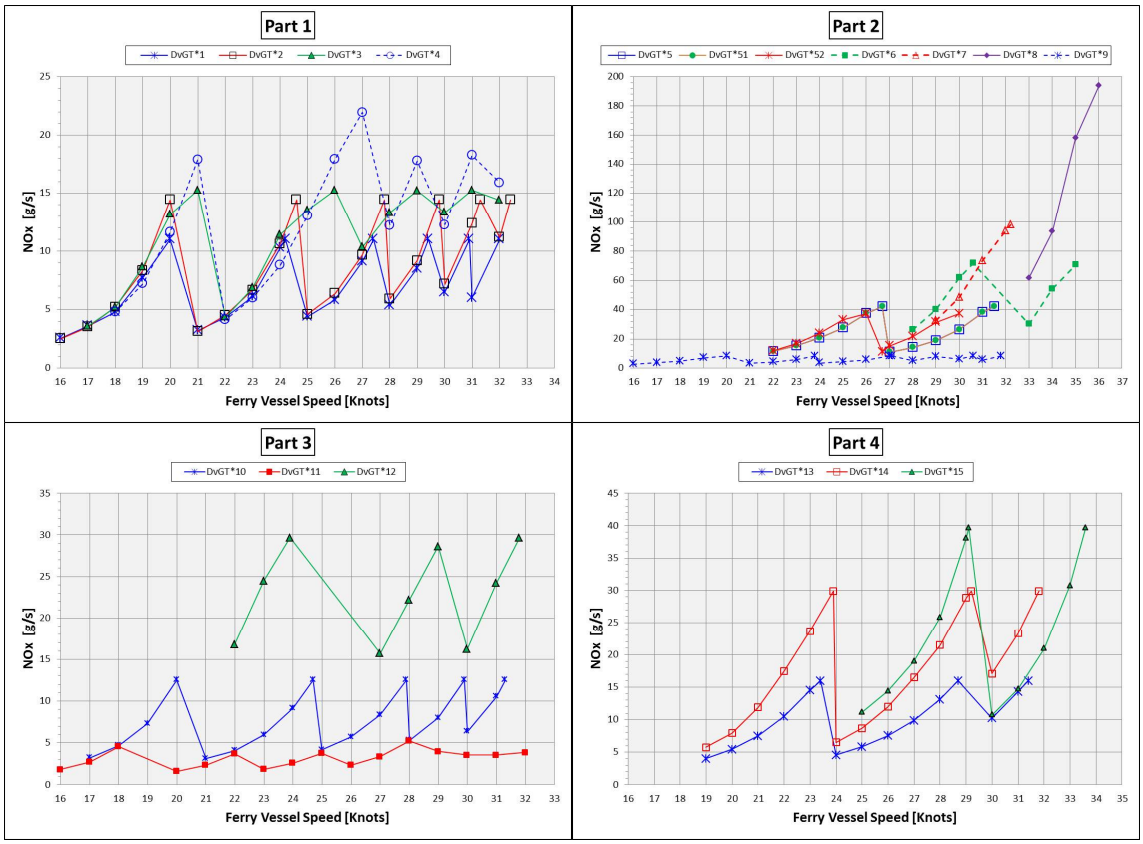

D.2.6 Selected Derivative GT Engines Performance Variation along one way Ferry Ship Voyage Route on Different Sea and Weather Conditions

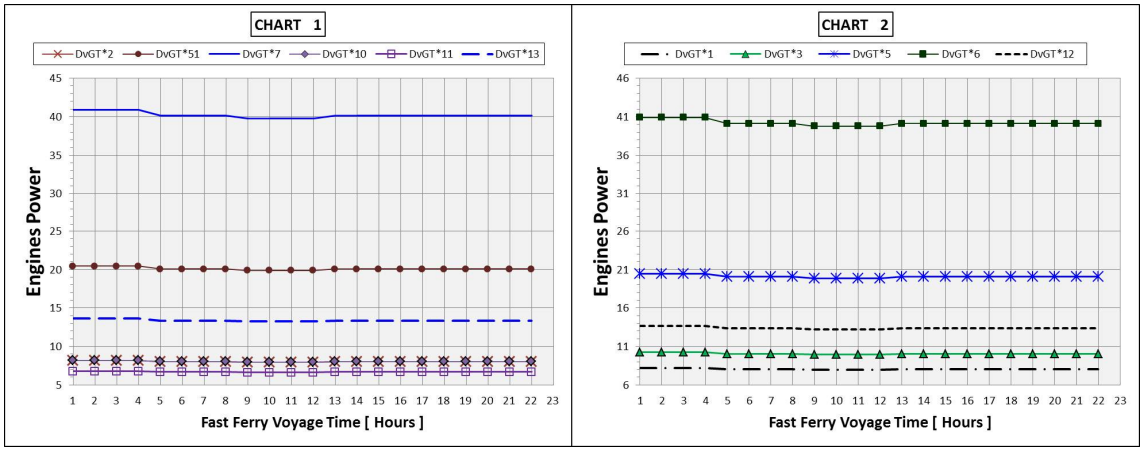

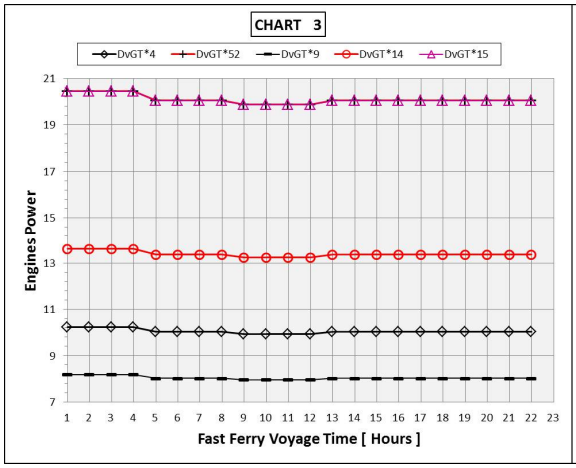
CHART 3
DvGT*4
DvGT*52
DvGT*9
DvGT*14
DvGT*15
Engines Power
Fast Ferry Voyage Time [Hours]

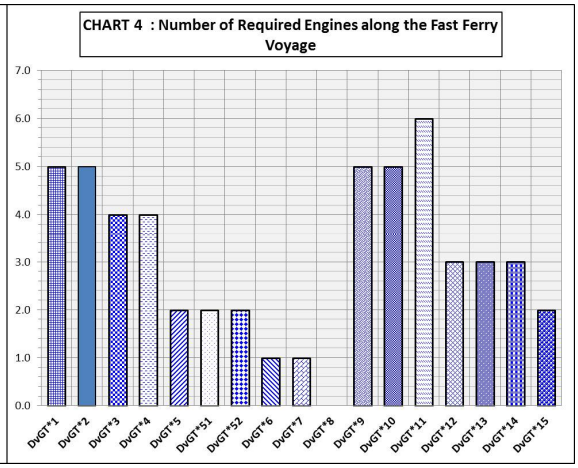
CHART 4 : Number of Required Engines along the Fast Ferry Voyage
DvGT*1
DvGT*2
DvGT*3
DvGT*4
DvGT*5
DvGT*51
DvGT*52
DvGT*6
DvGT*7
DvGT*8
DvGT*9
DvGT*10
DvGT*11
DvGT*12
DvGT*13
DvGT*14
DvGT*15

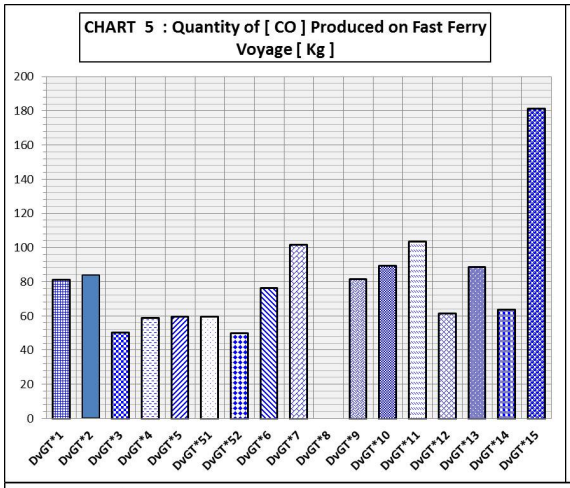
CHART 5 : Quantity of [CO] Produced on Fast Ferry Voyage [Kg]

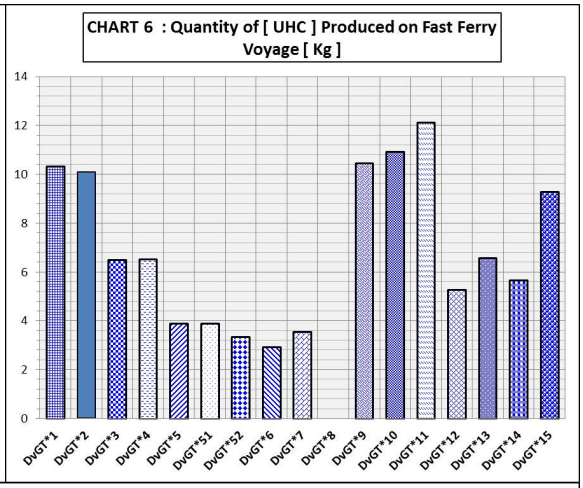
CHART 6 : Quantity of [UHC] Produced on Fast Ferry Voyage [Kg]

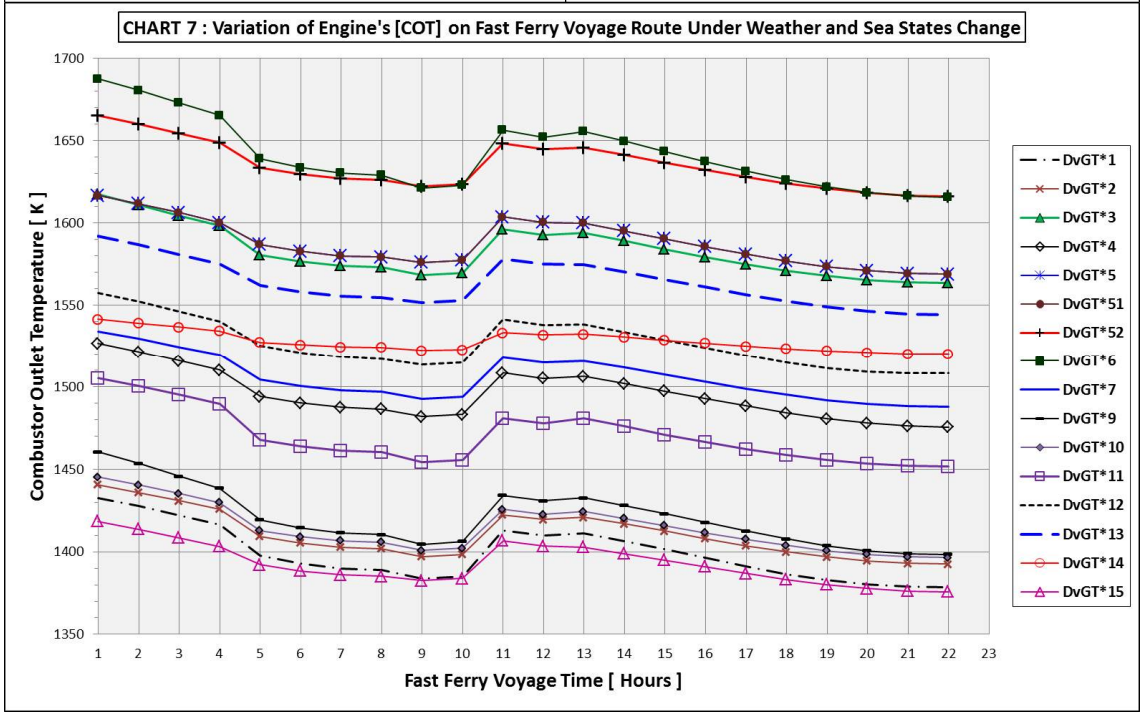
CHART 7 : Variation of Engine's [COT] on Fast Ferry Voyage Route Under Weather and Sea States Change
Combustor Outlet Temperature [K]
Fast Ferry Voyage Time [Hours]
DvGT*1
DvGT*2
DvGT*3
DvGT*4
DvGT*5
DvGT*51
DvGT*52
DvGT*6
DvGT*7
DvGT*9
DvGT*10
DvGT*11
DvGT*12
DvGT*13
DvGT*14
DvGT*15

D.2.7 Economics and Performance Comparison of Different Configurations of two Selected Models of Derivative GT Engines on one way Ferry Ship Voyage

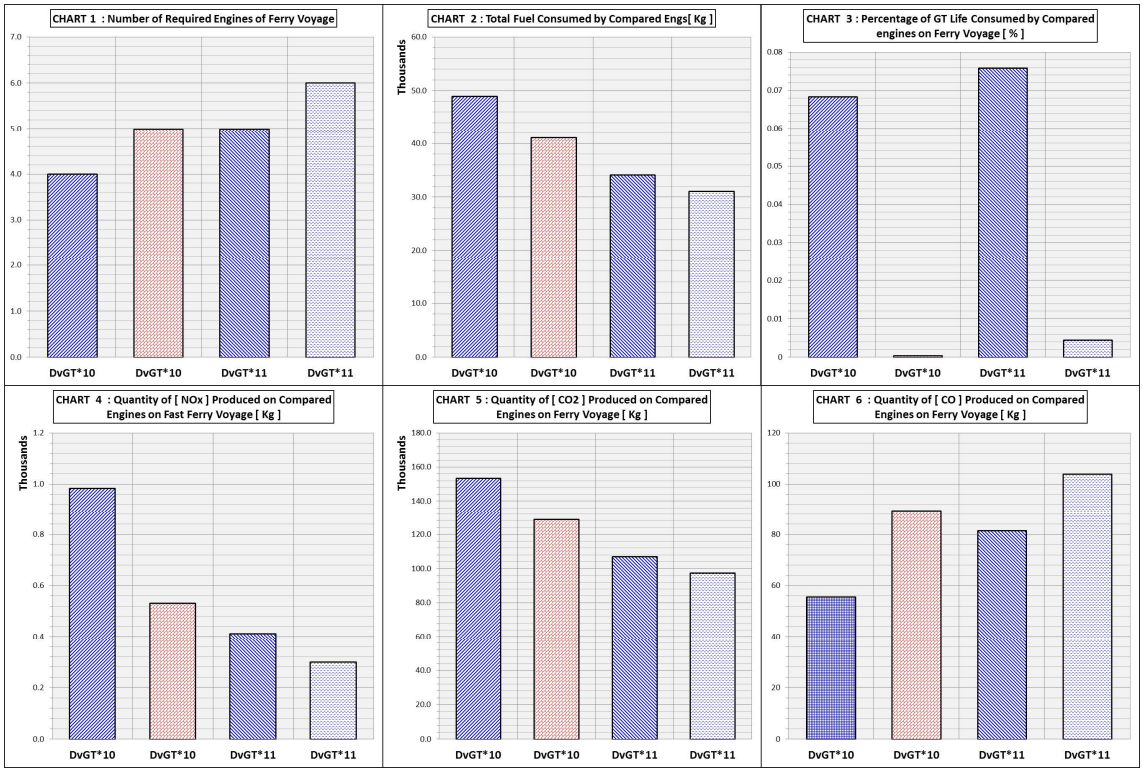

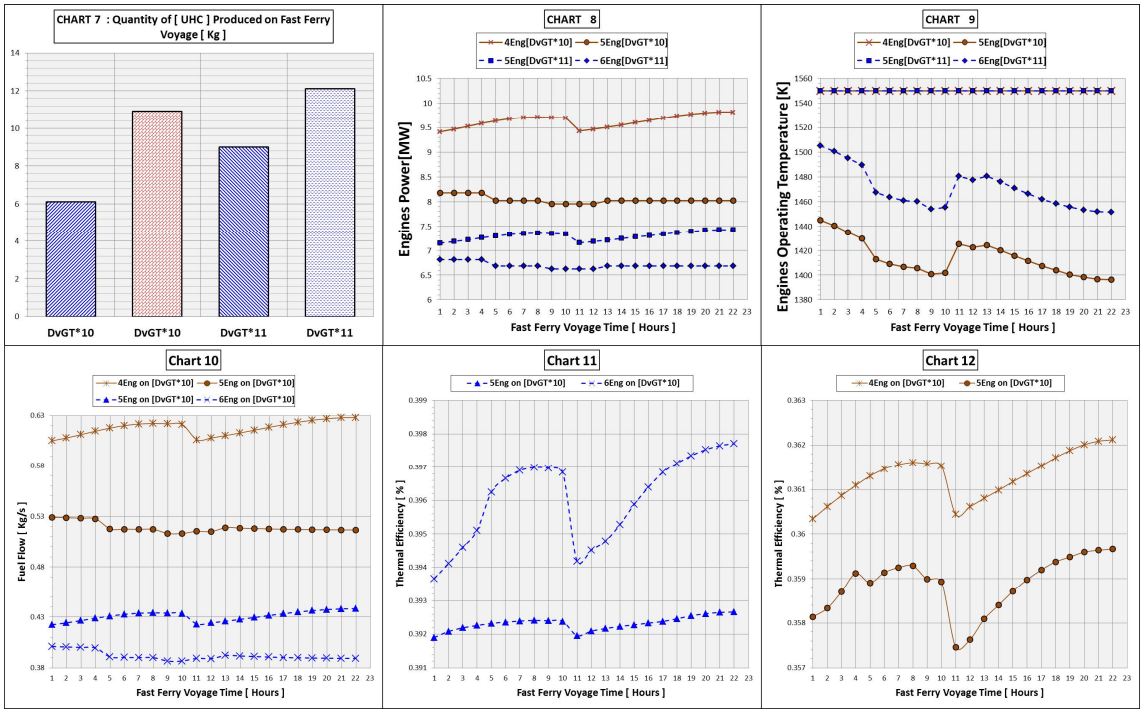

Appendix E Engines Input Data File (Turbomatch Models)

E.1 Maintaining (LP and HP) Components

E.1.1 Single-Spool Single-Shaft SC Engine [IPT] Model

```
! TURBOMATCH MODEL DATA FILE FOR: AERO-
DERIVATIVE ENGINE DERIVED FROM CUAV 130
AIRCRAFT ENGINE
MODELLED BY ABDELMANAM ABAAD
////
OD SI KE VA FP
-1
-1
INTAKE S1, 2      D1-4            R300
COMPRE S2, 3      D18-24          R302 V18 V19
PREMAS S3, 21, 4   D25 -28
ARITHY            D120-124
COMPRE S4, 5      D29-35          R303 V29
ARITHY            D250-255
PREMAS S5, 22, 6   D36 -39
PREMAS S22, 24, 23 D40 -43
PREMAS S6, 25, 7   D44 -47
BURNER S7, 8      D48-50          R304
MIXEES S8, 25, 9
MIXEES S9, 23, 10
ARITHY            D140-147
TURBIN S10, 11    D51 -58, 147, 59        V51 V52
NOZCON S11, 12, 1 D83             R306
ARITHY            D230-235
ARITHY            D240-245
ARITHY            D250-255
ARITHY            D260-265
ARITHY            D270-275
!*************************
! FOR EMMISION CALCULATION
!*************************
ARITHY            D330-335
ARITHY            D340-345
ARITHY            D350-357
ARITHY            D360-365
ARITHY            D370-378
!*************************
ARITHY            D500-505
ARITHY            D515-522
ARITHY            D523-530
ARITHY            D551-556
ARITHY            D560-567
ARITHY            D570-577
ARITHY            D701-706
ARITHY            D710-717
ARITHY            D720-727
ARITHY            D580-585
!****************************
! FOR Heat Output CALCULATION
!****************************
ARITHY            D600-605
ARITHY            D610-618
ARITHY            D620-628
ARITHY            D630-637
ARITHY            D640-648
!****************************
!                 W18 Tex Tstack Q
PLOTBD            D605, 585,627,648
!                 W7 P7 T7 Wf Alt DT W COT TET
! PLOTBD          D335, 378, 365, 357, 1,
2,255,275,245
!                 Alt Tamb W22 COT TET Q
! PLOTBD          D1, 235,265,275,245,648
!                 LPC W2 Ta COT TET Tex HC1 HPT Q
! PLOTBD          D20,
505,235,275,245,585,530,577,648
PERFOR  S1,0,0    D51,84-86,306,300,304,0,0,0,0,0,0
CODEND
DATA ITEMS////
! INTAKE
1 0.0         ! INTAKE ALTITUDE
2 0.0         ! ISA DEVIATION
3 0.0         ! MACH NO
4 0.9951      ! PRESSURE RECOVERY
! HP COMPRESSOR1
18   0.85     ! Z Parameter
19   1.0      ! Relative ND rotational Speed
20   7.11     ! Compressor Pressure Ratio
21   0.9      ! Isentropic Efficiency
22   0.0      ! Error Selection
23   5.0      ! Compressor Map Number
24   0.0      ! ANGLE
!  BLEEDING VALVE
25 0.04568     ! BLEEDING RATIO
26 0.0        ! MASS FLOW LOSS
27 0.0        ! PRESSURE FACTOR
28 0.0        ! PRESSURE LOSS
! HP COMPRESSOR2
29   0.85     ! Z Parameter
30   1.0      ! Relative ND rotational Speed
31   2.11     ! Compressor Pressure Ratio
32   0.88     ! Isentropic Efficiency
33   0.0      ! Error Selection
34   4.0      ! Compressor Map Number
35   0.0      ! ANGLE
!  TOTAL COOLING BLEED FOR HPT & LPT
SEALING
36 0.145       ! ROTORS COOLING
37 0.0        ! MASS FLOW LOSS
38 1.0        ! PRESSURE FACTOR
39 0.0        ! PRESSURE LOSS
!  SPLIT COOLING BLEED FOR LPT SEALING)
40 0.31      !% HPT SEALING AND % LPT
41 0.0       ! MASS FLOW LOSS
42 0.0       ! PRESSURE FACTOR
43 0.0       ! PRESSURE LOSS
! BURNER INTERNAL BYPASS COOLING
44 0.0        ! BYPASS RATIO
45 0.0        ! MASS FLOW LOSS
46 0.0        ! PRESSURE FACTOR
47 0.0        ! PRESSURE LOSS
!  BURNER
48    0.048    ! Fractional pressure Loss DP/P
49    0.9999   ! COMBUSTION EFFICIENCY
50   -1.0      ! FUEL FLOW
!  HP TURBINE
51 5437943.5   ! AUX.WORK
52 -1.0        ! REL NON-D MASS FLOW
53 -1.0        ! REL NON-D SPEED
54 0.90        ! EFFICIENCY
55 -1.0        ! REL ROT.SPEED (COMP TURB=-1)
56 1.0         ! COMP NO. FROM LOW END
57 5.0         ! TURBINE MAP
58 1000.0       ! POWER LAW
59 0.0         ! NGV ANGLE RELATIVE TO D
! NOZCON
```

```
83   -1.0      ! THROAT AREA
! PERFOR
84    1.0      ! PROPELLER
EFFICIENCY
85    0.0      ! SCALING INDEX
86    0.0      ! REQUIRED THRUST
!  ARITHY: HPC1 SPEED = HPC2
SPEED
120 5.0        ! COPY
121 -1.0
122 30.0       ! HPC2 SPEEDD
123 -1.0
124 19.0       ! HPC1 SPEED
!  ARITHY: HPT WORK = HPC1
WORK + HPC2 WORK
140 1.0        ! ADD
141 -1.0
142 147      ! HPT WORK
143 -1.0
144 302      ! HPC1 WORK
145 -1.0
146 303      ! HPC2 WORK
! ARITHY COPY D235=Tamb
230 5
231 -1
232 235
233 1
234 6
! ARITHY COPY D245=TET
240 5
241 -1
242 245
243 10
244 6
! ARITHY W2 IN Kg/s
250 11
251 -1
252 255
253 2
254 2
! ARITHY W4 IN Kg/s
260 11
261 -1
262 265
263 4
264 2
! ARITHY COPY 275=COT
270 5
271 -1
272 275
273 8
274 6
!*************************
! FOR EMMISION CALCULATION
!*************************
! ARITHY W7 IN Kg/s
330 11
331 -1
332 335
333 7
334 2
! ARITHY W8 IN Kg/s
340 11
341 -1
342 345
343 8
344 2
! ARITHY Wf= (W8-W7)
350 2
351 -1
352 357
353 -1
354 345
355 -1
356 335
! ARITHY COPY T7=365
360 5
361 -1
362 365
363 7
364 6
! ARITHY P7 in (Pa)
370 3
371 -1
372 378
373 7
374 4
375 -1
376 377
377 101325.0
!*************************
! ARITHY W2 IN Kg/s
500 11
501 -1
502 505
503 2
504 2
! ARITHY: (W2*SQRT T2)
515 15
516 -1
517 522
518 -1
519 505
520 2
521 6
! ARITHY: (W2*SQRT T2)/P2
523 4
524 -1
525 530
526 -1
527 522
528 2
529 4
! ARITHY W10 IN Kg/s
551 11
552 -1
553 556
554 10
555 2
! ARITHY: (W10*SQRT T10)
560 15
561 -1
562 567
563 -1
564 556
565 10
566 6
! ARITHY: (W10*SQRT T10)/P10
570 4
571 -1
572 577
573 -1
574 567
575 10
576 4
! ARITHY COPY 585=T12
580 5
581 -1
582 585
583 12
584 6
!*************************
! FOR Heat Output CALCULATION
!*************************
! ARITHY W12 IN Kg/s
600 11
601 -1
602 605
603 12
604 2
! ARITHY (W12*Cp)
610 3
611 -1
612 618
613 -1
614 605
615 -1
616 617
617 1150.0
! ARITHY (Tex-Tout)
620 2
621 -1
622 628
623 12
624 6
625 -1
626 627
627 400.0
! ARITHY Q=W12*Cp*(Tex-Tstack)
630 3
631 -1
632 637
633 -1
634 618
635 -1
636 628
! ARITHY Q IN MW
640 4
641 -1
642 648
643 -1
644 637
645 -1
646 647
647 1000000.0
!*************************
-1
1 2 27.04      ! INLET MASS FLOW
8 6 1308.92    ! COMBUSTION
OUTLET TEMPERATURE
-1
-3
```

E.1.2 Single-Spool Two-shaft SC Engine [FPT] Model

```
! TURBOMATCH MODEL DATA FILE FOR: AERO-
DERIVATIVE ENGINE DERIVED FROM CUAV 130
AIRCRAFT ENGINE
MODELLED BY ABDELMANAM ABAAD
////
OD SI KE VA FP
-1
-1
INTAKE S1, 2      D1-4            R300
COMPRE S2, 3      D18-24          R302 V18 V19
PREMAS S3, 21, 4   D25 -28
ARITHY            D120-124
COMPRE S4, 5      D29-35          R303 V29
PREMAS S5, 22, 6   D3 6-39
PREMAS S22, 24, 23 D40 -43
PREMAS S6, 25, 7   D44 -47
BURNER S7, 8      D48-50          R304
MIXEES S8, 25, 9
MIXEES S9, 23, 10
ARITHY            D140-147
TURBIN S10, 11    D51 -58, 147, 59         V52
DUCTER S11, 12    D69-72          R305
MIXEES S12, 24, 13
TURBIN S13, 14    D73-82              V73 V74
NOZCON S14, 15, 1 D83             R306
ARITHY            D230-235
ARITHY            D240-245
ARITHY            D250-255
ARITHY            D260-265
ARITHY            D270-275
!*************************
! FOR EMMISION CALCULATION
!*************************
ARITHY            D330-335
ARITHY            D340-345
ARITHY            D350-357
ARITHY            D360-365
ARITHY            D370-378
!*************************
ARITHY            D500-505
ARITHY            D515-522
ARITHY            D523-530
ARITHY            D551-556
ARITHY            D560-567
ARITHY            D570-577
ARITHY            D701-706
ARITHY            D710-717
ARITHY            D720-727
ARITHY            D580-585
!*****************************
! FOR Heat Output CALCULATION
!*****************************
ARITHY            D600-605
ARITHY            D610-618
ARITHY            D620-628
ARITHY            D630-637
ARITHY            D640-648
!*****************************
!                 W18 Tex Tstack Q
PLOTBD            D605, 585,627,648
!                  W7 P7 T7 Wf Alt DT W COT TET
! PLOTBD     D335, 378, 365, 357, 1, 2,255,275,245
            ! Alt Tamb W22 COT TET Q
! PLOTBD          D1, 235,265,275,245,648
PERFOR  S1,0,0    D73,84-86,306,300,304,0,0,0,0,0,0
CODEND
DATA ITEMS////
! INTAKE
1 0.0          ! INTAKE ALTITUDE
2 0.0          ! ISA DEVIATION
3 0.0          ! MACH NO
4 0.9951       ! PRESSURE RECOVERY
! HP COMPRESSOR1
18   0.85      ! Z Parameter
19   1.0       ! Relative ND rotational Speed
20   7.11      ! Compressor Pressure Ratio
21   0.9       ! Isentropic Efficiency
22   0.0       ! Error Selection
23   5.0       ! Compressor Map Number
24   0.0       ! ANGLE
!  BLEEDING VALVE
25 0.04568         ! BLEEDING RATIO
26 0.0         ! MASS FLOW LOSS
27 1.0         ! PRESSURE FACTOR
28 0.0         ! PRESSURE LOSS
! HP COMPRESSOR2
29   0.85      ! Z Parameter
30   1.0       ! Relative ND rotational Speed
31   2.11      ! Compressor Pressure Ratio
32   0.88      ! Isentropic Efficiency
33   0.0       ! Error Selection
34   4.0       ! Compressor Map Number
35   0.0       ! ANGLE
!  TOTAL COOLING BLEED FOR HPT & LPT
SEALING
36 0.145        ! ROTORS COOLING
37 0.0         ! MASS FLOW LOSS
38 1.0         ! PRESSURE FACTOR
39 0.0         ! PRESSURE LOSS
!  SPLIT COOLING BLEED FOR LPT SEALING)
40 0.31       !% HPT SEALING AND % LPT
41 0.0        ! MASS FLOW LOSS
42 1.0        ! PRESSURE FACTOR
43 0.0        ! PRESSURE LOSS
! BURNER INTERNAL BYPASS COOLING
44 0.0         ! BYPASS RATIO
45 0.0         ! MASS FLOW LOSS
46 0.0         ! PRESSURE FACTOR
47 0.0         ! PRESSURE LOSS
!  BURNER
48    0.048    ! Fractional pressure Loss DP/P
49    0.9999   ! COMBUSTION EFFICIENCY
50   -1.0      ! FUEL FLOW
!  HP TURBINE
51 0.0         ! AUX.WORK
52 -1.0        ! REL NON-D MASS FLOW
53 -1.0        ! REL NON-D SPEED
54 0.8815        ! EFFICIENCY
55 -1.0        ! REL ROT.SPEED (COMP TURB=-1)
56 1.0         ! COMP NO. FROM LOW END
57 5.0         ! TURBINE MAP
58 -1.0        ! POWER LAW
59 0.0         ! NGV ANGLE RELATIVE TO D
!  PT INLET DUCT
69 0.0
70 0.02
71 0.0
72 0.0
!  POWER TURBINE
73 5619688.0   ! Auxiliary Work
74 0.8         ! Relative ND Mass Flow
75 0.6         ! Relative ND Rotational Speed
76 0.90        ! Isentropic efficiency
77 1.0         ! Relative Rotational Speed
78 0.0         ! Compressor number
79 4.0         ! Map Number
```

```
80 1000.0      ! Power Law index
81 -1.0        ! Compressor Work
82 0.0         ! NGV ANGLE RELATIVE TO DP ANGLE
! NOZCON
83   -1.0      ! THROAT AREA
! PERFOR
84    1.0      ! PROPELLER EFFICIENCY
85    0.0      ! SCALING INDEX
86    0.0      ! REQUIRED THRUST
!  ARITHY: HPC1 SPEED = HPC2 SPEED
120 5.0        ! COPY
121 -1.0
122 30.0       ! HPC2 SPEEDD
123 -1.0
124 19.0       ! HPC1 SPEED
!  ARITHY: HPT WORK = HPC1 WORK + HPC2
WORK
140 1.0         ! ADD
141 -1.0
142 147       ! HPT WORK
143 -1.0
144 302       ! HPC1 WORK
145 -1.0
146 303       ! HPC2 WORK
! ARITHY COPY D235=Tamb
230 5
231 -1
232 235
233 1
234 6
! ARITHY COPY D245=TET
240 5
241 -1
242 245
243 10
244 6
! ARITHY W2 IN Kg/s
250 11
251 -1
252 255
253 2
254 2
! ARITHY W4 IN Kg/s
260 11
261 -1
262 265
263 4
264 2
! ARITHY COPY 275=T8
270 5
271 -1
272 275
273 8
274 6
!**************************
! FOR EMMISION CALCULATION
!**************************
! ARITHY W7 IN Kg/s
330 11
331 -1
332 335
333 7
334 2
! ARITHY W8 IN Kg/s
340 11
341 -1
342 345
343 8
344 2
! ARITHY Wf=(W8-W7)
350 2
351 -1
352 357
353 -1
354 345
355 -1
356 335
! ARITHY COPY T7=365
360 5
361 -1
362 365
363 7
364 6
! ARITHY P7 in (Pa)
370 3
371 -1
372 378
373 7
374 4
375 -1
376 377
377 101325.0
!**************************
! ARITHY W2 IN Kg/s
500 11
501 -1
502 505
503 2
504 2
! ARITHY: (W2*SQRT T2)
515 15
516 -1
517 522
518 -1
519 505
520 2
521 6
! ARITHY: (W2*SQRT T2)/P2
523 4
524 -1
525 530
526 -1
527 522
528 2
529 4
! ARITHY W10 IN Kg/s
551 11
552 -1
553 556
554 10
555 2
! ARITHY: (W10*SQRT T10)
560 15
561 -1
562 567
563 -1
564 556
565 10
566 6
! ARITHY: (W10*SQRT T10)/P10
570 4
571 -1
572 577
573 -1
574 567
575 10
576 4
! ARITHY COPY 585=T15
580 5
581 -1
582 585
583 15
584 6
!**************************
! FOR Heat Output CALCULATION
```

```
!****************************
! ARITHY W15 IN Kg/s
600 11
601 -1
602 605
603 15
604 2
! ARITHY (W15*Cp)
610 3
611 -1
612 618
613 -1
614 605
615 -1
616 617
617 1150.0
! ARITHY (Tex-Tstack)
620 2
621 -1
622 628
623 15
624 6
625 -1
626 627
627 400.0
! ARITHY Q=W15*Cp*(Tex-Tout)
630 3
631 -1
632 637
633 -1
634 618
635 -1
636 628
! ARITHY Q IN MW
640 4
641 -1
642 648
643 -1
644 637
645 -1
646 647
647 1000000.0
! ARITHY W13 IN Kg/s
701 11
702 -1
703 706
704 13
705 2
! ARITHY: (W13*SQRT T13)
710 15
711 -1
712 717
713 -1
714 706
715 13
716 6
! ARITHY: (W13*SQRT T13)/P13
720 4
721 -1
722 727
723 -1
724 717
725 13
726 4
-1
1 2 27.04       ! INLET MASS FLOW
8 6 1308.92     ! COMBUSTION OUTLET
TEMPERATURE
-1
-3
```

E.1.3 Two-Spool Two-shaft SC Engine [IPT]

```
! TURBOMATCH MODEL DATA FILE FOR: AERO-
DERIVATIVE ENGINE DERIVED FROM CUAV 130
AIRCRAFT ENGINE
MODELLED BY ABDELMANAM ABAAD
////
OD SI KE VA FP
-1
-1
INTAKE S1, 2      D1-4            R300
COMPRE S2, 3      D5-11           R301 V5 V6
DUCTER S3, 4      D12 -15
COMPRE S4, 5      D18-24          R302 V18 V19
PREMAS S5, 21, 6   D25 -28
ARITHY          D120-124
COMPRE S6, 7      D29-35          R303 V29
PREMAS S7, 22, 8   D36 -39
PREMAS S22, 24, 23 D40 -43
PREMAS S8, 25, 9   D44 -47
BURNER S9, 10     D48-50          R304
MIXEES S10, 25, 11
MIXEES S11, 23, 12
ARITHY          D140-147
TURBIN S12, 13    D51 -58, 147, 59          V52
MIXEES S13, 24, 14
TURBIN S14, 15    D60 -67, 301, 68          V60 V61
NOZCON S15, 16, 1  D83            R306
ARITHY          D200-205
ARITHY          D230-235
ARITHY          D240-245
ARITHY          D250-255
ARITHY          D260-265
ARITHY          D270-275
!*************************
! FOR EMMISION CALCULATION
!*************************
ARITHY          D330-335
ARITHY          D340-345
ARITHY          D350-357
ARITHY          D360-365
ARITHY          D370-378
!*************************
ARITHY          D500-505
ARITHY          D510-518
ARITHY          D520-528
ARITHY          D530-537
ARITHY          D540-548
ARITHY          D600-605
ARITHY          D606-613
ARITHY          D614-621
ARITHY          D625-630
ARITHY          D631-638
ARITHY          D639-646
ARITHY          D650-655
ARITHY          D656-663
ARITHY          D664-671
ARITHY          D675-680
ARITHY          D681-688
ARITHY          D689-696
ARITHY          D700-705
ARITHY          D706-713
ARITHY          D714-721
ARITHY          D725-730
ARITHY          D731-738
ARITHY          D739-746
!             LPC HC1 HC2 HPT LPT Q
! PLOTBD          D621, 646,671,696,721,548
!             LPC W T7 COT TET HC1 HC2 HPT Q
! PLOTBD   D7, 227,245,275,235,646,671,696,548
!              W9 P9 T9 Wf Alt DT W COT TET
PLOTBD      D335, 378, 365, 357, 1, 2,255,275,235
PERFOR  S1,0,0     D60,84-
86,306,300,304,0,0,0,0,0,0
CODEND
DATA////
1    0.0      ! ALTITUDE
2    0.0      ! DEV FROM STAND TEMPERATURE
3    0.0      ! MACH NUMBER
4    0.9951   ! PRESSURE RECOVERY
! LP COMPRESSORE
5    0.75     ! Z PARAMETER
6    -1.0     ! Relative ND rotational Speed
7    2.0      ! Compressor Pressure Ratio
8    0.89     ! Isentropic Efficiency
9    0.0      ! Error Selection
10   5.0      ! Compressor Map Number
11   0.0      ! ANGLE
! DIFUSSER
12   0.0      ! Switch Set
13   0.0      ! Total pressure Loss/Inlet total Pressure
Dp/P
14   0.0      ! Combustion Efficiency
15   0.0      ! Limiting Value of Fuel Flow
! HP COMPRESSOR1
18   0.85     ! Z Parameter
19   1.0      ! Relative ND rotational Speed
20   7.11     ! Compressor Pressure Ratio
21   0.9      ! Isentropic Efficiency
22   0.0      ! Error Selection
23   5.0      ! Compressor Map Number
24   0.0      ! ANGLE
!  BLEEDING VALVE
25 0.04568    ! BLEEDING RATIO
26 0.0        ! MASS FLOW LOSS
27 1.0        ! PRESSURE FACTOR
28 0.0        ! PRESSURE LOSS
! HP COMPRESSOR2
29   0.85     ! Z Parameter
30   1.0      ! Relative ND rotational Speed
31   2.11     ! Compressor Pressure Ratio
32   0.88     ! Isentropic Efficiency
33   0.0      ! Error Selection
34   4.0      ! Compressor Map Number
35   0.0      ! ANGLE
!  TOTAL COOLING BLEED FOR HPT & LPT
SEALING
36 0.145       ! ROTORS COOLING
37 0.0        ! MASS FLOW LOSS
38 1.0        ! PRESSURE FACTOR
39 0.0        ! PRESSURE LOSS
!  SPLIT COOLING BLEED FOR LPT SEALING)
40 0.31      !% HPT SEALING AND % LPT
41 0.0       ! MASS FLOW LOSS
42 1.0       ! PRESSURE FACTOR
43 0.0       ! PRESSURE LOSS
! BURNER INTERNAL BYPASS COOLING
44 0.0        ! BYPASS RATIO
45 0.0        ! MASS FLOW LOSS
46 0.0        ! PRESSURE FACTOR
47 0.0        ! PRESSURE LOSS
!  BURNER
48    0.048    ! Fractional pressure Loss DP/P
49    0.9999   ! COMBUSTION EFFICIENCY
50   -1.0      ! FUEL FLOW
!  HP TURBINE
51 0.0        ! AUX.WORK
52 -1.0        ! REL NON-D MASS FLOW
53 -1.0        ! REL NON-D SPEED
54 0.90        ! EFFICIENCY
```

```
55 -1.0        ! REL ROT.SPEED (COMP TURB=-1)
56 2.0         ! COMP NO. FROM LOW END
57 5.0         ! TURBINE MAP
58 -1.0        ! POWER LAW
59 0.0         ! NGV ANGLE RELATIVE TO D
!  LP TURBINE
60 17256750.0   ! AUXILIARY WORK
61 -1.0        ! REL NON-D MASS FLOW
62 -1.0        ! REL NON-D SPEED
63 0.9053        ! ISENTROPIC EFFICIENCY
64 -1.0        ! REL ROT.SPEED
65 1.0         ! COMPRESSOR NUMBER
66 4.0         ! TURBINE MAP NUMBER
67 1000.0        ! POWER LOW INDEX
68 0.0         ! NGV ANGLE RELATIVE TO D.
! NOZCON
83   -1.0      ! THROAT AREA
! PERFOR
84    1.0      ! PROPELLER EFFICIENCY
85    0.0      ! SCALING INDEX
86    0.0      ! REQUIRED THRUST
!  ARITHY: HPC1 SPEED = HPC2 SPEED
120 5.0        ! COPY
121 -1.0
122 30.0        ! HPC2 SPEED
123 -1.0
124 19.0        ! HPC1 SPEED
!  ARITHY: HPT WORK = HPC1 WORK + HPC2
WORK
140 1.0         ! ADD
141 -1.0
142 147       ! HPT WORK
143 -1.0
144 302       ! HPC1 WORK
145 -1.0
146 303       ! HPC2 WORK
! ARITHY COPY T4=205
200 5! COPY
201 -1
202 205
203 4
204 6
! ARITHY COPY 235=T12
230 5
231 -1
232 235
233 12
234 6
! ARITHY COPY 245=T7
240 5
241 -1
242 245
243 7
244 6
! ARITHY W2 IN Kg/s
250 11
251 -1
252 255
253 2
254 2
! ARITHY W11 IN Kg/s
260 11
261 -1
262 265
263 11
264 2
! ARITHY COPY 275=T10
270 5
271 -1
272 275
273 10
274 6
!**************************
! FOR EMMISION CALCULATION
!**************************
! ARITHY W9 IN Kg/s
330 11
331 -1
332 335
333 9
334 2
! ARITHY W10 IN Kg/s
340 11
341 -1
342 345
343 10
344 2
! ARITHY Wf= (W10-W9)
350 2
351 -1
352 357
353 -1
354 345
355 -1
356 335
! ARITHY COPY T9=365
360 5
361 -1
362 365
363 9
364 6
! ARITHY P9 in (Pa)
370 3
371 -1
372 378
373 9
374 4
375 -1
376 377
377 101325.0
!**************************
! ARITHY W18 IN Kg/s
500 11
501 -1
502 505
503 18
504 2
! ARITHY (W18*Cp)
510 3
511 -1
512 518
513 -1
514 505
515 -1
516 517
517 1150.0
! ARITHY (Tex-Tout)
520 2
521 -1
522 528
523 18
524 6
525 -1
526 527
527 400.0
! ARITHY Q=W18*Cp*(Tex-Tout)
530 3
531 -1
532 537
533 -1
534 518
535 -1
536 528
! ARITHY Q IN MW
540 4
541 -1
```

```
542 548
543 -1
544 537
545 -1
546 547
547 1000000.0
! ARITHY W2 IN Kg/s
600 11
601 -1
602 605
603 2
604 2
! ARITHY: (W2*SQRT T2)
606 15
607 -1
608 613
609 -1
610 605
611 2
612 6
! ARITHY: (W2*SQRT T)/P2
614 4
615 -1
616 621
617 -1
618 613
619 2
620 4
! ARITHY W4 IN Kg/s
625 11
626 -1
627 630
628 4
629 2
! ARITHY: (W4*SQRT T4)
631 15
632 -1
633 638
634 -1
635 630
636 4
637 6
! ARITHY: (W4*SQRT T4)/P4
639 4
640 -1
641 646
642 -1
643 638
644 4
645 4
! ARITHY W6 IN Kg/s
650 11
651 -1
652 655
653 6
654 2
! ARITHY: (W6*SQRT T6)
656 15
657 -1
658 663
659 -1
660 655
661 6
662 6
! ARITHY: (W6*SQRT T6)/P6
664 4
665 -1
666 671
667 -1
668 663
669 6
670 4
! ARITHY W12 IN Kg/s
675 11
676 -1
677 680
678 12
679 2
! ARITHY: (W12*SQRT T12)
681 15
682 -1
683 688
684 -1
685 680
686 12
687 6
! ARITHY: (W12*SQRT T12)/P12
689 4
690 -1
691 696
692 -1
693 688
694 12
695 4
! ARITHY W14 IN Kg/s
700 11
701 -1
702 705
703 14
704 2
! ARITHY: (W14*SQRT T14)
706 15
707 -1
708 713
709 -1
710 705
711 14
712 6
! ARITHY: (W14*SQRT T14)/P14
714 4
715 -1
716 721
717 -1
718 713
719 14
720 4
! ARITHY W16 IN Kg/s
725 11
726 -1
727 730
728 16
729 2
! ARITHY: (W16*SQRT T16)
731 15
732 -1
733 738
734 -1
735 730
736 16
737 6
! ARITHY: (W16*SQRT T16)/P16
739 4
740 -1
741 746
742 -1
743 738
744 16
745 4
-1
1 2 48.45
10 6 1630.7256
-1
-3
```

E.1.4 Two-Spool Three-Shaft SC Engine [FPT]

```
! TURBOMATCH MODEL DATA FILE FOR: AERO-
DERIVATIVE ENGINE DERIVED FROM CUAV 130
AIRCRAFT ENGINE
MODELLED BY ABDELMANAM ABAAD
////
OD SI KE VA FP
-1
-1
INTAKE S1, 2      D1-4            R300
COMPRE S2, 3      D5-11           R301 V5 V6
DUCTER S3, 4      D12 -15
COMPRE S4, 5      D18-24          R302 V18 V19
PREMAS S5, 21, 6  D25 -28
ARITHY            D120-124
COMPRE S6, 7      D29-35          R303 V29
PREMAS S7, 22, 8  D36 -39
PREMAS S22, 24, 23 D40 -43
PREMAS S8, 25, 9  D44 -47
BURNER S9, 10     D48-50          R304
MIXEES S10, 25, 11
MIXEES S11, 23, 12
ARITHY            D140-147
TURBIN S12, 13    D51 -58, 147, 59          V52
MIXEES S13, 24, 14
TURBIN S14, 15    D60 -67, 301, 68          V61
DUCTER S15, 16    D69 -72
TURBIN S16, 17    D73-82              V73 V74
NOZCON S17, 18, 1 D83             R306
ARITHY            D200-205
ARITHY            D230-235
ARITHY            D240-245
ARITHY            D250-255
ARITHY            D260-265
ARITHY            D270-275
ARITHY            D280-285
!*****************************
! FOR EMMISION CALCULATION
!*****************************
ARITHY            D330-335
ARITHY            D340-345
ARITHY            D350-357
ARITHY            D360-365
ARITHY            D370-378
!*****************************
ARITHY            D379-384
ARITHY            D385-392
ARITHY            D393-400
ARITHY            D500-505
ARITHY            D515-522
ARITHY            D523-530
ARITHY            D551-556
ARITHY            D560-567
ARITHY            D570-577
ARITHY            D701-706
ARITHY            D710-717
ARITHY            D720-727
!*****************************
! FOR Heat Output CALCULATION
!*****************************
ARITHY            D600-605
ARITHY            D610-618
ARITHY            D620-628
ARITHY            D630-637
ARITHY            D640-648
!*****************************
!                 W18 Tex Tstack Q
PLOTBD            D605, 285,627,648
!                  W9 P9 T9 Wf Alt DT W COT TET
! PLOTBD       D335, 378, 365, 357, 1, 2,384,275,235
PERFOR  S1,0,0    D73,84-
86,306,300,304,0,0,0,0,0,0
CODEND
DATA////
1   0.0      ! ALTITUDE
2   0.0      ! DEV FROM STAND TEMPERATURE
3   0.0      ! MACH NUMBER
4   0.9951   ! PRESSURE RECOVERY
! LP COMPRESSORE
5   0.85     ! Z PARAMETER
6   -1.0     ! Relative ND rotational Speed
7   2.0      ! Compressor Pressure Ratio
8   0.89     ! Isentropic Efficiency
9   0.0      ! Error Selection
10  5.0      ! Compressor Map Number
11  0.0      ! ANGLE
! DIFUSSER
12  0.0      ! Switch Set
13  0.0      ! Total pressure Loss/Inlet total Pressure
Dp/P
14  0.0      ! Combustion Efficiency
15  0.0      ! Limiting Value of Fuel Flow
! HP COMPRESSOR1
18  0.85     ! Z Parameter
19  1.0      ! Relative ND rotational Speed
20  7.11     ! Compressor Pressure Ratio
21  0.9      ! Isentropic Efficiency
22  0.0      ! Error Selection
23  5.0      ! Compressor Map Number
24  0.0      ! ANGLE
!  BLEEDING VALVE
25 0.04568   ! BLEEDING RATIO
26 0.0       ! MASS FLOW LOSS
27 1.0       ! PRESSURE FACTOR
28 0.0       ! PRESSURE LOSS
! HP COMPRESSOR2
29  0.85     ! Z Parameter
30  1.0      ! Relative ND rotational Speed
31  2.11     ! Compressor Pressure Ratio
32  0.88     ! Isentropic Efficiency
33  0.0      ! Error Selection
34  4.0      ! Compressor Map Number
35  0.0      ! ANGLE
!  TOTAL COOLING BLEED FOR HPT & LPT
SEALING
36 0.145     ! ROTORS COOLING
37 0.0       ! MASS FLOW LOSS
38 1.0       ! PRESSURE FACTOR
39 0.0       ! PRESSURE LOSS
!  SPLIT COOLING BLEED FOR LPT SEALING)
40 0.31      !% HPT SEALING AND % LPT
41 0.0       ! MASS FLOW LOSS
42 1.0       ! PRESSURE FACTOR
43 0.0       ! PRESSURE LOSS
! BURNER INTERNAL BYPASS COOLING
44 0.0       ! BYPASS RATIO
45 0.0       ! MASS FLOW LOSS
46 0.0       ! PRESSURE FACTOR
47 0.0       ! PRESSURE LOSS
!  BURNER
48   0.048   ! Fractional pressure Loss DP/P
49   0.9999  ! COMBUSTION EFFICIENCY
50   -1.0    ! FUEL FLOW
!  HP TURBINE
51 0.0       ! AUX.WORK
52 -1.0      ! REL NON-D MASS FLOW
53 -1.0      ! REL NON-D SPEED
54 0.90      ! EFFICIENCY
55 -1.0      ! REL ROT.SPEED (COMP TURB=-1)
```

```
56 2.0        ! COMP NO. FROM LOW END
57 5.0        ! TURBINE MAP
58 -1.0       ! POWER LAW
59 0.0        ! NGV ANGLE RELATIVE TO D
!  LP TURBINE
60 0.0        ! AUXILIARY WORK
61 -1.0        ! REL NON-D MASS FLOW
62 -1.0        ! REL NON-D SPEED
63 0.91        ! ISENTROPIC EFFICIENCY
64 -1.0        ! REL ROT.SPEED
65 1.0        ! COMPRESSOR NUMBER
66 4.0        ! TURBINE MAP NUMBER
67 -1.0        ! POWER LOW INDEX
68 0.0        ! NGV ANGLE RELATIVE TO D.
!  PT INLET DUCT
69 0.0
70 0.02
71 0.0
72 0.0
!  POWER TURBINE
73 17256648.0! Auxiliary Work
74 0.8       ! Relative ND Mass Flow
75 0.6       ! Relative ND Rotational Speed
76 0.91      ! Isentropic efficiency
77 1.0       ! Relative Rotational Speed
78 0.0       ! Compressor number
79 4.0       ! Map Number
80 1000.0     ! Power Law index
81 -1.0       ! Compressor Work
82 0.0
! NOZCON
83   -1.0      ! THROAT AREA
! PERFOR
84    1.0      ! PROPELLER EFFICIENCY
85    0.0      ! SCALING INDEX
86    0.0      ! REQUIRED THRUST
!  ARITHY: HPC1 SPEED = HPC2 SPEED
120 5.0       ! COPY
121 -1.0
122 30.0       ! HPC2 SPEED
123 -1.0
124 19.0       ! HPC1 SPEED
!  ARITHY: HPT WORK = HPC1 WORK + HPC2
WORK
140 1.0        ! ADD
141 -1.0
142 147       ! HPT WORK
143 -1.0
144 302       ! HPC1 WORK
145 -1.0
146 303       ! HPC2 WORK
! ARITHY COPY T4=205
200 5! COPY
201 -1
202 205
203 4
204 6
! ARITHY COPY 235=TET
230 5
231 -1
232 235
233 12
234 6
! ARITHY COPY 245=T7
240 5
241 -1
242 245
243 7
244 6
! ARITHY W2 IN Kg/s
250 11
251 -1
252 255
253 2
254 2
! ARITHY W11 IN Kg/s
260 11
261 -1
262 265
263 11
264 2
! ARITHY COPY 275=COT
270 5
271 -1
272 275
273 10
274 6
! ARITHY COPY 285=Tex
280 5
281 -1
282 285
283 18
284 6
!*************************
! FOR EMMISION CALCULATION
!*************************
! ARITHY W9 IN Kg/s
330 11
331 -1
332 335
333 9
334 2
! ARITHY W10 IN Kg/s
340 11
341 -1
342 345
343 10
344 2
! ARITHY Wf= (W10-W9)
350 2
351 -1
352 357
353 -1
354 345
355 -1
356 335
! ARITHY COPY T9=365
360 5
361 -1
362 365
363 9
364 6
! ARITHY P9 in (Pa)
370 3
371 -1
372 378
373 9
374 4
375 -1
376 377
377 101325.0
!*****************************
! ARITHY W2 IN Kg/s
379 11
380 -1
381 384
382 2
383 2
! ARITHY: (W2*SQRT T2)
385 15
386 -1
387 392
388 -1
389 375
390 2
391 6
```

```
! ARITHY: (W2*SQRT T2)/P2
393 4
394 -1
395 400
396 -1
397 392
398 2
399 4
! ARITHY W4 IN Kg/s
500 11
501 -1
502 505
503 4
504 2
! ARITHY: (W4*SQRT T4)
515 15
516 -1
517 522
518 -1
519 505
520 4
521 6
! ARITHY: (W4*SQRT T4)/P4
523 4
524 -1
525 530
526 -1
527 522
528 4
529 4
! ARITHY W12 IN Kg/s
551 11
552 -1
553 556
554 12
555 2
! ARITHY: (W12*SQRT T12)
560 15
561 -1
562 567
563 -1
564 556
565 12
566 6
! ARITHY: (W12*SQRT T12)/P12
570 4
571 -1
572 577
573 -1
574 567
575 12
576 4
!**************************
! FOR Heat Output CALCULATION
!**************************
! ARITHY W18 IN Kg/s
600 11
601 -1
602 605
603 18
604 2
! ARITHY (W16*Cp)
610 3
611 -1
612 618
613 -1
614 605
615 -1
616 617
617 1150.0
! ARITHY (Tex-Tout)
620 2
621 -1
622 628
623 18
624 6
625 -1
626 627
627 400.0
! ARITHY W12*Cp*(Tex-Tout)
630 3
631 -1
632 637
633 -1
634 618
635 -1
636 628
! ARITHY Q IN MW
640 4
641 -1
642 648
643 -1
644 637
645 -1
646 647
647 1000000.0
!**************************
! ARITHY W14 IN Kg/s
701 11
702 -1
703 706
704 14
705 2
! ARITHY: (W14*SQRT T14)
710 15
711 -1
712 717
713 -1
714 706
715 14
716 6
! ARITHY: (W14*SQRT T14)/P14
720 4
721 -1
722 727
723 -1
724 717
725 14
726 4
-1
1 2 48.45
10 6 1630.7256
-1
-3
```

E.1.5 Two-Spool 2-Shaft I/C Engine [IPT]

```
! TURBOMATCH MODEL DATA FILE FOR: AERO-
DERIVATIVE ENGINE DERIVED FROM CUAV 130
AIRCRAFT ENGINE
MODELLED BY ABDELMANAM ABAAD
////
OD SI KE VA FP
-1
-1
INTAKE S1, 2      D1-4            R300
COMPRE S2, 3      D5-11           R301 V5 V6
DUCTER S3, 4      D12 -15
COMPRE S4, 5      D18-24          R302 V18 V19
PREMAS S5, 21, 6  D25 -28
ARITHY            D120-124
COMPRE S6, 7      D29-35          R303 V29
PREMAS S7, 22, 8  D36 -39
PREMAS S22, 24, 23 D40 -43
PREMAS S8, 25, 9  D44 -47
BURNER S9, 10     D48-50          R304
MIXEES S10, 25, 11
MIXEES S11, 23, 12
ARITHY            D140-147
TURBIN S12, 13    D51 -58, 147, 59          V52
MIXEES S13, 24, 14
TURBIN S14, 15    D60 -67, 301, 68          V60 V61
NOZCON S15, 16, 1 D83             R306
ARITHY            D210-215
ARITHY            D220-225
ARITHY            D230-235
ARITHY            D240-247
ARITHY            D250-257
ARITHY            D260-265
ARITHY            D270-275
ARITHY            D280-285
!*************************
! FOR EMMISION CALCULATION
!*************************
ARITHY            D330-335
ARITHY            D340-345
ARITHY            D350-357
ARITHY            D360-365
ARITHY            D370-378
!*************************
! FOR Exhaust Heat Q (MW) CAL
!*************************
ARITHY            D500-505
ARITHY            D510-518
ARITHY            D520-528
ARITHY            D530-537
ARITHY            D540-548
!*************************
ARITHY            D600-605
ARITHY            D606-613
ARITHY            D614-621
ARITHY            D625-630
ARITHY            D631-638
ARITHY            D639-646
ARITHY            D650-655
ARITHY            D656-663
ARITHY            D664-671
ARITHY            D675-680
ARITHY            D681-688
ARITHY            D689-696
ARITHY            D700-705
ARITHY            D706-713
ARITHY            D714-721
!               Wex Tex Tstack Q T4
PLOTBD            D505, 285,527,548,235
!          W9 P9 T9 Wf A D IADT COT TET
! PLOTBD D335, 378, 365, 357, 1, 2,247,265,275
!              Alt DT W Tam IADT ICDT COT TET
! PLOTBD       D1, 2,605,215,247,257,265,275
!                Tex LPC HC1 HC2 HPT LPT Q
! PLOTBD       D285, 621,646,671,696,721,548
PERFOR  S1,0,0    D60,84-
86,306,300,304,0,0,0,0,0,0
CODEND
DATA////
1   0.0          ! ALTITUDE
2   0.0          ! DEV FROM STAND TEMPERATURE
3   0.0          ! MACH NUMBER
4   0.9951       ! PRESSURE RECOVERY
! LP COMPRESSORE
5   0.85     ! Z PARAMETER
6   -1.0     ! Relative ND rotational Speed
7   3.5      ! Compressor Pressure Ratio
8   0.89     ! Isentropic Efficiency
9   0.0      ! Error Selection
10  5.0      ! Compressor Map Number
11  0.0      ! ANGLE
! INTERCOOLER (SPRINT)
12  2.0      ! Switch Set
13  0.03     ! Total pressure Loss/Inlet total Pressure
Dp/P
14  0.5      ! Combustion Efficiency
15  0.0      ! Limiting Value of Fuel Flow
! HP COMPRESSOR1
18  0.85     ! Z Parameter
19  0.85     ! Relative ND rotational Speed
20  7.11     ! Compressor Pressure Ratio
21  0.9      ! Isentropic Efficiency
22  0.0      ! Error Selection
23  5.0      ! Compressor Map Number
24  0.0      ! ANGLE
!  BLEEDING VALVE
25 0.04568    ! BLEEDING RATIO
26 0.0        ! MASS FLOW LOSS
27 1.0        ! PRESSURE FACTOR
28 0.0        ! PRESSURE LOSS
! HP COMPRESSOR2
29  0.85     ! Z Parameter
30  0.85     ! Relative ND rotational Speed
31  2.11     ! Compressor Pressure Ratio
32  0.88     ! Isentropic Efficiency
33  0.0      ! Error Selection
34  4.0      ! Compressor Map Number
35  0.0      ! ANGLE
!  TOTAL COOLING BLEED FOR HPT & LPT
SEALING
36 0.145      ! ROTORS COOLING
37 0.0        ! MASS FLOW LOSS
38 1.0        ! PRESSURE FACTOR
39 0.0        ! PRESSURE LOSS
!  SPLIT COOLING BLEED FOR LPT SEALING)
40 0.31      !% HPT SEALING AND % LPT
41 0.0       ! MASS FLOW LOSS
42 1.0       ! PRESSURE FACTOR
43 0.0       ! PRESSURE LOSS
! BURNER INTERNAL BYPASS COOLING
44 0.0        ! BYPASS RATIO
45 0.0        ! MASS FLOW LOSS
46 0.0        ! PRESSURE FACTOR
47 0.0        ! PRESSURE LOSS
!  BURNER
48   0.048    ! Fractional pressure Loss DP/P
49   0.9999   ! COMBUSTION EFFICIENCY
50   -1.0     ! FUEL FLOW
!  HP TURBINE
```

```
51 0.0        ! AUX.WORK
52 -1.0       ! REL NON-D MASS FLOW
53 -1.0       ! REL NON-D SPEED
54 0.90       ! EFFICIENCY
55 -1.0       ! REL ROT.SPEED (COMP TURB=-1)
56 2.0        ! COMP NO. FROM LOW END
57 5.0        ! TURBINE MAP
58 -1.0       ! POWER LAW
59 0.0        ! NGV ANGLE RELATIVE TO D
!  LP TURBINE
60 31268678.0  ! AUXILIARY WORK
61 -1.0       ! REL NON-D MASS FLOW
62 -1.0       ! REL NON-D SPEED
63 0.91       ! ISENTROPIC EFFICIENCY
64 -1.0       ! REL ROT.SPEED
65 1.0        ! COMPRESSOR NUMBER
66 4.0        ! TURBINE MAP NUMBER
67 1000.0        ! POWER LOW INDEX
68 0.0        ! NGV ANGLE RELATIVE TO D.
! NOZCON
83   -1.0      ! THROAT AREA
! PERFOR
84    1.0      ! PROPELLER EFFICIENCY
85    0.0      ! SCALING INDEX
86    0.0      ! REQUIRED THRUST
!  ARITHY: HPC1 SPEED = HPC2 SPEED
120 5.0       ! COPY
121 -1.0
122 30.0       ! HPC2 SPEEDD
123 -1.0
124 19.0       ! HPC1 SPEED
!  ARITHY: HPT WORK = HPC1 WORK + HPC2
WORK
140 1.0        ! ADD
141 -1.0
142 147      ! HPT WORK
143 -1.0
144 302      ! HPC1 WORK
145 -1.0
146 303      ! HPC2 WORK
! ARITHY COPY Tamb=215
210 5! COPY
211 -1
212 215
213 1
214 6
! ARITHY COPY T3=225
220 5! COPY
221 -1
222 225
223 3
224 6
! ARITHY COPY T4=235
230 5! COPY
231 -1
232 235
233 4
234 6
! ARITHY COPY IADT=(T4-Tamb)
240 2! COPY
241 -1
242 247
243 -1
244 235
245 1
246 6
! ARITHY COPY ICDT= (T3-T4)
250 2! COPY
251 -1
252 257
253 3
254 6
255 4
256 6
! ARITHY COPY COT=265
260 5! COPY
261 -1
262 265
263 10
264 6
! ARITHY COPY TET=275
270 5! COPY
271 -1
272 275
273 12
274 6
! ARITHY COPY Tex=285
280 5! COPY
281 -1
282 285
283 16
284 6
!*************************
! FOR EMMISION CALCULATION
!*************************
! ARITHY W9 IN Kg/s
330 11
331 -1
332 335
333 9
334 2
! ARITHY W10 IN Kg/s
340 11
341 -1
342 345
343 10
344 2
! ARITHY Wf=(W10-W9)
350 2
351 -1
352 357
353 -1
354 345
355 -1
356 335
! ARITHY COPY T9=365
360 5
361 -1
362 365
363 9
364 6
! ARITHY P9 in (Pa)
370 3
371 -1
372 378
373 9
374 4
375 -1
376 377
377 101325.0
!*****************************
! FOR Q (MW) Exhaust Heat CalcS
!*****************************
! ARITHY W16 IN Kg/s
500 11
501 -1
502 505
503 16
504 2
! ARITHY (W16*Cp)
510 3
511 -1
512 518
513 -1
514 505
515 -1
```

```
516 517
517 1150.0
! ARITHY (Tex-Tout)
520 2
521 -1
522 528
523 16
524 6
525 -1
526 527
527 400.0
! ARITHY Q=W16*Cp*(Tex-Tout)
530 3
531 -1
532 537
533 -1
534 518
535 -1
536 528
! ARITHY Q IN MW
540 4
541 -1
542 548
543 -1
544 537
545 -1
546 547
547 1000000.0
!*****************************
! ARITHY W2 IN Kg/s
600 11
601 -1
602 605
603 2
604 2
! ARITHY: (W2*SQRT T2)
606 15
607 -1
608 613
609 -1
610 605
611 2
612 6
! ARITHY: (W2*SQRT T)/P2
614 4
615 -1
616 621
617 -1
618 613
619 2
620 4
! ARITHY W4 IN Kg/s
625 11
626 -1
627 630
628 4
629 2
! ARITHY: (W4*SQRT T4)
631 15
632 -1
633 638
634 -1
635 630
636 4
637 6
! ARITHY: (W4*SQRT T4)/P4
639 4
640 -1
641 646
642 -1
643 638
644 4
645 4
! ARITHY W6 IN Kg/s
650 11
651 -1
652 655
653 6
654 2
! ARITHY: (W6*SQRT T6)
656 15
657 -1
658 663
659 -1
660 655
661 6
662 6
! ARITHY: (W6*SQRT T6)/P6
664 4
665 -1
666 671
667 -1
668 663
669 6
670 4
! ARITHY W12 IN Kg/s
675 11
676 -1
677 680
678 12
679 2
! ARITHY: (W12*SQRT T12)
681 15
682 -1
683 688
684 -1
685 680
686 12
687 6
! ARITHY: (W12*SQRT T12)/P12
689 4
690 -1
691 696
692 -1
693 688
694 12
695 4
! ARITHY W14 IN Kg/s
700 11
701 -1
702 705
703 14
704 2
! ARITHY: (W14*SQRT T14)
706 15
707 -1
708 713
709 -1
710 705
711 14
712 6
! ARITHY: (W14*SQRT T14)/P14
714 4
715 -1
716 721
717 -1
718 713
719 14
720 4
-1
4 6 358.993       ! Intercooler Outlet Temperature
1 2 82.2439      ! Inlet Mass Flow
10 6 1630.7256   ! Combustor Outlet Temperature
-1
-3
```

E.1.6 Two-Spool Three-Shaft I/C Engine [FPT]

```
! TURBOMATCH MODEL DATA FILE FOR: AERO-
DERIVATIVE ENGINE DERIVED FROM CUAV 130
AIRCRAFT ENGINE
MODELLED BY ABDELMANAM ABAAD
////
OD SI KE VA FP
-1
-1
INTAKE S1, 2       D1-4              R300
COMPRE S2, 3       D5-11             R301 V5 V6
DUCTER S3, 4       D12 -15
COMPRE S4, 5       D18-24            R302 V18 V19
PREMAS S5, 21, 6   D25 -28
ARITHY             D120-124
COMPRE S6, 7       D29-35            R303 V29
PREMAS S7, 22, 8   D36 -39
PREMAS S22, 24, 23 D40 -43
PREMAS S8, 25, 9   D44 -47
BURNER S9, 10      D48-50            R304
MIXEES S10, 25, 11
MIXEES S11, 23, 12
ARITHY             D140-147
TURBIN S12, 13     D51 -58, 147, 59          V52
MIXEES S13, 24, 14
TURBIN S14, 15     D60 -67, 301, 68          V61
DUCTER S15, 16     D69-72            R305
TURBIN S16, 17     D73-82                V73 V74
NOZCON S17, 18, 1  D83               R306
ARITHY             D210-215
ARITHY             D220-225
ARITHY             D230-235
ARITHY             D240-247
ARITHY             D250-257
ARITHY             D260-265
ARITHY             D270-275
ARITHY             D280-285
!*************************
! FOR EMMISION CALCULATION
!*************************
ARITHY             D330-335
ARITHY             D340-345
ARITHY             D350-357
ARITHY             D360-365
ARITHY             D370-378
!*************************
! FOR Exhaust Heat Q (MW) CAL
!*************************
ARITHY             D500-505
ARITHY             D510-518
ARITHY             D520-528
ARITHY             D530-537
ARITHY             D540-548
!*************************
ARITHY             D600-605
ARITHY             D606-613
ARITHY             D614-621
ARITHY             D625-630
ARITHY             D631-638
ARITHY             D639-646
ARITHY             D650-655
ARITHY             D656-663
ARITHY             D664-671
ARITHY             D675-680
ARITHY             D681-688
ARITHY             D689-696
ARITHY             D700-705
ARITHY             D706-713
ARITHY             D714-721
!                Wex Tex Tstack Q T4
PLOTBD             D505, 285,527,548,235
!                  W9 P9 T9 Wf A D IADT COT TET
! PLOTBD      D335, 378, 365, 357, 1, 2,247,265,275
!                Alt DT W Tam IADT ICDT COT TET
! PLOTBD             D1, 2,605,215,247,257,265,275
!                  Tex LPC HC1 HC2 HPT LPT Q
! PLOTBD             D285, 621,646,671,696,721,548
PERFOR  S1,0,0     D73,84-
86,306,300,304,0,0,0,0,0,0
CODEND
DATA////
1   0.0          ! ALTITUDE
2   0.0          ! DEV FROM STAND TEMPERATURE
3   0.0          ! MACH NUMBER
4   0.9951       ! PRESSURE RECOVERY
! LP COMPRESSORE
5   0.85     ! Z PARAMETER
6   0.9      ! Relative ND rotational Speed
7   3.5      ! Compressor Pressure Ratio
8   0.89     ! Isentropic Efficiency
9   0.0      ! Error Selection
10  5.0      ! Compressor Map Number
11  0.0      ! ANGLE
! INTERCOOLER (SPRINT)
12  2.0      ! Switch Set
13  0.03     ! Total pressure Loss/Inlet total Pressure
Dp/P
14  0.5      ! Combustion Efficiency
15  0.0      ! Limiting Value of Fuel Flow
! HP COMPRESSOR1
18  0.85     ! Z Parameter
19  0.85     ! Relative ND rotational Speed
20  7.11     ! Compressor Pressure Ratio
21  0.9      ! Isentropic Efficiency
22  0.0      ! Error Selection
23  5.0      ! Compressor Map Number
24  0.0      ! ANGLE
!  BLEEDING VALVE
25 0.04568    ! BLEEDING RATIO
26 0.0       ! MASS FLOW LOSS
27 1.0       ! PRESSURE FACTOR
28 0.0       ! PRESSURE LOSS
! HP COMPRESSOR2
29  0.85     ! Z Parameter
30  0.85     ! Relative ND rotational Speed
31  2.11     ! Compressor Pressure Ratio
32  0.88     ! Isentropic Efficiency
33  0.0      ! Error Selection
34  4.0      ! Compressor Map Number
35  0.0      ! ANGLE
!  TOTAL COOLING BLEED FOR HPT & LPT
SEALING
36 0.145      ! ROTORS COOLING
37 0.0       ! MASS FLOW LOSS
38 1.0       ! PRESSURE FACTOR
39 0.0       ! PRESSURE LOSS
!  SPLIT COOLING BLEED FOR LPT SEALING)
40 0.31      !% HPT SEALING AND % LPT
41 0.0       ! MASS FLOW LOSS
42 1.0       ! PRESSURE FACTOR
43 0.0       ! PRESSURE LOSS
! BURNER INTERNAL BYPASS COOLING
44 0.0       ! BYPASS RATIO
45 0.0       ! MASS FLOW LOSS
46 0.0       ! PRESSURE FACTOR
47 0.0       ! PRESSURE LOSS
!  BURNER
48   0.048   ! Fractional pressure Loss DP/P
49   0.9999  ! COMBUSTION EFFICIENCY
50  -1.0     ! FUEL FLOW
!  HP TURBINE
```

```
51 0.0        ! AUX.WORK
52 -1.0       ! REL NON-D MASS FLOW
53 -1.0       ! REL NON-D SPEED
54 0.90       ! EFFICIENCY
55 -1.0       ! REL ROT.SPEED (COMP TURB=-1)
56 2.0        ! COMP NO. FROM LOW END
57 5.0        ! TURBINE MAP
58 -1.0       ! POWER LAW
59 0.0        ! NGV ANGLE RELATIVE TO D
!  LP TURBINE
60 0.0   ! AUXILIARY WORK
61 -1.0        ! REL NON-D MASS FLOW
62 -1.0        ! REL NON-D SPEED
63 0.91        ! ISENTROPIC EFFICIENCY
64 -1.0        ! REL ROT.SPEED
65 1.0         ! COMPRESSOR NUMBER
66 5.0         ! TURBINE MAP NUMBER
67 -1.0        ! POWER LOW INDEX
68 0.0         ! NGV ANGLE RELATIVE TO D.
!  PT INLET DUCT
69 0.0
70 0.03
71 0.0
72 0.0
!  POWER TURBINE
73 31596822.0! Auxiliary Work
74 0.8        ! Relative ND Mass Flow
75 0.6        ! Relative ND Rotational Speed
76 0.92       ! Isentropic efficiency
77 1.0        ! Relative Rotational Speed
78 0.0        ! Compressor number
79 4.0        ! Map Number
80 1000.0     ! Power Law index
81 -1.0       ! Compressor Work
82 0.0        ! NGV ANGLE RELATIVE TO D
! NOZCON
83   -1.0      ! THROAT AREA
! PERFOR
84    1.0      ! PROPELLER EFFICIENCY
85    0.0      ! SCALING INDEX
86    0.0      ! REQUIRED THRUST
!  ARITHY: HPC1 SPEED = HPC2 SPEED
120 5.0       ! COPY
121 -1.0
122 30.0       ! HPC2 SPEEDD
123 -1.0
124 19.0       ! HPC1 SPEED
!  ARITHY: HPT WORK = HPC1 WORK + HPC2
WORK
140 1.0        ! ADD
141 -1.0
142 147      ! HPT WORK
143 -1.0
144 302      ! HPC1 WORK
145 -1.0
146 303      ! HPC2 WORK
! ARITHY COPY Tamb=215
210 5! COPY
211 -1
212 215
213 1
214 6
! ARITHY COPY T3=225
220 5! COPY
221 -1
222 225
223 3
224 6
! ARITHY COPY T4=235
230 5! COPY
231 -1
232 235
233 4
234 6
! ARITHY COPY IADT=(T4-Tamb)
240 2! COPY
241 -1
242 247
243 -1
244 235
245 1
246 6
! ARITHY COPY ICDT= (T3-T4)
250 2! COPY
251 -1
252 257
253 3
254 6
255 4
256 6
! ARITHY COPY COT=265
260 5! COPY
261 -1
262 265
263 10
264 6
! ARITHY COPY TET=275
270 5! COPY
271 -1
272 275
273 12
274 6
! ARITHY COPY Tex=285
280 5! COPY
281 -1
282 285
283 18
284 6
!*****************************************
! FOR EMMISION CALCULATION
!*****************************************
! ARITHY W9 IN Kg/s
330 11
331 -1
332 335
333 9
334 2
! ARITHY W10 IN Kg/s
340 11
341 -1
342 345
343 10
344 2
! ARITHY Wf=(W10-W9)
350 2
351 -1
352 357
353 -1
354 345
355 -1
356 335
! ARITHY COPY T9=365
360 5
361 -1
362 365
363 9
364 6
! ARITHY P9 in (Pa)
370 3
371 -1
372 378
373 9
374 4
375 -1
376 377
377 101325.0
```

```
!************************************
*****
! FOR Q (MW) Exhaust Heat
Calcs
!************************************
*****
! ARITHY W18 IN Kg/s
500 11
501 -1
502 505
503 18
504 2
! ARITHY (W18*Cp)
510 3
511 -1
512 518
513 -1
514 505
515 -1
516 517
517 1150.0
! ARITHY (Tex-Tout)
520 2
521 -1
522 528
523 18
524 6
525 -1
526 527
527 400.0
! ARITHY Q=W18*Cp*(Tex-Tout)
530 3
531 -1
532 537
533 -1
534 518
535 -1
536 528
! ARITHY Q IN MW
540 4
541 -1
542 548
543 -1
544 537
545 -1
546 547
547 1000000.0
!************************
! ARITHY W2 IN Kg/s
600 11
601 -1
602 605
603 2
604 2
! ARITHY: (W2*SQRT T2)
606 15
607 -1
608 613
609 -1
610 605
611 2
612 6
! ARITHY: (W2*SQRT T)/P2
614 4
615 -1
616 621
617 -1
618 613
619 2
620 4
! ARITHY W4 IN Kg/s
625 11
626 -1
627 630
628 4
629 2
! ARITHY: (W4*SQRT T4)
631 15
632 -1
633 638
634 -1
635 630
636 4
637 6
! ARITHY: (W4*SQRT T4)/P4
639 4
640 -1
641 646
642 -1
643 638
644 4
645 4
! ARITHY W6 IN Kg/s
650 11
651 -1
652 655
653 6
654 2
! ARITHY: (W6*SQRT T6)
656 15
657 -1
658 663
659 -1
660 655
661 6
662 6
! ARITHY: (W6*SQRT T6)/P6
664 4
665 -1
666 671
667 -1
668 663
669 6
670 4
! ARITHY W12 IN Kg/s
675 11
676 -1
677 680
678 12
679 2
! ARITHY: (W12*SQRT T12)
681 15
682 -1
683 688
684 -1
685 680
686 12
687 6
! ARITHY: (W12*SQRT T12)/P12
689 4
690 -1
691 696
692 -1
693 688
694 12
695 4
! ARITHY W14 IN Kg/s
700 11
701 -1
702 705
703 14
704 2
! ARITHY: (W14*SQRT T14)
706 15
707 -1
708 713
709 -1
710 705
711 14
712 6
! ARITHY: (W14*SQRT T14)/P14
714 4
715 -1
716 721
717 -1
718 713
719 14
720 4
-1
4 6 358.993      ! Intercooler
Outlet Temperature
1 2 82.2439      ! Inlet Mass Flow
10 6 1630.7256   ! Combustor
Outlet Temperature
-1
-3
```

E.1.7 Single-Spool 1ShConv-[HE] [IPT] GT Engine

```
! TURBOMATCH MODEL DATA FILE FOR: AERO-
DERIVATIVE ENGINE DERIVED FROM CUAV 130
AIRCRAFT ENGINE
MODELLED BY ABDELMANAM ABAAD
////
OD SI KE VA FP
-1
-1
INTAKE S1, 2      D1-4            R300
COMPRE S2, 3      D18-24          R302 V18 V19
PREMAS S3, 21, 4   D25 -28
ARITHY            D120-124
COMPRE S4, 5      D29-35          R303 V29
PREMAS S5, 22, 6   D36 -39
PREMAS S22, 24, 23 D40 -43
HETCOL S6, 7      D90 -93
PREMAS S7, 25, 8   D44 -47
BURNER S8, 9      D48-50          R304
MIXEES S9, 25, 10
MIXEES S10, 23, 11
ARITHY            D140-147
TURBIN S11, 12    D51 -58, 147, 59        V51 V52
HETHOT S6, 12, 13 D95 -98
NOZCON S13, 14, 1 D83             R306
ARITHY            D230-235
ARITHY            D240-245
ARITHY            D250-255
ARITHY            D260-265
ARITHY            D270-275
ARITHY            D280-285
ARITHY            D290-295
!**************************
! FOR EMMISION CALCULATION
!**************************
ARITHY            D330-335
ARITHY            D340-345
ARITHY            D350-357
ARITHY            D360-365
ARITHY            D370-378
!**************************
ARITHY            D500-505
ARITHY            D515-522
ARITHY            D523-530
ARITHY            D551-556
ARITHY            D560-567
ARITHY            D570-577
ARITHY            D580-585
!**************************
!FOR Exhaust Heat Q(MW) CAL
!**************************
ARITHY            D600-605
ARITHY            D610-618
ARITHY            D620-628
ARITHY            D630-637
ARITHY            D640-648
!**************************
!                Wex Tex Tstack Q HETin DHEC
PLOTBD             D605, 585,627,648,275,297
!               Wc Pc Tc Wf Alt DT W COT TET
! PLOTBD   D335, 378, 365, 357, 1, 2,215,255,265
!               COT TET T15 Tex HC1 HPT Q DHEC
! PLOTBD          D255, 265,275,285,530,577,648,297
!               COT TET T12 Tex Q DHEC
! PLOTBD             D255, 265,275,285,648,295
PERFOR  S1,0,0    D51,84-86,306,300,304,0,0,0,0,0,0
CODEND
DATA ITEMS////
! INTAKE
1 0.0         ! INTAKE ALTITUDE
2 0.0         ! ISA DEVIATION
3 0.0         ! MACH NO
4 0.9951      ! PRESSURE RECOVERY
! HP COMPRESSOR1
18   0.85     ! Z Parameter
19   -1.0     ! Relative ND rotational Speed
20   7.11     ! Compressor Pressure Ratio
21   0.9      ! Isentropic Efficiency
22   0.0      ! Error Selection
23   5.0      ! Compressor Map Number
24   0.0      ! ANGLE
!  BLEEDING VALVE
25 0.04568     ! BLEEDING RATIO
26 0.0        ! MASS FLOW LOSS
27 0.0        ! PRESSURE FACTOR
28 0.0        ! PRESSURE LOSS
! HP COMPRESSOR2
29   0.85     ! Z Parameter
30   -1.0     ! Relative ND rotational Speed
31   2.11     ! Compressor Pressure Ratio
32   0.88     ! Isentropic Efficiency
33   0.0      ! Error Selection
34   4.0      ! Compressor Map Number
35   0.0      ! ANGLE
!  TOTAL COOLING BLEED FOR HPT & LPT
SEALING
36 0.145       ! ROTORS COOLING
37 0.0        ! MASS FLOW LOSS
38 1.0        ! PRESSURE FACTOR
39 0.0        ! PRESSURE LOSS
!  SPLIT COOLING BLEED FOR LPT SEALING)
40 0.31       !% HPT SEALING AND % LPT
41 0.0        ! MASS FLOW LOSS
42 0.0        ! PRESSURE FACTOR
43 0.0        ! PRESSURE LOSS
! BURNER INTERNAL BYPASS COOLING
44 0.0        ! BYPASS RATIO
45 0.0        ! MASS FLOW LOSS
46 0.0        ! PRESSURE FACTOR
47 0.0        ! PRESSURE LOSS
!  BURNER
48    0.048    ! Fractional pressure Loss DP/P
49    0.9999   ! COMBUSTION EFFICIENCY
50   -1.0      ! FUEL FLOW
!  HP TURBINE
51 5242601.0    ! AUX.WORK
52 -1.0       ! REL NON-D MASS FLOW
53 -1.0       ! REL NON-D SPEED
54 0.90       ! EFFICIENCY
55 -1.0       ! REL ROT.SPEED (COMP TURB=-1)
56 1.0        ! COMP NO. FROM LOW END
57 5.0        ! TURBINE MAP
58 1000.0     ! POWER LAW
59 0.0        ! NGV ANGLE RELATIVE TO D
! HETCOL
90 0.02
91 0.9
92 3.0
93 0.0
! HETHOT
95 0.03
96 0.9
97 3.0
98 0.0
! NOZCON
83   -1.0     ! THROAT AREA
! PERFOR
84    1.0     ! PROPELLER EFFICIENCY
85    0.0     ! SCALING INDEX
```

```
86    0.0       ! REQUIRED THRUST
!  ARITHY: HPC1 SPEED = HPC2 SPEED
120 5.0        ! COPY
121 -1.0
122 30.0       ! HPC2 SPEEDD
123 -1.0
124 19.0       ! HPC1 SPEED
!  ARITHY: HPT WORK = HPC1 WORK + HPC2
WORK
140 1.0        ! ADD
141 -1.0
142 147      ! HPT WORK
143 -1.0
144 302      ! HPC1 WORK
145 -1.0
146 303      ! HPC2 WORK
! ARITHY COPY D205=Tamb
200 5
201 -1
202 205
203 1
204 6
! ARITHY W2 IN Kg/s
210 11
211 -1
212 215
213 2
214 2
! ARITHY COPY Wb=(W3-W4)
220 2
221 -1
222 227
223 3
224 2
225 4
226 2
! ARITHY COPY D245=COLD HE Tin
230 5
231 -1
232 235
233 6
234 6
! ARITHY COPY D255=COLD HE Tout
240 5
241 -1
242 245
243 7
244 6
! ARITHY COPY D265=COT
250 5
251 -1
252 255
253 9
254 6
! ARITHY COPY D275=TET
260 5
261 -1
262 265
263 10
264 6
! ARITHY COPY D285=HOT HE Tin
270 5
271 -1
272 275
273 12
274 6
! ARITHY COPY D295=HOT HE Tout
280 5
281 -1
282 285
283 13
284 6
! ARITHY DHEC=D297=(HE Tin-HPC Tout)
290 2.0! Sub
291 -1
292 297
293 12
294 6
295 6
296 6
!**************************
! FOR EMMISION CALCULATION
!**************************
! ARITHY W8 IN Kg/s
330 11
331 -1
332 335
333 8
334 2
! ARITHY W9 IN Kg/s
340 11
341 -1
342 345
343 9
344 2
! ARITHY Wf=(W9-W8)
350 2
351 -1
352 357
353 -1
354 345
355 -1
356 335
! ARITHY COPY T8=365
360 5
361 -1
362 365
363 8
364 6
! ARITHY P8 in (Pa)
370 3
371 -1
372 378
373 8
374 4
375 -1
376 377
377 101325.0
!**************************
! ARITHY W2 IN Kg/s
500 11
501 -1
502 505
503 2
504 2
! ARITHY: (W2*SQRT T2)
515 15
516 -1
517 522
518 -1
519 505
520 2
521 6
! ARITHY: (W2*SQRT T2)/P2
523 4
524 -1
525 530
526 -1
527 522
528 2
529 4
! ARITHY W11 IN Kg/s
551 11
552 -1
553 556
554 11
```

```
555 2
! ARITHY: (W11*SQRT T11)
560 15
561 -1
562 567
563 -1
564 556
565 11
566 6
! ARITHY: (W11*SQRT T11)/P11
570 4
571 -1
572 577
573 -1
574 567
575 11
576 4
! ARITHY COPY 585=Tex
580 5
581 -1
582 585
583 14
584 6
!*****************************
! FOR Q (MW) Exhaust Heat CalcS
!*****************************
! ARITHY W14 IN Kg/s
600 11
601 -1
602 605
603 14
604 2
! ARITHY (W14*Cp)
610 3
611 -1
612 618
613 -1
614 605
615 -1
616 617
617 1150.0
! ARITHY (Tex-Tout)
620 2
621 -1
622 628
623 14
624 6
625 -1
626 627
627 400.0
! ARITHY Q=W14*Cp*(Tex-Tout)
630 3
631 -1
632 637
633 -1
634 618
635 -1
636 628
! ARITHY Q IN MW
640 4
641 -1
642 648
643 -1
644 637
645 -1
646 647
647 1000000.0
-1
1 2 27.04       ! INLET MASS FLOW
9 6 1308.92     ! COMBUSTION OUTLET
TEMPERATURE
-1
-3
```

E.1.8 Single-Spool 2Sh Conv-[HE] [FPT] GT Engine

```
! TURBOMATCH MODEL DATA FILE FOR: AERO-
DERIVATIVE ENGINE DERIVED FROM CUAV 130
AIRCRAFT ENGINE
MODELLED BY ABDELMANAM ABAAD
////
OD SI KE VA FP
-1
-1
INTAKE S1, 2      D1-4            R300
COMPRE S2, 3      D18-24          R302 V18 V19
PREMAS S3, 21, 4   D25 -28
ARITHY            D120-124
COMPRE S4, 5      D29-35          R303 V29
PREMAS S5, 22, 6   D36 -39
PREMAS S22, 24, 23 D40 -43
HETCOL S6, 7      D90 -93
PREMAS S7, 25, 8   D44 -47
BURNER S8, 9      D48-50          R304
MIXEES S9, 25, 10
MIXEES S10, 23, 11
ARITHY            D140-147
TURBIN S11, 12    D51 -58, 147, 59        V52
DUCTER S12, 13    D69-72          R305
MIXEES S13, 24, 14
TURBIN S14, 15    D73-82              V73 V74
HETHOT S6, 15, 16 D95 -98
NOZCON S16, 17, 1 D83             R306
ARITHY            D200-205
ARITHY            D210-215
ARITHY            D220-227
ARITHY            D230-235
ARITHY            D240-245
ARITHY            D250-255
ARITHY            D260-265
ARITHY            D270-275
ARITHY            D280-285
ARITHY            D290-297
!**************************
! FOR EMMISION CALCULATION
!**************************
ARITHY            D330-335
ARITHY            D340-345
ARITHY            D350-357
ARITHY            D360-365
ARITHY            D370-378
!**************************
ARITHY            D500-505
ARITHY            D515-522
ARITHY            D523-530
ARITHY            D551-556
ARITHY            D560-567
ARITHY            D570-577
ARITHY            D580-585
!**************************
! FOR Exhaust Heat Q(MW) CAL
!**************************
ARITHY            D600-605
ARITHY            D610-618
ARITHY            D620-628
ARITHY            D630-637
ARITHY            D640-648
!**************************
!                 Wex Tex Tstack Q HETin DHEC
PLOTBD             D605, 585,627,648,275,297
!                Wc Pc Tc Wf Alt DT W COT TET
! PLOTBD    D335, 378, 365, 357, 1, 2,215,255,265
!                COT TET T15 Tex HC1 HPT Q DHEC
! PLOTBD     D255, 265,275,285,530,577,648,297
!              Alt DT COT TET T15 Tex Q DHEC Wb
! PLOTBD        D1, 2,255,265,275,285,648,297,227
PERFOR  S1,0,0    D73,84-86,306,300,304,0,0,0,0,0,0
CODEND
DATA ITEMS////
! INTAKE
1 0.0          ! INTAKE ALTITUDE
2 0.0          ! ISA DEVIATION
3 0.0          ! MACH NO
4 0.9951       ! PRESSURE RECOVERY
! HP COMPRESSOR1
18   0.85      ! Z Parameter
19   -1.0      ! Relative ND rotational Speed
20   7.11      ! Compressor Pressure Ratio
21   0.9       ! Isentropic Efficiency
22   0.0       ! Error Selection
23   5.0       ! Compressor Map Number
24   0.0       ! ANGLE
!  BLEEDING VALVE
25 0.04568      ! BLEEDING RATIO
26 0.0         ! MASS FLOW LOSS
27 0.0         ! PRESSURE FACTOR
28 0.0         ! PRESSURE LOSS
! HP COMPRESSOR2
29   0.85      ! Z Parameter
30   1.0       ! Relative ND rotational Speed
31   2.11      ! Compressor Pressure Ratio
32   0.88      ! Isentropic Efficiency
33   0.0       ! Error Selection
34   4.0       ! Compressor Map Number
35   0.0       ! ANGLE
!  TOTAL COOLING BLEED FOR HPT & LPT
SEALING
36 0.145        ! ROTORS COOLING
37 0.0         ! MASS FLOW LOSS
38 1.0         ! PRESSURE FACTOR
39 0.0         ! PRESSURE LOSS
!  SPLIT COOLING BLEED FOR LPT SEALING)
40 0.31       !% HPT SEALING AND % LPT
41 0.0        ! MASS FLOW LOSS
42 0.0        ! PRESSURE FACTOR
43 0.0        ! PRESSURE LOSS
! BURNER INTERNAL BYPASS COOLING
44 0.0         ! BYPASS RATIO
45 0.0         ! MASS FLOW LOSS
46 0.0         ! PRESSURE FACTOR
47 0.0         ! PRESSURE LOSS
!  BURNER
48    0.048    ! Fractional pressure Loss DP/P
49    0.9999   ! COMBUSTION EFFICIENCY
50   -1.0      ! FUEL FLOW
!  HP TURBINE
51   0.0       ! AUX.WORK
52 -1.0        ! REL NON-D MASS FLOW
53 -1.0        ! REL NON-D SPEED
54 0.90        ! EFFICIENCY
55 -1.0        ! REL ROT.SPEED (COMP TURB=-1)
56 1.0         ! COMP NO. FROM LOW END
57 5.0         ! TURBINE MAP
58 -1.0      ! POWER LAW
59 0.0         ! NGV ANGLE RELATIVE TO D
!  PT INLET DUCT
69 0.0
70 0.03
71 0.0
72 0.0
!  POWER TURBINE
73 5607600.0! Auxiliary Work
74 0.8       ! Relative ND Mass Flow
75 0.6       ! Relative ND Rotational Speed
```

```
76 0.91    ! Isentropic efficiency
77 1.0     ! Relative Rotational Speed
78 0.0     ! Compressor number
79 4.0     ! Map Number
80 1000.0    ! Power Law index
81 -1.0     ! Compressor Work
82 0.0     ! NGV ANGLE RELATIVE TO D
! HETCOL
90 0.02
91 0.9
92 3.0
93 0.0
! HETHOT
95 0.03
96 0.9
97 3.0
98 0.0
! NOZCON
83   -1.0     ! THROAT AREA
! PERFOR
84    1.0     ! PROPELLER EFFICIENCY
85    0.0     ! SCALING INDEX
86    0.0     ! REQUIRED THRUST
!  ARITHY: HPC1 SPEED = HPC2 SPEED
120 5.0       ! COPY
121 -1.0
122 30.0       ! HPC2 SPEEDD
123 -1.0
124 19.0       ! HPC1 SPEED
!  ARITHY: HPT WORK = HPC1 WORK + HPC2
WORK
140 1.0        ! ADD
141 -1.0
142 147      ! HPT WORK
143 -1.0
144 302      ! HPC1 WORK
145 -1.0
146 303      ! HPC2 WORK
! ARITHY COPY D205=Tamb
200 5
201 -1
202 205
203 1
204 6
! ARITHY W2 IN Kg/s
210 11
211 -1
212 215
213 2
214 2
! ARITHY COPY Wb=(W3-W4)
220 2
221 -1
222 227
223 3
224 2
225 4
226 2
! ARITHY COPY D245=COLD HE Tin
230 5
231 -1
232 235
233 6
234 6
! ARITHY COPY D255=COLD HE Tout
240 5
241 -1
242 245
243 7
244 6
! ARITHY COPY D265=COT
250 5
251 -1
252 255
253 9
254 6
! ARITHY COPY D275=TET
260 5
261 -1
262 265
263 11
264 6
! ARITHY COPY D285=HOT HE Tin
270 5
271 -1
272 275
273 15
274 6
! ARITHY COPY D295=HOT HE Tout
280 5
281 -1
282 285
283 16
284 6
! ARITHY DHEC=D297=(HE Tin-HPC Tout)
290 2! Subtract
291 -1
292 297
293 15
294 6
295 6
296 6
!**************************
!FOR EMMISION CALCULATION
!**************************
! ARITHY W8 IN Kg/s
330 11
331 -1
332 335
333 8
334 2
! ARITHY W9 IN Kg/s
340 11
341 -1
342 345
343 9
344 2
! ARITHY Wf=(W9-W8)
350 2
351 -1
352 357
353 -1
354 345
355 -1
356 335
! ARITHY COPY T8=365
360 5
361 -1
362 365
363 8
364 6
! ARITHY P8 in (Pa)
370 3
371 -1
372 378
373 8
374 4
375 -1
376 377
377 101325.0
!**************************
! ARITHY W2 IN Kg/s
500 11
501 -1
502 505
503 2
```

```
504 2
! ARITHY: (W2*SQRT T2)
515 15
516 -1
517 522
518 -1
519 505
520 2
521 6
! ARITHY: (W2*SQRT T2)/P2
523 4
524 -1
525 530
526 -1
527 522
528 2
529 4
! ARITHY W11 IN Kg/s
551 11
552 -1
553 556
554 11
555 2
! ARITHY: (W11*SQRT T11)
560 15
561 -1
562 567
563 -1
564 556
565 11
566 6
! ARITHY: (W11*SQRT T11)/P11
570 4
571 -1
572 577
573 -1
574 567
575 11
576 4
! ARITHY COPY 585=Tex
580 5
581 -1
582 585
583 16
584 6
!*****************************
! FOR Q (MW) Exhaust Heat CalcS
!*****************************
! ARITHY W16 IN Kg/s
600 11
601 -1
602 605
603 16
604 2
! ARITHY (W16*Cp)
610 3
611 -1
612 618
613 -1
614 605
615 -1
616 617
617 1150.0
! ARITHY (Tex-Tout)
620 2
621 -1
622 628
623 16
624 6
625 -1
626 627
627 400.0
! ARITHY Q=W16*Cp*(Tex-Tout)
630 3
631 -1
632 637
633 -1
634 618
635 -1
636 628
! ARITHY Q IN MW
640 4
641 -1
642 648
643 -1
644 637
645 -1
646 647
647 1000000.0
-1
1 2 27.04       ! INLET MASS FLOW
9 6 1308.92     ! COMBUSTION OUTLET
TEMPERATURE
-1
-3
```

E.1.9 Single Spool 2Sh non-Conv [HE] [FPT] GT Engine

```
! TURBOMATCH MODEL DATA FILE FOR: AERO-
DERIVATIVE ENGINE DERIVED FROM CUAV 130
AIRCRAFT ENGINE
MODELLED BY ABDELMANAM ABAAD
////
OD SI KE VA FP
-1
-1
INTAKE S1, 2      D1-4            R300
COMPRE S2, 3      D18-24          R302 V18 V19
PREMAS S3, 21, 4   D25 -28
ARITHY            D120-124
COMPRE S4, 5      D29-35          R303 V29
PREMAS S5, 22, 6   D36 -39
PREMAS S22, 24, 23 D40 -43
HETCOL S6, 7 D90 -93
PREMAS S7, 25, 8   D44 -47
BURNER S8, 9      D48-50          R304
MIXEES S9, 25, 10
MIXEES S10, 23, 11
ARITHY            D140-147
TURBIN S11, 12 D51 -58, 147, 59         V52
HETHOT S6, 12, 13 D95 -98
DUCTER S13, 14 D69 -72
MIXEES S14, 24, 15
TURBIN S15, 16    D73-82              V73 V74
NOZCON S16, 17, 1 D83             R306
ARITHY            D200-205
ARITHY            D210-215
ARITHY            D220-227
ARITHY            D230-235
ARITHY            D240-245
ARITHY            D250-255
ARITHY            D260-265
ARITHY            D270-275
ARITHY            D280-285
ARITHY            D290-297
!**************************
! FOR EMMISION CALCULATION
!**************************
ARITHY            D330-335
ARITHY            D340-345
ARITHY            D350-357
ARITHY            D360-365
ARITHY            D370-378
!**************************
ARITHY            D500-505
ARITHY            D515-522
ARITHY            D523-530
ARITHY            D551-556
ARITHY            D560-567
ARITHY            D570-577
ARITHY            D580-585
!**************************
!FOR Exhaust Heat Q(MW) CAL
!**************************
ARITHY            D600-605
ARITHY            D610-618
ARITHY            D620-628
ARITHY            D630-637
ARITHY            D640-648
!**************************
!                 Wex Tex Tsk Q HETin DHEC
PLOTBD            D605, 585,627,648,275,297
!                Wc Pc Tc Wf Alt DT W COT TET
! PLOTBD          D335, 378, 365, 357, 1,
2,215,255,265
!                COT TET T12 Tex HC1 HPT Q DHEC
! PLOTBD          D255, 265,275,285,530,577,648,297
!                Alt DT COT TET T15 Tex Q DHEC Wb
! PLOTBD          D1, 2,255,265,275,285,648,297,227
PERFOR  S1,0,0    D73,84-86,306,300,304,0,0,0,0,0,0
CODEND
DATA ITEMS////
! INTAKE
1 0.0         ! INTAKE ALTITUDE
2 0.0         ! ISA DEVIATION
3 0.0         ! MACH NO
4 0.9951      ! PRESSURE RECOVERY
! HP COMPRESSOR1
18   0.85     ! Z Parameter
19   1.0      ! Relative ND rotational Speed
20   7.11     ! Compressor Pressure Ratio
21   0.9      ! Isentropic Efficiency
22   0.0      ! Error Selection
23   5.0      ! Compressor Map Number
24   0.0      ! ANGLE
!  BLEEDING VALVE
25 0.04568     ! BLEEDING RATIO
26 0.0         ! MASS FLOW LOSS
27 0.0         ! PRESSURE FACTOR
28 0.0         ! PRESSURE LOSS
! HP COMPRESSOR2
29   0.85     ! Z Parameter
30   1.0      ! Relative ND rotational Speed
31   2.11     ! Compressor Pressure Ratio
32   0.88     ! Isentropic Efficiency
33   0.0      ! Error Selection
34   4.0      ! Compressor Map Number
35   0.0      ! ANGLE
!  TOTAL COOLING BLEED FOR HPT & LPT
SEALING
36 0.145       ! ROTORS COOLING
37 0.0         ! MASS FLOW LOSS
38 1.0         ! PRESSURE FACTOR
39 0.0         ! PRESSURE LOSS
!  SPLIT COOLING BLEED FOR LPT SEALING)
40 0.31       !% HPT SEALING AND % LPT
41 0.0        ! MASS FLOW LOSS
42 0.0        ! PRESSURE FACTOR
43 0.0        ! PRESSURE LOSS
! BURNER INTERNAL BYPASS COOLING
44 0.0         ! BYPASS RATIO
45 0.0         ! MASS FLOW LOSS
46 0.0         ! PRESSURE FACTOR
47 0.0         ! PRESSURE LOSS
!  BURNER
48    0.048    ! Fractional pressure Loss DP/P
49    0.9999   ! COMBUSTION EFFICIENCY
50   -1.0      ! FUEL FLOW
!  HP TURBINE
51 0.0         ! AUX.WORK
52 -1.0        ! REL NON-D MASS FLOW
53 -1.0        ! REL NON-D SPEED
54 0.90        ! EFFICIENCY
55 -1.0        ! REL ROT.SPEED (COMP TURB=-1)
56 1.0         ! COMP NO. FROM LOW END
57 5.0         ! TURBINE MAP
58 -1.0        ! POWER LAW
59 0.0         ! NGV ANGLE RELATIVE TO D
!  PT INLET DUCT
69 0.0
70 0.02
71 0.0
72 0.0
!  POWER TURBINE
73 4384399.5! Auxiliary Work
74 0.8     ! Relative ND Mass Flow
```

```
75 0.6      ! Relative ND Rotational Speed
76 0.91     ! Isentropic efficiency
77 1.0      ! Relative Rotational Speed
78 0.0      ! Compressor number
79 4.0      ! Map Number
80 1000.0   ! Power Law index
81 -1.0     ! Compressor Work
82 0.0      ! NGV ANGLE RELATIVE TO D
! HETCOL
90 0.02
91 0.9
92 3.0
93 0.0
! HETHOT
95 0.03
96 0.9
97 3.0
98 0.0
! NOZCON
83   -1.0      ! THROAT AREA
! PERFOR
84    1.0      ! PROPELLER EFFICIENCY
85    0.0      ! SCALING INDEX
86    0.0      ! REQUIRED THRUST
!  ARITHY: HPC1 SPEED = HPC2 SPEED
120 5.0       ! COPY
121 -1.0
122 30.0       ! HPC2 SPEEDD
123 -1.0
124 19.0       ! HPC1 SPEED
!  ARITHY: HPT WORK = HPC1 WORK + HPC2
WORK
140 1.0        ! ADD
141 -1.0
142 147      ! HPT WORK
143 -1.0
144 302      ! HPC1 WORK
145 -1.0
146 303      ! HPC2 WORK
! ARITHY COPY D205=Tamb
200 5
201 -1
202 205
203 1
204 6
! ARITHY W2 IN Kg/s
210 11
211 -1
212 215
213 2
214 2
! ARITHY COPY Wb=(W3-W4)
220 2
221 -1
222 227
223 3
224 2
225 4
226 2
! ARITHY COPY D245=COLD HE Tin
230 5
231 -1
232 235
233 6
234 6
! ARITHY COPY D255=COLD HE Tout
240 5
241 -1
242 245
243 7
244 6
! ARITHY COPY D265=COT
250 5
251 -1
252 255
253 9
254 6
! ARITHY COPY D275=TET
260 5
261 -1
262 265
263 11
264 6
! ARITHY COPY D285=HOT HE Tin
270 5
271 -1
272 275
273 12
274 6
! ARITHY COPY D295=HOT HE Tout
280 5
281 -1
282 285
283 13
284 6
! ARITHY DHEC=D297=(HE Tin-HPC Tout)
290 2! Subtract
291 -1
292 297
293 12
294 6
295 6
296 6
!*************************
! FOR EMMISION CALCULATION
!*************************
! ARITHY W8 IN Kg/s
330 11
331 -1
332 335
333 8
334 2
! ARITHY W9 IN Kg/s
340 11
341 -1
342 345
343 9
344 2
! ARITHY Wf=(W9-W8)
350 2
351 -1
352 357
353 -1
354 345
355 -1
356 335
! ARITHY COPY T8=365
360 5
361 -1
362 365
363 8
364 6
! ARITHY P8 in (Pa)
370 3
371 -1
372 378
373 8
374 4
375 -1
376 377
377 101325.0
!*************************
! ARITHY W2 IN Kg/s
500 11
501 -1
502 505503 2
```

```
504 2
! ARITHY: (W2*SQRT T2)
515 15
516 -1
517 522
518 -1
519 505
520 2
521 6
! ARITHY: (W2*SQRT T2)/P2
523 4
524 -1
525 530
526 -1
527 522
528 2
529 4
! ARITHY W11 IN Kg/s
551 11
552 -1
553 556
554 11
555 2
! ARITHY: (W11*SQRT T11)
560 15
561 -1
562 567
563 -1
564 556
565 11
566 6
! ARITHY: (W11*SQRT T11)/P11
570 4
571 -1
572 577
573 -1
574 567
575 11
576 4
! ARITHY COPY 585=Tex
580 5
581 -1
582 585
583 16
584 6
!*****************************
! FOR Q(MW) Exhaust Heat Calcs
!*****************************
! ARITHY W16 IN Kg/s
600 11
601 -1
602 605
603 16
604 2
! ARITHY (W16*Cp)
610 3
611 -1
612 618
613 -1
614 605
615 -1
616 617
617 1150.0
! ARITHY (Tex-Tout)
620 2
621 -1
622 628
623 16
624 6
625 -1
626 627
627 400.0
! ARITHY Q=W16*Cp*(Tex-Tout)
630 3
631 -1
632 637
633 -1
634 618
635 -1
636 628
! ARITHY Q IN MW
640 4
641 -1
642 648
643 -1
644 637
645 -1
646 647
647 1000000.0
-1
1 2 27.04       ! INLET MASS FLOW
9 6 1308.92     ! COMBUSTION OUTLET
TEMPERATURE
-1
25 0.0        !******** (Bleed Valve CLOSED)
***************
1 -400.0      ! %%%%%%%%%%(COT is
Changed)%%%%%%%%%%%%%%%%%%
-1
-3
```

E.1.10 Two-Spool 3-Shaft Conventional HEx Cycle [FPT] Engine

```
! TURBOMATCH MODEL DATA FILE FOR: AERO-
DERIVATIVE ENGINE DERIVED FROM CUAV 130
AIRCRAFT ENGINE
MODELLED BY ABDELMANAM ABAAD
////
OD SI KE VA FP
-1
-1
INTAKE S1, 2      D1-4            R300
COMPRE S2, 3      D5-11           R301 V5 V6
DUCTER S3, 4      D12 -15
COMPRE S4, 5      D18-24          R302 V18 V19
PREMAS S5, 21, 6  D25 -28
ARITHY            D120-124
COMPRE S6, 7      D29-35          R303 V29
PREMAS S7, 22, 8  D36 -39
PREMAS S22, 24, 23 D40 -43
HETCOL S8, 9      D9 0-93
PREMAS S9, 25, 10  D44 -47
BURNER S10, 11     D48-50         R304
MIXEES S11, 25, 12
MIXEES S12, 23, 13
ARITHY            D140-147
TURBIN S13, 14    D51 -58, 147, 59        V52
MIXEES S14, 24, 15
TURBIN S15, 16     D60 -67, 301, 68       V61
DUCTER S16, 17     D69 - 72
TURBIN S17, 18     D73-82             V73 V74
HETHOT S8, 18, 19  D95 -98
NOZCON S19, 20, 1  D83             R306
ARITHY            D200-205
ARITHY            D210-215
ARITHY            D220-227
ARITHY            D230-235
ARITHY            D240-245
ARITHY            D250-255
ARITHY            D260-265
ARITHY            D270-275
ARITHY            D280-285
ARITHY            D290-297
!**************************
!FOR EMMISION CALCULATION
!**************************
ARITHY            D330-335
ARITHY            D340-345
ARITHY            D350-357
ARITHY            D360-365
ARITHY            D370-378
!**************************
ARITHY            D500-505
ARITHY            D515-522
ARITHY            D523-530
ARITHY            D551-556
ARITHY            D560-567
ARITHY            D570-577
ARITHY            D580-585
ARITHY            D700-705
ARITHY            D706-713
ARITHY            D714-721
!**************************
! FOR Exhaust Heat Q (MW) CAL
!**************************
ARITHY            D600-605
ARITHY            D610-618
ARITHY            D620-628
ARITHY            D630-637
ARITHY            D640-648
!**************************
!                 Wex Tex Tsk Q HETin DHEC
PLOTBD            D605, 585,627,648,275,297
!                 Wc Pc Tc Wf Alt DT COT TET DHEC
! PLOTBD          D335, 378, 365, 357, 1, 2, 255, 265,
297
!                 COT TET T18 Tex Q DHEC
! PLOTBD          D255, 265,275,285,648,297
!                 COT TET T16 HC1 HC2 HPT Q DHEC
! PLOTBD          D255, 265,275,530,577,721,648,297
PERFOR  S1,0,0    D73,84-86,306,300,304,0,0,0,0,0,0
CODEND
DATA ITEMS////
! INTAKE
1 0.0         ! INTAKE ALTITUDE
2 0.0         ! ISA DEVIATION
3 0.0         ! MACH NO
4 0.9951      ! PRESSURE RECOVERY
! LP COMPRESSORE
5    0.85     ! Z PARAMETER
6    0.85     ! Relative ND rotational Speed
7    1.3      ! Compressor Pressure Ratio
8    0.89     ! Isentropic Efficiency
9    0.0      ! Error Selection
10   5.0      ! Compressor Map Number
11   0.0      ! ANGLE
! DIFUSSER
12   0.0      ! Switch Set
13   0.0      ! Total pressure Loss/Inlet total Pressure
Dp/P
14   0.0      ! Combustion Efficiency
15   0.0      ! Limiting Value of Fuel Flow
! HP COMPRESSOR1
18   0.85     ! Z Parameter
19   0.8      ! Relative ND rotational Speed
20   7.11     ! Compressor Pressure Ratio
21   0.9      ! Isentropic Efficiency
22   0.0      ! Error Selection
23   5.0      ! Compressor Map Number
24   0.0      ! ANGLE
!  BLEEDING VALVE
25 0.04568    ! BLEEDING RATIO
26 0.0        ! MASS FLOW LOSS
27 0.0        ! PRESSURE FACTOR
28 0.0        ! PRESSURE LOSS
! HP COMPRESSOR2
29   0.85     ! Z Parameter
30   0.8      ! Relative ND rotational Speed
31   2.11     ! Compressor Pressure Ratio
32   0.88     ! Isentropic Efficiency
33   0.0      ! Error Selection
34   4.0      ! Compressor Map Number
35   0.0      ! ANGLE
!  TOTAL COOLING BLEED FOR HPT & LPT
SEALING
36 0.145      ! ROTORS COOLING
37 0.0        ! MASS FLOW LOSS
38 1.0        ! PRESSURE FACTOR
39 0.0        ! PRESSURE LOSS
!  SPLIT COOLING BLEED FOR LPT SEALING)
40 0.31       !% HPT SEALING AND % LPT
41 0.0        ! MASS FLOW LOSS
42 0.0        ! PRESSURE FACTOR
43 0.0        ! PRESSURE LOSS
! BURNER INTERNAL BYPASS COOLING
44 0.0        ! BYPASS RATIO
45 0.0        ! MASS FLOW LOSS
46 0.0        ! PRESSURE FACTOR
47 0.0        ! PRESSURE LOSS
!  BURNER
48    0.048   ! Fractional pressure Loss DP/P
```

```
49    0.9999    ! COMBUSTION EFFICIENCY
50   -1.0       ! FUEL FLOW
!  HP TURBINE
51   0.0        ! AUX.WORK
52 -1.0         ! REL NON-D MASS FLOW
53 -1.0         ! REL NON-D SPEED
54 0.90         ! EFFICIENCY
55 -1.0         ! REL ROT.SPEED (COMP TURB=-1)
56 2.0          ! COMP NO. FROM LOW END
57 5.0          ! TURBINE MAP
58 -1.0         ! POWER LAW
59 0.0          ! NGV ANGLE RELATIVE TO D
!  LP TURBINE
60 0.0    ! AUXILIARY WORK
61 -1.0         ! REL NON-D MASS FLOW
62 -1.0         ! REL NON-D SPEED
63 0.91         ! ISENTROPIC EFFICIENCY
64 -1.0         ! REL ROT.SPEED
65 1.0          ! COMPRESSOR NUMBER
66 5.0          ! TURBINE MAP NUMBER
67 -1.0        ! POWER LOW INDEX
68 0.0          ! NGV ANGLE RELATIVE TO D.
!  PT INLET DUCT
69 0.0
70 0.02
71 0.0
72 0.0
!  POWER TURBINE
73 8751524.0! Auxiliary Work
74 0.8       ! Relative ND Mass Flow
75 0.6       ! Relative ND Rotational Speed
76 0.9203    ! Isentropic efficiency
77 1.0       ! Relative Rotational Speed
78 0.0       ! Compressor number
79 4.0       ! Map Number
80 1000.0    ! Power Law index
81 -1.0      ! Compressor Work
82 0.0       ! NGV ANGLE RELATIVE TO D
! HETCOL
90 0.02
91 0.9
92 3.0
93 0.0
! HETHOT
95 0.03
96 0.9
97 3.0
98 0.0
! NOZCON
83   -1.0       ! THROAT AREA
! PERFOR
84    1.0       ! PROPELLER EFFICIENCY
85    0.0       ! SCALING INDEX
86    0.0       ! REQUIRED THRUST
!  ARITHY: HPC1 SPEED = HPC2 SPEED
120 5.0        ! COPY
121 -1.0
122 30.0        ! HPC2 SPEEDD
123 -1.0
124 19.0        ! HPC1 SPEED
!  ARITHY: HPT WORK = HPC1 WORK + HPC2
WORK
140 1.0         ! ADD
141 -1.0
142 147       ! HPT WORK
143 -1.0
144 302       ! HPC1 WORK
145 -1.0
146 303       ! HPC2 WORK
! ARITHY COPY D205=Tamb
200 5
201 -1
202 205
203 1
204 6
! ARITHY W2 IN Kg/s
210 11
211 -1
212 215
213 2
214 2
! ARITHY COPY Wb= (W5-W6)
220 2
221 -1
222 227
223 5
224 2
225 6
226 2
! ARITHY COPY D245=COLD HE Tin
230 5
231 -1
232 235
233 8
234 6
! ARITHY COPY D255=COLD HE Tout
240 5
241 -1
242 245
243 9
244 6
! ARITHY COPY D265=COT
250 5
251 -1
252 255
253 11
254 6
! ARITHY COPY D275=TET
260 5
261 -1
262 265
263 13
264 6
! ARITHY COPY D285=HOT HE Tin
270 5
271 -1
272 275
273 18
274 6
! ARITHY COPY D295=HOT HE Tout
280 5
281 -1
282 285
283 19
284 6
! ARITHY DHEC=D297=(HE Tin-HPC Tout)
290 2! Subtract
291 -1
292 297
293 18
294 6
295 8
296 6
!*************************
! FOR EMMISION CALCULATION
!*************************
! ARITHY W10 IN Kg/s
330 11
331 -1
332 335
333 10
334 2
! ARITHY W11 IN Kg/s
340 11
341 -1
```

```
342 345
343 11
344 2
! ARITHY Wf= (W11-W10)
350 2
351 -1
352 357
353 -1
354 345
355 -1
356 335
! ARITHY COPY T10=365
360 5
361 -1
362 365
363 10
364 6
! ARITHY P10 in (Pa)
370 3
371 -1
372 378
373 10
374 4
375 -1
376 377
377 101325.0
!*************************
! ARITHY W4 IN Kg/s
500 11
501 -1
502 505
503 4
504 2
! ARITHY: (W4*SQRT T4)
515 15
516 -1
517 522
518 -1
519 505
520 4
521 6
! ARITHY: (W4*SQRT T4)/P4
523 4
524 -1
525 530
526 -1
527 522
528 4
529 4
! ARITHY W6 IN Kg/s
551 11
552 -1
553 556
554 6
555 2
! ARITHY: (W6*SQRT T6)
560 15
561 -1
562 567
563 -1
564 556
565 6
566 6
! ARITHY: (W6*SQRT T6)/P6
570 4
571 -1
572 577
573 -1
574 567
575 6
576 4
! ARITHY COPY 585=Tex
580 5
581 -1
582 585
583 19
584 6
!*****************************
! FOR Q (MW) Exhaust Heat
CalcS
!*****************************
! ARITHY W19 IN Kg/s
600 11
601 -1
602 605
603 19
604 2
! ARITHY (W19*Cp)
610 3
611 -1
612 618
613 -1
614 605
615 -1
616 617
617 1150.0
! ARITHY (Tex-Tout)
620 2
621 -1
622 628
623 19
624 6
625 -1
626 627
627 400.0
! ARITHY Q=W19*Cp*(Tex-Tout)
630 3
631 -1
632 637
633 -1
634 618
635 -1
636 628
! ARITHY Q IN MW
640 4
641 -1
642 648
643 -1
644 637
645 -1
646 647
647 1000000.0
!*****************************
! ARITHY W13 IN Kg/s
700 11
701 -1
702 705
703 13
704 2
! ARITHY: (W13*SQRT T13)
706 15
707 -1
708 713
709 -1
710 705
711 13
712 6
! ARITHY: (W13*SQRT T13)/P13
714 4
715 -1
716 721
717 -1
718 713
719 13
720 4
-1
1 2 33.7071      ! INLET MASS
FLOW
11 6 1423.5      ! COMBUSTION
OUTLET TEMPERATURE
-1
-3
```

E.1.11 Two-Spool 3Shaft non-Conventional Hex Cycle [FPT] Engine

```
! TURBOMATCH MODEL DATA FILE FOR: AERO-
DERIVATIVE ENGINE DERIVED FROM CUAV 130
AIRCRAFT ENGINE
MODELLED BY ABDELMANAM ABAAD
////
OD SI KE VA FP
-1
-1
INTAKE S1, 2      D1-4            R300
COMPRE S2, 3      D5-11           R301 V5 V6
DUCTER S3, 4      D12 -15
COMPRE S4, 5      D18-24          R302 V18 V19
PREMAS S5, 21, 6   D25
ARITHY          D120-124
COMPRE S6, 7      D29-35          R303 V29
PREMAS S7, 22, 8   D36 -39
PREMAS S22, 24, 23 D40 -43
HETCOL S8, 9      D90 -93
PREMAS S9, 25, 10  D44 -47
BURNER S10, 11    D48-50          R304
MIXEES S11, 25, 12
MIXEES S12, 23, 13
ARITHY          D140-147
TURBIN S13, 14    D51 -58, 147, 59          V52
MIXEES S14, 24, 15
TURBIN S15, 16    D60 -67, 301, 68          V61
HETHOT S8, 16, 17  D95 -98
DUCTER S17, 18    D69 -72
TURBIN S18, 19    D73-82              V73 V74
NOZCON S19, 20, 1  D83            R306
ARITHY          D200-205
ARITHY          D210-215
ARITHY          D220-227
ARITHY          D230-235
ARITHY          D240-245
ARITHY          D250-255
ARITHY          D260-265
ARITHY          D270-275
ARITHY          D280-285
ARITHY          D290-297
!*************************
! FOR EMMISION CALCULATION
!*************************
ARITHY          D330-335
ARITHY          D340-345
ARITHY          D350-357
ARITHY          D360-365
ARITHY          D370-378
!*************************
ARITHY          D500-505
ARITHY          D515-522
ARITHY          D523-530
ARITHY          D551-556
ARITHY          D560-567
ARITHY          D570-577
ARITHY          D580-585
ARITHY          D700-705
ARITHY          D706-713
ARITHY          D714-721
!*************************
! FOR Exhaust Heat Q(MW) CAL
!*************************
ARITHY          D600-605
ARITHY          D610-618
ARITHY          D620-628
ARITHY          D630-637
ARITHY          D640-648
!*************************
!              Wex Tex Tsk Q HETin DHEC
PLOTBD          D605, 585,627,648,275,297
!             Wc Pc Tc Wf Alt DT W COT TET
! PLOTBD        D335, 378, 365, 357, 1,
2,215,255,265
!             LPC COT TET T16 Tex Q DHEC
! PLOTBD        D7, 255,265,275,285,648,297
!              COT TET T14 HC1 HC2 HPT Q DHEC
! PLOTBD        D255, 265,275,530,577,721,648,297
PERFOR  S1,0,0    D73,84-
86,306,300,304,0,0,0,0,0,0
CODEND
DATA////
1   0.0     ! ALTITUDE
2   0.0     ! DEV FROM STAND TEMPERATURE
3   0.0     ! MACH NUMBER
4   0.9951   ! PRESSURE RECOVERY
! LP COMPRESSORE
5   0.85    ! Z PARAMETER
6   0.85    ! Relative ND rotational Speed
7   2.0     ! Compressor Pressure Ratio
8   0.89    ! Isentropic Efficiency
9   0.0     ! Error Selection
10  5.0     ! Compressor Map Number
11  0.0     ! ANGLE
! DIFUSSER
12  0.0     ! Switch Set
13  0.0     ! Total pressure Loss/Inlet total Pressure
Dp/P
14  0.0     ! Combustion Efficiency
15  0.0     ! Limiting Value of Fuel Flow
! HP COMPRESSOR1
18  0.85    ! Z Parameter
19  -1.0    ! Relative ND rotational Speed
20  7.11    ! Compressor Pressure Ratio
21  0.9     ! Isentropic Efficiency
22  0.0     ! Error Selection
23  5.0     ! Compressor Map Number
24  0.0     ! ANGLE
!  BLEEDING VALVE
25 0.04568   ! BLEEDING RATIO
26 0.0       ! MASS FLOW LOSS
27 1.0       ! PRESSURE FACTOR
28 0.0       ! PRESSURE LOSS
! HP COMPRESSOR2
29  0.85    ! Z Parameter
30  -1.0    ! Relative ND rotational Speed
31  2.11    ! Compressor Pressure Ratio
32  0.88    ! Isentropic Efficiency
33  0.0     ! Error Selection
34  4.0     ! Compressor Map Number
35  0.0     ! ANGLE
!  TOTAL COOLING BLEED FOR HPT & LPT
SEALING
36 0.145     ! ROTORS COOLING
37 0.0       ! MASS FLOW LOSS
38 1.0       ! PRESSURE FACTOR
39 0.0       ! PRESSURE LOSS

!  SPLIT COOLING BLEED FOR LPT SEALING)
40 0.31      ! % HPT SEALING AND % LPT
41 0.0       ! MASS FLOW LOSS
42 1.0       ! PRESSURE FACTOR
43 0.0       ! PRESSURE LOSS
! BURNER INTERNAL BYPASS COOLING
44 0.0       ! BYPASS RATIO
45 0.0       ! MASS FLOW LOSS
46 0.0       ! PRESSURE FACTOR
47 0.0       ! PRESSURE LOSS
!  BURNER
```

```
48    0.048   ! Fractional pressure Loss DP/P
49    0.9999  ! COMBUSTION EFFICIENCY
50   -1.0     ! FUEL FLOW
!  HP TURBINE
51 0.0       ! AUX.WORK
52 -1.0       ! REL NON-D MASS FLOW
53 -1.0       ! REL NON-D SPEED
54 0.90       ! EFFICIENCY
55 -1.0       ! REL ROT.SPEED (COMP TURB=-1)
56 2.0       ! COMP NO. FROM LOW END
57 5.0       ! TURBINE MAP
58 -1.0       ! POWER LAW
59 0.0       ! NGV ANGLE RELATIVE TO D
!  LP TURBINE
60 0.0        ! AUXILIARY WORK
61 -1.0        ! REL NON-D MASS FLOW
62 -1.0        ! REL NON-D SPEED
63 0.91        ! ISENTROPIC EFFICIENCY
64 -1.0        ! REL ROT.SPEED
65 1.0        ! COMPRESSOR NUMBER
66 4.0        ! TURBINE MAP NUMBER
67 -1.0        ! POWER LOW INDEX
68 0.0        ! NGV ANGLE RELATIVE TO D.
!  PT INLET DUCT
69 0.0
70 0.02
71 0.0
72 0.0
!  POWER TURBINE
73 13086652.0! Auxiliary Work
74 0.8      ! Relative ND Mass Flow
75 0.6      ! Relative ND Rotational Speed
76 0.91     ! Isentropic efficiency
77 1.0      ! Relative Rotational Speed
78 0.0      ! Compressor number
79 4.0      ! Map Number
80 1000.0    ! Power Law index
81 -1.0      ! Compressor Work
82 0.0      ! NGV ANGLE RELATIVE TO D
! HETCOL
90 0.02
91 0.9
92 3.0
93 0.0
! HETHOT
95 0.03
96 0.9
97 3.0
98 0.0
! NOZCON
83   -1.0     ! THROAT AREA
! PERFOR
84    1.0     ! PROPELLER EFFICIENCY
85    0.0     ! SCALING INDEX
86    0.0     ! REQUIRED THRUST
! ARITHY: HPC1 SPEED = HPC2 SPEED
120 5.0       ! COPY
121 -1.0
122 30.0       ! HPC2 SPEED
123 -1.0
124 19.0       ! HPC1 SPEED
! ARITHY: HPT WORK = HPC1 WORK + HPC2
WORK
140 1.0        ! ADD
141 -1.0
142 147      ! HPT WORK
143 -1.0
144 302      ! HPC1 WORK
145 -1.0
146 303      ! HPC2 WORK
! ARITHY COPY D205=Tamb
200 5
201 -1
202 205
203 1
204 6
! ARITHY W2 IN Kg/s
210 11
211 -1
212 215
213 2
214 2
! ARITHY COPY Wb=(W5-W6)
220 2
221 -1
222 227
223 5
224 2
225 6
226 2
! ARITHY COPY D245=COLD HE Tin
230 5
231 -1
232 235
233 8
234 6
! ARITHY COPY D255=COLD HE Tout
240 5
241 -1
242 245
243 9
244 6
! ARITHY COPY D265=COT
250 5
251 -1
252 255
253 11
254 6
! ARITHY COPY D275=TET
260 5
261 -1
262 265
263 13
264 6

! ARITHY COPY D285=HOT HE Tin
270 5
271 -1
272 275
273 16
274 6
! ARITHY COPY D295=HOT HE Tout
280 5
281 -1
282 285
283 17
284 6
! ARITHY DHEC=D297= (HE Tin-HPC Tout)
290 2  ! Subtract
291 -1
292 297
293 16
294 6
295 8
296 6
!*************************
! FOR EMMISION CALCULATION
!*************************
! ARITHY W10 IN Kg/s
330 11
331 -1
332 335
333 10
334 2
! ARITHY W11 IN Kg/s
```

```
340 11
341 -1
342 345
343 11
344 2
! ARITHY Wf=(W11-W10)
350 2
351 -1
352 357
353 -1
354 345
355 -1
356 335
! ARITHY COPY T10=365
360 5
361 -1
362 365
363 10
364 6
! ARITHY P10 in (Pa)
370 3
371 -1
372 378
373 10
374 4
375 -1
376 377
377 101325.0
!**************************
! ARITHY W4 IN Kg/s
500 11
501 -1
502 505
503 4
504 2
! ARITHY: (W4*SQRT T4)
515 15
516 -1
517 522
518 -1
519 505
520 4
521 6
! ARITHY: (W4*SQRT T4)/P4
523 4
524 -1
525 530
526 -1
527 522
528 4
529 4
! ARITHY W6 IN Kg/s
551 11
552 -1
553 556
554 6
555 2
! ARITHY: (W6*SQRT T6)
560 15
561 -1
562 567
563 -1
564 556
565 6
566 6
! ARITHY: (W6*SQRT T6)/P6
570 4
571 -1
572 577
573 -1
574 567
575 6
576 4
! ARITHY COPY 585=Tex
580 5
581 -1
582 585
583 20
584 6
!*****************************
! FOR Q(MW) Exhaust Heat
CalcS
!*****************************
! ARITHY W20 IN Kg/s
600 11
601 -1
602 605
603 20
604 2
! ARITHY (W20*Cp)
610 3
611 -1
612 618
613 -1
614 605
615 -1
616 617
617 1150.0
! ARITHY (Tex-Tout)
620 2
621 -1
622 628
623 20
624 6
625 -1
626 627
627 400.0
! ARITHY Q=W20*Cp*(Tex-Tout)
630 3
631 -1
632 637
633 -1
634 618
635 -1
636 628
! ARITHY Q IN MW
640 4
641 -1
642 648
643 -1
644 637
645 -1
646 647
647 1000000.0
!*****************************
! ARITHY W13 IN Kg/s
700 11
701 -1
702 705
703 13
704 2
! ARITHY: (W13*SQRT T13)
706 15
707 -1
708 713
709 -1
710 705
711 13
712 6
! ARITHY: (W13*SQRT T13)/P13
714 4
715 -1
716 721
717 -1
718 713
719 13
720 4
-1
1 2 48.45      ! INLET MASS
FLOW
11 6 1630.73
-1
-3
```

E.1.12 Two-Spool 2-Shaft Conv-[ICR] Cycle Engine [IPT]

```
! TURBOMATCH MODEL DATA FILE FOR: AERO-
DERIVATIVE ENGINE DERIVED FROM CUAV 130
AIRCRAFT ENGINE
MODELLED BY ABDELMANAM ABAAD
////
OD SI KE VA FP
-1
-1
INTAKE S1, 2      D1-4            R300
COMPRE S2, 3      D5-11           R301 V5 V6
DUCTER S3, 4      D12 -15
ARITHY            D160-168
ARITHY            D169-173
COMPRE S4, 5      D18-24          R302 V18 V19
PREMAS S5, 21, 6   D25 -28
ARITHY            D120-124
COMPRE S6, 7      D29-35          R303 V29
PREMAS S7, 22, 8   D36 -39
PREMAS S22, 24, 23 D40 -43
HETCOL S8, 9      D90 -93
PREMAS S9, 25, 10  D44 -47
BURNER S10, 11    D48-50          R304
MIXEES S11, 25, 12
MIXEES S12, 23, 13
ARITHY            D140-147
TURBIN S13, 14    D51 -58, 147, 59          V52
MIXEES S14, 24, 15
TURBIN S15, 16    D60 -67, 301, 68          V61
DUCTER S16, 17    D69-72          R305
TURBIN S17, 18    D73-82              V73 V74
HETHOT S8, 18, 19  D95 -98
NOZCON S19, 20, 1  D83            R306
ARITHY            D200-205
ARITHY            D210-215
ARITHY            D220-225
ARITHY            D230-235
ARITHY            D240-245
ARITHY            D250-255
ARITHY            D260-265
ARITHY            D270-275
ARITHY            D280-285
ARITHY            D500-505
ARITHY            D510-518
ARITHY            D520-528
ARITHY            D530-537
ARITHY            D540-548
ARITHY            D600-605
ARITHY            D606-613
ARITHY            D614-621
ARITHY            D625-630
ARITHY            D631-638
ARITHY            D639-646
ARITHY            D650-655
ARITHY            D656-663
ARITHY            D664-671
ARITHY            D675-680
ARITHY            D681-688
ARITHY            D689-696
ARITHY            D700-705
ARITHY            D706-713
ARITHY            D714-721
              ! W  T3 T4 T7 COT TET T18 Tex Q
PLOTBD    D605, 205,215,235,255,265,275,285,548
!              TET T16 Tex LPC HC1 HC2 HPT LPT Q
! PLOTBD   D265, 275,285,621,646,671,696,721,548
!               LPC W T3 T4 T6 T7 T8 COT
! PLOTBD    D7, 605,205,215,225,235,245,255
PERFOR  S1,0,0  D73,84-86,306,300,304,0,0,0,0,0,0
CODEND
```

```
DATA////
1   0.0          ! ALTITUDE
2   0.0          ! DEV FROM STAND TEMPERATURE
3   0.0          ! MACH NUMBER
4   0.9951       ! PRESSURE RECOVERY
! LP COMPRESSORE
5   0.85     ! Z PARAMETER
6   -1.0     ! Relative ND rotational Speed
7   1.2      ! Compressor Pressure Ratio
8   0.89     ! Isentropic Efficiency
9   0.0      ! Error Selection
10  5.0      ! Compressor Map Number
11  0.0      ! ANGLE
! INTERCOOLER (SPRINT)
12  2.0      ! Switch Set
13  0.03     ! Total pressure Loss/Inlet total Pressure
Dp/P
14  0.8      ! Combustion Efficiency
15  0.0      ! Limiting Value of Fuel Flow
! HP COMPRESSOR1
18  0.85     ! Z Parameter
19  1.0      ! Relative ND rotational Speed
20  7.11     ! Compressor Pressure Ratio
21  0.9      ! Isentropic Efficiency
22  0.0      ! Error Selection
23  5.0      ! Compressor Map Number
24  0.0      ! ANGLE
!  BLEEDING VALVE
25 0.04568    ! BLEEDING RATIO
26 0.0        ! MASS FLOW LOSS
27 1.0        ! PRESSURE FACTOR
28 0.0        ! PRESSURE LOSS
! HP COMPRESSOR2
29  0.85     ! Z Parameter
30  1.0      ! Relative ND rotational Speed
31  2.11     ! Compressor Pressure Ratio
32  0.88     ! Isentropic Efficiency
33  0.0      ! Error Selection
34  4.0      ! Compressor Map Number
35  0.0      ! ANGLE
!  TOTAL COOLING BLEED FOR HPT & LPT
SEALING
36 0.145      ! ROTORS COOLING
37 0.0        ! MASS FLOW LOSS
38 1.0        ! PRESSURE FACTOR
39 0.0        ! PRESSURE LOSS
!  SPLIT COOLING BLEED FOR LPT SEALING)
40 0.31       !% HPT SEALING AND % LPT
41 0.0       ! MASS FLOW LOSS
42 1.0       ! PRESSURE FACTOR
43 0.0       ! PRESSURE LOSS
! BURNER INTERNAL BYPASS COOLING
44 0.0        ! BYPASS RATIO
45 0.0        ! MASS FLOW LOSS
46 0.0        ! PRESSURE FACTOR
47 0.0        ! PRESSURE LOSS
!  BURNER
48    0.048    ! Fractional pressure Loss DP/P
49    0.9999   ! COMBUSTION EFFICIENCY
50   -1.0      ! FUEL FLOW
!  HP TURBINE
51 0.0        ! AUX.WORK
52 -1.0       ! REL NON-D MASS FLOW
53 -1.0       ! REL NON-D SPEED
54 0.90       ! EFFICIENCY
55 -1.0       ! REL ROT.SPEED (COMP TURB=-1)
56 2.0        ! COMP NO. FROM LOW END
57 5.0        ! TURBINE MAP
58 -1.0       ! POWER LAW
```

```
59 0.0        ! NGV ANGLE RELATIVE TO D
!  LP TURBINE
60 0.0        ! AUXILIARY WORK
61 -1.0       ! REL NON-D MASS FLOW
62 -1.0       ! REL NON-D SPEED
63 0.91       ! ISENTROPIC EFFICIENCY
64 -1.0       ! REL ROT.SPEED
65 1.0        ! COMPRESSOR NUMBER
66 5.0        ! TURBINE MAP NUMBER
67 -1.0     ! POWER LOW INDEX
68 0.0        ! NGV ANGLE RELATIVE TO D.
!  PT INLET DUCT
69 0.0
70 0.02
71 0.0
72 0.0
!  POWER TURBINE
73 7200907.5    ! Auxiliary Work
74 0.8        ! Relative ND Mass Flow
75 0.6        ! Relative ND Rotational Speed
76 0.922       ! Isentropic efficiency
77 1.0        ! Relative Rotational Speed
78 0.0        ! Compressor number
79 4.0        ! Map Number
80 1000.0     ! Power Law index
81 -1.0       ! Compressor Work
82 0.0        ! NGV ANGLE RELATIVE TO D
! NOZCON
83   -1.0      ! THROAT AREA
! PERFOR
84    1.0      ! PROPELLER EFFICIENCY
85    0.0      ! SCALING INDEX
86    0.0      ! REQUIRED THRUST
! HETCOL
90 0.02
91 0.9
92 2.0
93 0.0

! HETHOT
95 0.03
96 0.9
97 2.0
98 0.0
!  ARITHY: HPC1 SPEED = HPC2 SPEED
120 5.0       ! COPY
121 -1.0
122 30.0       ! HPC2 SPEEDD
123 -1.0
124 19.0       ! HPC1 SPEED
!  ARITHY: HPT WORK = HPC1 WORK + HPC2
WORK
140 1.0        ! ADD
141 -1.0
142 147      ! HPT WORK
143 -1.0
144 302      ! HPC1 WORK
145 -1.0
146 303      ! HPC2 WORK
! ARITHY T4=Tamb+11.85
160 1
161 -1
162 168
163 1
164 6
165 -1
166 167
167 11.85
! ARITHY T4=168
169 5   ! COPY
170 4
171 6
172 -1
173 168
! ARITHY COPY T3=205
200 5! COPY
201 -1
202 205
203 3
204 6
! ARITHY COPY T4=215
210 5   ! COPY
211 -1
212 215
213 4
214 6
! ARITHY COPY T6=225
220 5   ! COPY
221 -1
222 225
223 6
224 6
! ARITHY COPY 235=T7
230 5
231 -1
232 235
233 7
234 6
! ARITHY COPY 245=T8
240 5
241 -1
242 245
243 8
244 6
! ARITHY COPY COT=255
250 5
251 -1
252 255
253 11
254 6
! ARITHY COPY TET=265
260 5! COPY
261 -1
262 265
263 13
264 6
! ARITHY COPY T18=275
270 5! COPY
271 -1
272 275
273 18
274 6
! ARITHY COPY Tex=285
280 5! COPY
281 -1
282 285
283 20
284 6
! ARITHY W20 IN Kg/s
500 11
501 -1
502 505
503 20
504 2
! ARITHY (W20*Cp)
510 3
511 -1
512 518
513 -1
514 505
515 -1
516 517
517 1150.0
! ARITHY (Tex-Tout)
520 2
521 -1
```

```
522 528
523 20
524 6
525 -1
526 527
527 400.0
! ARITHY Q=W20*Cp*(Tex-Tout)
530 3
531 -1
532 537
533 -1
534 518
535 -1
536 528
! ARITHY Q IN MW
540 4
541 -1
542 548
543 -1
544 537
545 -1
546 547
547 1000000.0
! ARITHY W2 IN Kg/s
600 11
601 -1
602 605
603 2
604 2
! ARITHY: (W2*SQRT T2)
606 15
607 -1
608 613
609 -1
610 605
611 2
612 6
! ARITHY: (W2*SQRT T)/P2
614 4
615 -1
616 621
617 -1
618 613
619 2
620 4
! ARITHY W4 IN Kg/s
625 11
626 -1
627 630
628 4
629 2
! ARITHY: (W4*SQRT T4)
631 15
632 -1
633 638
634 -1
635 630
636 4
637 6
! ARITHY: (W4*SQRT T4)/P4
639 4
640 -1
641 646
642 -1
643 638
644 4
645 4
! ARITHY W6 IN Kg/s
650 11
651 -1
652 655
653 6
654 2
! ARITHY: (W6*SQRT T6)
656 15
657 -1
658 663
659 -1
660 655
661 6
662 6
! ARITHY: (W6*SQRT T6)/P6
664 4
665 -1
666 671
667 -1
668 663
669 6
670 4
! ARITHY W13 IN Kg/s
675 11
676 -1
677 680
678 13
679 2
! ARITHY: (W13*SQRT T13)
681 15
682 -1
683 688
684 -1
685 680
686 13
687 6
! ARITHY: (W13*SQRT T13)/P13
689 4
690 -1
691 696
692 -1
693 688
694 13
695 4
! ARITHY W15 IN Kg/s
700 11
701 -1
702 705
703 15
704 2
! ARITHY: (W15*SQRT T15)
706 15
707 -1
708 713
709 -1
710 705
711 15
712 6
! ARITHY: (W15*SQRT T15)/P15
714 4
715 -1
716 721
717 -1
718 713
719 15
720 4
-1
1 2 30.846      ! Inlet Mass Flow
11 6 1362.8     ! Burner Outlet Temperature
-1
-3
```

E.1.13 Two-Spool Three-Shaft Conv-[ICR] Cycle Engine [FPT]

```
! TURBOMATCH MODEL DATA FILE FOR: AERO-
DERIVATIVE ENGINE DERIVED FROM CUAV 130
AIRCRAFT ENGINE
MODELLED BY ABDELMANAM ABAAD
////
OD SI KE VA FP
-1
-1
INTAKE S1, 2      D1-4          R300
COMPRE S2, 3      D5-11         R301 V5 V6
DUCTER S3, 4      D12 -15
COMPRE S4, 5      D18-24        R302 V18 V19
PREMAS S5, 21, 6  D25 -28
ARITHY            D120-124
COMPRE S6, 7      D29-35        R303 V29
PREMAS S7, 22, 8  D36 -39
PREMAS S22, 24, 23 D40 -43
HETCOL S8, 9      D90 -93
PREMAS S9, 25, 10  D44 -47
BURNER S10, 11    D48-50        R304
MIXEES S11, 25, 12
MIXEES S12, 23, 13
ARITHY            D140-147
TURBIN S13, 14    D51- 58, 147, 59      V52
MIXEES S14, 24, 15
TURBIN S15, 16    D60 -67, 301, 68      V61
DUCTER S16, 17    D69-72        R305
TURBIN S17, 18    D73-82            V73 V74
HETHOT S8, 18, 19  D95 -98
NOZCON S19, 20, 1  D83          R306
ARITHY            D160-165
ARITHY            D170-175
ARITHY            D180-187
ARITHY            D190-197
ARITHY            D200-205
ARITHY            D210-215
ARITHY            D220-227
ARITHY            D230-235
ARITHY            D240-245
ARITHY            D250-255
ARITHY            D260-265
ARITHY            D270-275
ARITHY            D280-285
ARITHY            D290-297
!*************************************
! FOR EMMISION CALCULATION
!*************************************
ARITHY            D330-335
ARITHY            D340-345
ARITHY            D350-357
ARITHY            D360-365
ARITHY            D370-378
!*********************************
ARITHY            D500-505
ARITHY            D515-522
ARITHY            D523-530
ARITHY            D551-556
ARITHY            D560-567
ARITHY            D570-577
ARITHY            D580-585
ARITHY            D700-705
ARITHY            D706-713
ARITHY            D714-721
!*************************************
! FOR Exhaust Heat Q (MW) CAL
!*************************************
ARITHY            D600-605
ARITHY            D610-618
ARITHY            D620-628
ARITHY            D630-637
ARITHY            D640-648
!*************************
!                 Wex Tex Tsk Q T4 HETin DHEC
PLOTBD            D605, 585,627,648,175,275,297
!               Wc Pc Tc Wf Alt DT COT TET DHEC
! PLOTBD          D335, 378, 365, 357, 1,
2,255,265,297
!               COT TET T18 Tex HC1 HC2 HPT Q
DHEC
! PLOTBD          D255,
265,275,285,530,577,721,648,297
!               Alt DT Tam COT DIA DLI DHEC Q
! PLOTBD          D1, 2,205,255,197,187,297,648
!                 Alt DT Tam DIA DLI DHEC Q Blv
! PLOTBD       D1, 2,205,197,187,297,648,227
PERFOR  S1,0,0    D73,84-86,306,300,304,0,0,0,0,0,0
CODEND
DATA ITEMS////
! INTAKE
1 0.0         ! INTAKE ALTITUDE
2 0.0         ! ISA DEVIATION
3 0.0         ! MACH NO
4 0.9951      ! PRESSURE RECOVERY
! LP COMPRESSORE
5    0.85     ! Z PARAMETER
6    0.8     ! Relative ND rotational Speed
7    1.3      ! Compressor Pressure Ratio
8    0.89     ! Isentropic Efficiency
9    0.0      ! Error Selection
10   5.0      ! Compressor Map Number
11   0.0      ! ANGLE
!  DUCTER
12   2.0      ! Switch Set
13   0.03     ! Total pressure Loss/Inlet total Pressure
Dp/P
14   0.8      ! Combustion Efficiency
15   0.0      ! Limiting Value of Fuel Flow
! HP COMPRESSOR1
18   0.85     ! Z Parameter
19   -1.0     ! Relative ND rotational Speed
20   7.11     ! Compressor Pressure Ratio
21   0.9      ! Isentropic Efficiency
22   0.0      ! Error Selection
23   5.0      ! Compressor Map Number
24   0.0      ! ANGLE
!  BLEEDING VALVE
25 0.04568     ! BLEEDING RATIO
26 0.0        ! MASS FLOW LOSS
27 0.0        ! PRESSURE FACTOR
28 0.0        ! PRESSURE LOSS
! HP COMPRESSOR2
29   0.85     ! Z Parameter
30   -1.0     ! Relative ND rotational Speed
31   2.11     ! Compressor Pressure Ratio
32   0.88     ! Isentropic Efficiency
33   0.0      ! Error Selection
34   4.0      ! Compressor Map Number
35   0.0      ! ANGLE
!  TOTAL COOLING BLEED FOR HPT & LPT
SEALING
36 0.145       ! ROTORS COOLING
37 0.0        ! MASS FLOW LOSS
38 1.0        ! PRESSURE FACTOR
39 0.0        ! PRESSURE LOSS
!  SPLIT COOLING BLEED FOR LPT SEALING)
40 0.31       !% HPT SEALING AND % LPT
41 0.0        ! MASS FLOW LOSS
```

```
42 0.0       ! PRESSURE
FACTOR
43 0.0       ! PRESSURE
LOSS
! BURNER INTERNAL
BYPASS COOLING
44 0.0       ! BYPASS RATIO
45 0.0       ! MASS FLOW
LOSS
46 0.0       ! PRESSURE
FACTOR
47 0.0       ! PRESSURE
LOSS
!  BURNER
48    0.048    ! Fractional
pressure Loss DP/P
49    0.9999   !
COMBUSTION EFFICIENCY
50   -1.0      ! FUEL FLOW
!  HP TURBINE
51   0.0       ! AUX.WORK
52 -1.0        ! REL NON-D
MASS FLOW
53 -1.0        ! REL NON-D
SPEED
54 0.90        ! EFFICIENCY
55 -1.0        ! REL
ROT.SPEED (COMP
TURB=-1)
56 2.0         ! COMP NO.
FROM LOW END
57 5.0         ! TURBINE MAP
58 -1.0        ! POWER LAW
59 0.0         ! NGV ANGLE
RELATIVE TO D
!  LP TURBINE
60 0.0    ! AUXILIARY WORK
61 -1.0        ! REL NON-D
MASS FLOW
62 -1.0        ! REL NON-D
SPEED
63 0.91        ! ISENTROPIC
EFFICIENCY
64 -1.0        ! REL
ROT.SPEED
65 1.0         ! COMPRESSOR
NUMBER
66 5.0         ! TURBINE MAP
NUMBER
67 -1.0       ! POWER LOW
INDEX
68 0.0         ! NGV ANGLE
RELATIVE TO D.
!  PT INLET DUCT
69 0.0
70 0.02
71 0.0
72 0.0
!  POWER TURBINE
73 8184656.5! Auxiliary Work
74 0.8       ! Relative ND
Mass Flow
75 0.6       ! Relative ND
Rotational Speed
76 0.92      ! Isentropic
efficiency
77 1.0       ! Relative
Rotational Speed
78 0.0       ! Compressor
number
79 4.0       ! Map Number
80 1000.0     ! Power Law
index
81 -1.0       ! Compressor
Work
82 0.0       ! NGV ANGLE
RELATIVE TO D
! HETCOL
90 0.02
91 0.9
92 3.0
93 0.0
! HETHOT
95 0.03
96 0.9
97 3.0
98 0.0
! NOZCON
83   -1.0      ! THROAT
AREA
! PERFOR
84    1.0      ! PROPELLER
EFFICIENCY
85    0.0      ! SCALING
INDEX
86    0.0      ! REQUIRED
THRUST
!  ARITHY: HPC1 SPEED =
HPC2 SPEED
120 5.0        ! COPY
121 -1.0
122 30.0       ! HPC2
SPEEDD
123 -1.0
124 19.0       ! HPC1 SPEED
!  ARITHY: HPT WORK =
HPC1 WORK + HPC2 WORK
140 1.0        ! ADD
141 -1.0
142 147      ! HPT WORK
143 -1.0
144 302      ! HPC1 WORK
145 -1.0
146 303      ! HPC2 WORK
! ARITHY T3=BD165
160 5! Add
161 -1
162 165
163 3
164 6
! ARITHY T4=175
170 5   ! COPY
171 -1
172 175
173 4
174 6
! ARITHY DLI=D187=(LPC
Tout-I/C Tout)
180 2! Sub
181 -1
182 187
183 3
184 6
185 4
186 6
! ARITHY D307= DIA =(I/C
Tout-Tamb)
190 2! Subtract
191 -1
192 197
193 4
194 6
195 1
196 6
! ARITHY COPY D205=Tamb
200 5
201 -1
202 205
203 1
204 6
! ARITHY W2 IN Kg/s
210 11
211 -1
212 215
213 2
214 2
! ARITHY COPY Wb=(W5-
W6)
220 2
221 -1
222 227
223 5
224 2
225 6
226 2
! ARITHY COPY
D245=COLD HE Tin
230 5
231 -1
232 235
233 8
234 6
! ARITHY COPY
D255=COLD HE Tout
240 5
241 -1
242 245
243 9
244 6
! ARITHY COPY D265=COT
250 5
251 -1
252 255
253 11
254 6
! ARITHY COPY D275=TET
260 5
261 -1
262 265
263 13
264 6
! ARITHY COPY D285=HOT
HE Tin
270 5
271 -1
272 275
273 18
274 6
! ARITHY COPY D295=HOT
HE Tout
280 5
281 -1
282 285
283 19
284 6
! ARITHY D297= DHEC =(HE
Tin-HPC Tout)
290 2! Subtract
291 -1
292 297
293 18
294 6
295 8
296 6
!*************************
```

```
! FOR EMMISION
CALCULATION
!*************************
! ARITHY W10 IN Kg/s
330 11
331 -1
332 335
333 10
334 2
! ARITHY W11 IN Kg/s
340 11
341 -1
342 345
343 11
344 2
! ARITHY Wf= (W11-W10)
350 2
351 -1
352 357
353 -1
354 345
355 -1
356 335
! ARITHY COPY T10=365
360 5
361 -1
362 365
363 10
364 6
! ARITHY P10 in (Pa)
370 3
371 -1
372 378
373 10
374 4
375 -1
376 377
377 101325.0
!*************************
! ARITHY W4 IN Kg/s
500 11
501 -1
502 505
503 4
504 2
! ARITHY: (W4*SQRT T4)
515 15
516 -1
517 522
518 -1
519 505
520 4
521 6
! ARITHY: (W4*SQRT T4)/P4
523 4
524 -1
525 530
526 -1
527 522
528 4
529 4
! ARITHY W6 IN Kg/s
551 11
552 -1
553 556
554 6
555 2
! ARITHY: (W6*SQRT T6)
560 15
561 -1
562 567
563 -1
564 556
565 6
566 6
! ARITHY: (W6*SQRT T6)/P6
570 4
571 -1
572 577
573 -1
574 567
575 6
576 4
! ARITHY COPY 585=Tex
580 5
581 -1
582 585
583 19
584 6
!*****************************
! FOR Q(MW) Exhaust Heat
CalcS
!*****************************
! ARITHY W19 IN Kg/s
600 11
601 -1
602 605
603 19
604 2
! ARITHY (W19*Cp)
610 3
611 -1
612 618
613 -1
614 605
615 -1
616 617
617 1150.0
! ARITHY (Tex-Tout)
620 2
621 -1
622 628
623 19
624 6
625 -1
626 627
627 400.0
! ARITHY Q=W19*Cp*(Tex-
Tout)
630 3
631 -1
632 637
633 -1
634 618
635 -1
636 628
! ARITHY Q IN MW
640 4
641 -1
642 648
643 -1
644 637
645 -1
646 647
647 1000000.0
!*****************************
! ARITHY W13 IN Kg/s
700 11
701 -1
702 705
703 13
704 2
! ARITHY: (W13*SQRT T13)
706 15
707 -1
708 713
709 -1
710 705
711 13
712 6
! ARITHY: (W13*SQRT
T13)/P13
714 4
715 -1
716 721
717 -1
718 713
719 13
720 4
-1
4 6 308.2003
1 2 32.969     ! Inlet Mass
Flow
11 6 1400.0     ! Burner Outlet
Temperature
-1
-3
```

E.1.14 Two-Spool Three-Shaft non-Conv [ICR] Cycle Engine [FPT]

```
! TURBOMATCH MODEL DATA FILE FOR: AERO-
DERIVATIVE ENGINE DERIVED FROM CUAV 130
AIRCRAFT ENGINE
MODELLED BY ABDELMANAM ABAAD
////
OD SI KE VA FP
-1
-1
INTAKE S1, 2      D1-4            R300
COMPRE S2, 3      D5-11           R301 V5 V6
DUCTER S3, 4      D12 -15
COMPRE S4,5       D18-24          R302 V18 V19
PREMAS S5, 21, 6   D25 -28
ARITHY            D120-124
COMPRE S6, 7      D29-35          R303 V29
PREMAS S7, 22, 8   D36 -39
PREMAS S22, 24, 23 D40 -43
HETCOL S8, 9   D90 -93
PREMAS S9, 25, 10   D44 -47
BURNER S10, 11      D48-50        R304
MIXEES S11, 25, 12
MIXEES S12, 23, 13
ARITHY            D140-147
TURBIN S13, 14    D51 -58, 147, 59        V52
MIXEES S14, 24, 15
TURBIN S15, 16     D60 -67, 301, 68       V61
HETHOT S8, 16, 17   D95 -98
DUCTER S17, 18     D69-72         R305
TURBIN S18, 19     D73-82             V73 V74
NOZCON S19, 20, 1   D83            R306
ARITHY            D150-155
ARITHY            D160-168
ARITHY            D170-175
ARITHY            D180-187
ARITHY            D190-197
ARITHY            D200-205
ARITHY            D210-215
ARITHY            D220-227
ARITHY            D230-235
ARITHY            D240-245
ARITHY            D250-255
ARITHY            D260-265
ARITHY            D270-275
ARITHY            D280-285
ARITHY            D290-297
!*************************
! FOR EMMISION CALCULATION
!*************************
ARITHY            D330-335
ARITHY            D340-345
ARITHY            D350-357
ARITHY            D360-365
ARITHY            D370-378
!*************************
ARITHY            D500-505
ARITHY            D515-522
ARITHY            D523-530
ARITHY            D551-556
ARITHY            D560-567
ARITHY            D570-577
ARITHY            D580-585
ARITHY            D700-705
ARITHY            D706-713
ARITHY            D714-721
!*************************
!FOR Exhaust Heat Q(MW) CAL
!*************************
ARITHY            D600-605
ARITHY            D610-618
ARITHY            D620-628
ARITHY            D630-637
ARITHY            D640-648
!*************************
!                 Wex Tex Tsk Q T4 HETin DHEC
PLOTBD            D605, 585,627,648,175,275,297
!                Wc Pc Tc Wf Alt DT COT TET DHEC
! PLOTBD           D335, 378, 365, 357, 1,
2,255,265,297
!                COT TET T16 Tex HC1 HC2 HPT Q
DHEC
! PLOTBD           D255,
265,275,285,530,577,721,648,297
!              LPC DT T4 COT TET T16 DIA DHEC Q
! PLOTBD           D7, 2,175,255,265,275,197,297,648
!               Alt DT Tam DIA DLI DHEC Q BIV
! PLOTBD            D1, 2,205,197,187,297,648,227
PERFOR  S1,0,0    D73,84-86,306,300,304,0,0,0,0,0,0
CODEND
DATA ITEMS////
! INTAKE
1 0.0         ! INTAKE ALTITUDE
2 0.0         ! ISA DEVIATION
3 0.0         ! MACH NO
4 0.9951      ! PRESSURE RECOVERY
! LP COMPRESSORE
5    0.85     ! Z PARAMETER
6    0.8      ! Relative ND rotational Speed
7    3.0      ! Compressor Pressure Ratio
8    0.89     ! Isentropic Efficiency
9    0.0      ! Error Selection
10   5.0      ! Compressor Map Number
11   0.0      ! ANGLE
!  DUCTER
12   2.0      ! Switch Set
13   0.03     ! Total pressure Loss/Inlet total Pressure
Dp/P
14   0.8      ! Combustion Efficiency
15   0.0      ! Limiting Value of Fuel Flow
! HP COMPRESSOR1
18   0.85     ! Z Parameter
19   -1.0     ! Relative ND rotational Speed
20   7.11     ! Compressor Pressure Ratio
21   0.9      ! Isentropic Efficiency
22   0.0      ! Error Selection
23   5.0      ! Compressor Map Number
24   0.0      ! ANGLE
!  BLEEDING VALVE
25 0.04568     ! BLEEDING RATIO
26 0.0         ! MASS FLOW LOSS
27 0.0         ! PRESSURE FACTOR
28 0.0         ! PRESSURE LOSS
! HP COMPRESSOR2
29   0.85     ! Z Parameter
30   -1.0     ! Relative ND rotational Speed
31   2.11     ! Compressor Pressure Ratio
32   0.88     ! Isentropic Efficiency
33   0.0      ! Error Selection
34   4.0      ! Compressor Map Number
35   0.0      ! ANGLE
!  TOTAL COOLING BLEED FOR HPT & LPT
SEALING
36 0.145       ! ROTORS COOLING
37 0.0         ! MASS FLOW LOSS
38 1.0         ! PRESSURE FACTOR
39 0.0         ! PRESSURE LOSS
!  SPLIT COOLING BLEED FOR LPT SEALING)
40 0.31       !% HPT SEALING AND % LPT
```

```
41 0.0       ! MASS FLOW LOSS
42 0.0       ! PRESSURE
FACTOR
43 0.0       ! PRESSURE LOSS
! BURNER INTERNAL BYPASS
COOLING
44 0.0       ! BYPASS RATIO
45 0.0       ! MASS FLOW
LOSS
46 0.0       ! PRESSURE
FACTOR
47 0.0       ! PRESSURE LOSS
!  BURNER
48    0.048    ! Fractional
pressure Loss DP/P
49    0.9999   ! COMBUSTION
EFFICIENCY
50   -1.0      ! FUEL FLOW
!  HP TURBINE
51   0.0       ! AUX.WORK
52 -1.0        ! REL NON-D MASS
FLOW
53 -1.0        ! REL NON-D
SPEED
54 0.90        ! EFFICIENCY
55 -1.0        ! REL ROT.SPEED
(COMP TURB=-1)
56 2.0         ! COMP NO. FROM
LOW END
57 5.0         ! TURBINE MAP
58 -1.0        ! POWER LAW
59 0.0         ! NGV ANGLE
RELATIVE TO D
!  LP TURBINE
60 0.0    ! AUXILIARY WORK
61 -1.0        ! REL NON-D
MASS FLOW
62 -1.0        ! REL NON-D
SPEED
63 0.91        ! ISENTROPIC
EFFICIENCY
64 -1.0        ! REL ROT.SPEED
65 1.0         ! COMPRESSOR
NUMBER
66 5.0         ! TURBINE MAP
NUMBER
67 -1.0       ! POWER LOW
INDEX
68 0.0         ! NGV ANGLE
RELATIVE TO D.
!  PT INLET DUCT
69 0.0
70 0.02
71 0.0
72 0.0
!  POWER TURBINE
73 21600906.0! Auxiliary Work
74 0.8       ! Relative ND Mass
Flow
75 0.6       ! Relative ND
Rotational Speed
76 0.92      ! Isentropic efficiency
77 1.0       ! Relative Rotational
Speed
78 0.0       ! Compressor number
79 4.0       ! Map Number
80 1000.0     ! Power Law index
81 -1.0       ! Compressor Work
82 0.0       ! NGV ANGLE
RELATIVE TO D
! HETCOL
90 0.02
91 0.9
92 3.0
93 0.0
! HETHOT
95 0.03
96 0.9
97 3.0
98 0.0
! NOZCON
83   -1.0      ! THROAT AREA
! PERFOR
84    1.0      ! PROPELLER
EFFICIENCY
85    0.0      ! SCALING INDEX
86    0.0      ! REQUIRED
THRUST
! ARITHY: HPC1 SPEED =
HPC2 SPEED
120 5.0        ! COPY
121 -1.0
122 30.0       ! HPC2 SPEEDD
123 -1.0
124 19.0       ! HPC1 SPEED
!  ARITHY: HPT WORK = HPC1
WORK + HPC2 WORK
140 1.0        ! ADD
141 -1.0
142 147        ! HPT WORK
143 -1.0
144 302        ! HPC1 WORK
145 -1.0
146 303        ! HPC2 WORK
! ARITHY T3=BD165
160 5! Add
161 -1
162 165
163 3
164 6
! ARITHY T4=175
170 5   ! COPY
171 -1
172 175
173 4
174 6
! ARITHY DLI=D187=(LPC Tout-
I/C Tout)
180 2! Sub
181 -1
182 187
183 3
184 6
185 4
186 6
! ARITHY D307= DIA =(I/C Tout-
Tamb)
190 2! Subtract
191 -1
192 197
193 4
194 6
195 1
196 6
! ARITHY COPY D205=Tamb
200 5
201 -1
202 205
203 1
204 6
! ARITHY W2 IN Kg/s
210 11
211 -1
212 215
213 2
214 2
! ARITHY COPY Wb= (W5-W6)
220 2
221 -1
222 227
223 5
224 2
225 6
226 2
! ARITHY COPY D245=COLD
HE Tin
230 5
231 -1
232 235
233 8
234 6
! ARITHY COPY D255=COLD
HE Tout
240 5
241 -1
242 245
243 9
244 6
! ARITHY COPY D265=COT
250 5
251 -1
252 255
253 11
254 6
! ARITHY COPY D275=TET
260 5
261 -1
262 265
263 13
264 6
! ARITHY COPY D285=HOT HE
Tin
270 5
271 -1
272 275
273 16
274 6
! ARITHY COPY D295=HOT HE
Tout
280 5
281 -1
282 285
283 17
284 6
! ARITHY D297= DHEC =(HE
Tin-HPC Tout)
290 2! Subtract
291 -1
292 297
293 16
294 6
295 8
296 6
!**************************
! FOR EMMISION
CALCULATION
!**************************
! ARITHY W10 IN Kg/s
330 11
331 -1
332 335
333 10
334 2
! ARITHY W11 IN Kg/s
340 11
341 -1
```

```
342 345
343 11
344 2
! ARITHY Wf=(W11-W10)
350 2
351 -1
352 357
353 -1
354 345
355 -1
356 335
! ARITHY COPY T10=365
360 5
361 -1
362 365
363 10
364 6
! ARITHY P10 in (Pa)
370 3
371 -1
372 378
373 10
374 4
375 -1
376 377
377 101325.0
!*************************
! ARITHY W4 IN Kg/s
500 11
501 -1
502 505
503 4
504 2
! ARITHY: (W4*SQRT T4)
515 15
516 -1
517 522
518 -1
519 505
520 4
521 6
! ARITHY: (W4*SQRT T4)/P4
523 4
524 -1
525 530
526 -1
527 522
528 4
529 4
! ARITHY W6 IN Kg/s
551 11
552 -1
553 556
554 6
555 2
! ARITHY: (W6*SQRT T6)
560 15
561 -1
562 567
563 -1
564 556
565 6
566 6
! ARITHY: (W6*SQRT T6)/P6
570 4
571 -1
572 577
573 -1
574 567
575 6
576 4
! ARITHY COPY 585=Tex
580 5
581 -1
582 585
583 19
584 6
!*****************************
! FOR Q(MW) Exhaust Heat
CalcS
!*****************************
! ARITHY W19 IN Kg/s
600 11
601 -1
602 605
603 19
604 2
! ARITHY (W19*Cp)
610 3
611 -1
612 618
613 -1
614 605
615 -1
616 617
617 1150.0
! ARITHY (Tex-Tout)
620 2
621 -1
622 628
623 19
624 6
625 -1
626 627
627 400.0
! ARITHY Q=W19*Cp*(Tex-Tout)
630 3
631 -1
632 637
633 -1
634 618
635 -1
636 628
! ARITHY Q IN MW
640 4
641 -1
642 648
643 -1
644 637
645 -1
646 647
647 1000000.0
!*****************************
! ARITHY W13 IN Kg/s
700 11
701 -1
702 705
703 13
704 2
! ARITHY: (W13*SQRT T13)
706 15
707 -1
708 713
709 -1
710 705
711 13
712 6
! ARITHY: (W13*SQRT T13)/P13
714 4
715 -1
716 721
717 -1
718 713
719 13
720 4
-1
4 6 360.0
1 2 70.4     ! Inlet Mass Flow
11 6 1635.3  ! Combustor Outlet
Temperature
-1
-3
```

E.2 Marinating HP Components

E.2.1 Two-Spool 3Shaft Simple Cycle [DDV] Engine [FPT]

```
! TURBOMATCH MODEL DATA FILE FOR: AERO-
DERIVATIVE ENGINE DERIVED FROM CUAV 130
AIRCRAFT ENGINE
MODELLED BY ABDELMANAM ABAAD
////
OD SI KE VA FP
-1
-1
INTAKE S1, 2       D1-4              R300
COMPRE S2, 3       D5-11             R301 V5 V6
DUCTER S3, 4       D12 -15
COMPRE S4, 5       D18-24            R302 V18 V19
PREMAS S5, 21, 6   D25 -28
ARITHY             D120-124
COMPRE S6, 7       D29-35            R303 V29
PREMAS S7, 22, 8   D36 -39
PREMAS S22, 24, 23 D40 -43
PREMAS S8, 25, 9   D44 -47
BURNER S9, 10      D48-50            R304
MIXEES S10, 25, 11
MIXEES S11, 23, 12
ARITHY             D140-147
TURBIN S12, 13     D51 -58, 147, 59          V52
MIXEES S13, 24, 14
TURBIN S14, 15     D60 -67, 301, 68          V61
DUCTER S15, 16     D69 -72
TURBIN S16, 17     D73-82                    V73 V74
NOZCON S17, 18, 1  D83               R306
ARITHY             D200-205
ARITHY             D230-235
ARITHY             D240-245
ARITHY             D250-255
ARITHY             D260-265
ARITHY             D270-275
ARITHY             D280-285
!*************************
! FOR EMMISION CALCULATION
!*************************
ARITHY             D330-335
ARITHY             D340-345
ARITHY             D350-357
ARITHY             D360-365
ARITHY             D370-378
!*************************
ARITHY             D379-384
ARITHY             D385-392
ARITHY             D393-400
ARITHY             D500-505
ARITHY             D515-522
ARITHY             D523-530
ARITHY             D551-556
ARITHY             D560-567
ARITHY             D570-577
ARITHY             D701-706
ARITHY             D710-717
ARITHY             D720-727
!****************************
! FOR Heat Output CALCULATION
!****************************
ARITHY             D600-605
ARITHY             D610-618
ARITHY             D620-628
ARITHY             D630-637
ARITHY             D640-648
!****************************
!                  W18 Tex Tstack Q
PLOTBD             D605, 285,627,648
!                  W9 P9 T9 Wf Alt DT W COT TET
! PLOTBD           D335, 378, 365, 357, 1,
2,384,275,235
PERFOR  S1,0,0     D73,84-
86,306,300,304,0,0,0,0,0,0
CODEND
DATA////
1   0.0      ! ALTITUDE
2   0.0      ! DEV FROM STAND TEMPERATURE
3   0.0      ! MACH NUMBER
4   0.9951   ! PRESSURE RECOVERY
! LP COMPRESSORE
5   0.85     ! Z PARAMETER
6   -1.0     ! Relative ND rotational Speed
7   2.53866  ! Compressor Pressure Ratio
8   0.89     ! Isentropic Efficiency
9   0.0      ! Error Selection
10  5.0      ! Compressor Map Number
11  0.0      ! ANGLE
! DIFUSSER
12  0.0      ! Switch Set
13  0.0      ! Total pressure Loss/Inlet total Pressure
Dp/P
14  0.0      ! Combustion Efficiency
15  0.0      ! Limiting Value of Fuel Flow
! HP COMPRESSOR1
18  0.85     ! Z Parameter
19  1.0      ! Relative ND rotational Speed
20  7.11     ! Compressor Pressure Ratio
21  0.9      ! Isentropic Efficiency
22  0.0      ! Error Selection
23  5.0      ! Compressor Map Number
24  0.0      ! ANGLE
!  BLEEDING VALVE
25 0.04568   ! BLEEDING RATIO
26 0.0       ! MASS FLOW LOSS
27 1.0       ! PRESSURE FACTOR
28 0.0       ! PRESSURE LOSS
! HP COMPRESSOR2
29  0.85     ! Z Parameter
30  1.0      ! Relative ND rotational Speed
31  2.11     ! Compressor Pressure Ratio
32  0.88     ! Isentropic Efficiency
33  0.0      ! Error Selection
34  4.0      ! Compressor Map Number
35  0.0      ! ANGLE
!  TOTAL COOLING BLEED FOR HPT & LPT
SEALING
36 0.145     ! ROTORS COOLING
37 0.0       ! MASS FLOW LOSS
38 1.0       ! PRESSURE FACTOR
39 0.0       ! PRESSURE LOSS
!  SPLIT COOLING BLEED FOR LPT SEALING)
40 0.31      !% HPT SEALING AND % LPT
41 0.0       ! MASS FLOW LOSS
42 1.0       ! PRESSURE FACTOR
43 0.0       ! PRESSURE LOSS
! BURNER INTERNAL BYPASS COOLING
44 0.0       ! BYPASS RATIO
45 0.0       ! MASS FLOW LOSS
46 0.0       ! PRESSURE FACTOR
47 0.0       ! PRESSURE LOSS
!  BURNER
```

```
48    0.048     ! Fractional pressure Loss DP/P
49    0.9999    ! COMBUSTION EFFICIENCY
50   -1.0       ! FUEL FLOW
!  HP TURBINE
51 0.0         ! AUX.WORK
52 -1.0        ! REL NON-D MASS FLOW
53 -1.0        ! REL NON-D SPEED
54 0.90        ! EFFICIENCY
55 -1.0        ! REL ROT.SPEED (COMP TURB=-1)
56 2.0         ! COMP NO. FROM LOW END
57 5.0         ! TURBINE MAP
58 -1.0        ! POWER LAW
59 0.0         ! NGV ANGLE RELATIVE TO D
!  LP TURBINE
60 0.0         ! AUXILIARY WORK
61 -1.0        ! REL NON-D MASS FLOW
62 -1.0        ! REL NON-D SPEED
63 0.91        ! ISENTROPIC EFFICIENCY
64 -1.0        ! REL ROT.SPEED
65 1.0         ! COMPRESSOR NUMBER
66 5.0         ! TURBINE MAP NUMBER
67 -1.0        ! POWER LOW INDEX
68 0.0         ! NGV ANGLE RELATIVE TO D.
!  PT INLET DUCT
69 0.0
70 0.02
71 0.0
72 0.0
!  POWER TURBINE
73 24864546.0! Auxiliary Work
74 0.8       ! Relative ND Mass Flow
75 0.6       ! Relative ND Rotational Speed
76 0.9114      ! Isentropic efficiency
77 1.0       ! Relative Rotational Speed
78 0.0       ! Compressor number
79 4.0       ! Map Number
80 1000.0     ! Power Law index
81 -1.0      ! Compressor Work
82 0.0
! NOZCON
83   -1.0      ! THROAT AREA
! PERFOR
84    1.0      ! PROPELLER EFFICIENCY
85    0.0      ! SCALING INDEX
86    0.0      ! REQUIRED THRUST
!  ARITHY: HPC1 SPEED = HPC2 SPEED
120 5.0        ! COPY
121 -1.0
122 30.0        ! HPC2 SPEEDD
123 -1.0
124 19.0        ! HPC1 SPEED
!  ARITHY: HPT WORK = HPC1 WORK + HPC2
WORK
140 1.0         ! ADD
141 -1.0
142 147       ! HPT WORK
143 -1.0
144 302       ! HPC1 WORK
145 -1.0
146 303       ! HPC2 WORK
! ARITHY COPY T4=205
200 5! COPY
201 -1
202 205
203 4
204 6
! ARITHY COPY 235=TET
230 5
231 -1
232 235
233 12
234 6
! ARITHY COPY 245=T7
240 5
241 -1
242 245
243 7
244 6
! ARITHY W2 IN Kg/s
250 11
251 -1
252 255
253 2
254 2
! ARITHY W11 IN Kg/s
260 11
261 -1
262 265
263 11
264 2
! ARITHY COPY 275=COT
270 5
271 -1
272 275
273 10
274 6
! ARITHY COPY 285=Tex
280 5
281 -1
282 285
283 18
284 6
!**************************
! FOR EMMISION CALCULATION
!**************************
! ARITHY W9 IN Kg/s
330 11
331 -1
332 335
333 9
334 2
! ARITHY W10 IN Kg/s
340 11
341 -1
342 345
343 10
344 2
! ARITHY Wf= (W10-W9)
350 2
351 -1
352 357
353 -1
354 345
355 -1
356 335
! ARITHY COPY T9=365
360 5
361 -1
362 365
363 9
364 6
! ARITHY P9 in (Pa)
370 3
371 -1
372 378
373 9
374 4
375 -1
376 377
377 101325.0
!**************************
! ARITHY W2 IN Kg/s
379 11
380 -1
381 384
382 2
```

```
383 2
! ARITHY: (W2*SQRT T2)
385 15
386 -1
387 392
388 -1
389 375
390 2
391 6
! ARITHY: (W2*SQRT T2)/P2
393 4
394 -1
395 400
396 -1
397 392
398 2
399 4
! ARITHY W4 IN Kg/s
500 11
501 -1
502 505
503 4
504 2
! ARITHY: (W4*SQRT T4)
515 15
516 -1
517 522
518 -1
519 505
520 4
521 6
! ARITHY: (W4*SQRT T4)/P4
523 4
524 -1
525 530
526 -1
527 522
528 4
529 4
! ARITHY W12 IN Kg/s
551 11
552 -1
553 556
554 12
555 2
! ARITHY: (W12*SQRT T12)
560 15
561 -1
562 567
563 -1
564 556
565 12
566 6
! ARITHY: (W12*SQRT T12)/P12
570 4
571 -1
572 577
573 -1
574 567
575 12
576 4
!****************************
! FOR Heat Output CALCULATION
!****************************
! ARITHY W18 IN Kg/s
600 11
601 -1
602 605
603 18
604 2
! ARITHY (W16*Cp)
610 3
611 -1
612 618
613 -1
614 605
615 -1
616 617
617 1150.0
! ARITHY (Tex-Tout)
620 2
621 -1
622 628
623 18
624 6
625 -1
626 627
627 400.0
! ARITHY W12*Cp*(Tex-Tout)
630 3
631 -1
632 637
633 -1
634 618
635 -1
636 628
! ARITHY Q IN MW
640 4
641 -1
642 648
643 -1
644 637
645 -1
646 647
647 1000000.0
!**************************
! ARITHY W14 IN Kg/s
701 11
702 -1
703 706
704 14
705 2
! ARITHY: (W14*SQRT T14)
710 15
711 -1
712 717
713 -1
714 706
715 14
716 6
! ARITHY: (W14*SQRT T14)/P14
720 4
721 -1
722 727
723 -1
724 717
725 14
726 4
-1
1 2 59.23      ! Inlet Mass Flow
10 6 1758.58   ! Combustion Outlet Temperature
-1
-3
```

E.2.2 Three-Spool Simple Cycle [DDV] GT Engines [IPT]

```
! TURBOMATCH MODEL DATA FILE FOR: AERO-
DERIVATIVE ENGINE DERIVED FROM CUAV 130
AIRCRAFT ENGINE
MODELLED BY ABDELMANAM ABAAD
////
OD SI KE VA FP
-1
-1
INTAKE S1, 2       D1-4              R300
COMPRE S2, 3       D5-11             R301 V5 V6
DUCTER S3, 4       D12 -15
COMPRE S4-5        D16-22            R302 V16 V17
DUCTER S5, 6       D23 -26
COMPRE S6, 7       D27-33            R303 V27 V28
PREMAS S7, 21, 8   D34 -37
ARITHY             D120-124
COMPRE S8, 9       D38-44            R304 V38
PREMAS S9, 22, 10  D45 -48
PREMAS S22, 24, 23 D49 -52
PREMAS S10, 25, 11 D53 -56
BURNER S11, 12     D57-59            R305
MIXEES S12, 25, 13
MIXEES S13, 23, 14
ARITHY             D140-147
TURBIN S14, 15     D60 -67, 147, 68          V61
MIXEES S15, 24, 16
TURBIN S16, 17     D69 -76, 302, 77          V70
TURBIN S17, 18     D78 -85, 301, 86          V78 V79
NOZCON S18, 19, 1  D101              R306
ARITHY             D215-220
ARITHY             D221-226
ARITHY             D230-235
ARITHY             D240-245
ARITHY             D250-255
ARITHY             D260-265
ARITHY             D270-275
ARITHY             D280-285
ARITHY             D500-505
ARITHY             D510-518
ARITHY             D520-528
ARITHY             D530-537
ARITHY             D540-548
ARITHY             D600-605
ARITHY             D606-613
ARITHY             D614-621
!              LPC W T3 T4 T6 T8 T9 COT TET
! PLOTBD    D7, 220,226,235,245,255,265,208,275
!               Tex LPC IPC HC1 HC2 HPT IPT LPT Q
! PLOTBD    D285, 621,646,671,696,721,746,771,548
PERFOR  S1,0,0     D78,102-
104,306,300,305,0,0,0,0,0,0
CODEND
DATA////
1    0.0       ! ALTITUDE
2    0.0       ! DEV FROM STAND TEMPERATURE
3    0.0       ! MACH NUMBER
4    0.9951     ! PRESSURE RECOVERY
! LP COMPRESSORE
5    0.85       ! Z PARAMETER
6   -1.0        ! Relative ND rotational Speed
7    1.2        ! Compressor Pressure Ratio
8    0.89       ! Isentropic Efficiency
9    0.0        ! Error Selection
10   5.0        ! Compressor Map Number
11   0.0        ! ANGLE
! INTERCOOLER (SPRINT)
12   0.0        ! Switch Set
13   0.0       ! Total pressure Loss/Inlet total Pressure
Dp/P
14   0.0       ! Combustion Efficiency
15   0.0       ! Limiting Value of Fuel Flow
! IP COMPRESSOR
16   0.85       ! Z Parameter
17   1.0        ! Relative ND rotational Speed
18   2.53       ! Compressor Pressure Ratio
19   0.9        ! Isentropic Efficiency
20   0.0        ! Error Selection
21   5.0        ! Compressor Map Number
22   0.0        ! ANGLE
! DIFFUSER
23   0.0        ! Switch Set
24   0.0        ! Total pressure Loss/Inlet total Pressure
Dp/P
25   0.0        ! Combustion Efficiency
26   0.0        ! Limiting Value of Fuel Flow
! HP COMPRESSOR1
27   0.85       ! Z Parameter
28   1.0        ! Relative ND rotational Speed
29   7.11       ! Compressor Pressure Ratio
30   0.9        ! Isentropic Efficiency
31   0.0        ! Error Selection
32   5.0        ! Compressor Map Number
33   0.0        ! ANGLE
!  BLEEDING VALVE
34   0.04568    ! BLEEDING RATIO
35   0.0        ! MASS FLOW LOSS
36   1.0        ! PRESSURE FACTOR
37   0.0        ! PRESSURE LOSS
! HP COMPRESSOR2
38   0.85       !Z Parameter
39   1.0        ! Relative ND rotational Speed
40   2.11       ! Compressor Pressure Ratio
41   0.88       ! Isentropic Efficiency
42   0.0        ! Error Selection
43   4.0        ! Compressor Map Number
44   0.0        ! ANGLE
!  TOTAL COOLING BLEED FOR HPT & LPT
SEALING
45   0.145      ! ROTORS COOLING
46   0.0        ! MASS FLOW LOSS
47   1.0        ! PRESSURE FACTOR
48   0.0        ! PRESSURE LOSS
!  SPLIT COOLING BLEED FOR LPT SEALING)
49   0.31       !% HPT SEALING AND % LPT
50   0.0        ! MASS FLOW LOSS
51   1.0        ! PRESSURE FACTOR
52   0.0        ! PRESSURE LOSS
! BURNER INTERNAL BYPASS COOLING
53   0.0        ! BYPASS RATIO
54   0.0        ! MASS FLOW LOSS
55   0.0        ! PRESSURE FACTOR56   0.0        !
PRESSURE LOSS
!  BURNER
57   0.048      ! Fractional pressure Loss DP/P
58   0.9999     ! COMBUSTION EFFICIENCY
59 -1.0        ! FUEL FLOW
!  HP TURBINE
60   0.0        ! AUX.WORK
61 -1.0        ! REL NON-D MASS FLOW
62 -1.0        ! REL NON-D SPEED
63   0.90       ! EFFICIENCY
64 -1.0        ! REL ROT.SPEED (COMP TURB=-1)
65   3.0        ! COMP NO. FROM LOW END
66   5.0        ! TURBINE MAP
67 -1.0        ! POWER LAW
68   0.0        ! NGV ANGLE RELATIVE TO D
!  IP TURBINE
69   0.0        ! AUXILIARY WORK
```

```
70 -1.0        ! REL NON-D
MASS FLOW
71 -1.0        ! REL NON-D
SPEED
72   0.91       ! ISENTROPIC
EFFICIENCY
73 -1.0        ! REL ROT.SPEED
74   2.0        ! COMPRESSOR
NUMBER
75   5.0        ! TURBINE MAP
NUMBER
76 -1.0        ! POWER LOW
INDEX
77   0.0        ! NGV ANGLE
RELATIVE TO D.
!  LP TURBINE
78 33026610.0   ! Auxiliary Work
79 -1.0        ! Relative ND Mass
Flow
80 -1.0        ! Relative ND
Rotational Speed
81   0.91       ! Isentropic
efficiency
82 -1.0        ! Relative Rotational
Speed
83   1.0        ! Compressor
number
84   4.0        ! Map Number
85 1000.0        ! Power Law
index
86   0.0        ! NGV ANGLE
RELATIVE TO D
! NOZCON
101 -1.0       ! THROAT AREA
! PERFOR
102 1.0        ! PROPELLER
EFFICIENCY
103 0.0        ! SCALING INDEX
104 0.0        ! REQUIRED
THRUST
!  ARITHY: HPC1 SPEED =
HPC2 SPEED
120 5.0        ! COPY
121 -1.0
122 39.0        ! HPC2 SPEEDD
123 -1.0
124 28.0        ! HPC1 SPEED
!  ARITHY: HPT WORK = HPC1
WORK + HPC2 WORK
140 1.0        ! ADD
141 -1.0
142 147        ! HPT WORK
143 -1.0
144 303        ! HPC1 WORK
145 -1.0
146 304        ! HPC2 WORK
! ARITHY COPY W1=220
215 5! COPY
216 -1
217 220
218 1
219 2
! ARITHY COPY T3=226
221 5   ! COPY
222 -1
223 226
224 3
225 6
! ARITHY COPY T4=235
230 5! COPY
231 -1
232 235
233 4
234 6
! ARITHY COPY T6=245
240 5! COPY
241 -1
242 245
243 6
244 6
! ARITHY COPY T8=255
250 5! COPY
251 -1
252 255
253 8
254 6
! ARITHY COPY T9=265
260 5! COPY
261 -1
262 265
263 9
264 6
! ARITHY COPY TET=275
270 5! COPY
271 -1
272 275
273 14
274 6
! ARITHY COPY Tex=285
280 5! COPY
281 -1
282 285
283 19
284 6
! ARITHY W19 IN Kg/s
500 11
501 -1
502 505
503 19
504 2
! ARITHY (W19*Cp)
510 3
511 -1
512 518
513 -1
514 505
515 -1
516 517
517 1150.0
! ARITHY (Tex-Tout)
520 2
521 -1
522 528
523 19
524 6
525 -1
526 527
527 400.0
! ARITHY Q=W19*Cp*(Tex-Tout)
530 3
531 -1
532 537
533 -1
534 518
535 -1
536 528
! ARITHY Q IN MW
540 4
541 -1
542 548
543 -1
544 537
545 -1
546 547
547 1000000.0
! ARITHY W2 IN Kg/s
600 11
601 -1
602 605
603 2
604 2
! ARITHY: (W2*SQRT T2)
606 15
607 -1
608 613
609 -1
610 605
611 2
612 6
! ARITHY: (W2*SQRT T)/P2
614 4
615 -1
616 621
617 -1
618 613
619 2
620 4
-1
1 2 69.02    ! Inlet Mass Flow
12 6 1864.33
-1
34 0.0!*****( Blow Off Bleed
Valve is OFF )*******
-1
-3
```

E.2.3 Three Spool Intercooled [DDV] GT Engines [IPT]

```
! TURBOMATCH MODEL DATA FILE FOR: AERO-
DERIVATIVE ENGINE DERIVED FROM CUAV 130
AIRCRAFT ENGINE
MODELLED BY ABDELMANAM ABAAD
////
OD SI KE VA FP
-1
-1
INTAKE S1, 2      D1-4            R300
COMPRE S2, 3      D5-11           R301 V5 V6
DUCTER S3, 4      D12 -15
COMPRE S4-5       D16-22          R302 V16 V17
DUCTER S5, 6      D23 -26
COMPRE S6, 7      D27-33          R303 V27 V28
PREMAS S7, 21, 8  D34 -37
ARITHY            D120-124
COMPRE S8, 9      D38-44          R304 V38
PREMAS S9, 22, 10 D45 -48
PREMAS S22, 24, 23 D49 -52
PREMAS S10, 25, 11 D53 -56
BURNER S11, 12    D57-59          R305
MIXEES S12, 25, 13
MIXEES S13, 23, 14
ARITHY            D140-147
TURBIN S14, 15    D60 -67, 147, 68        V61
MIXEES S15, 24, 16
TURBIN S16, 17    D69 -76, 302, 77        V70
TURBIN S17, 18    D78 -85, 301, 86        V78 V79
NOZCON S18, 19, 1 D101            R306
ARITHY            D210-215
ARITHY            D220-225
ARITHY            D230-235
ARITHY            D240-247
ARITHY            D250-257
ARITHY            D260-265
ARITHY            D270-275
ARITHY            D280-285
!*************************
! FOR EMMISION CALCULATION
!*************************
ARITHY            D330-335
ARITHY            D340-345
ARITHY            D350-357
ARITHY            D360-365
ARITHY            D370-378
!*************************
!*************************
! FOR Exhaust Heat Q(MW) CAL
!*************************
ARITHY            D500-505
ARITHY            D510-518
ARITHY            D520-528
ARITHY            D530-537
ARITHY            D540-548
!*************************
ARITHY            D600-605
ARITHY            D606-613
ARITHY            D614-621
ARITHY            D625-630
ARITHY            D631-638
ARITHY            D639-646
ARITHY            D650-655
ARITHY            D656-663
ARITHY            D664-671
ARITHY            D675-680
ARITHY            D681-688
ARITHY            D689-696
ARITHY            D700-705
ARITHY            D706-713
ARITHY            D714-721
!                 Wex Tex Tstack Q T4
PLOTBD            D505, 285,527,548,235
!                  W Alt DT Tam IADT ICDT COT TET
! PLOTBD           D605, 1, 2,215,247,257,265,275
!                 W9
! PLOTBD           D335
!                 P9 T9 Wf A D IADT COT TET
! PLOTBD           D378, 365, 357, 1, 2,247,265,275
!                 W9 P9 T9 Wf A D IADT COT TET
! PLOTBD           D335, 378, 365, 357, 1,
2,247,265,275
!                  W  Tam T3 T4
! PLOTBD           D605, 215,225,235
!                  Tex LPC HC1 HC2 HPT LPT Q
! PLOTBD           D285, 621,646,671,696,721,548
PERFOR  S1,0,0     D78,102-
104,306,300,305,0,0,0,0,0,0
CODEND
DATA////
1   0.0       ! ALTITUDE
2   0.0       ! DEV FROM STAND TEMPERATURE
3   0.0       ! MACH NUMBER
4   0.9951    ! PRESSURE RECOVERY
! LP COMPRESSORE
5   0.45      ! Z PARAMETER
6   -1.0      ! Relative ND rotational Speed
7   3.0       ! Compressor Pressure Ratio
8   0.89      ! Isentropic Efficiency
9   0.0       ! Error Selection
10  5.0       ! Compressor Map Number
11  0.0       ! ANGLE
! INTERCOOLER (SPRINT)
12  2.0       ! Switch Set
13  0.03      ! Total pressure Loss/Inlet total Pressure
Dp/P
14  0.5       ! Combustion Efficiency
15  0.0       ! Limiting Value of Fuel Flow
! IP COMPRESSOR
16  0.85      ! Z Parameter
17  1.0       ! Relative ND rotational Speed
18  2.53      ! Compressor Pressure Ratio
19  0.9       ! Isentropic Efficiency
20  0.0       ! Error Selection
21  5.0       ! Compressor Map Number
22  0.0       ! ANGLE
! DIFFUSER
23  0.0       ! Switch Set
24  0.0       ! Total pressure Loss/Inlet total Pressure
Dp/P
25  0.0       ! Combustion Efficiency
26  0.0       ! Limiting Value of Fuel Flow
! HP COMPRESSOR1
27  0.85      ! Z Parameter
28  1.0       ! Relative ND rotational Speed
29  7.11      ! Compressor Pressure Ratio
30  0.9       ! Isentropic Efficiency
31  0.0       ! Error Selection
32  5.0       ! Compressor Map Number
33  0.0       ! ANGLE
!  BLEEDING VALVE
34  0.04568   ! BLEEDING RATIO
35  0.0       ! MASS FLOW LOSS
36  1.0       ! PRESSURE FACTOR
37  0.0       ! PRESSURE LOSS
! HP COMPRESSOR2
38  0.85      ! Z Parameter
39  1.0       ! Relative ND rotational Speed
40  2.11      ! Compressor Pressure Ratio
```

```
41   0.88      ! Isentropic Efficiency
42   0.0       ! Error Selection
43   4.0       ! Compressor Map Number
44   0.0       ! ANGLE
!  TOTAL COOLING BLEED FOR HPT & LPT
SEALING
45   0.145     ! ROTORS COOLING
46   0.0       ! MASS FLOW LOSS
47   1.0       ! PRESSURE FACTOR
48   0.0       ! PRESSURE LOSS

!  SPLIT COOLING BLEED FOR LPT SEALING)
49   0.31      !% HPT SEALING AND % LPT
50   0.0       ! MASS FLOW LOSS
51   1.0       ! PRESSURE FACTOR
52   0.0       ! PRESSURE LOSS
! BURNER INTERNAL BYPASS COOLING
53   0.0       ! BYPASS RATIO
54   0.0       ! MASS FLOW LOSS
55   0.0       ! PRESSURE FACTOR
56   0.0       ! PRESSURE LOSS
!  BURNER
57   0.048     ! Fractional pressure Loss DP/P
58   0.9999    ! COMBUSTION EFFICIENCY
59 -1.0        ! FUEL FLOW
!  HP TURBINE
60   0.0       ! AUX.WORK
61 -1.0        ! REL NON-D MASS FLOW
62 -1.0        ! REL NON-D SPEED
63   0.90      ! EFFICIENCY
64 -1.0        ! REL ROT.SPEED (COMP TURB=-1)
65   3.0       ! COMP NO. FROM LOW END
66   5.0       ! TURBINE MAP
67 -1.0        ! POWER LAW
68   0.0       ! NGV ANGLE RELATIVE TO D
!  IP TURBINE
69   0.0       ! AUXILIARY WORK
70 -1.0        ! REL NON-D MASS FLOW
71 -1.0        ! REL NON-D SPEED
72   0.91      ! ISENTROPIC EFFICIENCY
73 -1.0        ! REL ROT.SPEED
74   2.0       ! COMPRESSOR NUMBER
75   5.0       ! TURBINE MAP NUMBER
76 -1.0        ! POWER LOW INDEX
77   0.0       ! NGV ANGLE RELATIVE TO D.
!  LP TURBINE
78 87013080.0  ! Auxiliary Work
79 -1.0        ! Relative ND Mass Flow
80 -1.0        ! Relative ND Rotational Speed
81   0.91      ! Isentropic efficiency
82 -1.0        ! Relative Rotational Speed
83   1.0       ! Compressor number
84   4.0       ! Map Number
85 1000.0      ! Power Law index
86   0.0       ! NGV ANGLE RELATIVE TO D
! NOZCON
101 -1.0       ! THROAT AREA
! PERFOR
102 1.0        ! PROPELLER EFFICIENCY
103 0.0        ! SCALING INDEX
104 0.0        ! REQUIRED THRUST
!  ARITHY: HPC1 SPEED = HPC2 SPEED
120 5.0        ! COPY
121 -1.0
122 39.0       ! HPC2 SPEEDD
123 -1.0
124 28.0       ! HPC1 SPEED
!  ARITHY: HPT WORK = HPC1 WORK + HPC2
WORK
140 1.0        ! ADD
141 -1.0
142 147        ! HPT WORK
143 -1.0
144 303        ! HPC1 WORK
145 -1.0
146 304        ! HPC2 WORK
! ARITHY COPY Tamb=215
210 5! COPY
211 -1
212 215
213 1
214 6
! ARITHY COPY T3=225
220 5! COPY
221 -1
222 225
223 3
224 6
! ARITHY COPY I/C Tout=235
230 5! COPY
231 -1
232 235
233 4
234 6
! ARITHY COPY IADT= (T4-Tamb)
240 2! COPY
241 -1
242 247
243 -1
244 235
245 1
246 6
! ARITHY COPY ICDT=(T3-T4)
250 2! COPY
251 -1
252 257
253 3
254 6
255 4
256 6
! ARITHY COPY COT=265
260 5! COPY
261 -1
262 265
263 12
264 6
! ARITHY COPY TET=275
270 5! COPY
271 -1
272 275
273 14
274 6
! ARITHY COPY Tex=285
280 5! COPY
281 -1
282 285
283 19
284 6
!*************************
! FOR EMMISION CALCULATION
!*************************
! ARITHY W11 IN Kg/s
330 11
331 -1
332 335
333 11
334 2
! ARITHY W12 IN Kg/s
340 11
341 -1
342 345
343 12
344 2
! ARITHY Wf= (W12-W11)
350 2
351 -1
```

```
352 357
353 -1
354 345
355 -1
356 335
! ARITHY COPY T11=365
360 5
361 -1
362 365
363 11
364 6
! ARITHY P11 in (Pa)
370 3
371 -1
372 378
373 11
374 4
375 -1
376 377
377 101325.0
!*****************************
! FOR Q (MW) Exhaust Heat
CalcS
!*****************************
! ARITHY W19 IN Kg/s
500 11
501 -1
502 505
503 19
504 2
! ARITHY (W19*Cp)
510 3
511 -1
512 518
513 -1
514 505
515 -1
516 517
517 1150.0
! ARITHY (Tex-Tout)
520 2
521 -1
522 528
523 19
524 6
525 -1
526 527
527 400.0
! ARITHY Q=W19*Cp*(Tex-Tout)
530 3
531 -1
532 537
533 -1
534 518
535 -1
536 528
! ARITHY Q IN MW
540 4
541 -1
542 548
543 -1
544 537
545 -1
546 547
547 1000000.0
!*****************************
! ARITHY W2 IN Kg/s
600 11
601 -1
602 605
603 2
604 2
! ARITHY: (W2*SQRT T2)
606 15
607 -1
608 613
609 -1
610 605
611 2
612 6
! ARITHY: (W2*SQRT T)/P2
614 4
615 -1
616 621
617 -1
618 613
619 2
620 4
! ARITHY W4 IN Kg/s
625 11
626 -1
627 630
628 4
629 2
! ARITHY: (W4*SQRT T4)
631 15
632 -1
633 638
634 -1
635 630
636 4
637 6
! ARITHY: (W4*SQRT T4)/P4
639 4
640 -1
641 646
642 -1
643 638
644 4
645 4
! ARITHY W6 IN Kg/s
650 11
651 -1
652 655
653 6
654 2
! ARITHY: (W6*SQRT T6)
656 15
657 -1
658 663
659 -1
660 655
661 6
662 6
! ARITHY: (W6*SQRT T6)/P6
664 4
665 -1
666 671
667 -1
668 663
669 6
670 4
! ARITHY W14 IN Kg/s
675 11
676 -1
677 680
678 14
679 2

! ARITHY: (W14*SQRT T14)
681 15
682 -1
683 688
684 -1
685 680
686 14
687 6
! ARITHY: (W14*SQRT T14)/P14
689 4
690 -1
691 696
692 -1
693 688
694 14
695 4
! ARITHY W16 IN Kg/s
700 11
701 -1
702 705
703 16
704 2
! ARITHY: (W16*SQRT T16)
706 15
707 -1
708 713
709 -1
710 705
711 16
712 6
! ARITHY: (W16*SQRT T16)/P16
714 4
715 -1
716 721
717 -1
718 713
719 16
720 4
-1
4 6 300.0    ! I/C Tout
1 2 168.9    ! Inlet Mass Flow
12 6 1830.9
-1
-3
```